animals

Special Issue Reprint

Wildlife Diseases

Pathology and Diagnostic Investigation

Edited by
Lorenzo Domenis and Serena Robetto

mdpi.com/journal/animals

MDPI

Wildlife Diseases: Pathology and Diagnostic Investigation

Wildlife Diseases: Pathology and Diagnostic Investigation

Guest Editors

Lorenzo Domenis
Serena Robetto

MDPI

Basel • Beijing • Wuhan • Barcelona • Belgrade • Novi Sad • Cluj • Manchester

Guest Editors

Lorenzo Domenis
Valle d'Aosta Department
Istituto Zooprofilattico
Sperimentale del Piemonte,
Liguria e Valle d'Aosta
Quart
Italy

Serena Robetto
Valle d'Aosta Department
Istituto Zooprofilattico
Sperimentale del Piemonte,
Liguria e Valle d'Aosta
Quart
Italy

Editorial Office
MDPI AG
Grosspeteranlage 5
4052 Basel, Switzerland

This is a reprint of the Special Issue, published open access by the journal *Animals* (ISSN 2076-2615), freely accessible at: https://www.mdpi.com/journal/animals/special_issues/ASWJ19MN20.

For citation purposes, cite each article independently as indicated on the article page online and as indicated below:

Lastname, A.A.; Lastname, B.B. Article Title. *Journal Name* **Year**, *Volume Number*, Page Range.

ISBN 978-3-7258-9175-7 (Hbk)
ISBN 978-3-7258-9176-4 (PDF)
https://doi.org/10.3390/books978-3-7258-9176-4

Cover image courtesy of Lorenzo Domenis
Acidophilic intra-cytoplasmatic inclusion bodies by Contagious Ecthyma Virus (ORFV) in alpine ibex (*Capra ibex*) - (Brightfield, HE, 100×)

© 2026 by the authors. Articles in this reprint are Open Access and distributed under the Creative Commons Attribution (CC BY) license. The reprint as a whole is distributed by MDPI under the terms and conditions of the Creative Commons Attribution-NonCommercial-NoDerivs (CC BY-NC-ND) license (https://creativecommons.org/licenses/by-nc-nd/4.0/).

Contents

About the Editors . . . . . **ix**

Lorenzo Domenis and Serena Robetto
Wildlife Diseases: Pathology and Diagnostic Investigation
Reprinted from: *Animals* **2026**, *16*, 1343, https://doi.org/10.3390/ani16091343 . . . . . **1**

Lorenzo Domenis, Marzia Pezzolato, Elena Biasibetti, Raffaella Spedicato and Serena Robetto
Gallbladder Carcinoma in a Eurasian Otter (*Lutra lutra*)
Reprinted from: *Animals* **2025**, *15*, 2484, https://doi.org/10.3390/ani15172484 . . . . . **4**

Piyaporn Eiamcharoen, Piyarat Khumraksa, Santi Ninwat, Tatsawan Suttiboon, Narissara Keawchana, Peerapon Sornying and Watcharapol Suyapoh
Novel Insight into Dugong Mortality: First Report of Systemic *Achromobacter xylosoxidans* Infection, Disseminated Intravascular Coagulation, and Associated Pathogenesis
Reprinted from: *Animals* **2025**, *15*, 2441, https://doi.org/10.3390/ani15162441 . . . . . **13**

Massimo Giangaspero, Salah Al Mahdhouri, Sultan Al Bulushi and Metaab K. Al-Ghafri
Wild Fauna in Oman: Foot-and-Mouth Disease Outbreak in Arabyan Oryx (*Oryx leucorix*)
Reprinted from: *Animals* **2025**, *15*, 2389, https://doi.org/10.3390/ani15162389 . . . . . **34**

Elisa Mazzotta, Claudia Zanardello, Giovanni De Zottis, Antonio Barberio, Mery Campalto, Federico Martignago, et al.
Diagnostic Approach and Pathological Characterization of Metastatic Intrahepatic Cholangiocarcinoma in a Captive Puma (*Puma concolor*)
Reprinted from: *Animals* **2025**, *15*, 1821, https://doi.org/10.3390/ani15121821 . . . . . **54**

Farkas Sükösd, István Lakatos, Ádám Ürmös, Réka Karkas, Ákos Sükösd, Gábor Palánki, et al.
When Antlers Grow Abnormally: A Hidden Disease Behind Common Cervid Trophy Deformities, Introducing Pedunculitis Chronica Deformans
Reprinted from: *Animals* **2025**, *15*, 1530, https://doi.org/10.3390/ani15111530 . . . . . **67**

Ella Cousins, Lucy Woolford, David McLelland, Sarah Brownrigg and Natasha Speight
Reference Values for Postmortem Examination of the Heart in the Macropod (*Macropodidae*) and Koala (*Phascolarctidae*)
Reprinted from: *Animals* **2025**, *15*, 1397, https://doi.org/10.3390/ani15101397 . . . . . **92**

Jaegyeong Shin, Nari Kim, Gwi-Ho Jeon, Taesik Yun, Byeong-Teck Kang and Dong-Hyuk Jeong
Diagnostic Application of Fluorine-18 Fluorodeoxyglucose Positron Emission Tomography/Computed Tomography in the Treatment of Oral Squamous Cell Carcinoma in an African Pygmy Hedgehog
Reprinted from: *Animals* **2024**, *14*, 3679, https://doi.org/10.3390/ani14243679 . . . . . **102**

Lorenzo Domenis, Raffaella Spedicato, Cristina Guidetti, Emanuele Carella and Serena Robetto
Different Types of Co-Infection by Contagious Ecthyma Virus, Enteropathogenic *Escherichia coli*, *Mycoplasma conjunctivae*, Ecto- and Endo-Parasites in Four Young Alpine Ibex (*Capra ibex*)
Reprinted from: *Animals* **2024**, *14*, 3666, https://doi.org/10.3390/ani14243666 . . . . . **109**

Zuleima Suárez-González, Jorge F. González, Manuel Arbelo, Eva Sierra, Ayoze Castro-Alonso, Julia N. Hernández, et al.
Parasitic Infections in Stranded Whales and Dolphins in Canary Islands (2018–2022): An Update
Reprinted from: *Animals* **2024**, *14*, 3377, https://doi.org/10.3390/ani14233377 . . . . . **122**

Ursula Siebert, Jan Lakemeyer, Martin Runge, Peter Lienau, Silke Braune, Edda Bartelt, et al.
Investigations on the Health Status and Infection Risk of Harbour Seals (*Phoca vitulina*) from Waters of the Lower Saxon Wadden Sea, Germany
Reprinted from: *Animals* **2024**, *14*, 2920, https://doi.org/10.3390/ani14202920 . . . . . **140**

Alessia Mariacher, Valentina Galietta, Gianni Massai, Francesco Bruni, Giovanni Ragionieri, Claudia Eleni and Gianluca Fichi
A Case of Epicardial Epidermoid Cyst in a Crested Porcupine
Reprinted from: *Animals* **2024**, *14*, 2706, https://doi.org/10.3390/ani14182706 . . . . . **161**

Laura Martino, María Cuvertoret-Sanz, Sarah Wilkinson, Alberto Allepuz, Albert Perlas, Llilianne Ganges, et al.
Serological Investigation for *Brucella ceti* in Cetaceans from the Northwestern Mediterranean Sea
Reprinted from: *Animals* **2024**, *14*, 2417, https://doi.org/10.3390/ani14162417 . . . . . **171**

Oana Irina Tanase, Geta Pavel, Ozana Maria Hritcu, Mihaela Anca Dascalu, Bianca Elena Bratuleanu, Cristina Mihaela Rimbu and Florentina Daraban Bocaneti
Disseminated Infection with *Aspergillus fumigatus* in a Scarlet Macaw Parrot (*Ara macao*)—A Case Report
Reprinted from: *Animals* **2024**, *14*, 2282, https://doi.org/10.3390/ani14152282 . . . . . **184**

Ilaria Prandi, Eva Dervas, Elena Colombino, Giuseppe Bonaffini, Stefania Zanet, Riccardo Orusa, et al.
Causes of Admission, Mortality and Pathological Findings in European Hedgehogs: Reports from Two University Centers in Italy and Switzerland
Reprinted from: *Animals* **2024**, *14*, 1852, https://doi.org/10.3390/ani14131852 . . . . . **192**

Alireza Rahmani Shahraki, João H. J. Bittar, Samantha M. Wisely and Juan M. Campos-Krauer
A Case of Severe Abomasal Sand Impaction in a Farmed White-Tailed Deer (*Odocoileus virginianus*) in Florida
Reprinted from: *Animals* **2024**, *14*, 1602, https://doi.org/10.3390/ani14111602 . . . . . **214**

Sydney L. Cottingham, An-Chi Cheng, Pedro H. de Oliveira Viadanna, Kuttichantran Subramaniam, William F. Craft, Marley E. Iredale, et al.
Mycobacterium kansasii Infection in a Farmed White-Tailed Deer (*Odocoileus virginianus*) in Florida, USA
Reprinted from: *Animals* **2024**, *14*, 1511, https://doi.org/10.3390/ani14101511 . . . . . **220**

Gabriela Muñoz, Vanessa Mendieta, Mauricio Ulloa, Belén Agüero, Cristian G. Torres, Lucas Kruger and Victor Neira
Lack of Highly Pathogenic Avian Influenza H5N1 in the South Shetland Islands in Antarctica, Early 2023
Reprinted from: *Animals* **2024**, *14*, 1008, https://doi.org/10.3390/ani14071008 . . . . . **226**

Caterina Raso, Valentina Galietta, Claudia Eleni, Marco Innocenti, Niccolò Fonti, Tiziana Palmerini, et al.
Ectopic Pregnancy and T-Cell Lymphoma in a Eurasian Red Squirrel (*Sciurus vulgaris*): Possible Comorbidity and a Comparative Pathology Perspective
Reprinted from: *Animals* **2024**, *14*, 731, https://doi.org/10.3390/ani14050731 . . . . . **235**

Šimun Naletilić, Ivan-Conrado Šoštarić-Zuckermann and Željko Mihaljević
Tumor and Tumor-like Lesions in Red Foxes (*Vulpes vulpes*) from Croatia
Reprinted from: *Animals* **2024**, *14*, 558, https://doi.org/10.3390/ani14040558 . . . . . **243**

Arturo Nicoletti, Paola Pregel, Laura Starvaggi Cucuzza, Enrico Bollo and Frine Eleonora Scaglione
A Health Status Update of *Myocastor coypus* in Northern Italy
Reprinted from: *Animals* **2024**, *14*, 245, https://doi.org/10.3390/ani14020245 . . . . . **254**

Elga Ersilia Tieri, Lucio Marino, Katiuscia Zilli, Cinzia Pompilii, Giovanni Di Teodoro, Antonio Cocco, et al.
Survey of *Mycobacterium* spp. in Eurasian Badgers (*Meles meles*) in Central Italy
Reprinted from: *Animals* **2024**, *14*, 219, https://doi.org/10.3390/ani14020219 . . . . . **264**

Sung Bin Lee, Adams Hei Long Yuen, Young Min Lee, Sang Wha Kim, Sunmin Kim, Cherry Tsz Ching Poon, et al.
Adhesive Bowel Obstruction (ABO) in a Stranded Narrow-Ridged Finless Porpoise (*Neophocaena asiaeorientalis sunameri*)
Reprinted from: *Animals* **2023**, *13*, 3767, https://doi.org/10.3390/ani13243767 . . . . . **276**

Eugenijus Jurgelėnas, Indrė Jasinevičiūtė and Linas Daugnora
Prevalence and Characterization of Dental and Skull-Bone Pathologies of the Raccoon Dog (*Nyctereutes procyonoides*) in Lithuania
Reprinted from: *Animals* **2023**, *13*, 2437, https://doi.org/10.3390/ani13152437 . . . . . **285**

Antonio Fernández, Nakita Câmara, Eva Sierra, Manuel Arbelo, Yara Bernaldo de Quirós, Paul D. Jepson, et al.
Cetacean Intracytoplasmic Eosinophilic Globules: A Cytomorphological, Histological, Histochemical, Immunohistochemical, and Proteomic Characterization
Reprinted from: *Animals* **2023**, *13*, 2130, https://doi.org/10.3390/ani13132130 . . . . . **300**

About the Editors

Lorenzo Domenis

Lorenzo Domenis, DVM (1989) and PhD (1993) at the University of Torino (Italy) and Master in Zooprophylaxis (1995) at the Istituto Zoopprofilattico of Brescia (Italy), since 2001 has been working as a veterinary officer at the Aosta Department/National Reference Centre of Wildlife Diseases (CeRMAS) of Istituto Zooprofilattico del Piemonte, Liguria e Valle d'Aosta. His main expertise fields, developed since his doctoral thesis on neuroreceptor nets in the naso-labial region of Italian insectivores (with particular attention to the Eimer's corpuscles in the mole) and then through employment in different public and private veterinary laboratories, focus on histopathology and bacteriology applied, in integrated form with parasitology and virology, to investigate diseases affecting free-ranging animals. Thanks to the location of his Department in the middle of the North-Western Italian Alps, he mainly deals with the diagnosis of infectious and neoplastic processes of wild mountain ungulates, carnivores and mustelids. Among these topics, his most relevant publications concerned different infectious diseases reports in chamois (caseosus lymphangytis by *Corynebacterium pseudotuberculosis*, meninngo-encephalitis by Border Disease Virus, pneumonia by *Nocardia otitidiscaviarum*); ibex (septicaemia by *Erysipelothryx rhusiopathiae*, contagious echtyma by ORF virus, cheratoconjuctivitis by *Mycoplasma mycoides* cluster); roe deer (tuberculosis by *Mycobacterium bovis*); wild boar (coinfection by *Trichinella britovi* and *Sarcocystis* spp.); various epithelial neoplasms in chamois, roe deer and otter; antibiotic resistance in wild fauna and the analytical protocol adopted for wild animals by his lab through the description of some model case reports of co-infections in alpine ruminants.

Serena Robetto

Serena Robetto graduated in Veterinary Medicine in 2002 and specialized in Swine Pathology in 2007 at the University of Torino (Italy). Since 2003 she has been dealing with wildlife pathology at the National Reference Centre of Wildlife Diseases (CeRMAS) of Istituto Zooprofilattico Sperimentale del Piemonte, Liguria e Valle d'Aosta (IZSPLV). She is involved in national and international scientific research on wild animal diseases and participated in the drafting and execution of several research projects funded by the Italian Ministry of Health, also serving as the scientific coordinator or project manager. Since 2019 she has had a permanent position as a veterinary officer at the IZSPLV – SS Patologia della fauna selvatica, and she is involved in diagnostic activities (necropsy, anatomopathological examination, parasitology, forensic pathology) related to wild animal diseases, especially in the passive surveillance of ungulates and wild carnivores. Her interests focus primarily on the monitoring of infectious diseases in wildlife and in the wildlife–livestock–human (WLH) interface, with particular interest for emerging and re-emerging viruses and parasites. In this context, she is author/co-author of scientific papers concerning zoonotic pathogens in wildlife, such as hepatitis E virus, coronavirus, *Sarcoptes scabiei*, and *Trichinella britovi*, as well as tick-borne pathogens in relation to the host and the environment. She also contributed to the reporting of the most interesting cases of wild animal diseases published in collaboration with CeRMAS.

animals

MDPI

Editorial

Wildlife Diseases: Pathology and Diagnostic Investigation

Lorenzo Domenis * and Serena Robetto

Istituto Zooprofilattico Sperimentale del Piemonte, Liguria e Valle d'Aosta, Via Bologna 148, 10154 Torino, Italy; serena.robetto@izsplv.it

* Correspondence: lorenzo.domenis@izsplv.it

In recent years, especially following the COVID-19 outbreak, wildlife studies and publications have focused on the roles of free-living animal species in the spillover of pathogens towards humans, livestock, and pets [1]. Recognizing the importance of this epidemiological aspect—widely acknowledged by the scientific community within One Health [2]—this Special Issue aimed to reconsider wild fauna as a genuine subject of veterinary and medico-legal investigation beyond its role as the (often healthy) carrier of zoonotic agents. From this perspective, we favored and selected articles reporting original cases of pathological processes (congenital, metabolic–degenerative, parasitic, infectious, and neoplastic) in free-ranging or captive wild animals (including exotic species), without neglecting non-pathological conditions (e.g., trauma and starvation), as well as studies related to their anatomical and physiological aspects. Special attention was devoted to the description of necropsy and histopathological findings, particularly important tools for supporting the damaging action of etiological factors identified and confirmed through strong diagnostic protocol (including bacteriological and virological examinations, biomolecular techniques, and clinical chemistry) and, ultimately, for distinguishing infectious diseases from asymptomatic infections.

Having evaluated the 24 manuscripts on the basis of animal species, marine mammals appear to have mainly been studied, including six articles referring to dugong (*Dugong dugon*), harbor seal (*Phoca vitulina*), narrow-ridged finless porpoise (*Neophocaena asiaeorientalis sunameri*) and different species of dolphins, whales, and wild ruminants, with six articles referring to oryx (*Oryx leucoryx*), different species of cervids, ibex (*Capra ibex*), and white-tailed deer (*Odocoileus virginianus*). The greater attention given to detecting diseases or abnormalities in these animal categories may be explained by considering the fact that they are frequently the objects of conservation projects with targeted surveillance (such as oryx and cetaceans), or, more generally, that large animal carcasses are more easily found in nature by humans (tourists, forest rangers, scholars, or naturalists), such as in the case of marine mammal strandings. When grouping the articles based on pathological process, reports about infectious and parasitic diseases prevail, with ten articles referring to *Achromobacter xylosidans* in dugong, the foot-and-mouth disease virus in oryx, *Brucella ceti* in cetaceans, orthomyxovirus H5N1 in Antarctic birds, *Mycobacterium* spp. in badger (*Meles meles*) and white-tailed deer, *Escherichia coli/Mycoplasma conjunctivae* co-infection in ibex, *Aspergillus fumigatus* in scarlet macaw parrot (*Ara Macau*), different bacteria in the lung of nutria (*Myocastor coypus*), and parasitic infections in whales and dolphins. These are followed by the topic of neoplastic diseases, with six articles referring to cholangiocarcinoma in puma (*Puma concolor*), gallbladder carcinoma in otter (*Lutra lutra*), squamous cell carcinoma in African pygmy hedgehog (*Atelerix albiventris*), epidermoid cyst in porcupine (*Hystrix cristata*), lymphoma in red squirrel (*Sciurus vulgaris*) and different tumor types and tumor-like lesions in fox (*Vulpes vulpes*). If the infection—often asymptomatic (as it is for

mycobacteria and orthomyxovirus H5N1)—by parasites, bacteria and viruses matches what we could logically hypothesize in free-ranging animals exposed to a hostile environment without veterinary care, the sequence of neoplasms in wildlife species deserves particular attention. Globally, wild animals share the same carcinogenic factors active in humans due to reduced natural habitats and increasing pollution, and can therefore actually be involved in neoplastic processes [3]. The growing interest in comparative oncology, traditionally oriented towards domestic animals (mainly dogs and cats) where spontaneous tumors are more frequent, is stimulating attention to alternative animal models among wild fauna. Apart from the known endemic neoplasms like, e.g., the facial tumor in Tasmanian devils (*Sarcophilus harrisii*), fibropapillomatosis in sea turtles (*Chelonia mydas*) and urogenital carcinoma in California sea lions (*Zalophus californianus*) [4], neoplastic diseases in wild animals are generally rather rare and obviously difficult to investigate due to the lack of anamnesis and evident impossibility of therapeutic/follow up verification. However, this very aspect makes them worthy of study, for example regarding possible different mechanisms for suppressing cancer—as found in elephants and sea sponges [5,6]—or the impact of carcinogenic factors in apparently pollution-free natural habitats, as observed in belugas (*Delphinapterus leucas*). Serving as evidence of the growing interest that the scientific community is dedicating to wild animals even on less conventional topics, the Special Issue is completed by some articles that deal with aspects not linked to traditional infectious or neoplastic diseases, such as congenital anomalies of cervid horns, dental and skull-bone pathologies of the racoon dog (*Nyctereutes procyonoides*); organic lesions due to sand impaction in white-tailed deer and adhesive intestinal obstruction in narrow-crested finless porpoise; particular anatomical or physiological features, such as the reference values for post-mortem examinations of the hearts of macropods (*Macropodidae*) and koalas (*Phascolarctidae*); and intracytoplasmic hepatocytes eosinophilic globules in cetaceans. Apart from cases of specific diseases or abnormalities, the main causes of death—especially in medium and small wild animals—remain traumatic events related to human activities (e.g., impact with vehicles and getting caught in fishing nets)—as evidenced not only by the present survey on the European hedgehog (*Erinaceus europaeus*), but also by other studies on, for example, otters, wolves and turtles—and starvation due a fatal combination of different and overlapping pathological processes (viral and bacteriological infections, parasitic diseases, pollution), especially when associated with periods of food scarcity [7].

As broadly evidenced by most articles in the Special Issue, the diagnostic activity on wild animals involves the application of hard protocol, where multiple disciplines, from biology and natural science to pathological anatomy and the most advanced biotechnological techniques, must be integrated to achieve the final goal; in other words, establishing the cause of death [8]. Diagnostic work, especially that performed on wild animals found dead in the environment, is rather complex and difficult; in the absence of any kind of anamnesis (as in the case of zoo animals or captive wildlife), the investigation is based exclusively on the anatomical–pathological findings and subsequent laboratory exams. Analyses, particularly bacteriological and histological exams, are often compromised by the poor quality of tissue, considering the fact that the time between death and finding the carcass is often particularly long, and even more so if the weather conditions are adverse (as can happen in summer for high temperatures). The lack of validated tests for wildlife, especially with regard to serological diagnostics, contributes to this difficulty [9]. Therefore, all case reports where advantageous circumstances (favorable climate, the absence of post-mortem animal predation, timely collection and analysis of the carcass) allowed for the achievement of a reliable diagnostic result are to be considered valuable opportunities that truly improve the knowledge of wildlife diseases.

https://doi.org/10.3390/ani16091343

In conclusion, we hope this Special Issue will be a valuable tool for training and educating future professionals involved in the study and management of wildlife—above all naturalists, foresters, veterinarians, and forensic pathologists—with a special perspective towards three main objectives; in other words, biodiversity and ecosystem conservation (the prevention of diseases as well as criminal activity, e.g., poaching, equally contributes to the welfare of wild populations and in particular of endangered species), the health of livestock and pets (threatened by the interspecies spillover of pathogens shared between domestic and wild fauna), and last but not least, public health protection (monitoring the health status of wildlife avoids the transmission of infectious agents by free-ranging animals to humans).

Data Availability Statement: No new data were created or analyzed in this study. Data sharing is not applicable to this article.

Conflicts of Interest: The authors declare no conflicts of interest.

References

1. David, Q. *Spillover: Animal Infections and the Next Human Pandemic*; W. W. Norton & Company: New York, NY, USA; London, UK, 2012; ISBN 978-0393066807.
2. Woods, R.; Reiss, A.; Cox-Witton, K.; Grillo, T.; Peters, A. The Importance of Wildlife Disease Monitoring as Part of Global Surveillance for Zoonotic Diseases: The Role of Australia. *Trop. Med. Infect. Dis.* **2019**, *4*, 29. [CrossRef] [PubMed] [PubMed Central]
3. Pesavento, P.A.; Agnew, D.; Keel, M.K.; Woolard, K.D. Cancer in wildlife: Patterns of emergence. *Nat. Rev. Cancer* **2018**, *18*, 646–661. Erratum in *Nat. Rev. Cancer* **2019**, *19*, 299. https://doi.org/10.1038/s41568-019-0113-0. [CrossRef] [PubMed]
4. McAloose, D.; Newton, A.L. Wildlife cancer: A conservation perspective. *Nat. Rev. Cancer* **2009**, *9*, 517–526. Erratum in *Nat. Rev. Cancer* **2009**, *9*, 605. [CrossRef] [PubMed] [PubMed Central]
5. Gaughran, S.J.; Pless, E.; Stearns, S.C. How elephants beat cancer. *eLife* **2016**, *5*, e21864. [CrossRef] [PubMed] [PubMed Central]
6. Calcabrini, C.; Catanzaro, E.; Bishayee, A.; Turrini, E.; Fimognari, C. Marine Sponge Natural Products with Anticancer Potential: An Updated Review. *Mar. Drugs* **2017**, *15*, 310. [CrossRef] [PubMed] [PubMed Central]
7. Domenis, L.; Spedicato, R.; Orusa, R.; Goria, M.; Sant, S.; Guidetti, C.; Robetto, S. The diagnostic activity on wild animals through the description of a model case report (caseous lymphadenitis by *Corynebacterium pseudotuberculosis* associated with *Pasteurella* spp. and parasites infection in an alpine ibex—*Capra ibex*). *Open Vet. J.* **2017**, *7*, 384–390. [CrossRef] [PubMed] [PubMed Central]
8. Daszak, P.; Cunningham, A.A.; Hyatt, A.D. Anthropogenic environmental change and the emergence of infectious diseases in wildlife. *Acta Trop.* **2001**, *78*, 103–116. [CrossRef] [PubMed]
9. Ryser-Degiorgis, M.-P. Wildlife health investigations: Needs, challenges and recommendations. *BMC Vet. Res.* **2013**, *9*, 223. [CrossRef] [PubMed] [PubMed Central]

Disclaimer/Publisher's Note: The statements, opinions and data contained in all publications are solely those of the individual author(s) and contributor(s) and not of MDPI and/or the editor(s). MDPI and/or the editor(s) disclaim responsibility for any injury to people or property resulting from any ideas, methods, instructions or products referred to in the content.

animals

MDPI

Case Report

Gallbladder Carcinoma in a Eurasian Otter (*Lutra lutra*)

Lorenzo Domenis *, Marzia Pezzolato, Elena Biasibetti, Raffaella Spedicato and Serena Robetto

Istituto Zooprofilattico Sperimentale del Piemonte, Liguria e Valle d'Aosta, Via Bologna 148, 10154 Torino, Italy; marzia.pezzolato@izsplv.it (M.P.); elena.biasibetti@izsplv.it (E.B.); raffaella.spedicato@izsplv.it (R.S.); serena.robetto@izsplv.it (S.R.)

* Correspondence: lorenzo.domenis@izsplv.it

Simple Summary: A gallbladder neoplasm, with secondary nodules in the liver, spleen and pancreas, was diagnosed in a Eurasian otter (*Lutra lutra*) found dead. Gross lesions, histological and immunohistochemical findings were consistent with a primary gallbladder carcinoma (GBC) of metastatic type; to the best of our knowledge, this is the first report of GBC in a Eurasian otter.

Abstract

An adult female Eurasian otter (*Lutra lutra*), introduced with another subject in the National Park of Gran Paradiso (Aosta Valley Region, Italy), was found dead. The necropsy found a mass involving mainly the gallbladder walls with other multicentric masses in the liver and pancreas. In addition to these, through the histological examination, other nodules were detected in the pancreas, with structure similar to gallbladder neoplasm. Histopathology diagnosed it as neoplasia composed of epithelioid cells, forming lobules of tubules and pseudoacini, with a very low mitotic count, discrete cellular pleomorphism, and prominent fibrous stroma. Neoplastic cells demonstrated positive immunoreactivity for cytokeratin and negative immunoreactivity for S100. Gross and histologic lesions and immunohistochemical findings were consistent with a primary gallbladder carcinoma (GBC) of metastatic type. GBC is a rare neoplasm in both humans and animals, sometimes associated with cholelithiasis and cholecystitis, with few reports in the veterinary literature especially in cattle, pigs, dogs and cats. To the best of our knowledge, this is the first report of GBC in a Eurasian otter.

Keywords: otter; *Lutra lutra*; gallbladder; carcinoma; neoplasm; metastatic

1. Introduction

Otters are amphibious mammals distributed almost all over the world, except for Australia and the most remote islands; they have been classified in family Mustelidae, subfamily Lutrinae, divided into seven genera—*Aonyx*, *Enhydra*, *Hydrictis*, *Lontra*, *Lutra*, *Lutrogale*, *Pteronura*—and 13 species. The European otter (*Lutra lutra*), a medium-sized (about 120 cm long) animal, lives in a very wide geographical area ranging from the Iberian Peninsula to Japan, including some North African countries such as Morocco, Tunisia and Algeria. Woodlands along rivers and lakes are its natural habitat and its diet consists mainly of freshwater fish (stickleback, brown trout, eel, and bullhead). When freshwater fish are less available, as also exhibited by other generalist predators, otters switch to alternative prey like amphibians (predominantly common frog), waterfowl, crayfish, and they even can eat water insects and vegetables [1,2]. Since the end of the 1950s, the

number of Eurasian otter has suffered a sharp decline mainly caused by numerous anthropogenic factors (pollution, poaching, habitat destruction). As a result, the species, already protected in Europe by the Berne Convention and Directive Habitat (92/43/CEE), has most recently been assessed for the IUCN Red List of Threatened Species in 2023 and listed as Near Threatened (NT) worldwide [3–5]. In Italy, as in some countries of Asia (India, Pakistan, Bangladesh, Myanmar, and Thailand), it is classified as "Endangered" (EN), with an estimated population of about 800–1000 individuals mostly located in some central-southern regions (Campania, Molise, Calabria, Basilicata and Puglia) [6]. In recent years, thanks to reintroduction projects, the otter has reappeared in some northern regions including Valle d'Aosta, Trentino (likely introduction from Austria) and Friuli Venezia Giulia (probable introduction from Slovenia) [7]. Similar to domestic animals, among the otters or Lutrinae, especially in the sea otter (*Enhydra lutris*) and river otter (*Lontra canadensis*), different types of neoplasms are described. The assessment of the bibliographic oncological reports of the last 20 years shows a clear prevalence of hematopoietic system involvement, with lymphomas (n = 13) of various types and sites [8–18], followed by leiomyomas (n = 5) [19–21], malignant melanomas (n = 3) [21–23], squamocellular carcinomas (n = 3) [21,24], fibrosarcomas (n = 3) [17,18], pheochromocytomas (n = 2) [19,25], pancreatic adenomas (n = 2) [21,26], pancreatic adenocarcinomas (n = 2) [21,27], hepatocellular adenomas (n = 2) [21,28], splenic sarcomas (n = 2) [21] and hemangiosarcomas (n = 2) [21]. Single cases are described for mammary gland adenoma and adenocarcinoma [21,22], mammary malignant spindle cell tumor [21], hepatocellular carcinoma [21], biliary adenoma and carcinoma [19,21], thymoma [29], thyroid adenoma and carcinoma [21,30], parathyroid adenoma [21], omental neuroendocrine carcinoma [21], renal carcinoma [21], chondrosarcoma [17], osteosarcoma [31], basal cell carcinoma [32], ovarian teratoma [33], malignant seminoma [34], leydigoma [21], Sertoli cell tumor [21], bronchoalveolar adenoma and carcinoma [21], soft tisue sarcoma [21], and choroid plexus carcinoma [21]. In order to contribute to the knowledge of the neoplastic processes of the Eurasian otter, for which there are few oncological reports—unlike for other otter species—we describe a carcinoma of the gallbladder (GBC) in an adult female of *Lutra lutra*, living in the Gran Paradiso National Park in North-Western Italian Alps. The case, being the first report of such a tumor in this species, adds a new entry to the causes of mortality among European otters. This contributes to the conservation of endangered animals and also to the field of comparative oncology.

2. Case Description

A recently deceased female adult otter, introduced in a protected area of Gran Paradiso National Park (Valle d'Aosta Region, Italy) about two years prior to death, was found and submitted for necropsy. The animal was in good physical condition; upon opening the carcass (Figure 1a), the gallbladder appeared as a dark-red cauliflower-like mass of about 8–10 cm in diameter (Figure 1b); on sectioning, no stones were detected in the lumen and the wall was markedly thickened and extensively infiltrated by lobules of firm, waxy and hard tissue with focal intraluminal projections (Figure 1c). Much less prominent nodular masses, having a similar appearance to gallbladder neoplasm and measured approximately 0.5 cm in diameter, were observed in the splenic (Figure 1d) and hepatic parenchyma. In addition to the macroscopically visible neoplastic lesions, all internal organs were submitted for histological examination. Tissues were fixed in 10% neutral buffered formalin, trimmed, routinely processed, embedded in paraffin blocks and cut at 3 +/− 5 μm slices. All sections were stained with haematoxylin and eosin and microscopically analyzed at different magnifications by the Olympus BX60 microscope and image captured by DP-Soft Version 2.1 software.

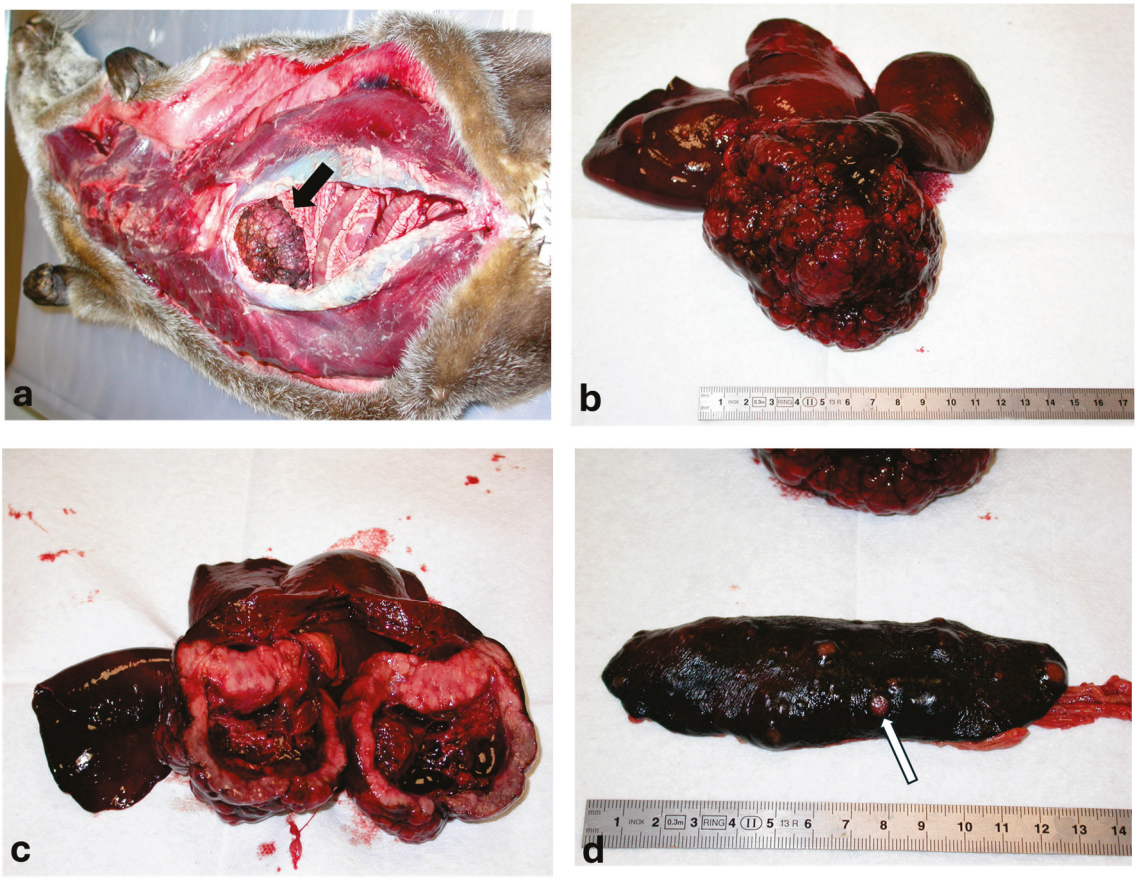


Figure 1. Gallbladder carcinoma—Otter (*Lutra lutra*). (**a**) Parahepatic mass at the opening of abdominal cavity (arrow); (**b**) Cauliflower neoplasia corresponding to gallbladder; (**c**) Section of neoplasm involving the gallbladder walls throughout; (**d**) Metastatic nodules of gallbladder neoplasm in the spleen (arrow).

To confirm the diagnosis, additional sections were cut on polarized slides and underwent immunohistochemical characterization. Primary antibodies directed against pan-cytokeratin (heat-induced epitope retrieval/HIER high pH, 1:50 dilution, AE1/AE3, mouse monoclonal; Dako) and S100 (HIER pH 6, 1:400 dilution Polyclonal Dako) were used. After deparaffinizing and rehydrating, HIER was performed with TriS-EDTA buffer, pH9-pH6 (S110), for 20 min at 97 °C in a water bath. Afterwards, the slides were treated with 3% hydrogen peroxide for 30 min, followed by two PBS washings and BSA incubation for 30 min. Each primary antibody was incubated for 30 min at room temperature. Then sections were covered with secondary antibody MACH 2 Universal HRP-Polymer Rabbit/mouse and incubated for 20 min at room temperature. The EnVision Peroxidase Dual Link System detection system (Dako, K4063) and DAB (3,3 diaminobenzidine tetrahydrochloride; Sigma, St. Louis, MO, USA) as chromogen were applied for 10 min. Then, sections were counterstained with Mayer's hematoxylin for 2 min and assembled according to routine methods. Each experimental run incorporated control specimens, including a positive control (a canine melanoma to confirm S100 antibody reactivity and a canine carcinoma to confirm cytokeratin antibody reactivity) and a negative control, obtained by omitting the primary antibody during the labelling process, to assess non-specific background staining.

The microscopic evaluation revealed in the gallbladder a neoplasia characterized by lobules, separated by thick fibrous connective trabeculae (Figure 2a) and consisting of acinar and pseudotubular structures, generally not associated with an evident mucinous secretion, supported by a fine fibrovascular stroma; neoplastic cells were characterized

by discrete anisocytosis, cytoplasm intensely eosinophilic, nuclei with chromatin finely dispersed and peripherally thickened, single voluminous nucleolus and mitotic rate of <2/10HPF (Figure 2b); in the context of neoplastic lobules large necrotic areas were present (Figure 2a). The nodules in the liver (Figure S1) and spleen (Figure 2c) were characterized by irregular peripheral fibrous capsule (more prominent in the liver), structure and cells similar to primary neoplasm, occasionally arranged in more solid sheets without lumina (Figure S2), and absence of necrotic foci. Neoplastic growth with the same features of hepatic and splenic masses was also detected in the pancreas (Figure 2d). Except for the liver parenchyma, showing intracellular cholestasis and diffuse lipidosis, histological lesions different from a neoplastic change were not observed in all internal organs. Regarding the immunohistochemical pattern, neoplastic cells showed a strong cytoplasmic positivity for cytokeratin while they were negative for S100 (Figure 3a,b). Given the histological findings (glandular structure and low mitotic index) and immunohistochemical pattern (cytokeratin-positivity), in addition to the presence of similar neoplastic nodules of smaller size in the liver, spleen and pancreas, the neoplasm—according to Cullen J.M [35]—has been classified as a malignant neoplasm of epithelial origin comparable to a primary gallbladder carcinoma (GBC) of metastatic type.

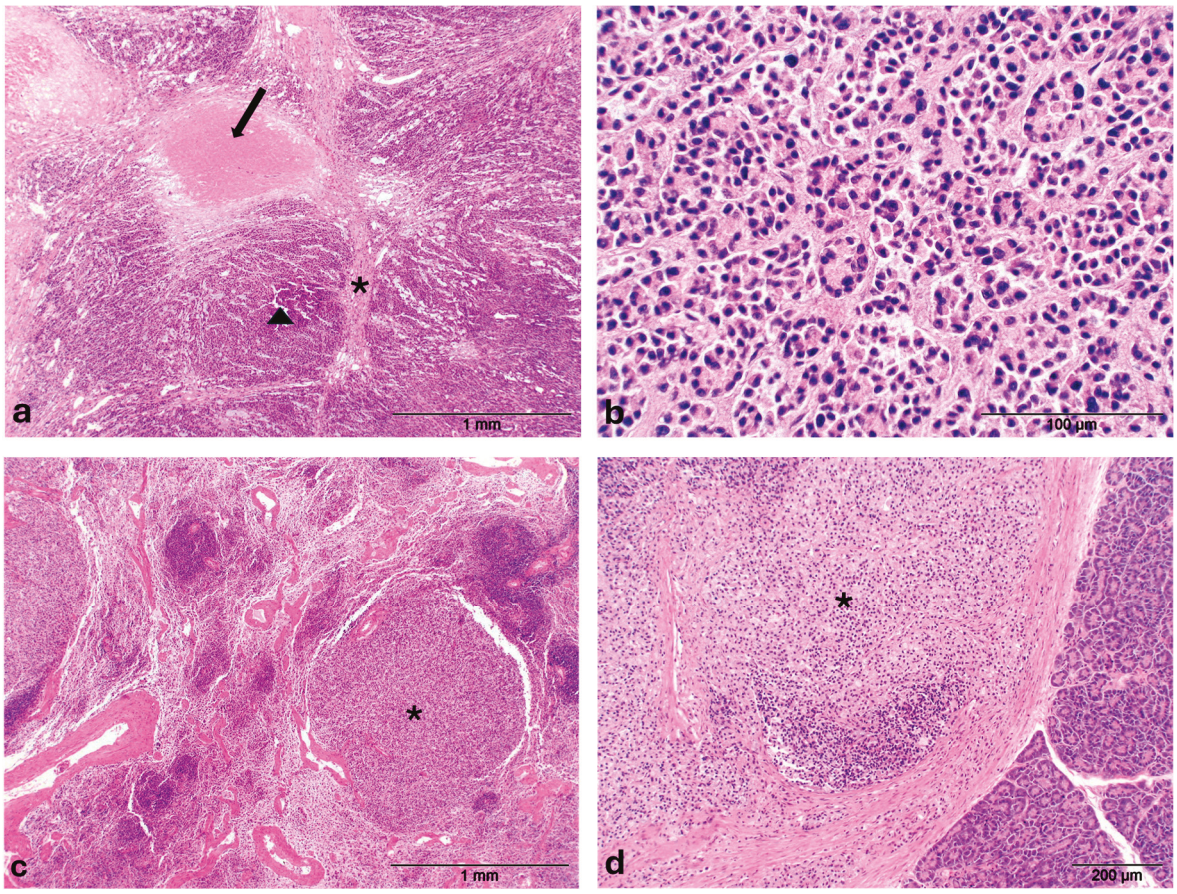


Figure 2. Gallbladder carcinoma—Otter (*Lutra lutra*). (**a**) Prominent fibrous trabeculae (asterisk) divide the neoplasia into lobules (triangle), occasionally associated with necrotic area (arrow); (**b**) Acini and pseudo-tubules supported by a fine fibrovascular stroma, characterized by absence of mitotic activity, not-evident mucinous secretion and moderate anisocytosis; (**c**) Metastatic nodule in the spleen (asterisk); (**d**) Metastatic nodule in the pancreas (asterisk).

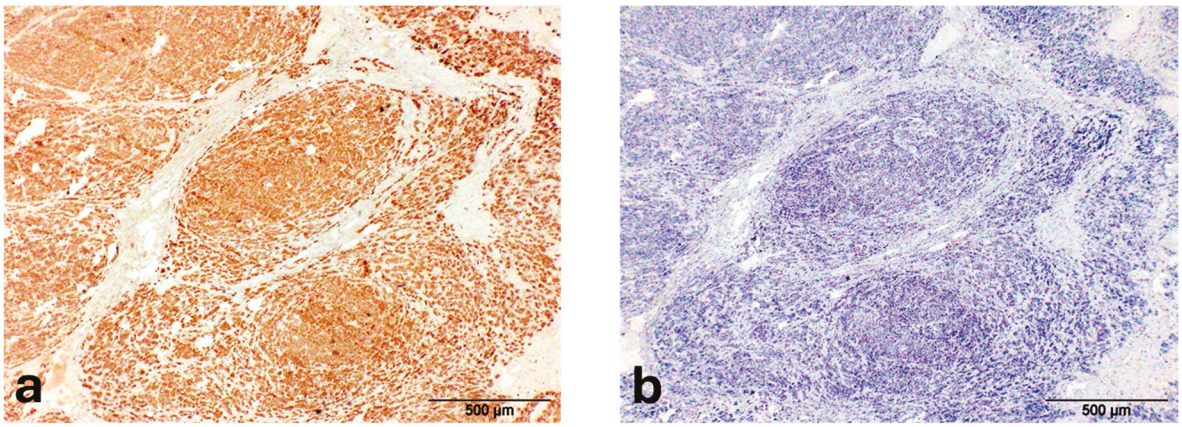


Figure 3. Gallbladder carcinoma—Otter (*Lutra lutra*) (**a**) GBC: Diffuse cytoplasmic positivity for cytokeratin; (**b**) GBC: S100 negativity.

In the absence of metastases to other vital organs like lungs and the limited secondary nodules in pancreas, spleen and liver, the death of the animal is probably attributable to the effects of the neoplastic process inside the gallbladder onto the hepatic parenchima (probably failure of the biliary system such as duct blockage with consequent hepatocytes damage).

3. Discussion

A neoplasm involving the gallbladder generally poses a problem of differential diagnosis between the three neoplasms commonly recognized in this anatomical district among the animals affected (cattle, pig, dog and cat) [35]. These are adenoma, carcinoma and neuroendocrine carcinoma (or carcinoid), but—given that GBC is essentially classified as extrahepatic cholangiocellular carcinoma—cholangiocarcinoma arising within intrahepatic biliary system should also be considered. Adenoma was excluded for the presence of metastases to the liver, spleen and pancreas; neuroendocrine carcinoma for the low mitotic activity and immunohistochemical characteristics (neuroendocrine carcinomas are identifiable immunohistochemically first for positivity to S100 as well as to chromogranin A and neuron-specific enolase). Regarding cholangiocellular carcinoma, an origin from bile ducts was not consistent with the absence of mucinous secretion and the low mitotic count, respectively abundant and high in typical intrahepatic cholangiocarcinomas [30]. The neoplasm observed in our case was consistent with a primary GBC for the following characteristics: (a) positivity for cytokeratin and negativity for S100 (this last result is reliable considering both the genomic loci encoding S100 proteins is highly conserved in mammals [36] and the same primary antibody we used tested positive for other neoplasm of otter, e.g., malignant melanoma [22]); (b) a structure similar to the GBCs described in the domestic animals, with acinar and tubular structures separated by thin fibrous stroma and a low mitotic count. As observed in some species such as dogs, despite the scarce mitotic activity and the moderate degree of differentiation, the behavior of GBCs is rather aggressive with a tendency to expand locally and then metastasize into the adjacent hepatic parenchyma and later on the serosal surfaces of the abdominal cavity, lymph nodes and lung [35].

GBC is quite rare in domestic animals [35]. In humans, it is the most common malignant neoplasm of the biliary tract worldwide and its risk factors have been statistically identified and listed as follows: demographic factors (advanced age, female gender, obesity, South America/India/Pakistan/Japan and Korea origin, genetic predisposition), gall bladder pathology/abnormalities (cholelithiasis, porcelain gall bladder, polyps, congenital biliary cysts, pancreaticobiliary anomalies), exposures (heavy metals, medication such

as methyldopa, isoniazid and estrogen, smoking) and infections (*Salmonella*, *Helicobacter*). Cholelithiasis is considered the main risk factor, with an 8.3 higher risk than the general population [37,38]. It is postulated that GBC may be intimately associated with large or numerous cholesterol gallstones that in the first instance may interfere with the mechanical functioning of the gallbladder. The size as well as the number of stones may contribute significantly to the promotion of filling defects of the gallbladder that may cause chronic mechanical damage to the gall bladder mucosa [39,40].

Similar to humans, even if the studies are more limited in animals (and completely missing in otters), it has been observed also in aged pigs that chronic cholecystitis associated with gallstones and/or bacterial infections may contribute to metaplastic changes and development of gallbladder neoplasms [41] while cholecystoliths are not commonly associated with GBC in dogs [42].

Excluding the female gender and the advanced age, for the GBC detected in this otter we have not identified other risk factors recognized in humans. Cholelythiasis as cholecystitis, which as mentioned above, mainly predisposes humans to GBC onset, is not frequently reported in otters and in any case never associated with neoplasms in the gallbladder [43,44]. The absence of stones and inflammatory processes supports the hypothesis that in this animal GBC was a spontaneous neoplasm not secondary to other pre-existing pathological conditions. Further research needs to demonstrate if the neoplasm was caused by exposure to carcinogenic chemical agents. However, it is possible to rule them out because there were not any industrial activities or other sources of pollution in the mountain ecosystem where the otter lived.

As with other wild animals, studies conducted in England, Germany and Italy indicate that the leading causes of mortality in European otters are traumatic events (e.g., road traffic accidents, bite wounds, etc.), accidents being mostly frequent in winter, and dog bites in summer. Infectious and non-infectious diseases (e.g., parasitic, viral or bacterial processes) are observed less frequently and typically as incidental findings in animals that died due to trauma [9,45,46]. Neoplasms are even more rarely reported; as noted in the Introduction, neoplasms in the European otter (*Lutra lutra*)—unlike the more frequently studied sea otter and river otter—are scarce and currently include only two malignant melanoma (one with concurrent trichoblastoma and mammary adenoma) [22,23], two lymphomas [8,9], one hepatocellular adenoma [28] and one undefined metastatic neoplasia in an Italian specimen [47].

4. Conclusions

Cancer is still a rare disease—generally not age related—in wildlife compared to captive animals; however, in recent years, also due to greater attention to the causes of mortality among the free-ranging species in a One Health perspective and biodiversity conservation, frequency of oncological reports is increasing. Toxin exposures, pollution, oncogenic pathogens, stress, immunosuppression and genetic anomalies can all contribute to neoplasm development in wild animals. Wild species at the interface between humans and the environment are growing, making wildlife sentinel for both animal and human health and so offering novel insights into potentially unique non-age-related mechanisms of carcinogenesis across species [48].

In this context, the GBC described in our case—the first such report in this species—adds new knowledge on neoplasm pathology in this mustelid and, more broadly, contributes to comparative oncology in wildlife.

Supplementary Materials: The following supporting information can be downloaded at: https://www.mdpi.com/article/10.3390/ani15172484/s1. Figure S1: Gallbladder carcinoma—Otter (*Lutra lutra*). Metastatic nodule of GBC in the liver (asterisk). Figure S2: Gallbladder carcinoma—Otter (*Lutra lutra*). Metastatic nodule of GBC in the liver arranged in solid sheets without lumina.

Author Contributions: Conceptualization, L.D.; formal analysis L.D., S.R., M.P. and E.B.; investigation, L.D. and S.R.; writing—original draft preparation, L.D.; writing—review and editing, L.D., S.R., R.S., M.P. and E.B.; supervision, L.D. All authors have read and agreed to the published version of the manuscript.

Funding: This research received no external funding.

Institutional Review Board Statement: Ethical review and approval were waived for this study because the research was conducted on a wild animal found dead inside a protected natural area.

Informed Consent Statement: Not applicable.

Data Availability Statement: Individual raw data collected are available on request from the corresponding author.

Acknowledgments: We thank Bruno Bassano and the Gran Paradiso National Park for reporting the case, Erica Minuzzo for English editing.

Conflicts of Interest: The authors declare no conflicts of interest.

References

1. Drake, L.E.; Cuff, J.P.; Bedmar, S.; McDonald, R.; Symondson, W.O.C.; Chadwick, E.A. Otterly delicious: Spatiotemporal variation in the diet of a recovering population of Eurasian otters (*Lutra lutra*) revealed through DNA metabarcoding and morphological analysis of prey remains. *Ecol. Evol.* **2023**, *13*, e10038. [CrossRef]
2. Peracino, V. Progetto Lontra Gran Paradiso. *IBEX J. Mt. Ecol. (Collana Sci. Parco Naz. Gran Parad.)* **1996**, *4*, 96.
3. Convention on the Conservation of European Wildlife and Natural Habitats (Bern Convention)—Decision 82/72/EEC. Available online: https://eur-lex.europa.eu/EN/legal-content/summary/bern-convention.html (accessed on 20 August 2025).
4. Council Directive 92/43/EEC of 21 May 1992 on the Conservation of Natural Habitats and of Wild Fauna and Flora. Available online: https://eur-lex.europa.eu/eli/dir/1992/43/oj/eng (accessed on 26 July 2025).
5. Red List of Threatened Species. Available online: https://www.iucnredlist.org (accessed on 26 July 2025).
6. Rondinini, C.; Battistoni, A.; Peronace, V.; Teofili, C. (Eds.) *Lista Rossa IUCN dei Vertebrati Italiani*; Comitato Italiano IUCN e Ministero dell'Ambiente e della Tutela del Territorio e del Mare: Roma, Italy, 2013.
7. Leoncini, F.; Semenzato, P.; Di Febbraro, M.; Loy, A.; Ferrari, C. Come back to stay: Landscape connectivity analysis for the Eurasian otter (*Lutra lutra*) in the western Alps. *Biodivers. Conserv.* **2023**, *32*, 653–669. [CrossRef]
8. Bartlett, S.L.; Imai, D.M.; Trnpkiewicz, J.G.; Garner, M.M.; Ogasawara, S.; Stokol, T.; Kiupel, M.; Abou-Madi, N.; Kollias, G.V. Intestinal lymphoma of granular lymphocytes in a fisher (*Martes pennanti*) and a Eurasian otter (*Lutra lutra*). *J. Zoo Wildl. Med.* **2010**, *41*, 309–315. [CrossRef] [PubMed]
9. Fusillo, R.; Romanucci, M.; Marcelli, M.; Massimini, M.; Della Salda, L. Health and Mortality Monitoring in Threatened Mammals: A First Post Mortem Study of Otters (*Lutra lutra* L.) in Italy. *Animals* **2022**, *12*, 609. [CrossRef] [PubMed]
10. Kim, J.H.; Kim, B.H.; Kim, J.H.; Yoo, M.J.; Kim, D.Y. Lymphosarcoma in a sea otter (*Enhydra lutris*). *J. Wildl. Dis.* **2002**, *38*, 616–617. [CrossRef]
11. Matt, C.L.; Mans, C.; Doss, G.; Pinkerton, M.; Elsmo, B. Splenic T-cell lymphoma in a North American River Otter (*Lontra canadensis*). *Open Vet. J.* **2020**, *10*, 272–275. [CrossRef] [PubMed]
12. Stedman, N.L.; Mills, Z.V. Splenic marginal zone lymphoma in an Asian small-clawed otter (*Aonyx cinerea*). *J. Zoo Wildl. Med.* **2014**, *45*, 719–722. [CrossRef]
13. Swenson, J.; Carpenter, J.W.; Janardhan, K.S.; Ketz-Riley, C.; Brinkman, E. Paresis in an Asian small clawed otter (*Aonyx cinereus*) associated with vertebral and ischial osteolysis caused by a malignant lymphangiosarcoma. *J. Zoo Wildl. Med.* **2008**, *39*, 236–243. [CrossRef]
14. Tanaka, N.; Izawa, T.; Kashiwagi-Yamamoto, E.; Kuwamura, M.; Ozaki, M.; Nakao, T.; Yamate, J. Primary cerebral T-cell lymphoma in a sea otter (*Enhydra lutris*). *J. Vet. Med. Sci.* **2013**, *75*, 1667–1669. [CrossRef]
15. Rebollada-Merino, A.; Canales, R.; Romani-Cremaschi, U.; Rodríguez-Bertos, A. Intestinal T-cell lymphoma in an Asian small-clawed otter: Case report and literature review of lymphoma in the subfamily *Lutrinae*. *J. Vet. Diagn. Investig.* **2023**, *35*, 72–75. [CrossRef]

16. McEntire, M.S.; Tang, K.N.; O'Connor, M.R.; Haulena, M. The management of lymphoproliferative neoplasia in four Northern Sea Otters (*Enhydra lutris kenyoni*). *J. Zoo Wildl. Med.* **2024**, *55*, 511–520. [CrossRef] [PubMed]
17. Burek-Huntington, K.A.; Mulcahy, D.M.; Doroff, A.M.; Johnson, T.O. Sarcomas in three tree-ranging northern sea otters *(Enhydra lutris kenyoni*) in Alaska. *J. Wildl. Dis.* **2012**, *48*, 483–487. [CrossRef]
18. Armwood, A.R.; Anderson, C.E.; Clauss, T.; Camus, A.C. Primary intracranial fibrosarcoma in a southern sea otter *Enhydra lutris nereis*. *Dis. Aquat. Organ.* **2020**, *138*, 207–213. [CrossRef] [PubMed]
19. Stetzer, E.; Williams, T.D.; Nightingale, J.W. Cholangiocellular adenocarcinoma, leiomyoma, and pheochromocytoma in a sea otter. *J. Am. Vet. Med. Assoc.* **1981**, *179*, 1283–1284. [CrossRef] [PubMed]
20. Williams, T.D.; Pulley, L.T. Leiomyomas in two sea otters, *Enhydra lutris*. *J. Wildl. Dis.* **1981**, *17*, 401–404. [CrossRef] [PubMed]
21. Righton, A.L.; Jungers, H.T.; Mena, A.J.; Stedman, N.L.; St Leger, J.; Langan, J.N.; Rainwater, K.L.; Aziz, N.; Delaney, M.A. Morbidity and mortality of Asian small-clawed otters (*Aonyx cinereus*) and North American river otters (*Lontra canadensis*) in US zoos and aquaria from 2000 to 2020: A survey of lesions in 2 popular otter species. *Vet. Pathol.* **2025**, *62*, 3009858251345828. [CrossRef]
22. Fuke, N.; Diep, N.V.; Hirai, T.; Suwanruengsri, M.; Izzati, U.Z.; Yamaguchi, R. Three neoplasms in a Eurasian otter (*Lutra lutra*): Malignant melanoma, trichoblastoma and mammary gland adenoma. *J. Vet. Med. Sci.* **2021**, *83*, 1661–1665. [CrossRef]
23. Weber, H.; Mecklenburg, L. Malignant melanoma in a Eurasian otter (*Lutra lutra*). *J. Zoo Wildl. Med.* **2000**, *31*, 87–90. [CrossRef]
24. van de Velde, N.; Demetrick, D.J.; Duignan, P.J. Primary pleural squamous cell carcinoma in a freeranging river otter (*Lontra canadensis*). *J. Wildl. Dis.* **2019**, *55*, 728–732. [CrossRef]
25. Schlanser, J.R.; Patterson, J.S.; Kiupel, M.; Hencken, C.; Sikarskie, J.G.; Harrison, T.M. Disseminated pheochromocytoma in a North American river otter (*Lontra canadensis*). *J. Zoo Wildl. Med.* **2012**, *43*, 407–411. [CrossRef] [PubMed]
26. Gaydos, J.K.; Delaney, M.A.; Raverty, S. Causes of Mortality in a Population of Marine-Foraging River Otters (*Lontra canadensis*). *J. Wildl. Dis.* **2020**, *56*, 941–946. [CrossRef]
27. Pinto, M.H.B.; Braga, T.R.C.; Blume, G.R.; Oliveira, L.B.; Chagas, N.T.C.D.; Souza, F.R.; Cassali, G.D.; Sant'Ana, F.J.F. Metastatic exocrine pancreatic adenocarcinoma in a giant otter (*Pteronura brasiliensis*). *Acta Vet. Hung.* **2023**, *71*, 41–45. [CrossRef]
28. Bae, I.H.; Pakhrin, B.; Jee, H.; Shin, N.S.; Kim, D.Y. Hepatocellular adenoma in a Eurasian otter (*Lutra lutra*). *J. Vet. Sci.* **2007**, *8*, 103–105. [CrossRef]
29. Pye, G.W.; White, A.; Robbins, P.K.; Burns, R.E.; Rideout, B.A. Preventive medicine success: Thymoma removal in an African spot-necked otter (*Lutra maculicollis*). *J. Zoo Wildl. Med.* **2010**, *41*, 732–734. [CrossRef] [PubMed]
30. Hsu, C.D.; Mathura, Y. Severe visceral pentastomiasis in an oriental small-clawed otter with functional thyroid carcinoma. *J. Vet. Med. Sci.* **2018**, *80*, 320–322. [CrossRef] [PubMed]
31. Rodriguez-Ramos Fernandez, J.; Thomas, N.; Dubielzig, R.; Drees, R. Osteosarcoma of the maxilla with concurrent osteoma in a southern sea otter (*Enhydra lutris nereis*). *J. Comp. Pathol.* **2012**, *147*, 391–396. [CrossRef]
32. Nakamura, K.; Tanimura, H.; Katsuragi, K.; Shibahara, T.; Kadota, K. Differentiated basal cell carcinoma in a Cape clawless otter (*Aonyx capensis*). *J. Comp. Pathol.* **2002**, *127*, 223–227. [CrossRef]
33. Zachary, J.F.; McDonald, S.C. Malignant ovarian teratoma in a spot-neck otter. *J. Am. Vet. Med. Assoc.* **1981**, *179*, 1279–1283. [CrossRef]
34. Reimer, D.C.; Lipscomb, T.P. Malignant seminoma with metastasis and herpesvirus infection in a free-living sea otter (*Enhydra lutris*). *J. Zoo Wildl. Med.* **1998**, *29*, 35–39. [PubMed]
35. Cullen, J.M. Tumors of the Liver and Gall Bladder. In *Tumors in Domestic Animals*, 5th ed.; Meuten, D.J., Ed.; John Wiley & Sons: Ames, IA, USA, 2017; pp. 622–623.
36. Sreejit, G.; Flynn, M.C.; Patil, M.; Krishnamurthy, P.; Murphy, A.J.; Nagareddy, P.R. S100 family proteins in inflammation and beyond. *Adv. Clin. Chem.* **2020**, *98*, 173–231.
37. Kanthan, R.; Senger, J.L.; Ahmed, S.; Kanthan, S.C. Gallbladder Cancer in the 21st Century. *J. Oncol.* **2015**, *2015*, 967472. [CrossRef] [PubMed]
38. Gupta, A.; Ammapelem, S.; Karamveer, S.; Arunkumar, V.; Prasoon, S. Gallbladder Carcinoma: A Comprehensive Review and Recent Updates. In *Hepatobiliary Medicine and Surgery—Gallbladder [Working Title]*; Lunevicius, R., Ed.; IntechOpen: London, UK, 2025. Available online: https://www.intechopen.com/online-first/1219270 (accessed on 26 June 2025).
39. Vitetta, L.; Sali, A.; Little, P.; Mrazek, L. Gallstones and gall bladder carcinoma. *Aust. N. Z. J. Surg.* **2000**, *70*, 667–673. [CrossRef]
40. Mathur, S.K.; Duhan, A.; Singh, S.; Aggarwal, M.; Aggarwal, G.; Sen, R.; Singh, S.; Garg, S. Correlation of gallstone characteristics with mucosal changes in gallbladder. *Trop. Gastroenterol.* **2012**, *33*, 39–44. [CrossRef]
41. Ushio, N.; Chambers, J.K.; Watanabe, K.I.; Kishimoto, T.E.; Shiga, T.; Li, J.Y.; Nakayama, H.; Uchida, K. Chronic Inflammatory and Proliferative Lesions of the Gallbladder in Aged Pigs. *Vet. Pathol.* **2020**, *57*, 122–131. [CrossRef]
42. MacLeod, A.N.; Reichle, J.K.; Szabo, D.; Cohen, E.B.; Artiles, C.; Fulkerson, C.V.; Kurihara, M.; Mattoon, J. Ultrasonographic Appearance of Gallbladder Neoplasia in 14 Dogs and 1 Cat. *Vet. Radiol. Ultrasound* **2023**, *64*, 537–545. [CrossRef] [PubMed]

43. Madsen, A.B.; Dietz, H.H.; Henriksen, P.; Clausen, B. Survey of Danish Free Living Otters *Lutra lutra*—A Consecutive Collection and Necroscopy of Dead Bodies. *IUCN Otter Spec. Group Bull.* **1999**, *16*, 65–76.
44. Wells, G.A.; Keymer, I.F.; Barnett, K.C. Suspected Aleutian disease in a wild otter (*Lutra lutra*). *Vet. Rec.* **1989**, *125*, 232–235. [CrossRef]
45. Simpson, V.R. Health status of otters (*Lutra lutra*) in south-west England based on postmortem findings. *Vet. Rec.* **1997**, *141*, 191–197. [CrossRef]
46. Rohner, S.; Wohlsein, P.; Prenger-Berninghoff, E.; Ewers, C.; Waindok, P.; Strube, C.; Baechlein, C.; Becher, P.; Wilmes, D.; Rickerts, V.; et al. Pathological Findings in Eurasian Otters (*Lutra lutra*) Found Dead between 2015–2020 in Schleswig-Holstein, Germany. *Animals* **2021**, *12*, 59. [CrossRef] [PubMed]
47. E' Morta la Lontra del Centro Visite di Pescasseroli. Available online: https://www.neveappennino.it/news/lontra-pescasseroli-pnalm (accessed on 23 July 2025).
48. Pesavento, P.A.; Agnew, D.; Keel, M.K.; Woolard, K.D. Cancer in wildlife: Patterns of emergence. *Nat. Rev. Cancer* **2018**, *18*, 646–661. [CrossRef] [PubMed]

Disclaimer/Publisher's Note: The statements, opinions and data contained in all publications are solely those of the individual author(s) and contributor(s) and not of MDPI and/or the editor(s). MDPI and/or the editor(s) disclaim responsibility for any injury to people or property resulting from any ideas, methods, instructions or products referred to in the content.

animals

MDPI

Article

Novel Insight into Dugong Mortality: First Report of Systemic *Achromobacter xylosoxidans* Infection, Disseminated Intravascular Coagulation, and Associated Pathogenesis

Piyaporn Eiamcharoen [1,†], Piyarat Khumraksa [2,†], Santi Ninwat [2], Tatsawan Suttiboon [3], Narissara Keawchana [4], Peerapon Sornying [4] and Watcharapol Suyapoh [4,5,*]

[1] Faculty of Veterinary Medicine, Kasetsart University, Bangkok 10900, Thailand; piyaporn.e@ku.th
[2] Marine and Coastal Resources Research Center (Lower Andaman Sea), Trang 92150, Thailand; piyarat.lmbc@gmail.com (P.K.); niwat@hotmail.com (S.N.)
[3] Marine and Coastal Resources Research Center (Lower Gulf of Thailand), Songkhla 90100, Thailand; tatsawanunderthesea@gmail.com
[4] Faculty of Veterinary Science, Prince of Songkla University, Songkhla 90110, Thailand; narissara.k@psu.ac.th (N.K.); peerapon.s@psu.ac.th (P.S.)
[5] Dugong and Seagrass Research Station, Prince of Songkla University, Songkhla 90112, Thailand
* Correspondence: watcharapol.s@psu.ac.th
† These authors contributed equally to this work.

Simple Summary: Dugongs are endangered marine mammals found in coastal areas of South-east Asia and Australia. In this study, we report the sudden death of a dugong calf that was rescued and cared for at a rehabilitation center in Thailand. Despite receiving treatment for dehydration and an eye condition, the calf died after developing signs of a severe and rapidly progressing illness. A detailed examination revealed a serious infection caused by *Achromobacter xylosoxidans*, a bacterium commonly found in water. The infection had spread throughout the body. We also found evidence of brain injury caused by harmful molecules known as reactive oxygen species. The bacteria were resistant to several antibiotics, which emphasizes the need for greater awareness in future rehabilitation practices. This is the first reported case of such an infection in a dugong. The findings raise concern about secondary opportunistic infections by this environmental bacterium, which may contaminate medical instruments, water systems, or even be transmitted through human contact. Understanding these risks can help improve infection prevention and the survival chances of stranded marine mammals in care.

Abstract

Dugongs (*Dugong dugon*), classified as vulnerable marine mammals, are increasingly impacted by infectious diseases, yet the role of septicemia and disseminated intravascular coagulation (DIC) in their mortality remains uncharacterized. This study aimed to investigate the pathological and microbiological features associated with an acute mortality event in a juvenile dugong during rehabilitation in southern Thailand. Comprehensive histopathological and microbiological analyses were conducted on tissue samples collected postmortem. Bacterial isolation and identification were performed using standard culture techniques and the VITEK-2 system. Histological examination revealed multisystemic lesions, including fibrin thrombi, hemorrhage, hepatocellular degeneration, pancreatic necrosis, lymphoid depletion, and neuronal damage. Oxidative stress and DNA damage were confirmed in brain tissues through immunofluorescence detection of 4-hydroxynonenal (4-HNE) and 8-hydroxy-2′-deoxyguanosine (8-oxodG). *Achromobacter xylosoxidans*, an opportunistic pathogen, was isolated from multiple organs, consistent with acute systemic infection. These findings represent the first evidence of septicemia-associated DIC in dugongs caused

by *A. xylosoxidans*, highlighting a previously undocumented cause of mortality in dugongs. The results emphasize the role of opportunistic bacteria in triggering oxidative damage and coagulopathy and underscore the importance of early detection and targeted therapeutic strategies to improve survival in stranded or rehabilitated dugongs.

Keywords: *Dugong dugon*; *Achromobacter xylosoxidans*; pathology; oxidative damage; disseminated intravascular coagulation; captive rehabilitation

1. Introduction

Dugongs (*Dugong dugon*) are the sole extant species of the Dugongidae family within the order Sirenia. According to the International Union for Conservation of Nature (IUCN) Red List of Threatened Species, global dugong populations are considered vulnerable to extinction [1]. This species is primarily found in a limited range extending from East Africa and the Middle East, across Southeast Asia to New Caledonia, and latitudinally from Okinawa Island in Japan to Australia [2,3]. Thailand is a renowned habitat for endangered dugongs, particularly around Muk and Talibong Islands in Trang Province, located in the Andaman Sea, where notable populations are found [4]. Currently, dugongs face various anthropogenic threats, including targeted or incidental captures, vessel collisions, and habitat degradation [5], in addition to non-anthropogenic challenges, such as infectious diseases [6], as similarly observed in cetaceans [7–10].

Infectious diseases are major contributors to the mortality of cetaceans and sirenians across various regions, including the Canary Islands, the Andaman Sea of Thailand, the Philippines, Brazil, Italy, and the Netherlands [6–8,11–13]. Many of the bacteria involved are pathogenic, and a considerable number are opportunistic organisms naturally harbored by marine mammal hosts [14,15]. Several of these bacteria, such as *Leptospira* spp., *Mycobacterium* spp., and *Vibrio* spp. have the potential to cause pathological changes and may also act as zoonotic agents, posing risks to both animal and human health [16–18]. Necropsy examinations of stranded cetaceans and sirenians often reveal infectious and inflammatory conditions, frequently associated with septicemia [6]. Instances of septicemia have been linked to several opportunistic bacterial pathogens, including *Streptococcus dysgalactiae*, *Morganella morganii*, and *Erysipelothrix rhusiopathiae* [19,20]. These pathogens typically arise in compromised individuals, often as a result of underlying factors such as parasitic infestations or environmental stressors [21]. Coagulation disorders are a recurrent and potentially fatal complication of septicemia, which can progress to disseminated intravascular coagulation (DIC) [22]. It has been reported primarily in pinniped species, such as New Zealand sea lions (*Phocarctos hookeri*) [23] and Northern elephant seals (*Mirounga angustirostris*) [24]. However, septicemia-induced DIC in dugongs during rehabilitation and the associated etiology of sepsis remain unreported.

This study aims to characterize the clinical, pathological, and microbial findings in a live stranded dugong calf with systemic *A. xylosoxidans* infection, to determine the pattern of oxidative damage and DIC associated with the infection.

2. Materials and Methods

2.1. Animal Signalment and History

On 10 August 2024, a live stranded male dugong calf was discovered on the east side of Koh Poda, Krabi Province, Thailand. Immediate assistance was provided, and the calf was transported by boat from the stranding site to Nopparat Thara Pier, then by truck to the nursery station at the Natural Resources and Environment Institute, Rajamangala

University of Technology Srivijaya, in Trang Province. The dugong calf had a body length of 102 cm and weighed 13.8 kg. Based on the body length and weight assessment, the calf was classified as a neonate, which typically exhibit body length ranging from 0.97 to 1.24 m and weight between 14 and 34 kg, according to Marsh et al. (1980) [25]. The observed dugong calf displayed small and short vibrissae sparsely distributed around the perioral region. Minor callosities were noted along the edges of the pectoral flippers. The umbilicus was completely closed. No dark green staining was observed on the horny plates of the upper and lower jaws within the oral cavity. Additionally, no fetal folds were present along the ventral surface. Based on these characteristics, the calf was estimated to be approximately two months old [25]. Upon initial examination, the calf was weak, dehydrated, and in poor bodily condition, with an estimated body condition score of 2/5, which was assessed according to the Dugong Necropsy Manual in Thailand [26]. In brief, the BCS assessment involved evaluating three parameters—cervical depression, dorsal musculature, and lateral body profile—and classifying the animal into one of five categories. A BCS of 1/5 (very thin) is characterized by a deep neck groove, a sharp vertebral outline, and an emaciated body profile; a BCS of 2/5 (thin) presents with a visible neck groove, a flattened back, and reduced body fullness; a BCS of 3/5 (healthy) shows no obvious neck groove, a slightly flattened but full back, and a gently rounded body profile; a BCS of 4/5 (overweight) is defined by the absence of a neck groove, a fully rounded back, and increased girth; and finally, a BCS of 5/5 (obese) is indicated by the absence of a neck groove, a broad and rounded back, and a markedly distended body. Clinical signs, including a concave neck, persistent suckling behavior indicative of hunger, and lethargy, suggested that the calf had been separated from its mother for several days. While precise estimation of the duration of fasting in dugong calves is limited due to the lack of species-specific data, these findings are consistent with at least 2–3 days of inadequate milk intake. Such signs reflect progressive undernutrition and dehydration, as documented in other mammalian and marine mammal neonates [27,28]. The left eye was opaqued, and the calf was unable to maintain balance in an upright position. The initial treatment focused on ocular therapy; however, the dugong calf developed acute clinical deterioration after one week of rehabilitation. Systemic enrofloxacin was administered empirically at a dosage of 5 mg/kg, intramuscularly, once daily (SID) from 21 August 2024 until death, based on clinical judgment and prior experience, as antimicrobial susceptibility results were not available during treatment. Despite 17 days of extensive therapy and rehabilitation, the animal's condition continued to decline, and the calf ultimately died. A necropsy was performed for further investigation, and antimicrobial susceptibility testing was conducted postmortem.

2.2. Necropsy

The dugong calf was necropsied following a standardized procedure [29,30]. Tissue samples were collected from multiple organs and anatomical sites, including the entire brain, trachea, lungs, heart, liver, gallbladder, pancreas, spleen, kidneys, adrenal glands, urinary bladder, lymph nodes, thymus, stomach, tongue, esophagus, intestines, skin from the area anterior and superior to the right eye, skeletal muscle with traumatic lesions, and both eyes, to enable comprehensive pathological evaluation. All specimens were subsequently preserved in 10% neutral buffered formalin [31].

2.3. Bacteriological Examination

Bacteriological analysis was performed on tissue samples from the lung, liver, spleen, kidney, brain and heart. The tissues were cultured on MacConkey agar (Oxoid, Thermo Fisher Scientific, Waltham, MA, USA) and incubated at 35 °C in a 5% CO_2 atmosphere.

Additionally, the samples were inoculated directly onto blood agar (Oxoid) and incubated at 35 °C. Further bacterial identification and characterization were conducted using the VITEK-2 Compact system (bioMérieux, Marcy l'Etoile, France) [32]. No polymerase chain reaction (PCR) assays were performed for bacterial identification. Antibiotic susceptibility testing was performed using the Kirby–Bauer disk diffusion method. Bacterial cultures were grown overnight on Mueller–Hinton (MH2) agar plates. Colonies were suspended in nutrient broth, and the turbidity of the suspension was measured using an optical spectrophotometer (λ = 600 nm). The optical density (OD) was adjusted to 0.25 or 0.50. A sterile cotton swab was dipped into the bacterial suspension, and a bacterial lawn was applied to the surface of the agar plates. Antibiotic disks (5 mm in diameter) were placed on top of the inoculated agar, ensuring the side containing the antimicrobial agent was facing down to ensure direct contact with the bacteria. The plates were then incubated at 37 °C for 48 h. The inhibition zones around the antibiotic disks were measured every 12 h, following the Kirby–Bauer test protocol [33].

2.4. Histopathology

Tissue samples were processed following standard histological procedures [34,35]. Briefly, the tissues underwent a graded dehydration process using ethanol. They were cleared with xylene to eliminate the alcohol and then embedded in paraffin wax to maintain structural integrity. Thin sections (4 μm) of the paraffin-embedded tissue were cut and stained with hematoxylin and eosin (H&E) for general morphological evaluation. The stained sections were subsequently mounted on glass slides under a coverslip for microscopic analysis.

2.5. Biomarker of Oxidative Damage

Double-immunofluorescence staining for 4-hydroxynonenal (4-HNE) and 8-hydroxydeoxyguanosine (8-oxodG) was utilized to evaluate the expression of reactive oxygen species (ROS) and to assess DNA damage. Paraffin-embedded tissue sections from lung, liver, spleen, kidney, heart, and brain were processed following the staining protocol described by Jantrakajorn et al. (2024) [36]. An antigen retrieval was performed using a citrate buffer (pH 6.0) in a high-pressure cooker for 10 min. To block non-specific binding, the sections were incubated with 1% normal horse serum in PBS for 45 min at room temperature. After blocking, the tissue sections were incubated overnight at 4 °C with a mixture of two primary antibodies. The first primary antibody, monoclonal mouse anti-4-hydroxynonenal (ab48506, Abcam, Cambridge, UK), was diluted 1:50, while the second, polyclonal goat anti-8-hydroxydeoxyguanosine (AB5830, Sigma-Aldrich, St. Louis, MO, USA), was used at a dilution of 1:200. Following incubation with the primary antibodies, the sections were washed with PBS and incubated with a mixture of secondary antibodies raised in different species: DyLight-488 Donkey Anti-mouse IgG (H + L) (Invitrogen, Waltham, MA, USA) and CF™ 555 Rabbit Anti-goat IgG (H + L) (Sigma-Aldrich, St. Louis, MO, USA), both diluted in 1% BSA, for 1 h at room temperature in the dark. The sections were then mounted with ProLong™ Gold Antifade Mountant containing DAPI (Thermo Fisher Scientific, Waltham, MA, USA) for DNA counterstaining. Fluorescence imaging was performed using a fluorescence microscope (ECLIPSE Ni-U, Nikon, Tokyo, Japan).

2.6. AI Tools Statement

Artificial intelligence tools (ChatGPT-4o, OpenAI) were used solely to assist in grammatical correction and language refinement. No AI tools were used for data analysis, content generation, or interpretation of results.

3. Results

3.1. Anamnesis, Clinical Examination, and Treatment

Following rescue, the dugong calf was transferred to a rehabilitation facility in Trang Province, Thailand. The calf was housed in a fiber circular tank, 1.20 m in depth with a total volume of 28,495 L, filled with natural saltwater (salinity 30 ppt) and a pH around 7.7 (Figure 1a). The water utilized for the care of the dugong calf was stored in a holding tank for 24 h prior to being transferred into the enclosures. There were two enclosures, which are used alternately on a daily basis. Water changes were performed at 100% capacity every day to maintain optimal conditions. The water was filtered continuously using sand filters, and warm water was added to maintain temperature at around 30 °C. The feeding regime initially consisted of a milk replacer formula for the first week. To mimic natural behavior where dugong mothers introduce seagrass to their calves, the veterinarian offered one or two leaves of lettuce prior to each tube feeding, as a form of behavioral enrichment and feeding stimulation. In the initial stage of rehabilitation, the dugong calf was primarily fed a milk formula consisting of 100 g of Milk Matrix 30/52, 100 g of puppy milk, 300 mL of coconut milk, and 35 mL of canola oil, all of which provided an energy intake of 50–80 kcal/kg per day. The formula was divided into four meals, given at 8 a.m., 12 p.m., 5 p.m., and 11 p.m., with a maximum of 300 mL of formula per feeding. In addition, each feeding was supplemented with B-complex vitamins, taurine, lactobacillus, and simethicone to support optimal health and development. After six days of formula feeding, the dugong calf exhibited symptoms of mild diarrhea, characterized by softer stools compared to those of healthy dugongs, as described by Ooi et al. [37], probably attributable to the lactose content in the puppy milk (Figure 1b). Consequently, experts recommended modifying the nutritional formula by eliminating the puppy milk and substituting it with 75 to 140 g of Milk Matrix 30/52 (adjusted according to the calf's body weight), 450 mL of coconut milk, and 35 mL of canola oil, administered in three divided feedings per day. The final feeding was replaced with 30 g of Oxbow (Critical Care—Herbivore, Oxbow Enterprises, Inc., Omaha, NE, USA) to enhance the calf's nutritional profile. This formulation adjustment was designed to minimize lactose consumption and optimize digestive function, supporting the calf's overall health and recovery during the rehabilitation process. Following this adjustment, the calf's stool returned to normal, with the feces appearing as soft, light yellowish pellets. The dugong's weight and overall condition gradually improved. However, on the morning of 27 August 2024, the dugong began to show signs of lethargy, floating still, and short breathing, and its breathing rate gradual increased beyond its normal respiratory range. After that, the calf had convulsions and pale mucous membrane, and the heart rate dropped before death on 28 August 2024. The total rehabilitated period was 17 days, and the daily weight record is shown in Figure 1c.

Upon admission, the dugong calf presented with severe dehydration and marked corneal opacity in the left eye. Within 24 h, initial stabilization efforts were made, including the administration of fluids and electrolytes to address the dehydration. Diazepam was also given for muscle relaxation, which resulted in an improvement in the animal's respiratory rate. Ophthalmic examination revealed significant corneal opacification and ulcerative keratitis with keratomalacia in the left eye, while the right eye appeared normal. The dugong was treated with the antibiotic, levofloxacin 0.5% (Cravit® ophthalmic solution Cravit, Santen Pharmaceutical Co., Osaka, Japan), four times daily. The dimension of the corneal opacity appeared reduced, and the calf showed a positive response to treatment. Blood tests revealed hypoproteinemia due to dehydration, elevated blood urea nitrogen (BUN) levels, and mild leukocytosis. Consequently, topical eye treatment was continued, and nutrition was managed via force-feeding through a stomach tube. The animal's condition remained stable, with normal heart and respiratory rates. However, on 27 August 2024,

the dugong's condition deteriorated after the water temperature dropped to 27 °C due to rainfall. Initially active, the calf began showing signs of distress around 4:30 a.m., with an increased respiratory rate and body tremors by 5 a.m. By 10:30 a.m., the respiratory rate had risen to over two breaths per minute, and additional signs of weakness were noted throughout the day, indicating a progressive decline in its health.

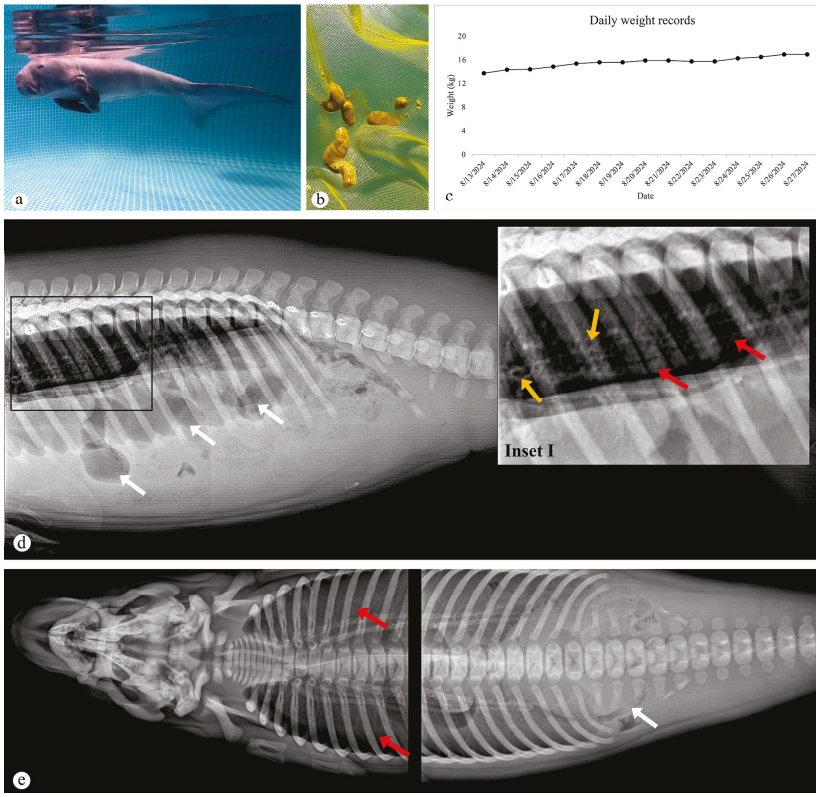


Figure 1. Captive rehabilitation and medical examination of the dugong calf (*Dugong dugon*): (**a**) The dugong was rehabilitated in a fiber circular tank; (**b**) Yellow, soft, unformed feces were present in piles, indicating diarrhea; (**c**) A graph depicting the daily weight of the dugong over a 17-day rehabilitation period; (**d**) Right lateral thoracolumbar radiograph showing an alveolar pattern (inset I, red arrow), bronchial pattern (inset I, yellow arrow) in the lung lobes, and intestinal gas (white arrow); (**e**) Dorsoventral thoracolumbar radiograph showing similar alveolar lung changes (red arrow) and intestinal gas (white arrow).

The right lateral thoracolumbar radiograph of the dugong revealed an alveolar and bronchial pattern in the lung lobes (Figure 1d, inset I), while the dorsoventral thoracolumbar radiograph showed similar alveolar changes involving both lung lobes (Figure 1e). In the abdomen, radiographic findings demonstrated radiopaque areas with gas-filled intestines floating within the peritoneal cavity (Figure 1d,e), suggestive of hydroperitoneum. The dugong showed increased pain and stiffness. A blood glucose test showed significantly decreased levels. Fluids were administered by an oral route and intravenous administration was also attempted. Pain medication and antibiotics were given. Immediate medication was administered, including diazepam (0.1 mg/kg, IM, SID), butorphanol (0.1 mg/kg, IM, SID), and enrofloxacin (5 mg/kg, IM, SID) up until death. Biochemical analyses showed severe hypoalbuminemia (1 g/L; reference ranges 17–47 g/L) and an increased BUN level (16 mg/dL; reference ranges 9–14 mg/dL). The fecal smear showed no evidence of parasitic infestation. Serum biochemistry reference intervals for live wild dugongs were based on the study by Lanyon et al. (2015) [38].

3.2. Necropsy and Histopathology Investigations

The postmortem evaluation indicated that the dugong calf's nutritional status was good (Figure 2a,b). Macroscopic examination of the skin and blubber throughout the body revealed no significant gross lesions. However, the right flipper above the elbow had localized subcutaneous congestion. Additionally, the musculature along the right dorsum had two areas of hemorrhage and necrosis, each approximately measuring 4 × 3 cm (Figure 2c,e). The pericardial sac contained 2.2 mL of serous fluid. Over 80% of the epicardium was contoured and edematous (Figure 2g). The cardiac chambers contained red blood clots. The lungs appeared grayish-pink, firm, mildly edematous, and non-collapsible, with blood oozing from the cut surface (Figure 2f). The trachea was fully occluded by frothy, turbid, dark red fluid and clots, particularly at the distal portion. The abdominal cavity contained 35 mL of serosanguineous fluid. The liver was congested, firm, and mottled dark brown to red (Figure 2h). The gallbladder was markedly distended, containing 7.5 mL of yellowish bile, with limited bile flow; however, no evidence of biliary tract obstruction was observed. The left eye was moderately shrunken and revealed corneal ulceration, characterized by an opened wound with superficial debris material, surrounded by corneal vascularization and granulation tissue (Figure 2i). The spleen had a rounded, bean-shaped appearance, and its cut surface exhibited diffuse reddening. Both kidneys and lymph nodes appeared unremarkable upon examination. Moderate congestion was noted in both the brain and intestines (Figure 2j).

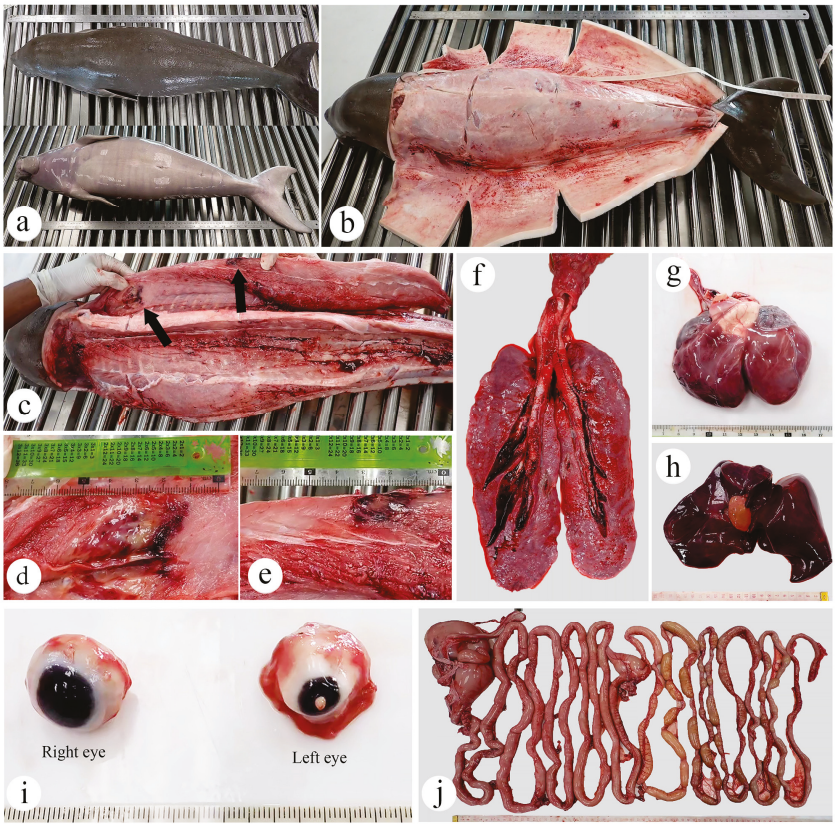


Figure 2. Gross necropsy findings of a dugong calf, *Dugong dugon*: (**a**) Dorsal and ventral views of the body; (**b**) Carcass opening revealing a thick layer of blubber; (**c**) Intramuscular hemorrhage and necrosis; (**d**) Close-up of deep myonecrosis in the anterior region; (**e**) Close-up of deep myonecrosis in the medial region; (**f**) Pulmonary edema and hemorrhage; (**g**) Fluid accumulation on the epicardium; (**h**) Hepatic congestion with gallbladder distention; (**i**) Corneal ulceration with debris material in the left eye; (**j**) Congested intestines.

3.2.1. Skin and Muscle

The skin of the dugong calf exhibited no significant gross lesions. Histopathological examination of the grossly hemorrhaged musculature revealed regionally extensive interstitial hemorrhage (Figure 3a). Muscle fibers varied in size and were rounded and variably shrunken, with some fibers appearing hyalinized, hypereosinophilic, or flocculent, and displaying central, prominent nuclei (myocyte degeneration, atrophy and regeneration). Occasionally, muscle fibers were fragmented with myocyte nuclear loss and prominent contraction bands (myonecrosis). Mild activation of satellite cells was observed. Infiltration of macrophages was evident in the degenerating and necrotic areas, with these cells containing fragments of broken muscle fibers (Figure 3b,c). Additionally, capillaries were lined by endothelial cells exhibiting hypertrophied nuclei.

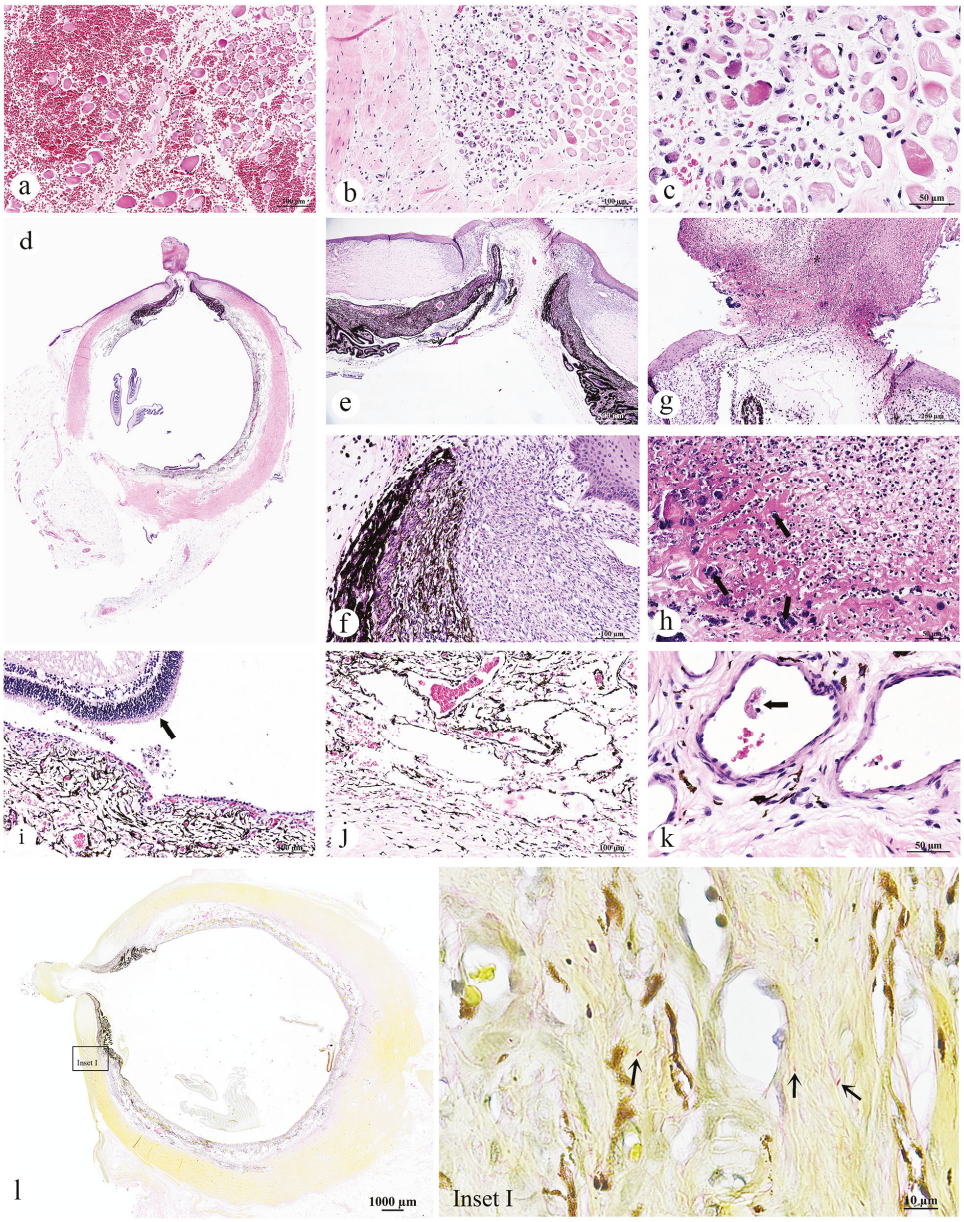


Figure 3. Photomicrographs of the muscular myonecrosis, atrophy, degeneration and hemorrhage, and corneal perforation of a dugong calf (*Dugong dugon*): (**a**) Interstitial hemorrhage of the musculature; (**b**) Muscle fiber degeneration and necrosis; (**c**) Damaged myofibers displayed a range of degenerative alterations, including variations in fiber size, swelling, hypereosinophilia, vacuolation (myofibrillolysis), and necrotic changes; (**d**) Subgross magnification view showing the entire globe with

corneal perforation subjacent to eosinophilic debris, along with the presence of anterior synechia; (**e**) Higher magnification of the anterior synechia; (**f**) Adhesion of the iris to the corneal stroma; (**g**) Close-up view of the adhesion site between the corneal debris and the globe; (**h**) Presence of bacterial colonies within the debris material (arrow); (**i**) Retinal detachment (arrow), with hypertrophy of the retinal pigmented epithelial layer; (**j**) The underlying choroid appeared congested, with mild hemorrhage, and was moderately expanded due to edematous fluid; (**k**) Fibrin thrombi in the vascular lumen (arrow); (**l**) Gram staining of the eye tissue showing a positive staining for Gram-negative rod-shaped bacteria (inset I, arrow) at the suspected site of infection. ((**a**–**k**) H&E staining; original magnification: (**d**) Subgross magnification, (**e**) ×4, scale bar = 500 μm; (**a**,**b**,**g**) ×10, scale bar = 250 μm; (**f**,**i**,**j**) ×20, scale bar = 100 μm; (**c**,**h**,**k**) ×40, scale bar = 50 μm; (**l**) gram staining; original magnification: (**l**) Subgross magnification, (**e**) ×4, scale bar = 1000 μm; (**l**) inset I ×100, scale bar = 100 μm).

Morphological diagnoses included the following:

- Skeletal muscle: Myositis and myonecrosis, multifocal, chronic-active, with myofiber degeneration and atrophy, myocyte regeneration, and histiocytic infiltration.

3.2.2. Eye

The left eye had eosinophilic necrotic material adhered to the outer surface of the ocular globe. Subjacent to this material, a corneal perforation was noted (Figure 3d). Surrounding the perforated site, the corneal stroma was circumferentially infiltrated by dense plump fibroblasts admixed proliferation of small caliber blood vessels, indicative of granulation tissue formation, surrounded by edematous collagenous stroma, infiltration of inflammatory cells, along with pale eosinophilic material, suspected to be fibrin. Inflammatory cells were principally lymphocytes, macrophages, and neutrophils. These components appeared to pull the iridal membranes cranially to appose to the cornea and caused the development of anterior synechia (Figure 3e,f). The rest of the corneal stroma had evidence of chronic pigmentary keratitis with epithelial hyperplasia and neovascularization, depicting by pigmentary incontinence, as well as formation of blood vessels scattered throughout. The exophytic eosinophilic material (Figure 3g,h) was composed of cellular debris, fibrin and bacterial colonies, consisting of cocci and bacilli (Figure 3h, arrow), suggesting a secondary infection. Such lesions are commonly associated with trauma or infection. The retina of left eye was detached, exhibiting hypertrophy (tombstoning) of the underlying retinal pigmented epithelium (Figure 3i, arrow). The underlying choroid appeared congested, with mild hemorrhage, and was moderately expanded due to edematous fluid (Figure 3j). Fibrin thrombi were present within the vascular lumen of this layer (Figure 3k). In contrast, the right eye showed no significant pathological findings. Gram staining of the eye revealed colonies of discrete Gram-negative rod-shaped bacteria at the inner choroid layer (Figure 3l, inset I).

Morphological diagnoses included the following:

- Left eye: Kerato-uveitis, chronic-active, suppurative and necrotizing, with corneal perforation, anterior synechia, retinal detachment, fibrin thrombi, and bacterial colonization (Gram-negative bacilli);
- Right eye: No significant lesions.

3.2.3. Gastrointestinal Organ and the Accessory Digestive Structures

Histopathological evaluation of the tongue, esophagus, stomach, intestine, liver, gallbladder, and pancreas revealed the following findings. No significant changes were observed in the tongue (Figure 4a). The esophagus had a mild thickening of keratinous layers with retained nuclei (parakeratotic hyperkeratosis) (Figure 4b). Examination of the stomach and intestinal tissues showed no remarkable mucosal alterations, although moderate congestion of the vasculature was evident (Figure 4c,d). The pancreas exhibited lysis of

the pancreatic parenchyma, though this did not extend into the peripancreatic adipose tissue. Areas of lytic necrosis were multifocal to coalescing, characterized by the loss of cellular architecture and replacement with eosinophilic cellular debris, karyorrhectic material, fibrin, hemorrhage, and edema (Figure 4e). Notably, no rimmed necrotic neutrophils or macrophage reactions were observed, suggesting a peracute necrosis process. Within the adjacent pancreatic parenchyma, acinar cells were either swollen with pale, vacuolated eosinophilic cytoplasm (indicating degeneration) or shrunken with hypereosinophilic cytoplasm, pyknotic nuclei, and the loss of zymogen granules (indicating single-cell death). Additionally, prominent changes were noted in the pancreatic vasculature, including interlobular capillaries, pancreatic arterioles, and small-caliber capillary vessels. The interlobular capillaries displayed discrete to extensive amorphous or meshwork-like deposits of finely granular, eosinophilic material (peracute fibrin thrombi), which were closely associated with lytic necrosis (Figure 4f, arrow). Within the necrotic foci, blood vessel vascular tunics were transmurally expanded by scant necrotic cellular debris, fibrin, hemorrhage, and edema (Figure 4g). In the liver, severe congestion was observed in scattered panlobular regions, accompanied by hepatocellular degeneration (Figure 4h).

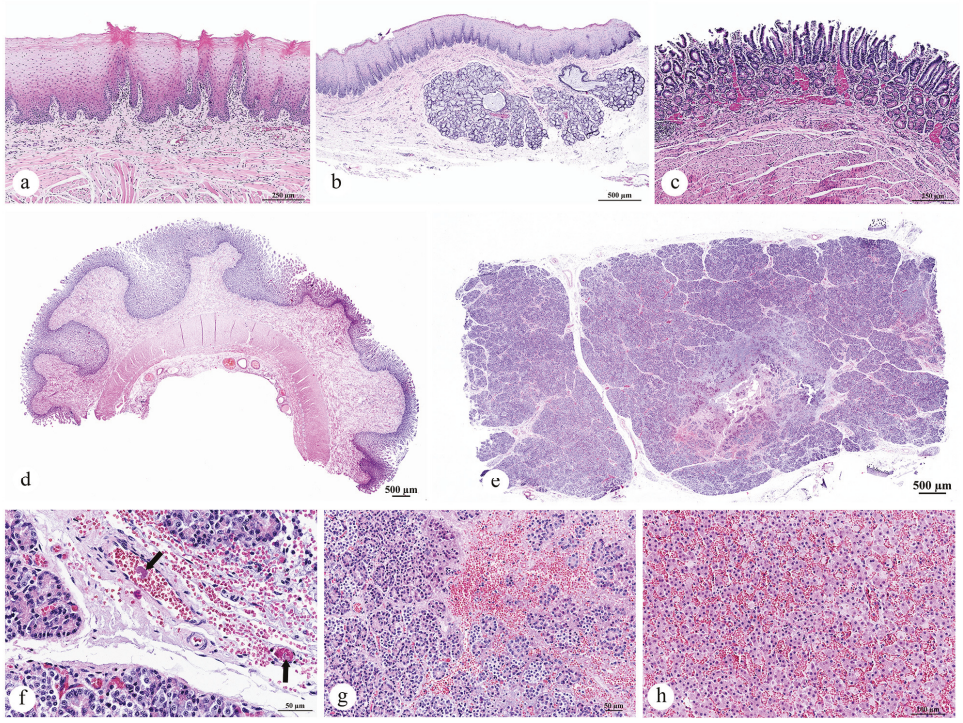


Figure 4. Photomicrographs of the gastrointestinal organs and accessory digestive structures of a dugong calf (*Dugong dugon*): (**a**) No significant changes observed in the architectural structure of the tongue; (**b**) No significant changes observed in the architectural structure of the esophagus; (**c**) Gastric congestion; (**d**) Intestinal congestion; (**e**) Moderate peracute pancreatic necrosis; (**f**) Presence of fibrin thrombi in the pancreatic interlobular capillaries (arrow); (**g**) Area of hemorrhage and necrosis within the pancreas; (**h**) Severe hepatic congestion. ((**a**–**h**) H&E staining; original magnification: (**b**,**d**,**e**) subgross magnification; (**a**,**c**) ×10, scale bar = 250 μm; (**h**) ×20, scale bar = 100 μm; (**f**,**g**) ×40, scale bar = 50 μm).

Morphological diagnoses including the following:

- Pancreas: Pancreatic necrosis, lytic, multifocal to coalescing, peracute, with fibrin thrombi and vascular necrosis;
- Liver: Congestion, multifocal to coalescing, moderate to severe, with hepatocellular degeneration;

- Esophagus: Parakeratotic hyperkeratosis, mild;
- Stomach and intestine: Congestion, mild;
- Tongue: No significant lesions.

3.2.4. Lymph Node, Thymus, and Spleen

The axillary lymph node exhibited marked enlargement, characterized by an increased accumulation of macrophages within the paracortex of the lymph node tissue, leading to paracortical hyperplasia (Figure 5a,b). Aggregates of neutrophils were often observed infiltrating the paracortex (Figure 5c). Additionally, prominent vascular congestion was observed throughout the lymph node (Figure 5c). The lymphatic vessels contained amorphous fibrin thrombi (Figure 5d, arrow). No notable alterations were detected in the thymus (Figure 5e). Examination of the spleen revealed a reduction in the size of the white pulp follicles, which were widely spaced by hypercellular red pulp. This red pulp was composed of erythrocytes interspersed with abundant homogeneous eosinophilic material, likely representing lysed erythrocytes. Furthermore, numerous neutrophils and scattered cellular debris were noted (Figure 5f).

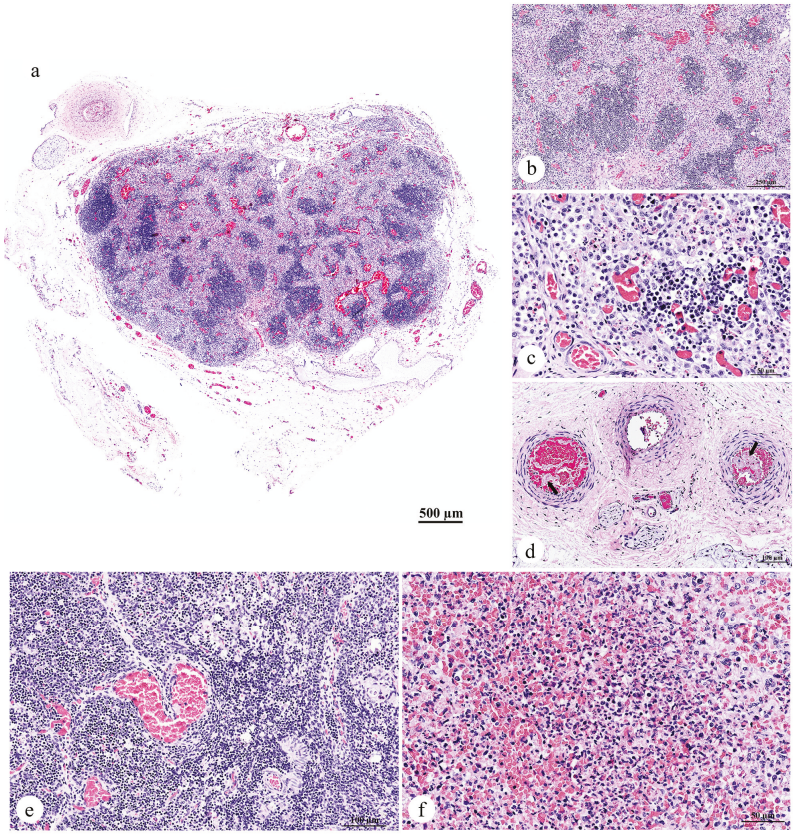


Figure 5. Photomicrographs of the lymphatic organs of a dugong calf (*Dugong dugon*): (**a**) Subgross magnification view showing expansion of the lymph node; (**b**) Higher magnification of the paracortical hyperplasia; (**c**) Lymph node congestion and infiltration of neutrophils in the paracortex; (**d**) Presence of fibrin thrombi in the lymphatic arterioles (arrow); (**e**) No significant changes observed in the architectural structure of the thymus; (**f**) Severe acute multifocal neutrophilic and necrotizing splenitis. ((**a**–**f**) H&E staining; original magnification: (**a**) subgross magnification; (**b**) ×10, scale bar = 250 μm; (**d**,**e**) ×20, scale bar = 100 μm; (**c**,**f**) ×40, scale bar = 50 μm).

Morphological diagnoses included the following:

- Lymph node: Lymphadenitis, neutrophilic and histiocytic, acute, multifocal to coalescing, with paracortical hyperplasia, vascular congestion, and fibrin thrombi;

- Spleen: Splenitis, neutrophilic and necrotizing, acute, multifocal, severe, with red pulp hypercellularity and white pulp depletion;
- Thymus: No significant lesions.

3.2.5. Cardiorespiratory System

Histopathological examination of the dugong calf revealed no significant lesions in the heart (Figure 6a). However, the trachea and lung sections exhibited notable alterations. In the lung, approximately 75% of the tissue exhibited congestion, with minimal hemorrhage. These regions contained dense accumulations of erythrocytes, along with aggregates of eosinophilic proteinaceous edema fluid, plump vacuolated macrophages, and epithelial detachment. Flattened "squames" or desquamated fetal skin cells, typically found in the amniotic fluid, were observed within an alveolus, alongside hemorrhage and epithelial detachment (Figure 6b). Additionally, marked changes were observed in the pulmonary vasculature, including the arterioles and alveolar capillaries, which showed discrete to extensive deposits of amorphous eosinophilic material, suggestive of peracute fibrin thrombi (Figure 6c). In the trachea, there was excessive mucus accumulation, mixed with epithelial debris and extravasated red blood cells (Figure 6d). In the bronchial lumens, a moderate accumulation of macrophages, lymphocytes, and neutrophils, along with mixed mucus, was observed (Figure 6e). The bronchial mucosa showed mild infiltration by lymphocytes, histiocytes and neutrophils. Inflammatory cells had transmigrated through the epithelium, extending into the submucosa and adjacent pulmonary parenchyma, and variably filling the bronchiolar and parabronchial areas (Figure 6f).

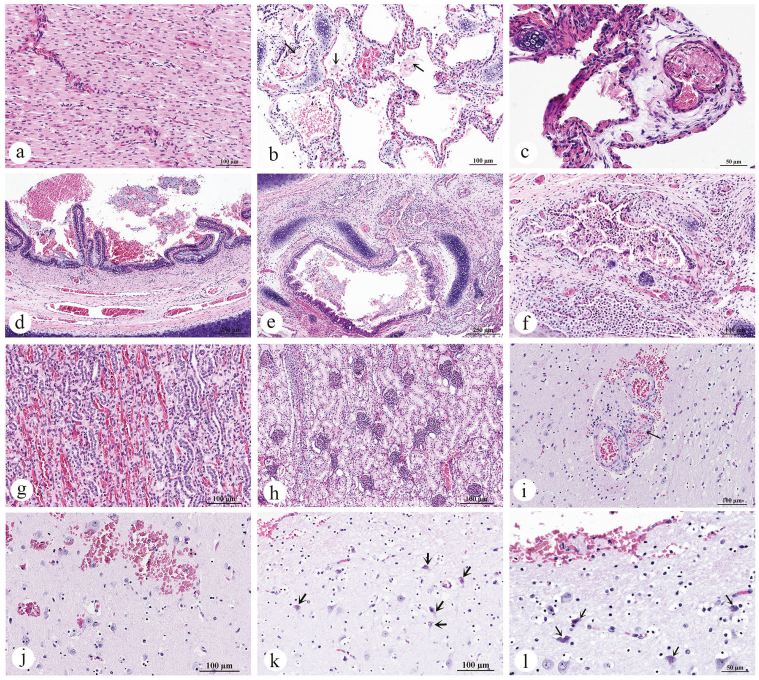


Figure 6. Photomicrographs of the heart, lung, kidney, and brain of a dugong calf (*Dugong dugon*): (**a**) The heart with no significant architectural changes; (**b**) Desquamated fetal skin cells (arrow) observed within an alveolus, alongside hemorrhage and epithelial detachment; (**c**) Fibrin thrombi in the alveolar capillaries (arrow); Excessive mucus mixed with red blood cells and epithelial debris in tracheal lumen (**d**), bronchial lumen (**e**); (**f**) Inflammation of the bronchus and adjacent pulmonary parenchyma; (**g**) Congestion noted in the renal medulla; (**h**) Congestion observed in the renal cortex and glomeruli; (**i**) Fibrin thrombi in a brain venule (arrow); (**j**) Hemorrhage in the neuroparenchyma; (**k**) Neuronal degeneration and necrosis (arrow); (**l**) Higher magnification of neuronal degeneration and necrosis (arrow). ((**a**–**l**) H&E staining; original magnification: (**d**,**e**) ×10, scale bar = 250 μm; (**a**,**b**,**f**–**k**) ×20, scale bar = 100 μm; (**c**,**l**) ×40, scale bar = 50 μm).

Morphological diagnoses included the following:

- Lung: Pulmonary congestion and edema, acute, multifocal to coalescing, with pulmonary hemorrhage, intra-aveolar squames (aspiration), and fibrin thrombi;
- Trachea: Intraluminal mucus and epithelial debris;
- Bronchi/bronchioles: Bronchopneumonia, lymphohistiocytic and neutrophilic, mild to moderate, with mucosal and submucosal inflammation;
- Heart: Congestion, no significant lesions.

3.2.6. Adrenal Glands, Kidneys, and Urinary Bladder

The adrenal glands, kidneys, and urinary bladder exhibited minimal pathological changes. Notable congestion was observed primarily in the vasculature and glomeruli of the kidneys, affecting both the renal cortex and medulla (Figure 6g,h). However, no fibrin thrombi were detected within the renal vasculature.

Morphological diagnoses included the following:

- Kidneys: Congestion, multifocal, mild to moderate;
- Urinary bladder: No significant lesions;
- Adrenal glands: No significant lesions.

3.2.7. Brain

Histopathological examination of the cerebrum, brainstem, and cerebellum revealed that some vessels, primarily veins and venules, contained well-organized thrombi composed of neutrophils and red blood cells (Figure 6i). The endothelium of the affected vessels was disrupted, and expanded by fibrinoid material, as well as areas of frank hemorrhage extending beyond the vessel walls. The surrounding neuroparenchyma exhibited microhemorrhage (Figure 6j). There was no evidence of inflammation in the affected vessels. Neurons in the affected regions exhibited cellular alterations and cell death, characterized by degeneration, increased eosinophilia, and karyolysis (Figure 6k,l).

Morphological diagnoses included the following:

- Cerebrum, brainstem, and cerebellum: Thromboembolic vasculopathy with fibrinoid necrosis and microhemorrhages, multifocal, with neuronal degeneration and necrosis.

The histopathological findings are summarized in Table 1 to facilitate clearer visualization and comparison of lesion types across different tissues.

Table 1. Comparative summary of lesion types observed in different organs of the dugong calf.

Tissue/Organ	Congestion	Hemorrhage	Necrosis	Cellular Infiltration	Fibrin Thrombi in Capillary
Musculoskeletal system					
Skeletal muscle	✓	✓	✓	✓	
Nervous and sensory system					
Brain	✓	✓	✓		✓
Eye	✓	✓		✓	
Digestive system					
Tongue	✓				
Esophagus	✓				
Stomach	✓				
Intestine	✓				
Pancreas	✓	✓	✓	✓	✓
Liver	✓				
Lymphatic system					
Lymph node	✓			✓	✓
Spleen	✓			✓	✓

Table 1. *Cont.*

Tissue/Organ	Congestion	Hemorrhage	Necrosis	Cellular Infiltration	Fibrin Thrombi in Capillary
Thymus	✓				
Urinary system					
Kidney	✓				
Urinary bladder	✓				
Endocrine system					
Adrenal gland	✓				
Cardiorespiratory system					
Heart	✓				
Trachea	✓	✓		✓	✓
Bronchi/bronchioles	✓	✓		✓	✓
Alveolar	✓	✓		✓	✓

3.3. Bacteriological Analysis and Antibiotic Susceptibility Testing

Bacteriological analysis was conducted on samples obtained from major organs, including the lung, liver, spleen, kidney, heart, and brain. The results revealed the growth of a single bacterial colony on the agar plates. Subsequent sub-culturing and Gram staining identified the bacterium as a Gram-negative rod, which was further characterized as *Achromobacter xylosoxidans* through species identification. Antibiotic susceptibility testing indicated that the isolate was resistant to amikacin, cefazolin, ceftriaxone, and oxytetracycline. It exhibited intermediate resistance to enrofloxacin and marbofloxacin, while being susceptible to amoxicillin–clavulanic acid, doxycycline, imipenem, and sulfa-trimethoprim (Table 2). The resistance profile of *Achromobacter xylosoxidans* in this case indicates limited efficacy of commonly used antibiotics such as aminoglycosides, cephalosporins, and oxytetracycline. Intermediate resistance to fluoroquinolones further complicates treatment choices. While susceptibility to drugs like amoxicillin–clavulanic acid and imipenem offers potential options, this highlights the need for culture-based antibiotic selection in dugong rehabilitation to improve therapeutic success and minimize resistance development.

Table 2. Bacteriological analysis using VITEK-2 Compact system and antibiotic susceptibility testing the Kirby–Bauer disk diffusion method.

Antibiotic	Concentration (μg) of the Antibiotic in Disc	Zone of Inhibition (mm)		
		Resistant	Intermediate	Sensitive
Amoxicillin–clavulanic acid	20/10	-	-	23
Amikacin	30	12	-	-
Cefazolin	30	13	-	-
Ceftriaxone	30	12	-	-
Doxycycline	30	-	-	20
Enrofloxacin	5	-	19	-
Imipenem	10	-	-	27
Marbofloxacin	5	-	17	-
Oxytetracycline	30	13	-	-
Sulfa-trimethoprim	1.25/23.7	-	-	26

3.4. Immunofluorescence Analysis of Oxidative Damage

Immunofluorescence staining was performed using 4-hydroxynonenal (4-HNE) and 8-hydroxydeoxyguanosine (8-oxodG) markers to investigate the impact of peracute DIC-induced oxidative stress and DNA damage on cellular structures in major organs, including the lung, liver, spleen, kidney, heart, and brain. Based on visual assessment, cells positive for 4-HNE exhibited a cytoplasmic staining pattern, whereas 8-oxodG-positive cells displayed nuclear staining. In the brain, 4-HNE expression was initially detected in neuronal

cells, with increased expression observed in regions displaying heightened neuronal degeneration. A significant upregulation of 8-oxodG expression was also identified in the brain. Notably, areas with intense 4-HNE expression also exhibited prominent co-expression of 8-oxodG, indicating concurrent oxidative damage and DNA damage in these regions. In contrast, no expression of either 4-HNE or 8-oxodG was detected in the lung, liver, spleen, kidney, or heart tissues. These findings suggest that, in the context of per-acute DIC in the dugong calf, the brain is the primary organ affected by oxidative stress and DNA damage (Figure 7). The co-localization of 4-HNE and 8-oxodG in neuronal regions suggests that oxidative stress and DNA damage may play a crucial role in initiating or exacerbating neuronal death, contributing to the observed mortality. While oxidative damage has the potential to drive neuroinflammation, such a response typically requires sufficient time for inflammatory cells to infiltrate and respond to free radical-induced injury. Therefore, in this peracute case, the lack of inflammatory cell infiltration likely reflects the rapid progression of the disease, which limited the development of a typical neuroinflammatory response.

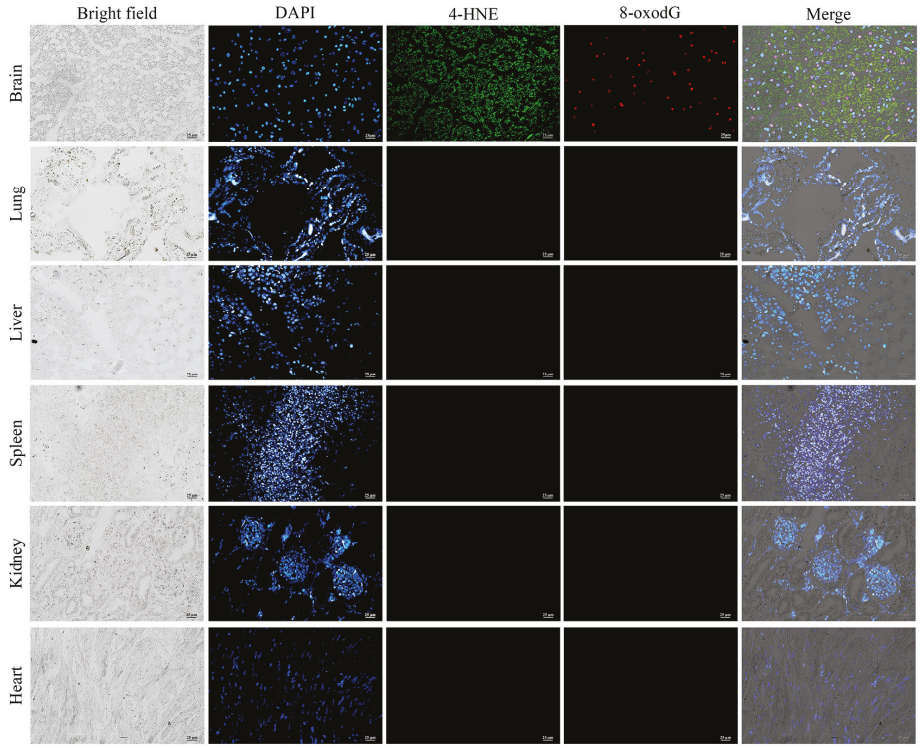


Figure 7. Expression of reactive oxygen species (4-HNE) and damaged DNA (8-oxodG) in different organs of the *Achromobacter xylosoxidans*-infected dugong calf. Panels from left to right show bright field, DAPI-stained nuclei, 4-HNE labeled with DyLight-488 (Invitrogen, Waltham, MA, USA (green), 8-oxodG labeled with CF™ 555 (Sigma-Aldrich, St. Louis, MO, USA) (red), and the merged image of the four panels. Co-localization of 4-HNE (green), 8-oxodG (red), and DAPI (blue) was observed exclusively in the brain tissue of the affected dugong calf. The purple spots represent the co-localization of damaged nuclei associated with DNA damage. (Immunofluorescence: DyLight-488 for 4-HNE (green), CF™ 555 for 8-oxodG (red), DAPI counterstain for nuclei (blue); original magnification, ×40; scale bar represents 50 μm).

4. Discussion

This study presents the first documented case of acute systemic infection and DIC in a dugong calf associated with *Achromobacter xylosoxidans*. This bacterium is an opportunistic Gram-negative organism commonly found in aquatic environments. [39]. It is a well-recognized pathogen in humans, known to cause sepsis and septicemia, particularly in neonates and immunocompromised individuals [40–42]. Although reports of *A.*

xylosoxidans infection in animals are limited, it has been implicated in cases of endocarditis and joint disease in dogs [43,44]. To the best of our knowledge, this is the first report of *A. xylosoxidans* infection in a dugong and the first to demonstrate its potential to induce DIC in marine mammals. This finding is particularly noteworthy in the context of systemic bacterial infections, which are relatively common among sirenians, particularly in manatees. Several bacterial pathogens have been identified in the Florida manatee (*Trichechus manatus latirostris*), including *Salmonella enterica*, which has been associated with lesions in the renal, respiratory, lymphatic, and skeletal systems [45]. *Clostridium* spp. have also been implicated in cases of septicemia and endotoxemia [46], while *Mycobacterium marinum* and *M. kansasii* have been reported to cause disseminated tuberculosis [47]. However, none of these previous reports have involved *A. xylosoxidans*, highlighting the novelty and significance of the present case. In addition to identifying the pathogen, this study also characterized its antimicrobial resistance profile, which has important implications for postmortem diagnosis, epidemiological surveillance, and understanding the potential risks posed by opportunistic aquatic pathogens. Antibiotic susceptibility testing demonstrated a multidrug-resistant profile, with the isolate exhibiting resistance to several commonly used antibiotics, including amikacin, cefazolin, ceftriaxone, and oxytetracycline. This resistance pattern aligns with previously reported findings [48,49], which attribute antimicrobial resistance in *A. xylosoxidans* to both intrinsic and acquired mechanisms, such as the production of β-lactamases, overexpression of efflux pumps, and biofilm formation, all of which contribute to significant therapeutic challenges [50,51]. In this case, the pathogen's dissemination, combined with the calf's immature immune system, is likely to have accelerated the onset of DIC and multi-organ failure. Impairment of immune system function increases susceptibility to opportunistic infections, particularly in neonates or immunocompromised individuals [52]. As reported in similar studies on cetaceans, such immunosuppression may result from synergistic factors including stress, exposure to heavy metals and environmental pollutants, or concurrent infections [53–55]. These findings underscore growing concerns regarding environmental influences on host immunity, the emergence of antimicrobial resistance in aquatic pathogens, and the need for targeted therapeutic strategies in vulnerable marine mammals.

Furthermore, this case emphasizes the importance of reviewing and enhancing rehabilitation protocols to minimize the risk of opportunistic bacterial contamination. Potential sources of *A. xylosoxidans* in the rehabilitation environment may include contaminated water supplies, feeding equipment, or even human handling [56,57]. Given the bacterium's ubiquitous presence in aquatic settings and its ability to form and persist in biofilms [58], special attention should be given to hygiene practices, sterilization procedures, and water quality management within rehabilitation facilities. To better understand and control such infections, further systematic environmental screening for bacterial contaminants should be conducted, particularly on water systems and feeding apparatus, to help identify the origin of infection and guide appropriate preventive strategies.

DIC is characterized by systemic activation of coagulation, impaired anticoagulant pathways, and suppression of fibrinolysis, leading to widespread microvascular thrombosis followed by consumptive coagulopathy and multiple organ dysfunction syndrome [59]. In our study, extensive histopathological lesions were observed, particularly, fibrin thrombi in the pulmonary, pancreatic, and cerebral vessels, along with hemorrhage and necrosis in multiple organs, leading to multiorgan failure and death. These findings are hallmark features of DIC [60]. Additionally, severe ocular lesions, including corneal perforation with Gram-negative bacterial colonization and retinal detachment, suggest a localized initial site of infection that may have served as a portal for systemic bacterial dissemination. Previous studies have indicated that microbial colonization following ocular trauma or

via hematogenous spread can facilitate the onset of systemic infections [61]. Moreover, hepatobiliary sepsis has been reported in human cases of ocular infections, supporting a possible association between ocular pathology and systemic bacterial invasion [62]. Thus, the ocular lesions observed in this dugong calf may represent portal of entry, an early clinical indicator of an underlying, progressing systemic infection. Despite supportive care during rehabilitation, the calf's immune immaturity, indicated by severe leukocytosis and hypoalbuminemia. This pattern is associated with the acquisition and severity of infectious diseases, and intact innate and adaptive immune responses [63]. Like in other young animals, this neonate possessed underdeveloped immune mechanisms, rendering it susceptible to opportunistic pathogens under environmental or nutritional stress [64,65]. These immunological limitations probably contributed to the progression of infection and the eventual onset of fatal DIC in this case.

The pathogenesis observed in this case is consistent with microvascular thrombosis, which probably resulted in tissue hypoxia, subsequently triggering inflammatory responses and activation of coagulation cascade mechanisms previously described in the context of DIC [59]. A key component of this pathological process appears to be hypoxia-induced oxidative stress, which damages the vascular endothelium and leads to elevated intracellular levels of reactive oxygen species (ROS) [66,67]. Notably, dysfunction of the mitochondrial electron transport chain under hypoxic conditions is considered a major source of excessive ROS production [61]. These elevated ROS levels can inflict significant damage to cellular components, including lipids, proteins, and DNA [68]. In the present study, immunofluorescence staining indicated this pathophysiological mechanism by revealing marked oxidative and DNA damage, particularly within the brain tissue. This localization suggests that the brain was a primary target of systemic dysfunction and is likely to have contributed substantially to the mortality observed in this case.

5. Conclusions

This case represents the first documented occurrence of *Achromobacter xylosoxidans*–associated septicemia leading to DIC in a dugong (*Dugong dugon*) calf. The findings underscore the increased susceptibility of juvenile dugongs, whose immunological immaturity predisposes them to opportunistic environmental pathogens. The rapid progression from the onset of clinical signs to fatal systemic infection emphasizes the necessity for prompt diagnostic investigation and immediate therapeutic intervention. Furthermore, this report highlights the critical importance of rigorous biosecurity and infection control measures within rehabilitation facilities to mitigate the risk of pathogen exposure. It also supports the implementation of vigilant monitoring, early diagnostic testing, and prophylactic strategies. These observations contribute valuable insights to the limited literature on dugong pathology and carry important implications for improving clinical management and conservation efforts for stranded marine mammals.

Author Contributions: Conceptualization, P.E. and W.S.; methodology, P.E., P.K., T.S., N.K., P.S. and W.S.; software, W.S.; validation, P.E. and W.S.; formal analysis, P.E. and W.S.; investigation, P.E., P.K. and W.S.; resources, P.K., T.S. and S.N.; data curation, P.E. and W.S.; writing—original draft preparation, P.E., P.K. and W.S.; writing—review and editing, P.E. and W.S.; visualization, W.S.; supervision, W.S.; project administration, P.E. and W.S.; funding acquisition, P.E. and W.S. All authors have read and agreed to the published version of the manuscript.

Funding: This research was supported by National Science, Research and Innovation Fund (NSRF) and Prince of Songkla University (Grant No. VET6801015S).

Institutional Review Board Statement: All procedures involving the use of surplus animal tissues were conducted in compliance with institutional guidelines and relevant regulations. The experimental protocol was reviewed and approved by the Institutional Animal Care and Use Committee (IACUC) of Prince of Songkla University (Approval No. MHESI 68014/1236). The committee determined that the protocol met the criteria for exemption under Exempt Determination Research. Date of Approval: 6 September 2024.

Informed Consent Statement: Not applicable.

Data Availability Statement: The data presented in this study are available on request from the corresponding author (W.S.).

Acknowledgments: We would like to express our sincere appreciation to the Department of Marine and Coastal Resources for providing the data used in this study. We are also deeply grateful to all veterinarians and caretakers who participated in the care and rehabilitation of the dugong. Additionally, we extend our heartfelt thanks to Prince of Songkla University and Kasetsart University for their support, particularly the contributions of their technical and veterinary staff. Artificial intelligence tools (ChatGPT-4o, OpenAI) were used solely to assist with grammatical correction and language refinement during manuscript preparation.

Conflicts of Interest: The authors declare no conflicts of interest.

Abbreviations

The following abbreviations are used in this manuscript:

4-HNE	4-hydroxynonenal
8-oxodG	8-hydroxy-2′-deoxyguanosine
DIC	Disseminated intravascular coagulation
DNA	Deoxyribonucleic acid
IM	Intramuscular
IUCN	International Union for Conservation of Nature
ROS	Reactive oxygen species
SID	Semel in die, which is Latin for “once a day” or “once daily”
°C	Degrees Celsius

References

1. IUCN Red List of Threatened Species. *Dugong Dugon*. Available online: https://www.iucnredlist.org/species/6909/160756767 (accessed on 25 June 2025).
2. Hines, E.; Adulyanukosol, K.; Poochaviranon, S.; Somany, P.; Ath, L.; Cox, N.; Symington, K.; Tun, T.; Ilangakoon, A.; Iongh, H.; et al. *Conserv . Dugongs Asia Pac.* **2012**, *58*, 58–76.
3. Panyawai, J.; Prathep, A. A systematic review of the status, knowledge, and research gaps of dugong in Southeast Asia. *Aquat. Mamm.* **2022**, *48*, 203–222. [CrossRef]
4. Petcharat, A.; Lee, Y. Measuring the nonuse value of the dugong (*Dugong dugon*) in Thailand. *J. Asia-Pac. Biodivers.* **2020**, *13*, 62–69. [CrossRef]
5. Ng, S.Z.H.; Ow, Y.X.; Jaafar, Z. Dugongs (*Dugong dugon*) along hyper-urbanized coastlines. *Front. Mar. Sci.* **2022**, *9*, 945123. [CrossRef]
6. Daochai, C.; Sornying, P.; Keawchana, N.; Manmoo, S.; Khumraksa, P.; Kaewmong, P.; Ninwat, S.; Upanoi, T.; Sukkarun, P.; Suyapoh, W. Investigation into the causes of mortality in cetaceans and sirenian populations in the Andaman Sea, Thailand: A retrospective analysis spanning 2018–2023. *Vet. World* **2024**, *17*, 2889–2898. [CrossRef]
7. Casalone, C.; Mazzariol, S.; Pautasso, A.; Di Guardo, G.; Di Nocera, F.; Lucifora, G.; Ligios, C.; Franco, A.; Fichi, G.; Cocumelli, C.; et al. Cetacean strandings in Italy: An unusual mortality event along the Tyrrhenian Sea coast in 2013. *Dis. Aquat. Organ.* **2014**, *109*, 81–86. [CrossRef] [PubMed]
8. Sánchez-Sarmiento, A.M.; Carvalho, V.L.; Díaz-Delgado, J.; Ressio, R.A.; Fernandes, N.C.C.A.; Guerra, J.M.; Sacristán, C.; Groch, K.R.; Silvestre-Perez, N.; Ferreira-Machado, E.; et al. Molecular, serological, pathological, immunohistochemical and microbiological investigation of *Brucella* spp. in marine mammals of Brazil reveals new cetacean hosts. *Transbound. Emerg. Dis.* **2019**, *66*, 1674–1692. [CrossRef]

9. Díaz-Delgado, J.; Fernández, A.; Sierra, E.; Sacchini, S.; Andrada, M.; Vela, A.I.; Quesada-Canales, Ó.; Paz, Y.; Zucca, D.; Groch, K.; et al. Pathologic findings and causes of death of stranded cetaceans in the Canary Islands (2006–2012). *PLoS ONE* **2018**, *13*, e0204444. [CrossRef]
10. Leguia, M.; Garcia-Glaessner, A.; Muñoz-Saavedra, B.; Juarez, D.; Barrera, P.; Calvo-Mac, C.; Jara, J.; Silva, W.; Ploog, K.; Amaro, L.; et al. Highly pathogenic avian influenza A (H5N1) in marine mammals and seabirds in Peru. *Nat. Commun.* **2023**, *14*, 5489. [CrossRef]
11. Moore, J.E.; Read, A.J. A Bayesian uncertainty analysis of cetacean demography and bycatch mortality using age-at-death data. *Ecol. Appl.* **2008**, *18*, 1914–1931. [CrossRef] [PubMed]
12. IJsseldijk, L.L.; Camphuysen, K.C.; Keijl, G.O.; Troost, G.; Aarts, G. Predicting harbor porpoise strandings based on near-shore sightings indicates elevated temporal mortality rates. *Front. Mar. Sci.* **2021**, *8*, 668038. [CrossRef]
13. Obusan, M.C.M.; Caras, J.A.A.; Lumang, L.S.L.; Calderon, E.J.S.; Villanueva, R.M.D.; Salibay, C.C.; Siringan, M.A.T.; Rivera, W.L.; Masangkay, J.S.; Aragones, L.V. Bacteriological and histopathological findings in cetaceans that stranded in the Philippines from 2017 to 2018. *PLoS ONE* **2021**, *16*, e0243691. [CrossRef]
14. Buck, J.D.; Wells, R.S.; Rhinehart, H.L.; Hansen, L.J. Aerobic microorganisms associated with free-ranging bottlenose dolphins in coastal Gulf of Mexico and Atlantic Ocean waters. *J. Wildl. Dis.* **2006**, *42*, 536–544. [CrossRef]
15. Morris, P.J.; Johnson, W.R.; Pisani, J.; Bossart, G.D.; Adams, J.; Reif, J.S.; Fair, P.A. Isolation of culturable microorganisms from free-ranging bottlenose dolphins (*Tursiops truncatus*) from the southeastern United States. *Vet. Microbiol.* **2011**, *148*, 440–447. [CrossRef]
16. Obusan, M.C.M.; Villanueva, R.M.D.; Siringan, M.A.T.; Rivera, W.L.; Aragones, L.V. *Leptospira* spp. and *Toxoplasma gondii* in stranded representatives of wild cetaceans in the Philippines. *BMC Vet. Res.* **2019**, *15*, 372. [CrossRef]
17. Obusan, M.C.M.; Aragones, L.V.; Salibay, C.C.; Siringan, M.A.T.; Rivera, W.L. Occurrence of human pathogenic bacteria and *Toxoplasma gondii* in cetaceans stranded in the Philippines: Providing clues on ocean health status. *Aquat. Mamm.* **2015**, *41*, 149–166. [CrossRef]
18. Sukkarun, P.; Arnuphapprasert, A.; Khumraksa, P.; Daochai, C.; Jantrakajorn, S.; Keawchana, N.; Sornying, P.; Suyapoh, W. Identification and Pathological Assessment of Mycobacterium spp. Infections in Wild Marine Mammals from the Andaman Sea, Thailand. In Proceedings of the 26th Khon Kaen Veterinary Annual International Conference (KVAC), Khon Kaen, Thailand, 16–17 July 2025.
19. Jepson, P.; Baker, J.; Kuiken, T.; Simpson, V.; Kennedy, S.; Bennett, P. Pulmonary pathology of harbour porpoises (*Phocoena phocoena)* stranded in England and Wales between 1990 and 1996. *Vet. Rec.* **2000**, *146*, 721–728. [CrossRef] [PubMed]
20. Sierra, E.; Fernández, A.; Felipe-Jiménez, I.; Zucca, D.; Díaz-Delgado, J.; Puig-Lozano, R.; Câmara, N.; Consoli, F.; Díaz-Santana, P.; Suárez-Santana, C. Histopathological differential diagnosis of meningoencephalitis in cetaceans. *Front. Vet. Sci.* **2020**, *7*, 650. [CrossRef]
21. Gerba, C.P. Environmentally transmitted pathogens. In *Environmental Microbiology*, 3rd ed.; Pepper, I.L., Gerba, C.P., Gentry, T.J., Eds.; Academic Press: San Diego, CA, USA, 2015; Volume 10, pp. 509–550.
22. Semeraro, N.; Ammollo, C.T.; Semeraro, F.; Colucci, M. Sepsis-associated disseminated intravascular coagulation and thromboembolic disease. *Mediterr. J. Hematol. Infect. Dis.* **2010**, *2*, e2010024. [CrossRef] [PubMed]
23. Roe, W.; Rogers, L.; Pinpimai, K.; Dittmer, K.; Marshall, J.; Chilvers, B. Septicaemia and meningitis in sea lion pups with hypermucoviscous *Klebsiella pneumoniae*. *Vet. Microbiol.* **2015**, *176*, 301–308. [CrossRef] [PubMed]
24. Kaye, S.; Johnson, S.; Rios, C.; Fletcher, D.J. Coagulation and fibrinolysis in northern elephant seals. *Vet. Clin. Pathol.* **2017**, *46*, 589–596. [CrossRef]
25. Marsh, H. Age determination of the dugong (*Dugong dugon*) in northern Australia and its biological implications. *Rep. Int. Whal. Comm. Spec. Iss.* **1980**, *3*, 181–201.
26. Department of Marine and Coastal Resources (DMCR). *Dugong Necropsy Manual in Thailand*; Department of Marine and Coastal Resources: Bangkok, Thailand, 2013. (In Thai)
27. Abutarbush, S.M. *Veterinary Medicine—A Textbook of the Diseases of Cattle, Horses, Sheep, Pigs and Goats*, 10th ed.; Saunders Elsevier: Philadelphia, PA, USA, 2007; pp. 1830–1903.
28. Goudalier, C.; Mouillot, D.; Bernagou, L.; Boksmati, T.; Bristol, C.; Clark, H.; Herandarudewi, S.M.C.; Hocdé, R.; Koester, A.; McIvor, A.J.; et al. Drone photogrammetry reveals contrasting body conditions of dugongs across the Indo-Pacific. *Remote Sens. Ecol. Conserv.* 2025; *in press*. [CrossRef]
29. Pugliares, K.R.; Bogomolni, A.; Touhey, K.M.; Herzig, S.M.; Harry, C.T. *Marine Mammal Necropsy: An Introductory Guide*; NOAA Fisheries: Woods Hole, MA, USA, 2007.
30. Eros, C.; Marsh, H.; Bonde, R.; O'Shea, T.; Beck, C.; Recchia, C.; Dobbs, K.; Turner, M.; Lemm, S.; Pears, R. *Procedures for the Salvage and Necropsy of the Dugong*; GBRMPA Research Publication No. 85; Great Barrier Reef Marine Park Authority: Townsville, QLD, Australia, 2007.

31. Suyapoh, W.; Nilake, C.; Sriamad, A.; Assawakulkamneard, T.; Prasertsee, T.; Jantrakajorn, S. First report of *Streptococcus iniae* infection in cultured spotted scat (*Scatophagus argus*) in Thailand. *J. Fish Dis.* **2025**, e70031. [CrossRef]
32. Nakasone, I.; Kinjo, T.; Yamane, N.; Kisanuki, K.; Shiohira, C.M. Laboratory-based evaluation of the colorimetric VITEK-2 Compact system for species identification and of the advanced expert system for detection of antimicrobial resistances: VITEK-2 Compact system identification and antimicrobial susceptibility testing. *Diagn. Microbiol. Infect. Dis.* **2007**, *58*, 191–198. [CrossRef] [PubMed]
33. Bauer, A.; Kirby, W.; Sherris, J.C.; Turck, M. Antibiotic susceptibility testing by a standardized single disk method. *Am. J. Clin. Pathol.* **1966**, *45*, 493–496. [CrossRef] [PubMed]
34. Suyapoh, W.; Keawchana, N.; Sornying, P.; Tangkawattana, S.; Khirilak, P.; Jantrakajorn, S. Mixed Eimeria and Cryptosporidium infection and its effects on pathology and clinical outcomes in juvenile Asian seabass (*Lates calcarifer*) cultured in Thailand. *J. Fish Dis.* **2024**, *47*, e13914. [CrossRef]
35. Suyapoh, W.; Thaweechart, B.; Wae-asae, P.; Keawchana, N.; Sornying, P.; Manmoo, S.; Rakwong, P.; Jantrakajorn, S. Detection and pathological effects of intestinal parasites in spotted scat *Scatophagus argus*: *Filisoma* spp. and *Cryptosporidium* spp. as infective agents and their roles in fish inflammatory response. *J. Aquat. Anim. Health* **2025**, vsaf009. [CrossRef]
36. Jantrakajorn, S.; Keawchana, N.; Sornying, P.; Khirilak, P.; Suyapoh, W. Intestinal inflammation, oxidative damage, and pathogenesis of intestinal Cryptosporidium in juvenile Asian sea bass (*Lates calcarifer*). *J. World Aquacult. Soc.* **2024**, *56*, e13114. [CrossRef]
37. Ooi, V.; McMichael, L.; Hunter, M.E.; Takoukam Kamla, A.; Lanyon, J.M. A new DNA extraction method (HV-CTAB-PCI) for amplification of nuclear markers from open ocean-retrieved faeces of an herbivorous marine mammal, the dugong. *PLoS ONE* **2023**, *18*, e0278792. [CrossRef]
38. Lanyon, J.M.; Wong, A.; Long, T.; Woolford, L. Serum biochemistry reference intervals of live wild dugongs (*Dugong dugon*) from urban coastal Australia. *Vet. Clin. Pathol.* **2015**, *44*, 234–242. [CrossRef]
39. Steinberg, J.P.; Burd, E.M. Other gram-negative and gram-variable bacilli. In *Mandell, Douglas, and Bennett's Principles and Practice of Infectious Diseases*, 8th ed.; Bennett, J.E., Dolin, R., Blaser, M.J., Eds.; W.B. Saunders: Philadelphia, PA, USA, 2015; pp. 2667–2683.e2664.
40. Turel, O.; Kavuncuoglu, S.; Hosaf, E.; Ozbek, S.; Aldemir, E.; Uygur, T.; Hatipoğlu, N.; Siraneci, R. Bacteremia due to *Achromobacter xylosoxidans* in neonates: Clinical features and outcome. *Braz. J. Infect. Dis.* **2013**, *17*, 450–454. [CrossRef]
41. Pérez Barragán, E.; Sandino Pérez, J.; Corbella, L.; Orellana, M.A.; Fernández-Ruiz, M. *Achromobacter xylosoxidans* bacteremia: Clinical and microbiological features in a 10-year case series. *Rev. Esp. Quimioter.* **2018**, *31*, 268–273.
42. Rajni, E.; Kataria, S.; Sarna, M.K.; Garg, V.K. A case of bacteremia by *Achromobacter xylosoxidans* in an immunocompromised host and review of literature. *Arch. Med. Health Sci.* **2023**, *11*, 141–144. [CrossRef]
43. Steiner, V.; Rosel, A.C.; Ruppitsch, W.; Allerberger, F.; Carranza Valencia, A.; Markovic, M.; Luckschander-Zeller, N.; Szostak, M.P.; Spergser, J.; Loncaric, I.; et al. The first bacterial endocarditis due to *Achromobacter xylosoxidans* in a dog. *Pathogens* **2021**, *10*, 1580. [CrossRef]
44. Girling, S.L.; Innes, J.F. Infection of a total hip prosthesis in a dog caused by *Achromobacter (Alcaligenes) xylosoxidans*. *J. Small Anim. Pract.* **2006**, *47*, 747–750. [CrossRef]
45. Vorbach, B.S.; Rotstein, D.S.; Stacy, N.I.; Mavian, C.; Salemi, M.; Waltzek, T.B.; de Wit, M. Fatal systemic salmonellosis in a Florida manatee (*Trichechus manatus latirostris*). *J. Wildl. Dis.* **2017**, *53*, 930–933. [CrossRef]
46. Landsberg, J.H.; Tabuchi, M.; Rotstein, D.S.; Subramaniam, K.; Rodrigues, T.C.S.; Waltzek, T.B.; Stacy, N.I.; Wilson, P.W.; Kiryu, Y.; Uzal, F.A.; et al. Novel lethal clostridial infection in Florida manatees (*Trichechus manatus latirostris*): Cause of the 2013 unusual mortality event in the Indian River Lagoon. *Front. Mar. Sci.* **2022**, *9*, 841857. [CrossRef]
47. Sato, T.; Shibuya, H.; Ohba, S.; Nojiri, T.; Shirai, W. Mycobacteriosis in two captive Florida manatees (*Trichechus manatus latirostris*). *J. Zoo Wildl. Med.* **2003**, *34*, 184–188. [CrossRef]
48. Trancassini, M.; Iebba, V.; Citerà, N.; Tuccio, V.; Magni, A.; Varesi, P.; Biase, R.; Totino, V.; Santangelo, F.; Gagliardi, A.; et al. Outbreak of *Achromobacter xylosoxidans* in an Italian cystic fibrosis center: Genome variability, biofilm production, antibiotic resistance, and motility in isolated strains. *Front. Microbiol.* **2014**, *5*, 138. [CrossRef]
49. Isler, B.; Kidd, T.J.; Stewart, A.G.; Harris, P.; Paterson, D.L. Achromobacter infections and treatment options. *Agents Chemother.* **2020**, *64*, e01025-20. [CrossRef] [PubMed]
50. Chalhoub, H.; Kampmeier, S.; Kahl, B.C.; Van Bambeke, F. Role of efflux in antibiotic resistance of *Achromobacter xylosoxidans* and *Achromobacter insuavis* isolates from patients with cystic fibrosis. *Front. Microbiol.* **2022**, *13*, 895389. [CrossRef]
51. Nielsen, S.M.; Penstoft, L.N.; Nørskov-Lauritsen, N. Motility, biofilm formation and antimicrobial efflux of sessile and planktonic cells of *Achromobacter xylosoxidans*. *Pathogens* **2019**, *8*, 14. [CrossRef]
52. Fayyaz, H.; Zaman, A.; Rafiq, W.; Murtaza, M.H.; Ullah, I. Immunosuppression in infectious diseases: Causes and effects. In *Innate Immunity—New Perspectives and Therapeutic Opportunities*; Lasfar, A., Ed.; IntechOpen: London, UK, 2024; pp. 1–15. [CrossRef]

53. Koch, M.S.; da Silva, V.P.; Bracarense, A.P.F.R.L.; Domit, C. Environmental aspects and diseases related to immunosuppression in cetaceans: A concise review. *Semina: Ciênc. Agrár.* **2018**, *39*, 2897–2917. [CrossRef]
54. Marsili, L.; Di Guardo, G.; Mazzariol, S.; Casini, S. Insights into cetacean immunology: Do ecological and biological factors make the difference? *Front. Immunol.* **2019**, *10*, 1219. [CrossRef]
55. Chen, F.; Jiang, F.; Ma, J.; Alghamdi, M.A.; Zhu, Y.; Yong, J.W.H. Intersecting planetary health: Exploring the impacts of environmental stressors on wildlife and human health. *Ecotoxicol. Environ. Saf.* **2024**, *283*, 116848. [CrossRef]
56. Amoureux, L.; Bador, J.; Fardeheb, S.; Mabille, C.; Couchot, C.; Massip, C.; Salignon, A.L.; Berlie, G.; Varin, V.; Neuwirth, C. Detection of *Achromobacter xylosoxidans* in hospital, domestic, and outdoor environmental samples and comparison with human clinical isolates. *Appl. Environ. Microbiol.* **2013**, *79*, 7142–7149. [CrossRef] [PubMed]
57. Yoon, S.H.; Kim, H.; Lim, S.M.; Kang, J.M. Nosocomial outbreak of *Achromobacter* spp. bacteremia due to germicide contamination: A systematic review. *Eur. Rev. Med. Pharmacol. Sci.* **2022**, *26*, 6374–6381. [CrossRef]
58. Jakobsen, T.H.; Hansen, M.A.; Jensen, P.O.; Hansen, L.; Riber, L.; Cockburn, A.; Kolpen, M.; Hansen, C.R.; Ridderberg, W.; Eickhardt, S.; et al. Complete genome sequence of the cystic fibrosis pathogen *Achromobacter xylosoxidans* NH44784-1996 complies with important pathogenic phenotypes. *PLoS ONE* **2013**, *8*, e68484. [CrossRef] [PubMed]
59. Gando, S.; Levi, M.; Toh, C.H. Disseminated intravascular coagulation. *J. Intensive Care* **2025**, *13*, 32–56. [CrossRef] [PubMed]
60. Papageorgiou, C.; Jourdi, G.; Adjambri, E.; Walborn, A.; Patel, P.; Fareed, J.; Elalamy, I.; Hoppensteadt, D.; Gerotziafas, G.T. Disseminated intravascular coagulation: An update on pathogenesis, diagnosis, and therapeutic strategies. *Clin. Appl. Thromb. Hemost.* **2018**, *24* (Suppl. S9), S8–S28. [CrossRef]
61. Deepthi, K.G.; Prabagaran, S.R. Ocular bacterial infections: Pathogenesis and diagnosis. *Microb. Pathog.* **2020**, *145*, 104206. [CrossRef]
62. Mak, C.Y.; Ho, M.; Iu, L.P.-l.; Sin, H.P.-y.; Chen, L.J.; Lui, G.; Brelen, M.E.; Young, A.L. Clinical features and treatment outcomes of endogenous *Klebsiella endophthalmitis*: A 12-year review. *Int. J. Ophthalmol.* **2020**, *13*, 1933–1940. [CrossRef]
63. Wiedermann, C.J. Hypoalbuminemia as surrogate and culprit of infections. *Int. J. Mol. Sci.* **2021**, *22*, 4496. [CrossRef]
64. Osorio, J.S. Gut health, stress, and immunity in neonatal dairy calves: The host side of host-pathogen interactions. *J. Anim. Sci. Biotechnol.* **2020**, *11*, 105. [CrossRef] [PubMed]
65. Sedney, C.J.; Harvill, E.T. The neonatal immune system and respiratory pathogens. *Microorganisms* **2023**, *11*, 1597. [CrossRef] [PubMed]
66. Yang, J.; Xu, J.; Xu, S.; Fan, Z.; Zhu, C.; Wan, J.; Yang, J.; Xing, X. Oxidative stress in acute pulmonary embolism: Emerging roles and therapeutic implications. *Thromb. J.* **2024**, *22*, 9. [CrossRef] [PubMed]
67. Wang, Q.; Zennadi, R. Oxidative stress and thrombosis during aging: The roles of oxidative stress in RBCs in venous thrombosis. *Int. J. Mol. Sci.* **2020**, *21*, 4259. [CrossRef]
68. Schieber, M.; Chandel, N.S. ROS function in redox signaling and oxidative stress. *Curr. Biol.* **2014**, *24*, R453–R462. [CrossRef]

Disclaimer/Publisher's Note: The statements, opinions and data contained in all publications are solely those of the individual author(s) and contributor(s) and not of MDPI and/or the editor(s). MDPI and/or the editor(s) disclaim responsibility for any injury to people or property resulting from any ideas, methods, instructions or products referred to in the content.

animals

MDPI

Article

Wild Fauna in Oman: Foot-and-Mouth Disease Outbreak in Arabyan Oryx (*Oryx leucorix*)

Massimo Giangaspero [1,2,*], Salah Al Mahdhouri [3], Sultan Al Bulushi [3] and Metaab K. Al-Ghafri [3]

[1] Faculty of Veterinary Medicine, University of Teramo, 64100 Teramo, Italy
[2] Parliamentary Assembly of the Mediterranean, Center for Global Studies, 47890 City of San Marino, San Marino
[3] Environment Authority, Muscat 100, Oman
* Correspondence: massimo.giangaspero@pam.int

Simple Summary: The Arabian oryx (*Oryx leucoryx*), a national symbol of Oman, was reintroduced in 1980 through a sanctuary in Al Wusta Governorate after its extinction in the wild in 1972. Managed by the Environment Authority, the population grew steadily, reaching 738 individuals by 2021, with no major health issues reported, and enabling limited rewilding efforts. Following a foot-and-mouth disease (FMD) outbreak in cattle, a vaccination program targeting serotypes A, O, and SAT 1 was applied, mainly to male oryx, from December 2023 to January 2024. In January 2025, a severe FMD outbreak struck the sanctuary. The disease spread rapidly (100% morbidity within two days), causing depression, inappetence, oral lesions, diarrhea, and high fatality rates. Treatment attempts were largely ineffective. Laboratory tests confirmed FMD, excluding other diseases. Of 669 oryx, 226 (33.8%) died, including 38.5% that had been vaccinated. This outbreak posed a major threat to decades of conservation progress. Enhanced biosecurity, vaccination strategies, and ongoing ecological research are essential to safeguard Oman's unique biodiversity.

Abstract

The Sultanate of Oman boasts remarkable biodiversity, exemplified by such species as the Arabian leopard (*Panthera pardus nimr*) and the Arabian oryx (*Oryx leucoryx*), national symbols that highlight the extensive conservation efforts required to protect the country's natural heritage. During decades, Omani authorities have taken significant measures to safeguard wildlife and preserve the natural environment. A sanctuary dedicated to the reintroduction of the Arabian Oryx, after extinction in nature in 1972, was established in 1980 in the Al Wusta Governorate under the patronage of the Royal Diwan and currently administrated by the recently established Environment Authority. During the almost 40 years since the reintroduction and the creation of the sanctuary, the oryx population has grown slowly but constantly. In 2021, the sanctuary hosted 738 oryx, allowing the start of the reintroduction of the species into the natural environment. Small groups of animals were released into the wild in selected areas. No animal health adverse events were recorded, and mortality was generally due to injuries received as a consequence of fighting, in particular during mating season. Standard veterinary care, including control of internal and external parasites, was regularly provided. In some occasions, immunization against certain diseases, such as clostridial infections, pasteurellosis, or mycoplasmosis, was also applied. In 2023, an FMD outbreak in cattle reported in Dhofar, about 500 km from the Al Wusta sanctuary, motivated specific prophylactic actions to prevent the risk of diffusion to oryx. From December 2023 to January 2024, an immunization program was undertaken using an FMD vaccine against serotypes A, O, and SAT 1, mostly in male oryx, while pregnant oryx were avoided for abortion risk due to handling. The following

year, in January 2025, a severe outbreak occurred in oryx herds held in the sanctuary. The rapid onset and the spread of clinical symptoms among animals (100% morbidity in the second day after the first appearance of signs in some individuals) were suggestive of a highly contagious disease. The animals suffered from severe depression and inappetence, rapidly followed by abundant salivation, erosions of the oral mucosa and tongue, and diarrhea, with a short course characterized by prostration and death of the animal in the most severe cases. Therapeutical attempts (administration of antibiotics and rehydration) were mostly ineffective. Laboratory investigations (ELISA and PCR) ruled out contagious bovine pleuropneumonia (CBPP), Johne's disease and Peste des petits ruminants (PPR). Both serology and antigen detection showed positiveness to foot-and-mouth disease (FMD). Out of a total population of 669 present in the sanctuary at the beginning of the outbreak, 226 (33.78%) oryx died. Despite the vaccinal status, the 38.49% of dead animals resulted being vaccinated against FMD. Taking into account the incalculable value of the species, the outbreak represented a very dangerous event that risked wiping out the decades of conservation efforts. Therefore, all the available means, such as accrued biosecurity and adequate prophylaxis, should be implemented to prevent the recurrence of such health risks. The delicate equilibrium of wild fauna in Oman requires study and support for an effective protection, in line with the national plan "Vision 2040", targeting the inclusion of the Sultanate within the 20 best virtuous countries for wildlife protection.

Keywords: Arabian Oryx; biosecurity; foot-and-mouth disease; reintroduction; vaccination

1. Introduction

The Sultanate of Oman, with its vast arid deserts and rugged mountain ranges, is home to an unexpectedly rich variety of remarkable wildlife. Among its most striking and iconic species is the majestic Arabian oryx or white oryx (*Oryx leucoryx*, Pallas, 1777). Four other species of oryx exist: the scimitar-horned oryx (*Oryx dammah*, Cretzschmar, 1827), the East African oryx (*Oryx beisa*, Rüppell, 1835), the fringed-eared oryx (*Oryx beisa callotis*, Thomas, 1892), and the Gemsbok (*Oryx gazella*, Linnaeus, 1758). The Arabian species is the smallest species of oryx (size 1.53–2.35 mt; weight 65–70 kg), able to live in most hostile conditions, perfectly adapted to a dry and arid environment, with white hair, very low perspiration and moisture loss, and a peculiar physiology allowing partial cooling of the brain and rise of body temperature up to 45 degrees without suffering [1].

The Arabian oryx (*Oryx leucoryx*) was extinct in the wild 50 years ago, mainly due to uncontrolled poaching [2]. Fortunately, the reintroduction was possible, at least in captivity, in some Arabian countries. Currently, only a few individuals are in the wild, and about 6,000 live in sanctuaries [3]. In Oman, for the purpose of reintroducing the Arabian oryx (*Oryx leucoryx*), in 1980, the Oryx Sanctuary was created, the first wildlife reserve and still the most relevant protected area in the country [2]. The sanctuary is located within the central desert and coastal hills in the Al Wusta Governorate, an area characterized by seasonal atmospheric conditions that support a unique desert ecosystem [4]. Since the global extinction in 1972, ten years after the death of the last oryx in Oman, the first animals born in American zoos could be reintroduced here in 1982 [2]. In 1994, the sanctuary was inscribed in the list of the United Nations Educational Scientific and Cultural Organization (UNESCO) World Heritage Centers (Dossier number 654), based on the criterium of a property of 2,750,000 ha, containing the most important and significant natural habitats for in situ conservation of biological diversity, including those containing threatened species of outstanding universal value from the point of view of science or conservation [5].

However, due to hydrocarbon exploitation, the protected area was drastically reduced by 90%, inducing UNESCO to delist the sanctuary in 2007 [6].

Since the first reintroduction of the animals, in a few decades, their number increased at the Al Wusta Sanctuary, reaching even good populations with over 900 individuals. This increase and the apparent absence of health problems allowed the start of the reintroduction of the species in the natural environment and small groups of animals have been released into the wild in selected areas. In addition, other species were introduced in the reserve, such as the Arabian sand gazelle (*Gazella marica*, Thomas, 1897), also known as reem gazelle. The sand gazelle was particularly prolific, and in 2021, the sanctuary hosted over 1150 Arabian sand gazelles, along with 738 Arabian oryx.

During the almost forty years of activity, no animal health adverse events were recorded, and mortality was generally due to injuries suffered as a consequence of fighting, particularly during mating season [2,7]. Standard veterinary care, including control of internal and external parasites, was regularly provided. On some occasions, immunization against certain diseases, such as clostridial infections, pasteurellosis, or mycoplasmosis, was also applied. Animals were fed with 55–70 kg of hay, 10 kg of lucerne, and 50 kg of concentrate daily. Fresh drinking water and salt blocks were available for the animals.

1.1. FMD in Oman

The infection was reported as present in the domestic animals in the country almost continuously. In the World Organization for Animal Health (WOAH) databases, the disease was declared to occur before 2005 and in the WHAIS since 2005, with two exceptions: absent during the second semester 2019 and the first semester 2024 and again present in the second semester 2024. However, concerning wild animals, FMD was reported absent until 2008, and later until 2024, no information was provided to WOAH [8].

1.2. The FMD Outbreak in Cattle in Dhofar

Infection with foot-and-mouth disease virus was formally reported to the World Organisation for Animal Health on the 1st of January 2023, under event ID number 5178. By immediate notification, as FMD is a listed disease, the Ministry of Agriculture of the Sultanate of Oman declared an official occurrence of FMD among domestic cattle from herds located near Salalah, in the southwestern administrative region of Dhofar. The reported cases were 5,100 and the deaths accounted for 23 bovines. By the vaccination of 5,100 heads, the outbreak was resolved and closed on the 28th of January 2023. The reason for notification was indicated as a new strain in the country and the virus was characterized as subtype SAT 2 by the analysis performed at the reference laboratory of Pirbright, UK, confirming the FMD event on the 28th of March 2023. This was the last notification from Oman to the WOAH (OIE) recorded in the WHAIS.

Currently, a prophylaxis program against FMD is undertaken at the country level for domestic animals, covering the 60% of cattle and sheep and goat populations, excluding dromedary camels. A vaccine against FMDV serotypes O, A, SAT 2, and Asia 1 was selected for the immunization of animals. Not all serotypes were considered for economic reasons, and serotype C is very rare and never reported in the country. FMDV serotype C has not been isolated by the network of WOAH/FAO reference laboratories for FMD since 2004, and no serotype C events have been reported to WOAH since then [8].

1.3. Extended Vaccination in Wildlife (Before Outbreak)

Considering that the FMD outbreak occurred in cattle from Dhofar, about 500 km from the Al Wusta sanctuary, to prevent the risk of virus diffusion, specific prophylactic actions were extended to the Arabian oryx. The FMD vaccination plan in Arabian oryx in Al Wusta was similar to the national program, but restricted to serotypes A, O, and SAT 1.

From December 2023 to January 2024, mainly male oryx were immunized, while, being in the middle of reproduction season, most of the females were excluded due to advanced pregnancy and effective risk of abortion if handled. However, the number of animals was consistent and in total, 465 oryx were vaccinated, including 102 females.

1.4. The FMD Outbreak in Oryx Population in Al Wusta

During about four weeks, from the 8 January to the 4 February 2025, a severe outbreak occurred in the Arabian oryx herds held in the sanctuary of Al Wusta. The rapid onset and the spread of clinical symptoms among animals (100% morbidity in the second day after the first appearance of signs in some individuals) were suggestive of a highly contagious disease. The animals suffered from severe depression and inappetence, rapidly followed by abundant salivation, erosions of the oral mucosa and tongue, and diarrhea, with a short course characterized by prostration and death of the animal in the most severe cases.

First, therapeutic attempts were applied. Treatments consisted of the administration of water soluble powder of oxytetracycline (Spectra cycline, Al Mutawwaj Veterinary Pharmaceutical Industries, Amman, Jordan) 1 g per 10 kg body weight (bw) for 3–6 days; oral administration of florfenicol (Introflor-100 oral, Holland, Viimsi, Estonia) 10 mg/kg bw in drinking water for 5 days; oral administration of gentamycin and tylosin association (Genta-Tylan, Travetco, Can Tho, Vietnam) 1 g/5 kg bw, continuous use for 3–5 days; injectable solutions of tylosine (Hangen-Tylo, Hanvet, Hanoi, Vietnam) via intra muscular (IM) injection 10 mL/50 kg bw, twice a day; selenium and vitamin E (Selephos, Topkim, Istambul, Turkey) 4 ml IM, 3–4 injections within 1 week; and non-steroidal anti-inflammatory drug containing ketoprofen, (Ketovet, Mobedco-Vet, Amman, Jordan) 3 mg/kg IM bw, once daily for up to 3–5 days and intravenous rehydration with saline solutions. In oryx, therapies did not provide evident beneficial effects, and in certain cases, it was not possible to administrate any medicinal product since the clinical course was too rapid and with fatal outcome.

Laboratory investigations have been conducted to ascertain the cause of the disease affecting the entire oryx population. Among different considered pathogens, laboratory tests confirmed only the presence of foot-and-mouth disease (FMD).

The other wild animal species present in the sanctuary were almost not affected by the ongoing outbreak in oryx. Out of the over 1150 sand gazelles (*Gazella marica*, Thomas, 1897) held in the Al Wusta natural reserve, only 20 cases with 4 deaths were reported. In this species, clinical cases were treated with doxycycline and tylosine administered per os by drinking water for 3 days, resulting in recovery. However, among female reems at full-term pregnancy, an increased fetal mortality was observed, with subsequent difficult delivery and mother death. Among Arabian gazelles (*Gazella arabica*, Lichtenstein, 1827) and Arabian mountain gazelles (*Gazella gazella cora*), only 1 fatal case was recorded in each species. Mortality was also reported in one blackbuck (*Antilope cervicapra*), also known as Indian antelope. In the ten llama (*Lama glama*, Linnaeus, 1758), living with the oryx, no clinical sings of disease were observed, despite new world camelids having been shown to be receptive to FMD infection [9].

The present study aimed to provide details of the FMD outbreak that occurred in Arabian oryx, the most deadly event never reported before in the species since its reintroduction from extinction in the wild. Taking into account the value of the wild fauna in the Sultanate, the overview of management difficulties related to breeding captive wild species is indicative of necessary conservation efforts and future prospects to address threats and challenges and protect animal health from epidemiological risks, with particular attention to the Arabian oryx and other vulnerable and endangered species.

2. Material and Methods

2.1. Animals

The Arabian oryx population was distributed in four different herds at the Al Wusta Sanctuary, Sultanate of Oman, accounting for a total of 669 individuals, 657 adults (312 males and 345 females), and 12 calves, recorded present on the 1 January 2025 (Table 1). As recorded in the animal register of the sanctuary and based on the monthly census performed by the staff, the animals were subdivided in 4 herds, held in four different enclosures, indicated as maha 1, 2, and 3 (Arabic female given name meaning half moon or beautiful eyes), and the fourth as HP. The herd in maha 1 was constituted only by adult males (n 163), while the other herds were mixed with both adult males and females (maha 2: M 53, F 171, and 8 calves; maha 3: M 46, F 144, and 4 calves; and HP: M 50 F 30).

Table 1. Arabian oryx population distributed in four different herds at the Al Wusta Sanctuary, Sultanate of Oman. A total of 669 oryx were reported from the four breeding areas on the 1 January 2025.

Herd/Enclosure	Number of Animals	Adults		Calves		Gender		
		Males	Females	Males	Females	Males	Females	%
Maha 1	163	163	0	0	0	163	0	24.36
Maha 2	232	53	171	3	5	56	176	34.68
Maha 3	194	46	144	0	4	46	148	29.00
HP	80	50	30	0	0	50	30	11.96
Total	669	312	345	3	9	315	354	100

Vaccinal campaign against FMD applied on Arabian oryx population, from the 26 December 2023 to the 22 January 2024, following the reported outbreak in cattle that occurred in Dhofar in January 2023 (Table 2). Each animal, a total of 465 individuals (M 363, F 102), was immunized with 2 mL subcutaneously (SC) with a polyvalent inactivated vaccine against FMD serotypes O, A, and SAT 2, commercialized for cattle, sheep, and goats (Vet. Ser. and Vacc. Res. Inst., Cairo, Egypt). One hundred vaccinated males were released into the wild from January 2024 to January 2025. The FMD vaccine was systematically administered simultaneously with a vaccine against enterotoxemia or hemorrhagic septicemia (Multiclostri 12P, Vac Sules, Canelones, Uruguay). Other animals were not protected for FMD, or immunized against other diseases (n 52) (clostridial infections, pasteurellosis, or mycoplasmosis), nor not immunized, especially pregnant females, to avoid risk of abortion due to handling.

Table 2. Vaccinal campaign against FMD applied on the Arabian oryx population at the Al Wusta Sanctuary, Sultanate of Oman, from the 26 December 2023 to the 22 January 2024, following the reported outbreak in cattle that occurred in Dhofar in January 2023. Each animal was immunized with 2 mL subcutaneously (SC) with a polyvalent inactivated vaccine against FMD serotypes O, A, and SAT 2, and commercialized for cattle, sheep, and goats (Vet. Ser. and Vacc. Res. Inst., Cairo, Egypt). * Animals not protected for FMD.

Vaccination	Number of Animals	Gender		
		Males	Females	%
Vaccine for FMD combined with enterotoxaemia	336	274	62	65
Vaccine for FMD combined with enterotoxaemia and hemorrhagic septicemia	129	89	40	25
Vaccine for other diseases only *	52	52	0	10
Total vaccinated	517	415	102	100

2.2. Monitoring of the Animals

Clinical examinations of animals showing abnormal behavior or apparent signs of illness were constantly performed by the staff to describe symptoms and eventual lesions. Morbidity and mortality rates were recorded daily. Some dead animals were necropsied to report gross lesions affecting internal organs. Due to the amplitude of the outbreak, implying relatively high numbers of deaths, and the lack of facilities available for use as a necropsy room and refrigerated chambers for carcasses, autopsies were conducted directly on the field and limited to approximative observations.

2.3. Samples

Sixteen samples were collected from clinically affected animals, 15 Arabian oryx and 1 sand gazelle (reem). Arabian oryx: twelve females, ear tag numbers 0094, 0098, 0447, 0464, 0500, 0994, 3, 245, 400, 405, 413, and 472; three males, ear tag numbers 83, 140, and one untagged; and sand gazelle: one untagged male.

Blood samples, collected from jugular vein in EDTA or silicone 10 mL tubes, and fresh feces, directly collected from the anus, were placed in an ice box and transported to the Central Laboratory for Animal Health, Directorate General of Animal Wealth, Ministry of Agricultural Wealth, Fisheries and Water Resources, Muscat, Sultanate of Oman. The tests were performed at the Biochemistry, Immunology, and Biotechnology sections of the Central Laboratory for Animal Health.

The first samples were collected on the 13th of January 2025, for complete blood count (CBC), kidney function test (KFT), liver function test (LFT), minerals, and parasitological screening. On the 15th of January, additional samples were collected for serological and antigen investigations.

2.4. Laboratory Tests

Hematology and hematochemistry

Complete blood count (CBC) analysis of blood samples from four oryx females (ear tags 0994, 400, 405, and 472) and one male (untagged) was achieved using an automated hematology analyzer (Sysmex XR-1000, Sysmex Corporation, Kobe, Japan). Red blood cells (RBC), white blood cells (WBC), and platelets (PLT) were counted with related parameters: mean corpuscular volume (MCV), nucleated RBC (NRBC), red cell distribution width standard deviation (RDW-SD), red cell distribution width coefficient of variations (RDW-CV), mean platelet volume (MPV), and platelet large cell ratio (P-LCR). Hemoglobin (Hb), mean corpuscular hemoglobin (MCH), corpuscular hemoglobin concentration (MCHC), as well as hematocrit (HCT) and procalcitonin (PCT) values were also obtained.

Blood samples for the analysis of biochemical parameters for a kidney function test (KFT), liver function test (LFT), and minerals were centrifuged at $2500\times g$ for 15 min. Serum and plasma were transferred into polypropylene micro-centrifuge tubes, which were stored at $-80\ ^{\circ}C$ until analysis. Serum ions, calcium, phosphorus, magnesium, copper, and iron, and a range of biochemical parameters, including serum albumin, alkaline phosphatase, bilirubin, creatinine, creatine kinase with N-acetyl cysteine (CK NAK), glucose, and urea, were analyzed with an automatic biochemistry analyzer (Chem 200, Gesan Production, Campobello di Mazara, Trapani, Italy) using absorbance photometry (enzymes and substrates). Values and means for various hematological and serum biochemical parameters were compared to values reported from apparently healthy animals referred to as normal reference limits [10–12].

Parasitology

Fecal samples were freshly collected directly from the rectal ampulla of five individual oryx (four females identified with ear tags 0094, 400, 405 and 472 and one untagged male),

to avoid contamination by eggs from the environment, using a plastic device for lambs. Three grams of feces from each animal were dissolved in water-saturated NaCl solution at room temperature (20 °C) to recover the eggs of gastrointestinal helminth parasites. Eggs were identified under light microscope.

Serology and Antigenic detection

Serum samples collected from 12 Arabian oryx (7 females, ear tags 0098, 0447, 0500, 0994, 3, 400, 405, 413, and 472, and 3 males, 2 identified with ear tags 83 and 140 and 1 untagged) were tested using commercial kits for antibodies against contagious bovine pleuropneumonia (CBPP) using the latex agglutination test (LAT), and for antibodies against FMDV non-structural proteins (NSP), Johne's disease (para-tuberculosis) and Peste des petits ruminants virus (PPRV), using enzyme linked immunosorbent assay (ELISA). Taking into account the applied vaccination against FMD in the oryx herd, discriminate infected from vaccinated animals (DIVA) diagnostic testing was used to detect the FMD infection/virus circulation in the vaccinated population. To assess exposure to FMDV during the outbreak in the captive Arabian oryx (*Oryx leucoryx*) population, serum samples were analyzed using the ID Screen® FMD NSP Competition ELISA kit (Innovative Diagnostics, Grabels, France), which is able to detect non capsid protein (3ABC NSP) antibodies in serum and plasma from all FMD-susceptible species. The ELISA was executed with coated 96-well flat-bottom microplates. Optical density (OD) reading was performed using a spectrophotometer at 450 nm (Microplate Reader 680, Bio-Rad, Hercules, CA, USA).

Real-time reverse transcription polymerase chain reaction (RT-qPCR) assay for FMDV and PPRV analysis was conducted on oral swabs collected from 9 Arabian oryx (7 females, ear tags 0098, 0447, 0464, 0500, 3, 245, and 413 and 2 males ear tags 83 and 140) and 1 sand gazelle (untagged male), using commercial test kits (FMDV dtec-RT-qPCR and PPRV dtec-RT-qPCR, Genetic analysis strategies SL, Orihuela, Spain). FMDV-specific RNA was detected targeting the conserved 3D RNA-dependent RNA polymerase gene of the virus. The tests were conducted following manufacturer instructions using a PCR thermal cycler (Mastercycler nexus X2, Eppendorf, Enfield, CT, USA).

3. Results

The monitoring of the Arabian oryx herds showed that clinical symptoms appeared first among the animals present in the maha 1 enclosure out of four, then rapidly diffused in the other three herds located in the other enclosures. The first sign of illness was inappetence. On the first day of the outbreak (the 8th of January 2025), the 25% of oryx showed inappetence. Then, on the third day, all other animals showed the same behavior, indicating a morbidity rate of 100%. Rapidly, other symptoms could be observed. Animals showed asthenia, reluctancy to move, preferring lying on the ground, and often acquiring abnormal postures, with head and neck turned backwards along the flank or extended limbs. Clinical symptoms were characterized by drooling (abundant salivation), limping (abnormal asymmetric gate), watery diarrhea (in some cases with mucus or blood-tinged), tympanism (inducing animals to kick their flanks), vomiting, in some cases bleeding from nostrils (Figure 1), and prostration and death in more severe cases (Figure 2). The severity of the clinical course was high among pregnant and calves, causing mortality among adults, especially at term of pregnancy (Figure 3), stillbirth (Figure 4), or early death of newborns, which was relatively high in other adult females and less severe in adult males.



Figure 1. Arabian oryx (*Oryx leucoryx*) at Al Wusta natural reserve showing epistaxis.



Figure 2. Dead Arabian oryx in poor body conditions. Ocular lesions are due to scavenger birds.



Figure 3. Arabian oryx female dead during delivery.



Figure 4. Stillbirth in Arabian oryx.

Lesions consisted in aphthae appearing in the oral cavity and evolving in erosive lesions. The erosions were observed on the gum of the upper lip, gingival mucosa (Figure 5), including peri dental gingiva, tongue (upper epithelium and lower mucosa) (Figure 6), and palate being eventually covered by necrotic caseous material (Figure 7). No animals showed lesions at the level of coronary band. The gastrointestinal tract was distended by accumulation of gas and presented serosal hemorrhages (Figure 8) and in some cases deposits of fibrinous exudate.



Figure 5. Erosions of gingiva with deposits of necrotic caseous material in Arabian oryx.



Figure 6. Severe erosions of the tongue and posterior necrotic caseous deposits in Arabian oryx.



Figure 7. Erosions of the palate in Arabian oryx.

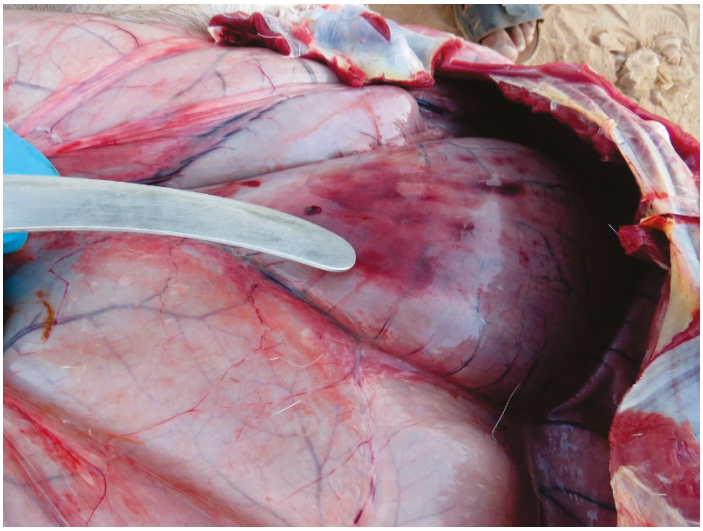


Figure 8. Gastrointestinal tract of Arabian oryx, distended by accumulation of gas and presenting hemorrhages on the serosa.

The mortality rate observed among animals held at the Al Wusta sanctuary, during the outbreak from the 8 January to the 4 February 2025, was high, particularly in the Arabian oryx population. The total death toll among Arabian oryx accounted for 226 animals, 82 males and 118 females, and another 26 animals for which gender was not recorded. This was equivalent to 33.78% of the entire population out of 669 animals present in the sanctuary at the beginning of the outbreak (as recorded on the 1 January 2025). With exception made for 24 untagged animals (6 males, 17 females, and 1 calf sex not reported), the majority of the dead oryx were identified by ear tag numbers, and most were documented individually by photos. Pregnancy and poor body conditions (malnutrition) appeared to be risk factors. Mortality was recorded also among vaccinated animals against FMD (n 87, 65 males, and 22 females, 38.49% of dead animals). Details on the vaccinal status of dead animals are given in Table 3. Observations in other species present in the sanctuary (reems, other gazelle species, blackbuck, and llamas) recorded fatal cases in four reems and one blackbuck. Details on mortality in animals are available in Supplementary Material Table S1.

Table 3. Vaccinal status of dead Arabian oryx (n 226) reported from 8 January to 4 February 2025 at the Al Wusta Sanctuary, Sultanate of Oman. * Animals not protected for FMD.

Vaccination	Number of Animals	Gender			
		Males	Females	Not Reported	%
Vaccine for FMD combined with enterotoxaemia	60	48	12	0	26.55
Vaccine for FMD combined with enterotoxaemia and hemorrhagic septicemia	27	17	10	0	11.94
Total vaccinated for FMD	87	65	22	0	38.49
Vaccine for other diseases only (four enterotoxaemia, five not specified) *	9	8	1	0	3.98
Total vaccinated	96	73	23	0	42.48
Unvaccinated *	105	3	77	25	46.46
Not reported	25	6	18	1	11.06
Total dead animals February 2025	226	82	118	26	100

The hematological profile of the animals, evaluated by CBC, KFT, and LFT, at the beginning of the outbreak, showed altered values, on the whole characteristic of a severe disease occurring. All considered, animals suffered from marked leucopenia (white blood cell count mean 6.13) with very low values, even lower than $4 \times 10^3/\mu L$, compared to the normal range from 11 to 14. Neutrophils were severely depleted, with an observed mean of 5.36%, instead of a normal range of 56.5–75.2%, while lymphocytes were augmented, showing a mean of 88.06% (normal range 20.5–28.4%), characteristic of an inflammatory process. Low values of red blood cells, hemoglobin, and platelets were also observed.

High values of bilirubin (mean 0.94 mg/dL, normal range 0.008–0.01), transaminases (GOT mean 118.58 U/L, GPT mean 59.68 U/L, compared to normal ranges of 47–63 and 35–45, respectively), and urea (mean 71.22 mg/dL, normal range 20–25) were consistent with acute hepato-renal sufferance. Additionally, elevated creatine kinase levels (mean 791.48, normal range 303–367) were indicative of kidney failure, in addition to underlying possible muscle damage or hearth issues, as well as the observed hypoalbuminemia (mean 3.24 g/dL, normal range 4.5–5.2) that could be related to nephrotic syndrome or extensive hepatic damage, while hypoglycemia (mean 83.23 mg/dL, normal range 119–150)

was probably an expression of the starvation of the animals. The detailed results of the hematological and serum biochemical analyses are reported in Table 4.

Table 4. Values and means for various hematological and serum biochemical parameters in adults Arabian oryx (*Oryx leukoryx*) compared to values reported from apparently healthy animals referred to as normal reference limits [10–12]. Numbers indicated in bold: abnormal values. ND: not determined.

Hematological Parameters								
Parameter (Unit)	**F 405**	**F 400**	**F 0994**	**F 472**	**M Unt.**	**Mean**	**Range**	**Normal**
WBC ($10^3/\mu L$)	**7.56** (−)	**3.73** (−)	**4.48** (−)	**6.65** (−)	**8.24** (−)	6.13	3.73–8.24	11–14
RBC ($10^6/\mu L$)	11.03	**8.79** (−)	**8.60** (−)	10.48	**8.01** (−)	9.38	8.01–11.03	9–17
Hb (g/dL)	15.8	**11.9** (−)	**12.8** (−)	**14.5** (−)	**11.7** (−)	13.34	11.7–15.8	15–17
HCT (%)	**54.5**	**41.2**	**44.0** (−)	50.3	**40.6** (−)	46.12	40.6–54.5	45–52
MCV (fL)	49.4	46.9	**51.2** (+)	48.0	**50.7** (+)	49.24	46.9–51.2	44–50
MCH (pg)	14.3	13.5	14.9	13.8	14.6	14.22	13.5–14.9	10–27
MCHC (g/dL)	**29.0** (−)	**28.9** (−)	**29.1** (−)	**28.8** (−)	**28.8** (−)	28.92	28.8–29.1	31–34
PLT ($10^3/\mu L$)	**169** (−)	**59** (−)	**33** (−)	**53** (−)	**360** (+)	134.8	33–360	183–327
RDW-SD (fL)	28.1	ND	29.9	ND	26.8	28.26	26.8–29.9	
RDW-CV (%)	23.3	22.6	21.4	23.9	19.4	22.12	19.4–23.9	
MPV (fL)	8.0	8.4	7.8	7.5	9.1	8.16	7.5–9.1	
P-LCR (%)	10.9	9.5	5.0	6.9	21.7	10.08	5.0–21.7	
PCT (%)	0.14	0.05	0.03	0.04	0.33	0.11	0.03–0.33	
NRBC ($10^3/\mu L$)	0.01 (0.1%)	0.01 (0.3%)	0.01 (0.2%)	0.01 (0.2%)	0.01 (0.1%)	0.01 (0.18%)	0.01 (0.1–0.3%)	
Neutrophyls ($10^3/\mu L$)	0.27 (3.5%)	0.68 (18.3%)	0.20 (4.5%)	0 (0%)	0.04 (0.5%)	0.23 (5.36%)	0–0.68 (0–18.3%)	0.55–2.68 (56.5–75.2%)
Lymphocytes ($10^3/\mu L$)	6.79 (89.8%)	2.82 (75.6%)	3.88 (86.6%)	6.28 (94.4%)	7.74 (93.9%)	5.50 (88.06%)	2.82–7.74 (75.6–94.4%)	0.70–0.79 (20.5–28.4%)
Monocytes ($10^3/\mu L$)	0.36 (4.8%)	0.21 (5.6%)	0.35 (7.8%)	0.31 (4.7%)	0.42 (5.1%)	0.33 (5.6%)	0.21–0.42 (4.7–7.8%)	0.03–0.04 (0.78–1.0%)
Eosinophyls ($10^3/\mu L$)	0.08 (1.1%)	0 (0%)	0 (0%)	0 (0%)	0 (0%)	0.01 (0.22%)	0–0.08 (0–1.1%)	0–0.10 (0–2.86%)
Basophyls ($10^3/\mu L$)	0.06 (0.8%)	0.02 (0.5%)	0.05 (1.1%)	0.06 (0.9%)	0.04 (0.5%)	0.04 (0.76%)	0.02–0.06 (0.5–1.1%)	0–0.06 (0–2.42%)
Serum Biochemical Parameters								
Parameter (Unit)	**F 405**	**F 400**	**F 0994**	**F 472**	**Mean**	**Range**	**Normal**	
Albumin (g/dL)	**3.84**	**2.68**	**2.56**	**3.90**	3.24	2.56–3.90	4.5–5.2	
Alkaline phosh (U/L)	**135.60**	**79.36**	**109.34**	**142.17**	116.61	79.36–142.17	111–115	
Bilirubine direct (mg/dL)	**0.35**	**0.90**	**1.85**	**0.67**	0.94	0.35–1.85	0.008–0.01	
Bilirubine total (mg/dL)	0.37	**1.14**	**2.89**	**0.80**	1.3	0.80–2.89	0.03–0.36	
CK NAK (U/L)	**691.72**	**783.10**	**902.24**	**788.88**	791.48	691.72–902.24	303–367	
Creatinine (mg/dL)	**1.86**	1.37	1.25	**1.83**	1.57	1.25–1.86	0.92–1.38	
Gamma GT (U/L)	8.71	11.61	14.30	9.33	10.98	8.71–14.30		
Glucose (mg/dL)	**80.24**	**77.81**	**78.51**	**96.39**	83.23	77.81–96.39	119–150	
GOT AST (U/L)	60.86	**211.87**	ND	**83.02**	118.58	60.86–211.87	47–63	
GPT ALT (U/L)	36.50	**49.34**	**109.03**	43.86	59.68	36.50–109.03	35–45	
Magnesium (mg/dL)	1.7	1.6	1.6	**1.9**	1.7	1.6–1.9	1.69–3	
Urea (mg/dL)	**36.3**	**147.4**	**42.3**	**58.9**	71.22	36.3–147.4	20–25	
Calcium (mg/dL)	**9.46**	8.34	**7.47**	8.73	8.5	7.47–9.46	8–9	
Copper (µg/dL)	88	77	77	95	84.25	77–95		
Iron (µg/dL)	78.18	36.65	49.14	71.48	58.86	36.65–78.18		
Phosphorus (mg/dL)	**7.67**	9.96	9.04	**3.91**	7.64	3.91–9.96	8–10	

The parasitological investigation was performed on fecal samples from Arabian oryx females identified by ear tags 0094, 400, and 405, and one untagged male, showing positiveness for *Nematodirus* spp. eggs (samples 0094 and 400 were highly positive). Females 0094 and 400 were also positive for *Eimeria* spp. oocysts. The sample from female 472 was negative for internal parasites.

The results of the serological and antigenic analyses are reported in Table 5. All serum samples collected from Arabian oryx (females 0994, 400, 405, and 472 and untagged male) were negative for antibodies against *Mycoplasma mycoides* subsp. *mycoides* small colonies, the causative agent of CBPP. Samples from Arabian oryx females (0098 and 413) and males (83 and 140) were negative for antibodies against *Mycobacterium avium paratuberculosis* (Johne's disease, para-tuberculosis), PPRV, and FMDV-NSP antibodies. The sample collected from Arabian oryx female, identified with ear tag number 3, was the only positive for anti-FMDV-NSP antibodies. The same sample showed a doubtful seroconversion against PPRV; thus, a request for a new sample after 2 weeks was formulated by the laboratory investigators, but the animal died before. Samples collected from two females (ear tags 0447 and 0500) were invalid for serological testing due to hemolysis. Blood samples obtained from six Arabian oryx females (0098, 245, 0447, 0464, 0500, and 3) were positive for FMDV RNA, showing cycle threshold (Ct) values ranging from 18.4 to 28.9, indicating active FMDV infection with moderate to high viral RNA loads in the tested oryx, while samples from three other Arabian oryx (female 413 and males 83 and 140) resulted negative. None of the tested Arabian oryx (females 0098, 245, 413, 0447, 0464, 0500, and 3, and males 83 and 140) showed positiveness for PPRV RNA. The sample collected from a sand gazelle male was negative for both FMDV and PPRV antigens.

Table 5. Results of serological screening for antibodies to contagious bovine pleuro polmonitis (CBPP), Johne's disease (JD), Peste des petits ruminants virus (PPRV), and foot-and-mouth disease virus (FMDV), and antigenic detection for PPRV and FMDV in animals from Al Wusta Sanctuary of the Sultanate of Oman. Ab: antibodies; and NE: not executed, in certain cases due to hemolysis.

Animal Species	**Gender**	**Ear Tag Number**	**Tests**					
			CBPP Ab	JD Ab	PPRV Ab	PPRV RNA	FMDV Ab	FMDV RNA
Arabian oryx	Female	0094	NE	NE	NE	NE	NE	NE
Arabian oryx	Female	0098	NE	Negative	Negative	Negative	Negative	**Positive**
Arabian oryx	Female	0447	NE	Hemolysis	Hemolysis	Negative	Hemolysis	**Positive**
Arabian oryx	Female	0464	NE	NE	NE	Negative	NE	**Positive**
Arabian oryx	Female	0500	NE	Hemolysis	Hemolysis	Negative	Hemolysis	**Positive**
Arabian oryx	Female	0994	Negative	NE	NE	NE	NE	NE
Arabian oryx	Female	3	NE	NE	Doubtful	Negative	**Positive**	**Positive**
Arabian oryx	Female	245	NE	NE	NE	Negative	NE	**Positive**
Arabian oryx	Female	400	Negative	NE	NE	NE	NE	NE
Arabian oryx	Female	405	Negative	NE	NE	NE	NE	NE
Arabian oryx	Female	413	NE	Negative	Negative	Negative	Negative	Negative
Arabian oryx	Female	472	Negative	NE	NE	NE	NE	NE
Arabian oryx	Male	83	NE	Negative	Negative	Negative	Negative	Negative
Arabian oryx	Male	140	NE	Negative	Negative	Negative	Negative	Negative
Arabian oryx	Male	Untagged	Negative	NE	NE	NE	NE	NE
Sand gazelle	Male	Untagged	NE	NE	NE	Negative	NE	Negative

4. Discussion

Foot-and-mouth disease (FMD) is a severe, highly contagious viral disease of livestock that has a significant economic impact. FMD is an OIE-listed disease, affecting cattle, swine, sheep, goats, and other cloven-hoofed ruminants, members of the order *Artiodactyla*. It is a

transboundary animal disease (TAD) [8]. There are seven viral serotypes (A, O, C, SAT1, SAT2, SAT3, and Asia1). Recent FMD outbreaks occurred in 2025 in Germany, Hungary, and Slovakia, countries officially free for 50 years, with subsequent application of strict trade restrictions on animals and animal products (including meat and dairy), as per WOAH rules [8], showing the constant potential of the disease for international spread, despite application of biosecurity measures. Oman is not officially FMD-free, as per WOAH, and the disease is present also in the neighboring countries of Yemen and Saudi Arabia, with animal health and international trade implications. In 2023, the risk of FMD introduction and spread in countries in the Near East and West Eurasia was evocated for serotype SAT2 (the same responsible of the outbreak in cattle in Dhofar), reminding us of the susceptibility of wild ruminants [13].

The FMDV serotype O, the most frequent in the region [14], has been recently introduced into the Arabian Peninsula on multiple occasions [15] and it was involved in one outbreak affecting the Arabian oryx in the United Arab Emirates (UAE) in 2015 [14] and in two other outbreaks affecting captive scimitar-horned oryx (*Oryx dammah*), a large Sahelo-Saharan antelope extinct in the wild, in UAE in 2013 and 2015 [16]. In another outbreak affecting scimitar-horned oryx, in UAE in 2013, the FMDV was a serotype A [16]. The Arabian oryx was previously documented as being a spill-over following outbreaks caused by serotype O [17,18]. In the case of the FMD outbreak in Al Wusta, even if the involved serotype was not determined, it is likely that the virus circulating in domestic animals was introduced into the captive oryx population. However, the epidemiological role of the Arabian oryx is still unknown, which calls for further studies [14].

Regarding the confirmatory diagnostics for FMD, virus isolation and histopathological examination represent the gold standard for definitive FMDV diagnosis. In addition, genetic characterization is crucial for understanding the molecular epidemiology and evolutionary dynamics of FMDV, especially in the context of a rare outbreak in a wildlife species such as the Arabian oryx. However, as this outbreak occurred under field conditions in a wildlife sanctuary located in a remote protected area with restricted handling protocols for endangered species, there were significant logistical, biosecurity, and practical limitations. Necessary facilities and cold chain, against high temperatures and rapid decomposition, were unavailable at the outbreak site. This prevented the collection of full necropsy samples and implementation of virus isolation, allowing only the collection of a limited number of samples. Ultimately, due to the acute nature of the outbreak, the focus was on rapid diagnosis and outbreak containment to minimize mortality and further spread.

In addition, sampling was constrained by the need to safely handle wild oryx and minimize stress. Standard sample size calculations (e.g., detecting a 1–5% prevalence at 95% confidence level in large herds) are theoretical and rarely met in such field settings. Samples were deliberately chosen to maximize the chance of detection (e.g., symptomatic or high-risk animals) from animals showing signs and being readily accessible and available at capture. This approach reflects accepted outbreak investigation practice in wildlife under field conditions [19–21]. Even with limited sampling, a positive result is highly indicative of an outbreak, and is possibly sufficient in the case of highly diffusive diseases such as FMD.

Nonetheless, despite the absence of virus isolation, several converging lines of evidence collectively support the conclusion of an FMD outbreak in Arabian oryx. Clinical signs in affected animals were highly characteristic of FMDV infection, including salivation and oral erosions, typical of the disease in cloven-hoofed species. The haematological profile was consistent with an acute severe infection of probable viral aetiology, also considering the low values of procalcitonin, which are elevated in case of bacterial or fungal infections.

All samples were processed in accordance with WOAH-recommended protocols and the diagnostic approach was aligned with WOAH recommendations for FMDV detec-

tion in wildlife settings, where PCR and NSP serology are acceptable when isolation is impractical [21].

The use of an FMD DIVA ELISA for the detection of NSP antibodies confirmed the exposure to active virus, ruling out vaccination as a cause. FMDV-specific RNA was detected using a RT-qPCR assay targeting the conserved 3D RNA-dependent RNA polymerase gene of the virus. This gene is commonly targeted in diagnostic protocols due to its high sequence conservation across all seven serotypes of FMDV and its suitability for pan-serotype detection. The assay employed follows the WOAH's recommended protocol, which has been widely validated for sensitivity and specificity in both domestic and wild cloven-hoofed species. Real-time RT-qPCR targeting the conserved 3D gene of FMDV yielded positive results in multiple samples, with Ct values between 18.4 and 28.9, indicating moderate to high viral RNA load. These Ct values are consistent with active FMDV infection. According to the standard interpretation for FMDV RT-qPCR targeting the 3D gene, Ct values ≤ 30 are typically considered strongly positive, as values are inversely proportional to the viral load, particularly when supported by clinical signs and other diagnostic evidence. In addition, the outbreak occurred concurrently with confirmed FMDV circulation in domestic livestock in the surrounding areas of Oman, supporting epidemiological plausibility.

4.1. Impact of FMD in Wild Fauna

FMD-susceptible wildlife species in the Near East and west Eurasia include wild sheep and goats, and several species of deer and antelope, including the mountain gazelles and the Arabian oryx [22]. While FMD has been reported in captive Arabian oryx, FMD has not been detected in wild populations [18,22].

FMD occurred in captive populations of Arabian oryx in Bahrain, UAE, and Saudi Arabia with high morbidity and mortality [14,22]. Three FMD outbreaks affecting Arabian Oryx were reported in 2015: one in Saudi Arabia, killing 21 animals out of 32 (65%), and two in UAE, where 12 died out of 44 (27%), and in the other, 30 animals died out of 210 (12.5%). From those reports, it appears that FMD is a deadly disease for the Arabian oryx, with mortality rates ranging between 12.5 and 65% of the affected population [14]. In the FMD outbreaks reported in captive scimitar-horned oryx (*Oryx dammah*) [16], despite high seroconversion rates (up to 78%) and presence of lesions as ulcers on the gum of the upper lip and coronary band characteristic of FMD infection, all animals were in good body condition, their feed intake was normal and they had very low mortality, which is attributable to FMD was noted in the population of nearly 4000 heads.

During the outbreak occurred in Al Wusta Sanctuary, in the daily examination that was ongoing in January 2025, Arabian oryx were identified exhibiting lesions partially compatible with FMD as aphthae and erosions on the oral mucosa, but no animals showed lesions at the level of feet. Sera were analyzed using an ELISA, which specifically measures antibodies directed at FMDV NSP. The results demonstrate that one animal tested was FMDV NSP-seropositive. All other animals were seronegative, probably due to the testing performed before seroconversion in recently infected animals. However, since the test has not been validated for the Arabian oryx species, results should be interpreted with caution. FMDV was also confirmed with real-time RT-PCR for antigen-detection in oral swabs. The results are compatible with an introduction of FMDV and rapid transmission of the virus due to its high contagiousness, which matched the observed clinical cases. Even if it was not possible to determine if FMD accounted for all the recorded mortality, this was considered highly probable also taking into account that no other pathogens were identified. Furthermore, FMD might have played an important role affecting fragile individuals, such as females at the late stage of pregnancy, newborns, or animals with general poor body

conditions, eventually being linked to heavy infestations with gastrointestinal parasites such as *Nematodirus* spp. The parasite exams performed in the present study were intended as ancillary data and reported for completeness; their identification was generally in line with expected parasite fauna [23,24]. However, parasites were unlikely to be the main cause of the outbreak, aside from possibly weakening overall body condition, and positive viral test results support our conclusion that the lesions were caused by FMDV.

It has been also noted that the overall health status of the animals decreased before the outbreak in concomitance with changes of feed supply, which was estimated to be of poorer quality in confronting the what was previously available by other feed business operators. Compared to the previous documented mortality rates, related to outbreaks involving limited numbers of animals, the mortality observed in the outbreak occurred in Al Wusta can be considered relatively high and suggests the circulation of a highly virulent FMD strain.

With concern to reem gazelle, native to the Middle East and originally inhabiting the Arabian and Syrian Deserts, it is now primarily found in the Arabian Peninsula, where it persists in the wild as small and isolated herds in Saudi Arabia, UAE, Oman, Yemen, Turkey, Kuwait, Iraq, Jordan, and Syria [25]. The population of mature wild sand gazelles is estimated at around 2150 individuals, classifying the species as vulnerable [26]. A substantially larger number is kept in captivity within reserves and breeding programs, such as Oman's Yalooni Breeding Center and Al Wusta Sanctuary, as well as notably in Abu Dhabi [26]. In Oman, the Arabian sand gazelle is among the predominant wild ruminant ungulates, and as with other wild ruminants, it is known to be susceptible to FMD. However, contrary to the observations in Arabian oryx, in the present study, only four cases of mortality were reported among the large herd of above 1,000 individuals housed in Al Wusta. In another FMD outbreak which occurred in UAE in 2013, the mortality in this species was very high, with deaths accounting for 663 animals out of a population of 1,095 gazelles (60.7%) [16].

4.2. Origine of the Infection in Oryx (Source of the Virus?)

Most of the domestic Omani animals, about the 70%, are raised in Dhofar [27,28], due to the favorable climate and availability of large pastures. The 225,000 bovines and the 187,000 dromedaries constitute the majority of the zootechnic resources of the region, along with less than 100,000 goats and donkeys. Apart from the national immunization plan against FMD, which covers 60% of the domestic large and small ruminant population (dromedaries are excluded), no other prophylactic programs are in place, and farmers are culturally averse. Pastures are freely shared by the different domestic species. Because of close intermingling, there are no barriers preventing disease transmission among animals. Furthermore, farmers often use natural reserves as grazing areas, allowing diseases to spread indirectly from domestic livestock to wildlife. Additionally, the high density of domestic animals increases the epidemiological risk, promoting the circulation of infectious diseases. Movements of live animals from Dhofar towards northern governorates for trade purposes are scarce, but the epidemiological risk exists and only a few animals are sufficient to spread pathogens, especially those with as highly diffusive potential as FMD.

According to the most recent update adopted in 2024 of the WOAH Terrestrial Animal Health Code (Article 8.8.1. General provisions) [8], many different species belonging to diverse taxonomic orders are known to be susceptible to infection with FMD virus. Their epidemiological significance depends upon the degree of susceptibility, the husbandry system, the density and extent of populations, and the contacts between them. For the purposes of the Terrestrial Code, FMD is defined as an infection of the following animals with FMDV: animals of the family *Suidae*; animals of the subfamilies *bovinae*, *caprinae*, and

antilopinae of the family *Bovidae* and family *Cervidae*; and *Camelus bactrianus*. Amongst the *Camelidae*, Bactrian camels and new world camelids have been shown to be susceptible [9]. According to WOAH, only Bactrian camels (*Camelus bactrianus*) are sufficiently susceptible to have potential for epidemiological significance. As per WOAH rules, dromedaries (*Camelus dromedarius*) are not formally susceptible species to infection with FMDV, while South American camelids are not considered to be of epidemiological significance [8]. Dromedaries are believed to be mostly resistant to clinical FMD, and virus isolation is difficult. Natural and experimental infections occurred in dromedaries; however, they are not believed to play a significant role in transmission to livestock [29]. Experimentally, dromedaries resulted from low susceptibility to inoculation with FMD virus serotype O [30]. Similar results were obtained by investigating the potential role of dromedary camels in the epidemiology of FMD also in Oman. Sera from local dromedaries that grazed with FMD-positive cattle and small ruminants were tested negative for antibodies against serotype O, suggesting that FMDV was not transmitted to dromedary camels [31]. However, in West Africa, serum samples from dromedaries were positive for FMD serotype A, suggesting that dromedaries may be susceptible to FMDV infection, even if likely not playing a significant role in the epidemiology of the disease [32]. In addition, no studies indicated camels to be resistant to the serotype SAT 1, reported to be circulating in Oman in 2023, and antibodies to all seven serotypes of FMDV have been found in domestic dromedary camels [33].

Nevertheless, small ruminants (goats) and especially dromedaries were observed frequently freely roaming very near, and even within, the perimeter of the sanctuary also during the FMD outbreak in oryx, suggesting high risk for naïve susceptible species. Indeed, the occurrence of the FMD outbreak in cattle in Dhofar in 2023, which was reported about 500 km from the Al Wusta Sanctuary, was seriously taken into account by the managers of the center. This motivated a subsequent vaccinal program to prevent the risk of diffusion to oryx. However, while mortality was expected among unvaccinated animals (46.46%), despite the vaccinal status, the 38.49% of dead animals were found to be vaccinated against FMD serotypes A, O, and SAT 1. It should be emphasized that the immunity provided by commercially available FMD vaccines is short and in order to obtain an effective protection of the animals, protocols require a second inoculation after 3 to 4 weeks, followed by a booster every six months. In addition, the specific circulating strains should be considered [14]. Another issue that appeared during the vaccination plan undertaken in the oryx population in Al Wusta was the handling of animals. In particular, the vaccination was given essentially to males, and females were only partially immunized since most of the adult females were pregnant and the risk of abortion due to stress caused by handling was considered high. This was reflected in the mortality rates among unvaccinated animals: the majority (96% of the animals for which the gender was reported) were females. In deaths among vaccinated animals, 75% were males and only 25% were females, simply because only a few females could be vaccinated. The various requirements and practical problems related to the handling of the animals constitute a challenge to effectively protect wildlife species.

4.3. Perspectives

A key recent milestone in advancing conservation efforts is Oman's future-oriented strategy, "Oman 2040" (Vision 2040). Prepared in 2019 under the Royal Directives of His Majesty Sultan Qaboos bin Said, this comprehensive 20-year, multisector plan outlines the nation's strategic priorities and directions for sustainable development. The defined priorities include environment and natural resources, targeting the inclusion of the Sultanate within the 20 best virtuous countries, in terms of environmental performance indicators, by 2040. This calls the full engagement of the Environment Authority of the Sultanate, estab-

lished in 2020, which is responsible for the protection and management of the wild fauna patrimony, particularly vulnerable and endangered species, also by research, awareness, and repopulation projects.

Nowadays, Oman remains a land of untamed, largely undiscovered natural beauty. Only a few data are available on wild animals, provided by some field reports and scientific studies. Only a few studies were focused to the Arabian oryx [1,2,7], with very limited information on diseases affecting the species. The present findings highlight not only the risk of FMD or other dangerous pathogens incurred in captive facilities in Oman and other neighboring countries in the Arabian Peninsula, but also underline the necessity to improve biosecurity and prevention by strengthening management standards and knowledge. Improved management requires the availability of adequate facilities. It is of the utmost importance for clinical therapies, surgical interventions, and rapid diagnostic testing (facilities for clinical examinations, treatments, surgery, necropsies, laboratory, and adequate equipment) for effective assistance to captive animals. This should be flanked by training the staff in the best practices. Improved knowledge requires design and implementation of research projects. The complexity of planned activities and expected results dictate the provision of dedicated human resources, equipment, and consumables. The objective of such activities should focus on the better understanding of animal health in wildlife. Such knowledge will allow for the improvement in the management of captive wild fauna, with beneficial effects on health and welfare, reducing diseases and mortality and sustaining repopulation strategies, taking into account the interconnection with domestic animals and related health risks.

5. Conclusions

Deserts, majestic mountains, and green landscapes are all part of the Sultanate of Oman, a small country with an abundance of biodiversity, a remarkable natural patrimony that should be preserved. In Oman, historically, the Asiatic lion (*Panthera leo persica*, Meyer, 1826) was also present [34]. The region experienced serious changes that affected the fauna, particularly in the context of the last century. The disappearance of selected species, such as the Arabian oryx (*Oryx leucoryx*) in 1972 [2], and the Asiatic cheetah (*Acinonyx jubatus venaticus*, Griffith, 1821) in 1977 [35], were indicative of these marked changes and serious threats affecting the natural environment of the country. Poaching was certainly the most important threat for wild fauna. In Oman, poaching not only led to the extinction of the oryx, but even hampered repopulation programs, especially during a period of heavy oryx hunting in 1996–1997. Despite that as per Ministerial Decision, the hunting of all species of the wild has been banned since 1993 [36], reports of law infringements [37] call attention to the threat to wildlife. However, even if the problem of uncontrolled hunting, as in the past, is still a reality and deserves efficient preventive measures, such as active monitoring of the territory by rangers and other public forces, risks related to animal health, as demonstrated by the present study, should be carefully taken into account and prevented with adequate resources and trained staff. The survival of endangered wildlife and the achievement of Oman's Vision 2040 program target can only be ensured by utilizing rational planning, research implementation, and natural resource management.

Supplementary Materials: The following supporting information can be downloaded at: https://www.mdpi.com/article/10.3390/ani15162389/s1, Table S1: Mortality in animals at Al Wusta Sanctuary of the Sultanate of Oman, from 8 January to 4 February 2025. Out of 669 presents in the sanctuary at the beginning of the outbreak (1 January 2025) (M 312; F 345; Calves 12) subdivided in 4 herds (in 1 only males 163; in 2 M 53 F 171 C 8; in 3 M 46 F 144 C 4 in 4 M 50 F 30), a total of 226 (33.78%) dead oryx were reported (images of ear tag numbers available for most of animals). In the same period were reported also deaths in 4 reems and 1 blackbuck.

Author Contributions: M.G. was responsible for the conceptualization, writing, review and editing, S.A.M. was responsible for the investigation and project administration, S.A.B. was responsible for the investigation and data curation and M.K.A.-G. contributed for the investigation and supervision of the present study. All authors have read and agreed to the published version of the manuscript.

Funding: This research received no external funding.

Institutional Review Board Statement: The research was performed in compliance with the Environment Agency, Sultanate of Oman, routine duties and responsibilities (statement dated 19 June 2025).

Informed Consent Statement: Not applicable.

Data Availability Statement: The article includes original contributions of the study and additional queries can be addressed to the corresponding author.

Acknowledgments: The authors would like to thank Adel Al Rahabi, Central laboratory, Muscat, Sultanate of Oman, Suwaibaq Humaid Al-Harsoosi and Abdullah Hamed Al-Harsoosi, Oryx Sanctuary (Al Wusta Wildlife Reserve), Environment Authority, Sultanate of Oman.

Conflicts of Interest: All authors declare that no competing financial interests or personal relationships influenced their work reported in the present study.

References

1. Hetem, R.S.; Strauss, W.M.; Ick, L.G.; Maloney, S.K.; Meyer, L.C.R.; Fuller, A.; Shobrak, M.; Mitchell, D. Selective brain cooling in Arabian oryx (*Oryx leucoryx*): A physiological mechanism for coping with aridity? *J. Exp. Biol.* **2012**, *215*, 3917–3924. [CrossRef] [PubMed]
2. Spalton, J.A. A brief history of the reintroduction of the Arabian oryx *Oryx leucoryx* into Oman 1980–1992. *Int. Zoo Yearb.* **1993**, *32*, 81–90. [CrossRef]
3. IUCN *Oryx leucoryx*. SSC Antelope Specialist Group. *IUCN Red List of Threatened Species*; IUCN: Gland, Switzerland, 2017. [CrossRef]
4. Patzelt, A. Synopsis of the Flora and Vegetation of Oman, with Special Emphasis on Patterns of Plant Endemism. *Abh. Braunschw. Wiss. Ges.* **2015**, 282–317.
5. UNESCO. *Arabian Oryx Sanctuary*; UNESCO: Paris, France, 2022. Available online: https://whc.unesco.org/en/list/654 (accessed on 20 May 2025).
6. UNESCO. *Oman's Arabian Oryx Sanctuary: First Site Ever to Be Deleted from UNESCO's World Heritage List*; UNESCO: Paris, France, 2007. Available online: https://whc.unesco.org/en/news/362 (accessed on 20 May 2025).
7. Goraya, K.; Al Rawahi, Q.; Al Balushi, S.; Al Saadi, H.; Al Rahbi, S.; Al Alawi, Z.; Hussain, M.H.; Hussain, M. Postmortem findings in captive sand Gazelle and Arabian Oryx at Al-Wusta Wildlife Reserve, Oman. *Pak. J. Zool.* **2021**, *53*, 1583–1586. [CrossRef]
8. WOAH. Foot and Mouth Disease. Listed Diseases, with Official Disease Status. 2025. Available online: https://www.woah.org/en/disease/foot-and-mouth-disease/ (accessed on 20 May 2025).
9. Larska, M.; Wernery, U.; Kinne, J.; Schuster, R.; Alexandersen, G.; Alexandersen, S. Differences in the susceptibility of dromedary and Bactrian camels to foot-and-mouth disease virus. *Epidemiol. Infect.* **2009**, *137*, 549–554. [CrossRef]
10. Vassart, M.; Greth, A. Hematological and Serum Chemistry Values for Arabian Oryx (*Oryx leucoryx*). *J. Wildl. Dis.* **1991**, *27*, 506–508. [CrossRef] [PubMed]
11. Hussein, M.F.; Al-Jumaah, R.S.; Homeida, A.; Alhaidary, A.A.; Alshaikh, M.A.; Garelnabi, A.; Mohamed, O.; Omer, S. Hemostatic profile, platelets, and blood constituents of the Arabian oryx (*Oryx leucoryx*). *Comp. Clin. Pathol.* **2010**, *19*, 585–591. [CrossRef]
12. Eljarah, A.; Ismail, Z.B. Hematology and serum biochemistry variables in apparently normal Arabian Oryx (*Oryx leucoryx*). *Vet. World* **2023**, *16*, 1369–1372. [CrossRef]
13. McLaws, M.; Ahmadi, B.V.; Condoleo, R.; Limon, G.; Kamata, A.; Arshed, M.; Rozstalnyy, A.; Rosso, F.; Dhingra, M. Risk of Foot-and-Mouth Disease SAT2 Introduction and Spread in Countries in the Near East and West Eurasia—FAO Qualitative Risk Assessment, FAO, Rome, Italy 2023. Available online: https://openknowledge.fao.org/server/api/core/bitstreams/667b4c4c-b80d-4206-bd5f-d432a02d7387/content (accessed on 20 May 2025).
14. Lignereux, L.; Alzahlawi, N.; Al Kharusi, Y.; Pesci, M.E. *Middle East Arabian Oryx Disease Survey*, 3rd ed.; Environment Agency: Abu Dhabi, United Arab Emirates, 2018. Available online: https://www.arabianoryx.org/wp-content/uploads/2022/07/Arabian-Oryx-disease-survey-3rd-edition-1.pdf (accessed on 20 May 2025).

15. Bachanek-Bankowska, K.; Di Nardo, A.; Wadsworth, J.; Mioulet, V.; Pezzoni, G.; Grazioli, S.; Knowles, N.J. Reconstructing the evolutionary history of pandemic foot-and-mouth disease viruses: The impact of recombination within the emerging O/ME-SA/Ind-2001 lineage. *Sci. Rep.* **2018**, *8*, 14693. [CrossRef] [PubMed]
16. Lignereux, L.; Chaber, A.L.; Saegerman, C.; Heath, L.; Knowles, N.J.; Wadsworth, J.; Mioulet, V.; King, D.P. Foot-and-mouth disease outbreaks in captive scimitar-horned oryx (*Oryx dammah*). *Transbound. Emerg. Dis.* **2020**, *67*, 1716–1724. [CrossRef]
17. Ostrowski, S.; Anajariyah, S. *2002 Middle East Arabian Oryx Disease Survey*; National Wildlife Research Center: Taif, Saudi Arabia, 2003.
18. Frölich, K.; Hamblin, C.; Jung, S.; Ostrowski, S.; Mwanzia, J.; Streich, W.J.; Anajariyah, S. Serologic surveillance for selected viral agents in captive and free-ranging populations of Arabian oryx (*Oryx leucoryx*) from Saudi Arabia and the United Arab Emirates. *J. Wildl. Dis.* **2005**, *41*, 67–79. [CrossRef]
19. Eltahir, Y.M.; Ishag, H.Z.A.; Wadsworth, J.; Hicks, H.M.; Knowles, N.J.; Mioulet, V.; King, D.P.; Mohamed, M.S.; Bensalah, O.K.; Yusof, M.F.; et al. Molecular Epidemiology of Foot-and-Mouth Disease Viruses in the Emirate of Abu Dhabi, United Arab Emirates. *Vet. Sci.* **2024**, *11*, 32. [CrossRef] [PubMed]
20. Ryser-Degiorgis, M.-P. Wildlife health investigations: Needs, challenges and recommendations. *BMC Vet. Res.* **2013**, *9*, 223. [CrossRef]
21. World Organisation for Animal Health. Training Manual on Wildlife Diseases Outbreak Investigations. Fourth Cycle Workshop for OIE National Focal Points for Wildlife. 2016. Available online: https://www.oie.int (accessed on 20 May 2025).
22. Weaver, G.V.; Domenech, J.; Thiermann, A.R.; Karesh, W.B. Foot and mouth disease: A look from the wild side. *J. Wildl. Dis.* **2013**, *49*, 759–785. [CrossRef]
23. Mohammed, O.B.; Alagaili, A.N.; Omer, S.A.; Hussein, M.F. Parasites of the Arabian Oryx (*Oryx leucoryx*, Pallas, 1777) and Their Prevalence in the Kingdom of Saudi Arabia. *Comp. Parasitol.* **2012**, *79*, 288–292. [CrossRef]
24. Pauling, C.D.; Oller, A.R.; Jackson, V. Fecal parasite identification by microscopy and PCR in scimitar-horned oryx, *Oryx dammah*, managed at two sites. *Int. J. Parasitol. Parasites Wildl.* **2016**, *5*, 312–320. [CrossRef]
25. Mallon, D.P.; Kingswood, S.C. *Antilopes—Enquête Mondiale et Plans D'action Régionaux, Partie 4: Afrique du Nord, Moyen-Orient et Asie. Cartes de Distribution*; UICN: Gland, Switzerland, 2001; p. 260.
26. IUCN *Gazella marica*. SSC Antelope Specialist Group. *IUCN Red List of Threatened Species*; e.T8977A50187738; IUCN: Gland, Switzerland, 2017.
27. Ministry of Agriculture. *Agriculture & Livestock Research—Five-Year Research Strategy 2011–2015*; Directorate General of Agriculture & Livestock Research, Ministry of Agriculture: Muscat, Oman, 2011; p. 52.
28. Food and Agriculture Organization (FAO) Crops and Livestock Products: Oman. FAO STAT, 2021. Available online: https://www.fao.org/faostat/en/#data/QCL (accessed on 20 May 2025).
29. Wernery, U.; Kaaden, O.R. Foot-and-mouth disease in camelids: A review. *Vet. J.* **2004**, *168*, 134–142. [CrossRef]
30. Alexandersen, S.; Wernery, U.; Nagy, P.; Frederiksen, T.; Normann, P. Dromedaries (*Camelus dromedarius*) are of Low Susceptibility to Inoculation with Foot-and-Mouth Disease Virus Serotype O. *J. Comp. Pathol.* **2008**, *139*, 187–193. [CrossRef] [PubMed]
31. Body, M.H.H.; Al-Senaidi, N.Y.A.; Al-Subhi, A.H.A.; Al-Maawali, M.G.; Ahmed, M.S.; Hussain, M.H. Foot and mouth disease virus serological study of dromedary camels in Oman. *Sci. Tech. Rev.* **2019**, *38*, 731–736. [CrossRef]
32. Ularamu, H.G.; Wungak, Y.S.; Lazarus, D.D.; Woma, T.Y.; Ehizibolo, D.O.; Dogonyaro, B.B.; Bwala, D.G.; Bakari, A.H.; Agom, D.; Onoja, M.A.; et al. Serological evidence of foot-and-mouth disease virus (FMDV) in camels (*Camelus dromedaries*) in Nigeria. *J. Vet. Med. Anim. Health* **2015**, *7*, 261–264. [CrossRef]
33. Yousef, M.R.; Mazloum, K.S.; Al-Nakhli, H.M. Serological evidence of natural exposure of camels (*Camelus dromedarius*) to foot and mouth disease virus. *Vet. World* **2012**, *5*, 197–200. [CrossRef]
34. Mallon, D.; Budd, K. *Regional Red List Status of Carnivores in the Arabian Peninsula*; IUCN: Cambridge, UK; Gland, Switzerland; Environment and Protected Areas Authority: Sharjah, United Arab Emirates, 2011; vi+49p.
35. Harrison, D.L. The mammal fauna of Oman with special reference to conservation and the Oman Flora and Fauna Survey. *J. Oman Stud.* **1983**, *6*, 329–339.
36. Insall, D.H. Oman. In *Antelopes: North Africa, the Middle East, and Asia. Global Survey and Regional Action Plans*; Mallon, D.P., Kingswood, S.C., Eds.; IUCN: Gland, Switzerland, 2001; Chapter 10.
37. Vaidya, S.K. 6 Suspect Gazelle Poachers Held in Oman. Gulf News 2013. Available online: http://gulfnews.com/news/gulf/oman/6-suspect-gazelle-poachers-held-in-oman-1.1204189 (accessed on 20 May 2025).

Disclaimer/Publisher's Note: The statements, opinions and data contained in all publications are solely those of the individual author(s) and contributor(s) and not of MDPI and/or the editor(s). MDPI and/or the editor(s) disclaim responsibility for any injury to people or property resulting from any ideas, methods, instructions or products referred to in the content.

animals

MDPI

Article

Diagnostic Approach and Pathological Characterization of Metastatic Intrahepatic Cholangiocarcinoma in a Captive Puma (*Puma concolor*)

Elisa Mazzotta [1,*], Claudia Zanardello [2], Giovanni De Zottis [2], Antonio Barberio [1], Mery Campalto [1], Federico Martignago [1], Giulia Maria De Benedictis [3], Carlo Guglielmini [3], Francesca Zanusso [3] and Greta Foiani [2,*]

[1] Istituto Zooprofilattico Sperimentale delle Venezie (IZSVe), Viale dell'Università 10, 35020 Legnaro, PD, Italy; abarberio@izsvenezie.it (A.B.); mcampalto@izsvenezie.it (M.C.); fmartignago@izsvenezie.it (F.M.)

[2] Laboratory of Histopathology (SCS3), Istituto Zooprofilattico Sperimentale delle Venezie (IZSVe), Viale dell'Università 10, 35020 Legnaro, PD, Italy; czanardello@izsvenezie.it (C.Z.); gdzottis@izsvenezie.it (G.D.Z.)

[3] Department of Animal Medicine, Productions and Health (MAPS), University of Padua, Viale dell'Università 12, 35020 Legnaro, PD, Italy; giuliamaria.debenedictis@unipd.it (G.M.D.B.); carlo.guglielmini@unipd.it (C.G.); francesca.zanusso@studenti.unipd.it (F.Z.)

* Correspondence: emazzotta@izsvenezie.it (E.M.); gfoiani@izsvenezie.it (G.F.)

Simple Summary: This report describes a case of intrahepatic cholangiocarcinoma with disseminated metastasis in a 16-year-old captive puma, highlighting the value of a comprehensive, multidisciplinary approach. It underscores the importance of clinical, diagnostic, and pathological collaboration in fully understanding the disease. The case provides important insights for veterinarians, pathologists, and wildlife specialists, emphasizing the need for integrated efforts in diagnosing and managing complex conditions in large felids under human care.

Abstract: A 16-year-old captive male puma (*Puma concolor*) presented with progressive weight loss and acute mild gastrointestinal symptoms. Clinical examination, and diagnostic imaging revealed abdominal, pleural, and pericardial effusion and nodular masses in multiple organs. Due to the clinical condition, multiple organ involvement, and a poor prognosis, compassionate euthanasia was chosen. Necropsy revealed abundant cavitary effusions and multiple yellow–white neoplastic masses involving the left hepatic lobes. Metastatic nodules were observed throughout the peritoneum, pericardium, kidney, spleen, and spermatic cord. Histologically, the tumor was characterized by tubular and acinar structures embedded in a desmoplastic stroma. Neoplastic cells were positive for pan-cytokeratins (CKs), CK7, and, to a lesser extent, CK20. The gross, histologic, and immunohistochemical findings were consistent with intrahepatic metastatic cholangiocarcinoma.

Keywords: captive felids; cholangiocarcinoma; clinical investigation; immunohistochemistry; metastatic; *Puma concolor*

1. Introduction

Cholangiocarcinomas (CCAs) are primary tumors of the biliary tract, originating from the intrahepatic or extrahepatic bile ducts or the gallbladder. These tumors have been reported in both domestic and wild animals [1,2], including captive large felids such as lions (*Panthera leo*) [3–5], leopards (*Panthera pardus*) [4,5], and tigers (*Panthera tigris*) [4], with only a single case documented in pumas (*Puma concolor*) [6]. In these species, CCAs are described as highly aggressive neoplasms, frequently metastasizing to distant organs.

Most reports in wild felids consist of case series or surveys from a zoologic institution, primarily focusing on post-mortem pathological findings [4,5]. In this report, we aim to document the diagnostic approach that led to the identification of a metastatic intrahepatic CCA in an elderly captive puma, including clinical evaluation, diagnostic imaging, and collateral microbiologic analysis, and to provide a characterization of its pathological features, highlighting the importance of a multidisciplinary approach to the management of these animals under human care.

2. Case Presentation

2.1. Clinical Report

A 16-year-old captive puma (*Puma concolor*, Linnaeus, 1771) presented with progressive weight loss, two days of decreased appetite, acute mild gastrointestinal signs (vomiting and diarrhea), listlessness, and reduced interaction. The animal came from a private wildlife collection comprising approximately 25 large felids. The puma used to live with two female pumas in an enclosure equipped with a nighttime shelter and various environmental enrichments (trees, a water pool, ropes, benches, stairs, etc.). The animal was routinely fed thermally treated raw meat, including rabbit, chicken, duck, and bovine sources. There were no relevant findings in the clinical history. Four years previously, a coprological examination had been positive for *Toxascaris leonina*, and the animal had received antiparasitic treatment accordingly and was annually checked for gastrointestinal parasites, with all subsequent controls testing negative. The animal was not regularly vaccinated. On visual examination, the animal was alert, ambulatory, and responsive to external stimuli. Abdominal distension was observed. Tachypnea and shallow respiration were noted with a respiratory rate of 32 breaths per minute. In order to perform a complete clinical evaluation, the animal was transferred to the Veterinary Teaching Hospital of the University of Padua (OVUD), where it was remotely anesthetized via intramuscular administration of a combination of dexmedetomidine (Dexdomitor, Vétoquinol Italia S.r.l., Forlì, Italy, 3 μg/kg), ketamine (Nimatek, Dechra Veterinary Products S.r.l., Torino, Italy, 2.5 mg/kg), midazolam (Midazolam Ibi, Ibi Istituto Biochimico Italiano Giovanni Lorenzini S.p.A., Aprilia, Italy, 0.2 mg/kg), and butorphanol (Dolorex, MSD Animal Health S.r.l., Segrate, Italy, 0.2 mg/kg). General anesthesia was maintained with an intravenous infusion of propofol (Proposure, Zoetis, Rome, Italy) to ensure an adequate depth of anesthesia throughout the diagnostic procedure. The animal was intubated, and supplemental oxygen was provided via an endotracheal tube. Physiological parameters were continuously monitored, and intravenous fluid therapy with Lactated Ringer's solution (Ringer Lattato, Salf S.p.A., Cenate Sotto, Italy) was administered at a rate of 2 mL/kg/h.

On admission, the animal weighed 55.4 kg, BCS < 3 [7,8], had marked abdominal distension, and was mildly dehydrated (estimated at approximately 5–6% of body weight loss based on clinical signs including delayed skin tenting and sticky mucous membranes). The mucous membranes were pale with a slightly increased capillary refill time (5 s). The popliteal lymph nodes were mildly enlarged, and both testicles appeared nodular and irregular on palpation. A complete blood count and serum biochemistry profile were performed, and the results reported a mild increase in the red blood cells count and hematocrit values (Table 1). Thoracic radiographies showed bilateral pleural and pericardial effusions (Figure 1).

Table 1. Hematological analyses were performed with the Sysmex XN1000-V analyzer (Sysmex Europe GmbH, Norderstedt, Germany). Biochemistry analyses were performed on serum through the Cobas c501 clinical chemistry analyzer with the related kit (Roche Diagnostics GmbH, Mannheim, Germany).

Hematology	**Value**
RBCs	9.96 M/µL
Hgb	14.8 g/dL
Hct	41.8%
MCV	42.0 fL
MCH	14.9 pg
MCHC	35.4 g/dL
RDW	21.2%
RBCs Morphology	Anisocytosis, Echinocytosis
WBCs	14.94 (10^3/µL)
NEUT	13.13 (10^3/µL)
LYMPH	0.72 (10^3/µL)
MONO	1.02 (10^3/µL)
EO	0.06 (10^3/µL)
BASO	0.01 (10^3/µL)
WBCs Morphology	Neutrophil Toxicity, Döhle bodies
PLT	329 (10^3/µL)
MPV	9.7 fL
Serum Biochemistry	**Value**
Total Proteins	71 g/L
Albumin	34 g/L
Globulin	37 g/L
Urea Nitrogen	25.2 mmol/L
Creatinine	284 µmol/L
Glucose	3.1 mmol/L
Cholesterol	4.25 mmol/L
Triglycerides	0.50 mmol/L
Total Bilirubin	4.84 µmol/L
Direct Bilirubin	2.55 µmol/L
Unconjugated Bilirubin	2.29 µmol/L
AST	50 U/L
ALT	34 U/L
ALP	19 U/L
GGT	8 U/L
Cholinesterase	4385 U/L
CK	229 U/L
Calcium	2.58 mmol/L

Table 1. *Cont.*

Hematology	Value
Phosphorus	1.65 mmol/L
Magnesium	1.27 mmol/L
Sodium	156 mmol/L
Potassium	4.53 mmol/L
Chlorine	115 mmol/L
Iron	55 µg/dL

RBCs (Red Blood Cells), Hgb (Hemoglobin), Hct (Hematocrit), MCV (Mean Corpuscular Volume), MCH (Mean Corpuscular Hemoglobin), MCHC (Mean Corpuscular Hemoglobin Concentration), RDW (Red Cell Distribution Width), WBCs (White Blood Cells), NEUT (Neutrophils), LYMPH (Lymphocytes), MONO (Monocytes), EO (Eosinophils), BASO (Basophils), PLT (Platelets), MPV (Mean Platelet Volume), AST (Serum Glutamic Oxaloacetic Transaminase), ALT (Serum Glutamic Pyruvic Transaminase), ALP (Alkaline Phosphatase), GGT (Gamma Glutamil Transferase), CK (Creatine Kinase).

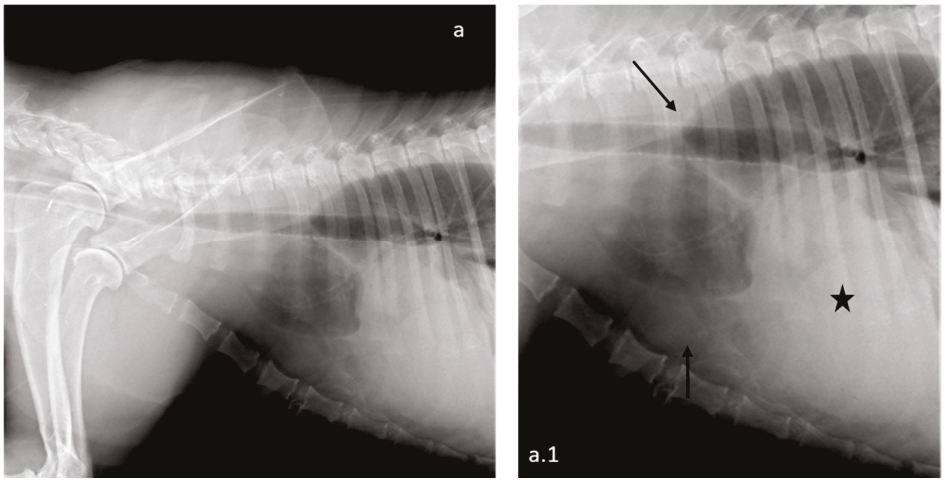


Figure 1. Thoracic radiographies: right lateral view (**a**) and details (**a.1**). The radiographic study is suggestive of severe bilateral pleural effusion, with dorsal mediastinal displacement and reduced pulmonary volume (arrows). Cardiac silhouette enlargement and increased radiopacity in the pericardial region are suggestive of pericardial effusion (star).

An APOCUS (Abdominal Point-Of-Care Ultrasound Scan) and an echocardiography were also performed. The APOCUS showed the presence of a large amount of free fluid in the abdominal cavity. The ultrasound examination also showed fluid accumulation in the thoracic cavity and pericardial space. Abdominal ultrasonography revealed hypoechoic masses within the left hepatic lobe, with heterogeneous internal echotexture and irregular margins, suggestive of a neoplastic process. Nodular lesions in the spleen and right testicle were detected.

On the Two-dimensional echocardiography, moderate pericardial effusion and moderate bi-atrial enlargement were visible (Figure 2). Other findings included pleural effusion associated with a distended caudal vena cava. A Doppler evaluation of transvalvular blood flow revealed mild–moderate mitral and tricuspid regurgitation. The combined absence of a recognizable P wave and irregular QRS complexes on simultaneous ECG tracing and the absence of the diastolic A wave on the pulsed-wave Doppler examination of the trans-mitral blood flow was suggestive of atrial fibrillation. No intrapericardial masses were visible.

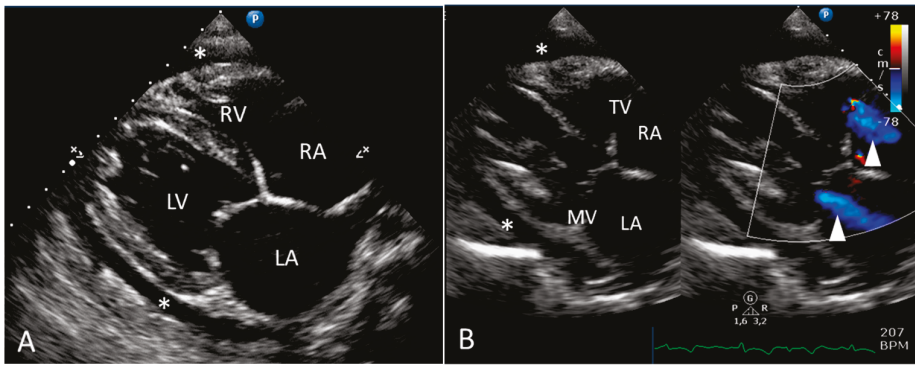


Figure 2. Two dimensional (2D) echocardiographic image (**A**) and combined 2D and color Doppler image (**B**) obtained from the right parasternal long axis view. The maximum depths in (**A**,**B**) are 16 cm and 15 cm, respectively. Moderate pericardial effusion (asterisks) and bi-atrial enlargement are evident (**A**). On Doppler interrogation of mitral and tricuspid blood flow (**B**), mild–moderate systolic regurgitant flow is visible (arrowheads). LA: left atrium; LV: left ventricle; MV: mitral valve; RA: right atrium; RV: right ventricle; TV: tricuspid valve.

Given the animal's serious clinical condition and the lack of viable therapeutic options to control or manage disease progression, euthanasia was chosen on compassionate grounds. The animal, anesthetized using the aforementioned protocol, was brought to a deep level of anesthesia and was subsequently administered a licensed euthanasia agent (Embutramide + Mebezonium Iodide + Tetracaine (Tanax®, MSD Animal Health S.r.l., Segrate, Italy) in accordance with animal welfare guidelines. Subsequently, the carcass was sent to the laboratories of the Istituto Zooprofilattico Sperimentale delle Venezie for necropsy and post-mortem diagnostic investigations.

2.2. Gross Pathology

At necropsy, approximately 2 L of abdominal sero-hemorrhagic effusion were observed. The left lateral and middle hepatic lobes were affected by whitish-yellow firm neoplastic masses (Figure 3a). The lateral lobe was severely enlarged and almost entirely occupied by the neoplasm (massive appearance), measuring 17.5 × 12 × 4 cm. The middle lobe was characterized by multiple coalescing nodules, with the largest (3.5 × 2 × 1.5 cm) displaying an umbilicated appearance. Small nodules (up to 1.5 cm in diameter) were also noted on the abdominal and pleural surfaces of the diaphragm (Figure 3c), on the mesentery, and on the surface of the spleen. The right spermatic cord was severely thickened due to the whitish nodular masses (Figure 3b), causing a displacement of the right testis and a focal irregular area characterized by a yellowish—brown and dry appearance. Mild catarrhal gastritis with hemorrhage, and catarrhal enteritis were noted. The kidneys showed multiple small, depressed nodules (2–3 mm) on the cortical surface (Figure 3d). Abundant sero-hemorrhagic pleural and moderate pericardial effusions were present in the thoracic cavity. Multiple neoplastic nodules were detected on both the visceral (Figure 3e) and parietal pericardial surfaces, with partial infiltration into the wall of the cranial vena cava. No gross lesions were observed on the central nervous system.

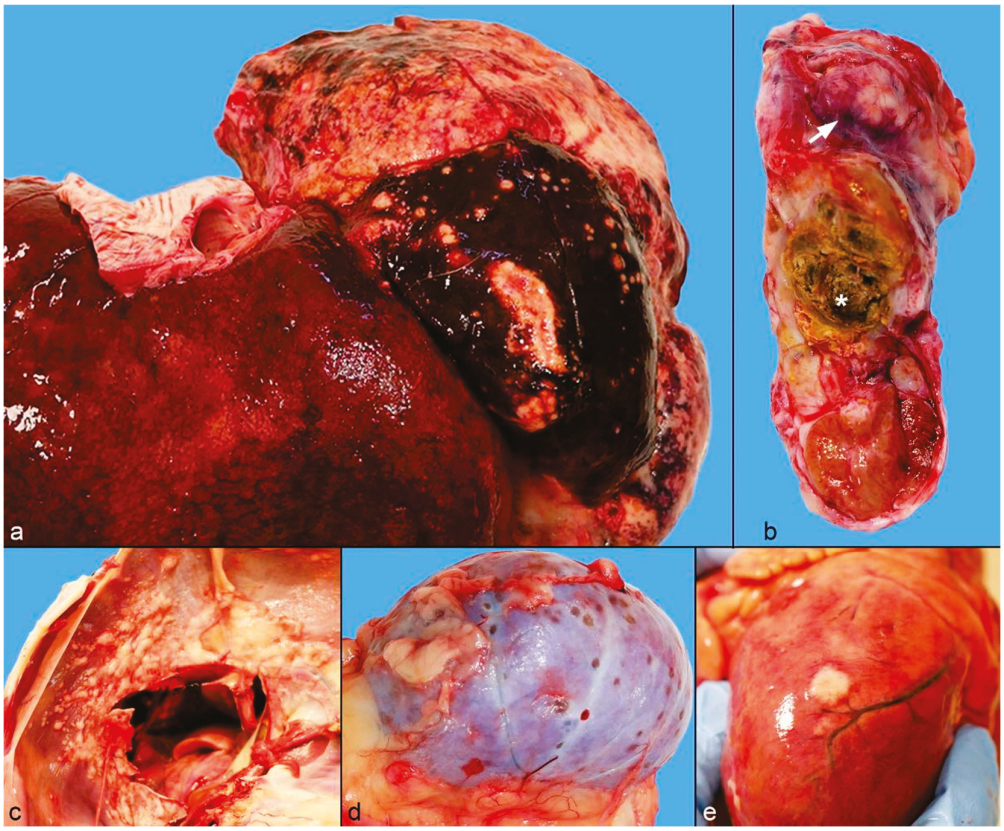


Figure 3. Gross findings of intrahepatic cholangiocarcinoma with disseminated metastases in a captive puma. (**a**) Whitish-yellow neoplastic masses in the left hepatic lobes. The left lateral lobe is severely enlarged and almost completely replaced by neoplasia. Multiple coalescing nodules, the largest with central depression and an umbilicated appearance, are visible in the left middle lobe. (**b**) Multiple whitish neoplastic nodules (arrow) are present within the spermatic cord, which is irregularly thickened, with an area of steatonecrosis (asterisk) and testis displacement. (**c**) Multiple coalescing whitish neoplastic nodules on the abdominal surface of the diaphragm. (**d**) Multiple small, depressed nodules on the cortical surface of the kidney. (**e**) Neoplastic nodule on the epicardium.

2.3. Cytological, Histological, and Immunohistochemical Findings

At necropsy, smears from the pericardial effusion were prepared for cytological analysis and stained with May Grünwald-Giemsa quick stain (MGG Quick Stain, code 04-090805M, Bio-Optica Milano S.p.A., Milan, Italy). Tissue samples from the liver, diaphragm, spermatic cord, testis, kidney, spleen, and heart were fixed in 10% neutral buffered formalin and processed for routine histopathologic examination.

Automated immunohistochemistry (IHC) was performed on the Discovery ULTRA system (Roche, Ventana Medical Systems Inc., Tucson, AZ, USA) using the primary antibodies anti-pan cytokeratin (CK, clone AE1-AE3, code M3515, Dako, Glostrup, Denmark), CK7 (clone OV-TL, code M7018, Dako), CK20 (clone Ks20.8, code M7019, Dako), and the von Willebrand factor (vWF, polyclonal antibody, code A0082, Dako, Glostrup, Denmark). Detailed information about the IHC protocols is listed in Table 2. After detection, sections were counterstained with Mayer's hematoxylin (Hematoxylin II, Ventana, Roche Diagnostics S.p.A., Monza, Italy).

Cytological smears from the pericardial effusion were composed of numerous cohesive clusters of cuboidal cells (Figure 4a). Occasional acinar structures with a central amorphous pink–violet material were observed. Neoplastic cells exhibited an intermediate to high nucleus-to-cytoplasm ratio, scant and occasionally vacuolated cytoplasm, round paracentral nuclei with unevenly granular chromatin, variably visible nucleoli, and moder-

ate anisokaryosis. These findings were consistent with an epithelial neoplasm. A mixed inflammatory infiltrate consisting mainly of neutrophils and macrophages was also present along with yellowish crystals (consistent with hematoidin and bilirubin).

Table 2. Antibody panels and immunohistochemistry protocols applied to the intrahepatic metastatic cholangiocarcinoma of a captive puma.

Antibody	Antigen Retrieval	Antibody Incubation	Detection System
Pan cytokeratin	CC1 [a,b]; 95 °C; 32 min	1:50; 24 min; RT	Discovery OmniMap anti Mouse HRP [b] 16 min; Discovery Chromomap DAB [b]
CK7	CC1; 95 °C; 64 min	1:20; 1 h; RT	Discovery Anti Mouse HQ [b] 36 °C 8 min; Discovery anti HQ HRP [b] 8 min; Discovery Chromomap DAB
CK20	CC1; 95 °C; 40 min	1:20; 1 h; 37 °C	Discovery Anti Mouse HQ 36 °C 8 min; Discovery anti HQ HRP 8 min; Discovery Chromomap DAB
von Willebrand factor (vWF)	Protease 2; 36 °C; 8 min	1:200; 32 min; RT	Discovery OmniMap anti Rabbit HRPb 16 min; Discovery Chromomap DAB [b]

DAB, 3′-3′-Diaminobenzidine; HRP, Horseradish Peroxidase; RT, room temperature. [a] CC1: cell conditioning solution 1 (pH 8.4). [b] Roche, Ventana Medical Systems (Tucson, AZ, USA).

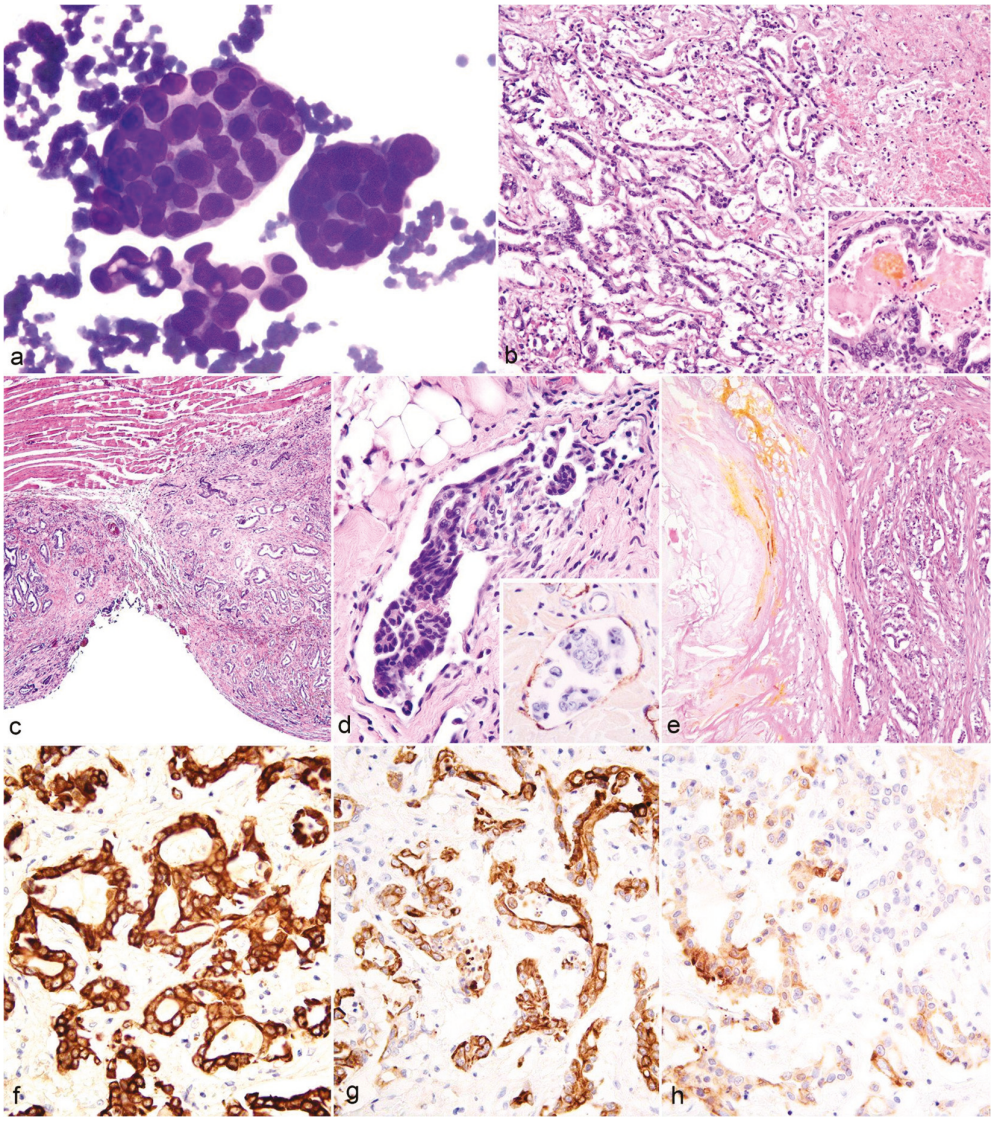


Figure 4. Cytologic, histologic, and immunohistochemical findings of intrahepatic cholangiocarcinoma with disseminated metastases in a captive puma. (**a**) Clusters of epithelial neoplastic cells in

cytological smears from the pericardial effusion, found using May Grünwald-Giemsa staining. (**b**) Liver: irregular neoplastic tubular structures lined a cuboidal to low columnar epithelium, with lytic necrosis and hemorrhage (right) and occasional intraluminal yellowish material, consistent with biliary pigment (inset). Hematoxylin and Eosin (H&E) stains: (**c**) neoplastic metastatic nodules on the diaphragmatic surface consisting of tubular and acinar structures and desmoplastic stroma. (**d**) Lymphovascular invasion of neoplastic cells within the vessels of the diaphragm (H&E), with endothelial immunohistochemical staining with the von Willebrand factor (inset, DAB Chromogen). (**e**) Neoplastic infiltration of the spermatic cord, adjacent to an area of steatonecrosis (left). (**f**) Diffuse strong cytoplasmic staining of neoplastic cells with pan-CKs AE1-AE3, DAB Chromogen. (**g**) Diffuse, intermediate-to-high intensity staining of neoplastic cells with CK7, DAB Chromogen. (**h**) Multifocal, low-to-moderate staining of neoplastic cells with CK20, DAB Chromogen.

Histologically, the liver showed an infiltrative, non-capsulated neoplastic epithelial neoplasm (Figure 4b) composed of tubular and acinar structures embedded in a variable amount of desmoplastic stroma. Neoplastic cells were cuboidal to low columnar, with scant eosinophilic cytoplasm and a large, round nucleus, with vesicular chromatin and variably prominent central nucleoli. The mitotic range was 0–5 per high power field (0.237 mm^2). The neoplastic tubules and acini contained proteinaceous material, necrotic debris, and sporadic yellowish material, consistent with biliary pigment (Figure 4b, inset). Extensive areas of necrosis and hemorrhage were noted. Similar neoplastic lesions were also observed in the diaphragm (on both the pleural and peritoneal surfaces) (Figure 3c), mesentery, spermatic cord, kidney, spleen, pericardium, and kidney. Neoplastic lymphovascular invasion was observed (Figure 4d), most frequently in the diaphragmatic metastatic nodules, and confirmed with von Willebrand factor (vWF) immunohistochemistry (IHC) for endothelial cells (Figure 4d inset).

The neoplastic cells in hepatic sections displayed diffuse strong cytoplasmic staining with pan-CKs (Figure 4f), diffuse CK7 staining of intermediate-to-high intensity (Figure 4g), and multifocal, low-to-moderate CK20 staining (Figure 4h). In the metastatic nodules, the pan-CKs were diffusely positive, while CK7 staining was less frequent and less intense, with a greater decrease in CK20 expression.

The histologic and immunohistochemical findings were consistent with an intrahepatic metastatic CCA.

2.4. Microbiological Findings

A microbiological examination for aerobic and anaerobic microorganisms was performed on specimens and swabs collected during the post-mortem examination. Tissue aspirates were collected from the liver and intestinal contents with sterile swabs (Copan Italia S.p.A., Brescia, Italy). Samples were then diluted in 1 mL of a nutrient broth (HIB, Heart Infusion Broth, Conda, Madrid, Spain), and 10 and 100 µL of bacterial suspensions were then inoculated into solid media and broths, respectively, as described below. The evaluation of aerobic microorganisms was conducted using a nutrient medium (BA, Blood Agar Base n°2, Biolife, Milan, Italy) with 5% defibrinated sheep blood (Allevamento Blood, Teramo, Italy), a nutrient broth (HIB), and selective *Enterobacteriaceae* media (McConkey agar, Oxoid, Basingstoke, UK). Cultures were inoculated and incubated at 37 ± 1 °C in aerobic conditions. An assessment of anaerobic microorganisms was performed using a nutrient medium (BA), selective media for *C. perfringens* (TSC Agar Base, Biolife, Milan, Italy), and a fluid Thioglycollate medium (THG, Liofilchem, Roseto degli Abruzzi, Teramo, Italy). The cultures were inoculated and incubated at 37 ± 1 °C under anaerobic conditions. *E. coli* was detected at low levels in the liver samples. From the intestinal swabs, coagulase-negative Staphylococci, *E. coli*, and *C. perfringens* were isolated.

A section of intestine (approximately 5 mm^3) was homogenized in 0.8 mL of Phosphate-Buffered Saline (PBS) supplemented with antibiotics (PBS-A: 10,000 IU/mL penicillin G,

10 mg/mL streptomycin, 5000 IU/mL nystatin, and 0.25 mg/mL gentamicin sulfate) using a Tissue Lyser (QIAGEN, Hilden, Germany) at 30 Hz for 3 min. One hundred microliters (100 µL) of the intestinal homogenate was used for viral DNA/RNA extraction, which was performed with the KingFisher™ Flex Purification System (Life Technologies, Carlsbad, CA, USA) and the ID Gene® Mag Universal Extraction Kit (IDvet, Grabels, France), following the manufacturer's instructions. The extracted DNA was tested for feline parvovirus (FPV) using a Real-Time PCR, targeting a region of the VP2 gene [9] with the QuantiFast Pathogen PCR + IC Kit (QIAGEN, Hilden, Germany). Meanwhile, the extracted RNA was tested for feline coronavirus (FCoV) using a Real-Time RT-PCR with the VetMAX™ FIP Dual IPC Kit (Thermo Fisher Scientific, Waltham, MA, USA). All molecular assays were performed on the CFX 96 Deep Well Real-Time PCR system (BioRad Laboratories Inc., Hercules, CA, USA). The intestinal sample tested negative for FPV and positive for FCoV in the Real-Time PCR and Real-Time RT-PCR assays [10].

3. Discussion

Captive populations of large felids often exhibit high stability due to dedicated care and long-term monitoring [1,11]. These animals are susceptible to several disorders caused by environmental influences, infectious agents, and genetic factors. These diseases can ultimately lead to the decline of these populations and the effectiveness of conservation strategies. Furthermore, it is important to assess the risk of zoonotic diseases affecting large cats in captivity, as they have the potential for a significant impact on human health both as environmental sentinels and susceptible hosts for infectious or zoonotic diseases [12–21].

Neoplastic diseases represent an important cause of morbidity and mortality in captive felids [1,5,22–26]. The increased longevity of wild captive animals is likely to contribute to the increased incidence of cancer in captive felids compared to their free-ranging counterparts [5,27]. In addition, the increased exposure to environmental pollutants, infectious agents, and genetic predisposition may promote the development of neoplastic disease [1,28,29].

Intrahepatic CCAs are malignant tumors that arise from the biliary duct epithelium and present either as a single mass or as coalescing, nodular proliferations on the surface of the liver and throughout the parenchyma [30]. Although primary hepatobiliary tumors are rare in domestic animals, CCAs seem to be the most common non-hematopoietic hepatic tumors in domestic cats [31]. In cats, CAAs originating from intrahepatic bile ducts are far more common than those arising from extrahepatic bile ducts or the gallbladder [30,32].

Cholangiocarcinoma typically occurs in domestic cats over 10 years of age and no consistent breed or sex predisposition has been reported [30]. However, some authors have suggested that there may be a higher prevalence in male cats [28,33].

Given the paucity of available reports, intrahepatic or extrahepatic CAA appears to be an infrequently documented condition in captive felids and is often associated with widespread metastases, although it may be underdiagnosed [3,6,34], and is often associated with widespread metastases. CCAs exhibit a highly invasive growth pattern and frequently metastasize in all species, with a reported metastasis rate of 78% in cats, according to one survey [30,35]. In captive pumas, digestive neoplasms, including hepatic tumors, are the most commonly reported after endocrine and neuroendocrine neoplasms [4]. Although rare cases of benign hepatic cholangioma have been documented, to the best of the author's knowledge, only a single case report of intrahepatic CCA in a captive puma has been reported thus far [4,6]. Similar to the present report, this case presented with a primary tumor characterized by both massive and multinodular growth, and multiorgan metastases to the lung, stomach, kidney, heart, and diaphragm [6].

In our case report, the histological appearance of the tumor, with tubular and acinar structures, allowed for the exclusion of hepatocellular carcinoma as a differential diagnosis, supported by the immunoreactivity to pan-CKs, and CK7 [36]. While canine CCAs have demonstrated a CK7+/CK20- immunophenotype, CK20 expression has been reported in the feline species, similar to our case [37].

In this case report, an elderly captive puma presented with mild gastrointestinal signs (vomiting and diarrhea), abdominal distension, and subtle respiratory changes. In the initial clinical assessment, the signs appeared relatively mild and non-specific. However, after sedation, palpation and a diagnostic evaluation revealed a far more severe clinical picture with chronic multiorgan involvement. Imaging studies revealed the presence of multiple cavitary effusions—including abdominal, pleural, and pericardial fluid—along with significant cardiopulmonary compromise. Other cardiac abnormalities included atrioventricular valve insufficiency, likely due to degenerative valve disease, and atrial fibrillation.

According to the recent literature [13,38–40], the hematology and biochemical findings indicate a mild increase in the total RBC count, as well as the hemoglobin and hematocrit values, which, contextualized within the clinical picture, may be associated with a mild to moderate state of dehydration [41]. Cell morphology reveals alterations indicative of an inflammatory or infectious state (anisocytosis, echinocytosis, neutrophil toxicity, Döhle bodies, and monocytosis) [42]. The biochemical parameters do not show any particular alterations. The intestine tested positive for FCoV and negative for FPV. Feline coronavirus is a ubiquitous RNA virus present in cats and non-domestic felid populations worldwide. FCoV is primarily an enteric virus, and infection is often asymptomatic or presents as enteritis, although outbreaks of feline infectious peritonitis (FIP) have been reported in captive felids [43–45]. In this report, the presence of FCoV, in the absence of FIP-related lesions, suggests an infection confined to the intestine, which may or may not have contributed to the gastrointestinal signs.

The etiology of bile duct tumors remains unclear, although several risk factors have been proposed to play a role in the development of CAAs in domestic animals and humans, including chronic inflammation of the biliary tract, cholestasis, fluke infestation, or chemical agents [46]. In humans, infection with the liver flukes *Opisthorchis viverrini* and *Clonorchis sinensis* has been recognized a risk factor for CCA in Southeast Asia [47,48]. Some studies in cats have suggested a similar association with *Clonorchis sinensis* infestation, but the limited data make it difficult to draw conclusions about the role of parasitism in the development of CCA in this species [30,49]. Ascarid, such as those caused by *Toxascaris leonina*, are not currently recognized as risk factors for hepatic neoplasia in felids. Carcinogenic chemicals, such as furans and nitrosamines, have been shown to induce CCA in laboratory rodents and dogs, respectively [50,51]. Chronic inflammation, regardless of cause, may stimulate increased biliary epithelial cell replication, which could facilitate tumor development over time [30]. In a survey of hepatic lesions in captive felids, non-neoplastic biliary tract alterations including biliary hyperplasia, cysts, and cholestasis were present in 35% of pumas, and portal hepatitis was present in 24% of cases [25,30]. However, no evidence of predisposing factors was identified in the present case.

4. Conclusions

To the best of our knowledge, this is the first reported case of CCA in a captive puma, documented through a comprehensive diagnostic investigation (ante- and post-mortem). The effective management of captive wild felids requires tailored diagnostic protocols to ascertain a diagnosis, both in vivo and post-mortem. A multidisciplinary team comprising veterinary clinicians, anesthetists, radiologists, infectious disease specialists, and patholo-

gists is essential. Furthermore, although the expertise of individual professionals is highly regarded, a knowledge gap emerges when considering the specific characteristics and management of chronic pathologies in these animals.

Author Contributions: Conceptualization, E.M., G.M.D.B. and G.F.; methodology, C.Z., A.B. and M.C.; validation, C.Z. and E.M.; formal analysis, E.M.; investigation, G.M.D.B., A.B. and E.M.; resources, G.M.D.B.; data curation, E.M. and G.F.; writing—original draft preparation, E.M. and G.F.; writing—review and editing, E.M., C.Z., G.M.D.B., C.Z., G.D.Z., M.C., F.M., A.B., C.G., F.Z. and G.F.; visualization, A.B.; supervision, E.M.; project administration, G.M.D.B.; funding acquisition G.M.D.B. All authors have read and agreed to the published version of the manuscript.

Funding: This research received no external funding.

Institutional Review Board Statement: Ethical review and approval were waived for this study because it was performed within the routine diagnostic activity of the Veterinary Teaching Hospital, at the University of Padua—OVUD and Istituto Zooprofilattico Sperimentale delle Venezie.

Informed Consent Statement: This study was performed during the clinical activity of the Veterinary Teaching Hospital, at the University of Padua—OVUD; the owner signed informed consent forms for the authorization to use personal data and privacy notices were also signed and collected. Clinical data and biological samples were collected by clinicians for diagnostic purposes at the request of the animal's owner. Gross pathology and histopathology images were collected and published with the animal owner's consent. The animal care and procedures are in accordance with the Directive 2010/63/EU of the European parliament and of the council of 22 September 2010 on the protection of animals for scientific purposes (National law: D.L. 26/2014).

Data Availability Statement: All the data are available in the present manuscript.

Acknowledgments: The authors express their gratefulness to Giacomo Ferrari and the staff of "*Wild Side of Magic, Tiger Experience*", to Annalisa Stefani for the hematological and biochemical analyses, and to Erica Melchiotti for the immunohistochemical analyses.

Conflicts of Interest: The authors declare no conflicts of interest.

References

1. Junginger, J.; Hansmann, F.; Herder, V.; Lehmbecker, A.; Peters, M.; Beyerbach, M.; Wohlsein, P.; Baumgärtner, W. Pathology in Captive Wild Felids at German Zoological Gardens. *PLoS ONE* **2015**, *10*, e0130573. [CrossRef] [PubMed]
2. Thalwitzer, S.; Wachter, B.; Robert, N.; Wibbelt, G.; Muller, T.; Lonzer, J.; Meli, M.L.; Bay, G.; Hofer, H.; Lutz, H. Seroprevalences to Viral Pathogens in Free-Ranging and Captive Cheetahs (Acinonyx Jubatus) on Namibian Farmland. *Clin. Vaccine Immunol.* **2010**, *17*, 232–238. [CrossRef] [PubMed]
3. Lepri, E.; Sforna, M.; Chiara, B.; Giovanni, V. Cholangiocarcinoma of intrahepatic bile ducts with disseminated metastases in an african lion (Panthera leo). *J. Zoo Wildl. Med.* **2013**, *44*, 509–512. [CrossRef] [PubMed]
4. Mathieu, A.; Garner, M.M. A Retrospective Study of Neoplasia in Nondomestic Felids in Human Care, with a Comparative Literature Review. *J. Zoo Wildl. Med.* **2021**, *52*, 413–426. [CrossRef]
5. D'Aquino, I.; Piegari, G.; Casciaro, S.M.; Prisco, F.; Rosato, G.; Silvestre, P.; Degli Uberti, B.; Capasso, M.; Laricchiuta, P.; Paciello, O.; et al. An Overview of Neoplasia in Captive Wild Felids in Southern Italy Zoos. *Front. Vet. Sci.* **2022**, *9*, 899481. [CrossRef]
6. Cho, H.-S.; Oh, Y. Cholangiocarcinoma with Multiple Organ Metastasis in a Captive Puma (*Puma concolor*). *Pak. J. Zool.* **2021**, *54*, 487–490. [CrossRef]
7. Daigle, C.L.; Brown, J.L.; Carlstead, K.; Pukazhenthi, B.; Freeman, E.W.; Snider, R.J. Multi-Institutional Survey of Social, Management, Husbandry and Environmental Factors for the SSP African Lion Panthera Leo Population: Examining the Effects of a Breeding Moratorium in Relation to Reproductive Success. *Int. Zoo Yearb.* **2015**, *49*, 198–213. [CrossRef]
8. Coon, C.A.C.; Nichols, B.C.; McDonald, Z.; Stoner, D.C. Effects of Land-Use Change and Prey Abundance on the Body Condition of an Obligate Carnivore at the Wildland-Urban Interface. *Landsc. Urban. Plan.* **2019**, *192*, 103648. [CrossRef]
9. Carrino, M.; Tassoni, L.; Campalto, M.; Cavicchio, L.; Mion, M.; Corrò, M.; Natale, A.; Beato, M.S. Molecular Investigation of Recent Canine Parvovirus-2 (CPV-2) in Italy Revealed Distinct Clustering. *Viruses* **2022**, *14*, 917. [CrossRef]

10. Decaro, N.; Elia, G.; Martella, V.; Desario, C.; Campolo, M.; Di Trani, L.; Tarsitano, E.; Tempesta, M.; Buonavoglia, C. A Real-Time PCR Assay for Rapid Detection and Quantitation of Canine Parvovirus Type 2 in the Feces of Dogs. *Vet. Microbiol.* **2005**, *105*, 19–28. [CrossRef]
11. Owston, M.A.; Ramsay, E.C.; Rotstein, D.S. Neoplasia in Felids at the Knoxville Zoological Gardens, 1979–2003. *J. Zoo Wildl. Med.* **2008**, *39*, 608–613. [CrossRef] [PubMed]
12. Larsson, M.H.M.A.; Flores, A.S.; Fedullo, J.D.L.; Teixeira, R.H.F.; Mirandola, R.M.S.; Ito, F.H.; Pessoa, R.B.; Itikawa, P.H. Biochemical Parameters of Wild Felids (Panthera Leo and Panthera Tigris Altaica) Kept in Captivity. *Semin. Agrar.* **2017**, *38*, 791–800. [CrossRef]
13. Dias, F.G.G.; de Brito, C.C.C.; Paulino Júnior, D.; Branco, C.H.; de Brito, V.J.S.C.; Tinasi, A.L.S.N.; Alves, M.Z.; Badoco, F.R.; Rodrigues, M.A. Parâmetros Hematológicos de Gatos Selvagens Das Espécies *Puma concolor*, Panthera Onca e Panthera Leo Mantidos Em Cativeiro. *Res. Soc. Dev.* **2022**, *11*, e35711629288. [CrossRef]
14. Mazzotta, E.; Foiani, G.; De Benedictis, G.M.; Fiore, E.; Natale, A.; Spagnolo, E.; Vascellari, M.; Cento, G.; Corrò, M. Salmonella Enteritidis Fatal Septicemia with Meningoencephalitis in a Tiger (Panthera Tigris) Cub. *Animals* **2022**, *12*, 2490. [CrossRef]
15. Bevins, S.N.; Carver, S.; Boydston, E.E.; Lyren, L.M.; Alldredge, M.; Logan, K.A.; Riley, S.P.D.; Fisher, R.N.; Vickers, T.W.; Boyce, W.; et al. Three Pathogens in Sympatric Populations of Pumas, Bobcats, and Domestic Cats: Implications for Infectious Disease Transmission. *PLoS ONE* **2012**, *7*, e31403. [CrossRef]
16. Terio, K.A.; Mitchell, E.; Walzer, C.; Schmidt-Küntzel, A.; Marker, L.; Citino, S. Diseases Impacting Captive and Free-Ranging Cheetahs. In *Cheetahs: Biology and Conservation: Biodiversity of the World: Conservation from Genes to Landscapes*; Academic Press: Cambridge, MA, USA, 2018; pp. 349–364. ISBN 9780128041208.
17. Martella, V.; Campolo, M.; Lorusso, E.; Cavicchio, P.; Camero, M.; Bellacicco, A.L.; Decaro, N.; Elia, G.; Greco, G.; Corrente, M.; et al. Norovirus in Captive Lion Cub (Panthera Leo). *Emerg. Infect. Dis.* **2007**, *13*, 1071–1073. [CrossRef]
18. Coleman, K.K.; Bemis, I.G. Avian Influenza Virus Infections in Felines: A Systematic Review of Two Decades of Literature. *Open Forum Infect. Dis.* **2025**, *12*, ofaf261. [CrossRef]
19. Redrobe, S.P. Avian Influenza H5N1: A Review of the Current Situation and Relevance to Zoos. *Int. Zoo Yearb.* **2007**, *41*, 96–109. [CrossRef]
20. Beirne, P. COVID-19 as an Anthroponosis: Toward a Nonspeciesist Criminology of Human-to-Animal Pathogen Transmission. *Int. J. Crime Justice Soc. Democr.* **2021**, *10*, 139–152. [CrossRef]
21. Fernández-Bellon, H.; Rodon, J.; Fernández-Bastit, L.; Almagro, V.; Padilla-Solé, P.; Lorca-Oró, C.; Valle, R.; Roca, N.; Grazioli, S.; Trogu, T.; et al. Monitoring Natural SARS-CoV-2 Infection in Lions (Panthera Leo) at the Barcelona Zoo: Viral Dynamics and Host Responses. *Viruses* **2021**, *13*, 1683. [CrossRef]
22. Schiffmann, C.; Unterhitzenberger, G.; Ortmann, S. Extrahepatic Biliary Tract Pathologies in Mammalian Species of Zoo Animals and Wildlife: A Review. *J. Basic Appl. Zool.* **2020**, *81*, 20. [CrossRef]
23. Grillini, M.; Frangipane di Regalbono, A.; Tessarin, C.; Beraldo, P.; Cassini, R.; Marchiori, E.; Simonato, G. Evidence of Dirofilaria Immitis in Felids in North-Eastern Italy. *Pathogens* **2022**, *11*, 1216. [CrossRef] [PubMed]
24. Ready, Z.C.; LoBato, D.; LaDouceur, E.; Garner, M.M.; Cushing, A.C. Melanocytic neoplasia in panthera species: Clinical presentations, pathologic findings and responses to treatment. *J. Zoo Wildl. Med.* **2023**, *53*, 844–854. [CrossRef] [PubMed]
25. Bernard, J.M.; Newkirk, K.M.; McRee, A.E.; Whittemore, J.C.; Ramsay, E.C. Hepatic Lesions in 90 Captive Nondomestic Felids Presented for Autopsy. *Vet. Pathol.* **2015**, *52*, 369–376. [CrossRef]
26. Kloft, H.M.; Ramsay, E.C.; Sula, M.M. Neoplasia in Captive Panthera Species. *J. Comp. Pathol.* **2019**, *166*, 35–44. [CrossRef]
27. Tidière, M.; Gaillard, J.-M.; Berger, V.; Müller, D.W.H.; Bingaman Lackey, L.; Gimenez, O.; Clauss, M.; Lemaître, J.-F. Comparative Analyses of Longevity and Senescence Reveal Variable Survival Benefits of Living in Zoos across Mammals. *Sci. Rep.* **2016**, *6*, 36361. [CrossRef]
28. Van Sprundel, R.G.H.M.; van den Ingh, T.S.G.A.M.; Guscetti, F.; Kershaw, O.; van Wolferen, M.E.; Rothuizen, J.; Spee, B. Classification of Primary Hepatic Tumours in the Cat. *Vet. J.* **2014**, *202*, 255–266. [CrossRef]
29. McAloose, D.; Newton, A.L. Wildlife Cancer: A Conservation Perspective. *Nat. Rev. Cancer* **2009**, *9*, 517–526. [CrossRef]
30. Cullen, J.M. Tumors of the Liver and Gallbladder. In *Tumors in Domestic Animals*; Wiley: Hoboken, NJ, USA, 2016; pp. 602–631.
31. Balkman, C. Hepatobiliary Neoplasia in Dogs and Cats. *Vet. Clin. N. Am. Small Anim. Pract.* **2009**, *39*, 617–625. [CrossRef]
32. Patnaik, A.K. A Morphologic and Immunocytochemical Study of Hepatic Neoplasms in Cats. *Vet. Pathol.* **1992**, *29*, 405–415. [CrossRef]
33. Post, G.; Patnaik, A.K. Nonhematopoietic Hepatic Neoplasms in Cats: 21 Cases (1983–1988). *J. Am. Vet. Med. Assoc.* **1992**, *201*, 1080–1082. [CrossRef] [PubMed]
34. Sakai, H.; Yanai, T.; Yonemaru, K.; Hirata, A.; Masegi, T. Gallbladder Adenocarcinomas in Two Captive African Lions (Panthera Leo). *J. Zoo Wildl. Med.* **2003**, *34*, 302–306. [CrossRef] [PubMed]
35. Carpenter, J.L.; Andrews, L.K.; Holzworth, J. Tumors and Tumor-like Lesions. In *Diseases of the Cat*; W.B. Saunders Company: Philadelphia, PA, USA, 1987; pp. 406–596. ISBN 0-7216-4863-4.

36. Ramos-Vara, J.A.; Miller, M.A.; Johnson, G.C. Immunohistochemical Characterization of Canine Hyperplastic Hepatic Lesions and Hepatocellular and Biliary Neoplasms with Monoclonal Antibody Hepatocyte Paraffin 1 and a Monoclonal Antibody to Cytokeratin 7. *Vet. Pathol.* **2001**, *38*, 636–643. [CrossRef] [PubMed]
37. Espinosa de Los Monteros, A.; Fernández, A.; Millán, M.Y.; Rodríguez, F.; Herráez, P.; Martín de Las Mulas, J. Coordinate Expression of Cytokeratins 7 and 20 in Feline and Canine Carcinomas. *Vet. Pathol.* **1999**, *36*, 179–190. [CrossRef]
38. Foster, G.W.; Cunningham, M.W. Hematology and Serum Chemistry Values for Free-Ranging Florida Panther Neonates with a Comparison to Adult Panther Values. *J. Wildl. Dis.* **2009**, *45*, 857–862. [CrossRef]
39. Hawkey, C.M.; Hart, M.G. Haematological Reference Values for Adult Pumas, Lions, Tigers, Leopards, Jaguars and Cheetahs. *Res. Vet. Sci.* **1986**, *41*, 268–269. [CrossRef]
40. Proverbio, D.; Perego, R.; Baggiani, L.; Ravasio, G.; Giambellini, D.; Spada, E. Hematological and Biochemical Reference Values in Healthy Captive Tigers (Panthera Tigris). *Animals* **2021**, *11*, 3440. [CrossRef]
41. Thrall, M.A.; Weiser, G.; Allison, R.W.; Campbell, T.W. *Veterinary Hematology, Clinical Chemistry, and Cytology*, 3rd ed.; John Wiley & Sons: Hoboken, NJ, USA, 2022; ISBN 978-1-119-28652-3.
42. Harvey, J.W. The Feline Blood Film: 2. Leukocyte and Platelet Morphology. *J. Feline Med. Surg.* **2017**, *19*, 747–757. [CrossRef]
43. Tasker, S.; Addie, D.D.; Egberink, H.; Hofmann-Lehmann, R.; Hosie, M.J.; Truyen, U.; Belák, S.; Boucraut-Baralon, C.; Frymus, T.; Lloret, A.; et al. Feline Infectious Peritonitis: European Advisory Board on Cat Diseases Guidelines. *Viruses* **2023**, *15*, 1847. [CrossRef]
44. Stout, A.E.; André, N.M.; Whittaker, G.R. Feline coronavirus and feline infectious peritonitis in nondomestic felid species. *J. Zoo Wildl. Med.* **2021**, *52*, 14–27. [CrossRef]
45. Stephenson, N.; Swift, P.; Moeller, R.B.; Worth, S.J.; Foley, J. Feline Infectious Peritonitis in a Mountain Lion (*Puma concolor*), California, USA. *J. Wildl. Dis.* **2013**, *49*, 408–412. [CrossRef] [PubMed]
46. Chapman, R.W. Risk Factors for Biliary Tract Carcinogenesis. *Ann. Oncol.* **1999**, *10*, S308–S312. [CrossRef]
47. Sripa, B.; Mairiang, E.; Thinkhamrop, B.; Laha, T.; Kaewkes, S.; Sithithaworn, P.; Tessana, S.; Loukas, A.; Brindley, P.J.; Bethony, J.M. Advanced Periductal Fibrosis from Infection with the Carcinogenic Human Liver Fluke Opisthorchis Viverrini Correlates with Elevated Levels of Interleukin-6. *Hepatology* **2009**, *50*, 1273–1281. [CrossRef]
48. Loeuillard, E.; Fischbach, S.R.; Gores, G.J.; Ilyas, S.I. Animal Models of Cholangiocarcinoma. *Biochim. Biophys. Acta-Mol. Basis Dis.* **2019**, *1865*, 982–992. [CrossRef] [PubMed]
49. Chang, H.P. Pathological Changes in the Intrahepatic Bile Ducts of Cats (Felis Catus) Infested with Clonorchis Sinensis. *J. Pathol. Bacteriol.* **1965**, *89*, 357–364. [CrossRef]
50. Maronpot, R.R.; Giles, H.D.; Dykes, D.J.; Irwin, R.D. Furan-Induced Hepatic Cholangiocarcinomas in Fischer 344 Rats. *Toxicol. Pathol.* **1991**, *19*, 561–570. [CrossRef]
51. Hirao, K.; Matsumura, K.; Imagawa, A.; Enomoto, Y.; Hosogi, Y. Primary Neoplasms in Dog Liver Induced by Diethylnitrosamine. *Cancer Res.* **1974**, *34*, 1870–1882.

Disclaimer/Publisher's Note: The statements, opinions and data contained in all publications are solely those of the individual author(s) and contributor(s) and not of MDPI and/or the editor(s). MDPI and/or the editor(s) disclaim responsibility for any injury to people or property resulting from any ideas, methods, instructions or products referred to in the content.

animals

MDPI

Article

When Antlers Grow Abnormally: A Hidden Disease Behind Common Cervid Trophy Deformities, Introducing Pedunculitis Chronica Deformans

Farkas Süközd [1,*,†], István Lakatos [2,3,†], Ádám Ürmös [4], Réka Karkas [5], Ákos Süközd [6], Gábor Palánki [7], Attila Arany Tóth [8], Károly Erdélyi [9], Mihály Misó [10], Péter Gőbölös [7], Katalin Posta [11], Ferenc Kovács [2], Szilamér Ferenczi [11,12], Győző Horváth [13], László Szemethy [13,‡] and Zsuzsanna Szőke [3,‡]

1 Department of Pathology, Albert Szent-Györgyi Medical School, University of Szeged, 6720 Szeged, Hungary
2 Department of Regional Game Management, Ministry of Agriculture, 1052 Budapest, Hungary; istvan.lakatos@am.gov.hu (I.L.); ferenc.kovacs@am.gov.hu (F.K.)
3 Agrobiotechnology and Precision Breeding for Food Security National Laboratory, Institute of Genetics and Biotechnology, Department of Animal Biotechnology, Hungarian University of Agriculture and Life Sciences, 2100 Godollo, Hungary; ferenczine.szoke.zsuzsanna@uni-mate.hu
4 Genome Integrity and DNA Repair Core Group, Hungarian Centre of Excellence for Molecular Medicine (HCEMM), 6728 Szeged, Hungary; adam.urmos@hcemm.eu
5 Department of Oncotherapy, University of Szeged, 6720 Szeged, Hungary; karkas.reka@med.u-szeged.hu
6 Department of Orthopaedics, Semmelweis University, 1083 Budapest, Hungary; sukosd.akos@semmelweis.hu
7 Gyulaj Forestry & Hunting Plc., 7090 Tamasi, Hungary; palanki@gyulajzrt.hu (G.P.); titkarsag@gyulaj.hu (P.G.)
8 Department of Surgery, University of Veterinary Medicine, 1078 Budapest, Hungary; aaranytoth@yahoo.com
9 HUN-REN Veterinary Medical Research Institute, 1143 Budapest, Hungary; erdelyi.karoly@vmri.hun-ren.hu
10 Guth Forestry, NYÍRERDŐ Forestry Co., 4400 Nyiregyhaza, Hungary; mihalym825@gmail.com
11 Department of Microbiology and Applied Biotechnology, Institute of Genetics and Biotechnology, Hungarian University of Agriculture and Life Sciences, 2100 Godollo, Hungary; posta.katalin@uni-mate.hu (K.P.); ferenczi.szilamer@koki.hun-ren.hu (S.F.)
12 Laboratory of Molecular Neuroendocrinology, Institute of Experimental Medicine, 1083 Budapest, Hungary
13 Institute of Biology, Faculty of Sciences, University of Pécs, 7624 Pecs, Hungary; hgypte@gamma.ttk.pte.hu (G.H.); szemethy.laszlo@pte.hu (L.S.)
* Correspondence: sukosd.farkas@gmail.com
† These authors contributed equally to this work.
‡ These authors contributed equally to this work.

Simple Summary: Antlers are the fastest regenerating bone tissue in the animal kingdom and serve as biological superstructures reflecting genetics, nutrition, environmental conditions, and the quality of wildlife management. The most common forms of antler abnormalities have traditionally been attributed to injuries sustained during mating fights. However, their pathological background has not been systematically investigated. By examining the skulls, pedicles, and antlers of three deer species, we identified a pathological condition—Pedunculitis Chronica Deformans (PCD)—with features overlapping previously reported cases in other cervids. Resembling chronic osteomyelitis, PCD likely arises from inflammation during antler casting and regrowth. We present a novel scoring system to assess the severity of lesions and offer detailed anatomical and pathological characterizations to aid diagnosis. Our findings challenge the long-held assumption that most antler deformities are trauma-related and highlight the need for standardized recognition and deeper investigation into deer health and antler biology.

Abstract: For centuries, the most prevalent antler abnormalities observed worldwide have been attributed to trauma. However, detailed pathological investigation of these cases has not yet been carried out. In free-living fallow deer (*Dama dama*), we identified a chronic osteomyelitis-like condition—Pedunculitis Chronica Deformans (PCD)—using pathological and radiological diagnostics. We propose that inflammation during post-casting wound

healing and consequent scar formation can trigger the development of PCD. In this study, we characterize the pathomorphology of PCD and introduce a scoring system to describe its severity. Furthermore, we describe the histoanatomy of the junction between the pedicle and the surrounding skin—an area essential for the integrity of the integument—which, when compromised, may predispose cervids to PCD. Our findings suggest that the most common antler abnormality results from a pathological fracture associated with PCD, which can be further complicated by fatal meningoencephalitis and brain abscesses. PCD-related lesions, while less frequently observed, can also be identified in roe deer (*Capreolus capreolus*) and red deer (*Cervus elaphus*), with species-specific differences. These findings overlap with cases reported in other cervid species, suggesting a more general disorder of antler formation. Describing this condition provides a basis for assessing its epidemiology and understanding its relevance to wildlife health.

Keywords: fallow deer antler; antler abnormality; pathological fracture; Pedunculitis Chronica Deformans; cervids

1. Introduction

Antlers are unique outgrowths that develop exclusively in males, with the exception of reindeer (*Rangifer tarandus*), specific to the Cervidae family that reflect the biological condition of the animal, exhibiting inherited phenotypes, nutritional status, environmental impacts, and the quality of wildlife management [1,2]. Notably, antlers represent the fastest-growing and regenerating bone tissue found in nature [1]. While antler abnormalities are rare [3], they hold significant value as trophies among hunters. The earliest scientific publication on antler deformities dates back to 1900 [4].

Rutting-related injuries and the resulting abnormal healing processes are currently regarded as the most widely accepted explanation for antler malformations [1,5–8]. The antler and pedicle together constitute a functional anatomical unit [9]. Consequently, it has been widely accepted that pedicle injuries are closely associated with antler deformities [6]. The factors that predispose this unit—primarily evolved for intraspecific combat [10,11]—to structural vulnerability remain poorly understood. Limb injuries have been reported to exert teratogenic effects on the contralateral antler, most likely via a complex and still obscure pathomechanism [1,5,6]. As secondary sexual characteristics, antlers are highly responsive to endocrine signals; in particular, reduced testosterone levels can induce distinct malformations such as “perruque-head”, “cactus buck”, or “antleroma”, which are generally distinguishable from other types of anomalies [12]. Moreover, nutritional factors, especially mineral intake, can significantly affect the integrity and quality of newly forming antlers [2].

Hungary is internationally recognized for the exceptional quality of its deer populations, with two world-record fallow deer (*Dama dama*) trophies originating from the northeastern region [13]. However, since the latter half of the 20th century, a notable increase in antler deformities has been observed in this species [14]. Similar abnormalities have also been observed in red deer (*Cervus elaphus*) and roe deer (*Capreolus capreolus*). Despite the significance of this issue, there are, unfortunately, no peer-reviewed English-language publications on the topic from Hungary or the broader Central European region. The only available source is a single case report published in the *Hungarian Veterinary Journal* over fifteen years ago, which did not include any epidemiological data [15]. In response, our research group was established as part of a government initiative to investigate and clarify the problem.

Additionally, such abnormalities have been noted among the elk (*Cervus canadensis*) population in Northern Arizona, including the Hualapai Indian Reservation [6]. Instances of comparable malformations were also documented on mule deer (*Odocoileus hemionus*) in central Utah in the mid-20th century [5], as well as in North-Central Kansas, where extreme antler malformations identical in morphology have been noted [12]. Particularly concerning are the distinctive osseous deformities involving the pedicle—the frontal bone outgrowth serving as the basis of the antler—and adjacent skull region. Such anomalies have been documented in white-tailed deer (*Odocoileus virginianus*) from Georgia, USA, where they were linked to peri-peduncular purulent inflammation and associated meningoencephalitis or intracranial abscess complications [16–18]. A comprehensive study conducted across 12 US states and four Canadian provinces found that 2.2% of 4500 white-tailed deer exhibited central nervous system inflammation coupled with pedicle, skull, and antler abnormalities [16]. This highly spatially variable disease was detected in 9 (35%) cases in a radio-collared male white-tailed deer population of 26 individuals aged 2.5 years or older in Kent County, Maryland, USA [19]. Despite these findings, the true extent and epidemiology of antler deformities remain unclear.

Without precise descriptions, it is not possible to distinguish between pathological abnormalities and physiological variants. In other words, proper treatment can only be carried out with the correct diagnosis. This approach allows the collection of a homogeneous group of diseased animals on which the causes can be properly investigated. Once identified, a treatment strategy can be developed. In addition, trophy evaluation procedures exclude cases showing such deformities, as the specimens concerned do not meet the criteria for standard evaluation https://cic-wildlife.org/about-the-tes-2/ (accessed on 18 May 2025). Consequently, the extent of these conditions remains underreported and poorly understood. Reliable epidemiological analysis requires a precise and consistently applicable phenotypic classification system, one that clearly distinguishes pathological changes from natural morphological variation and allows for straightforward subclassification, even in applied contexts such as trophy evaluation.

Our objective was to assemble a comprehensive collection of aberrant trophies from all three free-ranging cervid species in Hungary, focusing specifically on cases where the underlying cause could not be determined based on current scientific knowledge [1,5–8].

We hypothesized that the observable lesions could be graded by severity and, based on this assumption, developed a preliminary scoring system to characterize them. This system is intended as a foundation that can be refined through consensus-based classification using a larger sample set. In addition to macroscopic evaluation, we examined the surrounding soft tissues of both wet and dried antlers using histological and radiological methods, with the aim of identifying pathological patterns that might associate the lesions with known disease categories. We also sought to explore potential predisposing factors. Ultimately, if the constellation of findings supports the recognition of a distinct pathological entity, we intend to propose a formal nomenclature to ensure its clear and consistent identification in future research and evaluations.

2. Materials and Methods

2.1. Source of Anomalous and Normal Trophies

The study examined 50 *Dama dama* (DD) anomalous antler trophies collected between 2017 and 2021 from Hungary, Central Europe. A morphology control group (MCG) served as the basis of comparison to this evaluation, except for age, antler main beam length, and brow tine length. It comprised 24 trophies from Gúth, Hungary https://nyirerdo.hu/guthi-erdeszet/ (accessed on 18 May 2025), where no antler anomalies were reported during the same period. Trophies in both groups are from animals between 4 and 12 years

old. Additionally, five cases of roe deer (*Capreolus capreolus*, CC) and three cases of red deer (*Cervus elaphus*, CE) were analyzed. During the course of the trophy collection, it became evident that DD was considerably more affected than CC or CE and exhibited a broader spectrum of lesions compared to the latter two species. The observed overlap in the nature of distortions across species suggested that a common underlying process might be manifesting in species-specific ways. Consequently, we opted for a separate evaluation by species, applying the same diagnostic criteria. Given the notable differences in case numbers, we also employed distinct statistical approaches for each species. This strategy aimed to determine whether the phenomenon was species-specific or indicative of a broader condition affecting cervids in general.

The trophy-based age estimation was performed following established methods described in the literature [20,21]. The classic CIC (International Council for Game and Wildlife Conservation) trophy evaluation includes the assessment of age, antler beam length, and brow tine length measurements; therefore, we could use these data from the Hungarian Trophy Register (HTR) [22]. From this, a trophy register control group (TRCG) was formed from 2912 antler evaluation sheets, excluding those marked as "deformed", "injured pedicle", or "diseased pedicle".

2.2. Macroscopic Examinations

A standardized protocol was developed for the macroscopic evaluation. The morphological deviation of the trophy from the normal was evaluated for the roses (R), antlers (A), pedicle (P) and skull (S) with 3, 6, 7, and 6 parameters, respectively, for a total of 22 parameters on both sides in 24 healthy (MCG) and 50 abnormal cases (Table 1). An experienced wildlife manager (IL) with decades of trophy assessment experience and a consultant surgical pathologist (FS) conducted the initial assessments. To ensure inter-observer reliability, two additional trained observers (R.K. and A.S.) independently evaluated a subset of trophies.

Table 1. Detailed description of the RAPS features.

Rose	R1	Lack of continuity in the grain of the rose is longer than 5 mm but less than 1 cm.
	R2	Rose deformity (also visible on cast antlers).
	R3	Loss of rose granularity is greater than 1 cm.
Antler	A1	Supernumerary tine originating from the rose can be a sign of an extra antler bud.
	A2	Visually assessed length asymmetry between the left and right brow tines.
	A2.1	Difference from trophy register control group (TRCG), which is derived from data of the Hungarian Trophy Register after exclusions of cases marked abnormal.
	A3	Visually determined asymmetry in the main beam length between the two sides.
	A3.1	Difference relative to the TRCG.
	A4	Absence of antlers or aberrant antler beams.
Pedicle	P1	Pitting on the proximal surface of the pedicle.
	P2	The pedicle deformity characteristic of PCD in Fallow deer (*Dama dama*) is the deviation from the regular circle diameter more than 4 mm, also visible with the eye.
	P3	Shortening of the pedicle more than physiological.
	P4	Widening of the pedicle beyond the normal extent.
	P5	Peduncle fistula.
	P6	Free casting plane from which does not protrude any antler–bony protuberance.
	P7	More than fifty percent of the casting plane of the pedicle is in or below the plane of the skull, which is considered to be the absence of it.

Table 1. *Cont.*

Skull	S1	The pitting extends on the skull surface.
	S2	Spongy remodelation of skull bones where the cavities are larger than at intertrabecular spaces in spongious bone.
	S3	Discohesion along the interosseous suture.
	S4	Separation of the cortical bones is an independent sign of bone displacement.
	S5	A fistula mouth opens distant from the pedicle on the skull.
	S6	The center of the pedicle has shifted significantly, mostly towards the brow ridge.

Furthermore, the RAPS features were sorted into 4 severity grades based on their pathomorphological background (Table 2).

Table 2. Severity grades of the RAPS features.

Grade I	R1, A1, P1, S1
Grade II	P2, R2, A2, A2.1, P2, P3, P4, S2, S6
Grade III	R3, A3, A3.1, P5, P6, S4
Grade IV	A4, P7, S3, S4

We also analyzed a left abnormal antler in the velvet phase that was found incidentally within our study area. Above the frontal tine, an additional, aberrant branch of nearly equal length was observed. Near the site corresponding to the expected ablation surface, a highly irregular plane covered with blood coagulum was visible. The velvet skin showed no epithelial defects, fractures, or any abnormalities indicative of mechanical trauma.

2.3. Analysis of Pedicle Ellipticity

We tested whether PCD induces elliptical distortion of the pedicle using the minor (d) and major (D) axes of pedicles (modelled as ellipses). Ellipticity was quantified using the distance of the foci from the origin ($\sqrt{(D/2)^2 - (d/2)^2}$) and eccentricity ($foci\ distance/D$).

The diameters D and d were measured on both sides at the highest measurable plane of the pedicle in 33 healthy and 14 abnormal fallow deer (*Dama dama*) trophies using a caliper (see Table S5). In the healthy group, the average values for D and d were 44 mm and 41 mm, respectively, with an average calculated difference of 3.12 mm. In the abnormal group, the mean D was 64.4 mm and d was 47.4 mm, resulting in an average difference of 10.78 mm.

Both shape descriptors, ellipticity and eccentricity, showed statistically significant differences between the healthy and abnormal groups, as determined by two-sample Wilcoxon tests (p-values: 4.371×10^{-7} and 1.426×10^{-4}, respectively).

2.4. Microscopic Examinations

Five DD heads, each showing abnormality, both in the velvet phase and with fully ossified (dry) antlers, were collected. All specimens exhibited evident abnormalities on at least one antler side and included soft tissues such as skin, connective tissue, muscle, and brain. The proximal ca. 20 cm long segment of the antler, the whole antler in case of obvious abnormality, and the pedicle attached to the antler and the surrounding skull roof, including all soft tissues and brain, were cut out and fixed in 10% formalin for at least one week. These preserves were sawed into 4 mm thick slices with a meat industry band saw. Visible alterations were excised for microscopic examination. Electric decalcification using a Tissue-tek TDE 30 Decalcifier system (ref.: 1428 Sakura Finetek Europe, Alphen aan den

Rijn, The Netherlands) was used for three weeks with continuous monitoring. Samples that couldn't be sectioned after this time were further handled for one month in a solution of 70% ethanol containing 5% phenol or Q path DC3 (VWR ref.: 09128300. Vienna, Austria) for three weeks.

After decalcification, traditional pathological techniques (embedding in a paraffin block and making 5 micrometer sections) were employed, including Hematoxylin & Eosin, PAS, Warthin-Starry, Giemsa, Zhiel-Neelsen, and Wade-Fite staining to detect potential pathogens. In four cases of yearling stag trophies, parallel 4 mm thick slices were sawed from the pedicle, and after decalcification, microscopic examinations were conducted.

2.5. Radiological Examinations

Computed tomography (CT) images of 16 deer trophies and 2 complete heads with soft tissue were acquired with a single slice GE CT Scanner Model CT/e (GE Healthcare, Chicago, IL, USA). Acquisition parameters for CT images were as follows: helical mode, 512 × 512 matrix, 1 mm slice thickness, 1 mm image interval, 120 kVp, 20–120 mA, and bone convolution kernel. The preparations were placed in a prone position on the CT bed with the aid of foam wedges. Transverse images of the skull were obtained perpendicular to the hard palate. The scanned area ranged from the occipital bone to the mid-orbital region, including the antler tree. The osseous structures on DICOM images were evaluated using a window width of 4000 and a level of 400 HU.

2.6. Statistical Analysis

The presence of morphological anomalies (R, A, P, and S) was recorded with a value of 1 for presence and 0 for absence, separately for each side. A2.1 and A3.1 were considered as present if the brow tine and main beam length were lower than the bottom 20% and 5% quantiles of the distributions of brow tine and main beam length in the TRCG of the corresponding age and side. Pairwise comparisons between means, unless stated otherwise, were carried out using two-sample Wilcoxon tests, with Holm's multiple testing correction. Computations were performed using the R language and environment version 4.4.3 [23], figures were drawn using ggplot2 [24], ggpubr [25], ggraph [26], and pheatmap [27].

3. Results and Discussion

3.1. Epidemiology of Cervidae with Aberrant Trophies

The analysis of our Southern Hungarian non-species-selected aberrant trophy collection from 2017 to 2021 showed significant occurrences in antler anomalies in various free-living Cervidae species. The incidence of aberrant trophies among fallow deer (*Dama dama*, DD) was notably higher than in roe deer (*Capreolus capreolus*, CC) and red deer (*Cervus elaphus*, CE), with ten times more anomalies in DD compared to CC (50 vs. 5) and approximately 16 times more than CE (50 vs. 3). When adjusted for population density, DD appears to be impacted the most by these deformities: 34 times more frequently than CC and 50 times more than CE, suggesting a unique vulnerability (Figure 1, Table S1).

3.2. Health Condition of Fallow Deer (Dama dama) with Aberrant Trophies

In the Hungarian trophy register (HTR), data on age, main beam, and brow tine sizes are recorded for normal trophies from 2017 to 2020; a total of 2924 register sheets documented these parameters regarding our study region. Of these, 12 cases (0.4%) included pedicle abnormalities and were excluded from analysis. The remaining 2912 records formed our trophy register control group for brow tine and main beam sizes across age groups. This low incidence rate in records contrasts sharply with the 40–80% frequency of abnormalities observed during harvests in this region [14] (Figure 2a). The discrepancy

may be due to the lack of standardized methods for describing malformed trophies. Scoring systems such as those by the International Council for Game and Wildlife Conservation (CIC score, https://www.cic-wildlife.org (accessed on 18 May 2025)) and Boone and Crockett Club (B&C score, https://www.boone-crockett.org (accessed on 18 May 2025)) are well-suited for assessing healthy trophy sizes and forms but lack guidelines for classifying malformations (Figure 2b). Consequently, only sporadic notes on these anomalies appear in trophy evaluations. The remaining 2900 healthy cases formed our trophy register control group (TRCG), with an average age of 9 years, compared to an average age of 7.74 years for aberrant DD trophies ($p < 0.0001$) (Figure 2c,d).



Figure 1. A striking scene from Kocsola (Southern Hungary, Central Europe) showing three fallow deer (*Dama dama*) with antler development issues. Their upright head posture suggests that their antlers did not break off during fights but failed to develop properly. To compensate for the resulting weight imbalance, they developed hypertrophied neck muscles to maintain normal head position and vision (Photo: András Molnár).

3.3. Characteristics of Fallow Deer (Dama dama) Aberrant Trophies

Aberrant trophies exhibit pathological variations that are not observed under physiological conditions, for example, significant absence of rose granularity, remarkable differences between beam lengths, pedicle deformities, and skull abnormalities. Additionally, they often show the accumulation of unique anatomical variations rarely observed under normal circumstances, such as supernumerary tines. To characterize these abnormalities, which we dubbed RAPS features, we examined three malformations of the antler rose (R1–R3), six of the antler (A1, A2, A2.1, A3, A3.1, and A4), seven of the pedicle (P1–P7), and six of the surrounding skull (S1–S6), altogether 22 characteristics (Table 1). Since specific combinations of RAPS symptoms can also indicate disease severity, we established four grades of disease progression (Table 2 and Table S4, Figure 3) based on this framework, which can serve as a starting point for a consensus classification based on a larger cohort in the future.

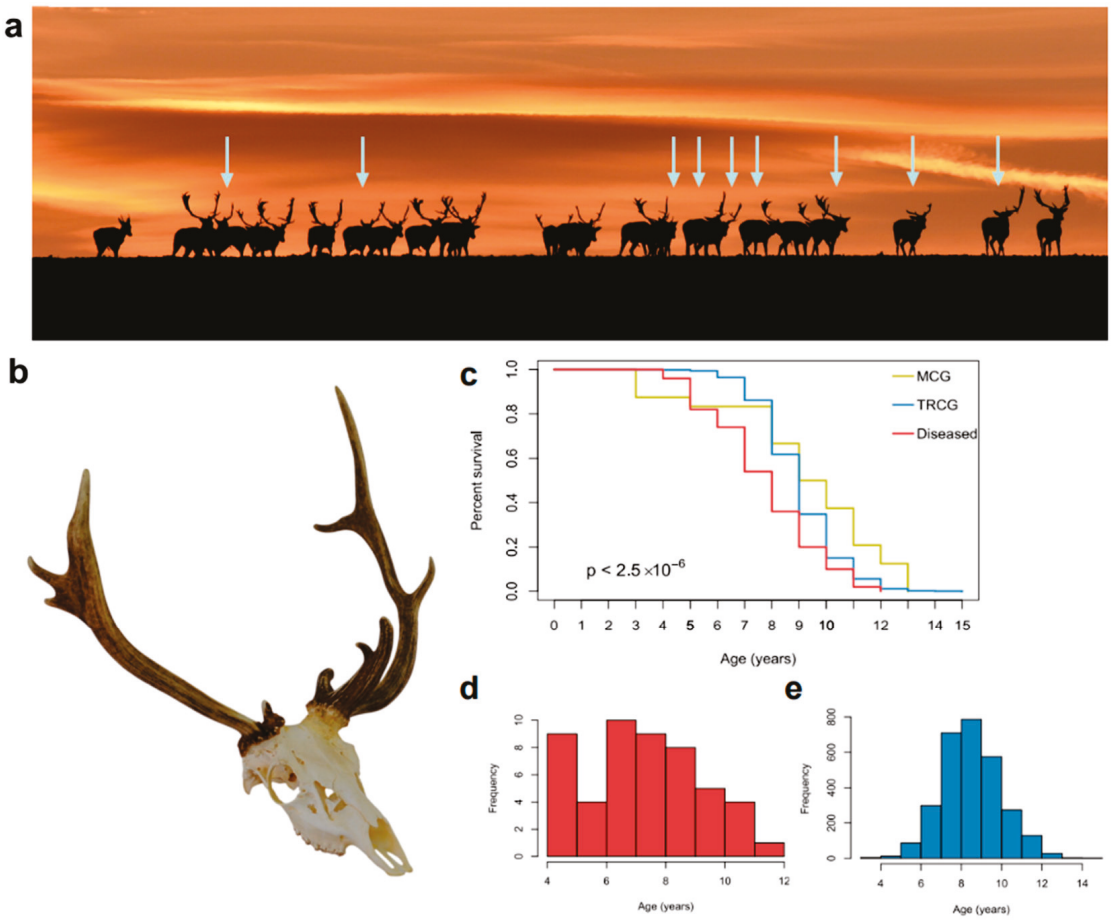


Figure 2. Antler abnormality in Southern Hungary. (**a**) A herd of fallow deer *(Dama dama*, DD) at sunset in the Kocsola region (Southern Hungary). Notably, 9 out of 23 individuals (39%) exhibit visible antler abnormalities (arrows) (Photo: Sándor Juhos). (**b**) Individuals with antler anomalies, like those shown in the photograph, are excluded from trophy evaluations, making it difficult to obtain reliable data on their prevalence. (**c**) Although hunting-related mortality is influenced by planned culling, it is still associated with the animal's health status. Kaplan-Meier survival analysis revealed reduced life expectancy for animals with deformed antlers compared with healthy members of Morphological (MCG, n = 50) and Trophy Register (TRCG, n = 2912) Control Group (Kaplan-Meier curves contrasted with log-rank test). (**d**) The average age of the healthy (not showing antler abnormality) individuals to be evaluated is 9 years. (**e**) Compared to an average age of 7.74 years for aberrant DD trophies ($p < 0.0001$).

We compared the frequency of RAPS features between a healthy morphological control group (MCG) and aberrant-antlered DD cohorts. On the MCG (24 trophies) from the control, we inspected 1056 morphological features, of which 16 (1.52%) showed anomalies. In contrast, among aberrant DD trophies (50 trophies, 2200 inspected features), 989 pathological features were detected (44.95%) (Table S4). The Fisher's exact test ($p < 0.0001$) confirmed that the RAPS characteristics were highly discriminative between these groups (Figure 4a). All of the RAPS features showed a consistently higher prevalence in the aberrant trophies than in the MCG, with 20 of the 22 being statistically significant discriminators (Pearson's Chi-square tests, see Table S4).

While antler abnormalities are generally considered unilateral lesions, our study suggests a bilateral condition (Table S4). The noticeable asymmetry likely reflects varying environmental factors, primarily infections and secondary traumas, as previously suggested [28]. This chronic process, which can span several years and multiple antler shedding cycles, becomes more pronounced on the side that is more severely affected.

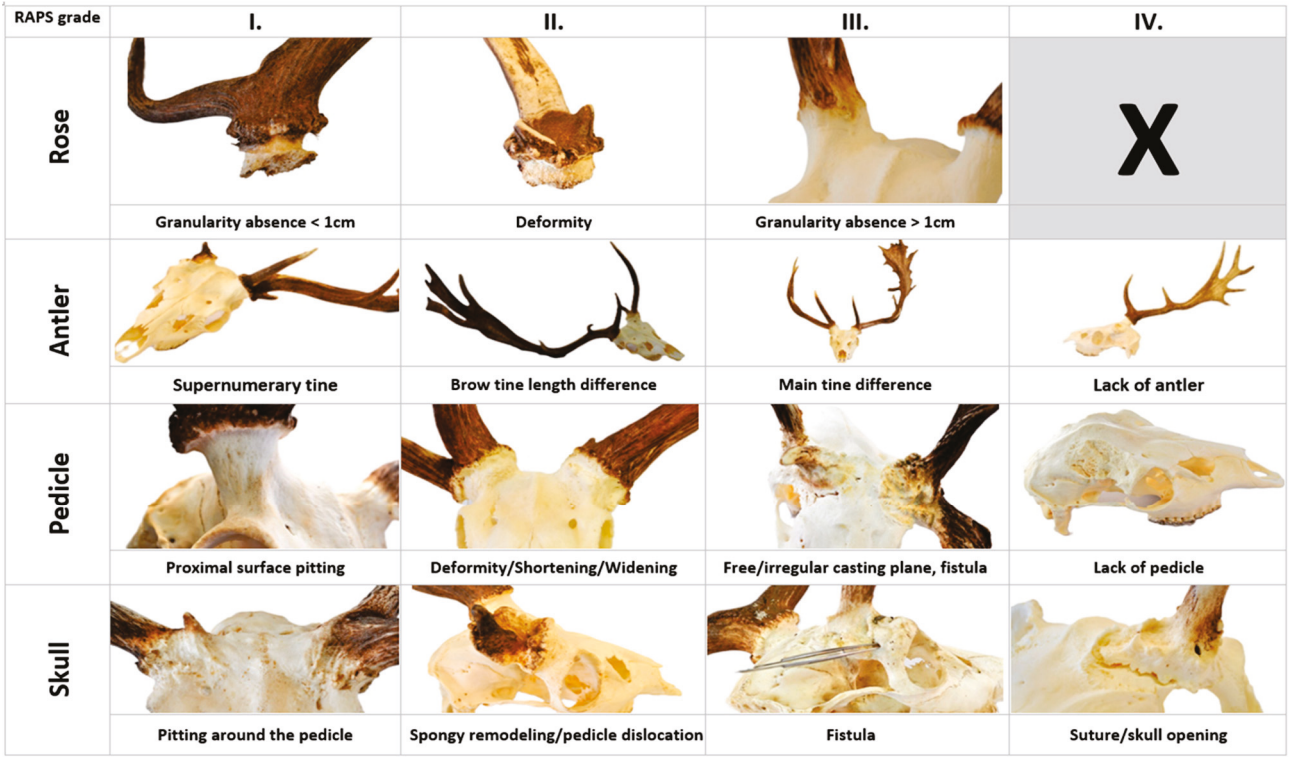


Figure 3. The assessment of the RAPS (rose/pedicle/antler/skull) features describes Pedunculitis Chronica Deformans (PCD) and its severity. The RAPS features can be grouped into three grades for the rose and four for the pedicle/antler/skull. **Grade I:** Lack of continuity in the grain of the rose is longer than 5 mm but less than 1 cm. (**R1**). A supernumerary tine originating from the rose can be a sign of an extra antler bud (**A1**). Pitting on the proximal surface of the pedicle (**P1**). The pitting extends to the skull surface (**S1**). **Grade II:** A deformity of the rose that is visible to the eye is a deviation from a regular circle. This is not independent of the pedicle deformity (**P2**) and visible on cast antlers, too (**R2**). The length difference between the two sides of the brow tines (**A2**) and the difference from the trophy register control group (**A2.1**), which is derived from data of the Hungarian trophy register after exclusion of cases marked abnormal (see text). The pedicle deformity characteristic of PCD in fallow deer (*Dama dama*) is a difference in the major and minor axis lengths of more than 4 mm, also visible by eye (**P2**). Shortening (**P3**) and widening (**P4**) of the pedicle beyond normal extent. Spongy remodeling of skull bones where the cavities are larger than at intertrabecular spaces in cancellous bone (**S2**) or visible in the center of the pedicle has shifted significantly, mostly towards the brow ridge (**S6**). **Grade III:** Loss of rose granularity is greater than 1 cm (**R3**). The difference in length of the main beams relative to each other (**A3**) and the difference relative to the Trophy Register Control group (**A3.1**). A pedicle fistula (**P5**, or a free casting plane without any protruding antler-bony structure (**P6**). A fistula mouth opens distant from the pedicle on the skull (**S4**). **Grade IV:** Absence of antlers or aberrant antler beams (**A4**). More than fifty percent of the casting plane of the pedicle is in or below the plane of the skull, which is considered to be the absence of it (**P7**). Discohesion along the interosseous suture (**S3**) or separation of cortical bone independently is a sign of bone displacement (**S4**).

In our study, the most frequently observed anomaly was compared to the TRCG—a reduction in antler main beam length (A3.1, 92%) (Figure 4b,c). Additionally, visible asymmetry between the main beam length was frequently noted (A3, 69%).

The second most frequent change was the pedicle surface pitting (P.1, 80%), particularly visible on the frontal area, described earlier by Davidson et al. as a hallmark of this anomaly [29]. Histological and radiological analyses revealed that this accompanies the superficial form of chronic osteomyelitis [30–32] (Figure 5d,e).

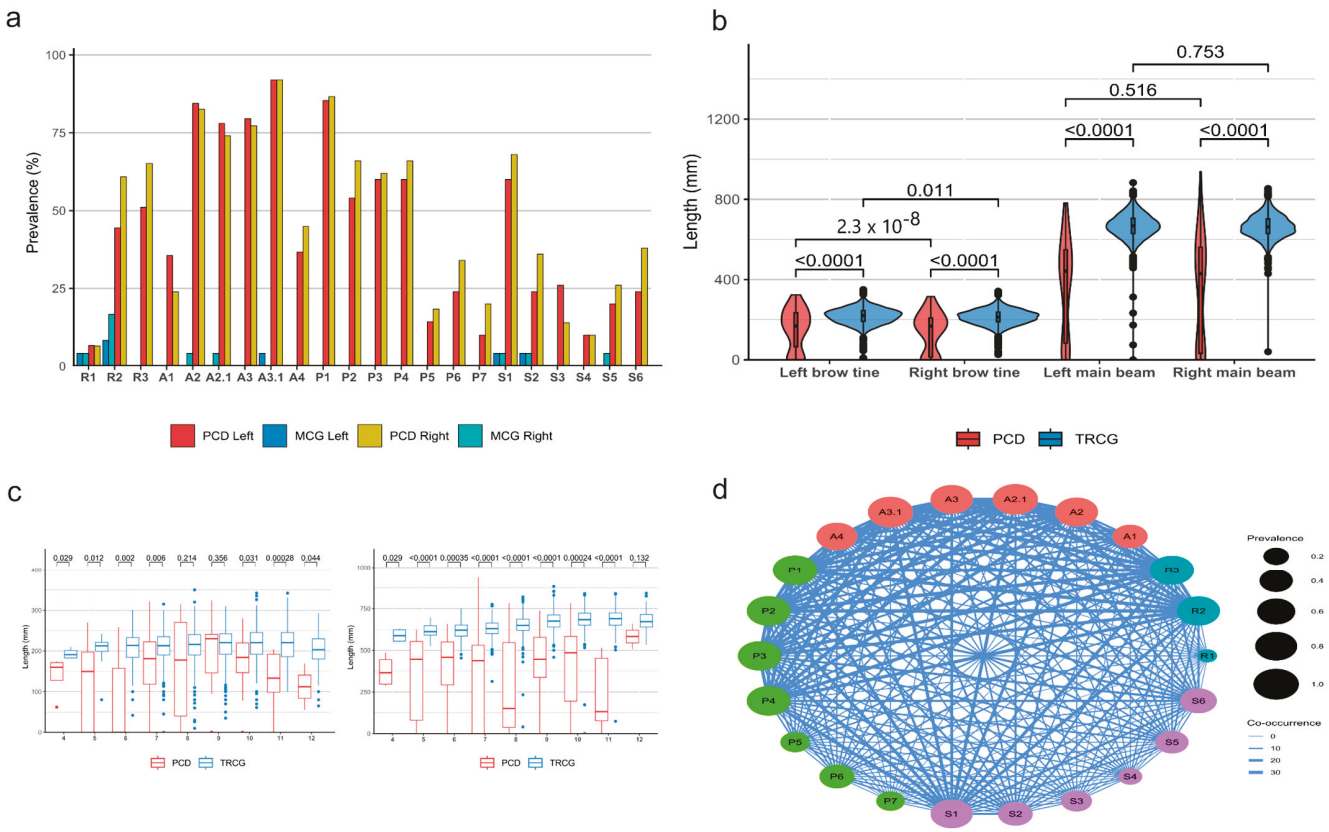


Figure 4. Prevalence of RAPS features representing anomalies of the rose (R), antler (A), pedicle (P), and skull (S) in fallow deer (*Dama dama*). (**a**) Fifty trophies with antler abnormalities (left side: red and right side: yellow) and 24 trophies from a healthy (morphological) control group (left side: blue and right side: teal) were evaluated. Some anomalies were observed in the healthy cohort, but at low frequency (Table S4). (**b**) Length differences between anomalous DD (red) and healthy (blue) brow tines and main beams by side in comparison to the trophy register control group (TRCG, n = 2912). Numbers represent p-values of two-sample Wilcoxon tests, with Holm's multiple testing correction. Differences between sides were non-significant in all but one of the comparisons (TRCG brow tine), reflecting the notion that such differences often arise as a result of normal physiology. (**c**) Differences in brow tine and main beam lengths between abnormal DD individuals and the TRCG by age group. Numbers represent p-values of two-sample Wilcoxon tests, with Holm's correction. Brow tine lengths were significantly different in most, and main beam lengths in all but one age of the groups. (**d**) The graph shows the co-occurrence of the RAPS symptom in the 50 anomalous DD trophies. The size of the nodes represents the prevalence of the symptom in the cohort, and the width of the edges represents the number of co-occurrences between the two symptoms. The data were aggregated by side (see also Figure S1).

This often extended to the adjacent skull (S1, 64%). The rose deformity (R2, 48%) and discontinuity of rose granularity greater than 1 cm (R3, 53%) were also prevalent, appearing in roughly half of the cases. A prior study has noted the association of R2 with unilateral antler deficiencies [28]. In our study, R2 was significantly associated with visible brow tine difference (A2, 76%), while R3 correlated with shortened brow tine (A2.1, 76%) and main beam (A3.1) length. Furthermore, both R2 and R3 were significantly associated with all pedicle and skull anomalies (Figure 4c and Table S4), indicating that the more severe rose abnormalities can act as an indicator of subcutaneous issues. The irregular, also called "dirty" casting plane (P6, 29%) in shed antlers is a well-documented phenomenon [1], associated with an insufficient testosterone peak [33]. However, only a third (29%) of the trophies displayed this characteristic, as many were collected outside the casting period. The shortening and widening of the pedicle is a physiological event that occurs with age [1,34].

Based on subjective judgment, shortening (P3) was considered more pronounced than normal in 61% of abnormal cases and widening (P4) in 63%. However, the pedicle deformity (P2), defined as a deviation from a regular circle shape, appeared in over half of our cases (60%), serving as a usable marker of disease recognition in DD but not in CC and CE. On average, the larger diameter of the near-circular cross-section in healthy antlers exceeded the smaller diameter by only 3.12 mm. In contrast, antlers from abnormal trophies showed a threefold greater difference, averaging 10.78 mm (Table S5). Both elliptical shape descriptors—ellipticity and eccentricity—differed significantly between the healthy and abnormal groups (p-values: 4.371×10^{-7} and 1.426×10^{-4}, respectively). To the best of our knowledge, these are the first results evaluating pedicle ellipticity, based on which we have proposed a 4 mm threshold between the diameters D and d. According to this criterion, 13 out of 66 antlers (19%) from the normal group fell within the abnormal range, while 3 out of 28 antlers (10%) from the PCD group did not exceed the threshold (Table S5). More precise conclusions will require further studies with larger sample sizes.

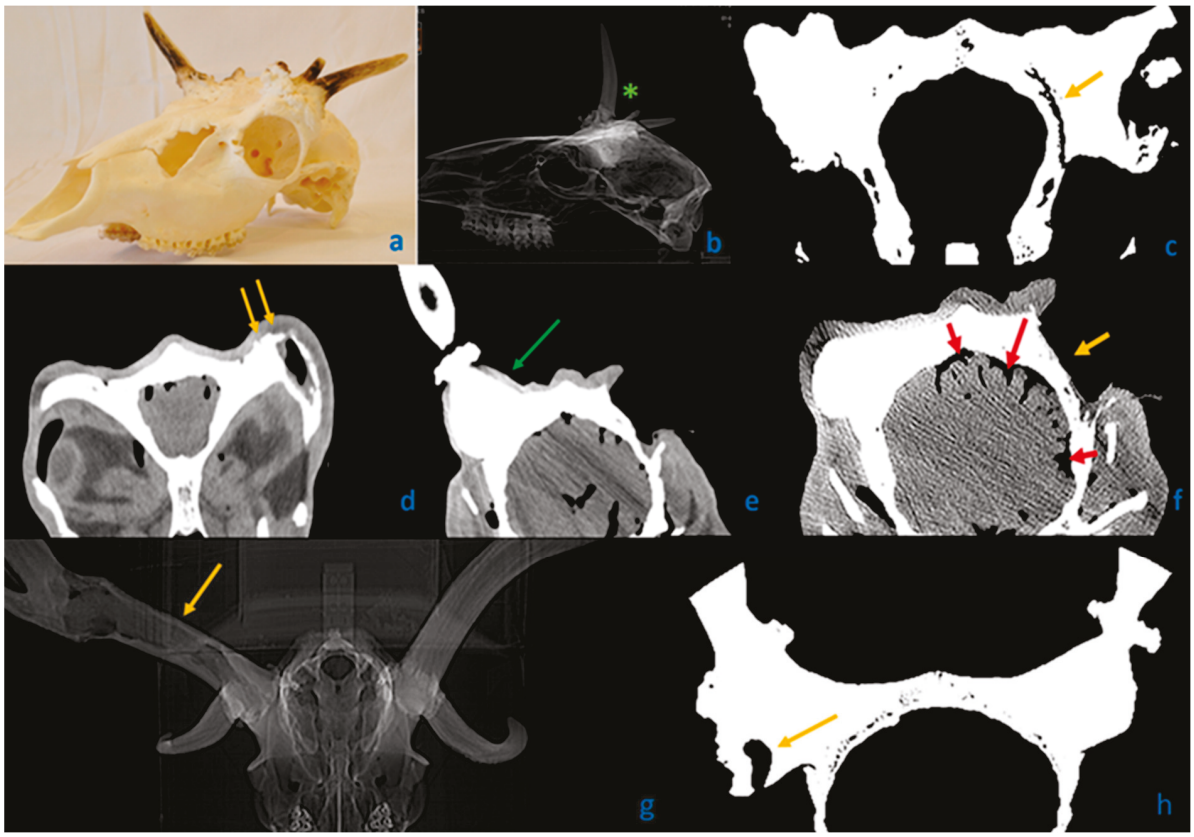


Figure 5. Computed tomography (CT) scans of three fallow deer (*Dama dama*) cases. (**a**–**c**) A trophy with severe involvement on both sides with aberrant antler beams (AAB). (**d**,**e**) Complete head with soft tissues. (**g**,**h**) The only case with cavity formation in an antler. (**a**) Bilateral loss of antlers with deformed pedicles and AAB. (**b**) Typically, no cavities are formed in AABs (marked with green asterisks). (**c**) Frontal scan through the antler pedicles. On the left side, not visible to the naked eye, a large gap-like cavity (yellow arrow) ran parallel to the cranial plane without displacement of the cranial bones. Development due to trauma is unlikely. (**d**) Whole head with soft tissues. Yellow arrows show the unevenness of the residual pedicle, suggestive of superficial chronic osteomyelitis. (**e**) The green arrow shows the deeper plane of the other side pedicle surface without significant radiographic abnormality. (**f**) In an even deeper plane, due to pus accumulation in the subcranial space, the widening of the sulci and thinning of the gyri (red arrows) suggest meningoencephalitis. The yellow arrow shows the lack of a pedicle. (**g**) Only one of our cases showed a cavity (yellow arrow) in the unilateral antler beam, which may indicate the death of the growth center cells during growth. (**h**) Necrotic cells may have exited through a fistula (yellow arrow) to the outside.

In extreme cases, lateral displacement of the remaining pedicle, often extending to the supraorbital ridge (S6, 31%) was observed, similarly to the phenomenon photographically documented in North Arizona elk (*Cervus canadensis*) populations by J.L. Rachlow [6]. These aberrant proliferation–remodelling features (P2 and S6) are similar to those described in our study, suggesting that it is not just a DD-specific phenomenon.

In our work, we defined "spikes" (a term used within the hunting community) as aberrant antler beams (AAB) to distinguish terminologically between diseased forms and healthy yearling stags without branched antlers. If nothing or only an AAB was present at a given site, we classified the specimen as "lacking antler" (A4, 40%). We considered a formation as an antler if the main beam exceeded the brow tine in length, with at least a rudimentary antler rose. CT scans revealed these structures to be generally solid, with only one case showing cavity formation (Figure 5g,h). In cases where pedicle blastemas are less involved, more pronounced growth can occur by incorporating unused nutrients and minerals, which become more available due to a reduced number of osteoblasts in other areas. We termed this process compensatory growth (CG). The effect might be analogous to contralateral antler growth following removal of the peri-peduncular periosteum described by Li et al. [35]. CG can be indicated by a significant difference in brow tine length due to a longer-than-normal brow tine on the healthy side.

Among the observed skull abnormalities, irregularities such as peri-peduncular skull surface pitting [29] (S1, 64%), spongious skull remodeling (S2, 30%), and the lateral displacement of the expanding pedicle (S6) suggest atypical resorption and proliferative processes cannot be solely attributed to trauma or displacement during healing. A morphological evidence of secondary healing of chronic osteomyelitis is fistula formation [30,36], which was detected on the pedicle (P5) in 16% of the cases and on the skull (S4) in 10% of the cases. The opening of sutures (S3, 20%), theoretically, might be a consequence of injury; however, it would not occur in isolation since it typically requires adjacent skull fractures and dislocations. Trauma-induced extensive detachment of the external cortical plate from the underlying bone layer would result in substantial displacement. Conversely, CT imaging (Figure 5c) of an aberrant trophy revealed that the gaps between cortical plates (S5, 23%) often aligned with the cranial contour, suggesting that the origin of this malformation is unrelated to trauma. The absence of any signs of sharp fracture lines—either with or without displacement—and the lack of callus formation or (at least) partially broken pedicle structures (f.e., regular circular cross-section, with a missing part) further support that these abnormalities are not typical traumatic injuries. If not only trophies are available but also soft tissues can be examined, the presence of abscess-like purulent inflammation is evidence of the underlying pathology (Figure 6d–f).

The prevailing hypothesis suggests that post-traumatic deformity within antler pedicles is a consequence of the misalignment of the broken surfaces since the periosteum and skin cannot hold them together properly [1,28]. Certain studies seemingly supported this theory by examining the mechanical disruption of the pedicle immediately after casting or of antlers during the velvet stage [1]. However, it is important to note that these experiments were limited to growing antlers, which may represent imperfect antler growth rather than the process of pathological healing after the breakout of dry antlers [37,38]. In our study, we examined one case where injury occurred during the velvet stage, which caused acute osteomyelitis, accompanied by re-epithelialization of the exposed velvet surface (Figure 7). This inflammation was localized within the injured area and its immediate vicinity, sparing the deeper marrow area in larger tines and avoiding extension to the pedicle. Consequently, healing produced a deformed antler with a size reduction proportional to the initial injury. In theory, a severe acute inflammation that reaches the pedicle could cause a fatal sepsis. A less severe process, confined to the antlers, can cause deformation

or breakage of branches [28,39]. However, animals mostly avoid injury during the velvet stage due to the innervated and sensitive nature of their antlers [1,28]. In the absence of chronic inflammation or bone remodeling, injuries at the velvet stage are not usually a significant cause of antler deformities; healthy antlers can regrow in the following year [1]. Our biobank reflects only one such case among other abnormal samples.



Figure 6. The difference between an obvious trauma-induced and a pathological fracture. (**a**) The top row of images shows the left antler broken out following a motor vehicle collision. (**b**) Condition after soft tissue removal. (**c**) The fracture surfaces were sharp and angular, with displacement of the cranial bone (arrow). (**d**) The bottom row shows the right antler and the site of the breakout, which occurred due to a fall following a hunter's gunshot. Under normal circumstances, a fracture should not occur in this case. However, an underlying disease, secondarily infected with pyogenic bacteria, weakened the bone structure to such an extent that it fractured even under minimal force. The surface of the breakout, which covered a large area, was rounded. (**e**) Loss of the left antler occurred earlier. (**f**) Most of the fracture surfaces were covered with greyish-white pus, indicating a superinfection with pyogenic bacteria.

3.4. Antler Anomalies in Roe Deer (Capreolus capreolus) Trophies

Our aberrant Cervidae trophy collection included five roe deer (*Capreolus capreolus*, CC) trophies exhibiting antler anomalies overlapping with symptoms of DD. The antlered population-based data [22] indicate that this species was affected 22 times less frequently than DD. However, we believe this observation does not accurately reflect the true prevalence of antler anomalies in CC populations. This is because normal trophies exhibit significant morphological variability, which can make it difficult to recognize aberrant ones. Additionally, obvious anomalies may lead to exclusion from the evaluation process (https://www.cicukteb.com/uk-species/index (accessed on 18 May 2025)).

Due to the limited number of cases, we categorized and analyzed the involvement of the rose (R), antler (A), pedicle (P), and skull (S) together. We assessed the RAPS features on five trophies on both sides and categorized the frequency of anomalies into three groups: Frequent (70–100%), moderately common (40–69%), rare (less than 39%) (Figure 8, Table S2) In two cases (CC4 and CC5), one of the antlers broke off during the hunt, indicating significant weakening of the bony structure that led to pathological fractures. In these cases, we were able to evaluate the broken part and compare it to the intact side. Overall, antler

anomalies were the most frequent alterations (63%), occurring more often than pedicle (27%) and skull (23%) anomalies. Interestingly, the incidence rate of rose anomalies (R1–R3) was much lower (21%) than in DD and CE. This could be a consequence of the absence of pedicle deformation (P2), which is common in DD. Since R2 is not independent of P2, this may explain the interspecies difference.

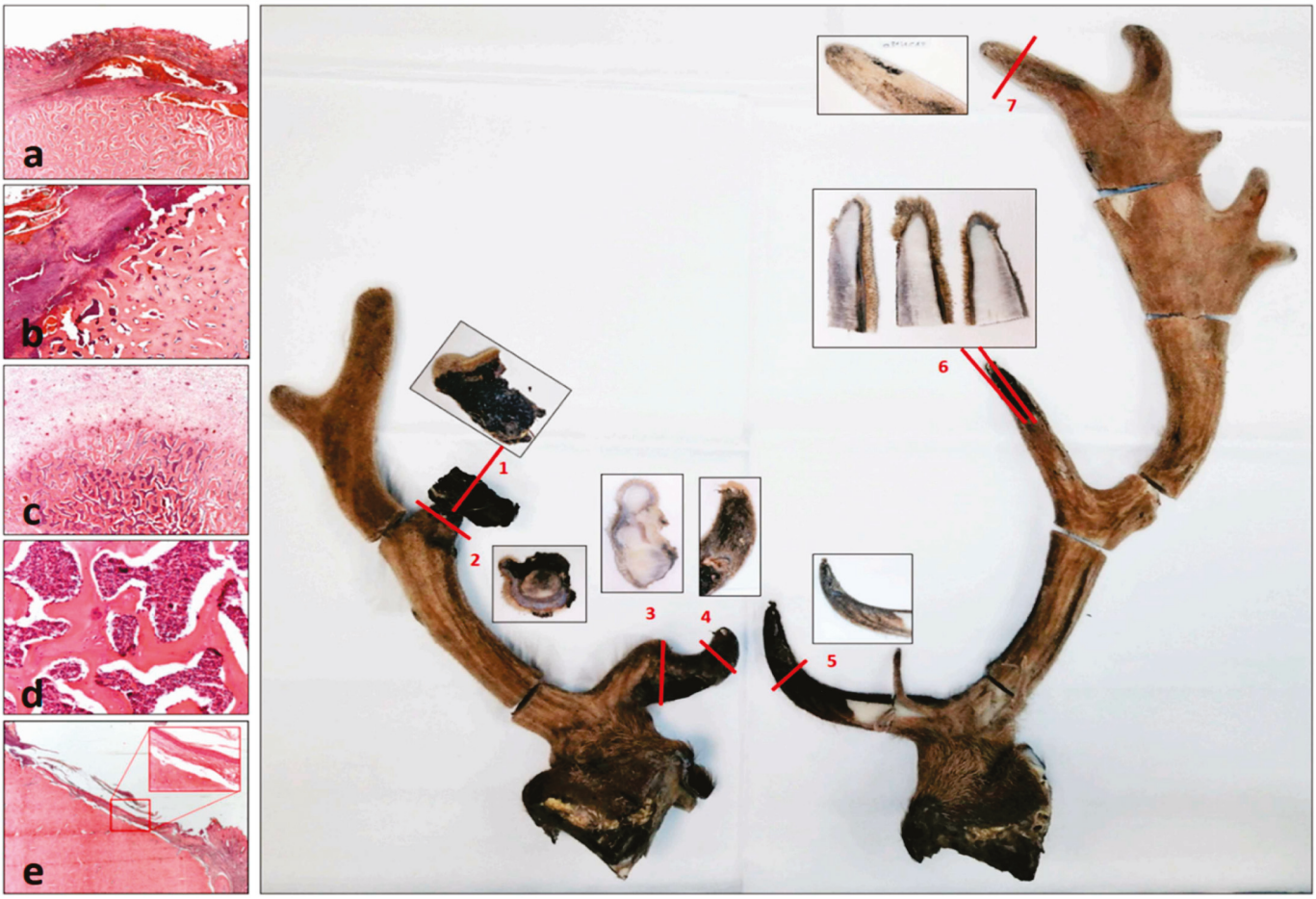


Figure 7. Microscopic examination of wounds caused by injury in the velvet phase, leading to antler deformity and asymmetry, suggests acute inflammation. The significant difference between the sides may be related to the different extent of the injuries and subsequent inflammation, and, therefore, a difference in the duration of the recovery period under which the antler could grow. The red numbers show the directions of the cut-offs for microscopic examination, and the adjacent images show the cut surfaces of the planes. (**a**) Subcutaneous hemorrhage and detachment from the bone surface are indications of injury (Cut 7). (**b**) The larger lesion was associated with necrosis of the skin and periosteum (upper left half of the figure). The superficially infiltrated blood layer confirmed that this was caused by trauma (Cut 2). (**c**) Inflammatory cells also reached the deep cancellous bone tissue (Cut 5). (**d**) The intertrabecular spaces of the cancellous bone were filled with acute inflammatory cells (neutrophil granulocytes) (Cut 5). (**e**) During re-epithelialization, the epithelium slides from the skin surface adjacent to the lesion to the free bone surface. The resulting contact is consistent with one of the histological components of the peduncular–dermal junction (PDJ) and is indicative of a longer period of regeneration. The inset shows a bony–epithelial contact area without the dermis. The gap is a retraction artifact formed during fixation (Cut 6).

This difference could be attributed to variations in osteoclast distribution in the pedicle. In CC, osteoclasts are concentrated narrowly around the casting plane, leading to a nearly flat shedding plane upon activation. In contrast, in DD, osteoclast distribution is more dispersed along the pedicle, resulting in a more uneven casting plane.

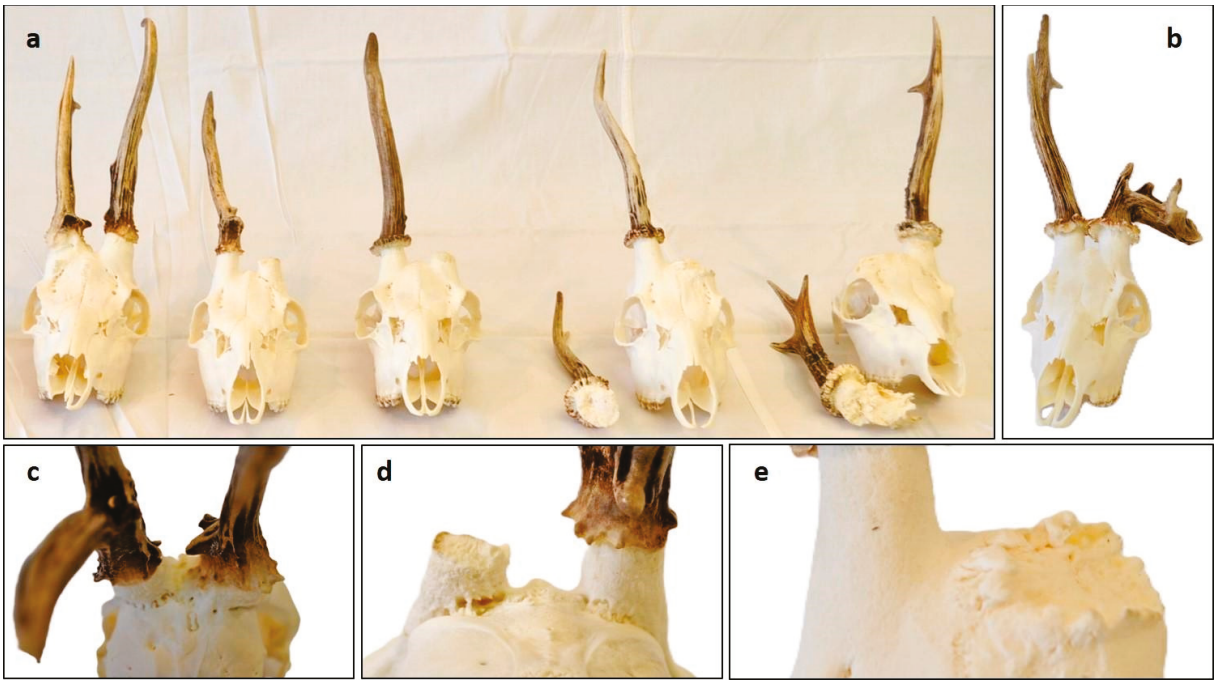


Figure 8. Pedunculitis Chronica Deformans (PCD) caused trophy anomalies on roe deer (*Capreolus capreolus*, CC). (**a**) Our five cases, ordered by severity, showed signs of PCD. (**b**) One velvet-phase injured CC with intact rose, pedicle, and skull; therefore, the deformity in the antlers is not due to PCD. (**c**) CC Case 1, as seen from behind. There are no brow tines or antler burrs on either side. (**d**) CC case 2 seen from behind. The distal pedicle surface showed pitting on both sides, more prominently on the side from which premature casting occurred. On this side, fissure formation between the pedicle and frontal bone and on the other side, the loss of burr granulation are evident. (**e**) On the left side of CC case 4, a margin crest developed on the broadening pedicle base, showing osteoblastic bone building activity.

3.5. Occurrence of RAPS Features in Red Deer (Cervus elaphus)

The antlered population density [22] adjusted data referred to 32 times less involvement in red deer (*Cervus elaphus*, CE) than fallow deer (*Dama dama*, DD) (Table S1). Despite the accessible low number of CE cases, RAPS features showed a significant overlap between these two species (Figure 9 and Table S3). A conspicuous weakening by abnormal remodeling of the pedicle at least on one side was visible in those CE cases. In one three-year-old stag case (CE 1), the right pedicle broke out (P6, P7) during the hunt. The fracture happened on the most proximal third of the pedicle immediately at the level of the skull, which showed spongious reconstruction (S2) of the outer and inner surfaces without dislocation of the flat bone lamels (Figure 9b,c). Further on, the holes in the inner surface of the pedicle did not arrange along a fault line, suggesting that this relatively large loss of bony material could not have been a consequence of trauma (Figure 9c). The pitting on the outer skull surface (S1) around the pedicle is a clear sign of chronic osteomyelitis (Figure 9d), which is a result of long-lasting inflammation, not acute trauma. The morphological evidence of this pathomechanism includes pitting of the distal part of the pedicle (P1) and skull surface (S1), or in serious cases, the spongious remodeling of this flat bone (S2). The improper wound healing with scar formation can lead to bone weakening, which can elicit distal pedicle, rose, and antler deformation or even loss (Figure 9e). One of the most conspicuous differences between CE and DD was the extent of spongious remodeling (Figure 9f). This was not only more prominent in CE, but involved the frontal bones extensively, even reaching the sutures in some cases (Figure 9g). This could be the consequence of the osteoclastic/osteoblastic activity (which is normally most prominent on the casting plane), not limited to pedicles,

but involving the surrounding part of the frontal bone. Additional features different from DD are the lack of deformation (P2), prominent shortening (P3), and widening (P4) of the pedicle, which can be explained by interspecies differences. In the case of DD, during bone remodeling by chronic osteomyelitis, the balance between osteolytic osteoclast activity and the proliferation activity of osteoblasts shifts in favor of the latter, as opposed to CE where the former can be more prominent.

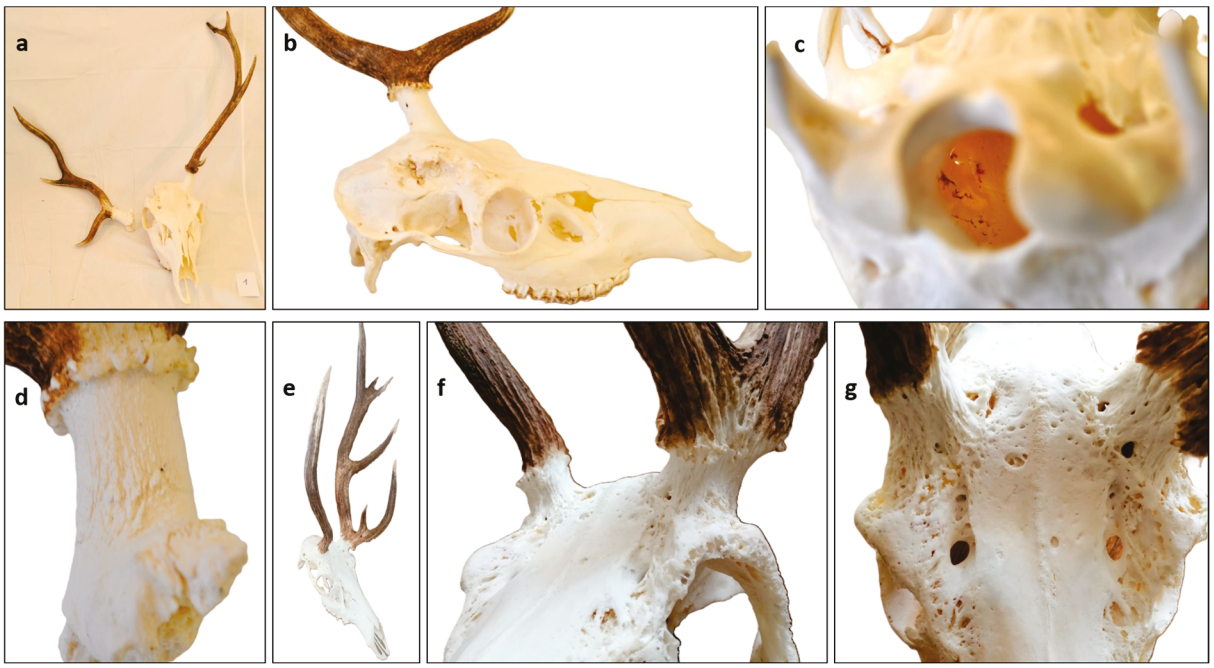


Figure 9. Signs of Pedunculitis Chronica Deformans (PCD) on red deer (*Cervus elaphus*, CE). (**a**–**d**) A two-year-old stag trophy with a broken-out right pedicle. The fracture happened during the hunt, therefore, we could examine both sides. (**a**) The fracture pattern serves as an example of juvenile PCD, where aseptic bone necrosis leads to pathological fracture. The right mean beam was shorter and less developed than the left. (**b**) The broad breaking surface involved most of the frontal bone and approached the orbital arch. (**c**) View through the foramen magnum towards the right pedicle base. The spongy perforations occurred without displacement of the skull bone surface and were not situated along a line of force, which could be a sign of a traumatic impact. (**d**) The broken-out pedicle showed remarkable pitting on the proximal two-thirds of its surface without deformation or loss of rose granulation. (**e**–**g**) A case of a five-year-old stag as an example where the inhibited cast wound healing could lead to an adult-type PCD. (**e**) The difference between the two sides was prominent, as only an aberrant antler beam developed on the right side. (There is no brow tine; therefore, we cannot consider it as an antler). (**f**) Total loss of rose granularity on both sides without pedicle shortening, broadening, or deformation, but surface irregularity is obvious. (**g**) The spongy bone remodeling due to osteoclast activation is a hallmark of PCD in CE. On both sides, more of the frontal bones were involved, and the disease was reaching the orbital arches too. In contrast to fallow deer (*Dama dama*), there is no bony crest formation and broadening of the pedicle, which could be a sign of elevated osteoblast activity.

3.6. Considerations for RAPS Score Assessment

Despite their rigorous applicability, the RAPS features cannot be treated as entirely independent variables due to inherent conflicts and contingencies. For instance, R1 and R2 are mutually exclusive events. Additionally, A2 and A3 were determined by comparing the two sides, and to maintain consistency, we assigned a score of 1 on both sides if present. However, this approach introduces an inherent bias into the downstream analysis by affecting the evaluation of laterality. Furthermore, our observations indicated that the age-stratified brow tine and main beam length distributions in the trophy register control

group (TRCG) were often skewed to the left. As a result, for the assessment of A2.1, we implemented a less stringent bottom 20% threshold, which allowed for a greater than 15% increase in sensitivity for this marker.

3.7. Healing of the Casting Wound

Upon casting, a wound corresponding to an open bone fracture forms at the detachment site. In healthy animals, this wound generally only leaves at most a small central scar after healing, and eventually is enclosed in velvet [40].

Wound healing is a complex and delicate process that can sometimes falter, leading to chronic, non-healing wounds. Common initiating factors in such cases include infection, persistent inflammation, immunosuppression, and impaired circulation, often working together to hinder recovery [40,41]. Despite the regenerative potential observed in antler wounds, research has not yet focused on the presence of inflammatory cells—essential indicators of immune activity—or on the morphological traits associated with pathological healing in antlers. In a non-sterile environment, wounds are susceptible to microbial colonization. This poses a risk to the ossification zone as bacteria can spread through the bloodstream, potentially causing osteomyelitis [28]. However, when the immune system is robust and wound closure is timely, inflammation is generally minimal and self-limiting, reflecting a natural resistance to chronic inflammation and infection; refer to the normal physiological conditions [40].

3.8. The Pedunculitis Chronica Deformans (PCD) Is a Consequence of Impaired Wound Healing

When tissue regeneration is impaired and immunosuppression occurs, wound healing disorders can develop. These conditions can trigger an inflammatory response that exceeds physiological levels, resulting in secondary or delayed wound healing, which is typically associated with excessive scar formation [41]. Instead of forming a uniform, continuous layer, the resulting scar tissue is a braided, irregular structure composed of fibrous bundles [42,43]. Such irregular scarring disrupts critical signaling pathways between the wound epidermis and the regenerating blastema [40]. The early chondrocytes, which originated from periosteal antlerogenic stem cells, form blastemas at the outer edges of the wound that develop into chondro-osseous columns during ossification [44,45]. The morphological examination of abnormal pedicles and AABs indicated that these structures originate from sparse, scattered residual osteoblasts and osteo-chondroid trabeculae in the irregular scar tissue.

The most obvious manifestation of this is the phenomenon described by Rachow et al., which is the “spike-on-one-side” (SOOS) [6], but it is not exclusively unilateral (Figure 5a,b and Figure 10a,b). In this condition, the pedicle periosteum undergoes appositional intramembranous ossification but widens unevenly due to scarring, often extending laterally and even approaching the orbital ridge (Figure 10c). This abnormal growth pattern results in further shortening and more pronounced bone loss in the pedicle, which can ultimately lead to a “hummel” stage (Figures 10d and 11). The “semi-hummel” condition can also occur: In this case, there is an antler on one side showing minor deviations only, while on the other side it cannot develop (Figures 1 and 10e). In place of the missing pedicle, usually only a widened bone ridge remained, which did not correspond to the morphology of a secondarily healed fracture. These trophies are thought to correspond to cases in which, despite a significant bilateral weight difference, the animals are able to keep their heads upright (Figure 1). In these cases, there is enough time for the development of a compensatory head-hold with neck muscle hypertrophy during the period of gradual weight gain on the intact side, providing an adequate visual field [46]. Sudden weight loss, observed during

non-simultaneous shedding, is associated with an oblique head position [47]. Unilateral antler loss due to trauma would cause the same.

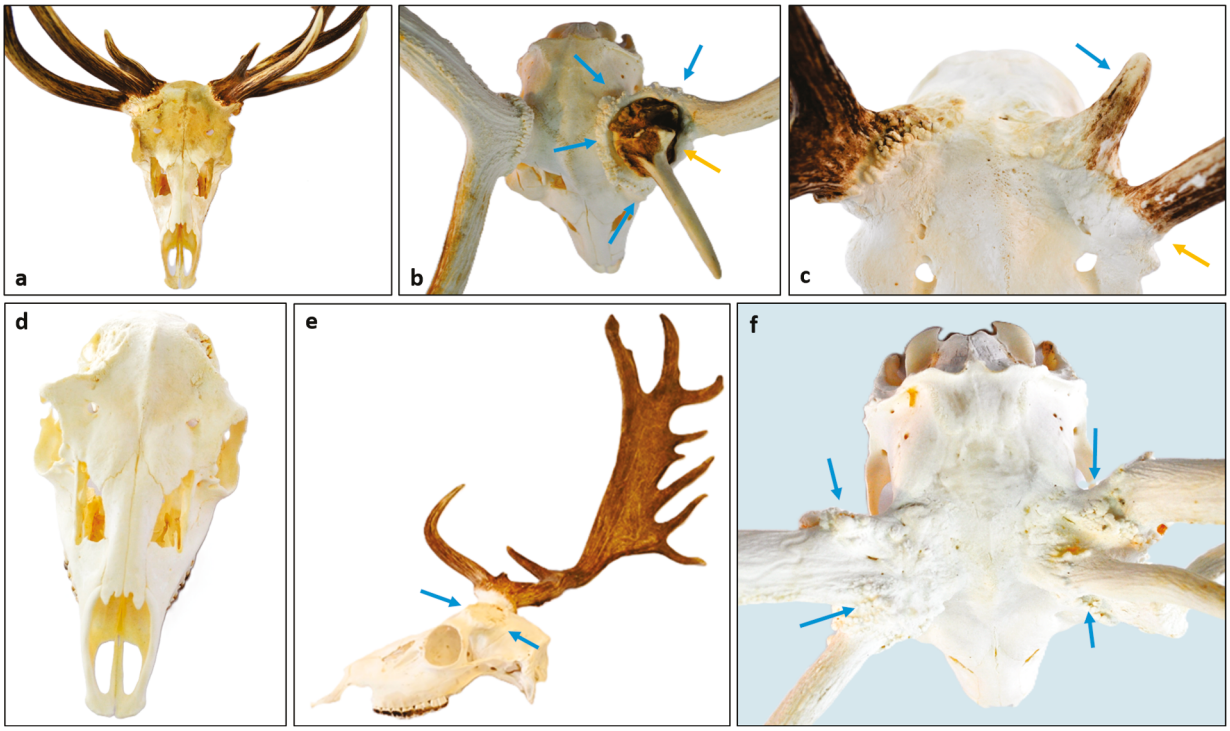


Figure 10. Morphological changes in Pedunculitis Chronica Deformans (PCD) suggest disrupted osteogenesis of the pedicle and antlers by scar tissue. (**a**) Bilateral aberrant antler beams (AAB) can be considered derivatives of antler-forming buds that have retained their developmental capacity between the dissecting scar tissues. They correspond to the phenomenon described as spike-on-one-side (SOOS) but can also be bilateral. (**b**) The top view of a velvet phase trophy shows intramembranous ossification (blue arrows) around the left, but it is not casted AAB (yellow arrow). In this case, the AAB caused the lateralization of ossification originating from the antlerogenic stem cells (ASC) of the chondro-osseous tissue. This process increases the diameter of the pedicle and moves it laterally. (**c**) In cases of severe ASC loss, little residual antler tissue can form (blue arrow), typically on the periphery, often located on the orbital arch (yellow arrow). (**d**) Bilateral total pedicle loss leads to the "hummel" condition. (**e**) In the place of the left pedicle, only a widened bone ridge-like edge remained (blue arrows), which did not correspond to secondary healing after fracture. The widening of the right pedicle is suggestive of PCD, and the long brow tine and massive palm formation can be considered compensatory growth. (**f**) A bony trophy can only indirectly evidence scar formation. However, its appearance with small nodules (blue arrows) corresponds to scars dissecting the chondro-osseous tissue.

The pathomechanism and morphological characteristics of the lesions described do not correspond to any known bone disease, including neoplastic transformations, but show notable similarities to Garré's sclerosing chronic non-suppurative osteomyelitis. This condition, which typically affects the mandible, is characterized by its "onion-skinning" bone deformation due to mild irritation or bacterial infection resulting from a proliferative periosteal reaction [48]. We have termed this unique condition Pedunculitis Chronica Deformans (PCD). In PCD, the osteoblasts of the peduncular surface ossify intramembranously but fail to form organized, parallel lamellar bone. Instead, they create irregular ridges derived from osseochondroid columns. The top of these ridges retains variable amounts of antlerogenic stem cells. PCD compromises the structural integrity of both the pedicle and the forming antler, occurring independently of any prior injury. The bony trophy can only

provide indirect evidence of scarring. However, the appearance of small osseous nodules is consistent with scars that dissect bone tissue (Figure 10f).



Figure 11. Trail camera footage from around the village of Szakcs (South Hungary, Middle Europe) from our study area. (**A**) This living "hummel" fallow deer (*Dama dama*) buck proves that the loss of antlers on both sides is survivable. (**B**) However, the survival time is questionable. The magnification shows a rather large loss of skull fragments on the left side.

Antler casting is primarily dependent on osteoclast activity across the pedicle, with the greatest extent of bone resorption occurring at the casting plane [40]. Under physiological conditions, this process does not result in complete regeneration; instead, the pedicle shortens while its diameter increases through appositional growth [1,40]. In case of healthy casting, the surface of the pedicle remains slightly concave and prickly due to fractured trabeculae, but the pedicle itself retains a circular cross-section and relatively smooth exterior [1]. However, during PCD, there is a notable reduction in both osteoblasts, which are essential for rebuilding the tissues, and also in osteoclasts involved in antler shedding. The distribution of osteoclasts becomes irregular and no longer concentrates exclusively on the casting plane, leading to an uneven casting surface. This disrupted remodeling weakens the pedicle structurally, which can render it incapable of supporting the developing antler, leading to fractures under the antler's weight even under the velvet phase (Figure 12). PCD is thus a primary contributor to pathological pedicle fractures. Differentiating whether the irregular shedding surface is a result of an atypical, remodeled casting plane or a pathological fracture requires close examination of the fracture surface and careful consideration of the timing relative to the antler shedding period. Previous work by U. Kierdorf and colleagues described an instance where a pathological condition was predisposed to the antler breakage following a velvet-stage injury, which compromised the antler but not the pedicle. They underscored that the underlying pathologic process is necessary in weakening the antler structure, thus predisposing it to fractures [28].

Thus, PCD can be defined as a chronic inflammation primarily affecting the pedicle tissue, caused by casting wound closure or enchondral ossification disturbance of the pedicle. The consequent scarring causes disturbance of pedicle and antler regeneration and weakening of their structure, creating the potential for pathological fracture, superinfection, and the development of fatal intracranial inflammation.

The etiology of PCD remains unknown. Although bacterial infection appears to be a likely cause [9–11], the possibility of secondary superinfection cannot be excluded. To the best of our knowledge, the involvement of other infectious agents has not been reported so far. The accumulation of toxic substances in antlers is a well-documented phenomenon [49–51]; however, their role in the development of antler or pedicle abnormalities remains unclear.

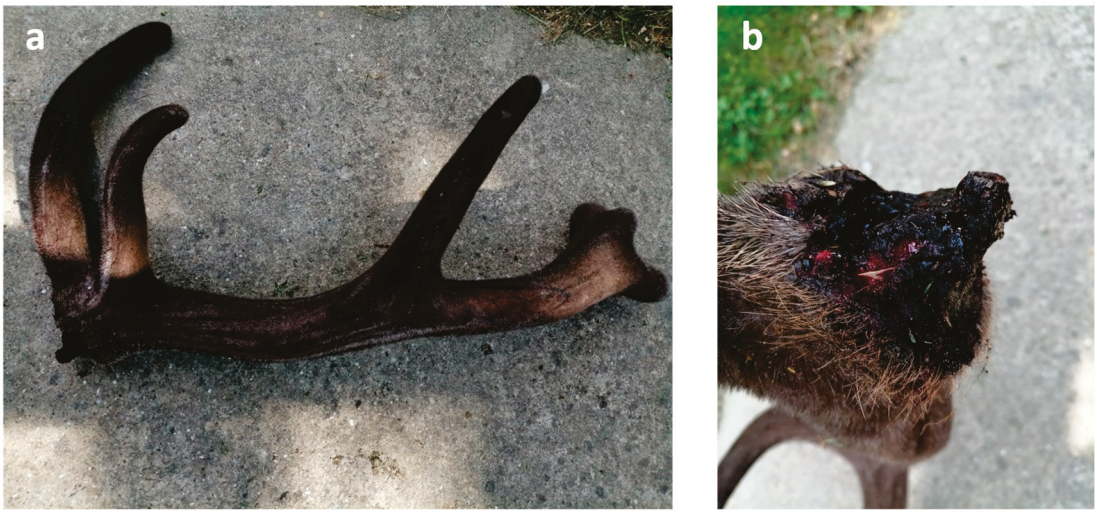


Figure 12. Antlers broken-out with an irregular plane in the velvet phase. (**a**) There is no evidence of a major traumatic force on the antler; therefore, it can be assumed that the pathological fracture was due to the antler's own weight. (**b**) An irregular fracture surface, which is incompatible with primary external trauma, formed above the casting plane.

3.9. Peduncular–Dermal Junction (PDJ); Structural and Pathological Insights

In diseased individuals, we observed a distinct macroscopic separation between the peri-peduncular soft tissues—including the skin, subcutaneous connective tissue, and periosteum—and the underlying bone (Figure 13h). This separation suggests that damage to a critical peripheral structural tight junction around the pedicle may contribute significantly to disease development.

In mammals, the only hitherto characterized bony structure that penetrates the integument is the tooth, whose anatomical structure, especially at the periodontal junction, is well-discussed [52]. This junction isolates the heterogeneous microbial flora of the oral cavity from the rest of the body through the specialized structure of the oral mucosa [52]. Antlers in *Cervidae* are bony structures that penetrate the integument when the velvet is shed and the continuity of the skin is interrupted [40]. This breach in the integument—the body's first line of defense—potentially exposes the animal to pathogens from the surrounding environment, particularly around the dry antler. We described the soft tissue components around the pedicle as an independent structure referred to as the pedunculo–dermal junction (PDJ), which we believe plays a crucial role in maintaining integumentary integrity. Microscopically, the PDJ is composed of three primary elements: (1) The direct connection of the distal edge of the epidermis without an intervening dermis or subcutaneous layer to the pedicle periosteum [44]; (2) Sharpey's fibers anchoring the periosteum firmly to the bone [53], and (3) the microscopic roughness of the distal peduncular bone surface, which is augmenting the contact area and potentially enhancing barrier strength (Figure 13a–g). Li et al. demonstrated that the distal third of the pedicle periosteum is more resistant to detachment than the proximal two-thirds [54], supporting our hypothesis that the PDJ is an independent histomorphological structural unit. In other words, segments of peri-peduncular soft tissue of different heights have different significance not only in antler regeneration [55] but also in the closure of the integument after casting of the velvet.

We found that damage to the PDJ caused periosteal-bone discohesion, allowing the accumulation of external contaminants, such as plant fibers in the resulting gap, and introducing pathogens, which bring about superinfections, triggering acute inflammation characterized by purulent exudate and tissue debris. The fibrotic remodeling of the connecting tissue leads to shrinkage of the surrounding elastic fiber matrix and the disruption

of Sharpey's fibers, creating a favorable environment for chronic inflammation around the pedicle (Figure 13h–o). The process can continue for several years, as evidenced by the case we identified in the velvet phase (Figure S2). The pathomechanism bears similarities to parodontitis, where persistent inflammation is exacerbated by compromised structural integrity [52].

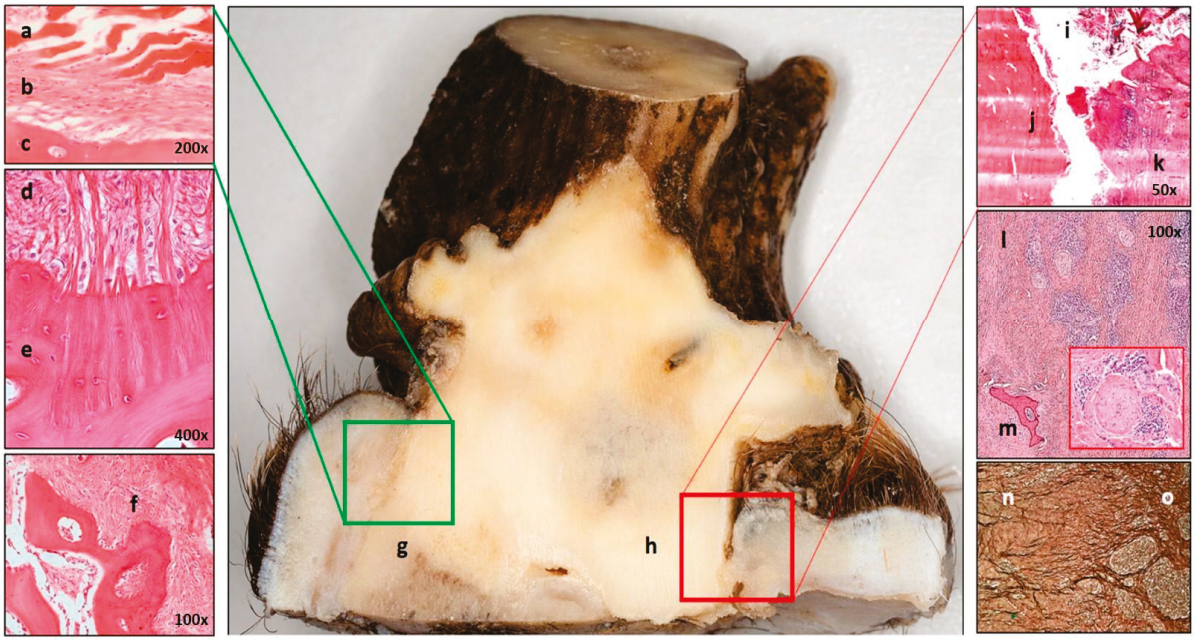


Figure 13. The peduncular–dermal junction (PDJ) and its damage on sagittally sectioned peduncle and peripeduncular soft tissue. The green square indicates healthy, and the red square indicates a diseased area from which excisions were made for microscopic examination. (**a**–**g**) On the left, the histological components of the PDJ are shown. The epidermis (**a**) is directly attached to the bone (**c**) surface without dermis (**b**). (**d**,**e**) Sharpey's fibres anchor the periosteum (**d**) to the bone (**e**). (**f**) At lower magnification, the bone surface roughness is visible, which increases the adhesion surface. The trabecular bone is on the left side of the picture; the periosteum is on the right. (**h**–**o**) Damage to the PDJ caused periosteal bone discohesion (**h**), allowing the accumulation of foreign, contaminated substances, such as plant fibres, purulent exudate, and tissue debris, in the resulting gap (**i**). Signs of superficial osteomyelitis are a surface covered with devitalized bone particles (**j**) and an accumulation of inflammatory cells in the skin, visible as a bluish discoloration (**k**). In the deeper soft tissue, a massive, predominantly perineural (see insert) and perivascular arrangement of lymphoplasmacytic inflammatory cell infiltration (**l**) with bone sequestrum (**m**) is seen. Chronic inflammation is characterized by fibrosis (**n**), which causes damage to the elastic fiber matrix (**o**) and disruption of Sharpey's fibers, resulting in further enlargement of the gap with shrinkage of the peripeduncular tissue.

4. Conclusions

To investigate the antler anomalies in Hungarian Cervidae populations—including fallow deer (*Dama dama*, DD), roe deer (*Capreolus capreolus*, CC), and red deer (*Cervus elaphus*, CE)—we described a chronic inflammatory disease—named Pedunculitis Chronica Deformans (PCD)—of the pedicle. As a result of our work, we have identified morphological characteristics that enable veterinarians, wildlife biologists, and game managers to recognize animals affected by this disease clearly. This paves the way for the collection of accurate epidemiological data and the establishment of homogeneous groups of affected individuals, which in turn will facilitate investigation into the underlying causes and may ultimately contribute to the development of potential treatment strategies. In this study, we introduce a morphological scoring system for this chronic osteomyelitis-like disease. Our work includes a detailed characterization of the peduncular–dermal junction (PDJ) as

a distinct anatomical structure, emphasizing its significance as a key factor in the initiation and progression of the disease. This study provides a more comprehensive understanding of these deformities and establishes a foundation for future diagnosis and treatment.

Supplementary Materials: The following supporting information can be downloaded at: https://www.mdpi.com/article/10.3390/ani15111530/s1, Figure S1: Heatmap of associations among RAPS (rose, R; antler A; pedicle, P; and skull, S) characteristics of the 50 studied fallow deer (*Dama dama*). Figure S2: Peduncular–dermal junction (PDJ) separation during the velvet phase. (a) Left side, the abnormal antler cut into pieces for fixation with its pedicle and surrounding skull roof. (b) Sagittal section of the velvet antler rose and pedicle. The skin–bone discohesion below the burr is visible (arrow). (c) On the other side of this section, the separation between the skin and pedicle is also visible, which is indicative of its extension. (d) The dark discoloration in the gap due to hemorrhage proves that the process occurred in a living animal. Table S1: The incidence of aberrant trophies among fallow deer *(Dama dama*, DD) was notably higher than in roe deer (*Capreolus capreolus*, CC) and red deer (*Cervus elaphus*, CE), with ten times more anomalies in DD than in CC (50 vs. 5) and approximately 16 times more than CE (50 vs. 3). When adjusted for population density, DD appeared to be impacted the most by these deformities: 34 times more frequently than CC and 50 times more than CE, suggesting a unique vulnerability. Table S2: Cervidae trophies collection, five roe deer (*Capreolus capreolus*, CC) trophies exhibited features characteristic of Pedunculitis Chronica Deformans (PCD). Table S3: Evaluation of Pedunculitis Chronica Deformans (PCD) signs on red deer (*Cervus elaphus*, CE). Table S4: Characterization of the Aberrant Trophies with RAPS (rose, R; antler A; pedicle, P; and skull, S) characteristics and their statistical evaluation. Table S5: Analysis of Pedicle Ellipticity among fallow deer (*Dama dama*, DD).

Author Contributions: Conceptualization, F.S., I.L., L.S. and Z.S.; data curation, Á.Ü., S.F., P.G. and F.K.; formal analysis, I.L., M.M. and G.H.; funding acquisition, F.S., P.G., F.K. and Z.S.; investigation, F.S., R.K., Á.S., G.P., A.A.T., K.E. and M.M.; methodology, F.S., A.A.T., K.E. and G.H.; project administration, Z.S.; resources, G.P., M.M. and P.G.; software, Á.Ü., Á.S. and G.H.; supervision, K.P., L.S. and Z.S.; validation, I.L., R.K., Á.S., G.P. and K.P.; visualization, Á.Ü. and R.K.; writing—original draft, F.S., I.L., Á.Ü., R.K., A.A.T., L.S. and Z.S.; writing—review and editing, G.P., S.F., P.G., K.P. and F.K. All authors have read and agreed to the published version of the manuscript.

Funding: The research was supported by the Department of Game Management, Ministry of Agriculture; Higher Education Institutional Excellence Programme, New National Excellence; Higher Education Institutional Excellence Programme, Thematic Excellence Programme 2020 "Institutional Excellence" sub-programme No. 3 "Innovation for sustainable life and environment" (PTE/119693/2020), The Hungarian National Laboratory Project, grant number RRF-2.3.1-21-2022-00007. FS was supported by the HUN-REN Excellence Programme, BRC Institute of Biochemistry.

Institutional Review Board Statement: According to the statement of the Institutional Review Board (NAIK MBK MÁB 004-09/2018), researchers collected samples from the carcasses of legally harvested fallow deer hinds. The carcasses were provided for the sampling by the authorized game managers, in full compliance with all ethical and legal regulations. Furthermore, Decision No. (TO-04H39/405-2/2020) of the Government Office of Tolna County, dated 5 June 2020, authorized the shooting of antlered fallow deer outside the hunting season for research purposes.

Informed Consent Statement: Not applicable.

Data Availability Statement: The original contributions presented in this study are included in the article/Supplementary Material. Further inquiries can be directed to the corresponding authors.

Acknowledgments: The authors of this article extend their appreciation to Gyulaj Forestry and Hunting Plc. for their support. The authors are grateful to Péter Zámbó, the State Secretary for Forestry and Land Affairs. The authors also thank Sándor Juhos, Bence Fábián and András Molnár for their contributions to photography.

Conflicts of Interest: István Lakatos, Ádám Ürmös, Réka Karkas, Ákos Sükösd, Attila Arany Tóth, Károly Erdélyi, Katalin Posta, Ferenc Kovács, Szilamér Ferenczi, Győző Horváth, László Szemethy, and Zsuzsanna Szőke have no conflicts of interest to declare. The funders had no role in the design of the study; in the collection, analyses, or interpretation of data; in the writing of the manuscript; or in the decision to publish the results. F.S. was supported by the HUN-REN Excellence Programme, BRC Institute of Biochemistry. The carcasses used in this study were provided for sampling by authorized game managers in full compliance with all relevant ethical and legal regulations: Gábor Palánki and Péter Gőbölös are employees of Gyulaj Forestry and Hunting Plc. Mihály Misó is an employee of Guth Forestry, a division of NYÍRERDŐ Forestry Co. These affiliations did not influence the design, conduct, or interpretation of the research.

Abbreviations

The following abbreviations are used in this manuscript:

AAB	aberrant antler beams
ASC	antlerogenic stem cell
B&C	Boone and Crockett Club
CC	*Capreolus capreolus* (roe deer)
CE	*Cervus elaphus* (red deer)
CIC	International Council for Game and Wildlife Conservation
CT	computed tomography
DD	*Dama dama* (fallow deer)
HTR	Hungarian trophy register
MCG	morphology control group
PCD	Pedunculitis Chronica Deformans
PDJ	peduncular–dermal junction
RAPS	rose, antler, pedicle, skull
SOOS	spike-on-one-side
TRCG	trophy register control group

References

1. Goss, R.J. *Deer Antlers: Regeneration, Function, and Evolution*; Academic Press: Cambridge, MA, USA, 1983. Available online: http://www.sciencedirect.com:5070/book/9780122930805/deer-antlers (accessed on 18 May 2025).
2. Landete-Castillejos, T.; Currey, J.; Estevez, J.; Fierro, Y.; Calatayud, A.; Ceacero, F.; Garcia, A.; Gallego, L. Do drastic weather effects on diet influence changes in chemical composition, mechanical properties and structure in deer antlers? *Bone* **2010**, *47*, 815–825. [CrossRef] [PubMed]
3. 'One in a Million' Three-Antler Deer Spotted in US-BBC News. Available online: https://www.bbc.com/news/world-us-canada-50440102 (accessed on 12 September 2022).
4. Rörig, A. Über Geweihentwickelung und Geweihbildung. *Arch. Für Entwicklungsmechanik Org.* **1900**, *10*, 618–644. [CrossRef]
5. Robinette, W.L.; Jones, D.A. Antler Anomalies of Mule Deer. *J. Mammal.* **1959**, *40*, 96–108. [CrossRef]
6. Rachlow, J.L.; Lee, R.M.; Riley, R.K. Abnormal Antlers and Pedicles on Rocky Mountain Elk in Northern Arizona. *Southwest. Nat.* **2003**, *48*, 147–153. [CrossRef]
7. Karns, G.R.; Ditchkoff, S.S. Trauma-induced malformed antler development in male white-tailed deer. *Wildl. Soc. Bull.* **2013**, *37*, 832–837. [CrossRef]
8. Karns, G.R.; Ditchkoff, S.S. Antler Breakage Patterns in White-tailed Deer. *J. Southeast. Assoc. Fish Wildl. Agencies* **2012**, *66*, 114–119.
9. Kierdorf, U.; Flohr, S.; Gomez, S.; Landete-Castillejos, T.; Kierdorf, H. The structure of pedicle and hard antler bone in the European roe deer (*Capreolus capreolus*): A light microscope and backscattered electron imaging study. *J. Anat.* **2013**, *223*, 364–384. [CrossRef]
10. Henshaw, J. Antlers—The Unbrittle Bones of Contention. *Nature* **1971**, *231*, 469. [CrossRef]
11. Currey, J.D.; Landete-Castillejos, T.; Estevez, J.; Ceacero, F.; Olguin, A.; Garcia, A.; Gallego, L. The mechanical properties of red deer antler bone when used in fighting. *J. Exp. Biol.* **2009**, *212*, 3985–3993. [CrossRef]
12. Kaufman, D.W.; Kaufman, G.A. Extreme Antler Malformation in a Mule Deer (*Odocoileus hemionus*) in Northcentral Kansas. *Trans. Kans. Acad. Sci.* **2019**, *122*, 275–278. [CrossRef]

13. Faragó, S.; Köller, J.; Zoltán, A. Természeti-vadászati örökségünk. In *A Legkiválóbb Vadásztrófeák*; Nimród Vadászújság: Budapest, Hungary, 2009.
14. Nimród-Mi Lesz Veled, Lábodi Dám?-Napjaink Dámgazdálkodási Problémái a SEFAG Zrt. Területén-Nimród-What Will Happen to You, the Fallow Deer of Labod?-The Problems of Fallow Deer Management in the Area of SEFAG LTD. Available online: https://nimrod.hu/hirek/milesz (accessed on 3 October 2023).
15. Gál, J.; Janosi, K.; Marosan, M.; Sugár, L. Purulent inflammation of the basis of antler in fallow deer (*Dama dama*) caused by Staphylococcus xylosus. *Magy. Allatorvosok Lapja* **2011**, *133*, 161–164.
16. Baumann, C.D.; Davidson, W.R.; Roscoe, D.E.; Beheler-Amass, K. Intracranial abscessation in white-tailed deer of North America. *J. Wildl. Dis.* **2001**, *37*, 661–670. [CrossRef] [PubMed]
17. Cohen, B.S.; Belser, E.H.; Killmaster, C.H.; Bowers, J.W.; Irwin, B.J.; Yabsley, M.J.; Miller, K.V. Epizootiology of Cranial Abscess Disease in White-Tailed Deer (*Odocoileus virginianus*) of Georgia, USA. *J. Wildl. Dis.* **2015**, *51*, 609–618. [CrossRef]
18. Timmons, J.; Shaub, M.; Scherer, L.; Gereg, I.; Maxwell, L.; Potts, L.; Stevens, M.; Vile, M.; Miller, E.A.; Niedringhaus, K.D. Pathologic Findings of Cranial Abscesses Involving the Pituitary Gland in Free-Ranging White-Tailed Deer (*Odocoileus virginianus*) in Pennsylvania. *Animals* **2025**, *15*, 409. [CrossRef]
19. Karns, G.R.; Lancia, R.A.; Deperno, C.S.; Conner, M.C.; Stoskopf, M.K. Intracranial Abscessation as a Natural Mortality Factor for Adult Male White-Tailed Deer (*Odocoileus virginianus*) in Kent County, Maryland, USA. *J. Wildl. Dis.* **2009**, *45*, 196–200. [CrossRef] [PubMed]
20. Hudson, R.J.; Drew, K.R.; Baskin, L.M. (Eds.) *Wildlife Production Systems: Economic Utilisation of Wild Ungulates*, 1st ed.; Cambridge University Press: Cambridge, UK, 2010.
21. Behaviour and Management of European Ungulates: Professor Marco Apollonio and Professor Rory Putman: 978-184995-122-7-Whittles Publishing. Available online: https://www.whittlespublishing.com/Behaviour_and_Management_of_European_Ungulates (accessed on 6 May 2025).
22. National Game Management Database. Available online: http://www.ova.info.hu/index-en.html (accessed on 10 May 2025).
23. R Core Team. *R: A Language and Environment for Statistical Computing*; R Foundation for Statistical Computing: Vienna, Austria, 2023. Available online: https://www.r-project.org/ (accessed on 5 February 2025).
24. Wickham, H. *ggplot2: Elegant Graphics for Data Analysis*; Use R! Springer International Publishing: Cham, Switzerland, 2016. [CrossRef]
25. Kassambara, A. ggpubr: "ggplot2" Based Publication Ready Plots; R Package Version 0.6.0; 2023. Available online: https://cran.r-project.org/web/packages/ggpubr/index.html (accessed on 5 February 2025).
26. Pedersen, T.L.; RStudio. ggraph: An Implementation of Grammar of Graphics for Graphs and Networks; R Package Version 2.2.1; 2024. Available online: https://cran.r-project.org/web/packages/ggraph/index.html (accessed on 5 February 2025).
27. Kolde, R. pheatmap: Pretty Heatmaps; R Package Version 1.0.12; 2019. Available online: https://cran.r-project.org/web/packages/pheatmap/index.html (accessed on 5 February 2025).
28. Kierdorf, U.; Kierdorf, H.; Konjević, D. Pathological fracture of a red deer antler secondary to purulent inflammation—A case report. *Vet. Arh.* **2013**, *83*, 347–356.
29. Davidson, W.R.; Nettles, V.F.; Hayes, L.E.; Howerth, E.W.; Couvillion, C.E. Epidemiologic features of an intracranial abscessation/suppurative meningoencephalitis complex in white-tailed deer. *J. Wildl. Dis.* **1990**, *26*, 460–467. [CrossRef]
30. Cierny, G.; Mader, J.T.; Penninck, J.J. A clinical staging system for adult osteomyelitis. *Clin. Orthop.* **2003**, *414*, 7–24. [CrossRef] [PubMed]
31. Tiemann, A.; Hofmann, G.O.; Krukemeyer, M.G.; Krenn, V.; Langwald, S. Histopathological Osteomyelitis Evaluation Score (HOES)—An innovative approach to histopathological diagnostics and scoring of osteomyelitis. *GMS Interdiscip. Plast. Reconstr. Surg. DGPW* **2014**, *3*, Doc08. [CrossRef]
32. Shed Antlers: Different Pedicle Types | Every Spring Deer Shed Their Antlers and Many Avid Sportsmen Take to the Woods to Find Sheds. Here We Take an In-Depth Look at the Different Shapes of... | By MSU Deer LabFacebook | Facebook. Available online: https://www.facebook.com/msu.deerlab/videos/shed-antlers-different-pedicle-types/188785065871222/ (accessed on 2 June 2024).
33. Bubenik, A.B. Epigenetical, Morphological, Physiological, and Behavioral Aspects of Evolution of Horns, Pronghorns, and Antlers. In *Horns, Pronghorns, and Antlers: Evolution, Morphology, Physiology, and Social Significance*; Bubenik, G.A., Bubenik, A.B., Eds.; Springer: New York, NY, USA, 1990; pp. 3–113. [CrossRef]
34. Kierdorf, U.; Stoffels, E.; Stoffels, D.; Kierdorf, H.; Szuwart, T.; Clemen, G. Histological studies of bone formation during pedicle restoration and early antler regeneration in roe deer and fallow deer. *Anat. Rec. Part A Discov. Mol. Cell. Evol. Biol.* **2003**, *273*, 741–751. [CrossRef]
35. Li, C.; Yang, F.; Sheppard, A. Adult stem cells and mammalian epimorphic regeneration-insights from studying annual renewal of deer antlers. *Curr. Stem Cell Res. Ther.* **2009**, *4*, 237–251. [CrossRef] [PubMed]

36. Sybenga, A.B.; Jupiter, D.C.; Speights, V.O.; Rao, A. Diagnosing Osteomyelitis: A Histology Guide for Pathologists. *J. Foot Ankle Surg.* **2020**, *59*, 75–85. [CrossRef]
37. Li, C. Residual antler periosteum holds the potential to partially regenerate lost antler tissue. *J. Exp. Zool. Part A Ecol. Integr. Physiol.* **2021**, *335*, 386–395. [CrossRef] [PubMed]
38. Li, C.; Suttie, J.M.; Clark, D.E. Morphological observation of antler regeneration in red deer (*Cervus elaphus*). *J. Morphol.* **2004**, *262*, 731–740. [CrossRef] [PubMed]
39. Agriculture and Natural Resources Marketing. Deer Ecology & Management Lab. Available online: https://www.msudeer.msstate.edu/ (accessed on 8 January 2025).
40. Kierdorf, U.; Kierdorf, H. Deer antlers—A model of mammalian appendage regeneration: An extensive review. *Gerontology* **2011**, *57*, 53–65. [CrossRef]
41. Stadelmann, W.K.; Digenis, A.G.; Tobin, G.R. Physiology and healing dynamics of chronic cutaneous wounds. *Am. J. Surg.* **1998**, *176*, 26S–38S. [CrossRef]
42. Jonathan Sherratt's Research: Scar Formation. Available online: https://www.macs.hw.ac.uk/~jas/researchinterests/scartissueformation.html (accessed on 18 May 2025).
43. Cumming, B.D.; McElwain, D.L.S.; Upton, Z. A mathematical model of wound healing and subsequent scarring. *J. R. Soc. Interface* **2009**, *7*, 19–34. [CrossRef]
44. Li, C.; Suttie, J.M.; Clark, D.E. Histological examination of antler regeneration in red deer (*Cervus elaphus*). *Anat. Rec. Part A Discov. Mol. Cell. Evol. Biol.* **2005**, *282A*, 163–174. [CrossRef]
45. Landete-Castillejos, T.; Kierdorf, H.; Gomez, S.; Luna, S.; García, A.; Cappelli, J.; Pérez-Serrano, M.; Pérez-Barbería, J.; Gallego, L.; Kierdorf, U. Antlers-Evolution, development, structure, composition, and biomechanics of an outstanding type of bone. *Bone* **2019**, *128*, 115046. [CrossRef]
46. Newman, B.A.; D'Angelo, G.J. A Review of Cervidae Visual Ecology. *Animals* **2024**, *14*, 420. [CrossRef]
47. Széchenyi, Z. A Szarvas Selejtezése (Selective Culling of Red Deer). Régi Vadászkönyvek. Available online: https://www.vadaszkonyv.com/szechenyi-zsigmond-a-szarvas-selejtezese/ (accessed on 3 January 2025).
48. Pathology Outlines-Osteomyelitis Overview. Available online: https://www.pathologyoutlines.com/topic/mandiblemaxillaosteomyelitis.html (accessed on 1 July 2024).
49. Kierdorf, U.; Kierdorf, H. Roe and red deer antlers as bioindicators of pollution of deer. *Vet Arh.* **2006**, *76*, S117–S129.
50. Ludolphy, C.; Kierdorf, U.; Kierdorf, H. Lead concentrations in antlers of European roe deer (*Capreolus capreolus*) from an agricultural area in Northern Germany over a 119-year period—A historical biomonitoring study. *Environ. Sci. Pollut. Res.* **2021**, *28*, 56069–56078. [CrossRef] [PubMed]
51. Lakatos, I.; Babarczi, B.; Molnár, Z.; Tóth, A.; Skoda, G.; Horváth, G.F.; Horváth, A.; Tóth, D.; Sükösd, F.; Szemethy, L.; et al. First Results on the Presence of Mycotoxins in the Liver of Pregnant Fallow Deer (*Dama dama*) Hinds and Fetuses. *Animals* **2024**, *14*, 1039. [CrossRef] [PubMed]
52. Nanci, A.; Bosshardt, D.D. Structure of periodontal tissues in health and disease. *Periodontology 2000* **2006**, *40*, 11–28. [CrossRef]
53. Harris, H.A. Bone Formation and the Osteoblast. *Lancet* **1928**, *212*, 489–493. [CrossRef]
54. Li, C.; Suttie, J.M. Tissue collection methods for antler research. *Eur. J. Morphol.* **2003**, *41*, 23–30. [CrossRef]
55. Li, C.; Yang, F.; Li, G.; Gao, X.; Xing, X.; Wei, H.; Deng, X.; Clark, D.E. Antler regeneration: A dependent process of stem tissue primed via interaction with its enveloping skin. *J. Exp. Zool. Part A Ecol. Genet. Physiol.* **2007**, *307*, 95–105. [CrossRef]

Disclaimer/Publisher's Note: The statements, opinions and data contained in all publications are solely those of the individual author(s) and contributor(s) and not of MDPI and/or the editor(s). MDPI and/or the editor(s) disclaim responsibility for any injury to people or property resulting from any ideas, methods, instructions or products referred to in the content.

animals

MDPI

Article

Reference Values for Postmortem Examination of the Heart in the Macropod (*Macropodidae*) and Koala (*Phascolarctidae*)

Ella Cousins [1], Lucy Woolford [1], David McLelland [2], Sarah Brownrigg [1] and Natasha Speight [1,*]

[1] School of Animal and Veterinary Sciences, Faculty of Sciences, Engineering and Technology, University of Adelaide, Roseworthy, SA 5371, Australia
[2] Zoos South Australia, Frome Rd., Adelaide, SA 5000, Australia
* Correspondence: natasha.speight@adelaide.edu.au

Simple Summary: Morphological assessment of the heart is an integral component of postmortem investigation of sudden death and cardiac disease in domestic animals and wildlife species. Reference values for these parameters have been published for domestic species, however, no postmortem reference values for these morphometrics are available for Australian marsupials, such as macropods (Macropodidae: kangaroos, wallabies, tree kangaroos, and others) and koalas (*Phascolarctos cinereus*). Species-specific reference values presented in this study facilitate objective and improved postmortem cardiac assessment in macropods and koalas.

Abstract: Morphometric cardiac reference values are reported for macropods and koalas (*Phascolarctos cinereus*). Body weight (BW), heart weight (HW), left ventricle (LV) wall, interventricular septum (S), right ventricle (RV) wall thickness, and LV+S and RV weights were measured at postmortem examination of 48 macropods and 32 koalas that had no evidence of cardiovascular disease. The HW/BW% (0.43–0.96%) and (LV+S)/RV (2.80–4.22) for macropods were comparable to domestic species. In koalas, the HW/BW% (0.25–0.51%) was lower, and the (LV+S)/RV (3.06–5.41) ranged higher than in macropods and domestic species. The LV:RV of koalas (1.0–10.8) was more variable than in macropods (1.17–4.27). Two macropods with cardiac disease were assessed on postmortem examination against the generated reference values. An adult male common wallaroo (*Osphranter robustus*) was found dead with copious serous peritoneal effusion, chronic passive hepatic congestion with centrilobular fibrosis, and dilation of the RV, while the LV:RV was elevated, supportive of RV thinning. A 21-year-old female zoo-housed Matschie's tree kangaroo (*Dendrolagus matschiei*) had a flaccid thin-walled RV, LV cardiomyocyte hypertrophy, interstitial myocardial fibrosis and myofiber degeneration, pulmonary oedema, and serous pericardial effusion. The (LV+S)/RV and LV:RV were elevated and RV:S decreased, supporting left hypertrophic cardiomyopathy. Species-specific reference values presented in this study facilitate objective and improved postmortem cardiac assessment in macropods and koalas.

Keywords: cardiovascular disease; diagnosis; kangaroo; morphology; morphometric; Phascolarctos

1. Introduction

Establishing health status and diagnosing disease can be challenging in native Australian marsupials, such as macropods (Macropodidae: kangaroos, wallabies, tree kangaroos, and others) and koalas (*Phascolarctos cinereus*). This is due to a lack of species-specific

parameters available to assess their often unique morphological characteristics. Given that some macropod species, and koalas, have an IUCN classification of 'endangered', due to threats such as habitat loss, motor vehicle accident, and disease [1–3], it is important to build upon our foundations of understanding of these parameters and their applications in wildlife veterinary medicine.

Morphological assessment of the heart is an integral component of postmortem investigation of sudden death and cardiac disease in domestic animals and wildlife species [4]. This involves macroscopic visual assessment for pathologic lesions, morphometric measurements, and histopathological evaluation of the endo-, myo-, and epicardium and the conduction system. Morphometric measurements include total heart weight, ventricular wall weights, and ventricular wall thicknesses [4,5]. Reference values for these parameters have been published for domestic species, including the dog, horse, cat, cow, goat, sheep, and pig [4]. However, no postmortem reference values for these morphometrics are available for Australian marsupials, such as macropods and koalas, recently highlighted as a significant obstacle in the investigation of cardiac disease in these species [6].

Macropods and koalas from the wild and those managed in human care internationally in zoological institutions are often the subjects of pathological investigations. The lack of reference values for cardiac morphometrics makes the diagnosis of cardiac disease, and specifically cardiomyopathies, i.e., those with absence of significance congenital or acquired valvular or vascular abnormality, or extrinsic or secondary (known systemic or etiological abnormalities) contributing factors, in these species difficult. Few studies describe normal cardiac anatomy and physiology in marsupials [7,8]. One study in wallabies and kangaroos suggested that heart rate, arterial pressure, and cardiac output were similar to those of domestic species of comparable size [9]. Detailed descriptions of the cardiovascular anatomy and physiology of the koala are lacking in the literature, with small numbers of published reports comparing koala anatomy with eutherian mammals [10–12].

In macropods, cardiac disease is most reported in association with nutritional myopathies, exertional myopathies, and infectious disease (e.g., encephalomyocarditis virus, *Toxoplasma gondii*, and *Neosporum caninum*) [13–15]. Reports of cardiomyopathies in marsupials are limited to individual case reports, small comparative studies, and zoological collection surveys, with morphometric assessment of the heart often limited or not performed at all. Hypertrophic cardiomyopathy has been diagnosed in a three-year-old, intact male Matschie's tree kangaroo (*Dendrolagus matschiei*) [16] and in two captive Bennett's wallabies (*Macropus rufogriseus rufogriseus*) [17]. Right-sided cardiac hypertrophy attributed to hypoxia of high altitude has been described in an adult male Bennett's wallaby held in a zoological collection situated at an altitude above 2000 m [18]. A degenerative cardiomyopathy of unspecified aetiology was reported in the eastern grey kangaroo (*Macropus giganteus*) [19]. More broadly, cardiovascular lesions suggestive of hypertension were identified in multiple western grey kangaroos from a single zoo. No aetiology was determined; however, lesions were characterised by arterial medial thickening and hypertrophy and increased tortuosity of renal arterioles. In koalas, cardiac failure has been reported secondary to an atrial septal defect [20]. The major challenge for clinicians and pathologists investigating cardiomyopathies, and cardiac disease more generally, in marsupials at postmortem is the lack of species-specific cardiac morphometric reference values. This often leads to a reliance on comparing individuals with conspecifics, which are generally few, if indeed available.

The aim of this study was to develop cardiac morphometric reference values for koalas and commonly examined macropod species to improve pathological assessment of the heart in these taxa.

2. Materials and Methods

Forty-eight macropods that had died of causes unrelated to cardiovascular disease were opportunistically sampled during routine postmortem examination, including four captive zoo-based wallabies and kangaroos that died or were euthanised due to health concerns, twenty rescued free-ranging kangaroos and wallabies with traumatic injuries necessitating euthanasia at referring veterinary clinics or zoos, and twenty-four free-ranging kangaroos that were euthanised under a permit issued by the South Australian Department of Environment of Water in accordance with the Animal Welfare Act 1985, for purposes not related to this study. By species, the study population comprised 12 red kangaroos (*Osphranter rufus*), 24 western grey kangaroos (*M. fuliginosus*), 8 tammar wallabies (*Notamacropus eugenii*), and 4 yellow-footed rock wallabies (*Petrogale xanthopus*); by sex, there were 29 females and 19 males (Table 1).

Table 1. Reference population for determination of macropod and koala cardiac morphometric intervals. TWC = tooth wear class.

		Western Grey Kangaroo (24)	Red Kangaroo (12)	Tammar Wallaby (8)	Yellow-Footed Rock Wallaby (4)	Koala (32)
Sex	Male	11	6	2	0	13
	Female	13	6	6	4	19
Age	Juvenile (<2 years)	9	2	3	0	TWC I = 2 TWC II = 3
	Adult (>2 years)	15	10	5	4	TWC III = 12 TWC I = 11 TWC V= 3

A total of 32 koalas, free ranging from the Mount Lofty Ranges region of South Australia (SA) or housed at Adelaide Zoo, SA, which had died of causes unrelated to cardiovascular disease, were obtained opportunistically for routine postmortem examination. Of these, 27 were euthanised on welfare grounds due to a dog attack or other trauma, and 5 had died due to other non-cardiovascular-related disease. Nineteen koalas were female and thirteen were male (Table 1). Of the 32 koalas, 31 had approximate age determined by tooth wear of the upper premolar, allowing evaluation by tooth wear class (TWC; I–V) [11]: TWC I, $n = 2$; class II, $n = 3$; class III, $n = 12$; class IV, $n = 11$; class V, $n = 3$.

Additionally, an adult male free-ranging common wallaroo (*Osphranter robustus*) (Case 1) found dead within the boundaries of an open-range zoo, and an adult female zoo-housed Matschie's tree kangaroo (Case 2) euthanised on welfare grounds due to deteriorating degenerative joint disease, were presented for postmortem examination. Both were found to have gross lesions suggestive of cardiac disease, and data were collected for opportunistic evaluation against the reference values generated here.

Following routine postmortem examination, the heart was transected approximately one-third the length of the ventricles above the apex, cleared of blood, weighed in toto, and fixed in 10% neutral buffered formalin. Left ventricular free wall (LV), interventricular septum (S), and right ventricular free wall (RV) widths were measured at the narrowest point of the free wall or septum at the site of transection (Figure 1). LV+S weight and RV weight were determined as per Robinson and Robinson, 2016 [4]. Minimum histopathology tissue sets included the heart, liver, and lung to screen for microscopic cardiac lesions and systemic lesions associated with cardiac insufficiency. A complete set of tissues was collected for histopathology for cases where the cause of death was not evident grossly. Formalin-fixed tissue samples were processed by routine histopathological techniques, embedded in paraffin, sectioned at 4 μm, and stained with haematoxylin and eosin (HE). Tissues were examined by using an Olympus BX43 microscope (Olympus, Tokyo, Japan).

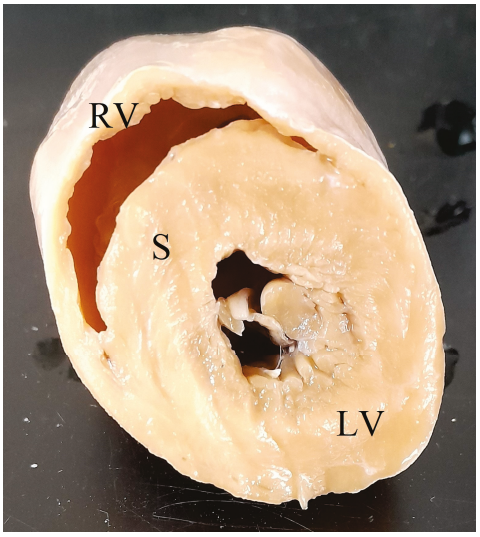


Figure 1. Transected koala heart showing right ventricular free wall (RV), interventricular septum (S), and left ventricular free wall (LV).

Mean, standard deviation (SD), and maximum and minimum values of HW/BW (%), (LV+S)/RV, LV:RV, LV:S, RV:S, (LV+S)/BW (%), and (LV+S)/HW (%) were determined for koalas, for all macropods, for kangaroos (*Osphranter* spp. and *Macropus* spp.), and for wallabies (*Notamacropus* spp. and *Petrogale* spp.) in Excel (Microsoft Corporation, Redmond, WA, USA, 2021). For 3/48 macropods and 26/32 koalas, heart weight and total body weight were not collected. All animals in the study populations were determined to be unaffected by cardiovascular disease. Data were also examined using Reference Value Advisor (National Veterinary School of Toulouse, Toulouse, Haute-Garonne, France; version 2.1) within Excel. Histograms were inspected visually for normality and detection of outliers. A tendency to retain rather than remove outlier values was adopted, unless there were determinable clinical or data integrity reasons for removal. No outliers were removed. For sex comparison, descriptive statistics were generated, and data were examined for normality using the Shapiro–Wilk test in SPSS v29 (IBM, New York, NY, USA). No outliers were removed. Non-parametric data were analysed using the Mann–Whitney U test, with statistical significance regarded as $p < 0.05$.

3. Results

3.1. Morphometric Reference Values

Heart weight as a percentage of total body weight for 45 macropods and 6 koalas is presented in Table 2. The ratios of the left ventricular free wall and septum weight to right ventricular free wall weight ((LV+S)/RV) are presented in Table 3. Ventricular wall width ratios (LV:RV, LV:S, and RV:S) for 48 macropods and 32 koalas are presented in Tables 4–6. Broad reference values for LV:RV were observed for both the macropod (1.17–4.27) and the koala (1.00–10.84), with koala values notably wider than the macropod. Additional values generated included LV+S weight as a percentage of total body weight (BW; Table 7) and as a percentage of total heart weight (HW; Table 8).

Table 2. Heart weight as a percentage of body weight for healthy macropods and koalas, within inclusion of published intervals for domestic species. YFRW = yellow-footed rock wallaby.

Species (*n*)	Mean (%)	Mean ± 2SD (%)	Min. (%)	Max. (%)
All Macropods (45)	0.69	0.43–0.96	0.50	1.13
Kangaroos—Red, Western grey (34)	0.68	0.43–0.93	0.50	1.13
Wallabies—YFRW, Tammar (11)	0.73	0.42–1.03	0.60	1.06
Tammar Wallaby (6) [14]	0.67	0.51–0.83	0.53	0.73
Koala (6)	0.38	0.25–0.51	0.31	0.49
Dog (21) [1]	0.71	0.43–0.99	n/a	n/a
Dog [2]	0.76	0.58–0.94	n/a	n/a
Horse (12) [1]	0.69	0.41–0.97	n/a	n/a
Cat (9) [1]	0.58	0.28–0.88	n/a	n/a
Cow (15) [1]	0.48	0.30–0.66	n/a	n/a
Goat (11) [1]	0.46	0.26–0.66	n/a	n/a
Sheep (8) [1]	0.41	0.17–0.65	n/a	n/a
Pig (8) [1]	0.40	0.32–0.48	n/a	n/a

Table 3. Left ventricular free wall and septum to right ventricular free wall weight ratios ((LV+S)/RV) for healthy macropods and koalas compared to published intervals for domestic species.

Species (*n*)	Mean	Mean ± 2SD	Min.	Max.
All Macropods (48)	3.52	2.80–4.22	2.68	4.28
Kangaroos—Red, Western grey (36)	3.42	2.80–4.03	2.68	4.04
Wallabies—YFRW, Tammar (12)	3.81	3.16–4.46	3.39	4.28
Koala (6)	4.23	3.06–5.41	3.77	5.29
Dog (21) [1]	3.26	2.39–5.12	n/a	n/a
Dog [2]	3.32	2.76–3.88	n/a	n/a
Horse (12) [1]	3.12	2.43–4.34	n/a	n/a
Cat (9) [1]	3.45	2.94–4.17	n/a	n/a
Cow (15) [1]	2.78	2.43–4.00	n/a	n/a
Goat (11) [1]	3.12	2.50–4.17	n/a	n/a
Sheep (8) [1]	3.33	2.63–4.45	n/a	n/a
Pig (8) [1]	2.94	2.38–3.84	n/a	n/a

Table 4. Left-to-right ventricular wall width ratios (LV:RV) determined at postmortem for healthy macropods, koalas, and dogs.

Species (*n*)	Mean	Mean ± 2SD	Min.	Max.
All Macropods	2.70 (48)	1.15–4.26	1.60	4.67
Kangaroos (Red, Western Grey)	2.51 (36)	1.20–3.78	1.60	4.00
Wallabies (YRFW, Tammar)	3.35 (12)	1.74–4.97	2.00	4.67
Koala	5.92 (32)	1.00–10.84	2.75	11.00
Dog [2]	2.13	1.80–2.46	n/a	n/a

Table 5. Left ventricular wall to septum width ratios for healthy macropods and koalas.

Species (*n*)	Mean	Mean ± 2SD	Min.	Max.
All Macropods (48)	1.08	0.77–1.40	0.83	1.67
Kangaroos—Red, Western Grey (36)	1.06	0.78–1.35	0.83	1.67
Wallabies—YFRW, Tammar (12)	1.14	0.77–1.51	0.89	1.50
Koala (32)	1.08	0.61–1.54	0.82	1.83

Table 6. Right ventricular wall to septum width ratios for healthy macropods and koalas.

Species (*n*)	Mean	Mean ± 2SD	Min.	Max.
All Macropods (48)	0.42	0.23–0.61	0.21	0.67
Kangaroos—Red, Western Grey (36)	0.44	0.27–0.62	0.29	0.67
Wallabies—YFRW, Tammar (12)	0.35	0.19–0.52	0.21	0.56
Koala (32)	0.21	0.00–0.43	0.09	0.67

Table 7. Left ventricle and septum weight as a percentage of body weight, (LV+S)/BW (%), for healthy macropods and koalas.

Species (*n*)	Mean (LV+S)/BW (%)	Mean ± 2SD	Min.	Max.
All Macropods (45)	0.43	0.25–0.60	0.30	0.74
Kangaroos—Red Western Grey (34)	0.42	0.25–0.59	0.30	0.74
Wallabies—YFRW, Tammar (11)	0.44	0.24–0.64	0.32	0.68
Koala (6)	0.22	0.16–0.29	0.19	0.22

Table 8. Left ventricle and septum weight as a percentage of heart weight, (LV+S)/HW (%), for healthy macropods and koalas.

Species (*n*)	Mean (LV+S)/HW (%)	Mean ± 2SD	Min.	Max.
All Macropods (48)	62.0	51.6–72.0	48.6	71.1
Kangaroos—Red, Western Grey (36)	62.0	52.2–72.4	49.1	71.1
Wallabies—YFRW, Tammar (12)	60.4	49.9–70.8	0.49	68.0
Koala (6)	59.5	46.5–72.5	51.7	69.5

For kangaroos, females showed a significantly higher HW/BW% than males (0.73% ± 0.03 vs. 0.63% ± 0.02; $p = 0.018$). Also, female koalas ($n = 13$) showed a significantly higher LV:RV width ratio (6.9 ± 0.7) than males ($n = 19$; 5.3 ± 0.6; $p = 0.037$) (Supplementary file S1).

3.2. Pathologic Cases

Cardiac measurements for two macropods suspected to have cardiac disease were compared with the reference values established in this study (Table 9). Case 1 was an adult male free-ranging common wallaroo (*Osphranter robustus*) that was found dead. The kangaroo was moderately underconditioned; however, body weight was not recorded. At postmortem examination, there was copious yellow serous fluid in the peritoneal cavity. The right ventricle was subjectively distended. For ventricular widths, LV:RV was elevated, supporting RV thinning, and LV:S was within reference values for all macropods but marginally elevated for kangaroos. Other available measurements were within the reference values. Microscopic examination of the left and right myocardium was unremarkable on HE and Masson's Trichrome stains. The liver was congested with marked chronic centrilobular and bridging fibrosis and subcapsular fibrosis with subcapsular congestion and hepatocellular atrophy, consistent with chronic passive congestion (Figure 2). Occasional aberrant ductular profiles were adjacent centrilobular fibrosis.

Table 9. Cardiac measurements for macropods with cardiac disease (H = higher and L = lower than reference values found in normal macropods in this study).

Case	BW (kg)	HW (gm)	HW/BW (%)	LV+S (gm)	RV (gm)	LV (mm)	S (mm)	RV (mm)	(LV+S)/RV	LV:RV	LV:S	RV:S
1. Wallaroo	n/a	328	n/a	211	71	21	15	5	2.99	4.20 (H)	1.40	0.33
2. Matschie's tree kangaroo	8.69	45.0	0.48	25.9	5.7	10	9.5	1.5	4.54 (H)	6.67 (H)	1.05	0.16 (L)

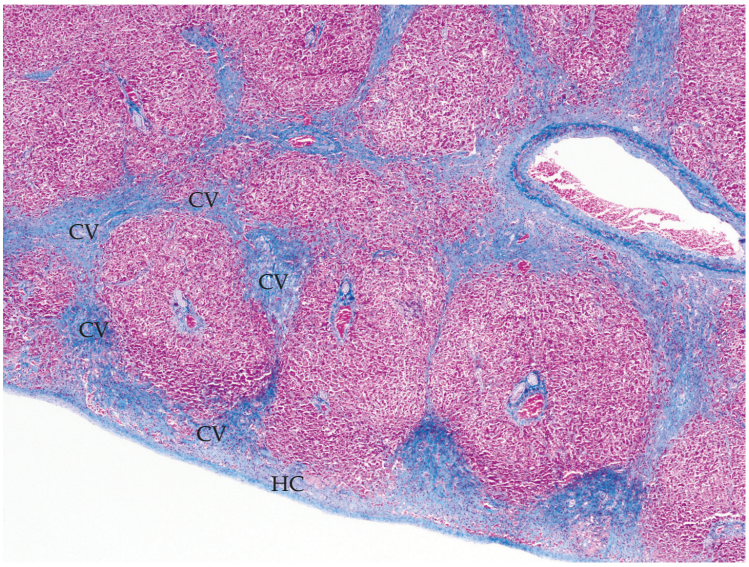


Figure 2. Case 1, common wallaroo (*O. robustus*), liver, Masson's Trichrome stain. There is marked expansion of fibrocollagenous connective tissue around central veins (CVs) with centrilobular bridging fibrosis and fibrous thickening of the hepatic capsule (HC).

Case 2 was a 21-year-old female zoo-housed Matschie's tree kangaroo weighing 8.69 kg. This geriatric kangaroo was euthanised due to deterioration of chronic vertebral osteoarthritis that had been managed with non-steroidal anti-inflammatory medication for the previous three years. At postmortem examination, the right ventricle was subjectively thin-walled and flaccid. The lungs oozed serous fluid on the cut section, and there was serosanguinous fluid in the large airways and pericardial sac. The (LV+S)/RV was elevated above reference values; however, HW/BW% was within the reference values. For ventricular wall ratios, LV:RV was elevated and RV:S decreased, suggesting left-side ventricular hypertrophy and/or thinning of the RV wall. Microscopically, there was moderate cardiomyocyte hypertrophy in the left ventricle, with multifocal interstitial myocardial fibrosis, myofiber degeneration, loss, and atrophy, with interstitial oedema (Figure 3). The lungs were diffusely congested, airways often flooded by proteinaceous fluid, with diapedesis and increased foamy macrophages, and haemosiderophages were not observed.

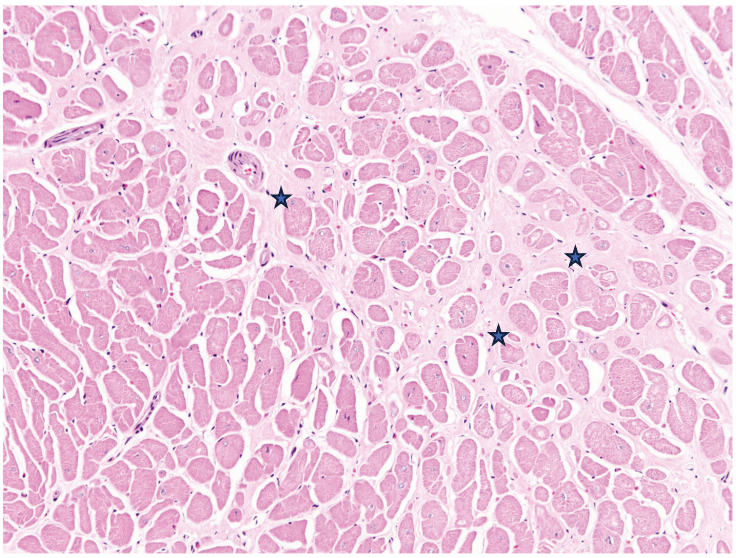


Figure 3. Case 2, Matschie's tree kangaroo (*D. matschiei*), left ventricular myocardium, haematoxylin and eosin stain. Cardiomyocytes are hypertrophic with increased variation in size. Mature fibrocollagenous connective tissue dissects between and isolates individual fibres (stars).

4. Discussion

Species-specific reference values facilitate objective assessment of the heart at postmortem. Determined reference values (mean ± 2SD) for heart weight as a percentage of body weight in macropods were similar to those determined previously for the tammar wallaby [21] and comparable to the domestic dog and horse. In contrast, koala reference values were lower with a narrower range than for macropods, dogs, and horses, but comparable to published reference values for the pig [1]. In the kangaroo, HW/BW% was greater in female than male kangaroos, contrasting to most domestic animals in which HW/BW% is typically greater in males than in females [4]. This most likely reflects sexual dimorphism in body size, with male red kangaroos and western grey kangaroos weighing 22–92 kg and 18–72 kg, respectively, compared to their female counterparts, with females of both species weighing between 17 kg and 39 kg [22,23].

The heart weight as a % of body weight is higher in more athletic species (horses and dogs) and is increased by training and exercise [4]. Kangaroos are athletic species, able to cover ground in short bursts at high speed [24]. Movements of >100 km have been recorded for individual red kangaroos from tagging and radio telemetry [25,26]. However, outside of drought periods when animals range more widely [27], these have been considered exceptions in a generally sedentary population where individuals move within home ranges of variable size [28]. In the koala, the lower heart weight as a % of body weight may reflect the relatively sedentary nature of these animals, which have been found to have a low metabolic rate, 74% of the predicted marsupial value [29].

The ratio of the left ventricle and septum weight to the right ventricular weight ((LV+S)/RV) is a key parameter used to assess the heart in domestic animals [4]. A ratio between 2.8 and 4.0 is considered normal in mature domestic animals, with a ratio > 4 indicating left ventricular hypertrophy, and a ratio < 2.8 suggesting right ventricular hypertrophy. For macropods, the reference values were comparable with domestic species; however, the koala values were broader, with a higher upper reference value.

Assessment of ventricular wall ratios is commonplace in postmortem assessment of the heart: in comparison to the domestic dog (1.80–2.46), a broader range of values was observed for LV:RV in both the macropod (1.165–4.27) and, notably, the koala (1.00–10.84), with the latter species showing an upper reference value and maximum twice that of macropods. It is possible that the broad reference values for LV:RV in the koala make this a less sensitive measure for the investigation of cardiac disease than in other species.

In Case 2, elevated (LV+S)/RV and LV:RV, and decreased RV:S, provided supportive evidence for left ventricular hypertrophy and left-sided congestive heart failure, alongside corroborative findings of myocardial hypertrophy with myofiber degeneration, and interstitial fibrosis, pulmonary oedema, and serous pericardial effusion. These findings were consistent with expected lesions in hypertrophic cardiomyopathy of felids and other domestic species [30]; however, HW/BW% was not increased in Case 2. For Case 1, elevated LV:RV lent further weight to grossly observed RV thinning and probable right-sided congestive heart failure, supported by chronic passive congestive and fibrotic changes in the liver and ascites observed grossly. Histopathological findings in the liver mirrored expected lesions in domestic animals with chronic right-sided congestive heart failure [30,31]. Hypertrophic cardiomyopathy has been previously described in two captive Bennett's wallabies [17]. Although body and heart weights were not published, reported (LV+S)/RV values of 5 and 8.2, for each wallaby, respectively, were elevated above the reference values determined in this study, lending further support for HCM in these individuals. Conversely, LV:RV, LV:S, and RV:S were within the RI generated here. Other reports of cardiomyopathies in macropods reviewed during this study did not include sufficient information to allow

assessment of hearts against generated reference values. Future studies will benefit from larger sample sizes and expansion of the number of species examined.

5. Conclusions

Reference values developed in this study facilitated improved and objective post-mortem cardiac assessment in macropods and koalas. As variation in heart morphology is expected across domestic species, it is likely that there is variation across the Macropodidae. This large superfamily includes kangaroos, wallabies, and the musky rat kangaroo (*Hypsiprymnodon moschatu*), which exhibit diversity in size, anatomy, and life histories [32]. Overall, however, these parameters will allow a better understanding of the occurrence and characteristics of cardiac disease in macropods and koalas.

Supplementary Materials: The following supporting information can be downloaded at: https://www.mdpi.com/article/10.3390/ani15101397/s1.

Author Contributions: Conceptualisation, N.S., D.M. and L.W.; methodology, N.S., D.M. and L.W.; formal analysis, E.C., S.B., N.S., D.M. and L.W.; resources, N.S., D.M. and L.W.; data curation, E.C., D.M., N.S., S.B. and L.W.; writing—original draft preparation, E.C., D.M., N.S., S.B. and L.W.; writing—review and editing, E.C., D.M., N.S., S.B. and L.W.; supervision, N.S., D.M. and L.W. All authors have read and agreed to the published version of the manuscript.

Funding: This research received no external funding. The authors are grateful to the financial support of the School of Animal and Veterinary Sciences, University of Adelaide, for histopathology slide preparation and processing.

Institutional Review Board Statement: Not applicable.

Informed Consent Statement: Not applicable.

Data Availability Statement: Data is contained within the article or Supplementary Material.

Acknowledgments: The authors wish to thank Zoos South Australia, Cleland Wildlife Park, and Gorge Wildlife Park for donation of macropod samples, and Adelaide Koala and Wildlife Centre and Zoos South Australia for koala samples. Thanks to Cheryl Day for skilful production of histology slides and Adrian Hines for assistance in necropsy.

Conflicts of Interest: The authors declare no conflicts of interest.

References

1. Gonzalez-Astudillo, V.; Henning, J.; Valenza, L.; Knott, L.; McKinnon, A.; Larkin, R.; Allavena, R. A necropsy study of disease and comorbidity trends in morbidity and mortality in the koala (*Phascolarctos cinereus*) in South-East Queensland, Australia. *Sci. Rep.* **2019**, *9*, 17494. [CrossRef] [PubMed]
2. Speight, K.N.; Hicks, P.; Graham, C.; Boardman, W.; Breed, W.G.; Manthorpe, E.; Funnell, O.; Woolford, L. Necropsy findings of koalas from the Mount Lofty Ranges population in South Australia. *Aust. Vet. J.* **2018**, *96*, 188–192. [CrossRef]
3. Woinarski, J.; Burbidge, A.A. *Phascolarctos cinereus* (amended version of 2016 assessment). *The IUCN Red List of Threatened Species* 2020: E.T16892A166496779. Available online: https://dx.doi.org/10.2305/IUCN.UK.2020-1.RLTS.T16892A166496779.en (accessed on 7 April 2025).
4. Robinson, W.; Robinson, N. Cardiovascular System. In *Jubb, Kennedy and Palmer's Pathology of Domestic Animals*, 6th ed.; Elsevier: Amsterdam, The Netherlands, 2015; Volume 3, pp. 1–101.
5. Turk, J.; Root, C. Necropsy of the Canine Heart: A Simple Technique for Quantifying Ventricular Hypertrophy and Valvular Alterations. *Am. J. Vet. Res.* **1983**, *5*, 905–910.
6. Fenton, H.; Rose, K. Macropods Heather Fenton and Karrie Rose in Hall J. In Proceedings of the Wildlife Health and Pathology Short Course, Sydney, NSW, Australia, 2024.
7. Sugishita, Y.; Iida, K.; O'Rourke, M.F.; Kelly, R.; Avolio, A.; Butcher, D.; Reddacliff, G. Echocardiographic and electrocardiographic study of the normal kangaroo heart. *Aust. N. Z. J. Med.* **1990**, *20*, 160–165. [CrossRef]
8. O'Rourke, M.F.; Avolio, A.P.; Nichols, W.W. The kangaroo as a model for the study of hypertrophic cardiomyopathy in man. *Cardiovasc. Res.* **1986**, *20*, 398–402. [CrossRef]

9. Maxwell, G.; Elliot, R.; Kneebone, G. Hemodynamics of kangaroos and wallabies. *Am. J. Physiol.* **1964**, *206*, 967–970. [CrossRef]
10. Forbes, W.A. On some points in the anatomy of koala (*Phascolarctos cinereus*). *Proc. Zool. Soc. London* **1881**, *17*, 180–195. [CrossRef]
11. Martin, R.W. Age-specific fertility in three populations of the koala, *Phascolarctos cinereus* Goldfuss, in Victoria. *Wildl. Res.* **1981**, *8*, 275–283. [CrossRef]
12. Owen, R. *On the Comparative Anatomy and Physiology of Vertebrates*; Longmans Green: London, UK, 1868; p. 915.
13. Rose, K.; McLelland, D.; Dixon, R.; Kirkland, P. Studies on the encephalomyocarditis virus in a zoological context. *Kokako* **2000**, *7*, 13.
14. Portas, T.J. Toxoplasmosis in macropodids: A review. *J. Zoo Wildl. Med.* **2010**, *41*, 1–6. [CrossRef]
15. Cronstedt-Fell, A.; Richter, B.; Voracek, T.; Kubber-Heiss, A. Neosporosis in a captive Parma wallaby (*Macropus parma*). *J. Comp. Pathol.* **2012**, *146*, 274–277. [CrossRef] [PubMed]
16. Fredholm, D.V.; Jones, A.E.; Hall, N.H.; Russell, K.; Heard, D.J. Successful management of hypertrophic cardiomyopathy in a Matschie's tree kangaroo (*Dendrolagus matschiei*). *J. Zoo Wildl. Med.* **2015**, *46*, 95–99. [CrossRef] [PubMed]
17. Stern, A.W.; Smith, S.; Snider, T.A. Hypertrophic cardiomyopathy in two captive Bennett's wallabies (*Macropus rufogriseus rufogriseus*). *J. Vet. Diagn. Investig.* **2009**, *21*, 889–892. [CrossRef] [PubMed]
18. Juan-Salles, C.; Martinez, L.S.; Rosas-Rosas, A.G.; Paras, A.; Martinez, O.; Hernandez, A.; Garner, M.M. Pulmonary arterial disease associated with right-sided cardiac hypertrophy and congestive heart failure in zoo mammals housed at 2100 m above sea level. *J. Zoo Wildl. Med.* **2015**, *46*, 825–832. [CrossRef]
19. Chineme, C.N.; Njoku, C.O.; Evbuoma, N. Degenerative cardiomyopathy in a captive kangaroo (*Macropus giganteus*). *J. Wildl. Dis.* **1978**, *14*, 52–53. [CrossRef]
20. Atwell, R.B.; Booth, R. Cardiac failure in a koala secondary to an atrial septal defect. *Aust. Vet. J.* **1990**, *67*, 272–273. [CrossRef]
21. Dawson, T.J.; Needham, A.D. Cardiovascular characteristics of two resting marsupials: An insight into the cardio-respiratory allometry of marsupials. *J. Comp. Physiol.* **1981**, *145*, 95–100. [CrossRef]
22. Dawson, T.J. *Kangaroos:Biology of the Largest Marsupials*; UNSW Press: Sydney, Australia, 1995.
23. Van Dyck, S.; Strahan, R. *The Mammals of Australia*, 3rd ed.; Reed New Holland: Sydney, Australia, 2008.
24. Dawson, T.J.; Taylor, C.R. Energetic cost of locomotion in kangaroos. *Nature* **1973**, *246*, 313–314. [CrossRef]
25. Bailey, P.; Best, L. A red kangaroo, *Macropus rufus*, recovered 25 years after marking in north-western New South Wales. *Aust. Mammal.* **1992**, *15*, 141. [CrossRef]
26. Bailey, P. The Red kangaroo, *Megaleia rufa* (Desmarest), in north western New South Wales. 1. Movements. *CSIRO Wildl. Res.* **1971**, *16*, 11–28. [CrossRef]
27. Norbury, G.L.; Norbury, D.C.; Oliver, A.J. Facultative behaviour in unpredictable environments: Mobility of red kangaroos in arid Western Australia. *J. Anim. Ecol.* **1994**, *63*, 410–418. [CrossRef]
28. McCullough, D.; McCullough, Y. *Kangaroos in Outback Australia: Comparative Ecology and Behavior of Three Coexisting Species*; Columbia University Press: New York, NY, USA, 2000.
29. Degabriele, R.; Dawson, T.J. Metabolism and heat balance in an arboreal marsupial, the koala (*Phascolarctos cinereus*). *J. Comp. Physiol. B Biochem. Syst. Environ. Physiol.* **1979**, *134*, 293–301. [CrossRef]
30. Miller, L.M.; Gal, A. Cardiovascular System and Lymphatic Vessels. In *Pathologic Basis of Veterinary Disease*, 10th ed.; Zachary, J.F., Ed.; Mosby: St. Louis, MO, USA, 2017; pp. 561–616.e561.
31. Cullen, J.M.; van den Ingh, T.S.; Bunch, S.E.; Rothuizen, J.; Washabau, R.J.; Desmet, V.J. Morphological classification of circulatory disorders of the canine and feline liver. In *WSAVA Standards for Clinical and Histological Diagnosis of Canine and Feline Liver Diseases*; Rothuizen, J., Bunch, S.E., Charles, J.A., Cullen, J.M., Desmet, V.J., Szatmári, V., Twedt, D.C., van den Ingh, T.S., Van Winkle, T., Washabau, R.J., Eds.; W.B. Saunders: Philadelphia, PA, USA, 2006; pp. 41–59.
32. Baker, A.; Gynther, I. *Strahan's Mammals of Australia*, 4th ed.; New Holland Publishers: Sydney, Australia, 2023.

Disclaimer/Publisher's Note: The statements, opinions and data contained in all publications are solely those of the individual author(s) and contributor(s) and not of MDPI and/or the editor(s). MDPI and/or the editor(s) disclaim responsibility for any injury to people or property resulting from any ideas, methods, instructions or products referred to in the content.

animals

MDPI

Case Report

Diagnostic Application of Fluorine-18 Fluorodeoxyglucose Positron Emission Tomography/Computed Tomography in the Treatment of Oral Squamous Cell Carcinoma in an African Pygmy Hedgehog

Jaegyeong Shin [1,†], Nari Kim [1,†], Gwi-Ho Jeon [2], Taesik Yun [1], Byeong-Teck Kang [1] and Dong-Hyuk Jeong [1,3,*]

[1] College of Veterinary Medicine, Chungbuk National University, Cheongju 28644, Republic of Korea; shinjk8646@naver.com (J.S.); queng91@gmail.com (N.K.); fermium@cbnu.ac.kr (T.Y.); kangbt@cbnu.ac.kr (B.-T.K.)
[2] Su Veterinary Clinic, Cheongju 28665, Republic of Korea; vet9530@naver.com
[3] Wildlife Center of Chungbuk, Cheongju 28116, Republic of Korea
* Correspondence: africabear@cbnu.ac.kr; Tel.: +82-10-4749-2061
† These authors contributed equally to this work.

Simple Summary: This case report evaluates the effectiveness of Fluorine-18 fluorodeoxyglucose positron emission tomography/computed tomography (18F-FDG PET/CT) in diagnosing tumor malignancy and assessing metastasis in an African pygmy hedgehog (*Atelerix albiventris*) with oral squamous cell carcinoma. Our findings suggest that 18F-FDG PET/CT can be a useful tool for assessing malignancy and metastasis in tumors in African pygmy hedgehogs.

Abstract: Neoplastic diseases are common in African pygmy hedgehogs (*Atelerix albiventris*), with squamous cell carcinoma (SCC) being the most prevalent oral tumor. Traditional imaging techniques like computed tomography (CT) have limitations in accurately defining tumor extent and detecting metastasis. In this study, a hedgehog with a suspected oral tumor underwent 18F-FDG PET/CT imaging, revealing a hypermetabolic lesion consistent with SCC and indications of metastatic activity. The lesion was too extensive for a lumpectomy, and suspected metastasis led to the decision for euthanasia due to the impracticability of further treatment. A histopathological examination after autopsy confirmed the diagnosis and metastatic spread, as suggested by PET/CT findings. This is the first case report demonstrating the potential use of 18F-FDG PET/CT in hedgehogs, facilitating the accurate staging and management of oral SCC. Further research is needed to establish PET/CT as a standard diagnostic tool for neoplastic diseases in hedgehogs.

Keywords: African pygmy hedgehog; *Atelerix albiventris*; oral squamous cell carcinoma; 18F-FDG PET/CT; metastasis assessment

1. Introduction

African pygmy hedgehogs (*Atelerix albiventris*) commonly develop neoplastic diseases, with retrospective studies indicating a prevalence ranging from 29% to 53% during necropsies [1–3]. These neoplasms are predominantly malignant (up to 85%) and often lead to a poor prognosis [1]. Among hedgehogs with oral neoplastic disease, squamous cell carcinoma (SCC) is the most prevalent type of neoplasm [1,4,5]. SCC metastasizes slowly, with pulmonary metastases occurring in a few cases [6]. Other neoplastic cases include peripheral odontogenic fibroma [7], osteoma [8], osteochondroma [9], osteosarcoma [4,8], and fibrosarcoma [1,10].

The spectrum of oral lesions typically observed in hedgehogs include both neoplastic and non-neoplastic growth [1,5,11]. A retrospective study on privately owned hedgehogs identified twenty-seven oral cavity masses, eight of which were non-neoplastic (gingival

hyperplasia), and nineteen neoplastic (seventeen SCCs and two mesenchymal tumors) [11]. This study states that histopathology is essential for a definitive diagnosis, although clinical signs, growth patterns, and anatomic location can aid in identifying SCC.

Treatment options for hedgehogs with SCC include chemotherapy [12], electrochemotherapy (ECT) [13], and lumpectomy [14], albeit with limited success due to metastasis. Computed tomography (CT) remains the primary tool for treatment planning; however, its limitations in accurately defining tumor extent and detecting metastasis are acknowledged [15].

In response to these limitations, positron emission tomography/computed tomography (PET/CT) has gained traction for head and neck cancer staging in humans [16] and cats [15,17], offering superior sensitivity for detecting cancer infiltration. PET/CT is a powerful tool for assessing metastatic disease, providing detailed metabolic and anatomical insights that aid in the precise staging and management of cancer [18].

The authors found no existing reports to date on the use of PET/CT for tumors in hedgehogs. Therefore, this case report evaluates the effectiveness of PET/CT in diagnosing tumor malignancy and evaluating tumor metastasis in hedgehogs with oral neoplastic diseases.

2. Case Description

A client-owned, 3-year-old male African pygmy hedgehog was first seen by a primary care veterinarian at Su Veterinary Clinic in July 2023 due to hyporexia. After the patient was anesthetized, a physical examination revealed that both the left mandibular and maxillary teeth were covered by a swollen, tumor-like gingiva. The patient was treated with prednisolone (PDS) (1 mg/kg orally (PO)), enrofloxacin (5 mg/kg PO), and famotidine (0.5 mg/kg PO) twice daily for 7 days.

A biopsy was performed on the damaged teeth and swollen gingiva to collect samples for histopathological examination. One sample from the teeth and five samples of gingival tissue, with depths ranging from 0.7 mm to 2.7 mm, were analyzed. Histopathological analysis revealed severe gingivitis and proliferative findings in the mucosal epithelial cells of the gingiva. The proliferative epithelial cells displayed bridge formations, proliferating in a cord-like growth pattern or forming islands. Keratin pearls and mitotic figures were not observed in this shallow sample. Based on these findings, acanthomatous ameloblastoma was diagnosed.

The oral mass in the gingival area continued to spread despite treatment and was subsequently treated with oclacitinib (0.6 mg/kg PO) for one day, along with PDS (1 mg/kg PO), clindamycin (5 mg/kg PO), and famotidine (0.5 mg/kg PO) for 7 days. All medications were administered twice daily. After 7 days, the oral mass appeared to be stable. Doxycycline (5 mg/kg PO) was added to the previous treatment regimen, administered twice daily for another 7 days, to prevent secondary infection. However, the mass began to spread again 29 days after the initial treatment began, prompting a switch from oclacitinib to toceranib (2.5 mg/kg PO) twice daily for one day. After two weeks, an abscess formed at the site of the tooth root, among the tumor sites, with a cheese-like consistency. As no improvement was observed, the patient was referred to Chungbuk National University Veterinary Teaching Hospital (CBNU-VTH) in October.

The patient had an overall swollen left side of the face and was unable to open his eyes. Forced breathing was confirmed, and an X-ray scan revealed gas accumulation in the intestines. After collecting blood samples from the cranial vena cava, a complete blood cell count (CBC) was performed using the ProCyte Dx (IDEXX, Westbrook, ME, USA) and blood chemistry tests were conducted using the VETSCAN VS2 (Zoetis, Parsippany, NJ, USA). The CBC results showed inflammation signs with increased neutrophil and monocyte counts. The blood chemistry results indicated impaired kidney and liver function, as evidenced by elevated levels of alanine transaminase, alkaline phosphatase, calcium, blood urea nitrogen, and globulin. The patient's blood glucose levels were very low, necessitating

oral glucose administration. Due to persistent severe pain responses, butorphanol was administered subcutaneously at a dosage of 0.1 mg/kg.

The PET/CT images in this study were acquired using the Discovery STE PET/CT system (General Electric Medical Systems, Waukesha, WI, USA). The patient was anesthetized with isoflurane using a mask and positioned in dorsal recumbency with the head immobilized to ensure accurate imaging. Following the induction of anesthesia, 0.17 mCi/kg of fluorodeoxyglucose (FDG) was administered intravenously via the cephalic vein. Low-dose CT images were acquired, followed by static PET images obtained 60 min post-injection. Whole-body PET images were acquired every 5 min per bed position. The PET image analysis was performed using OsiriX MD v10.0 (Pixmeo Sarl, Geneva, Switzerland). The regions of interest (ROIs) were manually delineated on the PET/CT fusion images. Metabolic activity of the ROIs was converted to a standardized uptake value (SUV) as follows: SUV = average tissue concentration of FDG (MBq/mL)/injected dose (MBq) per body weight (g). This resulted in a SUVmax of 10.31 and an SUVmean of 8.73 in the maxillary region. Furthermore, an SUVmax of 7.03 and SUVmean of 5.30 were observed in the left side of the lung (Figure 1). The lesion was deemed too extensive for lumpectomy, and metastasis to other areas, including the left lung, was suspected. Due to the impracticability of further treatment, euthanasia was chosen with the consent of the owner of the patient.

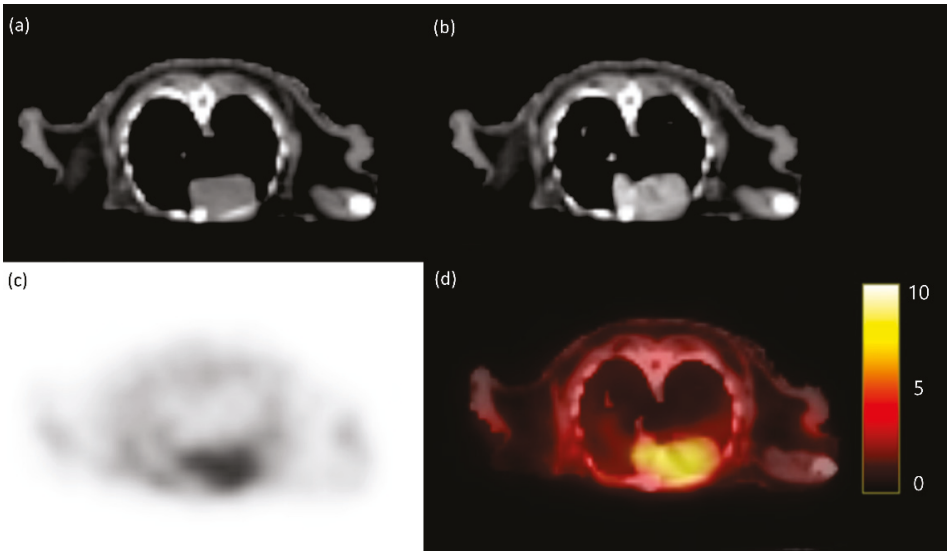


Figure 1. FDG-PET findings in a hedgehog (*Atelerix albiventris*) in the pulmonary region. Pre-contrast CT image (**a**), post-contrast CT image (**b**), FDG-PET (**c**), and PET/CT fusion (**d**) images. Pre-contrast CT image (**a**) showing anatomical structures without enhancement. Post-contrast CT image (**b**) demonstrating enhanced anatomical structures. FDG-PET image (**c**), where low and high FDG uptakes are represented by blackish and whitish colors. Fused FDG-PET/CT image (**d**) using a hot metal color scale, where low and high FDG uptakes are represented by blackish-to-reddish and yellowish colors. CT, computed tomography; FDG, 18F-fluorodeoxyglucose; PET, positron emission tomography.

Following euthanasia, a post-mortem examination was performed. The lesion site of the maxillary bone tumor corresponded to the area of high FDG uptake on the PET/CT (Figure 2). Additional PET/CT fused images from multiple planes (coronal, sagittal, and axial) of the maxillary regions were obtained to illustrate tracer uptake and distribution in the head (Supplementary Figure S1). Several other lesions were observed in the left eye, lungs, and kidneys. Samples were collected for histopathological analysis, including a cross-section of the oral tissue and skull where the protruding mass was most clearly visible, as well as ocular tissue and six cross-sections of the left lung.

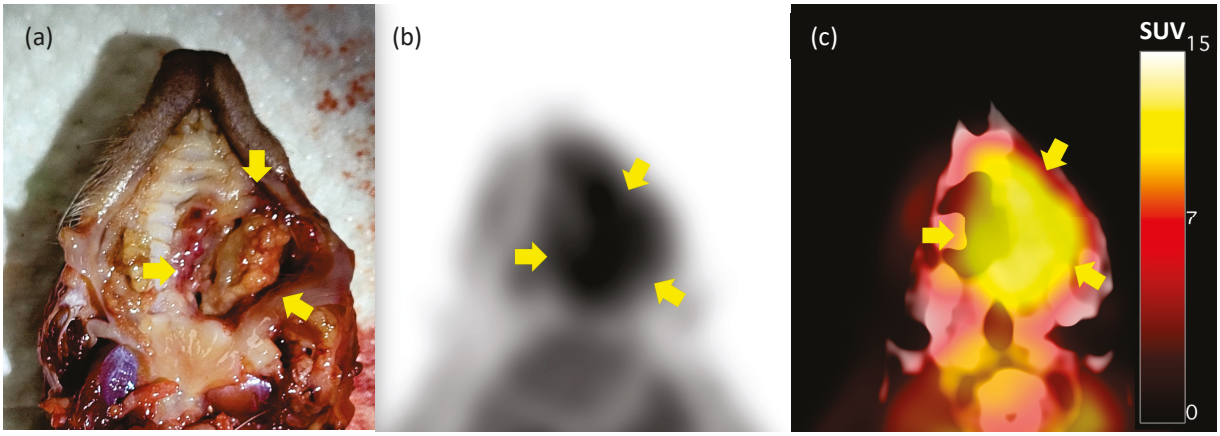


Figure 2. Necropsy and FDG-PET findings in a hedgehog (*Atelerix albiventris*) with an oral tumor. (**a**) An oral mass (arrows) found in the left maxillary region. FDG-PET (**b**) and PET/CT fusion (**c**) images. High FDG uptake is observed in the tumor lesion (arrows), and the maximal SUV of the lesion is 10.31.

The histological examination revealed a tumorous proliferation of epithelial cells in the oral tissue, characterized by marked cellular and nuclear pleomorphism, with 0–4 mitotic figures per high-power field (Figure 3a). The tumor cells aggressively infiltrated the inflamed muscular and connective tissues. They predominantly exhibited a stratified squamous epithelial cell morphology in an islet pattern, with the central formation of keratin pearls (Figure 3b).

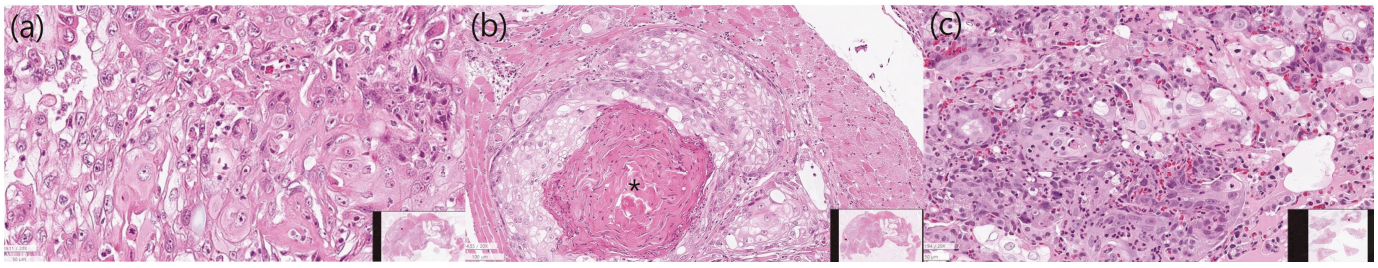


Figure 3. Photomicrographs of histopathological evaluation in oral (**a**,**b**) and lung (**c**) tissue of a hedgehog (*Atelerix albiventris*) with SCC. (**a**) Oral tissue: tumorous epithelial proliferation with nuclear pleomorphism and mitotic figures. Hematoxylin and eosin (H&E) stain. Scale bar = 50 µm. (**b**) Oral tissue: stratified squamous epithelial cells with a keratin pearl (asterisk). H&E stain. Scale bar = 100 µm. (**c**) Lung tissue: pulmonary edema and metastatic squamous cell carcinoma with inflammatory cell infiltration. H&E stain. Scale bar = 50 µm.

In the skull tissue, there was evident tumorous proliferation of epithelial cells similar to that observed at the primary site, along with pronounced cellular and nuclear pleomorphism. In the left ocular tissue, features consistent with SCC, nearly identical to the primary tumor, were observed in both the mass attached posteriorly to the retino-scleral complex and the mass adjacent to the optic disk. The tumors were growing inwards towards the inner part of the eye.

A histological examination of the left lung tissue revealed pulmonary edema and metastatic SCC (Figure 3c). Multifocal micronodular structures attributable to SCC were identified, showing histological features consistent with those of the primary tumors. Cells exhibiting a bizarre morphology with more than four nucleoli were observed. Furthermore, the infiltration of various inflammatory cells, including eosinophils, was observed within the tumor mass.

3. Discussion

To the best of our knowledge, this is the first case report to evaluate malignancy and metastasis to other organs in hedgehogs using PET/CT imaging. The tumor was assessed through a post-mortem histopathological examination to verify its consistency with the PET/CT results.

FDG-PET leverages the characteristic higher glucose metabolism of malignant tumors compared to that of normal tissues, making it a useful tool for cancer diagnosis, staging, and restaging [19]. Hybrid PET/CT enhances the diagnostic accuracy of FDG-PET and CT in cancer patients, influencing both diagnostic and therapeutic decisions in patient management [20]. This combined imaging enables a more accurate assessment of the location and metastasis of malignant tumors.

We investigated whether metabolic activity indicators can accurately assess the location and metastasis of oral squamous cell carcinoma (OSCC) in hedgehogs and whether this method could be applied. Due to their smaller organs compared with those of humans and cats, it was uncertain if tumor and metastasis evaluation using PET/CT imaging would be feasible. However, PET/CT imaging revealed severe malignancy of the oral tumor and detected metastasis in the left lung. The SUVmax and SUVmean values in the oral region were 10.31 and 8.33, respectively. In cats, previous records indicate that the SUVmax value in the oral region was 9.88, and the SUVmean value was 5.39 [15]. These similar values suggest the potential applicability of PET/CT for evaluating OSCC in hedgehogs. The PET/CT results indicated significant metabolic activity in the maxillary region, suggesting an aggressive lesion. Axial views also demonstrated tumor infiltration and turbinate bone lysis in the left nasal cavity. In the left lung, the SUVmax value was 7.03, and the SUVmean value was 5.30. No comparison with lung SUV values in PET/CT-imaged cats with OSCC was possible, as there were no lung metastasis cases reported; however, metastasis was inferred due to the high uptake in the lung area.

Consistent with the PET/CT imaging results, the post-mortem examination confirmed highly malignant masses in the oral cavity and lungs. Histopathological examination verified metastasis in the oral cavity, skull, eyes, and lungs. Before the patient was referred to CBNU-VTH, a superficial biopsy identified the tumor as being benign, diagnosing it as acanthomatous ameloblastoma. However, PET/CT imaging indicated malignancy, and a subsequent deeper biopsy confirmed the diagnosis of OSCC. This indicates that, without excising the tumor to its full depth, there is a risk of misdiagnosing SCC as another neoplasm. PET/CT can help prevent such misdiagnoses by assessing malignancy and evaluating metastasis.

The current best treatment methods for OSCC include lumpectomy, chemotherapy, and ECT, with metastasis evaluation being essential for accurate and efficient treatment planning. Even with successful surgery, the prognosis may be poor without metastasis evaluation, leading to postoperative mortality [1]. In this case, PET/CT imaging revealed that the lesion was too large for a lumpectomy, and metastasis in the lung was confirmed, rendering further treatment impossible. If an early diagnosis is made through PET/CT imaging in patients with an oral mass, more effective treatment could be achieved based on the evaluation of the malignancy and metastasis of the tumor.

A detailed evaluation of metastases in the oral cavity, nasal cavity, and eyes was impossible due to the reduced PET/CT resolution resulting from the small size of the hedgehog. This limitation allowed only for an approximate evaluation of metastasis in the other organs. However, this report suggests the potential use of PET/CT for assessing malignancy and metastasis in tumors in hedgehogs, including SCC.

4. Conclusions

This case report highlights the potential utilization of 18F-FDG PET/CT imaging in diagnosing and staging malignant tumors, specifically OSCC, in African pygmy hedgehogs (*Atelerix albiventris*). PET/CT imaging provided detailed metabolic and anatomical insights, revealing the severity of malignancy of the oral tumor and detecting lung metas-

tasis. Despite the resolution limitations of FDG uptake inherent to using human-sized PET/CT system for a small hedgehog, the imaging effectively identified the extent of the primary tumor and its metastases. These findings were confirmed through a post-mortem histopathological examination. This suggests that PET/CT imaging could play a crucial role in early diagnosis, accurate staging, and treatment planning for neoplastic diseases in hedgehogs, potentially improving clinical outcomes. Further research is needed to establish PET/CT as a standard diagnostic tool for tumors in hedgehogs, and to refine imaging techniques to allow for a better resolution and accuracy in small animals.

Supplementary Materials: The following supporting information can be downloaded at: https://www.mdpi.com/article/10.3390/ani14243679/s1, Figure S1: FDG-PET/CT images in a hedgehog (*Atelerix albiventris*) showing tracer uptake in the maxillary region. Coronal (**a**), Sagittal (**b**), and axial views (**c**–**f**) of FDG PET/CT fused images. Coronal view of the fused FDG–PET/CT image (**a**) demonstrating increased FDG uptake at the left maxillary region. Sagittal view of the fused FDG–PET/CT image (**b**), with dashed lines indicating the axial cross-section levels shown in (**c**–**f**). Axial views of fused FDG–PET/CT images at different levels (**c**–**f**), highlighting tumor infiltration and turbinate bone lysis (arrows) in the left nasal cavity.

Author Contributions: Conceptualization, N.K. and J.S.; methodology, T.Y. and B.-T.K.; software, T.Y.; validation, B.-T.K. and D.-H.J.; formal analysis, N.K.; investigation, N.K.; resources, G.-H.J.; data curation, N.K. and T.Y.; writing—original draft preparation, N.K. and J.S.; writing—review and editing, D.-H.J.; visualization, T.Y.; supervision, D.-H.J.; project administration, D.-H.J.; funding acquisition, D.-H.J. All authors have read and agreed to the published version of the manuscript.

Funding: This research was supported by the National Institute of Wildlife Disease Control and Prevention as a "Specialized Graduate School Support Project for Wildlife Diseases Specialist" (2024081308) and National Research Foundation of Korea (NRF) funded by the Ministry of Education (RS-2023-00244443).

Institutional Review Board Statement: Ethical review and approval were waived for this study because this was a retrospective case report.

Informed Consent Statement: Informed consent was obtained from animal's owner involved in the study.

Data Availability Statement: The data presented in this study are available on request from the corresponding author.

Conflicts of Interest: The authors declare no conflict of interest.

References

1. Raymond, J.T.; Garner, M.M. Spontaneous tumours in captive African hedgehogs (*Atelerix albiventris*): A retrospective study. *J. Comp. Pathol.* **2001**, *124*, 128–133. [CrossRef] [PubMed]
2. Done, L.B.; Dietze, M.; Cranfield, M.; Ialeggio, D. Necropsy lesions by body systems in African hedgehogs (*Atelerix albiventris*): Clues to clinical diagnosis. In Proceedings of the Joint Conference of the American Association of Zoo Veterinarians and the American Association of Wildlife Veterinarians, Oakland, CA, USA, 15–19 November 1992; pp. 15–19.
3. Raymond, J.T.; White, M.R. Necropsy and histopathologic findings in 14 African hedgehogs (*Atelerix albiventris*): A retrospective study. *J. Zoo Wildl. Med.* **1999**, *30*, 273–277. [PubMed]
4. Heatley, J.J.; Mauldin, G.E.; Cho, D.Y. A review of neoplasia in the captive African hedgehog (*Atelerix albiventris*). *Semin. Avian Exot. Pet. Med.* **2005**, *14*, 182–192. [CrossRef]
5. Pei-Chi, H.; Jane-Fang, Y.; Lin-Chiann, W. A retrospective study of the medical status on 63 African hedgehogs (*Atelerix albiventris*) at the Taipei Zoo from 2003 to 2011. *J. Exot. Pet Med.* **2015**, *24*, 105–111. [CrossRef]
6. Juan-Sallés, C.; Garner, M.M. Cytologic Diagnosis of Diseases of Hedgehogs. *Vet. Clin. N. Am. Exot. Anim. Pract.* **2007**, *10*, 51–59. [CrossRef] [PubMed]
7. Wozniak–Biel, A.; Janeczek, M.; Janus, I.; Nowak, N. Surgical resection of peripheral odontogenic fibromas in African pygmy hedgehog (*Atelerix albiventris*): A case study. *BMC Vet. Res.* **2015**, *11*, 145. [CrossRef] [PubMed]
8. Lennox, A.M.; Miwa, Y. Anatomy and disorders of the oral cavity of miscellaneous exotic companion mammals. *Vet. Clin. North Am. Exot. Anim. Pract.* **2016**, *19*, 929–945. [CrossRef] [PubMed]
9. Peauroi, J.R.; Lowestine, L.J.; Munn, R.J.; Wilson, D. Multicentric skeletal sarcomas associated with probable retrovirus particles in two African hedgehogs (*Atelerix albiventris*). *Vet. Pathol.* **1994**, *31*, 481–485. [CrossRef] [PubMed]

10. Okada, K.; Kondo, H.; Sumi, A.; Kagawa, Y. A retrospective study of disease incidence in African pygmy hedgehogs (*Atelerix albiventris*). *J. Vet. Med. Sci.* **2018**, *80*, 1504–1510. [CrossRef] [PubMed]
11. Del Aguila, G.; Torres, C.G.; Carvallo, F.R.; Gonzalez, C.M.; Cifuentes, F.F. Oral masses in African pygmy hedgehogs. *J. Vet. Diagn. Investig.* **2019**, *31*, 864–867. [CrossRef] [PubMed]
12. Bray, S.; Harrison, T.; Rodriguez Jr, C.O.; Johnson, A.; Wack, R.F. Oral squamous cell carcinoma in a greater hedgehog tenrec (*Setifer setosus*). *Vet. Rec. Case Rep.* **2016**, *4*, e000314. [CrossRef]
13. Spugnini, E.P.; Lanza, A.; Sebasti, S.; Baldi, A. Electrochemotherapy palliation of an oral squamous cell carcinoma in an African hedgehog (*Atelerix albiventris*). *Vet. Res. Forum* **2018**, *9*, 379–381. [CrossRef] [PubMed]
14. Mazlina, M.; Syahirah, A.A.; Salahuddin, M.A.; Haron, N.A.; Paul, B.T.; Bitrus, A.A.; Abba, Y.; Eric, L.T.C.; Peter, I.D.; Abraham, G.; et al. Series of clinical cases and management of histopathologically diagnosis of squamous cell carcinoma in African pygmy hedgehogs (*Atelerix albiventris*). *J. Vet. Malays.* **2020**, *32*, 19–23.
15. Randall, E.K.; Kraft, S.L.; Yoshikawa, H.; LaRue, S.M. Evaluation of 18F–FDG PET/CT as a diagnostic imaging and staging tool for feline oral squamous cell carcinoma. *Vet. Comp. Oncol.* **2013**, *14*, 2838. [CrossRef] [PubMed]
16. Schwartz, D.L.; Ford, E.; Rajendran, J.; Yueh, B.; Coltrera, M.D.; Virgin, J.; Anzai, Y.; Haynor, D.; Lewellyn, B.; Mattes, D.; et al. FDG–PET/CT imaging for preradiotherapy staging of head–and–neck squamous cell carcinoma. *Int. J. Radiat. Oncol. Biol. Phys.* **2005**, *61*, 129–136. [CrossRef] [PubMed]
17. Yoshikawa, H.; Randall, E.K.; Kraft, S.L.; Larue, S.M. Comparison between 2-(18) F-fluoro-2-deoxy-d-glucose positron emission tomography and contrast-enhanced computed tomography for measuring gross tumor volume in cats with oral squamous cell carcinoma. *Vet. Radiol. Ultrasound.* **2013**, *54*, 307–313. [CrossRef] [PubMed]
18. Ma, D.; Zhang, Y.; Shao, X.; Wu, C.; Wu, J. PET/CT for Predicting Occult Lymph Node Metastasis in Gastric Cancer. *Curr. Oncol.* **2022**, *29*, 6523–6539. [CrossRef] [PubMed]
19. Kelloff, G.J.; Hoffman, J.M.; Johnson, B.; Scher, H.I.; Siegel, B.A.; Cheng, E.Y.; Cheson, B.D.; O'shaughnessy, J.; Guyton, K.Z.; Mankoff, D.A.; et al. Progress and promise of FDG–PET imaging for cancer patient management and oncologic drug development. *Clin. Cancer. Res.* **2005**, *11*, 2785–2808. [CrossRef] [PubMed]
20. Bar-Shalom, R.; Yefremov, N.; Guralnik, L.; Gaitini, D.; Frenkel, A.; Kuten, A.; Altman, H.; Keidar, Z.; Israel, O. Clinical Performance of PET/CT in Evaluation of Cancer: Additional Value for Diagnostic Imaging and Patient Management. *J. Nucl. Med.* **2003**, *44*, 1200–1209. [PubMed]

Disclaimer/Publisher's Note: The statements, opinions and data contained in all publications are solely those of the individual author(s) and contributor(s) and not of MDPI and/or the editor(s). MDPI and/or the editor(s) disclaim responsibility for any injury to people or property resulting from any ideas, methods, instructions or products referred to in the content.

animals

MDPI

Case Report

Different Types of Co-Infection by Contagious Ecthyma Virus, Enteropathogenic *Escherichia coli*, *Mycoplasma conjunctivae*, Ecto- and Endo-Parasites in Four Young Alpine Ibex (*Capra ibex*)

Lorenzo Domenis *, Raffaella Spedicato, Cristina Guidetti, Emanuele Carella and Serena Robetto

Istituto Zooprofilattico Sperimentale del Piemonte, Liguria e Valle d'Aosta, Regione Amerique 7G, 11020 Quart, AO, Italy; raffaella.spedicato@izsplv.it (R.S.); emanuele.carella@izsplv.it (E.C.); serena.robetto@izsto.it (S.R.)
* Correspondence: lorenzo.domenis@izsto.it

Simple Summary: To deepen the knowledge about the perinatal pathology of the Alpine ibex (*Capra ibex*) and, at the same time, to evaluate its potential role in the interspecific transmission of diseases to other wild and domestic animals, including humans, we present the necropsy findings and subsequent analytic results obtained from four young ibex found dead in Valle d'Aosta, a region of northwestern Italy. The animals, with various co-infection patterns, were affected—showing typical gross and microscopical lesions in target organs and tissues—by contagious ecthyma virus (ORFV) (agent of a highly diffusive pustular dermatitis transmissible to small ruminants and humans), Enteropathogenic *Escherichia coli* (EPEC) (major etiological agent of infantile diarrhoea, especially in developing countries), *Mycoplasma conjunctivae* (MC) (cause of an ocular infection common to goats and sheep), various ectoparasites (ECP) (ticks and keds), and endoparasites (ENPs) (lung and intestinal nematodes, and coccidia).

Abstract: The research aimed to investigate the perinatal pathology of Alpine ibex (*Capra ibex*) through the study of four young subjects (at the age of 3 to 4 months) found dead in Valle d'Aosta, a region of northwestern Italy. The carcasses were submitted to necropsy followed by an examination of ecto- and endoparasites (ECP and ENP); samples from the gross lesions (in summary, cutaneous papilloma and crusts, ocular discharge, lobular haemorrhagic areas in the lungs, catarrhal–haemorrhagic enterocolitis) were analysed by bacteriological, histopathological, and biomolecular methods to define the etiological agent. The subjects, with various co-infection patterns, were affected by contagious ecthyma virus (ORFV) (agent of a highly diffusive pustular dermatitis transmissible to small ruminants and humans), Enteropathogenic *Escherichia coli* (EPEC) (major etiological agent of infantile diarrhoea especially in developing countries), *Mycoplasma conjunctivae* (MC) (cause of an ocular infection common to goats and sheep), various ECP (ticks and keds) and ENP (lung and intestinal nematodes, and coccidia). This study emphasises the potential role of the Alpine ibex in the transmission of infectious diseases to other animals such as to humans and, secondly, the need to apply diversified analytical approaches, with the commitment of various specialistic skills, in order to define, in detail, the various and frequently overlapping causes that led a free-ranging animal to the death.

Keywords: Alpine ibex (*Capra ibex*); contagious ecthyma; ectoparasites; endoparasites *Escherichia coli*; *Mycoplasma conjunctivae*

1. Introduction

The Alpine ibex (*Capra ibex*) is a wild mountain ruminant that, although almost completely extinct at the end of the 19th century, has reconquered a large part of its original territories thanks to conservation and awareness programmes, becoming the symbolic animal of the Italian Alps. As for other wild ungulates, the increase in the number has

led to an increasing sharing of pastures with domestic ruminants, especially goats and sheep, with a risk of interspecific transmission of several diseases and parasites [1]. For this reason, numerous epidemiological surveillance programmes have monitored the presence of particularly serious infectious diseases in ibex populations, transmissible to humans and animals, such as brucellosis, sarcoptic mange, blue tongue, pestivirus diseases, and paratuberculosis.

In order to further contribute to the knowledge of perinatal pathologies in this alpine ungulate, we describe four cases of co-infection in young ibex variously affected by contagious ecthyma virus (ORFV), Enteropathogenic *Escherichia coli* (EPEC), *Mycoplasma conjunctivae* (MC), ectoparasites (ECPs), and endoparasites (ENPs).

ORFV is an epitheliotropic virus belonging to the *Parapoxviridae* family that causes a highly contagious zoonotic pustular dermatitis, known as contagious ecthyma (CE). The infection has a worldwide distribution, primarily affecting domestic sheep and goats, and it is also reported in many wild ruminants: bighorn sheep (*Ovis canadiensis*), thinhorn sheep (*Ovis dallii*), Alaskan mountain goat (*Oreamnus americanus*), musk ox (*Ovibos moschatos*), reindeer (*Rangifer tarandus*), Sitka black-tailed deer (*Odocoileus hemionus sitkensis*), Sichuan takin (*Budorcas taxicolor tibetana*), chamois (*Rupicapra rupicapra*), Himalayan tahr (*Hemitragus jemlahicus*), serow (*Capricornus crispus*), white-tailed deer (*Odocoileus virginianus*), red deer (*Cervus elaphus*) [2–11]; in Italian Alpine ibex, CE has been detected several times in the Stelvio National Park, Central Alps [12]. ORFV is a zoonotic agent, and human infection from wild ruminants (especially common in hunters, foresters, veterinarians, biologists, and generally all professional categories most exposed to game) has been reported in America and Europe [10,13,14].

EPEC strains are defined as intimin (codified by the *eae* gene), containing diarrheagenic *Escherichia coli* that do not possess the Shiga toxin genes [15]; they are recognised as pathogens in humans, where they are a major etiological agent of infantile diarrhoea, especially in developing countries [16,17]. EPEC strains have been isolated from the faeces of a variety of domestic and wild animals, including many alpine ruminants such as red deer (*Cervus elaphus*), roe deer (*Capreolus capreolus*), chamois (*Rupicapra rupicapra*), and also Alpine ibex [18–22].

Mycoplasma conjunctivae is the causative agent of infectious keratoconjunctivitis (IKC), a highly contagious ocular infection that is common in sheep and goats (where it is also known as the "pinkeye" of domestic small ruminants). In the European Alps, IKC has often been observed in Alpine chamois (*Rupicapra r. rupicapra*) and Alpine ibex (*Capra ibex*), with several past outbreaks. Still, the disease has also been described in other wild Caprinae such as Pyrenean chamois (*Rupicapra r. pyrenaica*), Iberian ibex (*Capra pyrenaica*) and mouflon (*Ovis aries musimon*) in Spain, and *Hemitragus jemlahicus* in New Zealand [23–27].

Finally, ECP and ENP were investigated as a cause of loss of condition and even death in wild fauna; ECP (arthropods as ticks and mites) and ENP (lung and intestinal worms) are often hosted from wild ungulates and are usually detected in different species of ibex [28–32].

The cases reported are particularly interesting considering that it is quite exceptional for a laboratory to receive carcasses of wild Alpine ibex that died at high altitudes, that have a few months of life, and at the same time are in a state of conservation so good as to allow for processing samples and obtaining significant and reliable analytical results, especially for histological and bacteriological outcome.

2. Materials and Methods

2.1. Study Area and Animal Origin

Four carcasses of young Alpine ibex (*Capra ibex*) were carried to our laboratory for investigation of the cause of death. The animals, all coming from the territory of the Valle d'Aosta Region (north–western Italian Alps), were found dead (or in poor condition and then deceased or euthanized in a short time under veterinary supervision), respectively, in the following period, site, and altitude (Table 1): (1) end of August 2020, Valgrisenche

Valley, 1600 m a.s.l.; (2) beginning of August 2021, Valtournenche Valley, 1585 m a.s.l.; (3) at the end of August 2012, Gressoney Valley, 1700 m a.s.l.; (4) at the end of September 2012, Valpelline Valley, 2200 m a.s.l.

Table 1. Alpine ibex (subjects from 1 to 4). Origin, biometric data, gross lesions sites, and analytical results (M: male; F: female; n.a.: not analysed).

	Subject 1	**Subject 2**	**Subject 3**	**Subject 4**
Origin	Valgrisenche Valley	Valtournenche Valley	Gressoney Valley	Valpelline Valley
Altitude	1600 m a.s.l.	1585 m a.s.l.	1700 m a.s.l.	2200 m a.s.l.
Period/Year	August/2020	August/2021	August/2012	September/2012
Sex	M	F	M	M
Age	3 m	3 m	3 m	4 m
ECP	+	+	−	−
Lesions site	Skin, eye, tongue	Skin, intestine	Skin, tongue, intestine	Intestine
MC	+	−	+	n. a.
ORF virus	+	+	+	−
EPEC	/	+	n. a.	+
ENP	**−**	**+**	**n. a.**	**+**

2.2. Postmortem Examination and Diagnostic Protocol

All carcasses of ibexes were delivered to our laboratory in fresh and good condition. As usual, according to a diagnostic protocol consolidated at our laboratory, biometric surveys were initially conducted to establish the sex, weight, and age of the animals. During necropsy, macroscopic evaluation of the organs was performed, with a detailed description of gross lesions; every damaged organ or tissue (in our case, notably skin, eye, intestine, and lungs) was subjected to parasitological, bacteriological, histological, or molecular–virological analysis depending on the suspected etiological agent.

2.2.1. Parasitological Exams

A general objective examination of the skin surface was performed to verify the presence of ECPs; ECPs were identified using a stereomicroscope (Olympus SZ-40, (Olympus Optical Co., Ltd., Tokyo, Japan) comparing the morphological characteristics with a reference atlas [33–35]. For the differential diagnosis of cutaneous proliferative lesions, a skin scratch was routinely taken and then verified using the microscope, after maceration in KOH 20% solution, for the presence of mites (notably *Sarcopets scabiei*), which were always absent in all subjects. ENPs in faeces were examined by flotation, mixing a sample with $ZnSO_4$ 100% solution, which after filtration is capable of bringing light eggs (nematodes, cestodes, and coccidia) and heavy eggs (plathelminths) to the surface.

2.2.2. Bacteriological Exams

For skin lesions, Columbia Agar 5% Sheep Blood (CA), Mc Conkey Agar (MC), and RPF Agar were used (at 37 °C for 48 h in aerobiosis), while in the case of enterocolitis, the examination of the main intestinal pathogens was performed. In addition, XLD Agar and BGA Agar at 37 °C for 24 h in aerobiosis were used to detect *Salmonella* spp.; CCDA Agar at 42 °C for 48 h in microaerophilia was used to detect *Campylobacter* spp.; CIN Agar at 30 °C for 24 h in aerobiosis was used to detect *Yersinia* spp. The strains of *Escherichia coli* were confirmed by API 20 E Biomerieux (BioMerieux, Marcy l'Etoile, France) and subsequently typed for the *eae*, *stx1* and *stx2* genes, respectively, encoding the virulence factors intimin, Shiga-toxin 1, and Shiga-toxin 2, by the PCR-RT method described in the ISO/TS

13136/2012 [36] ("Horizontal method for the detection of Shiga toxin-producing *Escherichia coli* (STEC) and the determination of O157, O111, O26, O103 and O145 serogroups").

2.2.3. Histological Exams

The exam was applied according to the routine method to evaluate the microscopic lesions: fixation of pathological tissue pieces in buffered formalin 4%, paraffin embedding, trimming by microtome at a thickness of 4 µm, haematoxylin–eosin (HE) staining, and final mounting of the slides with Eukitt balsam [37]. The slides were observed in different magnifications with a light microscope Olympus BX60 (Olympus Optical Co., Ltd., Tokyo, Japan), and photos were captured using Olympus Camedia C-4040 Zoom (Olympus Optical Co., Ltd., Tokyo, Japan) and software Olympus DP Soft—Version 3.1.

2.2.4. Molecular Assays

When CE (refer to the results) was suspected, in addition to the routine bacteriological exam, an ORFV-specific PCR-RT was performed on skin lesions as follows. Briefly, DNA was extracted using the ExtractMe genomic DNA kit (Blirt, Gdańsk, Poland) following the manufacturer's instructions. The detection of ORFV strains was performed by end-point PCR using the Invitrogen™ Platinum™ Quantitative PCR SuperMix-UDG kit (Invitrogen, Waltham, MA, USA) and primers manufactured by Thermo Fisher Scientific (Norristown, PA, USA). The PCR mixture consisted of 500 nM of forward primers (5′-TACACGGAGTTGGCCGTGATCTTGTA-3′), 500 nM of reverse primers (5′-CGCCAAGTACAAGAAGCTGATGA-3′) specifically designed in a previous study [38], 5 µL of 10× buffer, 200 nM of dNTPs, 1.5 µM of $MgCl_2$, 0.5 U/µL of Taq polymerase, 3 µL of template, and 34 µL of DNase and RNase-free water in a total volume of 50 µL. The PCR cycling conditions on the Applied Biosystems 2720 Thermal Cycler (Life Technologies) consisted of an initial step at 95 °C for 4 min followed by 40 cycles at 94 °C for 15 s, 64 °C for 30 s, and 72 °C for 30 s [38]. The amplification products were run on a 1.8% agarose gel at 90 V for 60 min and analysed using the Amplisize Molecular Ruler (Bio-Rad, Hercules, CA, USA). PCR amplification of ORFV resulted in a 103 bp product.

In cases with ocular discharge with suspicion of IKC (or even without clinical signs, with the aim of monitoring the infection after past outbreaks as in Case 2), in addition to the routine bacteriological exam, the examination for MC was performed by using PCR as follows. Eye swabs, treated with 0.45 mL of lysis buffer (100 mM Tris–HCl, pH 8.5, 0.05 Tween 20, 0.24 mg/mL proteinase K), were incubated for 60 min at 60 °C and then heated to 95 °C for 15 min to extract DNA. The extracts were tested for the presence of MC DNA with a TaqMan qPCR, according to Vilei et al. [39]. The oligonucleotide primers and TaqMan fluorogenic probe were specific to the conserved 5′-terminal part of gene *lppS* of MC [40]. qPCR reactions were performed by using 2.5 µL of sample, 900 nM of *lppS* forward primer (5′-CAGCTGGTGTAGCACTTTTTGC-3′) and *lppS* reverse primer (5′-TTAACACCTATGCTCTCGTCTTTGA-3′), 300 nM of *lppS* probe (5′-TGCTTCGACTACCAAATATGATGGTGATCCTCT-3′), and TaqMan Universal PCR Master Mix at a 25 µL volume. PCR reactions were run on a StepOne Plus instrument (Thermofisher, Waltham, MA, USA) using the following cycling parameters: 1 step at 50 °C for 2 min and at 95 °C for 10 min, followed by 40 cycles consisting of denaturation at 95 °C for 15 s and extension at 60 °C for 1 min. Real-time fluorescence measurements were taken for each sample by using the StepOne™ Software v2.3 (Thermofisher, Waltham, MA, USA), and the PCR cycle number at which the fluorescent *lppS* signal crossed the threshold was recorded as Ct value (Figure S4).

3. Results

All the results are resumed in Table 1.

3.1. Biometry

Apart from Subject 2, which was a female, all animals were male. Considering (a) that the Alpine ibex breeding season is approximately between the end of May and the beginning of June, (b) the dates of discovery of the carcasses, (c) both the horn growth of about 4 cm length and the overall morphology (weight, length, height, and teeth), the age was estimated [41] at about 3 months for the subjects numbered 1, 2, and 3 (found towards mid-August), and about 4 months for Subject 4 (found towards the end of September); therefore, all subjects could be classified in the class of age 0, otherwise defined "yearlings" (kids born in the year).

3.2. Gross Lesions and Analytical Results

Subject number 1: the external physical examination revealed cachexia, the presence of papillomatous proliferative cutaneous lesions ("cauliflower-like"), heavily crusted and sometimes ulcerated, at the level of the tongue (Figure 1A), nostrils, labial rim and limb extremities (Figure 1B), abundant bilateral ocular discharge with focal corneal opacity, and ECPs attributable to *Melophagus rupicaprinus* (Figure 2). After opening the carcass, no macroscopically evident lesions were found on the internal organs. The virological and bacteriological examinations conducted on biopsies of the skin lesions confirmed the suspicion of CE, detecting ORFV (Figure S1) associated with *Staphylococcus aureus*. The histological examination shows parakeratotic and orthokeratotic hyperkeratosis associated with sero-cellular crusts, spongiosis, dyskeratosis, acanthosis, presence of intracytoplasmic acidophilic inclusion bodies surrounded by a clear halo, dermal hyperemia, and mixed sub-epidermal inflammation (Figure 1C–E). Eye swabs tested positive for MC (Figure S4).

Subject number 2: the external physical examination revealed cachexia, the presence of papillomatous proliferative cutaneous lesions, crusted and sometimes ulcerated, at the level of the nostrils, labial rim, and extremities of the limbs, non-severe bilateral ocular discharge, ECPs attributable to mallophages (*Melophagus rupicaprinus*), and ticks (*Ixodes ricinus*) (Figure 2A); the skin lesions were positive for ORFV (Figure S2) without any secondary bacterial infection and the histological examinations showed the same pictures as in Subject 1. After the opening of the carcass, lobular haemorrhagic areas in the lungs and catarrhal haemorrhagic enteritis were observed. Bacteriological and parasitological examinations of the intestine showed the presence of a nonhemolytic EPEC *eae* positive, *stx1*-*stx2* negative strain, associated with ENP, notably coccidia (Figure 2C) and strongyles (with the prevalence of *Nematodirus* spp. and *Ostertagia* spp.) (Figure 2D). The examination for other possible intestinal pathogens (*Salmonella* spp., *Campylobacter* spp., and *Yersinia* spp.), performed for differential diagnosis purposes, was negative. Eye swabs were negative for MC.

Subject number 3: the external physical examination revealed cachexia, the presence of papillomatous proliferative cutaneous lesions, with a crusted surface, at the level of the tongue, neck, sternal region, and extremities of the limbs; the skin lesions were positive for ORFV (Figure S3) without any secondary bacterial infection and with the same microscopical features as Case 1 and 2. After the opening of the carcass, catarrhal enteritis was observed but it was not possible to conduct further analytical investigations. Eye swabs tested positive for MC.

Subject number 4: the external physical examination revealed moderate cachexia and diarrhoea with faecal contamination of the perianal area. At the opening of the carcass, we observed severe catarrhal haemorrhagic enteritis characterised by dilation and congestion of the small intestine (Figure 3A), with haemorrhagic diarrhoeal stools associated with hyperplasia of the mesenteric lymph nodes and grey consolidated areas in the lung's parenchyma (Figure 4A). From the intestine, a haemolytic EPEC *eae* positive, *stx1*-*stx2* negative (Figure S5) strain was isolated, associated with the presence of coccidia. In histological examination, intense mixed cell inflammation (lymphocytes, plasma cells, macrophages) and hyperaemia of the intestinal mucosa with de-epithelialization of the apical portion of the villi were observed (Figure 3B,C). The examination for other possible intestinal pathogens (*Salmonella* spp., *Campylobacter* spp., and *Yersinia* spp.), performed for differential

diagnosis purposes, was negative. In the lung, typical pictures of verminous bronchopneumonia were detected (larvae and eggs of nematodes, hyperplasia of the smooth muscle septa, lymphohistiocytic inflammation, hyperplasia of BALT system) (Figure 4B). In this case, it was not possible to take ocular swabs for MC.

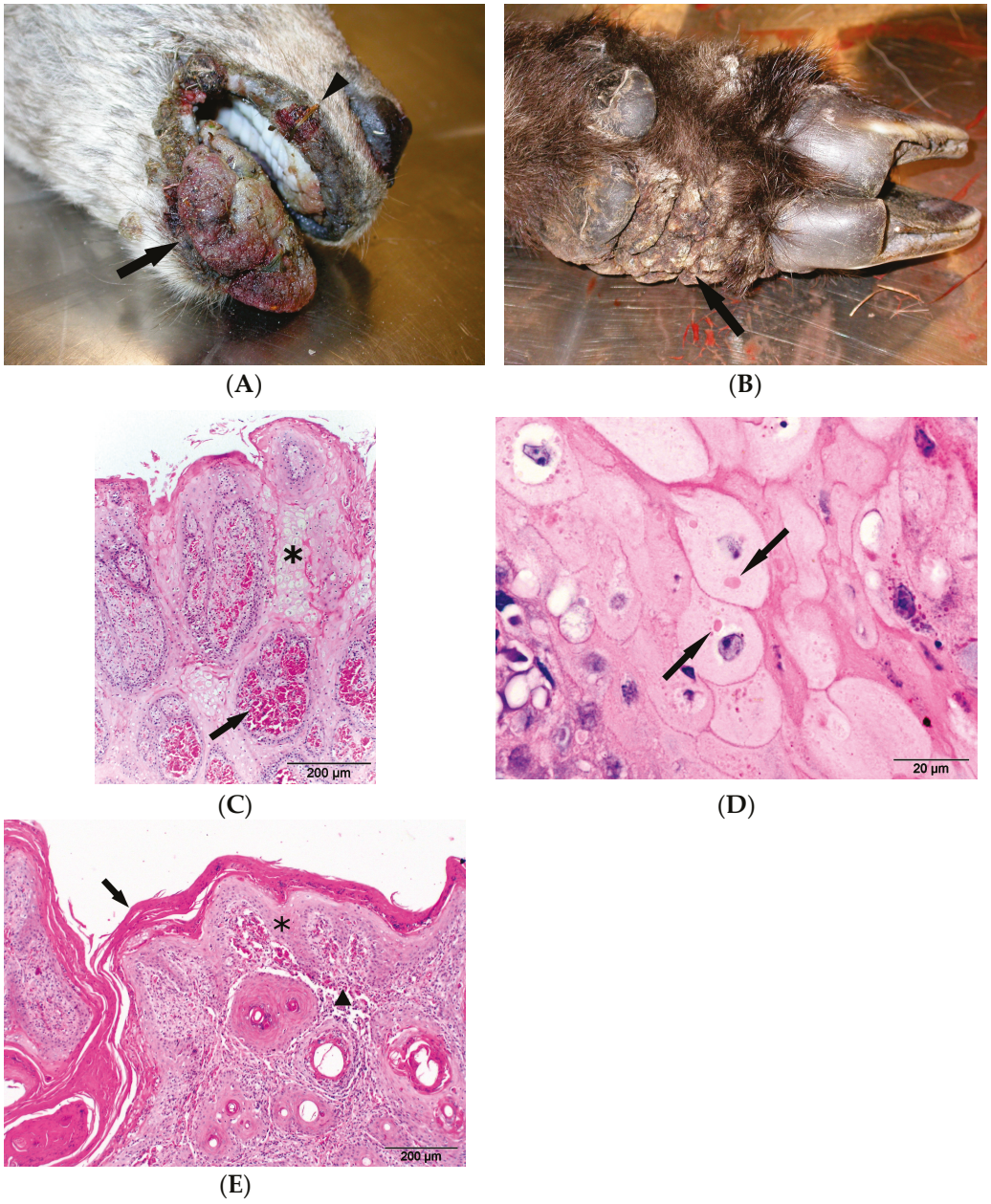


Figure 1. (**A**) Alpine ibex contagious ecthyma. Papillomatous proliferative lesion by ORFV, partially ulcerated and strongly hyperaemic, on the tongue (arrow) and upper lip (arrowhead)—(Subject 1). (**B**) Alpine ibex contagious ecthyma. Typical "cauliflower-like" papillomatous proliferative lesions (arrow) by ORFV, heavily crusted, at the extremities of the limbs, proximal to the nails—(Subject 1). (**C**) Alpine ibex contagious ecthyma. ORFV lesion in the tongue, characterised by epithelial proliferation with spongiosis (asterisk) and severe dilatation of the sub-epithelial vessel network (arrow)—(Subject 1). HE (10×). (**D**) Alpine ibex contagious ecthyma. Acidophilic intra-cytoplasmatic inclusion bodies by ORFV, with clear halo, inside epithelial spongiotic cells of the tongue mucosa (arrows)—(1). HE (100×). (**E**) Alpine ibex contagious ecthyma. Cutaneous proliferative lesions by ORFV, characterised by orthokeratotic hyperkeratosis (arrow), middle acanthosis (asterisk), dilatation of sub-epidermic vessel network, and mixed cells dermal phlogosis (triangle)—(Subject 2). HE (10×).

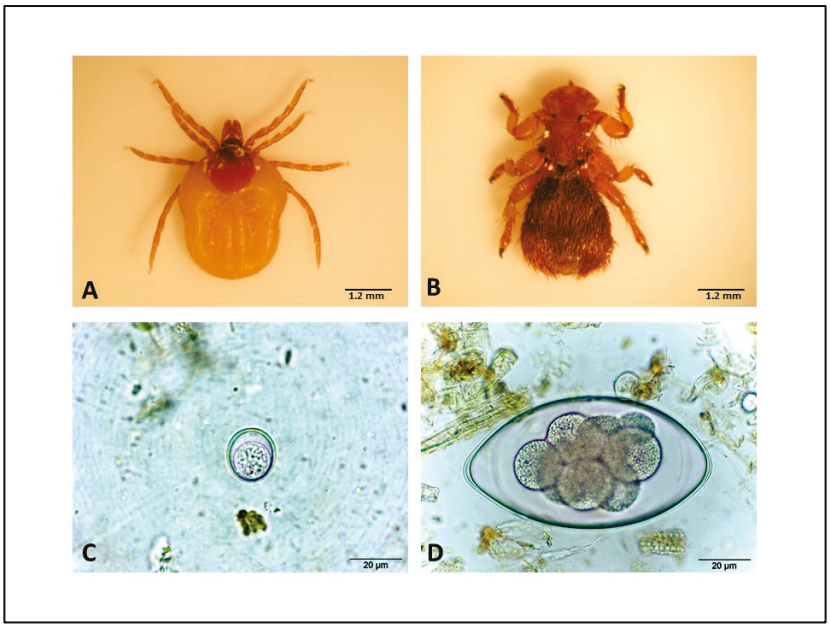
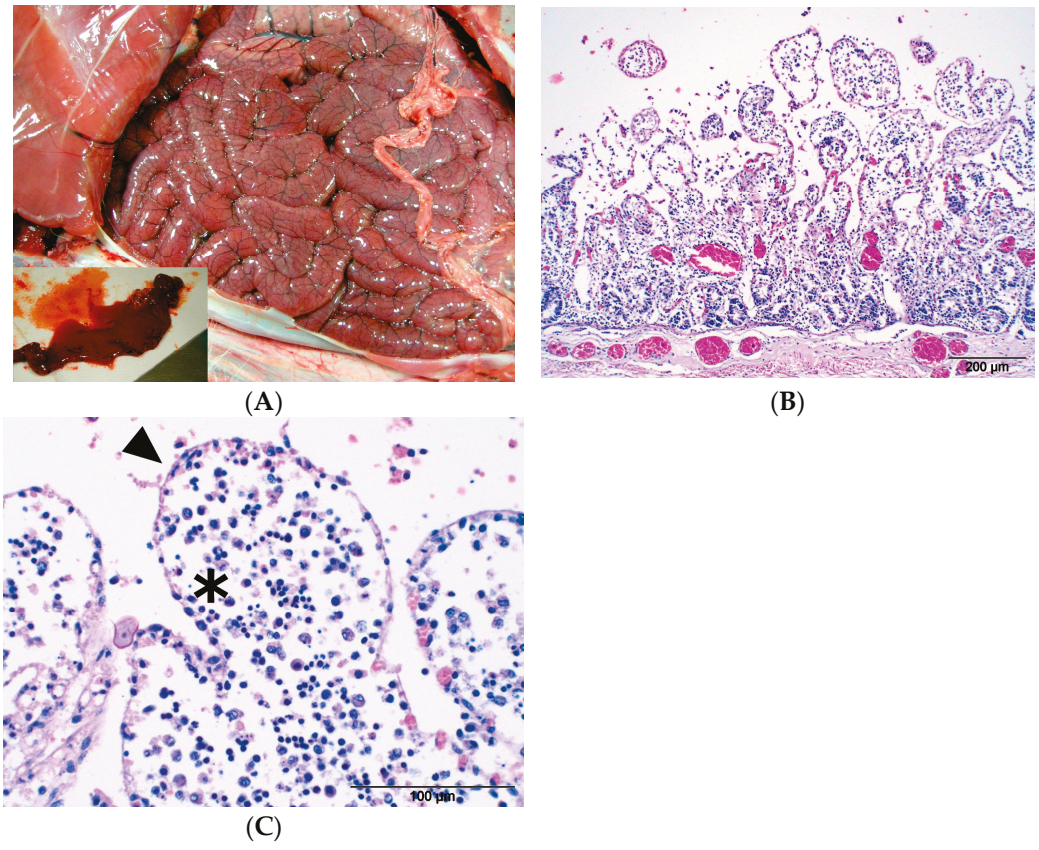
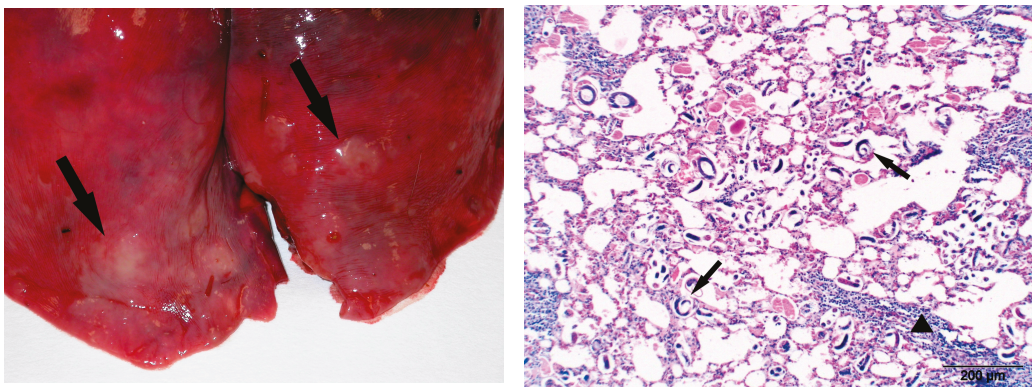


Figure 2. Alpine ibex ecto- and endo-parasites. *Ixodes ricinus* (**A**), *Melophagus rupicaprinus* (**B**), *Eimeria* spp., (**C**), *Nematodirus* spp. (**D**)—(Subjects 1, 2, 4).



(**A**) (**B**) (**C**)

Figure 3. (**A**) Alpine ibex enteritis by EPEC. The intestine appears oedematous, dilated, and congested, with diarrhoeic haemorrhagic content (insert)—(Subject 4). (**B**) Alpine ibex enteritis by EPEC. Acute phlogosis with a severe dilatation of lamina propria and sub-mucosa vessel network—(Subject 4). HE (10×). (**C**) Alpine ibex enteritis by EPEC. Intestinal villi show loss of epithelial surface cells (arrow), oedema, and mixed phlogosis with macrophages, monocytes, and neutrophils (asterisk)—(Subject 4). HE (40×).



(**A**) (**B**)

Figure 4. (**A**) Alpine ibex verminous bronchopneumonia. Parasitic lesions inside caudal lung lobes, characterised by multiple-coloured grey foci of consolidated parenchyma (arrows)—(Subject 4). (**B**) Alpine ibex verminous bronchopneumonia. Multiple appreciable nematodes larvae inside alveolar lumina (arrows) and hyperplasia of BALT system (triangle)—(Subject 4). HE (10×).

4. Discussion

Among the diseases, CE deserves particular attention as the most prevalent infection, present in 3 out of 4 subjects studied. The CE causative virus belongs to the genus *Parapox* (subfamily *Chordopoxvirinae*, family *Poxviridae*), which comprises four confirmed PPV species [11,12] recognised by the International Committee of Taxonomy of Viruses: the prototype member of virus (ORFV) endemic in most sheep- and goat-raising countries, the bovine papular stomatitis virus (BPSV), the pseudocowpox virus (PCPV) mainly infecting cattle, and Parapoxvirus of Red Deer in New Zealand (PVNZ); this last one is described by Robinson and Mercer [4]. The lesions we have observed in our cases are typical and completely comparable to those described by other authors in domestic and wild ruminants, as in ibex, infected by ORFV. The histological features demonstrate the pathological action of the virus replication in the skin and oral mucosa, which leads to proliferation, vacuolation, and swelling of the epithelial cells, with oedematous and granulomatous inflammation of the derma (cutis) or lamina propria (mucosa), especially when the infection is complicated by overlapping bacterial invasion (*Staphylococcus aureus* in Subject 1 or, as described in other wild ruminants, *Dermatophilus congolensis* or *Trueperella pyogenes* [2–12]). The severe highly vascularization and proliferation observed in the lesions are explained by the expression of proteins homologous to endothelial growth and permeability factor by ORFV, with both being angiogenesis regulators [42]. The painful ulcerated papillomas on the lips and tongue, also observable in domestic lambs or kids, can be particularly severe in young ibex. These animals live in the wild without access to medical treatment or veterinary care and these lesions can significantly impair the ability to suckle and graze, leading to the fatal outcome for starvation, especially in harsh winter months. As mentioned, the ORFV virus is a zoonotic agent that causes a self-limiting disease in humans, usually occurring as a single papule on a finger, hand, or other body part [2]. More important is the risk of spread of ORFV among domestic and wild animals by sharing pastures during the summer season (as frequently happens in our region), since sequencing and comparing the DNA of several isolates has repeatedly demonstrated [3,12] that the virus from many wild ruminants (ibex, chamois, Mountain goat, Dall's sheep, caribou) clusters with other Orthopoxvirus strains isolated from sheep and goats.

In two out of the four subjects, severe enterocolitis was demonstrated by EPEC strains, positive for the *eae* gene, in association with ENP (coccidia and strongyles); the key feature of EPEC pathogenesis is the production of "attaching and effacing" (A/E) lesions, which are characterised by the intimate adherence of the bacteria to the intestinal epithelium. The *eae* gene, located in the pathogenicity island "locus of enterocyte effacement" (LEE), encodes intimin, an outer membrane protein responsible for the adhesion. Depending

on the presence or absence of the EPEC adherence factor (EAF), plasmid EPEC is further divided into two subtypes: typical (tEPEC), more dominant in developing countries, and atypical (aEPEC), more important in developed countries [21]. Despite not having characterised the strains in addition to the *eae* and *stx* genes, the EPEC strains of our cases proved to be particularly aggressive and cytotoxic, causing the complete destruction of the intestinal epithelium with an outcome of haemorrhagic diarrhoea and, besides this, probably lung haemorrhages in Subject 2. EPEC are important human pathogens, representing one of the main causes of infantile diarrhoea in low-income countries to date, but with several outbreaks in the rest of the world mostly linked to food and water consumption [43,44]; considering that *E. coli* can survive for months in the environment, the possibility of transmission to humans by a wide variety of different sources (notably surface water contaminated by wild animal waste) must be taken into account [21,45]. As explained in the introduction, EPEC strains have been reported in many alpine ruminants; therefore, considering that most of these reports generally consist of monitoring based on stool samples without evidence of gastro-intestinal lesions, our cases become particularly interesting as they demonstrate the enteropathogenic action of EPEC in young Alpine ibex, similarly to what commonly happens, with very similar gross and microscopic lesions, for colibacillosis in livestock, especially young calves, lambs, and pigs [46,47].

MC has been detected in two subjects, one with a severe ocular discharge with corneal opacity and the other without evident ocular symptoms. For the last one, it is not possible to establish if it was a healthy carrier or an individual in the incubation phase, or, again, a subject cleared of a previous infection, considering that MC can establish different interactions with its hosts, resulting in very different clinical outcomes, as evident in our cases. When present, clinical signs of IKC are generally associated with ocular damage and inflammation, with visual impairment and blindness until, in more severe stages, staphyloma and perforation of the cornea; these symptoms are often fatal for wild fauna, for which blindness leads to death by starvation or more often by traumatic accident, frequently consequent to falling from a cliff [26]. Small domestic ruminants, mainly sheep, are traditionally assumed as the main reservoir of pathogens, while wild caprine, as chamois, were considered spillover hosts that cannot maintain IKC without the participation of domestic host [1]; however, a separate independent epidemiological cycle has been demonstrated in Iberian ibex [27], and Alpine ibex also seem to be a better candidate in playing a reservoir role complementary to domestic flocks [48]. Because MC is transmitted through direct contact and by flies, the IKC follows a seasonal pattern; like our subjects, both were found dead at the end of August, and the majority of cases were observed in summer, due to the increase in susceptible host densities, consequent to the birth of naive kids, and the abundance of insect vectors [49].

About parasitological findings, ECPs (various arthropods as insects, ticks, and mites) and ENPs as bronchopneumonia nematodes (*Muellerius* spp., *Protostrongylus* spp., *Neostrongylus* spp., *Cystocaulus* spp. and *Dictyocaulus* spp.), coccidia (*Eimeria* spp.), and gastro-intestinal nematodes (notably *Haemonchus* spp., *Marshallagia* spp., *Nematodirus* spp., *Ostertagia* spp., *Trichostrongylus* spp., *Teladorsagia* spp., *Capillaria* spp., *Trichuris* spp.) have been frequently identified in healthy animals among different species of ibex, as in both domestic and other wild ruminants [50–52]. Depending on the severity of the infection, age, immunological status, and predisposing factors of the host, progressive negative effects can be caused by different types of parasites, such as respiratory failure and secondary bacterial infections for lung nematodes or acute neonatal diarrhoea for coccidia. Parasites that do not cause disease outbreaks may lead to a constant loss of energetic resources with a decreased growth and survival rate [29]. In our opinion, the presence of ECPs and ENPs, each with their own specific pathogenic action more or less heavy, has certainly contributed to the fatal outcome of the three young Alpine ibexes found to be positive and already stressed by overlapping viral or/and bacterial infections.

5. Conclusions

The diagnostic work performed on wild animals found dead is rather complex and difficult; in the absence of any kind of anamnesis, investigation of the causes of death is based exclusively on the anatomical–pathological findings and subsequent laboratory exams. Analyses, especially bacteriological and histological, are often compromised by the poor quality of tissues, especially when the time between death and the finding of the carcass is particularly long, and even more if the weather conditions are adverse (as can happen in summer for high temperatures). The cases we have described, which are particularly lucky regarding the good quality of the young Alpine ibex' body conservation, confirm what has been gained through our experience; in other words, that wild animals generally die from a fatal combination of different pathological processes (viral and bacteriological infections, parasitic diseases, etc.), often associated with starvation in periods of food scarcity [53]. This reality requires a pathologist to apply diversified analytical approaches, with the commitment of various specialistic skills, in order to define, in detail, the various reasons that led the animal to death. Unlike domestic animals, wildlife is obviously not subject to regular health control and is, therefore, a potential reservoir of zoonoses. In Spain, it has been hypothesised that Iberian ibex could play a role in the maintenance of shared infectious diseases of animal health and conservation at the wildlife–livestock interface [54]. In this perspective, the detection of different pathogens in our study (ORFV, EPEC, MC, ECN, and ENP) reiterates that performing any diagnostic study on Italian Alpine ibex and, in general, wild animal carcasses is extremely important for the welfare of wild populations themselves, both for the monitoring of infections potentially transmissible to humans and finally for the control of the interspecies transmission of pathogens shared between domestic animals and wild fauna.

Supplementary Materials: The following supporting information can be downloaded at https://www.mdpi.com/article/10.3390/ani14243666/s1. Figure S1: Agarose gel electrophoresis of PCR products targeting ORFV for the Subject 1; Figure S2: Agarose gel electrophoresis of PCR products targeting ORFV for the Subject 2; Figure S3: Agarose gel electrophoresis of PCR products targeting ORFV for the Subject 3; Figure S4: PCR amplification plot for *lppS* gene DNA of *Mycoplasma conjunctivae* extracted from ocular swabs of Subject 1; Figure S5: The haemolytic strain of EPEC *eae* positive cultured on Columbia Agar 5% Sheep Blood from the intestine of Subject 4.

Author Contributions: Conceptualization, L.D.; methodology L.D.; investigation and analysis L.D., R.S., S.R., C.G. and E.C.; data curation, L.D. and R.S.; writing—original draft preparation, L.D.; writing—review and editing, L.D., R.S. and S.R.; supervision, L.D. All authors have read and agreed to the published version of the manuscript.

Funding: This research received no external funding.

Institutional Review Board Statement: Not applicable.

Informed Consent Statement: Not applicable.

Data Availability Statement: Individual raw data collected are available on request from the corresponding author.

Acknowledgments: We would like to thank M. Goria (Biotechnology Department of IZSPLV, Torino) for the analysis of the EPEC strains, R. Pelizzaro, A. Mosca and the Forest Rangers of Aosta Valley Region for presenting the ibex carcasses to our laboratory.

Conflicts of Interest: The authors declare no conflicts of interest.

References

1. Rossi, L.; Tizzani, P.; Rambozzi, L.; Moroni, B.; Meneguz, P.G. Sanitary emergencies at the wild/domestic caprines interface in Europe. *Animals* **2019**, *9*, 922. [CrossRef] [PubMed]
2. Spyrou, V.; Valiakos, G. Orf virus infection in sheep or goats. *Vet. Microbiol.* **2015**, *181*, 178–182. [CrossRef] [PubMed]
3. Tryland, M.; Beckmen, K.B.; Burek-Huntington, K.A.; Breines, E.M.; Klein, J. Orf virus infection in Alaskan mountain goats, Dall's sheep, muskoxen, caribou and Sitka black-tailed deer. *Acta Vet. Scand.* **2018**, *60*, 12. [CrossRef] [PubMed]

4. Robinson, A.J.; Mercer, A.A. Parapoxvirus of red deer: Evidence for its inclusion as a new member in the genus Parapoxvirus. *Virology* **1995**, *208*, 812–815. [CrossRef]
5. Friederichs, S.; Krebs, S.; Blum, H.; Lang, H.; Buttner, M. Parapoxvirus (PPV) of red deer reveals subclinical infection and confirms a unique species. *J. Gen. Virol.* **2015**, *96*, 1446–1462. [CrossRef] [PubMed]
6. Roess, A.A.; Galan, A.; Kitces, E.; Li, Y.; Zhao, H.; Paddock, C.D.; Adem, P.; Goldsmith, C.S.; Miller, D.; Reynolds, M.G.; et al. Novel deer-associated Parapoxvirus infection in deer hunters. *N. Engl. J. Med.* **2010**, *363*, 2621–2627. [CrossRef]
7. Roess, A.A.; McCollum, A.M.; Gruszynski, K.; Zhao, H.; Davidson, W.; Lafon, N.; Engelmeyer, T.; Moyer, B.; Godfrey, C.; Kilpatrick, H.; et al. Surveillance of Parapoxvirus among ruminants in Virginia and Connecticut. *Zoonoses Public Health* **2013**, *60*, 543–548. [CrossRef] [PubMed]
8. Scagliarini, A.; Vaccari, F.; Turrini, F.; Bianchi, A.; Cordioli, P.; Lavazza, A. Parapoxvirus Infections of Red Deer, Italy. *Emerg. Infect. Dis.* **2011**, *17*, 684–687. [CrossRef]
9. Horner, G.W.; Robinson, A.J.; Hunter, R.; Cox, B.T.; Smith, R. Parapoxvirus infections in New Zealand farmed red deer. *N. Z. Vet. J.* **1987**, *35*, 41–45. [CrossRef]
10. Kitchen, M.; Müller, H.; Zobl, A.; Windisch, A.; Romani, N.; Huemer, H. ORF virus infection in a hunter in Western Austria, presumably transmitted by game. *Acta Derm.-Venereol.* **2014**, *94*, 212–214. [CrossRef]
11. Scagliarini, A.; Casà, G.; Trentin, B.; Gallina, L.; Savini, F.; Morent, M.; Lavazza, A.; Puleio, R.; Buttaci, C.; Cannella, V.; et al. Evidence of zoonotic Poxviridae coinfection clinically diagnosed papillomas using a newly developed mini-array test. *J. Vet. Diagn. Investig.* **2016**, *28*, 59–64. [CrossRef] [PubMed]
12. Gallina, L.; Savini, F.; Casà, G.; Bertoletti, I.; Bianchi, A.; Gibelli, L.R.; Lelli, D.; Lavazza, A.; Scagliarini, A. Epitheliotropic Infections in Wildlife Ruminants from the Central Alps and Stelvio National Park. *Front. Vet. Sci.* **2020**, *30*, 229. [CrossRef] [PubMed]
13. Smith, K.J.; Skelton, H.G.; James, W.D.; Lupton, G.P. Parapoxvirus infections acquired after exposure to wildlife. *Arch. Dermatol.* **1991**, *127*, 79–82. [CrossRef] [PubMed]
14. Kuhl, J.T.; Huerter, C.J.; Hashish, H. A case of human orf contracted from a deer. *Cutis* **2003**, *71*, 288–290.
15. Alonso, C.A.; Mora, A.; Díaz, D.; Blanco, M.; González-Barrio, D.; Ruiz-Fons, F.; Simón, C.; Blanco, J.; Torres, C. Occurrence and characterization of stx and/or eae-positive *Escherichia coli* isolated from wildlife, including a typical EPEC strain from a wild boar. *Vet. Microbiol.* **2017**, *207*, 69–73. [CrossRef] [PubMed]
16. Cepeda-Molero, M.; Berger, C.N.; Walsham, A.D.S.; Ellis, S.J.; Wemyss-Holden, S.; Schüller, S.; Frankel, G.; Fernández, L.Á. Attaching and effacing (A/E) lesion formation by enteropathogenic *E. coli* on human intestinal mucosa is dependent on non-LEE effectors. *PLoS Pathog.* **2017**, *13*, e1006706.
17. Nataro, J.P.; Kaper, J.B. Diarrheagenic *Escherichia coli*. *Clin. Microbiol. Rev.* **1998**, *11*, 142–201. [CrossRef]
18. Smoglica, C.; Vergara, A.; Angelucci, S.; Festino, A.R.; Antonucci, A.; Moschetti, L.; Farooq, M.; Marsilio, F.; Di Francesco, C.E. Resistance Patterns, mcr-4 and OXA-48 Genes, and Virulence Factors of *Escherichia coli* from Apennine Chamois Living in Sympatry with Domestic Species, Italy. *Animals* **2022**, *12*, 129. [CrossRef]
19. Turchi, B.; Dec, M.; Bertelloni, F.; Winiarczyk, S.; Gnat, S.; Bresciani, F.; Viviani, F.; Cerri, D.; Fratini, F. Antibiotic Susceptibility and Virulence Factors in *Escherichia coli* from Sympatric Wildlife of the Apuan Alps Regional Park (Tuscany, Italy). *Microb. Drug Resist.* **2019**, *25*, 772–780. [CrossRef]
20. Hofer, E.; Cernela, N.; Stephan, R. Shiga toxin subtypes associated with Shiga toxin-producing *Escherichia coli* strains isolated from red deer, roe deer, chamois, and ibex. *Foodborne Pathog. Dis.* **2012**, *9*, 792–795. [CrossRef]
21. Chandran, A.; Mazumder, A. Prevalence of diarrhea-associated virulence genes and genetic diversity in *Escherichia coli* isolates from fecal material of various animal hosts. *Appl. Environ. Microbiol.* **2013**, *79*, 7371–7380. [CrossRef]
22. Obwegeser, T.; Stephan, R.; Hofer, E.; Zweifel, C. Shedding of foodborne pathogens and microbial carcass contamination of hunted wild ruminants. *Vet. Microbiol.* **2012**, *159*, 149–154. [CrossRef] [PubMed]
23. Giacometti, M.; Janovsky, M.; Belloy, L.; Frey, J. Infectious keratoconjunctivitis of ibex, chamois and other Caprinae. *Sci. Tech. Rev.* **2002**, *21*, 335–345. [CrossRef] [PubMed]
24. Tschopp, R.; Frey, J.; Zimmermann, L.; Giacometti, M. Outbreaks of infectious keratoconjunctivitis in alpine chamois and ibex in Switzerland between 2001 and 2003. *Vet Rec.* **2005**, *157*, 13–18. [CrossRef]
25. Grattarola, C.; Frey, J.; Abdo, E.M.; Orusa, R.; Nicolet, J.; Giacometti, M. *Mycoplasma conjunctivae* infections in chamois and ibexes affected with infectious keratoconjunctivitis in the Italian Alps. *Vet. Rec.* **1999**, *145*, 588–589. [CrossRef] [PubMed]
26. Fernández-Aguilar, X.; Cabezón, O.; Frey, J.; Velarde, R.; Serrano, E.; Colom-Cadena, A.; Gelormini, G.; Marco, I.; Mentaberre, G.; Lavín, S.; et al. Long-term dynamics of *Mycoplasma conjunctivae* at the wildlife-livestock interface in the Pyrenees. *PLoS ONE* **2017**, *12*, e0186069. [CrossRef] [PubMed]
27. Fernández-Aguilar, X.; Cabezón, Ó.; Granados, J.E.; Frey, J.; Serrano, E.; Velarde, R.; Cano-Manuel, F.J.; Mentaberre, G.; Ráez-Bravo, A.; Fandos, P.; et al. Postepizootic persistence of asymptomatic *Mycoplasma conjunctivae* infection in Iberian ibex. *Appl. Environ. Microbiol.* **2017**, *83*, e00690-17. [CrossRef]
28. Cassini, R.; Párraga, M.A.; Signorini, M.; Frangipane di Regalbono, A.; Sturaro, E.; Rossi, L.; Ramanzin, M. Lungworms in Alpine ibex (*Capra ibex*) in the eastern Alps, Italy: An ecological approach. *Vet. Parasitol.* **2015**, *214*, 132–138. [CrossRef] [PubMed]

29. Marreros, N.; Frey, C.F.; Willisch, C.S.; Signer, C.; Ryser-Degiorgis, M.P. Coprological analyses on apparently healthy Alpine ibex (*Capra ibex ibex*) from two Swiss colonies. *Vet. Parasitol.* **2012**, *186*, 382–389. [CrossRef] [PubMed]
30. Sarasa, M.; Serrano, E.; Soriguer, R.C.; Granados, J.E.; Fandos, P.; Gonzalez, G.; Joachim, J.; Pérez, J.M. Negative effect of the arthropod parasite, *Sarcoptes scabiei*, on testes mass in Iberian ibex, *Capra pyrenaica*. *Vet. Parasitol.* **2011**, *175*, 306–312. [CrossRef]
31. Yeruham, I.; Rosen, S.; Hadani, A.; Braverman, Y. Arthropod parasites of Nubian ibexes (*Capra ibex nubiana*) and gazelles (*Gazella gazella*) in Israel. *Vet. Parasitol.* **1999**, *83*, 167–173. [CrossRef] [PubMed]
32. Zanet, S.; Ferroglio, E.; Orlandini, F.; Bassano, B.; Battisti, E.; Brambilla, A. Bronchopulmonary Nematodes in Alpine Ibex: Shedding of First Stage Larvae Analyzed at the Individual Host Level. *Front. Vet. Sci.* **2021**, *8*, 663268. [CrossRef]
33. Cringoli, G.; Iori, A.; Rinaldi, L.; Veneziano, V.; Genchi, C. Zecche d'Italia. *Mappe Parassitol.* **2005**, *6*, 1–308.
34. Estrada-Peña, A.; Bouattour, A.; Camicas, J.L.; Walker, A.R. *Ticks of Domestic Animals in the Mediterranean Region: A Guide to Identification of Species*; University of Zaragoza: Zaragoza, Spain, 2004; pp. 1–221.
35. Tremblay, E. *Entomologia applicata. Da Ditteri Brachiceri (Caliptrati) a Sifanotteri e Strepsitteri*; Liguori: Napoli, Italy, 1997; Volume 3, pp. 1–140.
36. ISO/TS 13136/2012. Microbiology of Food and Animal Feed—Realtime Polymerase Chain Reaction (PCR)-Based Method for the Detection of Food-Borne Pathogens—Horizontal Method for the Detection of Shiga Toxin-Producing Escherichia coli (STEC) and the Determination of O157, O111, O26, O103 and O145 Serogroups. International Organization for Standardization: Geneva, Switzerland, 2012.
37. Lee, G.L. *Manual of Histologic Staining Methods of the Armed Forces Institute of Pathology*, 3rd ed.; Blakiston Division, McGraw-Hill: New York, NY, USA, 1968; pp. 1–258.
38. Bora, D.P.; Venkatesan, G.; Bhanuprakash, V.; Balamurugan, V.; Prabhu, M.; Siva Sankar, M.S.; Yogisharadhya, R. TaqMan real-time PCR assay based on DNA polymerase gene for rapid detection of Orf infection. *J. Virol. Methods* **2011**, *178*, 249–252. [CrossRef]
39. Vilei, E.M.; Bonvin-Klotz, L.; Zimmermann, L.; Ryser-Degiorgis, M.P.; Giacometti, M.; Frey, J. Validation and diagnostic efficacy of a TaqMan real-time PCR for the detection of *Mycoplasma conjunctivae* in the eyes of infected Caprinae. *J. Microbiol. Methods* **2007**, *70*, 384–386. [CrossRef] [PubMed]
40. Belloy, L.; Vilei, E.M.; Giacometti, M.; Frey, J. Characterization of LppS, an adhesin of *Mycoplasma conjunctivae*. *Microbiology* **2003**, *149*, 185–193. [CrossRef] [PubMed]
41. Mustoni, A.; Pedrotti, L.; Zanon, E.; Tosi, G. *Ungulati delle Alpi. Biologia, Riconoscimento, Gestione*; Nitida Immagine Editrice: Cles, Italy, 2002; pp. 1–539.
42. Ueda, N.; Inder, M.K.; Wise, L.M.; Fleming, S.B.; Mercer, A.A. Parapoxvirus of red deer in New Zealand encodes a variant of viral vascular endothelial growth factor. *Virus Res.* **2007**, *124*, 50–58. [CrossRef] [PubMed]
43. Lee, D.W.; Gwack, J.; Youn, S.K. Enteropathogenic *Escherichia coli* Outbreak and its Incubation Period: Is it Short or Long? *Osong Public Health Res. Perspect.* **2012**, *3*, 43–47. [CrossRef]
44. Kinnula, S.; Hemminki, K.; Kotilainen, H.; Ruotsalainen, E.; Tarkka, E.; Salmenlinna, S.; Hallanvuo, S.; Leinonen, E.; Jukka, O.; Rimhanen-Finne, R. Outbreak of multiple strains of non-O157 Shiga toxin-producing and enteropathogenic *Escherichia coli* associated with rocket salad, Finland, autumn 2016. *Euro Surveill.* **2018**, *23*, 1700666. [CrossRef] [PubMed]
45. Caprioli, A.; Morabito, S.; Brugère, H.; Oswald, E. Enterohaemorrhagic *Escherichia coli*: Emerging issues on virulence and modes of transmission. *Vet. Res.* **2005**, *36*, 289–311. [CrossRef]
46. Bardiau, M.; Muylaert, A.; Duprez, J.N.; Labrozzo, S.; Mainil, J.G. Prevalence, molecular typing, and antibiotic sensitivity of enteropathogenic, enterohaemorrhagic, and verotoxigenic *Escherichia coli* isolated from veal calves. *Tijdschr. Diergeneeskd.* **2010**, *135*, 554–558.
47. Janke, B.H.; Francis, D.H.; Collins, J.E.; Libal, M.C.; Zeman, D.H.; Johnson, D.D. Attaching and effacing *Escherichia coli* infections in calves, pigs, lambs, and dogs. *J. Vet. Diagn. Investig.* **1989**, *1*, 6–11. [CrossRef] [PubMed]
48. Ryser-Degiorgis, M.P.; Bischof, D.F.; Marreros, N.; Willisch, C.; Signer, C.; Filli, F.; Brosi, G.; Frey, J.; Vilei, E.M. Detection of *Mycoplasma conjunctivae* in the eyes of healthy, free-ranging Alpine ibex: Possible involvement of Alpine ibex as carriers for the main causing agent of infectious keratoconjunctivitis in wild Caprinae. *Vet. Microbiol.* **2009**, *134*, 368–374. [CrossRef]
49. Fernández-Aguilar, X.; López-Olvera, J.R.; Puig-Ribas, M.; Begovoeva, M.; Velarde, R.; Cardells, J.; Cabezón, Ó. *Mycoplasma conjunctivae* in insect vectors and anatomic locations related to transmission and persistence. *Vet. Microbiol.* **2019**, *228*, 7–11. [CrossRef]
50. Valldeperes, M.; Yerro, P.P.; López-Olvera, J.R.; Fandos, P.; Lavín, S.; Escofet, R.C.S.; Mentaberre, G.; León, F.J.C.; Espinosa, J.; Ráez-Bravo, A.; et al. Diseases of Iberian ibex (*Capra pyrenaica*). *Eur. J. Wildl. Res.* **2023**, *69*, 63. [CrossRef]
51. Pérez, J.M.; Granados, J.E.; Pérez, M.C.; Márquez, F.J.; Ferroglio, E.; Rossi, L. A survey of the gastrointestinal nematodes of Spanish ibex (*Capra pyrenaica*) in a high mountain habitat. *J. Parasitol.* **2003**, *89*, 315–318. [CrossRef]
52. Winter, J.; Rehbein, S.; Joachim, A. Transmission of Helminths between Species of Ruminants in Austria Appears More Likely to Occur than Generally Assumed. *Front. Vet. Sci.* **2018**, *5*, 30. [CrossRef]

53. Domenis, L.; Spedicato, R.; Orusa, R.; Goria, M.; Sant, S.; Guidetti, C.; Robetto, S. The diagnostic activity on wild animals through the description of a model case report (caseous lymphadenitis by *Corynebacterium pseudotuberculosis* associated with *Pasteurella* spp. and parasites infection in an alpine ibex—*Capra ibex*). *Open Vet. J.* **2017**, *7*, 384–390. [CrossRef] [PubMed]
54. Arenas, A.; García-Bocanegra, I. Spatiotemporal monitoring of selected pathogens in Iberian ibex (*Capra pyrenaica*). *Transbound. Emerg. Dis.* **2020**, *67*, 2259–2265.

Disclaimer/Publisher's Note: The statements, opinions and data contained in all publications are solely those of the individual author(s) and contributor(s) and not of MDPI and/or the editor(s). MDPI and/or the editor(s) disclaim responsibility for any injury to people or property resulting from any ideas, methods, instructions or products referred to in the content.

animals

MDPI

Article

Parasitic Infections in Stranded Whales and Dolphins in Canary Islands (2018–2022): An Update

Zuleima Suárez-González [1], Jorge F. González [2,*], Manuel Arbelo [1], Eva Sierra [1], Ayoze Castro-Alonso [1], Julia N. Hernández [2], Vidal Martín [3], Natalia Fraija-Fernández [4] and Antonio Fernández [1]

[1] Division of Histology and Veterinary Pathology, Atlantic Center for Cetacean Research, University Institute for Animal Health and Food Safety (IUSA), Veterinary School, University of Las Palmas de Gran Canaria (ULPGC), Transmontaña, Arucas, 35413 Canary Island, Spain; zuleima.suarez@ulpgc.es (Z.S.-G.); manuel.arbelo@ulpgc.es (M.A.); eva.sierra@ulpgc.es (E.S.); ayoze.castro@ulpgc.es (A.C.-A.); antonio.fernandez@ulpgc.es (A.F.)

[2] University Institute for Animal Health and Food Safety (IUSA), Veterinary School, University of Las Palmas de Gran Canaria (ULPGC), Transmontaña, Arucas, 35413 Canary Island, Spain; julia.hernandez@ulpgc.es

[3] Society for the Study of Cetacean in the Canary Archipelago (SECAC), Arrecife, Lanzarote, 35500 Canary Islands, Spain; vidal@cetaceos.org

[4] Marine Zoology Unit, Cavanilles Institute of Biodiversity and Evolutionary Biology, University of Valencia, 46980 Valencia, Spain; natalia.fraija@uv.es

* Correspondence: jorgefrancisco.gonzalez@ulpgc.es

Simple Summary: Cetaceans are considered indicator species for the health of the oceans. These wildlife animals are often parasitized by a wide range of species, including external and internal parasites. In turn, the parasites may provide valuable information in biological and ecological terms, where parasitic identification is a fundamental issue for etiological diagnosis, disease epidemiology and health assessment. Here, we update the record of parasites, by morphological identification, that are present in cetaceans stranded in the Canary Islands. Up to eighteen species and nine genera were identified in a wide range of hosts, both dolphins and whales, with different prevalence in each case. These data contribute and improve the general knowledge of the parasitic fauna in Canarian cetaceans, which requires special attention as an important source of information on host ecology and biology, as well as on the health status and imbalances that occur in the parasite–host association.

Abstract: The Canary Islands are considered a hot spot for marine species biodiversity. Each stranded cetacean has provided important scientific, biological and pathological information. The morphological identification of parasites in these stranded cetaceans is the main aim of the present article. An investigation to identify parasites was carried out in 233 stranded animals (2018–2022), which were submitted for necropsy. Adult and sub-adult/juvenile animals were the most parasitized age categories, and eighteen parasite species were morphologically identified, including nematodes (*Crassicauda grampicola*, *Crassicauda anthonyi*, *Halocercus delphini*, *Anisakis simplex*, *Stenurus globicephalae*, *Stenurus ovatus*), trematodes (*Nasitrema delphini*, *Oschmarinella rochebruni*, *Brachycladium atlanticum*, *Pholeter gastrophilus*), cestodes (*Clistobothrium delphini*, *Clistobothrium grimaldii)*, acanthocephalans *(Bolbosoma vasculosum*, *Bolbosoma capitatum*), protists (*Toxoplasma gondii*) and crustaceans (*Conchoderma auritum*, *Xenobalanus globicipitis*, *Pennella balaenoptera*), as well as nine genera: *Crassicauda* sp., *Halocercus* sp., *Anisakis* sp., *Stenurus* sp., *Nasitrema* sp., *Oschmarinella* sp., *Dyphyllobothrium* sp., *Cyamus* sp., *Conchoderma* sp., *and Sarcocystis* sp. These could not be identified at the species level. Differences in the host specificity of some parasites were observed, varying in prevalence. The accurate morphological identification of the parasites affecting these marine mammals is essential to understanding disease epidemiology, assessing cetacean populations' health status, and developing effective conservation and management strategies.

Keywords: cetaceans; conservation; parasites; identification; health

1. Introduction

Marine mammals in the Canary Islands, particularly cetaceans, serve as invaluable bioindicators of the marine ecosystem's environmental status, providing insights into pollution levels and ecological shifts [1–3]. Their health is impacted by various stressors, including parasitic infections [4–7], which may involve internal parasites (such as protists, nematodes, cestodes, trematodes, and acanthocephalans) and external parasites like crustaceans [8–10].

Parasites exert a substantial influence on the health of marine mammals and provide critical insights from both biological and ecological perspectives. They are considered indicators of health at the individual, population, and environmental levels [11–13]. Although parasitism **is** common in wildlife, host–parasite interactions can become unbalanced, leading to negative effects that range from debilitation to mortality and, in some instances, contribute to stranding events [14–17]. The severity of these effects depends on several factors, such as the host's immune status, parasite species and burden and the presence of additional pathogens [13,18,19].

Although few marine mammal parasites exhibit high pathogenicity, those with significant prevalence have been implicated in strandings and mortality [8,14,17]. For instance, worms such as the genus *Crassicauda* Leiper and Atkinson, 1914 [14,20–22] and various Pseudaliids Railliet & Henry, 1909 were found in the lungs and the pterygoid sacs [15,23]. Moreover, trematodes of the genus N*asitrema* Ozaki, 1935, have been observed in these sacs, which may be implicated in severe central nervous system lesions, directly leading to stranding and death [16,24–28]. In addition, other hepatic and pancreatic trematodes have been identified in a wide range of host species [29–33]. Some of these parasites in cetaceans have an important zoonotic relevance, posing risks to human health and the economy [3,12]. Notable examples include the nematode genus *Anisakis* Dujardin, 1845 and the zoonotic protist *Toxoplasma gondii* Nicolle & Manceaux, 1908 [34–37]. While cetaceans are not typically consumed directly by humans in most regions, infections can be associated with the ingestion of larvae through the consumption of raw or undercooked fish [38]. Additionally, cetaceans play an important role as potential reservoirs and sentinels for zoonotic parasitic agents, contributing to their maintenance and distribution within aquatic environments and participating in the natural transmission cycles of parasites and other infectious agents transmissible to humans [39,40].

Historically, research on the parasitic fauna in marine mammals has been limited, with most studies focusing on parasites found in stranded carcasses, often in advanced stages of decomposition, which complicates analysis [8,18,19,41,42]. Despite these challenges, this manuscript provides new records of parasite species and host interactions in cetaceans from the Canary Islands, contributing novel insights into previously undescribed associations in the region. In total, 31 different species of cetaceans, including 24 odontocetes and 7 mysticetes, have been identified in the Canary Islands by 2022 [43].

The accurate morphological identification of parasites infecting these marine mammals is essential for determining the etiology of parasitic diseases, conducting epidemiological investigations and assessing the health status of both individual animals and their populations [5]. In this study, we updated the genera and parasitic species that affect cetaceans in the Canary Islands, including odontocetes and mysticetes stranded between 2018 and 2022.

2. Materials and Methods

2.1. Necropsied Animals and Biological Data

Necropsies were performed on 233 stranded animals in the Canary Islands during the period 2018–2022. The necropsy protocol was carried out according to standard and innovative technological procedures [5,6]. Biological data, including species identification, biometrics, age category, sex and body condition, were recorded (Table 1). Age ranges were based on total body length and gonadal development, with individuals categorized as fetus/neonate, calf, juvenile, subadult or adult [5,6,44]. Body condition was assessed according to anatomical parameters and classified into four categories: good, moderate, poor and very poor [45].

Table 1. Prevalence of different species according to sex, age, body condition and total prevalence of infected animals stranded in Canary Islands between 2018 and 2022. A: adult; C: calf; F: female; G: good; J-Sad: juvenile–subadult; M: male; Md: moderate; N: neonate; ND: not determined; P: poor; VP: very poor.

	Parasitized Animals (%)	Sex (%)			Age (%)					Body Condition (%)				
		F	M	ND	N	C	J-Sad	A	ND	VP	P	Md	G	ND
Stenella coeruleoalba (n = 53/61)	87	40	58	2		11	29	58	2	6	30	47	8	9
Stenella frontalis (n = 44/51)	86	52	48		5	29	18	48		2	18	50	14	16
Delphinus delphis (n = 25/29)	86	52	48			16	16	68		8	56	16	4	16
Tursiops truncatus (n = 15/17)	88	47	53				33	60	7	13	33	27	13	14
Globicephala macrorhynchus (n = 13/15)	87	54	46			23	31	46			31	23	23	23
Grampus griseus (n = 7/11)	64	57	43			57	29		14	43	14	14		29
Kogia breviceps (n = 9/11)	82	33	67			11	33	56						
Physeter macrocephalus (n = 4/8)	50	75	25				75	25					50	50
Ziphius cavirostris (n = 8/8)	100	50	50				37	50	13	13	13	25	12	37
Steno bredanensis (n = 5/6)	83	60	40		20		20	60		20	40	20		20
Balaenoptera physalus (n = 1/3)	33		100			100					100			
Mesoplodon densirostris (n = 2/3)	67	50	50					100				100		
Mesoplodon europaeus (n = 1/3)	33		100					100				100		
Balaenoptera acutorostrata (n = 1/2)	50	100						100			100			
Lagenodelphis hosei (n = 1/2)	50		100			100						100		
Balaenoptera edeni (n = 1/1)	100		100				100						100	
Kogia sima (n = 1/1)	100	100						100						100
Peponocephala electra (n = 1/1)	100		100				100			100				

2.2. Parasite Analysis

Data on the parasite occurrence were obtained from the necropsy reports for all 233 animals examined. Each case included in this study was diagnosed through routine pathological and cause-of-death analyses of stranded cetaceans, performed at the Division of Histology and Animal Pathology, Institute for Animal Health (IUSA), within the Veterinary School at the Universidad de Las Palmas de Gran Canaria. Tissue samples were systematically collected during necropsy, fixed in 10% neutral buffered formalin, carved, routinely processed, embedded in paraffin, sectioned at 5 μm and stained with hematoxylin and eosin (HE) for light microscopic examination (Olympus BX51, Tokyo, Japan). Imaging was conducted using Camera software for DP21 (Ver.02.01.01.93) for pictures or figures (Olympus DP21, Tokyo, Japan). Direct parasite collection, however, was only possible for 57 animals stranded between 2020 and 2022. Complete individual parasites from these cases were preserved in 70% ethanol for subsequent laboratory morphological identification. Nematodes and acanthocephalans were cleared with a lactophenol solution to facilitate better observation of internal structures. Cestodes and trematodes were initially stained with acetocarmine, then dehydrated through a graded ethanol series, cleared with dimethyl phthalate and mounted in a permanent preparation using Canada balsam, following the methods previously used [46]. For detailed observation, a magnifying glass and, primarily, an optical microscope equipped with a monitor were employed. Motic® Images Plus 2.0 ML software and a Moticam digital camera were used to measure parasite length in μm. Parasites were morphologically identified using specific taxonomic guides and keys [25,47–58].

Microscopic protists were identified in histopathological tissue sections, with particular focus on tissues and organs known to harbor *Sarcocystis* (Lankester, 1882) and *Toxoplasma gondii* cysts [26,59,60]. *Toxoplasma gondii* was identified molecularly using a recently developed real-time PCR method described by Sierra et al. [26]. The PCR products obtained from positive cases were processed and sequenced according to Sierra et al. [26], and a BLAST search was performed to verify the identity of the PCR amplicons.

3. Results

3.1. Necropsied Animals and Biological Data

In the period 2018–2022, 233 animals were necropsied in the Canary Islands belonging to 18 different cetacean species. Animals in a very advanced state of decomposition were not included in this study. In total, 61 striped dolphins (*Stenella coeruleoalba)*, 51 Atlantic spotted

dolphins (*Stenella frontalis*), 29 common dolphins (*Delphinus delphis*), 17 bottlenose dolphins (*Tursiops truncatus*), 15 short-finned pilot whales (*Globicephala macrorhynchus*), 11 Risso's dolphins (*Grampus griseus*), 11 pygmy sperm whales (*Kogia breviceps*), 8 sperm whales (*Physeter macrocephalus*), 8 Cuvier's beaked whales (*Ziphius cavirostris*), 6 rough-toothed dolphins (*Steno bredanensis*), 3 fin whales (*Balaenoptera* physalus), 3 Blainville's beaked whales (*Mesoplodon densirostris*), 3 Gervais's beaked whales (*Mesoplodon europaeus*), 2 common minke whales (*Balaenoptera acutorostrata*), 2 Fraser's dolphins (*Lagenodelphis hosei*), 1 Bryde's whale (*Balaenoptera edeni*), 1 dwarf sperm whale (*Kogia sima*) and 1 melon-headed whale *(Peponocephala electra*) were analyzed. Stranded necropsied cetaceans and their respective biological data and stranding location are presented in Supplementary Table S1.

3.2. Parasite Analyses

Among the 233 animals necropsied, 192 (82%) were found to be parasitized by one or more species, including nematodes, trematodes, cestodes, acanthocephalans, crustaceans and protists. From the total parasitized animals, parasites were only obtained from 30% of the animals, and 18 parasitic species were identified. Many parasites could not be identified at the species level due to the poor condition of the preservation of the specimens. Table 1 shows the prevalence of parasitism among animals, categorized by sex, age and body condition. Generally, similar prevalence was observed between female and male animals, with the exception of sperm whales, likely due to the higher number of female than male strandings. In addition, adult and juvenile/sub-adult animals showed a higher parasitism rate among species with the most frequent strandings, such as the *D. delphis*, *S. frontalis*, *S. coeruleoalba* and *T. truncatus*. Furthermore, variable differences were observed in the body condition of these animals.

3.2.1. Nematodes

The nematode genus *Crassicauda* had a global prevalence of 43%. The highest prevalence was observed in *Z. cavirostris* (100%) and *S. frontalis* (61%) (Table 2). In *Z. cavirostris*, *Crassicauda anthonyi* Chabaud, 1962 was morphologically identified as responsible for renal parasitosis and vascular damage (Figure 1A), and *Crassicauda grampicola* Johnston & Mawson, 194 was identified parasitizing the pterygoids sacs in two *S. frontalis*, one *T. truncatus* and four *G. griseus* (Figure 1B). *Crassicauda* sp. was also found in the mammary glands, prostate and subcutaneous tissue of several odontocete species and one mysticete (*B. edeni*) (Table 3).

Additionally, the lungs of various stranded odontocetes were frequently parasitized, with the highest prevalence observed in *T. truncatus* (88%) and *D. delphis* (52%) (Table 2). *Halocercus delphini* Baylis & Daubney, 1925 was morphologically identified in two *S. coeruleoalba* (Figure 1C), while *Stenurus ovatus* (von Linstow, 1910) Baylis & Daubney, 1925 was found in four *T. truncatus*, diagnosed by its characteristic cuticle inflammation (Figure 1D). Although not identified at the species level, *Halocercus* sp. and *Stenurus* sp. were also detected in one *S. frontalis* and *S. coeruleoalba*, respectively. Nematodes in the pterygoid sacs were observed in 13% of the animals, with the highest prevalence in *G. macrorhynchus* (67%) (Table 2). *Stenurus globicephalae* Baylis et Daubney, 1925 was the only nematode species identified in the pterygoid sacs of three *G. macrorhynchus* and one *G. griseus* (Image 1e). The zoonotic nematode *Anisakis* sp. had an overall prevalence of 35% across 14 different odontocete species (Table 3), with the highest frequency observed in *K. breviceps* (72%) (Table 2). Both the dwarf sperm whale and melon-headed whale had a 100% prevalence of anisakiasis, although the number of strandings for these species was low (n = 1 for each). Adults of *A. simplex* were identified in one *D. delphis* (Figure 1F) and in the *P. electra*, leading to ulcerated areas. In addition, a species likely to be *A.* conf. *physeteris* was found in a *K. breviceps*, but confirmation was not possible due to the decomposition state of the carcass and the parasites.

Table 2. Numbers of host individuals parasitized over the number of animals analyzed according to each stranded cetacean species in the Canary Islands. B.a: *Balaenoptera acutorostrata*; B.e: *Balaenoptera edeni*; B.p: *Balaenoptera physalus*; D.d: *Delphinus delphis*; G.m: *Globicephala macrorhynchus*; G.g: *Grampus griseus*; K.b: *Kogia breviceps*; K.s: *Kogia sima*; L.h: *Lagenodelphis hosei*; M.d: *Mesoplodon densirostris*; M.e: *Mesoplodon europaeus*; P.e: *Peponocephala electra*; P.m: *Physeter macrocephalus*; S.c: *Stenella coeruleoalba*; S.f: *Stenella frontalis*; S.b: *Steno bredanensis*; T.t: *Tursiops truncatus*; Z.c: *Ziphius cavirostris*.

Parasites	S.c	S.f	D.d	T.t	G.m	G.g	K.b	P.m	Z.c	S.b	B.p	M.d	M.e	B.a	L.h	B.e	K.s	P.e
Nematodes																		
Crassicauda sp.	15/61	31/51	7/29	9/17	4/15	3/11	3/11	-	8/8	-	-	-	-	-	-	1/1	-	-
Crassicauda anthonyi	-	-	-	-	-	-	-	-	8/8	-	-	-	-	-	-	-	-	-
Crassicauda grampicola	-	2/51	-	1/17	-	4/11	-	-	-	-	-	-	-	-	-	-	-	-
Halocercus sp.	-	1/51	-	-	-	-	-	-	-	-	-	-	-	-	-	-	-	-
Halocercus delphini	2/61		-	-	-	-	-	-	-		-	-	-	-	-	-	-	-
Stenurus sp.	1/61	-	-	-	-	-	-	-	-	-	-	-	-	-	-	-	-	-
Stenurus ovatus	-	-	-	4/17	-	-	-	-	-	-	-	-	-	-	-	-	-	-
Stenurus globicephalae	-	-	-	-	3/15	1/11	-	-	-	-	-	-	-	-	-	-	-	-
Anisakis sp.	20/61	9/51	8/29	4/17	6/15	1/11	8/11	3/8	3/8	2/6	-		1/3	-	1/2	-	1/1	1/1
Anisakis simplex	-	-	1/29	-	-	-	-	-	-	-	-	-	-	-	-	-	-	1/1
Trematodes																		
Nasitrema sp.	7/61	8/51	9/29	12/17	-	-	1/11	-	-	3/6	-	-	-	-	-	-	-	-
Nasitrema delphini	2/61	-	1/29	3/17	-	-	-	-	-	-	-	-	-	-	-	-	-	-
Brachycladium atlanticum	3/61	-	1/29	-	-	-	-	-	-	-	-	-	-	-	-	-	-	-
Oschmarinella sp.	-	-	-	-	-	-	-	-	2/8	-	-	-	-	-	-	-	-	-
Oschmarinella rochebruni	2/61	2/51	1/29	1/17	-	-	-	-	-	1/6	-	-	-	-	-	-	-	-
Pholeter gastrophilus	36/61	11/51	11/29	10/17	7/15	1/11	-	-	-	3/6	-	-	1/3	-	-	-	1/1	-
Cestodes																		
Dyphyllobothrium sp.	7/61	-	-	-	-	-	-	-	-	-	-	-	-	-	-	-	-	-
Clistobothrium delphini	36/61	25/51	12/29	7/17	9/15	1/11	5/11	2/8	6/8	3/6	-	1/3	1/3	1/2		-	1/1	
Clistobothrium grimaldii	38/61	11/51	12/29	5/17	7/15	1/11	4/11	-	-	2/6	1/3	-	-	-	-	-	-	-
Acanthocephalans																		
Bolbosoma vasculosum	2/61	-	1/29	-	-	-	-		-	-		-	-	-	-	-	-	-
Bolbosoma capitatum	-	-	-	-	4/15	-	-	-	-	-	-	-	-	-	-	-	-	1/1
Crustaceans																		
Cyamus sp.	-	-	-	-	-	-	-	-	2/8	-	-	-	-	-	-	-	-	-
Pennella balaenoptera	2/61	-	-	1/17	-	-	1/11	-	1/8	1/6	-	-	-	-	-	1/1	-	1/1
Conchoderma sp.		1/51	2/29	1/17	1/15	-	-	-	2/8		-	-	-	-	-	-	-	-
Conchoderma auritum	-	-	-	-	-	-	-	-	1/8	-	-	-	-	-	-	-	-	-
Xenobalanus globicipitis	7/61	8/51	11/29	2/17	5/15	4/11	-	-	-	1/6	-	-	-	-	-	-	-	1/1
Protists																		
Sarcocystis sp.	4/61	4/51	6/29	-	-	-	-	2/8	-	-	-	-	-	-	-	-	-	-
Toxoplasma gondii	2/61	-	-	-	-	-	-	-	-	-	-	-	-	-	-	-	-	-

Table 3. Endoparasites and ectoparasites reported in the parasitized cetaceans during the period 2018–2022.

Parasites	Host	Site
Nematodes		
Crassicauda sp.	*B. edeni*, *D. delphis*, *G. macrorhynchus*, *G. griseus*, *K. breviceps*, *S. coeruleoalba*, *S. frontalis*, *T. truncatus*, *Z. cavirostris*	Mammary gland, Kidney, subcutanean tissue, prostate, pterygoid sacs
C. anthonyi	*Z. cavirostris*	Kidney
C. grampicola	*G. griseus*, *S. frontalis*, *T. truncatus*	Pterygoid sacs
Non-identified lungworms	*D. delphis*, *G. macrorhynchus*, *G. griseus*, *M. europaeus*, *S. coeruleoalba*, *S. frontalis*, *S. bredanensis*, *T. truncatus*	Lung
H. delphini	*S. coeruleoalba*	Lung
S. ovatus	*T. truncatus*	Lung
Stenurus globicephalae	*G. macrorhynchus*, *G. griseus*	Pterygoid sacs
Non-identified pterygoid sacs nematodes	*D. delphis*, *G. macrorhynchus*, *G. griseus*, *S. coeruleoalba*, *S. frontalis*, *S. bredanensis*, *T. truncatus*	Pterygoid sacs
Anisakis sp.	*D. delphis*, *G. macrorhynchus*, *G. griseus*, *K. breviceps*, *K. sima*, *L. hosei*, *M. europaeus*, *P. electra*, *P. macrocephalus*, *S. coeruleoalba*, *S. frontalis*, *S. bredanensis*, *T. truncatus*, *Z. cavirostris*	Digestive tract
A. simplex	*D. delphis*, *P. electra*	Digestive tract

Table 3. *Cont.*

Parasites	Host	Site
Trematodes		
Nasitrema sp.	*D. delphis*, *G. macrorhynchus*, *K. breviceps*, *S. coeruleoalba*, *S. frontalis*, *S. bredanensis*, *T. truncatus*	Pterygoid sacs, CNS
N. delphini	*D. delphis*, *S. coeruleoalba*, *T. truncatus*	Pterygoid sacs
Non-identified hepatic trematodes	*B. edeni*, *D. delphis*, *M. europaeus*, *S. coeruleoalba*, *S. frontalis*, *T. truncatus*, *Z. cavirostris*	Bile ducts
Non-identified pancreatic trematodes	*D. delphis*, *S. coeruleoalba*, *S. frontalis*, *T. truncatus*	Pancreas
B. atlanticum	*D. delphis*, *S. coeruleoalba*	Bile ducts, pancreas
O. rochebruni	*D. delphis*, *S. coeruleoalba*, *S. bredanensis*, *S. frontalis*, *T. truncatus*	Bile ducts, pancreas
P. gastrophilus	*D. delphis*, *G. macrorhynchus*, *G. griseus*, *K. sima*, *M. europaeus*, *S. coeruleoalba*, *S. frontalis*, *Steno bredanensis*, *T. truncatus*	Stomach
Cestodes		
Non-identified digestive cestodes	*D. delphis*, *G. macrorhynchus*, *G. griseus*, *P. electra*, *S. coeruleoalba*, *S. frontalis*, *T. truncatus*	Digestive tract
Diphyllobothrium Cobbold, 1858	*S. coeruleoalba*	Digestive tract
C. delphini	*B. acutorostrata*, *D. delphis*, *G. macrorhynchus*, *G. griseus*, *K. breviceps*, *K. sima*, *M. densirostris*, *M. europaeus*, *P. macrocephalus*, *S. coeruleoalba*, *S. frontalis*, *S. bredanensis*, *T. truncatus*, *Ziphius cavirostris*	Blubber
C. grimaldii	*B. physalus*, *D. delphis*, *G. macrorhynchus*, *G. griseus*, *K. breviceps*, *S. coeruleoalba*, *S. frontalis*, *S. bredanensis*, *T. truncatus*	Abdominal serous
Acanthocephalans		
Non-identified *acanthocephalans*	*D. delphis*, *G. macrorhynchus*, *M. europaeus*, *P. electra*, *S. coeruleoalba*, *S. frontalis*	Digestive tract
B. vasculosum	*D.delphis*, *S. coeruleoalba*	Digestive tract
B. capitatum	*G. macrorhynchus*, *P. electra*	
Ectoparasites		
Non-identified cyamids	*D. delphis*, *G. macrorhynchus*, *M. europaeus*, *P. macrocephalus*, *S. coeruleoalba*, *T. truncatus*, *Z. cavirostris*	Skin
Cyamus sp.	*Z. cavirostris*	Skin
Non-identified copepods	*B.edeni*, *K.breviceps*, *P.electra*, *S. coeruleoalba*, *S. bredanensis*, *T. truncatus*, *Z. cavirostris*	Skin
Pennella balaenoptera	*B. edeni*, *K. breviceps*, *P. electra*, *S. coeruleoalba*, *S. bredanensis*, *T.truncatus*, *Z. cavirostris*	Skin
Non-identified cirripedes	*D. delphis*, *G. griseus*, *P. macrocephalus*, *S. coeruleoalba*, *S. frontalis*, *T. truncatus*	Skin
Conchoderma sp.	*D. delphis*, *G. macrorhynchus*, *S. frontalis*, *Z. cavirostris*,	Skin
C. auritum	*Z. cavirostris*	Buccal commissure
Xenobalanus globicipitis	*D. delphis*, *G. macrorhynchus*, *G. griseus*, *P. electra*, *S. coeruleoalba*, *S. frontalis*, *S. bredanensis*, *T. truncatus*	Skin
Protists		
Sarcocystis sp.	*D. delphis*, *P. macrocephalus*, *S. coeruleoalba*, *S. frontalis*	Skeletal muscle
T. gondii	*S. coeruleoalba*	Systemic infection

3.2.2. Trematodes

The prevalence of *Nasitrema* spp. was 23%, predominantly affecting the pterygoid sacs and occasionally the central nervous system (CNS) in odontocetes (Table 3). The highest prevalence was observed in *T. truncatus* (71%) and *S. bredanensis* (50%) (Table 2). *Nasitrema delphini* Neiland, Rice, & Holden, 1970 was morphologically identified in three *T. truncatus*, two *S. coeruleoalba* and one *D. delphis* (Table 2 and Figure 2A).

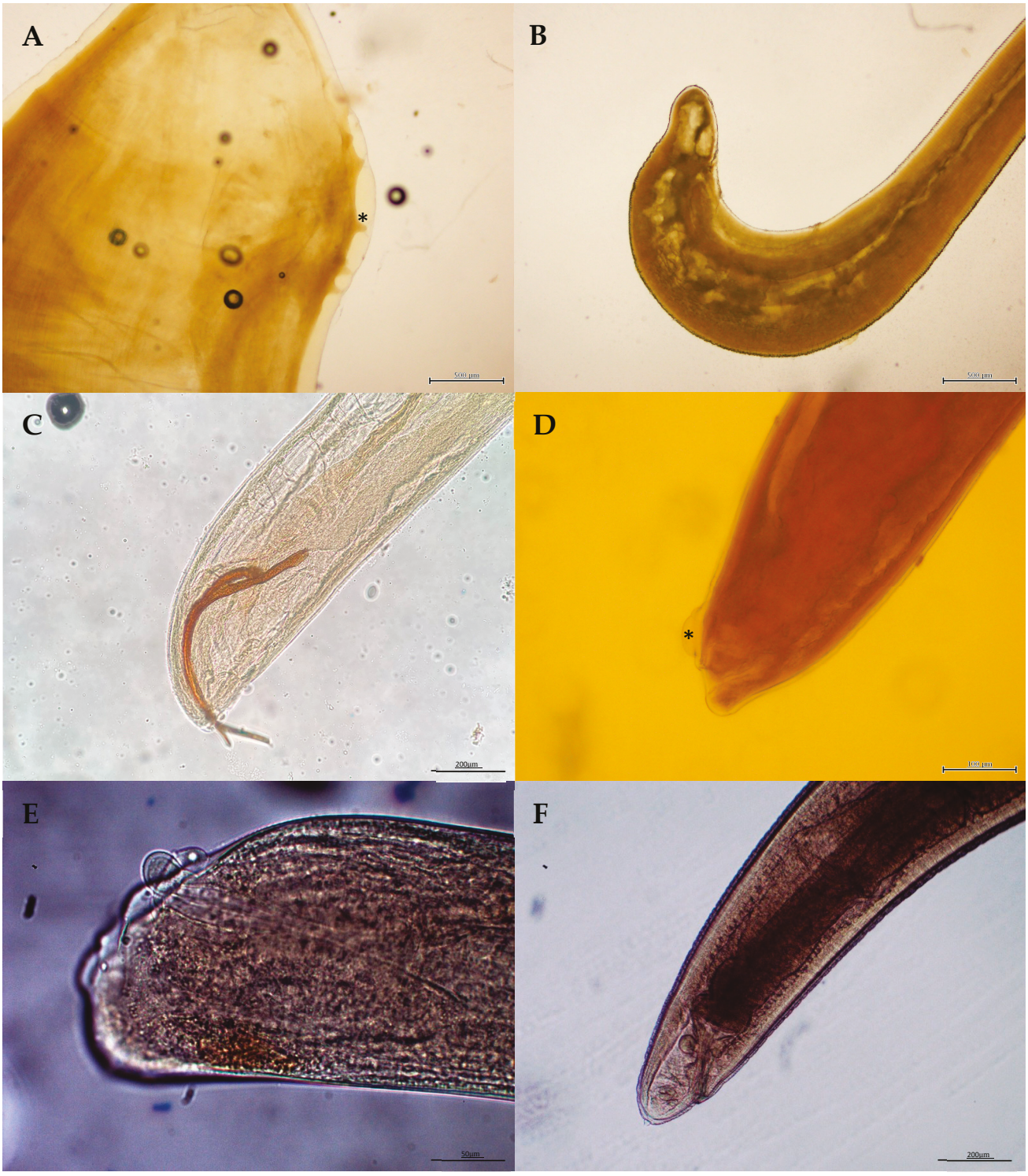


Figure 1. Microscopic views of the nematodes (**A**) Posterior end of a male (papillae in asterisk) of *Crassicauda anthonyi*. (**B**) Posterior end of a male of *Crassicauda grampicola* in the pterygoid sacs of *Grampus griseus*. (**C**) Posterior end of a male of *Halocercus delphini*. (**D**) Posterior end of a female of *Stenurus ovatus* (inflammation of the cuticle in asterisk). (**E**) Posterior end of a female *Stenurus globicephalae*. (**F**) Posterior end of a female of *Anisakis simplex*.

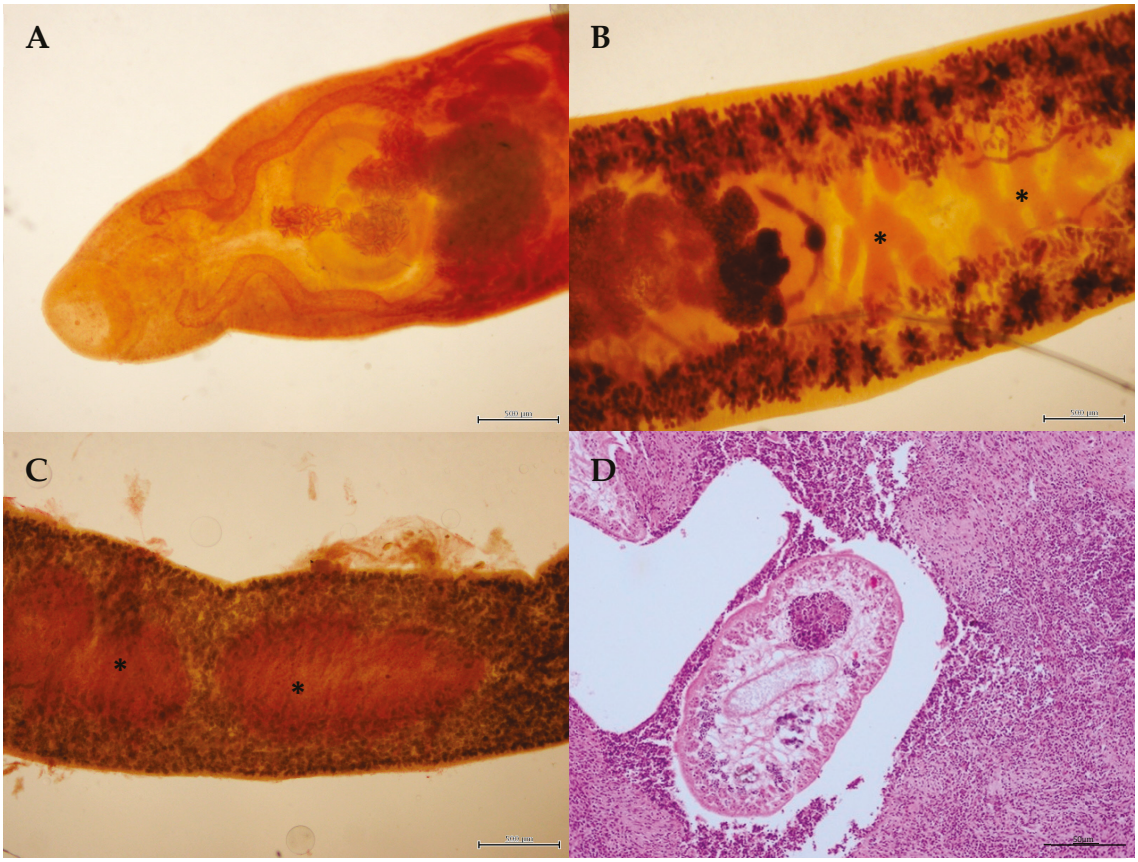


Figure 2. (**A**) Anterior end of *Nasitrema delphini*. (**B**) Detail of the posterior third quarter of the body of *Brachycladium atlanticum* showing the genitalia (testes in asterisks). (**C**) Detail of the middle third quarter of the body of *Oschmarinella rochebruni* showing the testes (asterisks). (**D**) Histological view of *Pholeter gastrophilus* in pyloric stomach leading to granulomatous gastritis. H-E stain.

Hepatic trematodes were found in 23% of the stranded marine mammals, primarily affecting the bile ducts, while pancreatic trematodes were detected in 24% of the animals. Varied prevalence was observed for liver flukes, with *D. delphis* and *G. macrorhynchus* showing higher infection rates in the pancreas. Among the stranded species, *S. coeruleoalba* and *S. frontalis* were the most frequently parasitized by liver and pancreatic trematodes. *Brachycladium atlanticum* (Abril, Balbuena and Raga, 1991) Gibson, 2005 (Figure 2B) was identified in *D. delphis* and three *S. coeruleoalba*, while *Oschmarinella rochebruni* (Poirier, 1886) Gibson & Bray, 1997 was morphologically identified in one *S. bredanensis*, two *S. coeruleoalba*, two *S. frontalis*, one *D. delphis* and one *T. truncatus*, affecting both the bile ducts and pancreas (Figure 2C). Brachycladiid trematodes, with an everted cirrus, compatible with the genus *Oschmarinella* were also collected in the bile ducts of two *Z. cavirostris*; however, their specific identity was not obtained. In addition, cysts of *Pholeter gastrophilus* (Kossack, 1910) Odhner, 1914 were found embedded in the mucosa, mainly in the glandular and pyloric regions of the stomach (Figure 2D), with the highest prevalences observed in *S. coeruleoalba* (59%) and *T. truncatus* (59%) (Table 2).

3.2.3. Cestodes

Cestodes were identified in the intestine of 16% of the stranded cetaceans analyzed in this study. However, only the genus *Diphyllobothrium* Cobbold, 1858 was identified in seven *S. coeruleoalba* (Table 2) due to the advanced decomposition state of these parasites and the absence of scolex and mature proglottids (Figure 3A). In addition, larval forms of the cestodes of *Clistobothrium delphini* (Bosc, 1802) Caira, Jensen, Pickering, Ruhnke & Gallagher, 2020 were detected in 14 different species, mainly in the anogenital region

(Figure 3B). *Clistobothrium grimaldii* (Moniez, 1889) Caira, Jensen, Pickering, Ruhnke & Gallagher, 2020 larvae were mainly observed in the abdominal serosa (Figure 3C). Both types of metacestodes were present in mysticetes and odontocetes, with varying prevalence across different host species (Table 2).



Figure 3. (**A**) Gravid proglottid of *Diphyllobothrium* sp. (**B**) *Clistobothrium delphini* cyst at subcutaneous tissue. (**C**) *Clistobothrium grimaldii* cyst in the abdominal serosa.

3.2.4. Acanthocephalans

Acanthocephalans were detected in only 8% of the stranded animals in seven different odontocete species (Table 3). Specifically, immature specimens of *Bolbosoma vasculosum* (Rudolphi, 1819) Porta, 1908 (Figure 4A) were identified in one *D. delphis* and two *S. coeruleoalba* (Table 2), while *Bolbosoma capitatum* (von Linstow, 1880) Porta, 1908 was identified in four *G. macrorhynchus* and one *P. electra* (Figure 4B). These parasites were embedded by their cephalic end in the gastric and intestinal mucosa.

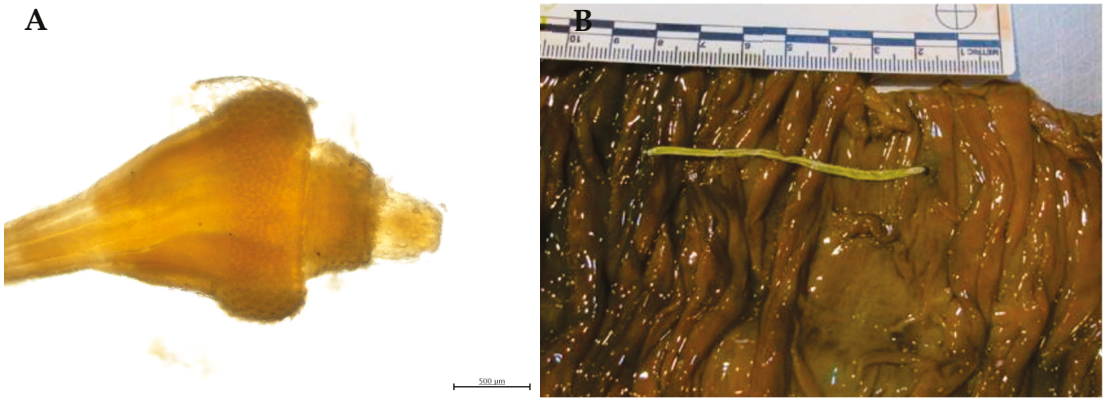


Figure 4. (**A**) Anterior end of *Bolbosoma vasculosum*. (**B**) *Bolbosoma capitatum* embedded in the intestinal mucosa of one short-finned pilot whale during necropsy.

3.2.5. Crustaceans

Ectoparasitic crustaceans were found in 44% of the stranded cetaceans, including cyamids, barnacles and copepods. Table 3 shows the parasitized host species and their location. Two specimens of the genus *Cyamus* Latreille, 1796 were identified in one *Z. cavirostris* (Figure 5A). Among the barnacles, *Conchoderma auritum* Linnaeus, 1767 was identified on a *Z. cavirostris* (Figure 5B), based on its ear-like extension in the capitulum, and *Conchoderma* sp. in five different species of odontocetes (Table 2). *Xenobalanus globicipitis* Steenstrup, 1852 was identified on eleven *D. delphis*, five *G. macrorhynchus*, four *G. griseus*, one *P. electra*, seven *S. coeruleoalba*, eight *S. frontalis*, one *S. bredanensis* and two *T. truncatus* (Table 2), primarily on the caudal, dorsal and pectoral fins (Figure 5C). At the same time, large-size copepods, *Pennella balaenoptera* Koren & Danielssen, 1877, were seen attached to the skin and embedded on the muscle (Figure 5D) in seven different host species (Tables 2 and 3).

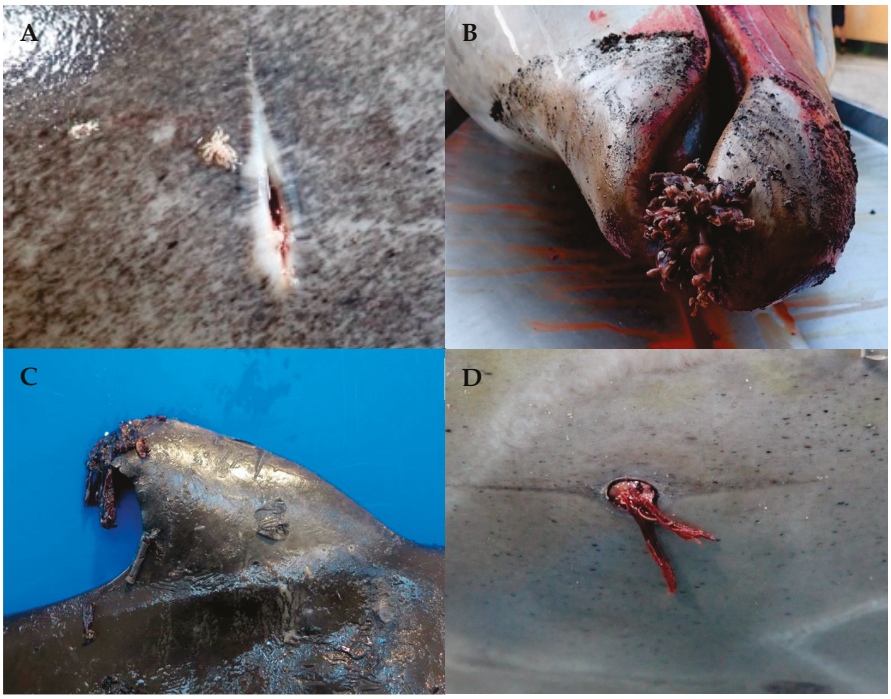


Figure 5. (**A**) *Cyamus* sp. associated with a linear injury in one *Ziphius cavirostris* during necropsy. (**B**) *Conchoderma auritum* attached to the rostral border of the mandible of a *Ziphius cavirostris*. (**C**) *Xenobalanus globicipitis* attached to the dorsal tail in a *Delphinus delphis*. (**D**) *Pennella balaenoptera* associated with ulceration in a *Ziphius cavirostris*.

3.2.6. Protists

Infection with the genus *Sarcocystis* was diagnosed in 8% of the animals based on histological examination, with revealed multifocal cysts within myofibers (Figure 6). No associated inflammatory processes were observed in any of the cases. *Toxoplasma gondii* was detected in two *S. coeruleoalba* during 2018–2022, with a total prevalence of 3% in this odontocete species (Table 2). Systemic toxoplasmosis was associated with an inflammatory reaction, and intracellular protist cysts were observed in the CNS (Figure 6B), as well as in the heart, skeletal muscle, adrenal glands, pancreas, liver, lung, spleen, pituitary, thyroid, genitourinary and digestive tracts through histopathological analysis in both animals. Molecular testing confirmed the presence of *T. gondii* in both animals.

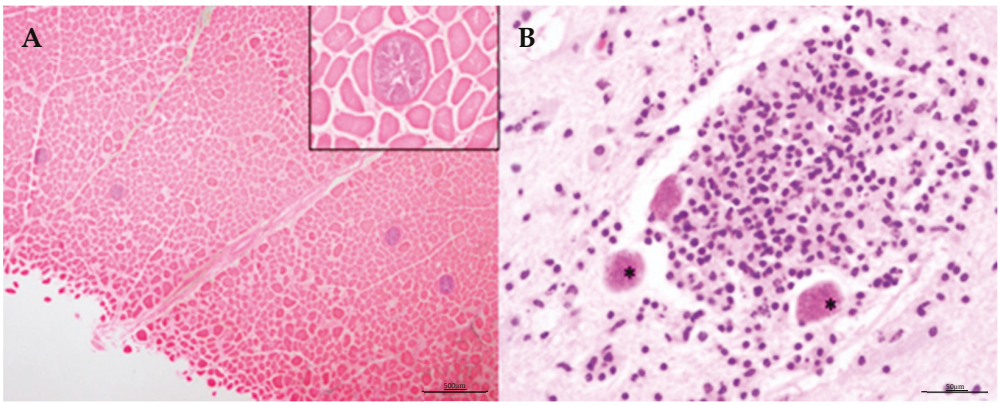


Figure 6. (**A**) Histological views of cysts of *Sarcocystis* sp. in the skeletal muscle. H-E stain. Inset: details of the cyst. x40 H-E. (**B**) Lymphohistiocytic to granulomatous inflammation with some associated *T. gondii* protist cysts (asterisk) of the CNS. H-E stain.

4. Discussion

The Canary Islands are recognized for their high natural value, attributed to their oceanographic characteristics, substantial cetacean biodiversity (comprising 31 species) and their strategic location along the migratory routes of numerous seasonal and a few resident cetacean species [43]. Parasitism in wildlife is prevalent, with cetaceans often hosting multiple parasitic species throughout their lives. In addition, these animals may experience infectious processes due to other pathogens, toxic exposure and various natural or anthropogenic factors, which can disrupt the balance in parasite–host interactions [10,18,61]. Anthropogenic activity in the Canary Islands has significantly increased, exposing marine mammals to various threats such as fishing nets, the ingestion of marine litter and vessel collisions [62–64]. The interaction between cetaceans and their parasites may have implications for disease transmission to other marine species and humans [65,66]. Therefore, comprehensive research on cetacean-associated parasites is crucial for understanding the ecological dynamics of these populations and for developing effective conservation and management strategies to preserve marine biodiversity in the region while assessing animal health. During the period 2018–2022, 233 cetacean carcasses from eighteen different marine mammal species were necropsied. The stranding of cetaceans in the Canary Islands can result from both natural and anthropogenic causes [5,6,67]. Of the cetaceans examined, 82% were found to be parasitized, with neonates being less frequently parasitized compared to juveniles/sub-adults or adults. This pattern likely reflects the increasing exposure to parasites that wildlife encounters throughout their lives [68]. While parasite prevalence was similar between males and females, in some cases, high parasite burdens were noted, compromising the health of the infected organ and the overall condition of the animal, depending on the parasite involved. However, no clear relationship was observed between parasitism and body condition in this study, which contrasts with findings from other research that have identified such associations [69].

Nematodes identified as *Crassicauda* spp. were associated with higher parasite burdens in this survey and severe lesions on host individuals. Relevant inflammatory responses were observed in the kidneys, muscles, prostate, mammary glands and pterygoid sacs of parasitized cetaceans, consistent with previous studies [20–22,70–73]. Despite the extensive lesions in the kidneys, characterized by a predominant eosinophilic response, parasitism did not alter the body condition. Special attention should be given to the inflammation of the pterygoid sacs, as lesions in this area have been proposed as a potential cause of strandings [74,75]. Nematodes of this genus were highly prevalent in the studied carcasses. Although crassicaudid species have been reported in a wide range of organs and tissues, including the vasculature, urogenital organs, placenta, mammary glands, cranial sinuses, lungs, musculature and subcutaneous fat layer [19], each species appears to exhibit a distinct tissue-specific localization and variability in host specificity. Thus, *Crassicauda anthonyi* appears to be a species-specific parasite of *Z. cavirostris*, primarily affecting the kidneys, as recently reported in Brazil [76], the Mediterranean Sea [77] and Japan [78]. Similarly, *Crassicauda grampicola* is known to have a strong affinity for *G. griseus*, particularly inhabiting the pterygoid sacs, where it can induce local inflammation, potentially contributing to strandings [15,21,79,80]. In our study, *C. grampicola* was identified in the pterygoid sacs of three odontocete species: *G. griseus*, *S. frontalis* and *T. truncatus*. The absence of nematodes in the pterygoid sacs of mysticete cetaceans in our study may be explained by the less frequent examination of their cranial regions, primarily due to logistical constraints. Additionally, this parasite species has been reported in other organs, such as the mammary gland of Atlantic white-sided dolphin (*Lagenorhynchus acutus*) [81] and the prostate gland in four different odontocete species in the Canary Islands [73]. However, in the present study, the identification of *C. grampicola* in reproductive organs was not possible. Finally, *C. boopis* is commonly known to parasitize the urinary tract of *B. physalus* [71,72,77,82], though in this case, the species-level identification of the *Crassicauda* sp. found in the fin whale was not achieved.

Pulmonary nematodes from the family Pseudaliidae are among the most commonly encountered parasites in cetaceans, with species of the genera *Halocercus*, *Stenurus* and *Pseudalius* being frequently reported [83]. In this study, *Halocercus delphini*, *Stenurus globicephala* and *Stenurus ovatus* were identified in four cetacean species. To the authors' knowledge, this represents the first morphological identification of these species in the Canary Islands. On the northwest coast of Spain, nematodes of the genus *Stenurus* were found to be the most prevalent in the lungs of stranded odontocetes, although they were also observed in the pterygoid sacs [84]. In the present study, *Stenurus globicephalae* was identified in *G. macrorhynchus* and *G. griseus*, while *Stenurus ovatus* and *Halocercus delphini* were exclusively found in *T. truncauts* and *S. coeruleoalba*, respectively. This aligns with the existing literature, which indicates that *Stenurus globicephala* is host-restricted to the clade Globicephalinae, whereas *Stenurus ovatus* and *Halocercus delphini* are associated with the clade Delphininae [84,85]. The findings of this survey support this observation; however, the low prevalence of these nematodes in our study underscores the need for further data to strengthen this hypothesis and provide more comprehensive insights into host–parasite relationships.

Anisakis spp. were commonly found in the forestomach of various hosts in this survey, as expected, across fourteen odontocete species. These nematodes were sometimes observed free in the stomach lumen, while in other cases, they were attached to the gastric mucosa. In some instances, inflammatory and ulcerated areas, hemorrhages and necrotic lesions were observed in the stomach, as previously described [36,86–88]. Such lesions caused by *Anisakis* spp. have also been documented in the Canary Islands [89]. Unfortunately, as noted in other studies [90], the poor conservation status of many of these worms made species identification difficult. However, *A. simplex* was identified in two animals from our study, a *D. delphis* and a *P. electra*, marking the first recorded instance of adult *A. simplex* in the *P. electra*, to the authors' knowledge. A clear pattern of host preference has been reported for *Anisakis* simplex, with a predominant infection in delphinids [91]. The presence of this zoonotic nematode in the Canary Islands is of particular importance, as it poses potential risks to the local fishing industry and public health and should be considered in local food safety regulations. Further investigation into the prevalence and impact of *Anisakis* spp. in this region is warranted.

Several trematodes are well-known pathogens in marine mammals, with some species causing significant health impacts. *Nasitrema delphini* has been previously reported, in a stranded *Mesoplodon densirostris* in the Canary Islands, associated with mild to severe sacculitis, neuritis, otitis and meningoencephalitis [27]. In this study, *N. delphini* was also detected in *D. delphis*, *S. coeruleoalba*, *T. truncatus* and, frequently in association with inflammatory lesions. In the liver and pancreas, *Brachycladium atlanticum* was primarily observed, as expected, in *S. coeruleoalba*, in line with previous findings from the Mediterranean Sea [92], and in *D. delphis*. *Oschmarinella rochebruni* was detected in several other members of the Delphinidae family, consistent with reports from other studies worldwide [19,92,93]. Less frequent is the presence of trematodes in the liver of *Z. cavirostris* [48,49,53,54]. Even though the trematode specimens were found in good conditions and some but not all specimens, had an everted cirrus, they were identified within the genus *Oschmarinella*, but specific identification was not possible. A more accurate diagnosis is necessary to confirm the species involve.

Diphyllobothrium Cobbold, 1858 is the only zoonotic cestodes known to infect marine mammals [94,95]. Although it has previously been recorded in the Canary Archipelago in *D. delphis*, *S. coeruleoalba* and *S. frontalis* [89]. However, during the five years of this study, it was only identified in *S. coeruleoalba*. Unsurprisingly, cysticercosis caused by *Clistobothrium delphini* and *Clistobothrium grimaldii* was commonly found in odontocetes in this survey. The presence of *C. grimaldii* in mysticetes, though less frequent [96], was also recorded, with this study marking the first documentation of this metacestode in a fin whale in the region.

Additionally, several other parasites were identified, including the lower-occurring acanthocephalans—eight percent in this survey—such *Bolbosoma vasculosum* and *Bolbosoma capitatum*. *Bolbosoma capitatum* has been documented in large odontocete species, being well known in *G. macrorhynchus* [97,98]. In addition, its presence in *P. electra* is considered in a new report within the Canary Islands, as previously described [98]. In contrast, *Bolbosoma vasculosum* has been reported in a wider range of odontocete species [97–101], reported in this survey in *D. delphis* and *S. coeruleoalba*. Additionally, accidental infections in humans involving parasites of this genus, particularly *Bolbosoma capitatum*, have been documented. The zoonotic potential of these acanthocephalans, similar to that of anisakiasis, is worth highlighting, especially in regions where raw fish consumption is common [37,102,103].

Concerning cyamids, only one specimen could be identified as *Cyamus* sp. Given the limited identification of these parasites, the use of other diagnostic techniques may be useful to confirm the species involved. Furthermore, this study presents the first recorded identification of *Conchoderna auritum* in a *Z. cavirostris* from the Canary Islands, previously reported only in Greek waters [104]. Similarly, *Xenobalanus globicipitis*, a barnacle frequently found in various odontocete species worldwide [97,105–110], including those in the Canary Islands, was also observed. These findings broaden the understanding of host–parasite interactions in the region and contribute to the growing body of knowledge on marine mammal parasitology.

Finally, protist cysts of *Sarcocystis* sp. were identified in the muscles of fifteen animals. This prevalence aligns with previous observations, and no inflammatory processes were associated with the presence of these cysts, suggesting that *Sarcocystis* sp. may not have significant pathological relevance [111]. The presence of *Toxoplasma gondii* was confirmed in two *S. coeruleoalba* through molecular and histopathological analyses, making the first reported case of *T. gondii* in *S. coeruleoalba* in the Canary Islands. Prior reports have identified *T. gondii* in *S. frontalis* within the region [5,6,26], where it has been associated with systemic infections and lesions similar to those observed in the current study. *T. gondii* is a notable pathogen and zoonotic protozoan that can cause severe lesions, significantly impacting animal health and potentially leading to stranding and death [26,59,112–116].

The parasitic fauna of cetaceans provides critical insights into host ecology and biology, serving as a valuable tool for understanding the impacts of parasites on cetacean health, which can influence stranding and mortality rates. Accurate parasite identification and health assessment are essential for elucidating imbalances in parasite–host interactions and serve as important biological and environmental indicators. This study has contributed to the knowledge of parasitic species affecting cetaceans stranded in the Canary Islands, including new reports of parasitic species and novel host records, thereby advancing our understanding of the parasitic fauna in this region.

5. Conclusions

The present study represents an update of the parasitic species and genera present in cetaceans, both odontocetes and mysticetes, stranded in the Canary Islands over the period between 2018 and 2022. At least eighteen parasitic species and nine genera were identified morphologically in cetaceans during this time.

Significant differences in parasitic prevalence were observed among the analyzed animals, with adult and juvenile/sub-adult animals being the most commonly parasitized, and the genus *Crassicauda*, the most frequently detected (43%).

These findings provide an overview of the current parasitism in cetaceans of the Canary Islands. Collection information on parasite diversity in cetaceans provides an important basis for understanding the impacts on the host and the ecology of the ecosystem. In addition, it allows us to carry out the monitoring of environmental changes over time, offering insights into potential shifts in the marine waters surrounding the Canary Islands, as well as the monitoring of the individual and population health of cetacean populations and their possible impact on human health.

Supplementary Materials: The following supporting information can be downloaded at https://www.mdpi.com/article/10.3390/ani14233377/s1: Table S1: Biological data and stranding location of 233 stranded and necropsied cetaceans. Sex: female (F), male (M), not determined (ND). Age: neonate (N), calf (C), juvenile–subadult (J), adult (A). Type of stranding (TS): dead (D), alive (Al). Body condition (BC): good (G), moderate (Md), poor (P), very poor (VP), not determined (ND). Conservation status (CS): very fresh (VF), fresh (F), moderate autolysis (MA), advanced autolysis (AA). Stranding location, islands (IS): Gran Canaria (GC), Fuerteventura (FV), Lanzarote (LZ), Tenerife (TF), La Gomera (LG), El Hierro (EH), La Palma (LP), La Graciosa (LGra).

Author Contributions: Conceptualization, Z.S.-G., J.F.G. and A.F.; methodology, Z.S.-G., J.F.G., M.A., E.S. and A.F.; formal analysis, Z.S.-G., M.A., E.S. and A.F.; investigation, Z.S.-G., J.F.G., M.A., E.S. and A.F.; resources, A.F.; writing—original draft preparation, Z.S.-G., M.A., E.S. and A.F.; writing—review and editing, J.F.G., M.A., E.S., A.C.-A., J.N.H., V.M., N.F.-F. and A.F.; supervision, A.F.; funding acquisition, A.F. All authors have read and agreed to the published version of the manuscript.

Funding: This research was funded by Canarian Agency for Research, Innovation, and Information Society (ACIISI) of the Regional Ministry of Universities, Science and Innovation and Culture and by European Social Fund Plus (ESF+) Integrated Operational Programme of the Canary Islands 2021–2027, axis 3 priority theme 74 (85%).

Institutional Review Board Statement: Under current Spanish legislation (Real Decreto 53/2013), ethical review was not required for this study. The research did not involve live animal experimentation; it was conducted on dead, stranded animals.

Informed Consent Statement: Not applicable.

Data Availability Statement: The data presented in this study are available within the article and the Supplementary Materials.

Acknowledgments: The authors would like to thank the Canary Islands Cetacean Stranding Network.

Conflicts of Interest: The authors declare no conflicts of interest.

References

1. Bossart, G.D. Marine mammals as sentinel species for oceans and human health. *Vet. Pathol.* **2011**, *48*, 676–690. [CrossRef] [PubMed]
2. Martín, V.; Servidio, A.; Tejedor, M.; Arbelo, M.; Brederlau, B.; Neves, S.; Perez-Gil, M.; Urquiola, E.; Perez-Gil, E.; Fernández, A. Cetaceans and conservation in the Canary Islands. In Proceedings of the 18th Biennial Conference on the Biology of Marine Mammals, Quebec City, QC, Canada, 12–16 October 2009; p. 153.
3. Perrin, W.F.; Würsig, B.; Thewissen, J.G.M. *Encyclopedia of Marine Mammals*; Academic Press: Cambridge, MA, USA, 2009; ISBN 9780123735539.
4. Domiciano, I.G.; Domit, C.; Broadhurst, M.K.; Koch, M.S.; Bracarense, A.P.F.R.L. Assessing disease and mortality among small cetaceans stranded at a world heritage site in Southern Brazil. *PLoS ONE* **2016**, *11*, e0149295. [CrossRef] [PubMed]
5. Díaz-Delgado, J.; Fernández, A.; Sierra, E.; Sacchini, S.; Andrada, M.; Vela, A.I.; Quesada-Canales, O.; Paz, Y.; Zucca, D.; Groch, K.; et al. Pathologic findings and causes of death of stranded cetaceans in the Canary Islands (2006–2012). *PLoS ONE* **2018**, *13*, e0204444. [CrossRef] [PubMed]
6. Arbelo, M.; De Los Monteros, A.E.; Herráez, P.; Andrada, M.; Sierra, E.; Rodríguez, F.; Jepson, P.D.; Fernández, A. Pathology and causes of death of stranded cetaceans in the Canary Islands (1999–2005). *Dis. Aquat. Org.* **2013**, *103*, 87–99. [CrossRef] [PubMed]
7. Berón-Vera, B.; Crespo, E.A.; Raga, J.A. Parasites in stranded cetaceans of Patagonia. *J. Parasitol.* **2008**, *94*, 946–948. [CrossRef]
8. Aznar, F.J.; Balbuena, J.A.; Fernández, M.; Raga, J.A. *Living Together: The Parasites of Marine Mammals*; Springer: Boston, MA, USA, 2002; pp. 385–423. ISBN 9781461505297.
9. Dailey, M.D. Parasites of Marine Mammals. In *Marine Parasitology*; Rohde, K., Ed.; CSIRO Publishing (Commonwealth Scientific and Industrial Research Organization): Collingwood, Australia, 2005; pp. 408–414. ISBN 0-643-09025-8.
10. Raga, J.A.; Fernández, M.; Balbuena, J.A.; Aznar, F.J. Parasites. In *Encyclopedia of Marine Mammals*; Academic Press: Cambridge, MA, USA, 2009; pp. 821–830.
11. Balbuena, J.A.; Aznar, F.J.; Fernández, M.; Raga, J.A. Parasites as indicators of social structure and stock identity of marine mammals. In *Whales, Seals, Fish and Man*; Elsevier Science: Amsterdam, The Netherlands, 1995; Volume 4, pp. 133–139. ISBN 0163-6995.
12. Evans, P.; Raga, J. *Marine Mammals: Biology and Conservation*; Springer: Berlin/Heidelberg, Germany, 2001; ISBN 978-0-306-46573-4.
13. Vidal-Martínez, V.M.; Pech, D.; Sures, B.; Purucker, S.T.; Poulin, R. Can parasites really reveal environmental impact? *Trends. Parasitol.* **2010**, *26*, 44–51. [CrossRef]

14. Balbuena, J.A.; Simpkin, A. role of *Crassicauda* sp. in natural mortality of pantropical spotted dolphins *Stenella attenuata*: A Reassessment. *Dis. Aquat. Org.* **2014**, *108*, 83–89. [CrossRef]
15. Cuvertoret-Sanz, M.; López-Figueroa, C.; O'Byrne, A.; Canturri, A.; Martí-Garcia, B.; Pintado, E.; Pérez, L.; Ganges, L.; Cobos, A.; Abarca, M.L.; et al. Causes of cetacean stranding and death on the Catalonian Coast (Western Mediterranean Sea), 2012–2019. *Dis. Aquat. Org.* **2020**, *142*, 239–253. [CrossRef]
16. Dailey, M.; Walker, W.A. Parasitism as a Factor (?) In Single Strandings of Southern California Cetaceans. *J. Parasitol.* **1978**, *64*, 593–596. [CrossRef]
17. O'Shea, T.J.; Homer, B.L.; Greiner, E.C.; Layton, A.W. *Nasitrema* sp. associated encephalitis in a striped dolphin (*Stenella coeruleoalba*) stranded in the gulf of Mexico. *J. Wildl. Dis.* **1991**, *27*, 706–709. [CrossRef]
18. Dailey, M.D. Parasitic Diseases. In *CRC Handbook of Marine Mammal Medicine*; CRC Press: Boca Raton, FL, USA, 2001; pp. 407–430.
19. Gibson, D.I.; Harris, E.A.; Bray, R.A.; Jepson, P.D.; Kuiken, T.; Baker, J.R.; Simpson, V.R. A survey of the helminth parasites of cetaceans stranded on the coast of England and Wales during the Period 1990–1994. *J. Zool.* **1998**, *244*, 563–574. [CrossRef]
20. Perrin, W.F.; Powers, J.E. Role of a nematode in natural mortality of spotted dolphins. *J. Wildl. Manag.* **1980**, *44*, 960–963. [CrossRef]
21. Zucca, P.; Di Guardo, G.; Pozzi Mucelli, R.; Scaravelli, D.; Francese, M. Use of computer tomography for imaging of *Crassicauda grampicola* in a Risso's dolphin (*Grampus griseus*). *J. Zoo. Wildl. Med.* **2004**, *35*, 391–394. [CrossRef]
22. Díaz-Delgado, J.; Fernández, A.; Xuriach, A.; Sierra, E.; Bernaldo de Quirós, Y.; Mompeo, B.; Pérez, L.; Andrada, M.; Marigo, J.; Catão-Dias, J.L.; et al. Verminous arteritis due to *Crassicauda* sp. in Cuvier's beaked whales (*Ziphius cavirostris*). *Vet. Pathol.* **2016**, *53*, 1233–1240. [CrossRef]
23. Moser, M.; Rhinehart, H. The lungworm, *Halocercus* spp. (Nematoda: Pseudaliidae) in cetaceans from California. *J. Wildl. Dis.* **1993**, *29*, 507–508. [CrossRef]
24. Degollada, E.; André, M.; Arbelo, M.; Fernández, A. Incidence, pathology and involvement of *Nasitrema* species in odontocete strandings in the Canary Islands. *Vet. Rec.* **2002**, *150*, 81–82. [CrossRef]
25. Neiland, K.A.; Rice, D.W.; Holden, B.L. Helminths of marine mammals, I. The genus *Nasitrema,* air sinus flukes of delphinid cetacea. *J. Parasitol.* **1970**, *56*, 305–316. [CrossRef]
26. Sierra, E.; Fernández, A.; Felipe-Jiménez, I.; Zucca, D.; Díaz-Delgado, J.; Puig-Lozano, R.; Câmara, N.; Consoli, F.; Díaz-Santana, P.; Suárez-Santana, C.; et al. Histopathological differential diagnosis of meningoencephalitis in cetaceans: Morbillivirus, Herpesvirus, *Toxoplasma gondii*, *Brucella* sp., and *Nasitrema* sp. *Front. Vet. Sci.* **2020**, *7*, 650. [CrossRef]
27. Felipe-Jiménez, I.; Fernández, A.; de Quirós, Y.B.; Arregui-Gil, M.; Puig-Lozano, R.; Arbelo, M.; Sierra, E. Cerebral nasitremiasis in a Blainville's beaked whale (*Mesoplodon densirostris*) stranded in the Canary Islands. *Res. Vet. Sci.* **2023**, *158*, 56–64. [CrossRef]
28. Phillips, A.C.N.; Suepaul, R. *Nasitrema* Species: A frequent culprit in melon-headed whale (*Peponocephala electra*) strandings in Trinidad. *Aquat. Mamm.* **2017**, *43*, 547–557. [CrossRef]
29. Abril, E.; Balbuena, J.A.; Raga, J.A. A new species of the genus *Zalophotrema* (Digenea: Campulidae), *Zalophotrema atlanticum* n. sp., from the liver of the striped dolphin *Stenella coeruleoalba* (Meyen, 1833) (Cetacea: Delphinidae) in Atlantic Waters. *Syst. Parasitol.* **1991**, *18*, 133–138. [CrossRef]
30. Demaree, R.S.; Critchfield, R.L.; Tinling, S.P. Liver sinuses of a beaked whale, *Mesoplodon stejnegeri* (Cetacea:Ziphiidae). *J. Helminthol. Soc. Wash.* **1997**, *64*, 183–187.
31. Fraija-Fernández, N.; Olson, P.D.; Crespo, E.A.; Raga, J.A.; Aznar, F.J.; Fernández, M. Independent host switching events by digenean parasites of cetaceans inferred from ribosomal DNA. *Int. J. Parasitol.* **2015**, *45*, 167–173. [CrossRef] [PubMed]
32. Jaber, J.R.; Pérez, J.; Arbelo, M.; Andrada, M.; Hidalgo, M.; Gómez-Villamandos, J.C.; Van Den Ingh, T.; Fernández, A. hepatic lesions in cetaceans stranded in the Canary Islands. *Vet. Pathol.* **2004**, *41*, 147–153. [CrossRef]
33. Raga, J.A. *Oschmarinella mascomai* n. Sp. (Trematoda: Campulidae) Parasite des canaux biliaires de *Stenella coeruleoalba* (Meyen, 1833) (Cetacea: Delphinidae) en Méditerranée. *Ann. Parasitol. Hum. Comp.* **1986**, *61*, 633–636. [CrossRef]
34. Jones, J.L.; Dubey, J.P. Waterborne Toxoplasmosis—Recent developments. *Exp. Parasitol.* **2010**, *124*, 10–25. [CrossRef]
35. Dubey, J.P.; Jones, J.L. *Toxoplasma gondii* infection in humans and animals in the United States. *Int. J. Parasitol.* **2008**, *38*, 1257–1278. [CrossRef]
36. Mattiucci, S.; Nascetti, G. Molecular systematics, phylogeny and ecology of anisakid nematodes. *Parasite* **2006**, *13*, 99–113. [CrossRef]
37. Arizono, N.; Kuramochi, T.; Kagei, N. Molecular and histological identification of the acanthocephalan *Bolbosoma* cf. capitatum from the human small intestine. *Parasitol. Int.* **2012**, *61*, 715–718.
38. Shamsi, S. Seafood-borne parasitic diseases: A "one-health" approach is needed. *Fishes* **2019**, *4*, 9. [CrossRef]
39. Specht, N.R.; Keve, G.; Fernández-Maldonado, C.; Caro, A.C.; Takács, N.; Kontschán, J.; Hornok, S. Molecular investigation of endoparasites of marine mammals (Cetacea: Mysticeti, Odontoceti) in the Western Mediterranean. *Front. Vet. Sci.* **2024**, *11*, 1431625. [CrossRef] [PubMed]
40. Dubey, J.P.; Zarnke, R.; Thomas, N.J.; Wong, S.K.; Van Bonn, W.; Briggs, M.; Thulliez, P. *Toxoplasma gondii*, *Neospora caninum, Sarcocystis neurona,* and *Sarcocystis canis*-like infections in marine mammals. *Vet. Parasitol.* **2003**, *116*, 275–296. [CrossRef] [PubMed]
41. Raga, J.; Balbuena, J.A.; Aznar, F.; Fernández, M. The impact of parasites on marine mammals: A review. *Parassitologia* **1997**, *39*, 293–296. [PubMed]

42. Gulland, F.M.D.; Hall, A.J. Is marine mammal health deteriorating? Trends in the global reporting of marine mammal disease. *Ecohealth* **2007**, *4*, 135–150. [CrossRef]
43. Cetáceos de Canarias. Secac. Available online: https://www.cetaceos.org/es/cetaceos-de-canarias/ (accessed on 1 August 2024).
44. IJsseldijk, L.L.; Brownlow, A.C.; Mazzariol, S. European best practice on cetacean post mortem investigation and tissue sampling. In Proceedings of the Joint ASCOBANS/ACCOBAMS 2019, 25th Meeting of the Advisory Committee, Stralsund, Germany, 17–19 September 2019.
45. Joblon, M.J.; Pokras, M.A.; Morse, B.; Harry, C.T.; Rose, K.S.; Sharp, S.M.; Niemeyer, M.E.; Patchett, K.M.; Sharp, W.B.; Moore, M.J. Body condition scoring system for delphinids based on short-beaked common dolphins (*Delphinus delphis*). *J. Mar. Anim. Ecol.* **2014**, *7*, 5–13.
46. Fraija-Fernández, N.; Aznar, F.; Raga, J.; Gibson, D.; Fernández, M. A new brachycladiid species (Digenea) from Gervais' beaked whale, *Mesoplodon europaeus* in North-Western Atlantic Waters. *Acta Parasitol.* **2014**, *59*, 510–517. [CrossRef]
47. Dailey, M.; Gilmartin, W. Diagnostic key to the parasites of some marine mammals. *Nav. Ocean. Syst. Cent.* **1980**, 41.
48. Delyamure, S.L. *Helminthofauna of Marine Mammals (Ecology and Phylogeny)*; Skrjabn, K.I., Ed.; Izdatel'stvo Akiademii Nauk SSSR: Moscow, Russia, 1955.
49. Gibson, D. Family Brachycladiidae Odhner, 1905. In *Keys to the Trematoda: Volume 2*; CABI Publishing: Wallingford, UK, 2005; pp. 641–652. ISBN 9780851995878.
50. Rajaguru, A.; Shantha, G. Association between the sessile barnacle *Xenobalanus globicipitis* (Coronulidae) and the bottlenose dolphin *Tursiops truncatus* (Delphinidae) form the bay of Bengal, India, with a summary of previous records from cetaceans. *Fish. Bull.* **1992**, *90*, 197–202.
51. Yamaguti, S. The Digenetic trematodes of vertebrates. *Syst. Helminthum* **1958**, *1*, 1–1575.
52. Nakagun, S.; Shiozaki, A.; Ochiai, M.; Matsuda, A.; Tajima, Y.; Matsuishi, T.; Kobayashi, Y. Prominent hepatic ductular reaction induced by *Oschmarinella macrorchis* in a Hubbs' beaked whale *Mesoplodon carlhubbsi*, with biological notes. *Dis. Aquat. Org.* **2018**, *127*, 177–192. [CrossRef]
53. Dailey, M.D. A new species of Digenea (Trematoda: Brachycladiidae) from the Gervais' beaked whale, *Mesoplodon europaeus*, with comments on other cetacean liver flukes. *Comp. Parasitol.* **2007**, *74*, 229–232. [CrossRef]
54. Skryabin, K.L. *Oschmarinella sobolevi* n. gen, n. sp. A New trematode from the liver of whales. *Dokl. Akad. Nauk. SSSR* **1947**, *57*, 857–859.
55. Chan, B.K.; Chen, Y.H. Distinguishing long-discussed cryptic species of the epibiotic goose-neck barnacle of the genus *Conchoderma* (Thoracicalcarea: Lepadidae) with integrative taxonomy. *Diversity* **2022**, *14*, 593. [CrossRef]
56. Hogans, W.E. Review of *Pennella* Oken, 1816 (Copepoda: Pennellidae) with a description of *Pennella benzi* sp. nov., a parasite of Escolar, *Lepidocybium flavobrunneum* (Pisces) in the northwest Atlantic Ocean. *Zootaxa* **2017**, *4244*, 1–38. [CrossRef]
57. Leung, Y.M. An illustrated key to the species of whale-lice (Amphipoda, Cyamidae), ectoparasites of Cetacea, with a guide to the literature. *Crustaceana* **1967**, *12*, 279–291. [CrossRef]
58. Costa, G.; Chubb, J.C.; Veltkamp, C.J. Cystacanths of *Bolbosoma vasculosum* in the black scabbard fish Aphanopus carbo, oceanic horse mackerel *Trachurus picturatus* and common dolphin *Delphinus delphis* from Madeira, Portugal. *J. Helminthol.* **2000**, *74*, 113–120. [CrossRef]
59. Díaz-Delgado, J.; Groch, K.R.; Ramos, H.G.C.; Colosio, A.C.; Alves, B.F.; Pena, H.F.J.; Catão-Dias, J.L. Fatal systemic toxoplasmosis by a novel non-archetypal *Toxoplasma gondii* in a Bryde's whale (*Balaenoptera edeni*). *Front. Mar. Sci.* **2020**, *7*, 336. [CrossRef]
60. Sierra, E.; Sánchez, S.; Saliki, J.T.; Blas-Machado, U.; Arbelo, M.; Zucca, D.; Fernández, A. Retrospective study of etiologic agents associated with nonsuppurative meningoencephalitis in stranded cetaceans in the Canary Islands. *J. Clin. Microbiol.* **2014**, *52*, 2390–2397. [CrossRef]
61. Moeller JR, R. Pathology of marine mammals with special reference to infectious diseases. In *Toxicology of Marine Mammals*; CRC Press: Boca Raton, FL, USA, 2002; pp. 15–49.
62. Puig-Lozano, R.; Fernández, A.; Saavedra, P.; Tejedor, M.; Sierra, E.; De la Fuente, J.; Xuriach, A.; Díaz-Delgado, J.; Rivero, M.A.; Andrada, M.; et al. Retrospective study of traumatic intra-interspecific interactions in stranded cetaceans, Canary Islands. *Front. Vet. Sci.* **2020**, *7*, 107. [CrossRef]
63. Puig-Lozano, R.; Fernández, A.; Sierra, E.; Saavedra, P.; Suárez-Santana, C.M.; De la Fuente, J.; Díaz-Delgado, J.; Godinho, A.; García-Álvarez, N.; Zucca, D.; et al. Retrospective study of fishery interactions in stranded cetaceans, Canary Islands. *Front. Vet. Sci.* **2020**, *7*, 567258. [CrossRef]
64. Sierra, E.; Fernández, A.; Espinosa De Los Monteros, A.; Arbelo, M.; Díaz-Delgado, J.; Andrada, M.; Herráez, P. Histopathological muscle findings may be essential for a definitive diagnosis of suspected sharp trauma associated with ship strikes in stranded cetaceans. *PLoS ONE* **2014**, *9*, e88780. [CrossRef] [PubMed]
65. Di Guardo, G.; Centelleghe, C.; Mazzariol, S. Cetacean host-pathogen interaction(s): Critical knowledge gaps. *Front. Immunol.* **2018**, *9*, 2815. [CrossRef] [PubMed]
66. Tomoo, O.; Kliks, M. Effects of marine mammal parasites on human health. *Int. J. Parasitol.* **1987**, *17*, 415–421. [CrossRef]
67. Santana, P.J.D. Patologías y causas de la muerte de los cetáceos varados en las Islas Canarias 2013–2018. Ph.D. Dissertation, University of Las Palmas de Gran Canaria, Las Palmas, Spain, 2023.
68. Kołodziej-Sobocińska, M. Factors affecting the spread of parasites in populations of wild european terrestrial mammals. *Mamm. Res.* **2019**, *64*, 301–318. [CrossRef]

69. Sánchez, C.A.; Becker, D.J.; Teitelbaum, C.S.; Barriga, P.; Brown, L.M.; Majewska, A.A.; Hall, R.J.; Altizer, S. On the relationship between body condition and parasite infection in wildlife: A Review and meta-analysis. *Ecol. Lett.* **2018**, *21*, 1869–1884. [CrossRef]
70. Baylis, H.A. LV.—Observations on the genus *Crassicauda*. *Ann. Mag. Nat. Hist.* **1920**, *5*, 410–419. [CrossRef]
71. Lambertsen, R. Taxonomy and distribution of a *Crassicauda* species (Nematoda: Spirurida) infecting the kidney of the common fin whale (*Balaenoptera physalus* Linne, 1758). *J. Parasitol.* **1985**, *71*, 485–488. [CrossRef]
72. Lempereur, L.; Delobelle, M.; Doom, M.; Haelters, J.; Levy, E.; Losson, B.; Jauniaux, T. *Crassicauda boopis* in a fin whale (*Balaenoptera physalus*) ship-struck in the Eastern North Atlantic Ocean. *Parasitol. Open* **2017**, *3*, e9. [CrossRef]
73. Suárez-Santana, C.M.; Sierra, E.; Díaz-Delgado, J.; Zucca, D.; de Quirós, Y.B.; Puig-Lozano, R.; Câmara, N.; De la Fuente, J.; de los Monteros, A.E.; Rivero, M.; et al. Prostatic lesions in odontocete cetaceans. *Vet. Pathol.* **2018**, *55*, 466–472. [CrossRef]
74. Nepote, F.T.A. *Lesões causadas pelos parasitas do gênero Crassicauda em crânios do boto Tursiops truncatus*; Federal University of Santa Catarina, Centre for Biological Sciences, Undergraduate Degree in Biological Sciences: Florianópolis, Brazil, 2020.
75. Van Bressem, M.-F.; Reyes, J.C.; Félix, F.; Echegaray, M.; Siciliano, S.; Di Beneditto, A.P.; Flach, L.; Viddi, F.; Avila, I.C.; Herrera, J.C.; et al. A preliminary overview of skin and skeletal diseases and traumata in small cetaceans from South American Waters. *Lat. Am. J. Aquat. Mamm.* **2007**, *6*, 7–42. [CrossRef]
76. Febronio, A.M.B.; Boos, G.S.; Batista, R.L.G.; Amorim, D.B.; Guimarães, J.P.; Bianchi, M.V.; Mariani, D.B.; Koproski, L.; Mari, C.; Parente, J.E.V.; et al. Crassicaudiasis in three geographically and chronologically distant Cuvier's beaked whales (*Ziphius cavirostris*) stranded off Brazil. *Int. J. Parasitol. Parasites Wildl.* **2021**, *16*, 262–269. [CrossRef] [PubMed]
77. Marcer, F.; Negrisolo, E.; Franzo, G.; Tessarin, C.; Pietrobelli, M.; Marchiori, E. Morphological and molecular characterization of adults and larvae of *Crassicauda* spp. (Nematoda: Spirurida) from Mediterranean fin whales *Balaenoptera physalus* (Linnaeus, 1758). *Int. J. Parasitol. Parasites Wildl.* **2019**, *9*, 258–265. [CrossRef] [PubMed]
78. Kumagai, T.; Shiozaki, A.; Tajima, Y. Molecular characterization of the parasitic nematode genus *Crassicauda*; larvae parasitic on the firefly squid and adults on beaked whales off the coast of Japan. *Int. J. Parasitol. Parasites Wildl.* **2023**, *20*, 56–62. [CrossRef] [PubMed]
79. Morimitsu, T.; Koono, M.; Hirai, T.; Kurita, T. Degeneration of the octavus nerve observed in a stranded Risso's dolphin (*Grampus griseus*), infested with *Crassicauda grampicola*. *Jpn. Cetology* **2010**, *20*, 7–12. [CrossRef] [PubMed]
80. Raga, J.A. Redescription of *Crassicauda grampicola* Johnston et. Mawson, 1941, (Nematoda: Spirurida), parasite of *Grampus griseus* (Cuvier, 1812) (Cetacea: Delphinidae). *Vie Milieu/Life Environ.* **1987**, 215–219.
81. Geraci, J.R.; Dailey, M.D.; St. Aubin, D.J. Parasitic mastitis in the Atlantic White-Sided Dolphin, *Lagenorhynchus acutus*, as a probable factor in herd productivity. *J. Fish. Res. Board Can.* **1978**, *35*, 1350–1355. [CrossRef]
82. Lambertsen, R.H. Crassicaudosis: A parasitic disease threatening the health and population recovery of large baleen whales. *Rev. Sci. Technol.* **1992**, *11*, 1131–1141. [CrossRef]
83. Measures, L.N. Lungworms of marine mammals. In *Parasitic Diseases of Wild Mammals*; John Wiley & Sons, Inc.: Hoboken, NJ, USA, 2001; pp. 279–300. ISBN 9780470377000.
84. Saldaña, A.; López, C.M.; López, A.; Covelo, P.; Remesar, S.; Martínez-Calabuig, N.; García-Dios, D.; Díaz, P.; Morrondo, P.; Díez-Baños, P.; et al. Specificity of *Stenurus* (Metastrongyloidea: Pseudaliidae) infections in odontocetes stranded along the North-West Spanish Coast. *Int. J. Parasitol. Parasites Wildl.* **2022**, *19*, 148–154. [CrossRef]
85. Pool, R.; Romero-Rubira, C.; Raga, J.A.; Fernández, M.; Aznar, F.J. Determinants of lungworm specificity in five cetacean species in the Western Mediterranean. *Parasit. Vectors* **2021**, *14*, 196. [CrossRef]
86. Geraci, J.R.; Aubin, D.J.S. Effects of parasites on marine mammals. *Int. J. Parasitol.* **1987**, *17*, 407–414. [CrossRef]
87. Motta, M.R.A.; Pinheiro, D.C.S.N.; Carvalho, V.L.; Viana, D.D.A.; Vicente, A.C.P.; Iñiguez, A.M. Gastric Lesions associated with the presence of *Anisakis* spp. Dujardin, 1845 (Nematoda: Anisakidae) in cetaceans stranded on the coast of Ceara, Brazil. *Biota Neotrop.* **2008**, *8*, 91–95. [CrossRef]
88. Van Beurden, S.J.; IJsseldijk, L.L.; Cremers, H.J.W.M.; Gröne, A.; Verheije, M.H.; Begeman, L. Anisakis Spp. Induced Granulomatous Dermatitis in a harbour porpoise Phocoena phocoena and a bottlenose dolphin Tursiops truncatus. *Dis. Aquat. Org.* **2015**, *112*, 257–263. [CrossRef] [PubMed]
89. Jaber, J.R.; Pérez, J.; Arbelo, M.; Zafra, R.; Fernández, A. Pathological and immunohistochemical study of gastrointestinal lesions in dolphins stranded in the Canary Island. *Vet. Rec.* **2006**, *159*, 410–414. [CrossRef] [PubMed]
90. Di Azevedo, M.I.N.; Carvalho, V.L.; Iñiguez, A.M. First Record of the anisakid nematode *Anisakis nascettii* in the Gervais' beaked whale *Mesoplodon europaeus* from Brazil. *J. Helminthol.* **2016**, *90*, 48–53. [CrossRef]
91. Cipriani, P.; Palomba, M.; Giulietti, L.; Marcer, F.; Mazzariol, S.; Santoro, M.; Alburqueque, R.A.; Covelo, P.; López, A.; Santos, M.B.; et al. Distribution and genetic diversity of *Anisakis* spp. in cetaceans from the northeast Atlantic Ocean and the Mediterranean Sea. *Sci. Rep.* **2022**, *12*, 13664. [CrossRef]
92. Mateu, P.; Raga, J.A.; Aznar, F.J. Host specificity of *Oschmarinella rochebruni* and *Brachycladium atlanticum* (Digenea: Brachycladiidae) in five cetacean species from western mediterranean waters. *J. Helminthol.* **2011**, *85*, 12–19. [CrossRef]
93. LeDuc, R. Delphinids, Overview. In *Encyclopedia of Marine Mammals*; Elsevier Ltd.: Amsterdam, The Netherlands, 2009; pp. 298–302. ISBN 9780123735539.
94. Dupouy-Camet, J.; Peduzzi, R. Helminth-trematode: *Diphyllobothrium*. *Encycl. Food Saf.* **2014**, *2*, 130–133. [CrossRef]

95. Fraija-Fernández, N.; Waeschenbach, A.; Briscoe, A.G.; Hocking, S.; Kuchta, R.; Nyman, T.; Littlewood, D.T.J. Evolutionary transitions in broad tapeworms (Cestoda: Diphyllobothriidea) revealed by mitogenome and nuclear ribosomal operon phylogenetics. *Mol. Phylogenetics Evol.* **2021**, *163*, 107262. [CrossRef]
96. Aznar, F.J.; Agustí, C.; Littlewood, D.T.J.; Raga, J.A.; Olson, P.D. Insight into the role of cetaceans in the life cycle of the Tetraphyllideans (Platyhelminthes: Cestoda). *Int. J. Parasitol.* **2007**, *37*, 243–255. [CrossRef]
97. Carvalho, V.L.; Bevilaqua, C.M.L.; Iñiguez, A.M.; Mathews-Cascon, H.; Ribeiro, F.B.; Pessoa, L.M.B.; de Meirelles, A.C.O.; Borges, J.C.G.; Marigo, J.; Soares, L.; et al. Metazoan parasites of cetaceans off the northeastern coast of Brazil. *Vet. Parasitol.* **2010**, *173*, 116–122. [CrossRef]
98. Colón-Llavina, M.M.; Mignucci-Giannoni, A.A.; Mattiucci, S.; Paoletti, M.; Nascetti, G.; Williams, E.H. Additional records of metazoan parasites from caribbean marine mammals, including genetically identified anisakid nematodes. *Parasitol. Res.* **2009**, *105*, 1239–1252. [CrossRef] [PubMed]
99. Pendergraph, G.E. First report of the acanthocephalan *Bolbosoma vasculosum* (Rudolphi, 1819) from the pygmy sperm whale, *Kogia breviceps*. *J. Parasitol.* **1971**, *57*, 1109. [CrossRef] [PubMed]
100. McAlpine, D.F.; Murison, L.D.; Hoberg, E.P. New records for the pygmy sperm whale, *Kogia breviceps* (Physeteridae) from Atlantic Canada with notes on diet and parasites. *Mar. Mamm. Sci.* **1997**, *13*, 701–704. [CrossRef]
101. Mignucci-Giannoni, A.A.; Hoberg, E.P.; Sigel-Causey, D.; Williams, E.H., Jr. Metazoan parasites and other symbionts of cetaceans in the Caribbean. *J. Parasitol.* **1998**, *84*, 939–946. [CrossRef] [PubMed]
102. Kaito, S.; Sasaki, M.; Goto, K.; Matsusue, R.; Koyama, H.; Nakao, M.; Hasegawa, H. A case of small bowel obstruction due to infection with *Bolbosoma* sp. (*Acanthocephala: Polymorphidae*). *Parasitol. Int.* **2019**, *68*, 14–16. [CrossRef]
103. Beaver, P.C.; Otsuji, T.; Otsuji, A.; Yoshimura, H.; Uchikawa, R.; Sato, A. Acanthocephalan, probably *Bolbosoma*, from the peritoneal cavity of man in Japan. *Am. J. Trop. Med. Hyg.* **1983**, *32*, 1016–1018. [CrossRef]
104. Foskolos, I.; Tourgeli Provata, M.; Frantzis, A. First record of *Conchoderma auritum* (Cirripedia: Lepadidae) on *Ziphius cavirostris* (Cetacea: Ziphiidae) in Greece. *Ann. Ser. Hist. Nat.* **2017**, *27*, 29–34. [CrossRef]
105. Carrillo, J.M.; Overstreet, R.M.; Raga, J.A.; Aznar, F.J. Living on the edge: Settlement patterns by the symbiotic barnacle *Xenobalanus globicipitis* on small cetaceans. *PLoS ONE* **2015**, *10*, e0127367. [CrossRef]
106. Flach, L.; Van Bressem, M.-F.; Pitombo, F.; Aznar, F. Emergence of the epibiotic barnacle *Xenobalanus globicipitis* in Guiana dolphins after a morbillivirus outbreak in Sepetiba Bay, Brazil. *Estuar. Coast. Shelf. Sci.* **2021**, *263*, 107632. [CrossRef]
107. Oliveira, J.B.; Morales, J.A.; González-Barrientos, R.C.; Hernández-Gamboa, J.; Hernández-Mora, G. Parasites of cetaceans stranded on the pacific coast of Costa Rica. *Vet. Parasitol.* **2011**, *182*, 319–328. [CrossRef]
108. Ryazanov, S.; Ryazanova, T. Risso's Dolphin (*Grampus griseus*) in Russia with note on *Xenobalanus globicipitis*. *Mar. Biodivers.* **2023**, *53*, 71. [CrossRef]
109. Ten, S.; Moreno-Colom, P.; Raga, J.; Aznar, F. Xenobalanus globicipitis as an indicator of cetacean hydrodynamics: Spatial distribution and aggregation on the flukes of striped dolphins, Stenella coeruleoalba. In Proceedings of the 21th European Association of Aquatic Mammals Conference (Virtual EAAM, 2021), Virtual, 11–13 March 2021.
110. Whitehead, T.O.; Rollinson, D.P.; Reisinger, R.R. Pseudostalked barnacles, *Xenobalanus globicipitis,* attached to killer whales, *Orcinus orca*, in South African waters. *Mar. Biodivers.* **2015**, *45*, 873–876. [CrossRef]
111. Sierra, E.; Espinosa de los Monteros, A.; Fernández, A.; Díaz-Delgado, J.; Suárez-Santana, C.; Arbelo, M.; Sierra, M.A.; Herráez, P. Muscle pathology in free-ranging stranded cetaceans. *Vet. Pathol.* **2017**, *54*, 298–311. [CrossRef] [PubMed]
112. Resendes, A.R.; Almería, S.; Dubey, J.P.; Obón, E.; Juan-Sallés, C.; Degollada, E.; Alegre, F.; Cabezón, O.; Pont, S.; Domingo, M. Disseminated toxoplasmosis in a mediterranean pregnant Risso's dolphin (*Grampus griseus*) with transplacental fetal infection. *J. Parasitol.* **2002**, *88*, 1029–1032. [CrossRef]
113. Costa-Silva, S.; Sacristán, C.; Gonzales-Viera, O.; Díaz-Delgado, J.; Sánchez-Sarmiento, A.M.; Marigo, J.; Groch, K.R.; Carvalho, V.L.; Ewbank, A.C.; Colosio, A.C.; et al. *Toxoplasma gondii* in cetaceans of Brazil: A histopathological and immunohistochemical survey. *Rev. Bras. De Parasitol. Vet.* **2019**, *28*, 395–402. [CrossRef]
114. Mazzariol, S.; Marcer, F.; Mignone, W.; Serracca, L.; Goria, M.; Marsili, L.; Di Guardo, G.; Casalone, C. Dolphin Morbillivirus and *Toxoplasma gondii* coinfection in a mediterranean fin whale (*Balaenoptera physalus*). *BMC Vet. Res.* **2012**, *8*, 20. [CrossRef]
115. Dubey, J.P.; Murata, F.H.A.; Cerqueira-Cézar, C.K.; Kwok, O.C.H.; Grigg, M.E. Recent epidemiologic and clinical importance of *Toxoplasma gondii* infections in marine mammals: 2009–2020. *Vet. Parasitol.* **2020**, *288*, 109296. [CrossRef]
116. Di Guardo, G.; Proietto, U.; Di Francesco, C.E.; Marsilio, F.; Zaccaroni, A.; Scaravelli, D.; Casalone, C. Cerebral toxoplasmosis in striped dolphins (*Stenella coeruleoalba*) stranded along the Ligurian Sea coast of Italy. *Vet. Pathol.* **2010**, *47*, 245–253. [CrossRef]

Disclaimer/Publisher's Note: The statements, opinions and data contained in all publications are solely those of the individual author(s) and contributor(s) and not of MDPI and/or the editor(s). MDPI and/or the editor(s) disclaim responsibility for any injury to people or property resulting from any ideas, methods, instructions or products referred to in the content.

animals

MDPI

Article

Investigations on the Health Status and Infection Risk of Harbour Seals (*Phoca vitulina*) from Waters of the Lower Saxon Wadden Sea, Germany

Ursula Siebert [1,*], Jan Lakemeyer [1], Martin Runge [2], Peter Lienau [3], Silke Braune [2], Edda Bartelt [4], Miguel L. Grilo [1] and Ralf Pund [4]

[1] Institute for Terrestrial and Aquatic Wildlife Research (ITAW), University of Veterinary Medicine Hannover Foundation (TiHo), 25761 Buesum, Germany; jlow66@yahoo.de (J.L.); mgrilo@ralvt.pt (M.L.G.)
[2] Food and Veterinary Institute Braunschweig/Hannover, Lower Saxony State Office for Consumer Protection and Food Safety (LAVES), 30173 Hannover, Germany; martin.runge@laves.niedersachsen.de (M.R.); silke.braune@laves.niedersachsen.de (S.B.)
[3] Seehundstation Nationalpark-Haus Norden-Norddeich, 26506 Norden, Germany; pl@seehundstation-norddeich.de
[4] Institute for Fish and Fishery Products Cuxhaven, LAVES, 27472 Cuxhaven, Germany; edda.bartelt@laves.niedersachsen.de (E.B.); poststelle.iff-cux@laves.niedersachsen.de (R.P.)
* Correspondence: ursula.siebert@tiho-hannover.de; Tel.: +49-511-8568158

Simple Summary: Harbour seals from the Wadden Sea area of Lower Saxony, Germany were investigated for their health status and causes of death for the first time. In newborn seals, weakness and emaciation were the main findings, most likely caused by a separation from the mother. After the weaning period, pulmonary parasitosis and bronchopneumonia were the most frequent pathological findings. These investigations emphasize the importance of a health monitoring programme for this top predator species in the Wadden Sea, as it can provide critical insights into changes in the ecosystem. Monitoring harbour seals, which are sentinel species, will support the implementation of the Trilateral Wadden Sea Agreement and the Marine Framework Directive to protect this important marine environment.

Abstract: Harbour seals (*Phoca vitulina*) are the most common pinniped species in the Wadden Sea of Schleswig-Holstein, Hamburg and Lower Saxony, Germany. Their numbers have recovered after significant depletion due to viral outbreaks and effects of anthropogenic activities like pollution and habitat disturbance. Within the Wadden Sea National Park of Lower Saxony the harbour seal is protected. As a top predator in the Wadden Sea ecosystem, the harbour seal is a sentinel species for the state of the environment. Between 2015 and 2017, a total of 80 stranded dead harbour seals were collected along the coastline of Lower Saxony and submitted for pathological investigations. Of these, 70 seals were born in the same year (0–7 months, age group 1) and eight in the previous year (8–19 months, age group 2), due to high mortality rates in these age groups. However, two perennial animals were also available for examination during this period, one of which was in good nutritional condition. Many of the seals that had been mercy-killed and found dead were in poor nutritional status. Histopathological, microbiological, parasitological and virological examinations were conducted on 69 individuals (86% (69/80)) in a suitable state of preservation. Respiratory tract parasitosis, cachexia, and bronchopneumonia were the most common causes of death or disease. Overall, there was no evidence of a relapse of a viral disease outbreak. Macrowaste, such as plastic waste or fishery-related debris, were not found in any gastrointestinal tract of the animals examined. There was also no evidence of grey seal predation. Weakness and cachexia were prominent causes of disease and death in harbour seals found within a few weeks after birth, but bronchopneumonia and septicaemia also developed in slightly older animals. Frequently found microbial pathogens in seals from Lower Saxony were similar to those found in other studies on seals from the Wadden Sea region in Schleswig-Holstein, for example streptococci and *Escherichia coli*/v. *haemolytica*, *Brucella* spp. and *Erysipelothrix rhusiopathiae*, potentially human pathogenic germs. The results of the examinations of dead harbour seals from Lower Saxony show that pathological investigations on a representative

number of animals deliver urgently needed information on the health status of the population. The results represent an important contribution to the state of the top predators of the Wadden Sea as part of the obligations within the Trilateral Wadden Sea Agreement, Oslo and Paris Convention for the Protection of the Marine Environment of the North-East Atlantic (OSPAR) and the Marine Framework Directive. The investigations should be continued as a matter of urgency and the stranding network should be expanded.

Keywords: harbour seal; pathology; microbiology; virology; parasitology; population health; infectious diseases; zoonosis

1. Introduction

The harbour seal (*Phoca vitulina*) is the most common seal species in the Lower Saxon Wadden Sea in northwestern Germany [1]. After hunting was banned in the mid-1970s, the decreased harbour seal population recovered slowly [2]. Also, chemical pollution and habitat disturbance were claimed to have a negative effect in the 1970s and 1980s [3,4]. The seal population was severely devastated and depleted by epidemics in 1988/89 and in 2002 due to phocine distemper virus (PDV), which induced pneumonia and subsequent secondary bacterial infections as the main cause of death [5]. Due to the PDV epidemic in 1988, the total number of harbour seals counted in the Wadden Sea during the moult in August dropped from an estimated 10,000 individuals in 1988 to 4544 in 1989, while the drop in 2002 was from 20,975 to 10,817 [1,5]. In 2014, the harbour seals in the Wadden Sea were struck by an influenza infection (H10N7) for the first time [6,7]. After these outbreaks, the population recovered again and the total number of harbour seals counted in the Wadden Sea during the moult in August 2023 reached 22,621 individuals [1]. Since 1991, harbour seals have been protected under the Agreement on the Conservation of Seals in the Wadden Sea (WSSA) which was concluded under the auspices of the UN Convention on the Conservation of Migratory Species of Wild Animals (Bonn Convention, CMS). The International Union for Conservation of Nature (IUCN) conservation status of the harbour seal in the Baltic Sea protected areas (HELCOM) is highly endangered, while the current status in the North Sea is reported to be endangered (IUCN).

Epidemiological health investigations, especially on the impact of infectious diseases were largely lacking when the first seal die-off started in 1988/89 [5,8]. A stranding network was established for the Wadden Sea coast of Schleswig-Holstein, and systematic pathological investigations were conducted, as increased knowledge on the health status of harbour seals was needed to improve the conservation status [8]. It was demonstrated that harbour seals regularly suffered from parasitic and bacterial infections [6] causing bronchopneumonia, hepatitis, gastroenteritis and septicaemia. Some of the potentially zoonotic bacteria such as *Brucella* spp. or *Erysipelothrix rhusiopathiae* were frequently found in live and dead harbour seals [6].

Human activities, such as shipping [9], offshore-constructions [4], marine litter and microplastic [10,11] as well as chemical pollution [4], may have a negative impact on the growth and health of the Wadden Sea harbour seal populations. Nonetheless, growing grey seal populations may also have a negative influence through grey seal predation and rape [12,13] as well as fatal mating attempts [14] and feeding competition [15].

Contrary to the waters of Schleswig-Holstein, epidemiological information on the health status of harbour seals from Lower Saxony is lacking. Therefore, the Lower Saxony Ministry of Food, Agriculture and Consumer Protection launched a research project allowing researchers to examine seals for their state of health, with special focus on the detection of zoonotic and infectious agents, macrowaste and evidence of grey seal predation. This study aimed to provide results that could be incorporated into the development of infection and hygiene management plans. In addition, the results serve the obligations within the Tri-

lateral Wadden Sea Agreement, Oslo and Paris Convention for the Protection of the Marine Environment of the North-East Atlantic (OSPAR) and the Marine Framework Directive.

2. Materials and Methods

For this study, the collection of stranded seals on the Wadden Sea coast of Lower Saxony was organised by the Seal Station in Norden-Norddeich (Norden, Germany). This institution is responsible for managing communication with local Wadden Sea Hunting Wardens in charge of handling seals in accordance with Lower Saxony Law (individuals trained by the state of Lower Saxony to monitor seal populations and to perform mercy-killing by shooting when animals present conditions not reversible by the rehabilitation process) and collect dead seals for analysis. The collection period for individuals included in this study (n = 80) lasted from January 2015 to May 2017. The project's timeline included two collection phases: the first began in January 2015 and lasted until June 2015 (n = 25) and the second began in July 2016 and lasted until May 2017 (n = 55). Locations where seals were found are shown in Figure 1, these ranging from the river Ems in the western coastal part of Lower Saxony to Cuxhaven located in the eastern part of Lower Saxony, including the East Frisian Islands.

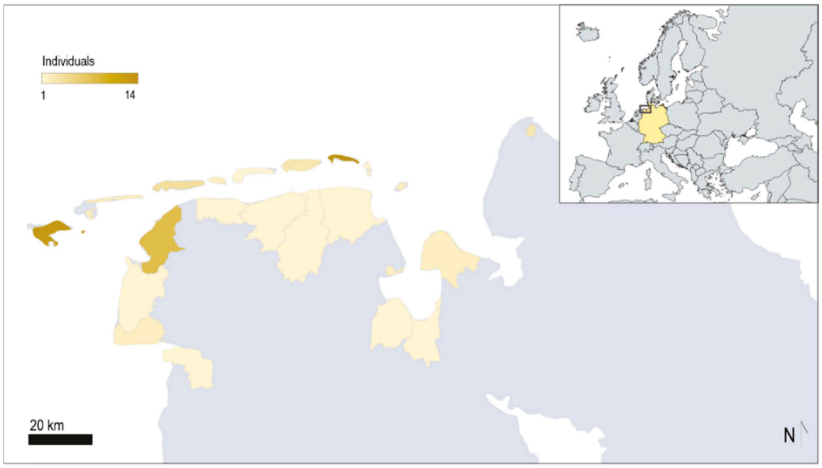


Figure 1. Locations of 80 harbour seals found on the Wadden Sea coast between 2015 and 2017 in the state of Lower Saxony, Germany. Europe map created with mapchart.net (accessed 1 January 2024). Lower Saxony map created with Microsoft Excel 2019 (©Microsoft, Albuquerque, NM, USA).

Seal carcasses (except for two individuals originating from Döse Beach, Cuxhaven, which were analysed without freezing) were stored at −20 °C in freezers distributed along the coast, at the Seal Station in Norden-Norddeich and at the Institute of Fish and Fishery Products (Cuxhaven, Germany) of the Lower Saxon State Office for Consumer Protection and Food Safety (Wardenburg, Germany). The investigated animals included both seals found dead (36.3%, n = 29) and mercy-killed ones (63.7%, n = 51). Mercy-killing was either performed by Wadden Sea Hunting Wardens trained by the State of Lower Saxony in the field or by the rehabilitation centre team prior to admission to the rehabilitation centre when the animal did not present a stable condition for a successful rehabilitation and release into the wild. Post-mortem analysis was either conducted at the Institute for Fish and Fishery Products (n = 42 seals) or at the Institute for Terrestrial and Aquatic Wildlife Research, University of Veterinary Medicine Hannover (Büsum, Germany; n = 38).

Each individual was evaluated in a necropsy examination following guidelines by the European Cetacean Society adapted for necropsies of small cetaceans and seals [8,16]. The status of decomposition of the animals was recorded and scored as follows: 1—fresh; 2—initial autolysis; 3—moderate autolysis; 4—advanced autolysis; 5—severe autolysis [8,16]. The carcasses were weighed and measured (see Figure 2) and the sex of the animal was recorded [8,16]. Age determination was based on the carcass discovery date in relation-

ship to time of year, length and weight [8]. Three age categories were established based on the previous characteristics: (I) animals born in the same year of death (0–7 months); (II) animals born in the year before death (8–19 months); (III) animals older than 19 months (>19 months) [10]. The carcasses were examined for the existence of external lesions, while all available organs were examined macroscopically for specific alterations [8,16]. The nutritional status was based on the individual's length (total length, standard length and reduced length; Figure 2), body weight, state of the musculature and blubber thickness determined at different locations and divided into good, moderate and emaciated (Figure 3) [8].

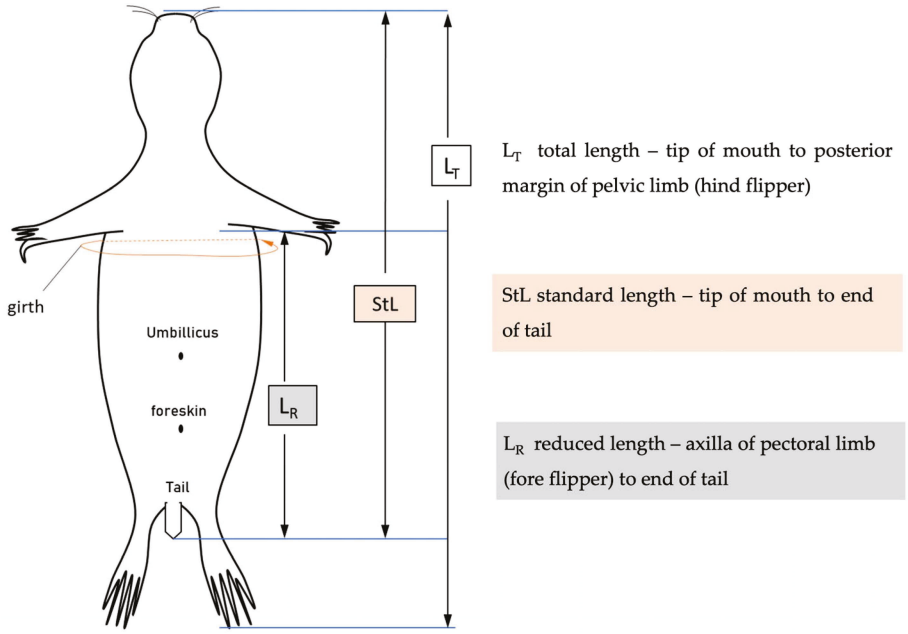


Figure 2. Reference points of the length measurements obtained in the post-mortem analysis of dead seals.

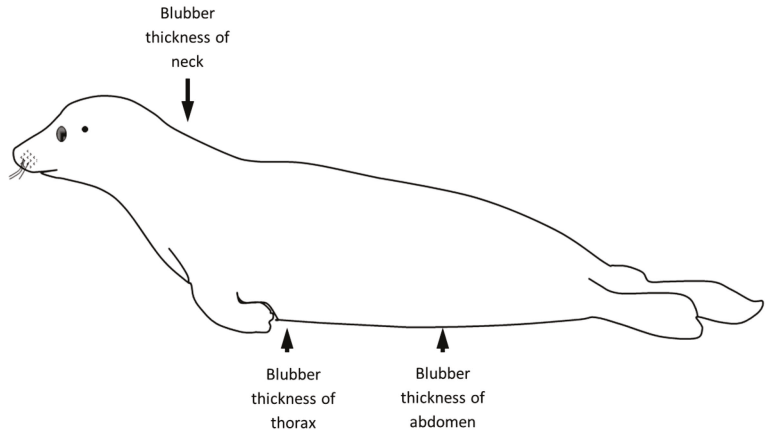


Figure 3. Reference points of the blubber thickness measurements (fatty tissue of the subcutis, blubber) in seals.

For histopathological investigations, samples measuring $1 \times 1 \times 1$ cm^3 were taken from the lung, trachea, stomach, intestine, heart, liver, pancreas, thyroid and adrenal glands, kidney, urinary bladder, testis, uterus, ovary, spleen, lymph nodes, skeletal muscle, skin and if possible brain and eye and then fixed in 10% buffered formalin and embedded in paraffin wax (Engelbrecht Medizin- und Labortechnik GmbH, Edermünde, Germany). Organ sections were cut (5 µm) and stained with routine haematoxylin and eosin stain (HE). Histopathological analysis was performed at the Institute for Fish and Fishery Products.

Parasites detected macroscopically were collected and fixed in 70% ethanol. Prior to identification, parasites were cleared with lactophenol. Identification was performed by light (Leica DM2500 LED, Leica Camera AG, Wetzlar, Germany) and binocular microscopy (Stereo-Zoom-Microscope MSZ5000-T, A. Krüss Optronic GmbH, Hamburg, Germany) [8].

Sampling for bacteriological and mycological analysis was performed either by collection of selected organs or collection of samples with swabs with transport medium (Meus S.r.l., Piove di Sacco, Italy). Sampled organs included brain, heart, intestine (small intestine and colon), kidneys, lungs, liver, reproductive organs, skin and spleen [8,17]. In some cases, swabs were additionally collected from inflamed tissue, for example tracheal mucosa or skin. Organ samples were stored at −20 °C and swabs were stored at 4 °C until further processing to prevent autolysis as well as overgrowth with external bacteria or fungi to maintain the originally sampled microbial flora.

Bacteriological and mycological examinations were carried out at the Veterinary Institute of the Lower Saxony State Office for Consumer Protection and Food Safety (Hannover, Germany). For culture purposes, sampled organs were decontaminated by heating the surface, and fresh cube-shaped sections (approximately 5 mm edge length) were streaked onto agar media. Swabs were plated directly onto the media.

Blood agar containing 5% defibrinated sheep blood (Oxoid Deutschland GmbH, Wesel, Germany) was used as non-selective media, water-blue metachrome-yellow lactose agar (Gassner agar; Oxoid Deutschland GmbH, Wesel, Germany) to detect Enterobacteriaceae. Additionally, selective media were used to isolate *Vibrio* spp. via thiosulphate-citrate-bile salts-sucrose (TCBS) agar (Merck KGaA, Darmstadt, Germany), *Brucella* spp. by use of agar base with *Brucella*-selective supplement (Oxoid Deutschland GmbH, Wesel, Germany), *Erysipelothrix rhusiopathiae* with agar described in [8], *Yersinia* spp. by means of Cefsulodin-Irgasan-Novobiocin (CIN) agar (Oxoid Deutschland GmbH, Wesel, Germany), *Salmonella* spp. through modified semi-solid Rappaport-Vassiliadis (MSRV) agar, brilliant green agar and Xylose-Lysine-Desoxycholate (XLD) agar (Oxoid Deutschland GmbH, Wesel, Germany). *Clostridia* spp. were cultured on Schaedler agar (Oxoid Deutschland GmbH, Wesel, Germany). For selective culturing of fungi Sabouraud agar (Oxoid Deutschland GmbH, Wesel, Germany) was used.

The different culture media were incubated according to the respective methods necessary for culturing each organism. *Brucella* selective agar was incubated in an atmosphere of 10% CO_2 for at least five days; Sabouraud agar at 28–30 °C for three-14 days (8)S, TCBS agar for two-five days at 25 °C, *Erysipelothrix rhusiopathiae* selective agar medium for 24–48 h at 37 °C, *Yersinia* spp. selective CIN agar for 48 h at 30 °C, MSRV agar for 24 and 48 h at 41 °C, XLD agar for 24 h at 37 °C and Schaedler agar for 24–48 h at 37 °C under anaerobic conditions in a jar using AnaeroGen™ gas sachets (Oxoid Deutschland GmbH, Wesel, Germany). Colonies were subcultured. Pure cultures were identified using standard morphological and biochemical methods as well as matrix-assisted laser desorption ionisation time-of-flight mass spectrometry (MALDI-TOF MS, Bruker Daltonics GmbH & Co. KG, Bremen, Germany). *Salmonella* isolates were identified to the serogroup by agglutination to *Salmonella* antisera (sifin diagnostics GmbH, Berlin, Germany).

Samples for virological analysis were obtained through the collection of tracheal swabs with transport Virocult medium (Sigma-Virocult®, Medical Wire & Equipment Co, Corsham, UK). Swabs were stored at 4 °C until investigation. Virological analyses were carried out at the Institute for Virology, University of Veterinary Medicine Hannover, Hannover, Germany. Virological analysis included the determination of influenza viruses, phocine herpesvirus and phocine distemper virus by qPCR [17–21]. RNA extractions for virus were performed using the IndiMag Pathogen Kit w/o plastics (Cat.-No.: SP947257, Leipzig, Germany) with homogenisation of the tissue samples in the BeadMill 24 (Thermo Fisher Scientific Inc., Waltham, MA, USA) using the Lysing Matrix M (MP Biomedicals, LC, Santa Ana, CA, USA) and buffer RA1 + ß-Mercaptoethanol (Macherey-Nagel GmbH & Co. KG, Düren, Germany). All screenings were made by qRT-PCR with the generic morbillivirus primers, as described by [18]. The morbillivirus qRT-PCR was performed

with the QuantiTect SYBR Green RT-PCR Kit (Qiagen GmbH, Hilden, Germany). Each reaction consisted of 12.5 µL QuantiTect SYBR Green RT-PCR Mastermix (Qiagen GmbH), 1 µL forward primer (20 pmol) MVP2202, 1 µL reverse primer (20 pmol) MVP2480, 0.25 µL reverse transcriptase, 5.25 µL H2O and 5 µL RNA. Detection of Influenza virus RNA was conducted using the Qiagen QuantiTect Probe RT-PCR kit [19,20]. Details for analyses of phocine herpesvirus are described in [21]. Reactions were performed based on a mixture of 12.5 µL QuantiTect Probe RT-PCR mix, 2.0 µL primer and probe mix (NP-1448-F: 25 µL, NP-1543-R: 25 µL, NP-1473-FAM: 3 µL, H2O: 147 µL), 2 µL GFP mix, 0.25 µL RT-Mix, 3.25 µL H2O, 5 µL sample. For both assays cycling conditions were set at 50 °C at 30 min, 95 °C at 15 min, 40 cycles of 30 s at 95 °C, 30 s at 56 °C and 30 s at 72 °C.

3. Results

3.1. Origin, State of Preservation, Age and Sex Determination, Morphometric Analyses

In total, 53.7% (*n* = 43/80) of the animals were found stranded in the coastal areas of the mainland of the state of Lower Saxony, while 46.3% (*n* = 37/80) were retrieved in the East Frisian Islands.

The state of preservation of the animals included in this study is shown in Figure 4. Due to a very advanced decomposition status (state of preservation 5), six (7.5%) of the examined seals were considered unsuitable for histopathological and microbiological analyses. For the eight animals presenting an advanced autolysis (preservation status 4), partial histopathological and microbiological analyses were performed in half of the animals found dead, while in the other half only morphometric data were retrieved. One animal (preservation status 2) was subjected to terrestrial predation and lacked all internal abdominal and most of the thoracic organs and was therefore excluded from the pathological analysis. In total, 69 animals (86%) were evaluated.

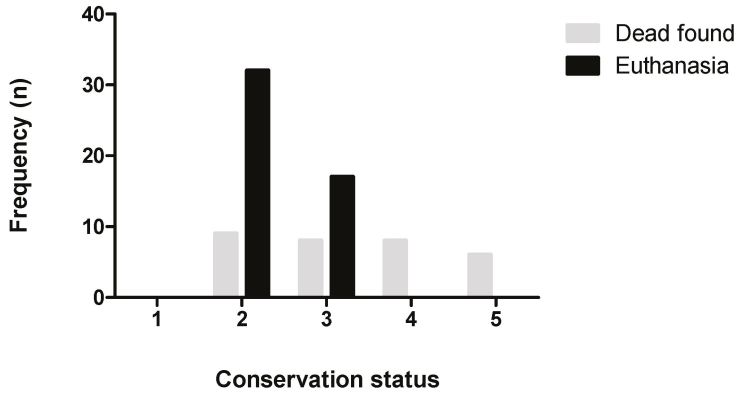


Figure 4. Preservation status of the seals included in this study (*n* = 80): 1—fresh, 2—first signs of autolysis, 3—moderate autolysis, 4—advanced autolysis, 5—macerated or advanced autolysis. Graph produced using GraphPad Prism1 (GraphPad Software, San Diego, CA, USA, version 5.01).

Sex and age determination were performed for all individuals, while morphometric data were retrieved when possible (Table 1). From the studied sample, 87.5% (*n* = 70/80) were individuals born in the same year they died, 10% (*n* = 8/80) had been born in the previous year, and 2.5% (*n* = 2/80) were older than 19 months. Most individuals were females (58.75%, *n* = 47/80).

Table 1. Sex, morphometry and nutritional status data of examined seals in relation to the age class. [1] Mean and standard deviation, [2] Total count, [3] Coefficient of variation, [4] Minimum and maximum values.

		Age Classes			
		I 0–6 Months	**II 7–19 Months**	**III >19 Months**	**Total**
Sex	Male	28 (35%)	5 (6.25%)	0 (0%)	33 (41.25%)
	Female	42 (52.5%)	3 (3.75%)	2 (2.5%)	47 (58.75%)
	Total	70 (87.5%)	8 (10%)	2 (2.5%)	80 (100%)
Morphometry	Body weight BW (kg)	10.06 ± 4.90 [1] (70) [2] 48.7% [3] 5.20–18.80 [4]	18.21 ± 2.92 (8) 16.0% 12.4–21.9	62.80 ± 3.69 (2) 6.3% 60.0–65.5	80 (100%)
	Total length L_T (cm)	89.28 ± 8.84 (67) 9.1% 72–115	105.16 ± 6.42 (8) 6.1% 94.3–112.0	158.00 ± 1.41 (2) 0.9% 157.0–159.0	77 (96.25%)
	Standard length L_{St} (cm)	77.66 ± 9.60 (67) 12.4% 45–100	94.50 ± 6.70 (8) 7.1% 80.5–100.0	137.0 (1) - -	76 (95%)
	Reduced length L_{red} (cm)	50.32 ± 5.98 (69) 11.9% 42.00–70.00	60.69 ± 4.64 (8) 7.6% 50.5–64.5	86.5 (1) - -	78 (97.5%)
	Girth axilla A (cm)	48.98 ± 9.51 (67) 19.4% 38.0–66.0	67.25 ± 5.98 (8) 8.9% 56.0–77.0	99.0 (1) - -	76 (95%)
	Blubber thickness thorax (mm)	7.7 ± 3.8 (67) 49.5% 0.0–15	12.13 ± 5.00 (8) 41.2 6.0–22.0	40.0 (1) - -	76 (95%)
	Blubber thickness neck (mm)	7.9 ± 4.1 (66) 51.5% 0.0–18.0	12.38 ± 3.02 (8) 24.4% 8.0–17.0	33.0 (1) - -	75 (93.75%)
	Blubber thickness abdomen (mm)	6.4 ± 3.4 mm (34) 52.6% 1.0–13.0	11.40 ± 5.99 (5) 52.5% 10.0–13.0	- - -	39 (48.75%)
Nutritional status	Good	14 (17.5%)	5 (6.25%)	1 (1.25%)	20 (25%)
	Moderate	6 (7.5%)	0 (0%)	0 (0%)	6 (7.5%)
	Emaciated	50 (62.5%)	3 (3.75%)	1 (1.25%)	54 (67.5%)
	Total	70 (87.5%)	8 (10%)	2 (2.5%)	80 (100%)

3.2. Assessment of Health Status

3.2.1. Nutritional Status

From all 80 individuals, the majority of examined seals presented an emaciated status (67.5%, $n = 54/80$). These animals presented cachexia and severe muscle atrophy. Most of the individuals were younger than six months. Overall, 25% ($n = 20/80$) of the individuals presented a good nutritional status.

3.2.2. Pathological Findings

Pathological findings collected during necropsies of the 69 examined seals are summarised in Table 2.

Table 2. Pathological findings in examined harbour seals (n = 69).

System/Region	Organ	Pathological Findings	Frequency
Respiratory system	Lungs and Bronchi	Pulmonary oedema	46 (67%)
		Pulmonary emphysema	44 (64%)
		Pulmonary parasitic infection	29 (42%)
		Bronchopneumonia/pneumonia	29 (42%)
		Atelectasis	21 (30%)
		Pulmonary haemorrhage	8 (12%)
		Congestion/hyperaemia	3 (4%)
	Larynx	Oedema	1 (1%)
	Trachea	Tracheitis	8 (12%)
		Oedema	1 (1%)
Thoracic cavity	Mediastinum	Mediastinal haemorrhage	9 (13%)
		Mediastinal emphysema	9 (13%)
Cardiovascular system	Blood vessels	Patent ductus arteriosus	5 (7%)
		Periarteritis	1 (1%)
	Heart	Auricular and ventricular parasitic infection	8 (12%)
		Right-sided cardiac failure	2 (3%)
		Perforation of the heart (secondary to gunshot)	1 (1%)
Gastrointestinal system	Teeth	Teeth deformation	1 (1%)
	Stomach	Gastritis	8 (12%)
		Gastric parasitic infection	4 (6%)
		Gastric haemorrhage	3 (4%)
	Intestines	Intestinal parasitic infection	7 (10%)
		Enteritis	15 (22%)
		Diarrhoea	12 (17%)
	Liver and Bile ducts	Hepatic congestion	17 (25%)
		Hepatic steatosis	3 (4%)
		Hepatic haemorrhage	2 (3%)
		Hepatitis	1 (1%)
Reproductive and Urinary system	Vagina and Uterus	Vaginitis/vulvitis	3 (4%)
		Endometritis/myometritis	1 (1%)
	Penis	Balanoposthitis	3 (4%)
	Umbilicus	Incomplete closure	10 (14%)
		Omphalitis	7 (10%)
	Kidneys	Renal congestion	3 (4%)
		Subcapsular renal haematoma	2 (3%)
		Renal cysts	1 (1%)
	Bladder	Urine sediment	3 (4%)
		Cystitis	2 (3%)
Locomotor system	Musculature	Muscular atrophy	44 (64%)
		Subcutaneous haematoma	6 (9%)
	Bones and articulations	Arthritis/polyarthritis	1 (1%)
		Open comminuted fracture with dislocation	1 (1%)
Skin and subcutis	Skin	Wounds of the skin and subcutis	1 (1%)
Haematopoietic and endocrine system	Spleen	Hyperplasia of the white pulp	4 (6%)

Respiratory System

In 29 examined seals (42%), a nematode infection was observed in the bronchial tree (Figure 5). The majority of respiratory parasitic infections were recorded in the younger individuals (age class I, n = 22), while no cases were recorded in the older animals (age class III).

Respiratory parasitosis ranged in terms of severity presentation (mild to severe). Two animals in the age classes I and II presented minor parasitic infections, seven had moderate parasitic infections, and the majority (n = 20) displayed severe parasitic infections in the respiratory system. This finding was particularly evident in animals of age class I (n = 16) which simultaneously presented good nutritional status. Parasites retrieved from the trachea (Figure 5), large main bronchi and smaller pulmonary bronchi were identified as roundworms *Otostrongylus circumlitus*. The largest nematodes (Figure 6) were up to 14.5 cm long (average) and had a diameter of 2 mm (unfixed). Often, lungworms were also isolated from the larynx and stomach.

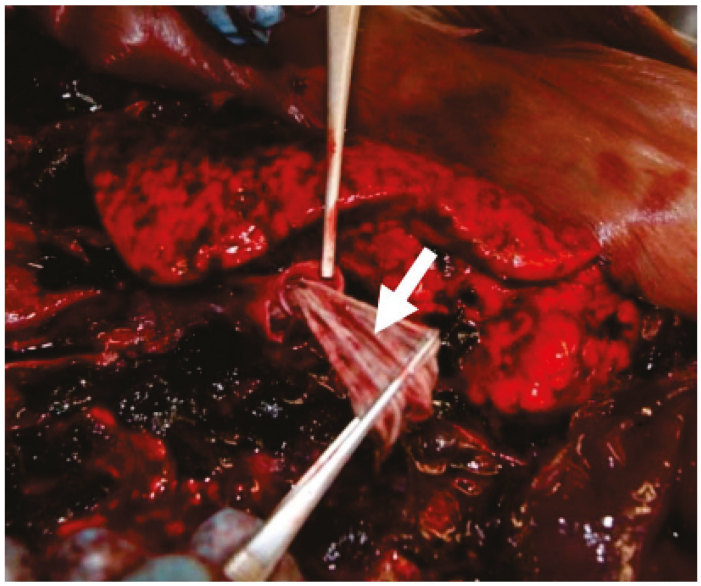


Figure 5. Severe lungworm infection with complete obstruction of the right main bronchus by pulmonary nematodes (arrow).

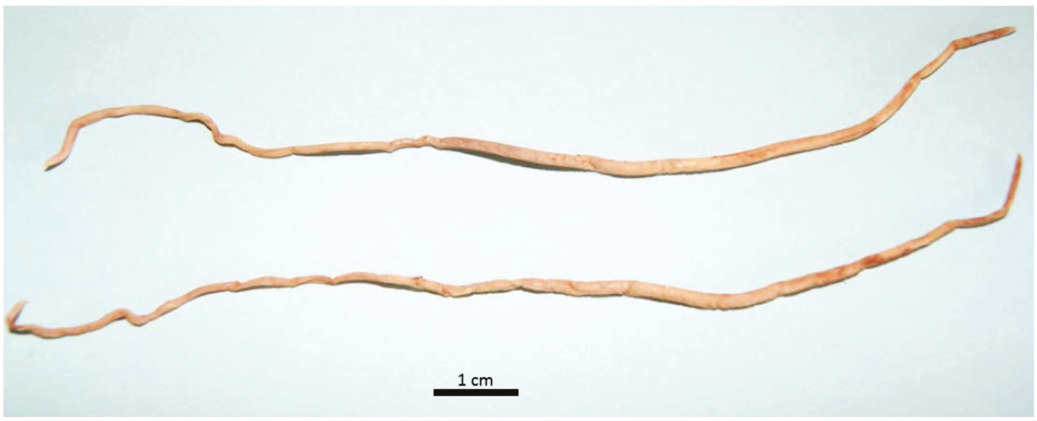


Figure 6. Roundworms (*Otostrongylus circumlitus*) isolated from the trachea and fixed in 70% ethanol.

In all animals with respiratory parasitic infections, bronchopneumonia or pneumonia was detected. Several types of inflammation could be diagnosed, including catarrhal-purulent or -haemorrhagic, granulomatous-necrotising, purulent-necrotising, and alveolar-interstitial. In most cases, pathological changes included several types of inflammatory lesions within the same animals (Figures 7 and 8).

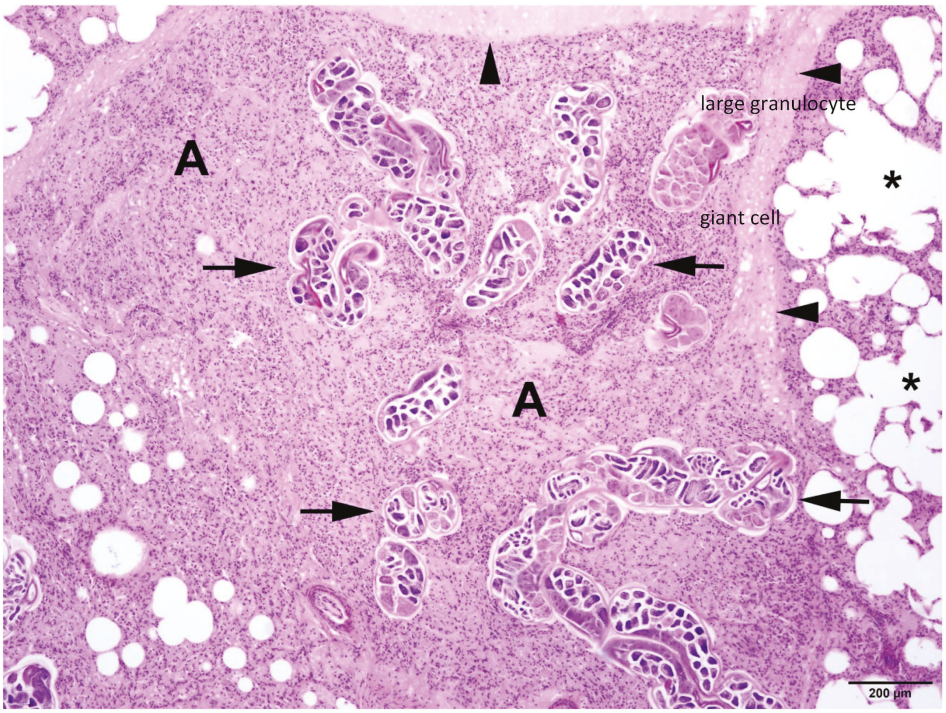


Figure 7. Harbour seal, lung: severe pulmonary endoparasitosis with nematodes in the parenchyma (arrows) associated with lobular atelectasis (A). Additionally, there is a moderate interstitial oedema (arrowheads) and an alveolar emphysema in the adjacent pulmonary tissue (asterisks). HE (4×).

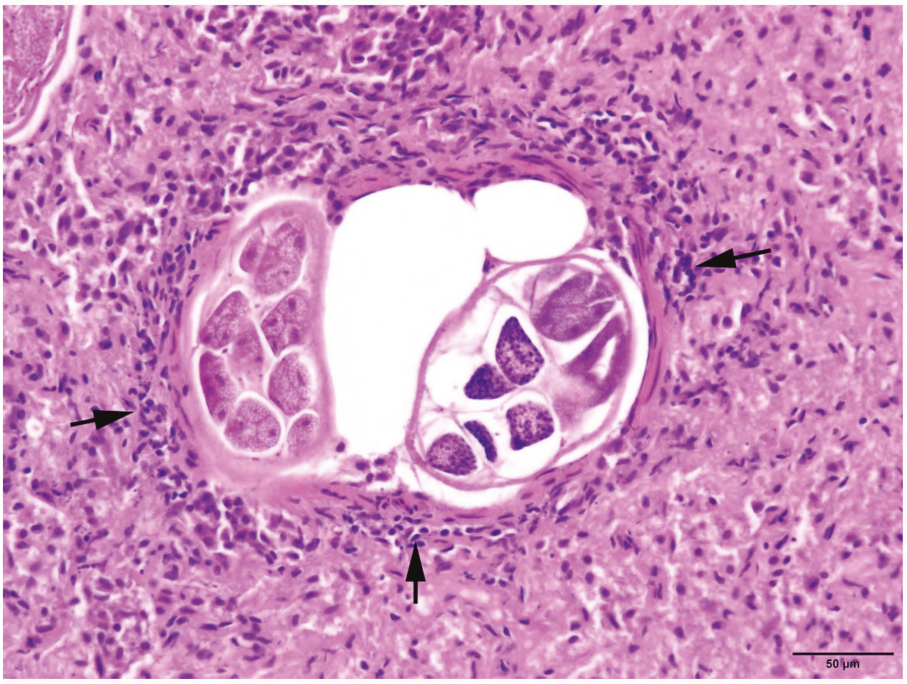


Figure 8. Harbour seal, lung: Bronchiolus with intraluminal nematodes and mild chronic peribronchitis (arrows). HE (20×).

The presence of red-grey-brown marbled lungs were associated with respiratory parasitic infections and/or bronchopneumonia, while tracheitis was recorded in eight individuals. Bilateral red-grey-brown marbled lungs were remarkably frequent, often resulting from agonal blood aspiration secondary to lesions existent in the lung tissue. Most cases were recorded in age class I animals (n = 21) and to a lesser extent in animals in

age class II (n = 8), which constitute the individuals presenting the more severe respiratory parasitic infections.

Different severity grades of alveolar/interstitial pulmonary emphysema (pathological accumulation of gas in the alveoli and/or cell spaces) could be detected in 44 animals often associated with parasitic infection and bronchopneumonia (Figure 9). Pulmonary atelectasis (collapse of alveoli) was found in 21 individuals. In 46 animals, alveolar/interstitial pulmonary oedema (pathological fluid accumulation in the alveoli and/or cell spaces) was recorded, with alveolar oedema present in 37 animals.

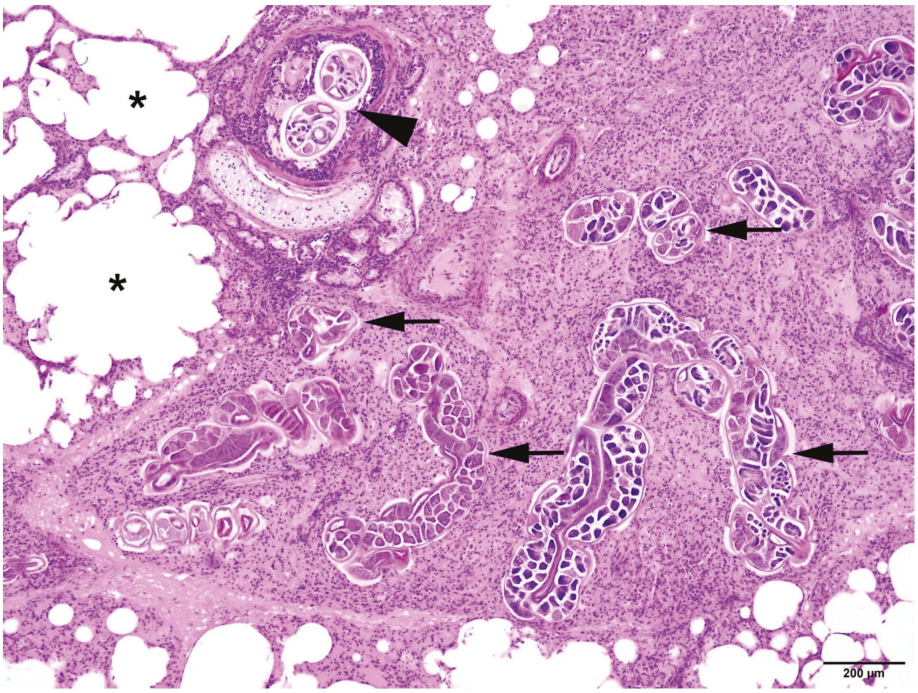


Figure 9. Harbour seal, lung: severe pulmonary endoparasitosis with nematodes in a bronchus (arrowhead) and in the parenchyma (arrows) with associated atelectasis. Adjacent pulmonary tissue displays alveolar emphysema (asterisks). HE (4×).

Cardiovascular System

Parasitic infections by *Otostrongylus circumlitus* were detected in the heart of eight seals (12%). The nematodes were mostly located in the right side of the heart (atrium and ventricle). Five animals in age class I (representing around 7% of the animals in this age class) presented a persistent ductus arteriosus. After incision, it was observed that the blood vessel was obstructed by a white-greyish mass. Differentiation between a physiological obstruction or a thrombus (i.e., white thrombus, separation thrombus) could not be concluded. One animal showed signs of periarteritis.

Gastrointestinal System

In several animals, parasitic nematodes were retrieved from the gastrointestinal system (stomach: n = 4 and intestines: n = 7). However, it was not completely clear in some cases whether these findings corresponded to gastrointestinal parasites (*Pseudoterranova decipiens* and/or *Contracaecum osculatum*) or to pulmonary parasites (*Otostrongylus circumlitus*) that were coughed up and swallowed by the animal while it was alive. Ultimately, the simultaneous presence of morphologically similar parasites in the respiratory system and in the gastrointestinal system, without observed parasite attachment in the gastrointestinal mucosa and associated lesion patterns, was considered evidence for this phenomenon. Figure 10 shows a gastric parasitic infection. In eight animals (12%), gastritis was present. Half of these animals presented a concomitant gastric parasitic infection.

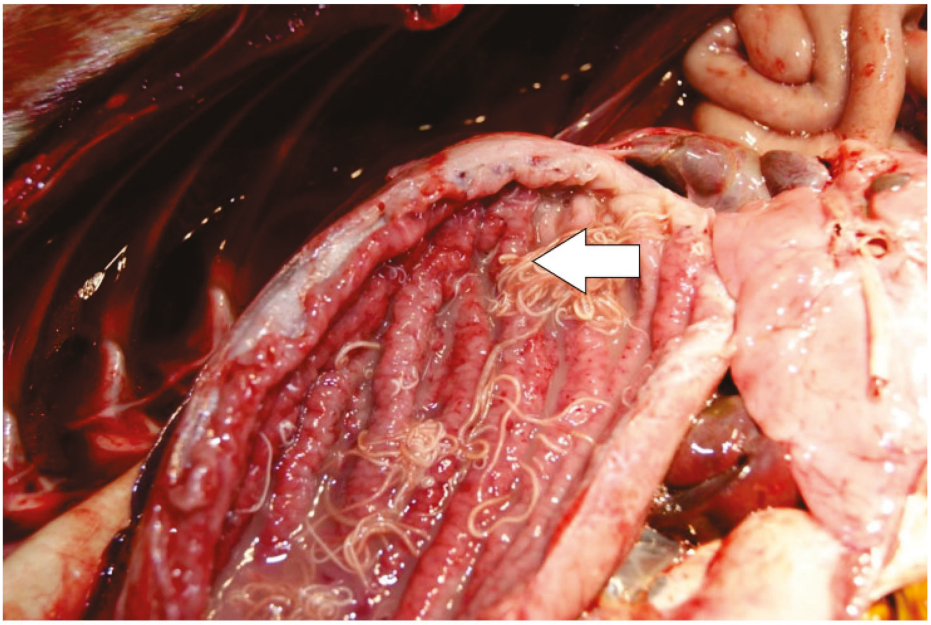


Figure 10. Severe gastric parasitic infection. Several roundworms (arrow) were found in the lumen of the stomach. The gastric mucosa is hypertrophied, forming broad increased folds and shows signs of petechiation (pin-point sized haemorrhages).

In 15 seals (22%), enteritis was evident, with the intestines presenting inflammation of the mucosa. In 12 of these seals, the affected animals also presented diarrhoea (unformed faeces) in the rectal area, with extensive contamination of the perianal area (fur and skin) (Figure 11). Regarding the underlying causes for enteritis, inflammatory and malabsorption statuses (the latter secondary to prolonged starvation) were considered.



Figure 11. Seal, ventral view. Perianal area contaminated with diarrhoea (black arrows). Posterior right flipper showing an open fracture involving the tarsal and metatarsal bones, with partial shattering, bone dislocation and dislocated fracture ends. In the fracture area, there is severe skin and subcutaneous tissue loss (10 × 8 cm). One of the metatarsal bones (white arrowheads) protrudes from the open wound, while parts of the tarsal bones (white arrow) can also be observed.

Regarding findings in the liver, hepatic congestion due to passive congestive hyperaemia was observed in 17 (25%) animals. Most individuals where this alteration was detected belonged to age group I. Three animals (4%) presented hepatic steatosis, and

hepatic haemorrhage was detected in two individuals (3%). Hepatitis was diagnosed in one animal (1%), and jaundice in another animal (1%).

Kidney, Reproductive Organs, Navel

In 10 animals from age group I, partial or complete patency of the navel was found, with three of these animals showing an infection of the navel. In another case, a firm, movable, 0.5 cm increase in circumference was found in the navel area. During microscopic examination, scar tissue was found, presumably because of a past infection (Figure 12). In three female harbour seals, inflammation of the uterus and vagina as well as bleeding in the vulva/vagina were encountered. In one of these three animals, the inflammation of the uterus encompassed the endo- and myometrium. Inflammation of the glans penis was found in three male animals. Urinary bladder inflammation was diagnosed in two animals. Another three seals had grit in the bladder.

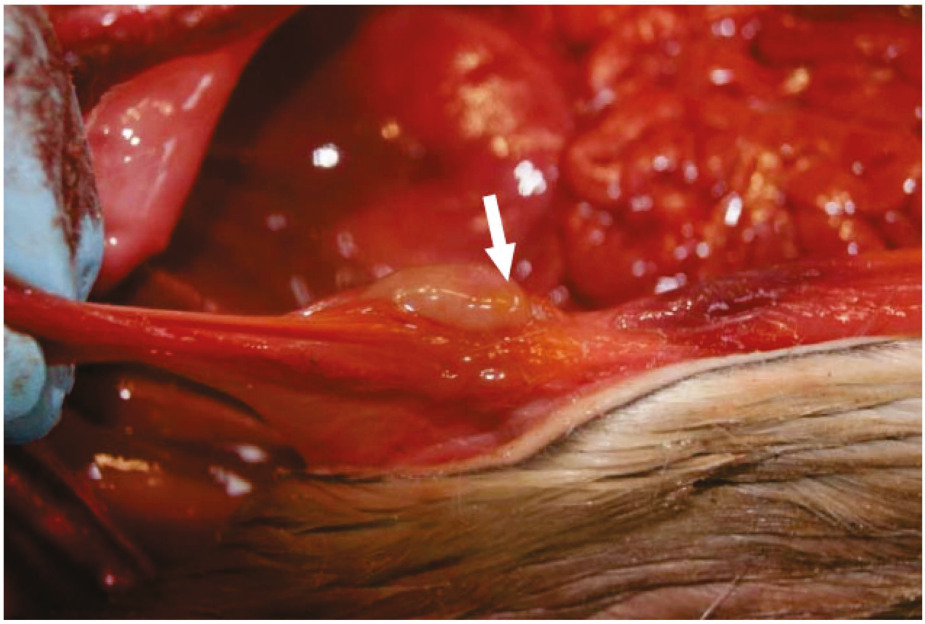


Figure 12. Seal, suppurative inflammation of the navel; when cut, a yellowish-grey and slightly viscous mass protruded (umbilical abscess, arrow).

Eyes, Ears, Central Nervous System (CNS)

One animal was missing both eyes due to bird scavenging damage, one seal displayed catarrhal conjunctivitis on both eyes and another animal had bilateral corneal ulcers.

Skeletal Muscles

All cachectic seals (n = 44) showed reduced blubber as well as muscle atrophy, of which 41 (93.2%) belonged to age group I.

Joints and Bones

Diffuse purulent arthritis was located in one animal. Another animal had an open comminuted fracture of the right rear flipper in the area of the tarsal and metatarsal bones with luxation of the metatarsalia—tarsalia (Figure 10) associated with 5–10 cm long, 4–8 cm wide and 0.5–1 cm deep skin wounds of reddish-brownish colour in the fracture area. In the case of another seal, the perforations of the os occipitale and os interparietale of the skull were of unknown origin. Furthermore, one animal developed a joint abscess of the tarsal joint.

Skin and Hypodermis

Four of the seals examined showed wounds on the skin of the limbs and abdominal skin, varying in size between 0.5–8 cm length, 0.5–2 cm width and 0.2–0.7 cm depth (Figure 13). Subcutaneous haematomas on the abdominal wall and head were found in six harbour seals.

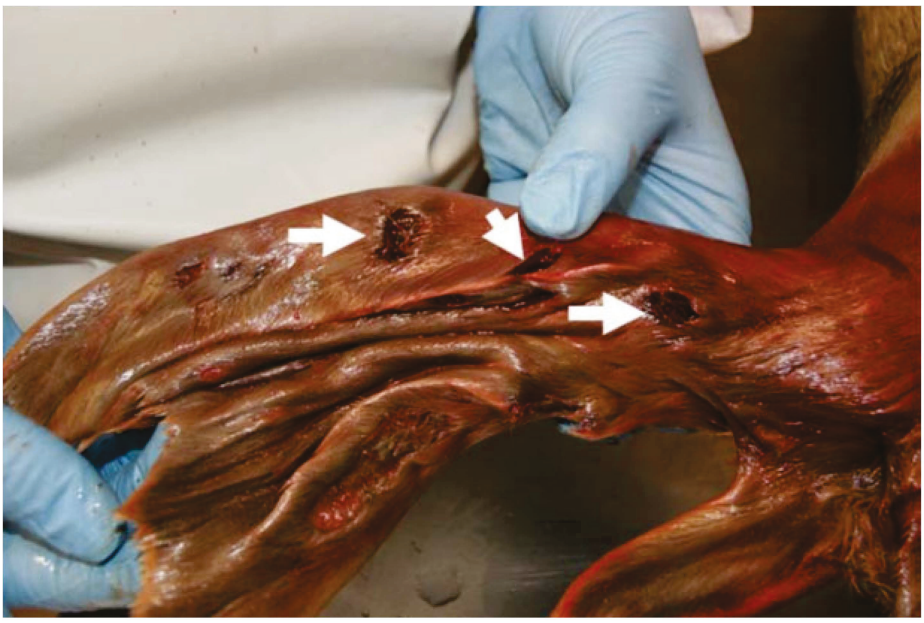


Figure 13. One seal showed superficial to 0.5–2 cm lesions on different parts of the skin (polytrauma); in the plantar metatarsal region of the right posterior flipper, there are clearly visible, fresh, up to 10 euro cent-sized, round-ovoid, bleeding, 0.2–0.5 cm deep skin wounds (arrows).

3.3. Bacteriological and Mycological Results

Various tissues (brain, eye, skin/subcutaneous tissue, sexual organs, intestines, bladder, liver/bile ducts, lungs, heart, navel, kidneys, lymph nodes) and various swab samples (including lungs, musculoskeletal system, skin) were sampled from the necropsied animals. In the 73 seals examined, this corresponded to 730 microbiological samples.

Among the potentially pathogenic bacteria, α- and ß-haemolytic were the most common streptococci, including *Streptococcus* (*S.*) *phocae*. Furthermore, *Escherichia coli* and *Escherichia coli* variatio (var.) *haemolytica* were diagnosed frequently (Table 3). The bacteria detected were associated with various diseases, especially bronchopneumonia and septicaemia. *Arcanobacterium phocae* could also be detected in the investigated harbour seals. *Brucella* (*B.*) *pinnipedialis* was isolated from the organs of three harbour seals. Human pathogenic bacteria such as *Erysipelothrix rhusiopathiae* and *Salmonella enterica* subsp. *enterica* ser. *typhimurium* were isolated from the organs of two seals each.

Other bacteria such as *Acinetobacter* sp., *Clostridium perfringens*, *Moraxella* sp., *Pantoea* sp., *Proteus* sp., *Pseudomonas* sp. and *Serratia* sp. were also detectable in various organs. In addition to bacteria, yeast (*Candida* sp.) and mold (*Aspergillus fumigatus*) were diagnosed. All findings are listed in Table 3.

Table 3. Findings of the microbiological examinations in different organs in 73 harbour seals from Lower Saxony, Germany. Number indicates the bacterial or fungal isolates.

	Organ											
Bacteria and Fungi	**Intestine**	**Genitalia**	**Skin**	**Heart**	**Liver**	**Lung**	**Spleen**	**Organ Pool**	**Swabs**	**CNS**	**Total Results**	**Number of Harbour Seals**
Number of investigated harbour seals												73
Bacteriological und mycological differentiations:												
Acinetobacter pittii						1				1	2	1
Acinetobacter lwoffii				1	1	1					3	1
Acinetobacter johnsonii				1		1					2	1
Acinetobacter sp.				1							1	1
Aerococcus viridans				3	3	4					10	4
Arcanobacterium phocae				1		2					3	2
Arcanobacterium phocisimile				1		2					3	3
Aspergillus fumigatus				1							1	1
Unknown bacterium	1			2		1					4	4
Brevundimonas diminuta				1							1	1
Brucella pinnipedialis		2			2						4	3
Burkholderia cepacia				1							1	1
Candida zeylanoides			1								1	1
Carnobacterium maltaromaticum				2	2	2					6	2
Clostridium bifermentans	5										5	5
Clostridium perfringens	46										46	46
—of these *Clostridium perfringens* type A	38										38	38
—of these *Clostridium perfringens* type D	1										1	1
Clostridium sordellii	9										9	9
Clostridium sp.	1										1	1
Clostridium tertium								1			1	1
Coliform bacteria				3	3	3					9	3
Corynebacterium jeikeium				1		1					2	1
Corynebacterium pseudodiphteriticum				1	1						2	1
Cronobacter malonaticus				1	1	1					3	1
Enterobacter cloacae				1	1						2	1
Enterobacter sp.				1	1	1					3	1
Enterococcus avium				3	1	2					6	3
Enterococcus durans					1						1	1
Enterococcus faecalis	2			7	5	6					20	11

Table 3. *Cont.*

	Organ											
Bacteria and Fungi	**Intestine**	**Genitalia**	**Skin**	**Heart**	**Liver**	**Lung**	**Spleen**	**Organ Pool**	**Swabs**	**CNS**	**Total Results**	**Number of Harbour Seals**
Enterococcus faecium				1	1	1					3	2
Erwinia herbicola					1						1	1
Erysipelothrix rhusiopathiae								2			2	2
Escherichia coli	1			5	4	6					16	6
Escherichia coli (haemolytic)				4	3	3					10	5
Ewingella americana						1					1	1
Gardnerella vaginalis				3		2					5	3
Gemella haemolysans				1	1	2					4	2
Gemella morbillorum				1		2					3	2
Hafnia alvei				1	1	1					3	1
Yeasts			1								1	1
Moraxella sp.				3	3	3					9	3
Morganella morganii					1						1	1
Indistinguishable germs				2	3	2					7	5
Indistinguishable germs (fungus)			1								1	1
Oceanobacillus oncorhynchi					1						1	1
Pantoea sp.				1							1	1
Pasteurella sp.				1		1					2	1
Penicillium sp.			1								1	1
Pseudomonas aeruginosa						1					1	1
Pseudomonas fluorescens				6	6	6					18	8
Pseudomonas lundensis				2	2	2					6	3
Pseudomonas proteolytica					1						1	1
Pseudomonas putida				3	3	3					9	4
Pseudomonas sp.				1	1	1					3	1
Psychrobacter phenylpyruvicus				3	4	2					9	4
Rahnella aquatilis				1	1		1	1			4	3
Raoultella ornithinolytica	1										1	1
Salmonella typhimurium	2			1	1	1		1			6	2
Serratia grimesii				2							2	2
Serratia liquefaciens				4	3	4					11	4
Serratia marcescens	1			1	1	1					4	2
Serratia plymuthica				1		1					2	1
Serratia sp.				1	1	1					3	1

Table 3. *Cont.*

Bacteria and Fungi	Organ											
	Intestine	Genitalia	Skin	Heart	Liver	Lung	Spleen	Organ Pool	Swabs	CNS	Total Results	Number of Harbour Seals
Serratia ureilytica				1	1	1					3	1
Staphylococcus sp.				2	3	3					8	4
Streptococcus equi spp. *equi*									1		1	1
Streptococcus gallolyticus						1					1	1
Streptococcus phocae				14	7	19					40	19
Streptococcus sanguinis				1	1	1					3	1
Streptococcus sp.						1					1	1
Torulaspora delbrueckii			1								1	1
Vagococcus fluvialis				1	1	1					3	1
Vibrio alginolyticus	1							1			2	1
Anaerobic bacteria negative	18										18	18
Brucella negative		64			66			70		69	269	71
Francisella negative					71		71				142	71
Erysipelothrix rhusiopathiae negative								69			69	69
Fish pathogenic pathogens (Flavobacteria, non-motile *Aeromonas*)				71	70	71					212	71
Salmonella negative	66							69			135	69
Vibrio negative	68							70			138	70
Yersinia negative	70				71		71				212	71
Non-specific bacteria									1		1	1
Bacterial investigation negative				26	26	21					73	29
Mycological investigation negative			8								8	8
Total results	400	66	13	198	400	245	143	284	2	70	1821	46

3.4. Virological Results

No signs of viral infection were observed during necropsies and histopathological examinations. A total of 73 seals were tested for seal distemper, seal herpes virus and influenza virus by means of PCR. PCRs provided negative diagnostics in all animals.

3.5. Parasitological Investigations

Of the 69 seals examined for parasites, 29 displayed parasitic infections in the respiratory system. The animals affected by lungworms were especially the yearlings (n = 22) with a body mass between 6 and 19 kg (for further details, see Table 4). The macroscopic and microscopic examinations showed an infection of the respiratory tract with *Otostrongylus circumlitus*. The infection was regularly concomitant with pneumonia or bronchopneumonia. Heavy parasitic infection of the lung also resulted in *Otostrongylus circumlitus* found in the heart, stomach and intestine through coughing and swallowing.

Table 4. Number, sex ratio, body weight and standard lengths of parasites in the respiratory system of investigated harbour seals (♂= male, ♀= female).

Age	Body Weight [kg]	Total Length [cm]	Standard Length [cm]	Number N	Sex Ratio
age class 1	13.1 ± 2.5	96.6 ± 8.1	85.1 ± 8.0	22	9 ♂; 13 ♀
age class 2	17.7 ± 2.7	104.8 ± 6.8	93.7 ± 6.8	7	4 ♂; 3 ♀

3.6. Causes of Disease and Death

The majority of the seals shot and found dead had a bad nutritional status. This could have been caused by infectious diseases, general debility in young animals or loss of the mother. Signs of septicaemia, such as generalised intravascular thrombi present as a result of DIC (disseminated intravascular coagulopathy), petechial haemorrhages in serous membranes as well as generalised or multiple organ infarctions were not observed in any of the necropsied animals. The most common causes of disease and death in the harbour seals of the Lower Saxon dead animal monitoring were parasitosis of the respiratory tract, followed by cachexia and bronchopneumonia.

4. Discussion

The health assessment of harbour seals was mainly based on dead animals, with examinations of yearlings (n = 70) and animals born in the year before their death (n = 8). This is due to the high morbidity and mortality rates in these age classes, affecting many harbour seal populations [1,5]. However, during this period there were also two perennial animals for examination, one of which was in good preservation status.

Most of the mercy-killed seals and those found dead displayed poor nutritional status and health. The main causes were infectious diseases and weakness during life in young animals, most likely due to maternal separation. Separation during the lactation period can be caused by human disturbances or the illness or death of the mother. In order to minimize human–seal interaction, the National Park authorities of the Wadden Sea, the seal stations, the Common Wadden Sea Secretariat and exhibition centres regularly provide information about the sensitivity of the newborn animals [1].

Disease and death in the examined harbour seals were especially induced by parasitosis of the respiratory tract, cachexia and bronchopneumonia. Those findings are in accordance with harbour seals examined in other regions in the North and Baltic Seas as well as North America [6]. Parasitosis of the respiratory tract and bronchopneumonia are also the most common pathological findings in harbour porpoises in the North Sea [22–24].

Overall, there was no evidence of a renewed, epidemic virus-related seal die-off neither in Lower Saxony nor in Schleswig-Holstein. However, combined health examinations of dead and alive seals in Schleswig-Holstein have shown that certain parameters, such as blood values [25], antibody and antigen detection for distemper [17] and influenza virus [9] should also be conducted in living animals in Lower Saxony in order to ensure a likewise assessment of older seals. Given the ongoing H1N5 influenza infections in wild bird populations, it can be expected that more positive cases will be found in marine mammals in the North Sea.

No macrowaste, such as plastic debris or fishing nets, was found in the gastrointestinal tract or on the fur, as described for animals from Schleswig-Holstein and Mecklenburg-Western Pomerania [10]. In the future, microplastic analyses should be introduced for animals from Lower Saxony, as previous analyses in different regions showed contamination by microplastic, which is of potential concern [11,26,27].

Furthermore, there were no characteristic indications of injuries from predators, as frequently found in Schleswig-Holstein [12,13] or harbour porpoises from Dutch and Belgian waters [28,29]. The lesions observed in the harbour seals from Lower Saxony are most likely due to bites from other seals or possibly dogs or blunt trauma.

When comparing the examination results with those of harbour seals from Schleswig-Holstein, it becomes clear that the examination material was also dominated by yearlings and the previous year's animals [8]. In the animals found around the period of birth, general debility and cachexia were also major causes of disease and death. Bronchopneumonia and septicaemia affected slightly older animals as well. Frequently found microbial pathogens in Schleswig-Holstein were also streptococci and *Escherichia coli* var. *haemolytica* [6].

This study detected *B. pinnipedialis* in the gonads of Lower Saxon harbour seals for the first time. The importance of *B. pinnipedialis* as a causative agent of marine mammal diseases and the risk potential as zoonotic pathogen are discussed in further research studies [8]. With *Brucella* sp. [6,30,31] and *Erysipelothrix rhusiopathiae* [32,33], potentially human pathogenic germs were found in both the states of Lower Saxony and Schleswig-Holstein, which always admonish to adhere to a careful handling of dead and alive seals.

Streptococcus phocae was also isolated during disease outbreaks on a salmon farm in 2005 [34]. This pathogen was first identified in 1997 in harbour seals in Scotland and later also in other marine species isolated from skin lesions such as wounds and abscesses [35]. In marine mammals, the pathogen was proven for the first time in 1994 [8,36]. Overall, streptococci are important pathogenic bacteria in marine mammals, also including zoonotic species such as *Streptococcus halichoeri* and *S. iniae* [36], warranting close monitoring.

A handout was compiled for the training of the Wadden Sea Game Wardens, which was used as part of the training courses at the seal station Norddeich. The information about the project should also be included in future exhibitions in the seal station and the national park buildings. The results of this study, which involved post-mortem examinations of a representative sample of dead harbour seals from Lower Saxony, contribute valuable insights into the health status of these top predators in the Wadden Sea. These findings will support efforts under the Trilateral Wadden Sea Agreement, OSPAR, and the Marine Framework Directive. These investigations should be continued, and the stranding network expanded as a matter of urgency.

5. Conclusions

This study underscores the importance of systematic pathological investigations, as basic knowledge of the health status and causes of death are needed to ensure the discovery of known infectious agents, including zoonotic pathogens. The causes of die-offs are identified more quickly when the health status of animals in specific areas is known. In addition, knowledge of infectious agents informs necessary adaptations to hygiene protocols when handling seals. Pathological investigations help to understand changes in the health of the Wadden Sea harbour seal population living in an environment affected by anthropogenic impacts like shipping, offshore-construction, ammunition, chemical pollution and marine litter. These results should encourage stakeholders to conduct annual health monitoring, as long-term studies are needed to understand the impacts of climate change, pollution, human activity, and habitat disruption, and to ensure adapted future management and protection strategies.

Author Contributions: Conceptualisation, U.S., P.L., E.B. and R.P.; methodology, U.S., J.L., M.R., S.B., M.L.G. and R.P.; validation, U.S., J.L., M.R., S.B., M.L.G. and R.P.; formal analysis, U.S., J.L., M.R., S.B., M.L.G. and R.P.; investigation, U.S., J.L., M.R., S.B., M.L.G. and R.P.; resources, U.S., P.L. and E.B.; data curation, U.S., J.L., P.L., M.R., S.B., M.L.G. and R.P.; writing—original draft preparation, R.P., U.S., M.L.G. and J.L.; writing—review and editing, all authors; visualisation, R.P., M.L.G. and U.S.; supervision, U.S. and E.B.; project administration, U.S. funding acquisition, U.S., P.L., R.P. and E.B. All authors have read and agreed to the published version of the manuscript.

Funding: This research was funded by the Lower Saxony Ministry of Food, Agriculture and Consumer Protection, Germany. We acknowledge financial support by the Open Access Publication Fund of the University of Veterinary Medicine Hannover, Foundation.

Institutional Review Board Statement: Not applicable.

Informed Consent Statement: Not applicable.

Data Availability Statement: The data supporting the conclusions of this article are available upon request to the authors.

Acknowledgments: We would like to thank the gamekeepers and helpers from the seal station Norddeich for the collection of carcasses. We would also like to acknowledge all technicians and scientists at LAVES and ITAW who helped with necropsies and analyses of the samples. We are very thankful to Peter Wohlsein, Institute for Pathology of the University of Veterinary Medicine Hannover for the help with the histological slides.

Conflicts of Interest: The authors declare no conflicts of interest. The funders had no role in the design of the study, in the collection, analyses or interpretation of data, in the writing of the manuscript or in the decision to publish the results.

References

1. Galatius, A.; Brasseur, S.; Hamm, T.; Jeß, A.; Meise, K.; Meyer, J.; Schop, J.; Siebert, U.; Stejskal, O.; Teilmann, J.; et al. Survey results of harbour seals in the Wadden Sea in 2023. In *The Population Continues to Decline*; Common Wadden Sea Secretariat: Wilhelmshaven, Germany, 2023.
2. Reijnders, P.J.H. The effect of hunting on the further existence of a harbour seal population in the Dutch Wadden Sea. *Z. Säugetierkd.* **1983**, *48*, 50–54.
3. Brouwer, A.; Reijnders, P.J.H.; Koeman, J.H. Polychlorinated biphenyl (PCB) contaminated fish induces vitamin A and thyroid hormone deficiency in the common seal (*Phoca vitulina*). *Aquat. Toxicol.* **1989**, *15*, 99–106. [CrossRef]
4. Siebert, U.; Müller, S.; Gilles, A.; Sundermeyer, J.; Narberhaus, I. Chapter VII Species Profiles marine mammals. In *Threatened Biodiversity in the German North and Baltic Seas—Sensitivities towards Human Activities and the Effects of Climate Change*; Narberhaus, I., Krause, J., Bernitt, J., Eds.; Nature Conservation and Biodiversity: Bonn-Bad Godesberg, Germany, 2012; pp. 487–542.
5. Härkönen, T.; Dietz, R.; Reijnders, P.; Teilmann, J.; Harding, K.; Hall, A.; Brasseur, S.; Siebert, U.; Goodman, S.J.; Jepson, P.D.; et al. A review of the 1988 and 2002 phocine distemper virus epidemics in European harbour seals. *Dis. Aquat. Org.* **2006**, *68*, 115–130. [CrossRef] [PubMed]
6. Colegrove, K.M.; Burek-Huntington, K.A.; Roe, W.; Siebert, U. Pinnipediae. In *Pathology of Wildlife and Zoo Animals*; Terio, K.A., McAloose, D., St. Leger, J., Eds.; Academic Press: New York, NY, USA, 2018; Chapter 23; pp. 569–592.
7. Krog, J.S.; Hansen, M.S.; Holm, E.; Hjulsager, C.K.; Chriél, M.; Pedersen, K.; Andresen, L.O.; Abildstrøm, M.; Jensen, T.H.; Larsen, L.E. Influenza A (H10N7) virus in dead harbour seals, Denmark. *Emerg. Infect. Dis.* **2015**, *21*, 684–687. [CrossRef] [PubMed]
8. Siebert, U.; Wohlsein, P.; Lehnert, K.; Baumgärtner, W. Pathological findings in harbour seals (*Phoca vitulina*): 1996–2005. *J. Comp. Path.* **2007**, *137*, 47–58. [CrossRef]
9. Mikkelsen, L.; Johnson, M.; Wisniewska, D.M.; van Neer, A.; Siebert, U.; Madsen, P.T.; Teilmann, J. Long-term sound and movement recording tags to study natural behavior and reaction to ship noise of seals. *Ecol. Evol.* **2019**, *9*, 2588–2601. [CrossRef]
10. Unger, B.; Herr, H.; Viquerat, S.; Gilles, A.; Burkhardt-Holm, P.; Siebert, U. Opportunistically collected data from aerial surveys reveal spatio-temporal distribution patterns of marine debris in German waters. *Environ. Sci. Poll. Res.* **2020**, *28*, 2893–2903. [CrossRef]
11. Philipp, C.; Unger, B.; Siebert, U. Occurrence of Microplastics in Harbour Seals (*Phoca vitulina*) and Grey Seals (*Halichoerus grypus*) from German Waters. *Animals* **2022**, *12*, 551. [CrossRef]
12. van Neer, A.; Gross, S.; Kesselring, T.; Wohlsein, P.; Leitzen, E.; Siebert, U. Behavioural and pathological insights into a case of active cannibalism by a grey seal (*Halichoerus grypus*) on Helgoland, Germany. *J. Sea Res.* **2019**, *148–149*, 12–16. [CrossRef]
13. van Neer, A.; Gross, S.; Kesselring, T.; Grilo, M.L.; Ludes-Wehrmeister, E.; Roncon, G.; Siebert, U. 2021. Assessing seal carcasses potentially subjected to grey seal predation. *Sci. Rep.* **2021**, *11*, 694. [CrossRef]
14. Rohner, S.; Hülskötter, K.; Gross, S.; Wohlsein, P.; Abdulmawjood, A.; Plötz, M.; Verspohl, J.; Haas, L.; Siebert, U. Male grey seal commits fatal sexual interaction with adult female harbour seals in the German Wadden Sea. *Sci. Rep.* **2020**, *10*, 13679. [CrossRef] [PubMed]
15. Heße, E.; Siebert, U.; Gilles, A. Trophic ecology of marine mammals with competition potential under resource-limited conditions in the southern North Sea. *Front. Mar. Sci.* **2024**. submitted.
16. IJsseldijk, L.L.; Brownlow, A.C.; Mazzariol, S. Best Practice on Cetacean Postmortem Investigation and Tissue Sampling. Bonn, Monaco: ASCOBANS and ACCOBAMS Document, ASCOBANS MOP9/Doc.6.2.5b. Available online: https://accobams.org/wp-content/uploads/2021/07/Best-practices-on-cetacean-post-mortem-investigation.pdf (accessed on 14 December 2023).
17. Ludes-Wehrmeister, E.; Dupke, C.; Harder, T.C.; Baumgärtner, W.; Haas, L.; Teilmann, J.; Dietz, R.; Jensen, L.F.; Siebert, U. Phocine distemper virus (PDV) seroprevalence as predictor for future outbreaks in harbour seals. *Vet. Microbiol.* **2016**, *183*, 43–49. [CrossRef] [PubMed]
18. Stokholm, I.; Puryear, W.; Sawatzki, K.; Knudsen, S.W.; Terkelsen, T.; Becher, P.; Siebert, U.; Olsen, M.T. Emergence and radiation of distemper viruses in terrestrial and marine mammals. *Proc. R. Soc. B* **2021**, *288*, 20211969. [CrossRef]
19. Bodewes, R.; Bestebroer, T.M.; van der Vries, E.; Verhagen, J.H.; Herfst, S.; Koopmans, M.P.; Fouchier, R.A.M.; Pfankuche, V.M.; Wohlsein, P.; Siebert, U.; et al. Avian Influenza A (H10N7) Virus–Associated Mass Deaths among Harbor Seals. *Emerg. Inf. Dis.* **2015**, *21*, 720–722. [CrossRef]

20. Postel, A.; King, J.; Kaiser, F.K.; Kennedy, J.; Lombardo, M.S.; Reineking, W.; de Roi, M.; Harder, T.; Pohlmann, A.; Gerlach, T.; et al. Infections with Highly Pathogenic Avian Influenza A Virus (HPAIV) H5N8 in Harbor Seals at the German North Sea Coast. *Emerg. Microb. Inf.* **2022**, *11*, 725–729. [CrossRef]
21. VanDevanter, D.R.; Warrener, P.; Bennett, L.; Schultz, E.R.; Coulter, S.; Garber, R.L.; Rose, T.M. Detection analysis of diverse herpesviral species by consensus primer PCR. *J. Clin. Microbiol.* **1996**, *34*, 1666–1671. [CrossRef]
22. Jauniaux, T.; Petitjean, D.; Brenez, C.; Borrens, M.; Brosens, L.; Haelters, J.; Tavernier, T.; Coignoul, F. Post-mortem findings and causes of death of harbour porpoises (*Phocoena phocoena*) stranded from 1990 to 2000 along the coastlines of Belgium and Northern France. *J. Comp. Pathol.* **2002**, *126*, 243–253. [CrossRef]
23. Jepson, P.D.; Baker, J.R.; Kuiken, T.; Simpson, V.R.; Kennedy, S.; Bennett, P.M. Pulmonary pathology of harbour porpoises stranded in England and Wales between 1990 and 1996. *Vet. Rec.* **2000**, *146*, 721–728. [CrossRef]
24. IJsseldijk, L.L.; Scheidat, M.; Siemensma, M.L.; Couperus, B.; Leopold, M.F.; Morell, M.; Grone, A.; Kik, M.J.L. Challenges in the assessment of bycatch: Postmortem findings in harbor porpoises (*Phocoena phocoena*) retrieved from gillnets. *Vet. Pathol.* **2021**, *58*, 405–415. [CrossRef]
25. Hasselmeier, I.; Fonfara, S.; Driver, J.; Siebert, U. Differential hematology profiles differential hematology profiles of free-ranging, rehabilitated, and captive harbor seals (*Phoca vitulina*) of the German North Sea. *Aquat. Mam.* **2008**, *34*, 149–156. [CrossRef]
26. Rebolledo, B.E.L.; Van Franeker, J.A.; Jansen, O.E.; Brasseur, S.M.J.M. Plastic ingestion by harbour seals (*Phoca vitulina*) in The Netherlands. *Mar. Pollut. Bull.* **2013**, *67*, 200–202. [CrossRef] [PubMed]
27. Browne, M.A.; Galloway, T.; Thompson, R. Microplastic-an emerging contaminant of potential concern? *Integr. Environ. Assess. Manag.* **2007**, *3*, 559–561. [CrossRef] [PubMed]
28. Bouveroux, T.; Kiszka, J.J.; Heithaus, M.R.; Jauniaux, T.; Pezeril, S. Direct evidence for gray seal (*Halichoerus grypus*) predation and scavenging on harbor porpoises (*Phocoena phocoena*). *Mar. Mammal Sci.* **2014**, *30*, 1542–1548. [CrossRef]
29. Leopold, M.F.; Begeman, L.; van Bleijswijk, J.D. Exposing the grey seal as a major predator of harbour porpoises. *Proc. R. Soc. B* **2015**, *282*, 20142429. [CrossRef]
30. Sohn, A.H.; Probert, W.S.; Glaser, C.A.; Gupta, N.; Bollen, A.W.; Wong, J.D.; Grace, E.M.; McDonald, W.C. Human neurobrucellosis with intracerebral granuloma caused by a marine mammal *Brucella* spp. *Emerg. Inf. Dis.* **2003**, *9*, 485–488. [CrossRef]
31. McDonald, W.L.; Jamaludin, R.; Mackereth, G.; Hansen, M.; Humphrey, S.; Short, P.; Taylor, T.; Swingler, J.; Dawson, C.E.; Whatmore, A.M.; et al. Characterization of a *Brucella* sp. strain as a marine-mammal type despite isolation from a patient with spinal osteomyelitis in New Zealand. *J. Clin. Microb.* **2006**, *44*, 4363–4370. [CrossRef]
32. Hunt, T.D.; Ziccardi, M.H.; Gulland, F.M.; Yochem, P.K.; Hird, D.W.; Rowles, T.; Mazet, J.A. Health risks for marine mammal workers. *Dis. Aqua. Org.* **2008**, *81*, 81–92. [CrossRef]
33. Waltzek, T.B.; Cortés-Hinojosa, G.; Wellehan, J.F., Jr.; Gray, G.C. Marine mammal zoonoses: A review of disease manifestations. *Zoonoses Public Health* **2012**, *59*, 521–535. [CrossRef]
34. Avendaño-Herrera, R.; Suarez, R.; Lazo, E.; Bravo, D.; Llegues, K.O.; Romalde, J.L.; Godoy, M.G. Genome sequence of *Streptococcus phocae* subsp. *salmonis strain C-4T, isolated from Atlantic salmon (Salmo salar). Genome Announc.* **2014**, *2*, 10–1128.
35. Numberger, D.; Siebert, U.; Fulde, M.; Valentin-Weigand, P. Streptococcal infections in marine mammals. *Microorganisms* **2021**, *9*, 350. [CrossRef] [PubMed]
36. Skaar, I.; Gaustad, P.; Tønjum, T.; Holm, B.; Stenwig, H. *Streptococcus phocae* sp. nov., a new species isolated from clinical specimens from seals. *Int. J. Sys. Evol. Microbiol.* **1994**, *44*, 646–650. [CrossRef] [PubMed]

Disclaimer/Publisher's Note: The statements, opinions and data contained in all publications are solely those of the individual author(s) and contributor(s) and not of MDPI and/or the editor(s). MDPI and/or the editor(s) disclaim responsibility for any injury to people or property resulting from any ideas, methods, instructions or products referred to in the content.

animals

MDPI

Case Report

A Case of Epicardial Epidermoid Cyst in a Crested Porcupine

Alessia Mariacher [1,*,†], Valentina Galietta [2,†], Gianni Massai [3], Francesco Bruni [4], Giovanni Ragionieri [3], Claudia Eleni [2] and Gianluca Fichi [3]

[1] Istituto Zooprofilattico Sperimentale delle Regioni Lazio e Toscana, UOT Toscana Sud, Viale Europa 30, 58100 Grosseto, Italy
[2] Istituto Zooprofilattico Sperimentale delle Regioni Lazio e Toscana, UOC Diagnostica Generale, Via Appia Nuova 1411, 00178 Rome, Italy; valentina.galietta@izslt.it (V.G.); claudia.eleni@izslt.it (C.E.)
[3] Istituto Zooprofilattico Sperimentale delle Regioni Lazio e Toscana, UOT Toscana Sud, Viale Toselli 12, 53100 Siena, Italy; gianluca.fichi@izslt.it (G.F.)
[4] Veterinary Practitioner, 53100 Siena, Italy
* Correspondence: alessia.mariacher@izslt.it; Tel.: +39-0564-456249
† These authors contributed equally to this work.

Simple Summary: One male adult crested porcupine was found moribund in the province of Siena (Tuscany, Central Italy), and died soon after being recovered by a wildlife rescue service. At necropsy, a rounded nodule was noted on the surface of the heart. Differential diagnoses included abscess, systemic tuberculosis, parasitic cyst, and neoplasia. Histology was performed on the lesion, revealing a cystic formation in the epicardium. The cyst was lined by stratified squamous epithelium and was filled with lamellar keratin without hair shafts. The lesion was diagnosed as an epicardial epidermoid cyst (EC). EC are most commonly found in the skin, both in human and animal patients, although rarely they can occur in various internal organs. However, cardiac EC has not been reported before in animals. To the best of our knowledge, this is the first report of EC in a wild animal species.

Abstract: The crested porcupine (*Hystrix cristata*) is present in central Italy with an estimated population of 1800 individuals. Despite the local abundance, little data are available on the diseases affecting free-ranging individuals. We describe a case of an epidermoid cyst (EC) in a male adult porcupine found in the municipality of Sovicille, province of Siena (Tuscany). At necropsy, a firm rounded nodule was noted on the left ventricle wall. Histological examination revealed a cystic formation lined by stratified squamous epithelium. The cyst was filled with lamellar keratin, while hair shafts were not present. The adjacent epicardium was infiltrated by lymphoplasmacytic cells in reaction to the rupture of the cyst with the spilling of keratinaceous debris. The lesion was diagnosed as a ruptured epicardial epidermoid cyst. EC are most commonly found in the skin, both in human and animal patients, though infrequently, they can occur in any internal organ. Cardiac EC has not been reported in domestic animals, and this is the first report of EC in a wild animal species. Clinical veterinarians should consider the possibility of similar cardiac lesions in captive subjects since the long lifespan of these rodents could allow the growth of the cyst with the compression of the adjacent tissues.

Keywords: choristoma; heart; heterotopia; histopathology; *Hystrix cristata*

1. Introduction

The crested porcupine (*Hystrix cristata*) outside of Africa is currently present in mainland Italy, Sicily, and Sardinia [1,2]. In the Italian peninsula, the species distribution is continuous in the central regions, while the distribution in the northern and southern regions is more fragmentary [3]. Species abundance in Tuscany was estimated to be 1803 individuals by Franchini and colleagues [4] through presence data obtained from camera traps, direct observations, and road-killing casualties.

Despite the local abundance and widespread presence in the Italian territory, little data are available on the health status of the crested porcupine population or on the common medical issues that can affect free-ranging individuals. It is reported that adult or subadult individuals are more frequently hospitalized in wildlife rescue centers, while a lower number of porcupettes gets rescued [5]; nonetheless, there are no reports of individual clinical assessments or pathologic data of the animals rescued in these facilities. The majority of the published works so far refer to parasitological studies in injured or road-killed porcupines, without the mention of clinical- or pathological- associated pictures. Cavallero et al. [6] performed a morphometrical and molecular analysis of *Trichocephalus* spp., in an attempt to identify distinct lineages infecting the species. Coppola and colleagues [7] reported a high prevalence of *Giardia* spp. on fecal samples, along with other less represented parasites (*Cryptosporidium* spp., *Trichocephalus* spp., gastrointestinal strongyles, Capillariids, and coccidian oocysts). In a study based on external examination only, 24% of the observed porcupines were infested by different species of fleas and/or ticks, with a higher prevalence for *Ixodes ricinus* and *Pulex irritans* [8], while a single case of sarcoptic mange was described with both gross and microscopic description in a female porcupine from southern Italy [9]. In addition, a case of a traumatic wound infested by *Calliphora vicina* larvae was reported in a juvenile female [10].

A case of systemic tuberculosis by *Mycobacterium bovis* was described in an adult male porcupine: at necropsy, pleuropneumonia with nodular lesions and mediastinal lymphadenitis were noted. Histologically, the lesions consisted of diffusive granulomatous foci, surrounded by epithelioid cells and giant multinucleated Langhans-type cells containing rod-shaped Z-N positive bacteria. The porcupine was regarded as a spill-over host in this instance [11]. A histopathological study was also conducted in a case of disseminated granulomatous pneumonia in a juvenile female porcupine, where cystic structures were observed, consistent with adiaspiromycosis by *Emmonsia crescens*, as further confirmed by a PCR assay [12]. *L. interrogans* serogroup Pomona serovar Pomona was isolated from one case of interstitial nephritis in a porcupette, leading the authors to hypothesize that the porcupine may represent a new host for this zoonotic bacterium [13].

As for viral infections, an outbreak of Encephalomyocarditis Virus (EMCV) infection in a captive setting and an RT-PCR positivity for Hepatitis E Virus in wild porcupines were also reported [14,15]. Gross and microscopic lesions were only described for EMCV, and consisted of interstitial myocarditis with grossly visible necrotic foci, and lymphocytic meningoencephalitis [14].

In this work, we describe the gross and microscopic findings that were found during the analysis of a specimen of an adult male porcupine, which was found dead in the province of Siena (Tuscany, Central Italy) in the spring of 2024. The examination of the subject revealed a small cardiac mass, whose histological diagnosis was a ruptured epicardial epidermoid cyst (EC). A description of the lesion and similar findings described in the literature in different animal species are provided.

2. Materials and Methods

In April 2024, a free-ranging crested porcupine was found moribund on the roadside in the municipality of Sovicille, in the province of Siena (Tuscany, Central Italy) (geographic coordinates: 43°29′05.5″ N, 11°00′05.3″ E). The animal was recovered by a wildlife rescue veterinary service but died in two days. The carcass was refrigerated at 4 °C and delivered within 12 h to the Istituto Zooprofilattico Sperimentale of Latium and Tuscany, Siena, for the investigation of the cause of death.

The autopsy was performed by veterinarian pathologists within 4 h, following the international standard procedures [16]. The carcass was identified following the literature description [17], and examined for any external abnormality and post-mortem lesions. After dissection, the internal organs were examined for any gross lesion. Parasitological, mycological, and bacteriological examinations were performed from external lesions, while internal organs, such as the lungs, spleen, liver, kidney, and pericardium, were

submitted for bacteriological examination. Feces were collected and conserved at 4 °C for parasitological examination.

Inocula from skin lesions and subcutaneous lesions, the lungs, spleen, liver, kidney, and pericardium were taken with a sterilized loop and plated onto Blood Agar and MacConkey Agar plates (IZSLT, Rome, Italy), and aerobically and anaerobically incubated at 37 °C for 24 h. Taxonomical analyses according to Bergey's Manual of Determinative Bacteriology [18] were conducted on the developed bacterial colonies. Briefly, the morphological characteristics of the colonies, Gram staining, and catalase and oxidase results were considered. For bacterial identification, the biochemical reactions were performed on API test strips (Biomerieux TM, Marcy-l'Étoile, France). Inocula from the skin were taken with a sterilized loop and plated on Sabouraud Dextrose Agar and incubated at 30 °C for 7 days, for mycological examination. After 7 days, the morphology of the fungi colonies was examined, and cell observation was performed through microscopic examination after Cotton Blue Lactophenol fresh staining [19]. Parasitological external and internal investigations were conducted, including the gross examination, and the examination of skin scraping samples, using a dissecting microscope after digestion through 10% potassium hydroxide [20].

A fecal sample was collected from the rectum and qualitatively examined according to previously published methods [21]. Samples of skin, subcutaneous lymph nodes, and heart were collected during the necropsy, fixed in 10% neutral buffered formalin, embedded in paraffin wax, sectioned at 4 μm, stained with Haematoxylin and Eosin (HE) and examined histologically under a light microscope.

3. Results

The subject under examination was identified as an adult male porcupine. The carcass was well preserved and free from colonization by cadaveric entomofauna. At necropsy, an external inspection revealed the presence of multiple wide skin erosions and ulcers, particularly severe in the maxillary and frontal regions (Figure 1a). Several abscesses in the subcutis and skeletal muscles were noted. Some abscesses formed fistulous tracts emerging at the neck and groin regions. After skin removal, another abscess was observed on the external surface of the right chest wall (Figure 1b). Generalized lymphadenopathy with enlarged and hyperaemic lymph nodes was present. In the thoracic cavity, chronic bilateral pneumonia with the consolidation of lung lobes was observed, along with pericarditis and myocarditis. In addition, on the epicardium of the left ventricle, a firm, rounded, raised whitish nodule, approximately 1 cm in size, was noted (Figure 2).



Figure 1. (**a**) Crested porcupine, head. Full-thickness ulceration of the skin in the frontal, maxillary, and nasal regions; (**b**) crested porcupine, right rib cage. After the removal of the skin (reflected on the right side of the image), a rounded mass of about 4 cm in diameter with a pasty consistency is observed on the caudal right rib cage, which at the cut surface is diagnosed as a non-calcified abscess.

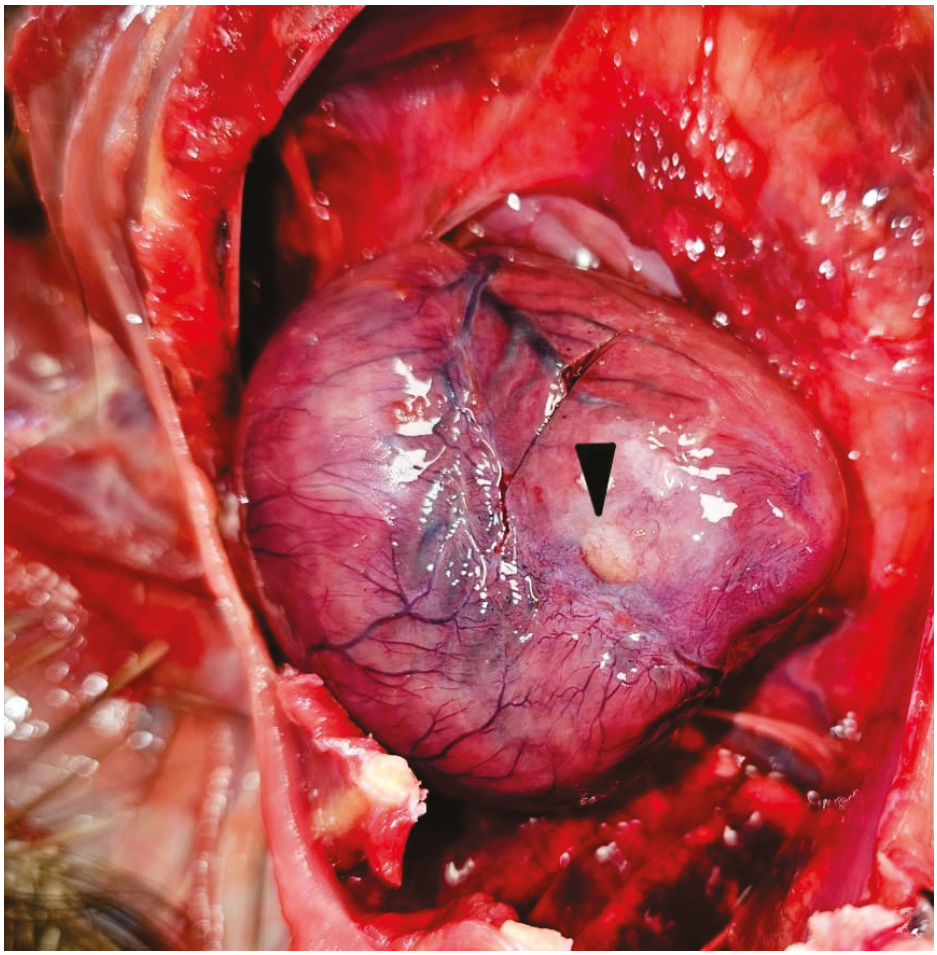


Figure 2. Crested porcupine, heart. A rounded whitish mass of approximately 1 cm in diameter is visible on the left ventricle wall (arrowhead).

Concerning bacteriology tests, *Staphylococcus aureus*, and *Streptococcus agalactiae* were identified after culturing from cutaneous lesions, while *S. agalactiae* was also isolated from abscesses in the subcutis and skeletal muscles, and in the intracardial blood clot. No pathogenic dermatophytes or ectoparasites were evidenced from skin lesions. At the parasitological examination of the carcass and feces, no internal parasites or eggs/oocysts were found. Differential diagnoses for the heart nodule, at this time, included abscess, nodular mycobacterial lesion, parasitic cyst, and neoplasia.

Histologically, the skin and subcutaneous tissue exhibited severe diffuse deep pyogranulomatous dermatitis and panniculitis (Figure 3), with numerous colonies of cocci. A similar inflammatory pattern was observed in the lymph nodes, presenting as severe multifocal pyogranulomatous lymphadenitis.

The histological examination of the heart revealed a mild diffuse lymphoneutrogranulocytic epicarditis and multifocal myocarditis. In the epicardium, a cystic formation was also observed. The cyst was lined by a well-differentiated stratified squamous epithelium (Figure 4) and contained lamellar keratin. Hair shafts were not present in the lumen of the cyst. The wall appeared discontinuous, with keratin spilling outward from the cyst. Additionally, a moderately loose fibrovascular stroma surrounding the cyst was diffusely infiltrated by lymphocytes, plasma cells, and a few neutrophils. The lesion was diagnosed as a ruptured epidermoid cyst.

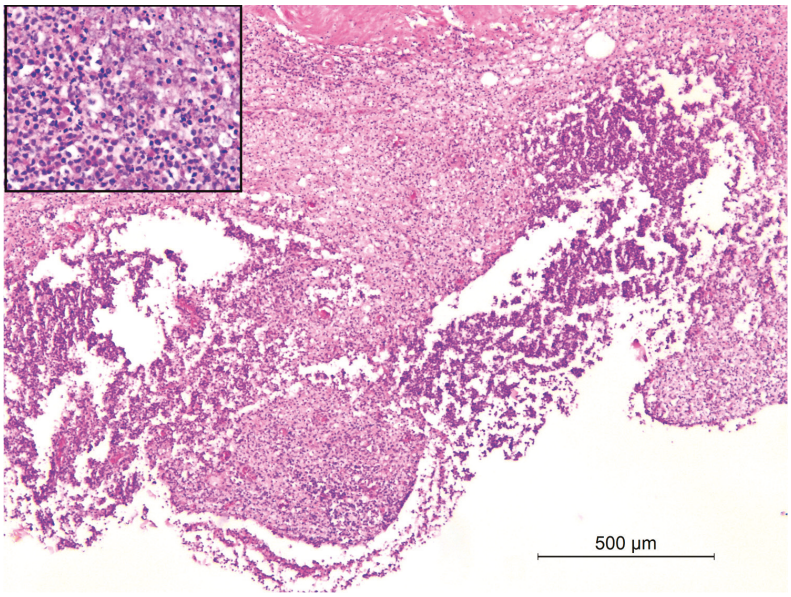


Figure 3. Subcutis adjacent to a skin abscess, crested porcupine. Severe diffuse pyogranulomatous panniculitis. Inset: detail of lesion with cellular debris, numerous degenerate neutrophils, epithelioid macrophages, and fewer lymphocytes and plasma cells (H&E, 5×).

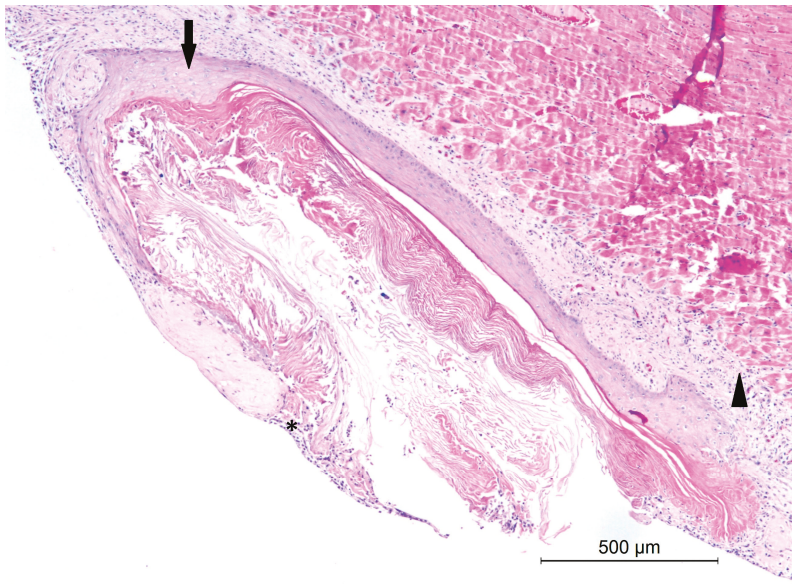


Figure 4. Epidermoid cyst, heart, crested porcupine. The histological section shows a cystic structure growing in the epicardium (arrowhead), with a wall of well-differentiated stratified squamous epithelium (arrow), which appears discontinuous with keratin spilling (asterisk) and moderate lymphocytic and neutrophilic infiltration (H&E, 5×).

4. Discussion

The porcupine specimen examined in this case report was primarily affected by diffuse skin lesions (pyogranulomatous dermatitis, ulcers, and abscesses) and generalized lymphadenitis. *S. aureus* and *S. agalactiae* were cultured from cutaneous lesions, a finding that is difficult to interpret since these bacteria are commensal skin bacteria and opportunistic pathogens in terrestrial mammals [22]. However, since *S. agalactiae* was also isolated from the intracardial blood clot, it is possible that the subject was suffering from septicemia related to severe skin lesions. Multiple skin abscesses were previously described in a case of sarcoptic mange in a porcupine, but in this case, we excluded this diagnosis based on

external findings, a negative search for ectoparasites, and the results of the histological examination, which did not reveal hyperplasia, hyperkeratosis, or mites [9]. The cause of the observed lesions cannot be determined unequivocally; however, we hypothesize that the subject may have been affected by episodes of intraspecific aggression with consequent traumatic and penetrating lesions from quills, as could be suggested, for example, by the presence of an abscess in the rib cage [23]. However, the most interesting aspect of the case is the finding of a peculiar lesion at the cardiac level.

The presence of differentiated noncardiac tissue in the heart is commonly referred to as cardiac heterotopia [24]. Intracardiac heterotopias are uncommon and, in almost all the cases reported in human medicine, the main aberrant tissue is of epithelial origin [25]. One type of cardiac heterotopia commonly reported in veterinary medicine is bovine myocardial epithelial inclusions, which consist of single to multiple foci of squamous to cuboidal epithelial cells, usually located in the left ventricle wall [26,27]. When heterotopic tissue is organized in discrete masses, it is rather referred to as a choristoma.

Epidermoid cysts (ECs) are rare, congenital, slow-growing, benign masses that arise from heterotopic epithelium. Grossly, these masses are usually described as rounded to oval, firm or with a soft core, with a smooth surface, and well circumscribed [28]. The macroscopic appearance can lead to a differential diagnosis of abscess [29], parasitic cyst, or malignancy [30]. At the histopathologic examination, EC is lined by a well-differentiated stratified squamous epithelium that resembles a normal epidermis and can contain the intraluminal breakdown products of desquamated epithelial cells, such as keratin, cholesterol crystals, or granules [31–33].

ECs are most commonly found in the skin, both in human and animal patients, though infrequently they can occur in any internal organ. Non-integumentary EC in human patients has been described in the brain, spleen, and gonads, with the cardiac location being a rarer occurrence [34,35]. In veterinary medicine, the most commonly reported locations are intracranial, intraspinal, and intraosseous, although many other organs, both in the thoracic and abdominal cavity, have been described as the possible sites of EC development, such as the rumen, intestine, spleen, and gonads (Table 1). However, cardiac EC has not been reported before in domestic animals, and there are no reports of EC in wild animal species.

Table 1. Anatomic locations of non-cutaneous epidermoid cysts reported in different animal species.

Animal Species	Anatomic Location	Reference
Dog	Nasopharynx	[36,37]
	Brain	[31,38–44]
	Spinal cord	[32,45–48]
	Diploe	[49]
	Bone	[50–54]
	Pelvic retroperitoneal space	[55]
	Intestine	[56,57]
	Spleen	[30]
	Mammary gland	[58]
Cat	Brain	[59]
	Intestine	[60]
	Lung	[61]
Cattle	Ovary	[29]
	Rumen	[62]
Rats, Mice	Brain and spinal cord	[63,64]
Horse	Intracranial	[65,66]
	Intra-articular	[67]
	Bone	[68,69]
Rabbit	Testis	[70]

Various hypotheses have been advanced regarding the origin of EC, which could be congenital (from the inclusion of ectodermal elements during embryological development) or acquired later in life, possibly as a result of penetrating injuries (including surgical procedures) or foreign body reactions. These latter events would allow the implantation of epidermal fragments in locations favorable to their growth [41,51]. In our case, it is not possible to determine a congenital or acquired origin of the described lesion, since we have no elements of the animal's history, nor from comparison with other cases, to support one hypothesis or the other. However, considering the observed skin lesions and the presence of multiple subcutaneous abscesses, we cannot exclude that porcupine quills, which can reach up to 30–40 cm in length [71], could have acted as foreign bodies in previous intraspecies conflicts.

It is possible that the mass had been growing over a certain time due to desquamation leading to an accumulation of keratinaceous material at the center of the cyst [34]. Furthermore, in the present case, the cyst wall appeared discontinuous, with keratin spilling outward and causing a lymphoplasmacytic and neutrogranulocytic infiltrate in the surrounding epicardium. Also in some previously reported cases, the EC wall was ruptured, resulting in the microscopic pictures of granulomatous nature consistent with foreign body reactions [53,59,67]. Even when the cyst wall is apparently intact, mild inflammation of the stroma surrounding the EC has been described [36,41,62], while the inflammatory component is usually absent in simple epithelial cysts [72].

The clinical significance of epicardial EC in the present case is doubtful. Since the mass did not occupy a significant space in the pericardial sac, and apparently it was not limiting the heart ventricular capacity, this may represent an incidental finding. However, since the porcupine has one of the longest lifespans among rodents (up to 28 years in captivity) [73], a space-occupying lesion in the heart could generate cardiovascular dysfunctions if allowed sufficient time for its growth. The possibility of similar cardiac lesions in captive subjects should be considered by wildlife or zoo veterinarians, since based on the lifespan of these rodents, the growth of the EC with the compression of the adjacent tissues could be expected.

5. Conclusions

Despite its widespread presence in Italy and its high protection status, the crested porcupine has been scarcely studied from a clinical and pathological point of view. In this report, we describe the case of a porcupine in which, in addition to the presence of a generalized infection by Gram-positive bacteria, a small whitish mass was observed in the epicardium of the left ventricle. The mass was histologically diagnosed as an epidermoid cyst. To the best of the authors' knowledge, this is the first case of cardiac epidermoid cyst in an animal patient and the first description in a wild species. The possibility of the development and growth of epidermoid cysts in captive porcupines, or in rescued subjects with a history of previous intraspecific conflicts involving the penetration of quills, should be considered by clinical veterinarians, since the long lifespan of these rodents may allow for the growth of EC with the compression of the adjacent tissues.

Author Contributions: Investigation, A.M., V.G., G.M., F.B., G.R., C.E. and G.F.; writing—original draft preparation, A.M. and V.G.; writing—review and editing, A.M., V.G., G.M., F.B., G.R., C.E. and G.F. All authors have read and agreed to the published version of the manuscript.

Funding: This research received no external funding.

Institutional Review Board Statement: This study did not require ethical approval.

Informed Consent Statement: Not applicable.

Data Availability Statement: The original contributions presented in the study are included in the article; further inquiries can be directed to the corresponding author.

Conflicts of Interest: The authors declare no conflicts of interest.

References

1. Amori, G.; De Smet, K. *Hystrix cristata*. The IUCN Red List of Threatened Species. 2016. Available online: https://doi.org/10.2305/IUCN.UK.2016-2.RLTS.T10746A22232484.en (accessed on 11 August 2024).
2. Milana, G.; Viviano, A.; Mori, E. Porcupines in Italian islands: Update on the distribution of *Hystrix cristata* in Sardinia. *Mammalia* **2023**, *87*, 162–165. [CrossRef]
3. Mori, E.; Ficetola, G.F.; Bartolomei, R.; Capobianco, G.; Varuzza, P.; Falaschi, M. How the South was won: Current and potential range expansion of the crested porcupine in Southern Italy. *Mamm. Biol.* **2021**, *101*, 11–19. [CrossRef]
4. Franchini, M.; Viviano, A.; Frangini, L.; Filacorda, S.; Mori, E. Crested porcupine (*Hystrix cristata*) abundance estimation using Bayesian methods: First data from a highly agricultural environment in central Italy. *Mammal Res.* **2022**, *67*, 187–197. [CrossRef]
5. Coppola, F.; Dari, C.; Vecchio, G.; Aloisi, M.; Romeo, G.; Biliotti, C.; Felicioli, A. Porcupettes Management at Wildlife Rescue Centers and Liberation into the Wild: Implications for Post-Liberation Success. *Animals* **2023**, *13*, 1546. [CrossRef] [PubMed]
6. Cavallero, S.; Di Filippo, M.M.; Mori, E.; Viviano, A.; De Liberato, C.; Sforzi, A.; D'amelio, S.; Berrilli, F. Morphological and molecular characterization of *Trichuris* sp. (nematoda: Trichuridae) in crested porcupines (*Hystrix cristata*; Rodentia: Hystricidae) from Italy. *Diversity* **2021**, *13*, 628. [CrossRef]
7. Coppola, F.; Maestrini, M.; Berrilli, F.; Guadano Procesi, I.; Felicioli, A.; Perrucci, S. First report of *Giardia duodenalis* infection in the crested porcupine (*Hystrix cristata* L., 1758). *Int. J. Parasitol. Parasites Wildl.* **2020**, *11*, 108–113. [CrossRef]
8. Mori, E.; Sforzi, A.; Menchetti, M.; Mazza, G.; Lovari, S.; Pisanu, B. Ectoparasite load in the crested porcupine *Hystrix cristata* Linnaeus, 1758 in Central Italy. *Parasitol. Res.* **2015**, *114*, 2223–2229. [CrossRef]
9. Amato, B.; Capucchio, M.T.; Fiasconaro, M.; Biasibetti, E.; Lastra, A.; Scaravelli, D.; Di Marco Lo Presti, V. A Case of Sarcoptic Mange in a crested porcupine (*Hystrix cristata*) from the Nebrodi Mountains (Sicily). *J. Comp. Pathol.* **2017**, *156*, 138. [CrossRef]
10. Scaravelli, D.; Senini, C.; Bonacci, T. First case of traumatic myiasis caused by *Calliphora vicina* in a crested porcupine *Hystrix cristata* L. in Italy. *J. Entomol. Acarol. Res.* **2017**, *49*, 81–84. [CrossRef]
11. Cambiotti, V.; Angeloni, G.; Conquista, M.; Rossi, G.; Galosi, L.; Manuali, E.; Pavone, S.; Barboni, R.C.; Papa, P.; Faccenda, L.; et al. Systemic bovine tuberculosis in a crested porcupine (*Hystrix cristata*) in the Marche region, italy. *J. Wildl. Dis.* **2021**, *57*, 705–707. [CrossRef] [PubMed]
12. Morandi, F.; Galuppi, R.; Buitrago, M.J.; Delogu, M.; Lowenstine, L.J.; Panarese, S.; Benazzi, C.; Sarli, G. Disseminated Pulmonary adiaspiromycosis in a Crested Porcupine (*Hystrix cristata* Linnaeus, 1758). *J. Wildl. Dis.* **2012**, *48*, 523–525. [CrossRef] [PubMed]
13. Cilia, G.; Bertelloni, F.; Coppola, F.; Turchi, B.; Biliotti, C.; Poli, A.; Parisi, F.; Felicioli, A.; Cerri, D.; Fratini, F. Isolation of *Leptospira* serovar *Pomona* from a crested porcupine (*Hystrix cristata*, L., 1758). *Vet. Med. Sci.* **2020**, *6*, 985–991. [CrossRef] [PubMed]
14. Cardeti, G.; Mariano, V.; Eleni, C.; Aloisi, M.; Grifoni, G.; Sittinieri, S.; Dante, G.; Antognetti, V.; Foglia, E.A.; Cersini, A.; et al. Encephalomyocarditis virus infection in *Macaca sylvanus* and *Hystrix cristata* from an Italian rescue centre for wild and exotic animals. *Virol. J.* **2016**, *13*, 193. [CrossRef] [PubMed]
15. Pirani, S.; Pierini, I.; Manuali, E.; Bazzucchi, M.; De Mia, G.M.; Giammarioli, M. Paslahepevirus balayani (Hepatitis E Virus) in Italian Nonungulate Wildlife: Molecular Detection and Characterization of an Isolate from a Crested Porcupine (*Hystrix cristata*). *J. Wildl. Dis.* **2023**, *59*, 460–464. [CrossRef]
16. Woodford, M.H.; Keet, D.F.; Bengis, R.G. *Post-Mortem Procedures for Wildlife Veterinarians and Field Biologists*; OIE: Paris, France, 2001.
17. Walid, M.F. The Crested Porcupine *Hystrix cristata* (Linnaeus, 1758) in Misurata, Libyya. *J. Ecol. Nat. Environ.* **2011**, *3*, 228–231.
18. Bergey, D.H. *Bergey's Manual of Determinative Bacteriology*; Williams & Wilkins: Baltimore, MD, USA, 1994.
19. Rebell, G.; Taplin, D. *Dermatophytes: Their Recognition and Identification*; University of Miami Press: Coral Gables, FL, USA, 1970.
20. OIE. Mange. In *Manual of Diagnostic Tests and Vaccines for Terrestrial Animals*; OIE: Paris, France, 2019; Chapter 3.9.7.
21. Mariacher, A.; Santini, A.; Del Lesto, I.; Tonon, S.; Cardini, E.; Barone, A.; Eleni, C.; Fichi, G.; Perrucci, S. Endoparasite infections of the european hedgehog (*Erinaceus europaeus*) in central Italy. *Animals* **2021**, *11*, 3171. [CrossRef]
22. Ross, A.A.; Rodrigues Hoffmann, A.; Neufeld, J.D. The skin microbiome of vertebrates. *Microbiome* **2019**, *7*, 79. [CrossRef]
23. Švara, T.; Zdovc, I.; Gombač, M.; Pogačnik, M. Quill injury—Cause of death in a captive Indian crested porcupine (*Hystrix indica*, KERR, 1792). *Maced. Vet. Rev.* **2015**, *38*, 119–122. [CrossRef]
24. Bundza, A.; Dukes, T.W. Some heterotopic tissue remnants in domestic animals. *Can. Vet. J.* **1978**, *19*, 322–324.
25. Ariza, S.; Rafel, E.; Castillo, J.A.; Garcia-Canton, J.A. Intracardiac heterotopia—Mesenchymal and endodermal. *Br. Heart J.* **1978**, *40*, 325–327. [CrossRef] [PubMed]
26. Nordstoga, K.; Aleksandersen, M. Epithelial Inclusions in the Bovine Myocardium. *Vet. Pathol.* **1988**, *25*, 525–526. [CrossRef] [PubMed]
27. Baker, D.C.; Schmidt, S.P.; Langheinrich, K.A.; Cannon, L.; Smart, R.A. Bovine Myocardial Epithelial Inclusions. *Vet. Pathol.* **1993**, *30*, 82–88. [CrossRef] [PubMed]
28. Vail, D.M.; Withrow, S.J. Tumors of the Skin and Subcutaneous Tissues. In *Withrow & MacEwen's Small Animal Clinical Oncology*; W.B. Saunders: St. Louis, MO, USA, 2007; pp. 375–401. [CrossRef]
29. Edwards, J.F. Three Cases of Ovarian Epidermoid Cysts in Cattle. *Vet. Pathol.* **2002**, *39*, 744–746. [CrossRef]
30. Lee, N.; Kim, D.Y.; Kim, Y.J.; Kim, D.Y. Splenic epidermoid cyst in a dog. *J. Vet. Diagnostic Investig.* **2023**, *35*, 209–211. [CrossRef]
31. Kornegay, J.N.; Gorgacz, E.J. Intracranial Epidermoid Cysts in Three Dogs. *Vet. Pathol.* **1982**, *19*, 646–650. [CrossRef]

32. Devathasan, D.; Murakami, M.; Miller, M.A.; Thomovsky, S.A.; Lewis, M.J. Case Report: Recurrence of an Extradural Spinal Epidermoid Cyst Following Surgical Excision in a Dog. *Front. Vet. Sci.* **2022**, *9*, 871023. [CrossRef]
33. Hagr, A.; Laberge, J.M.; Nguyen, L.T.; Emil, S.; Bernard, C.; Patenaude, Y. Laparoscopic excision of subdiaphragmatic epidermoid cyst: A case report. *J. Pediatr. Surg.* **2001**, *36*, 1–2. [CrossRef]
34. Leef, G.; Davis, K.; Wu, K.C.; Mukherjee, M.; Madrazo, J.A. Right Atrial Epidermoid Cyst: An Unusual Mass Discovered in the Workup for Arrhythmia in Pregnancy. *Case* **2021**, *5*, 408–411. [CrossRef]
35. Wang, J.X.; Chen, Y.X.; Chen, X.Y.; Wang, H.Y.; Zhao, S.H. Epidermoid cyst in the atrial septum: A rare entity with unique imaging features. *Eur. Hear. J.—Case Rep.* **2022**, *6*, ytac267. [CrossRef]
36. Murgia, D.; Pivetta, M.; Bowlt, K.; Volmer, C.; Holloway, A.; Dennis, R. Intranasal epidermoid cyst causing upper airway obstruction in three brachycephalic dogs. *J. Small Anim. Pract.* **2014**, *55*, 431–435. [CrossRef] [PubMed]
37. Ellison, G.W.; Donnell, R.L.; Daniel, G.B. Nasopharyngeal epidermal cyst in a dog. *J. Am. Vet. Med. Assoc.* **1995**, *207*, 1590–1592. [CrossRef] [PubMed]
38. Mawdesley-Thomas, L.E.; Hague, P.H. An intra-cranial epidermoid cyst in a dog. *Vet. Rec.* **1970**, *87*, 133–134. [CrossRef]
39. Kawaminami, A.; Tawaratani, T.; Nakazawa, M.; Uchimoto, H.; Sumi, N. A case of muItiloculated, intracranial epidermoid cyst in a beagle dog. *Lab. Anim.* **1991**, *25*, 226–227. [CrossRef] [PubMed]
40. Platt, S.R.; Graham, J.; Chrisman, C.L.; Adjiri-Awere, A.; Clemmons, R.M. Canine intracranial epidermoid cyst. *Vet. Radiol. Ultrasound* **1999**, *40*, 454–458. [CrossRef] [PubMed]
41. MacKillop, E.; Schatzberg, S.J.; De Lahunta, A. Intracranial epidermoid cyst and syringohydromyelia in a dog. *Vet. Radiol. Ultrasound* **2006**, *47*, 339–344. [CrossRef]
42. Steinberg, T.; Matiasek, K.; Brühschwein, A.; Fischer, A. Imaging diagnosis—Intracranial epidermoid cyst in a doberman pinscher. *Vet. Radiol. Ultrasound* **2007**, *48*, 250–253. [CrossRef]
43. De Decker, S.; Davies, E.; Benigni, L.; Wilson, H.; Pelligand, L.; Rayner, E.L.; Shihab, N.; Volk, H.A. Surgical Treatment of an Intracranial Epidermoid Cyst in a Dog. *Vet. Surg.* **2012**, *41*, 766–771. [CrossRef]
44. Konar, M.; Horvat, B.; Lorinson, D. Magnetic resonance imaging—A method for in vivo tissue diagnosis of epidermoid cysts in dogs? *Kleintierpraxis* **2001**, *46*, 645.
45. Tomlinson, J.; Higgins, R.J.; LeCouteur, R.A.; Knapp, D. Intraspinal epidermoid cyst in a dog. *J. Am. Vet. Med. Assoc.* **1988**, *193*, 1435–1436.
46. Cappello, R.; Lamb, C.R.; Rest, J.R. Vertebral epidermoid cyst causing hemiparesis in a dog. *Vet. Rec.* **2006**, *158*, 865–867. [CrossRef]
47. Shamir, M.H.; Lichovsky, D.; Aizenberg, I.; Chrisman, C.L. Partial surgical removal of an intramedullary epidermoid cyst from the spinal cord of a dog. *J. Small Anim. Pract.* **1999**, *40*, 439–442. [CrossRef] [PubMed]
48. Lipitz, L.; Rylander, H.; Pinkerton, M.E. Intramedullary epidermoid cyst in the thoracic spine of a dog. *J. Am. Anim. Hosp. Assoc.* **2011**, *47*, e145–e149. [CrossRef] [PubMed]
49. Lee, S.; Jang, M.; Mann, F.A.; Choi, S.; Lee, J.K.; Kim, J.K. Intradiploic epidermoid cyst in a dog. *J. Am. Vet. Med. Assoc.* **2020**, *257*, 183–188. [CrossRef] [PubMed]
50. Liu, S.K.; Dorfman, H.D. Intraosseous Epidermoid Cysts in Two Dogs. *Vet. Pathol.* **1974**, *11*, 230–234. [CrossRef]
51. Frank, H.; Kirchhof, N.; Biesenbach, W.; Frese, K. Intraosseous epidermoid cysts of the toe phalanx in dogs. *Berl. Munch. Tierarztl. Wochenschr.* **1995**, *108*, 73–76.
52. Featherstone, H.; Llabres Diaz, F. Maxillary bone epithelial cyst in a dog. *J. Small Anim. Pract.* **2003**, *44*, 541–545. [CrossRef]
53. Vagias, M.; Cassidy, J.P.; Skelly, C.; Mullins, R.A. Intraosseous epidermoid cysts of adjacent digits in a dog. *BMC Vet. Res.* **2020**, *16*, 1–9. [CrossRef]
54. Homer, B.L.; Ackerman, N.; Woody, B.J.; Green, R.W. Intraosseous epidermoid cysts in the distal phalanx of two dogs. *Vet. Radiol. Ultrasound* **1992**, *33*, 133–137. [CrossRef]
55. Annoni, M.; Botazzoli, A.; Bertazzolo, W. Short communication: Retroperitoneal epidermoid cyst in a dog. *Vet. Rec.* **2013**, *173*, 220. [CrossRef]
56. Shimamura, S.; Kainuma, R.; Kimura, K.; Okamura, Y.; Kobayashi, S.; Katayama, M.; Sato, R.; Yasuda, J. Epidermoid cyst of the ileum in a miniature dachshund dog. *Can. Vet. J.* **2014**, *55*, 366–368. [PubMed]
57. Ogden, J.A.; Heng, H.G.; Ramos-Vara, J.A. Epidermoid cysts associated with the gastrointestinal tract in a dog. *J. Small Anim. Pract.* **2022**, *63*, 163. [CrossRef] [PubMed]
58. Viscone, É.A.; Nakagaki, K.Y.R.; Wronski, J.G.; Nunes, M.M.; Cassali, G.D. Epidermoid Cyst in the Bitch Mammary Gland. *Acta Sci. Vet.* **2023**, *51*, 21–24. [CrossRef]
59. Mazaro, R.D.; Lorenzetti, D.M.; Paz, M.C.; Fighera, R.A. Intracranial epidermoid cyst in a cat. *Cienc. Rural* **2021**, *51*, 1990–1993. [CrossRef]
60. Niederhäuser, S.; Schaffartzik, A.; Tschuor, F.; Baeumlin, Y.; Kühn, N.; Glaus, T. Intestinal epidermoid cyst in a cat. *Schweiz. Arch. Tierheilkd.* **2015**, *157*, 559–562. [CrossRef] [PubMed]
61. Milli, U.H.; Haziroglu, R. Pulmonary epidermoid cysts in a cat. *Vet. Rec.* **1990**, *127*, 287.
62. Ohfuji, S. Epidermoid cysts of the rumen in a holstein-friesian steer. *J. Comp. Pathol.* **2014**, *151*, 80–82. [CrossRef]
63. Nobel, T.A.; Nyska, A.; Pirak, M.; Skolnik, M.; Meshorer, A. Epidermoid cysts in the central nervous system of mice. *J. Comp. Pathol.* **1987**, *97*, 357–359. [CrossRef]

64. Kulwich, B.A. Epidermoid Cysts in the Central Nervous System of Rats and Mice: An Incidental Finding in Toxicity/Oncogenicity Studies. *Vet. Pathol.* **1994**, *31*, 475–478. [CrossRef]
65. Peters, M.; Brandt, K.; Wohlsein, P. Intracranial epidermoid cyst in a horse. *J. Comp. Pathol.* **2003**, *129*, 89–92. [CrossRef]
66. Kelly, D.F.; Watson, W.J.B. Epidermoid cyst of the brain in the horse. *Equine Vet. J.* **1976**, *8*, 110–112. [CrossRef] [PubMed]
67. Hibner-Szaltys, M.; Hann, M.J.; Woods, S.C.C.; Rocchigiani, G.; Stack, J.D. Diagnosis and arthroscopic removal of an intra-articular epidermoid cyst in the distal interphalangeal joint of a 15-year-old horse. *Equine Vet. Educ.* **2023**, *35*, e290–e295. [CrossRef]
68. Camus, A.C.; Burba, D.J.; Valdes, M.A.; Taylor, H.W. Intraosseous epidermoid cyst in a horse. *J. Am. Vet. Med. Assoc.* **1996**, *209*, 632–633. [CrossRef] [PubMed]
69. Headley, S.A.; Kummala, E.; Saarinen, H.; Tupamäki, A.; Tulamo, R.M. Diagnostic exercise: Intraosseous epidermoid cysts in the third phalanx of a dressage mare. *Vet. Pathol.* **2009**, *46*, 355–357. [CrossRef] [PubMed]
70. Wijnands, M. Multiple epidermoid cysts in the testis of a New Zealand White rabbit: A case report. *Exp. Toxicol. Pathol.* **2012**, *64*, 873–874. [CrossRef] [PubMed]
71. Mori, E.; Maggini, I.; Menchetti, M. When quills kill: The defense strategy of the crested porcupine *Hystrix cristata* L., 1758. *Mammalia* **2014**, *78*, 229–234. [CrossRef]
72. Davidson, H.J.; Blanchard, G.L. Periorbital epidermoid cyst in the medial canthus of three dogs. *J. Am. Vet. Med. Assoc.* **1991**, *198*, 271–272. [CrossRef]
73. Weigl, R. *Longevity of Mammals in Captivity: From the Living Collections of the World*; Schweizerbart Science Publishers: Stuttgart, Germany, 2005.

Disclaimer/Publisher's Note: The statements, opinions and data contained in all publications are solely those of the individual author(s) and contributor(s) and not of MDPI and/or the editor(s). MDPI and/or the editor(s) disclaim responsibility for any injury to people or property resulting from any ideas, methods, instructions or products referred to in the content.

animals

MDPI

Article

Serological Investigation for *Brucella ceti* in Cetaceans from the Northwestern Mediterranean Sea

Laura Martino [1,*], María Cuvertoret-Sanz [2], Sarah Wilkinson [2], Alberto Allepuz [1], Albert Perlas [1], Llilianne Ganges [3], Lola Pérez [4] and Mariano Domingo [1]

[1] Departament de Sanitat i Anatomia Animals, Facultat de Veterinària, Universitat Autònoma de Barcelona, 08193 Bellaterra, Spain; alberto.allepuz@uab.cat (A.A.); mariano.domingo@uab.cat (M.D.)
[2] Servei de Diagnòstic de Patologia Veterinària, Facultat de Veterinària, Universitat Autònoma de Barcelona, 08193 Bellaterra, Spain; maria-cuvertoret@idexx.com (M.C.-S.); sarah@vetscape.co.za (S.W.)
[3] IRTA—Institut de Recerca en Sanitat Animal, Programa de Sanitat Animal, Centre de Recerca en Sanitat Animal (CReSA), 08193 Bellaterra, Spain; llilianne.ganges@irta.cat
[4] Facultat de Veterinària de Barcelona, Universitat Autònoma de Barcelona, 08193 Bellaterra, Spain; lola.perez@uab.cat
* Correspondence: laura.martinog@autonoma.cat

Simple Summary: *Brucella ceti* is a marine bacterium that causes neurological, reproductive and skeletal disease in free-ranging cetaceans. Its zoonotic potential and importance for wild animals has prompted, over the years, the search for a reliable diagnostic method to detect antibodies and infer the level of infection. In this work, we perform an exploratory serological study on cetaceans stranded in the Northwestern Mediterranean Sea. Antibody levels were higher in animals with confirmed *Brucella* disease and infection in juveniles and in animals with chronic morbilliviral infection. This provides the first seroprevalence estimation in this area and reaffirms the active circulation of *Brucella* in wild cetaceans.

Abstract: Neurobrucellosis in cetaceans, caused by *Brucella ceti*, is a relevant cause of death in striped dolphins (*Stenella coeruleoalba*) from the Mediterranean Sea. Serological tests are not used as a routinary technique for the diagnosis of this infection. We briefly describe the pathological findings of nine free-ranging stranded cetaceans diagnosed with *Brucella* disease or infection in our veterinary necropsy service from 2012 to 2022. The findings included focal diskospondylitis and non-suppurative meningitis, choroiditis and radiculitis. Additionally, an exploratory serological study was conducted in sixty-six frozen sera collected in the period 2012–2022 from fifty-seven striped dolphins, five Risso's dolphins (*Grampus griseus*), two common bottlenose dolphins (*Tursiops truncatus*), one common dolphin (*Delphinus delphis*) and one pilot whale (*Globicephala melas*) to compare antibody levels in *Brucella*-infected (n = 8) and non-infected (n = 58) animals, classified by the cause of death, sex, age class and cetacean morbillivirus (CeMV) infection status. The authors hypothesized that active infection in cases of neurobrucellosis would elicit a stronger, detectable humoral response compared to subclinical infections. We performed a commercial competition ELISA (cELISA) using serial serum dilutions for each sample, considering a percentage of inhibition (PI) of $\geq$40% as positive. A titer of 1:160 was arbitrarily determined as the seropositivity threshold. Seropositive species included striped dolphins and Risso's dolphins. Seroprevalence was higher in animals with neurobrucellosis (87.5%) compared to the overall seroprevalence (31.8%) and to other causes of death, indicating, likely, a high sensitivity but low specificity for neurobrucellosis. Animals with chronic CeMV seemed to have higher seroprevalences, as well as juveniles, which also had a higher disease prevalence. These results indicate, as in other studies, that antibodies are not decisive against clinical brucellosis, although they may indicate a carrier state, and that CeMV may influence *Brucella* epidemiology. More research is required to elucidate the epidemiology and pathogenesis and to resolve the complicated host–pathogen interaction in *Brucella* species.

Keywords: brucellosis; serology; antibodies; ELISA; morbillivirus; dolphin; stranding; necropsy

1. Introduction

Brucellosis in cetaceans was first described in 1994 [1] and is caused by *Brucella ceti* [2]. Since then, infection and disease associated with *B. ceti* have been increasingly recognized in many cetacean species worldwide [3,4], and brucellosis is considered an emerging threat for odontocetes and mysticetes [5]. In the Mediterranean Sea, cetacean brucellosis was first diagnosed in 2013, and more cases have been reported since then [6–10], but serological evidence of exposure was already detected in dolphins stranded along the Mediterranean coast of Spain in 1997–1999 [11], suggesting that Mediterranean dolphins were already exposed to the pathogen at that time. Disease due to *B. ceti* in cetaceans can occur as neurobrucellosis, reproductive disease, spinal diskospondylitis or abscesses (frequently cutaneous and subcutaneous) [4]. However, in many other instances, serological evidence of infection has been found in asymptomatic cetaceans, and *B. ceti* has been isolated from tissues of apparently healthy cetaceans, suggesting that *Brucella*-infected cetaceans may overcome initial infection and survive or become *Brucella* carriers (see for review [3,4]). Health assessment of wild cetacean populations is usually conducted through necropsy of stranded dolphins and laboratory investigation. Since the first description of disease associated with *B. ceti* in the Catalan Mediterranean coast [8], we have intensified efforts to detect *Brucella* in stranded cetaceans. In this paper we describe the cases of brucellosis detected in the period 2012 to 2022 in the Northwestern Mediterranean coast. Moreover, we perform an exploratory serological analysis using a commercial cELISA to compare the antibody levels between infected and non-infected animals to determine if animals with *Brucella*-associated lesions have higher antibody titers than potential subclinical carriers. Serological results were compared by age groups, sex, and cetacean morbillivirus (CeMV) status, with a special emphasis on striped dolphins. CeMV is assessed routinely in all cetaceans, and in *Brucella* cases, the coinfections were investigated because of the reports of coinfection in other areas [12] and to explore the effect CeMV infection has on anti-*Brucella* antibody production. The general aims were to provide information about the epidemiology and pathogenesis of *B. ceti* infection and to evaluate its impact on cetacean species in the area.

2. Materials and Methods

2.1. Cases Investigated and Necropsy Procedure

A total of 123 cetaceans stranded along the Catalan coast during the period 2012–2022 were necropsied at the Universitat Autònoma de Barcelona, according to standard procedures [13]. Necropsied species included striped dolphins (*Stenella coeruleoalba*) (n = 97), common bottlenose dolphins (*Tursiops truncatus*) (n = 11), Risso's dolphins (*Grampus griseus*) (n = 10), common dolphins (*Delphinus delphis*) (n = 2), a fin whale (*Balaenoptera physalus*), a pilot whale (*Globicephala melas*) and a Cuvier's beaked whale (*Ziphius cavirostris*). Condition code ranged from 1 to 3 (animals in overt autolysis were not transported for necropsy) following the scale of Kuiken and García-Hartmann 1991 [14]. Retrieval of cerebrospinal fluid (CSF) was routinely attempted from the atlanto-occipital joint, or directly from the lateral ventricle after extraction of the brain. Frozen samples and swabs from multiple organs were collected for bacteriological and molecular investigations. A complete set of organs was sampled for histopathology, fixed in 10% neutral buffered formalin and routinely processed. Routine immunohistochemistry and RT-PCR for surveillance of CeMV were performed on lung, diaphragmatic lymph node and brain [15]. Cause of death was determined using a combination of computed tomography scan, complete necropsy, routine histopathology of multiple organs, CeMV PCR and immunohistochemistry (IHC) and, when required, microbiological culture (see [15] for details). After the determination of the cause of death, animals were classified in different groups: bycatch, neurobrucellosis, CeMV, PEM (polioencephalomalacia of unknown origin), mother–calf separation, infectious/inflammatory

causes, sinusitis by *Crassicauda grampicola*, other and unknown. "Infectious/inflammatory" cause of death comprised peritonitis, septicemia, protozoal infections, severe parasitism (other than *C. grampicola*), diskospondylitis, mucormycosis, bacterial meningoencephalitis (negative *Brucella* culture), necrotizing enteritis, erysipelas and meningoencephalitis of unknown origin. "Other" included animals dying from tension pneumothorax, abortion and muscular degeneration.

2.2. Serology for Brucella

Blood retrieval was attempted by cardiac puncture as soon as possible after reception of each cadaver with a 20 mL syringe and a 16G, 1.7 × 133 mm catheter needle (Angiocath™, BD, REF 382259, Franklin Lakes, NJ, USA) and portioned in vacutainer plain tubes. Blood was centrifuged at 2500× *g* for 10 min, and serum was aliquoted in 1 mL cryotubes and frozen at −80 °C until use.

For the present serological study, available serum samples from 2012 to 2022 (n = 66; 57 striped dolphins, 5 Risso's dolphins, 2 common bottlenose dolphins, 1 common dolphin and 1 pilot whale) were defrosted (see Supplementary File S1 for all cetacean samples). A commercial blocking ELISA (INgezim *Brucella* Compac, INGENASA, Madrid, Spain) was used following the manufacturer's instructions. This competitive ELISA test (*Brucella* cELISA) is a multispecies kit developed for detection of blocking antibodies against LPS of *Brucella* abortus in domestic ruminants and swine serum samples, using a peroxidase-conjugated secondary monoclonal antibody directed to the LPS of *B. abortus*. The dilution of the serum sample for cetaceans is not established for the test and, therefore, sera were diluted as recommended by the manufacturer for ovine and caprine sera (1:5), bovine and porcine sera (1:10), and additionally at 1:20, 1:40, 1:80 and 1:160. Serum of culture-confirmed *Brucella*-infected cases (n = 8) were further diluted to 1:320, 1:640, 1:1280, 1:2560, 1:5120 and 1:10240. Optical density (OD) values were measured at 450 nm within 5 min after the addition of stop solution using a spectrophotometer (FLx800, Bio-Tek Instruments, Winooski, VT, USA). OD values were used to calculate the final results, read as a percentage of inhibition (PI) in comparison to positive and negative control sera included in the kit, with the formula PI = 100 × [1 − (OD test sample/OD negative control)], where OD = optical density. Following the procedures of the test, a sample was classified as positive if the PI in the well was ≥40%.

The possible association between the level of hemolysis and the *Brucella* cELISA result was investigated in a non-published preliminary study. Briefly, the level of hemolysis was visually graded in the first dilution of samples when dispensed onto the ELISA plate into group 1 (non-hemolyzed or slightly hemolyzed serum) and group 2 (hemolyzed serum or hemolyzed blood). A comparison of positive and negative results in *Brucella* cELISA (for 1:20 dilutions and 1:40 dilutions) with the hemolysis score was performed with the Wilcoxon two-sample test (Epi Info Package, www.cdc.gov/epiinfo/index.html (accessed on 19 August 2024)).

2.3. Brucella Isolation

Brucella isolation, the gold standard for brucellosis diagnosis, was attempted in dolphins with compatible lesions, a positive reaction to Rose Bengal Test or with CeMV infection. Samples used for *Brucella* isolation were frozen swabs from the lateral cerebral ventricle, periventricular cerebral tissue, cerebrospinal fluid (CSF), spleen, mesenteric lymph node, or swabs from spondylytic lesions. Bacterial culture was performed as previously described [8]. Briefly, tissue samples were superficially sterilized, homogenized in saline buffer and cultured in plates of both Farrell and CITA selective media. Isolates were identified as marine *Brucella* using a Bruce-ladder PCR [16]. Confirmation of *Brucella ceti* as the isolated species was conducted by a multiplex PCR adapted from Bruce-ladder [16].

2.4. Age Determination

The age of the 57 striped dolphins with serological analysis was estimated using a Gompertz formula established for this species in the Northwestern Mediterranean Sea [17]. Subsequently, animals were divided into four age ranges (fetus, calves, juveniles and adults), considering adulthood as being above 6 years [18].

2.5. Data Analysis

Differences between antibody titers in striped dolphins, grouped by their cause of death and age, were compared in two-way contingency tables and using Fisher's test. R software (version 4.4.0) was used to introduce data and elaborate the tables and StatCalc tool, from EpiInfo (version 7.2.6.0), to retrieve significance of the results. Significance was considered with p-value < 0.05.

3. Results

3.1. Pathological Investigation

See Supplementary File S2 for biometrical data, cause of death and ancillary test results in the 123 cetaceans. Nine cases of infection by *Brucella ceti* were detected among the one hundred twenty-three (7.3%) necropsied cetaceans, eight striped dolphins and one common bottlenose dolphin. Seven of the nine dolphins stranded alive and died shortly thereafter (n = 4) or were euthanized due to bad prognosis (n = 3). Five of them showed neurological signs, disorientation or abnormal swimming before death (301/12, 319/16, 368/19, 314/19 and 333/22). Biometric and stranding data from the nine cetaceans with brucellosis are shown in Table 1, and the stranding location is depicted in Figure 1. In two animals, the meningeal turbidity was visible grossly, and in one there was a mild hydrocephalus (Figure 2). Seven striped dolphins had neurobrucellosis, characterized by a severe diffuse or multifocal non-suppurative meningitis or meningoencephalitis, in some cases more intense in the cerebellum and brainstem (Figure 3), and including choroiditis and radiculoneuritis. The other striped dolphin showed a subacute systemic CeMV infection, with an intense encephalitis and less meningeal involvement. Morbilliviral encephalitis was considered the cause of death in this dolphin. The common bottlenose dolphin had ankylosing spondylitis. Macroscopic and microscopic findings of the *Brucella*-infected cases are summarized in Table 2.

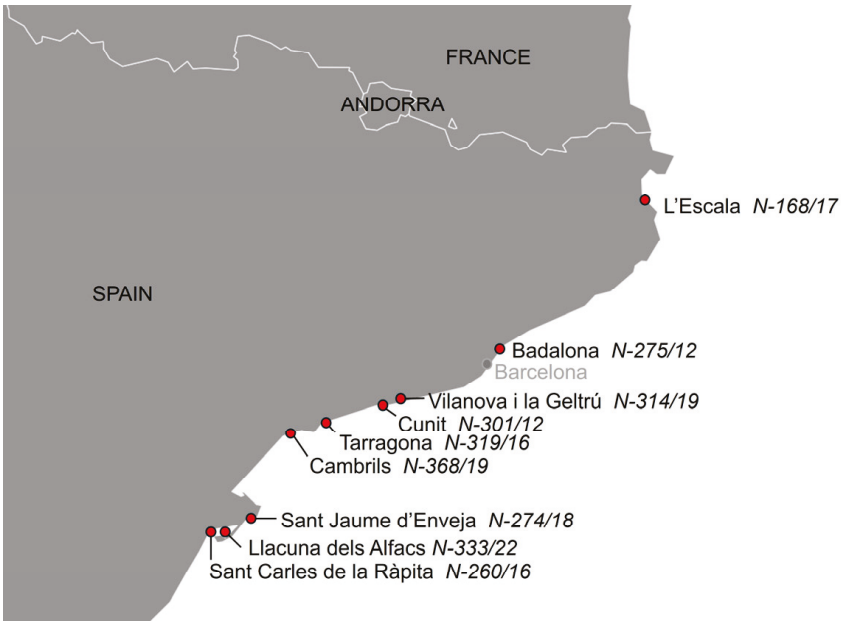


Figure 1. Map showing the stranding location of 9 cetaceans with *Brucella* infection, 7/9 of them with neurobrucellosis.

Table 1. Biometric data and stranding information of the 9 dolphins with brucellosis. J = juvenile. Ad = adult. D = found dead. A = stranded alive. All animals are striped dolphins except N-275/12, which is a common bottlenose dolphin.

ID	Date	Place of Stranding	Age Class	Age Estimation	Length (cm)	Weight (kg)	Sex	A/D
N-275/12	23 May 2012	Badalona	Ad	-	300	Unknown	M	D
N-301/12	3 June 2012	Cunit	Ad	6.25	184	54.5	F	A
N-260/16	19 June 2016	Sant Carles de la Ràpita	J	3.88	170	39.5	F	D
N-319/16	8 September 2016	Tarragona	J	5.35	180	47	F	A
N-168/17	18 April 2017	L'Escala	Ad	10.39	193	79	M	A
N-274/18	24 June 2018	Sant Jaume d'Enveja	J	2.43	152	38	M	A
N-314/19	1 September 2019	Vilanova i la Geltrú	J	2.8	159	41	F	A
N-368/19	12 October 2019	Cambrils	J	5.23	175	47	M	A
N-333/22	22 September 2022	Llacuna dels Alfacs	Ad	6.15	180	47.5	M	A

Table 2. Summary of the signalment and pathological findings in 8 striped dolphins and a bottlenose dolphin (N-275/12) (*, previously published in [8]) diagnosed with brucellosis or with *Brucella* infection. CSF = cerebrospinal fluid. Only lesions attributable to *Brucella ceti* or relevant to cause of death are included.

ID	Macroscopic Lesions	Histopathology	*Brucella* Culture	Others	Cause of Death	Available Serum
N-275/12 *	Chronic suppurative diskospondylitis Multifocal brain malacia	Mycotic pyogranulomatous-necrotizing meningoencephalomyelitis	**Positive** (vertebral abscess)	Mycotic encephalitis	Mycotic encephalitis	No
N-301/12 *	Not relevant	Non-suppurative meningoencephalitis, diffuse, more intense in cerebellum, brainstem and spinal cord; choroiditis; radiculoneuritis	**Positive** (brain)	-	Neurobrucellosis	Yes
N-260/16	Emaciation; cerebral edema; absence of recent ingesta	Non-suppurative meningoencephalitis, diffuse, more intense in brainstem; choroiditis; radiculoneuritis, multifocal and milder	**Positive** (brain)	-	Neurobrucellosis	Yes
N-319/16	Low body condition; absence of recent ingesta; meningeal congestion	Non-suppurative meningoencephalitis	**Positive** (brain, ventricle swab)	CeMV intensely positive (RT-PCR and IHC)	CeMV encephalitis	Yes
N-168/17	Absence of recent ingesta; meningeal and CSF turbidity	Non-suppurative meningitis, more intense in brainstem and cerebellum	**Positive** (lateral ventricle swab, spinal cord, mesenteric LN, brain, CSF)	-	Neurobrucellosis	Yes
N-274/18	Loss of body condition; brain edema and meningeal hemorrhage	Non-suppurative meningitis, diffuse, with multifocal encephalitis; choroiditis	**Positive** (lateral ventricle swab)	*Aeromonas sobria* and *P. damselae* in lung, liver, CNS	Neurobrucellosis	Yes
N-314/19	CSF turbidity; brain edema and meningeal hemorrhage; mild hydrocephalus	Non-suppurative meningoencephalitis, more intense in brainstem, cerebellum and thalamus; choroiditis; radiculoneuritis, multifocal and milder	**Positive** (CSF)	-	Neurobrucellosis	Yes
N-368/19	Emaciation; absence of recent ingesta; CSF turbidity	Non-suppurative meningitis, localized in brainstem and, with less intensity, cerebellum	Negative (contaminated sample) **PCR intensely positive** in CSF.	-	Neurobrucellosis	Yes
N-333/22	Slight loss of body condition; absence of regent ingesta; brain edema; meningeal and CSF turbidity	Non-suppurative meningitis, localized in brainstem and cerebellum, choroiditis	**Positive** (brain, CSF)	-	Neurobrucellosis	Yes

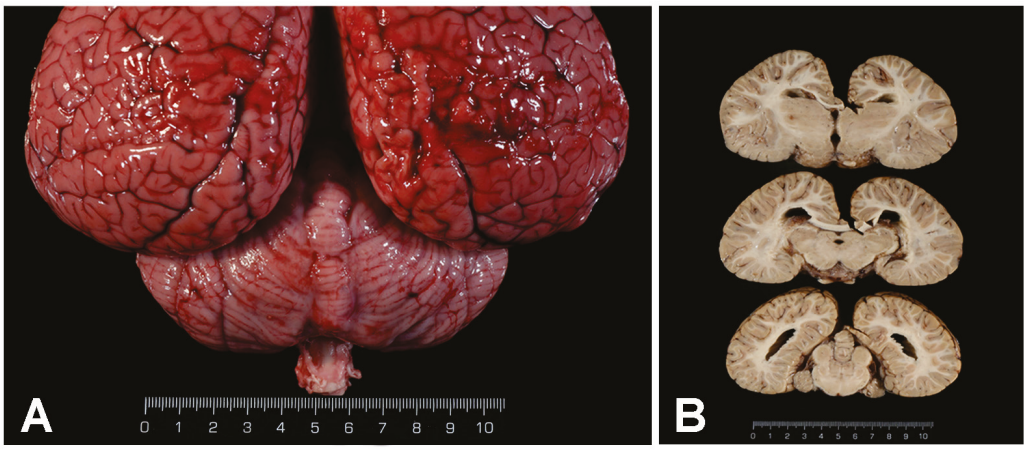


Figure 2. Gross findings in striped dolphins with neurobrucellosis. Scale is in cm. (**A**) Brain, fresh, dorsal view. Cerebellar meninges are turbid. Histologically, there was a lymphoplasmacytic meningitis. Case N-333/22. (**B**) Brain, formalin-fixed. Mild dilation of the ventricular system (hydrocephalus). Case N-314/19.

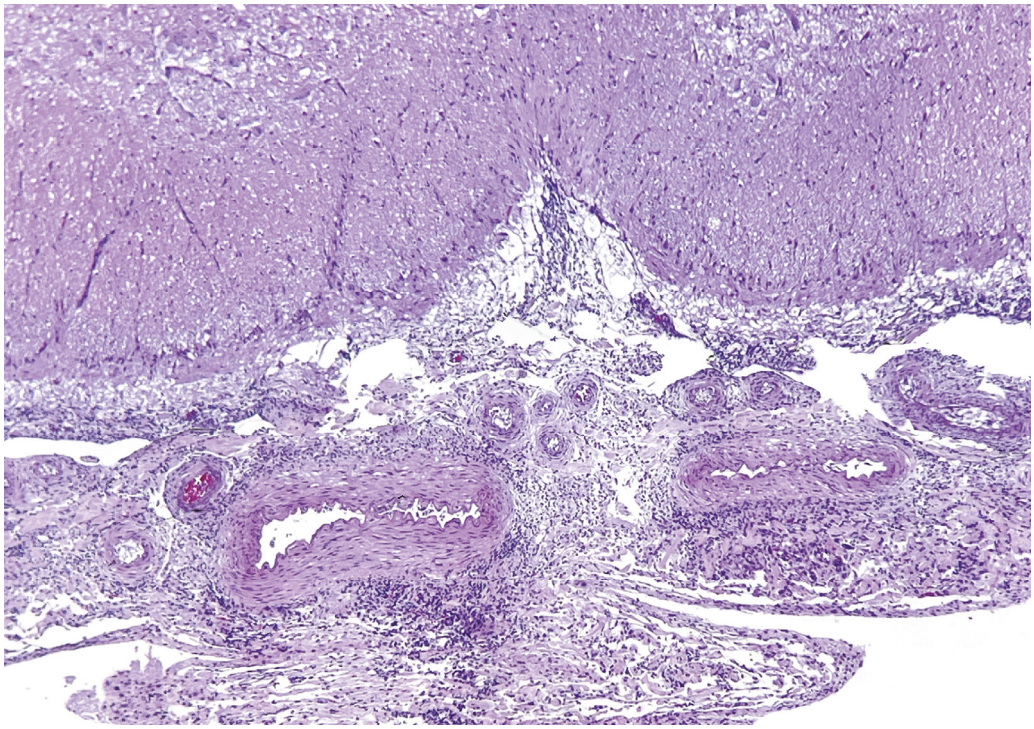


Figure 3. Spinal cord and meninges, hematoxylin and eosin stain. A severe subacute-chronic lymphoplasmacytic meningitis is the hallmark of neurobrucellosis. Case N-333/22.

3.2. Culture of Brucella

Brucella culture was attempted in 25 cetaceans, including cases with compatible histological lesions, epididymitis or a positive Rose Bengal test. Three additional dolphins with a positive result in a qPCR against *Brucella* in brain tissue were included. *Brucella ceti* was isolated in 8/25 cetaceans (six striped dolphins with neurobrucellosis, one striped dolphin with subacute morbilliviral encephalitis, and the common bottlenose dolphin with diskospondylitis). In the striped dolphins, *Brucella* was cultured from CNS samples (brain, CSF, ventricle swabs, spinal cord), or mesenteric lymph node, and in the bottlenose dolphin, from the diskospondylitic lesion [8] (see Table 2). The diagnosis of neurobrucellosis in an additional striped dolphin (N-368/19) was based on highly compatible lesions and

a low Ct result in the *Brucella* qPCR in CSF. Culture was attempted but the sample was contaminated due to storage problems. A positive *Brucella* PCR result has prompted the inclusion of this case in the neurobrucellosis group for the serological analysis.

The level of haemolysis did not affect the results of the cELISA in our samples from well-preserved cetacean carcasses, as tested in the preliminary study.

3.3. Serological Investigation

A multispecies cELISA was used in an exploratory study to detect antibodies against the LPS of *Brucella* sp. in sixty-six cetaceans, with eight of them infected with *Brucella*. This test has not been validated for cetaceans, and there is no cut-off established to consider one sample as positive or negative. Furthermore, a panel of reference sera of infected and non-infected cetaceans is not available at present. As a consequence, the sensitivity (Se) and specificity (Sp) of the test for cetaceans are unknown. All dolphins were tested at serial dilutions from 1:5 to 1:160, and the last dilution with a PI $\geq$ 40% was arbitrarily considered the titer of that serum sample, given the fact that the majority of cetaceans (seven of eight) with *Brucella* isolation were positive at the 1:160 dilution. However, a high proportion of sera (21 of 66; 31.8%) were still positive (PI $\geq$ 40%) at the 1:160 dilution (see Figure 4). The overall *Brucella* antibody estimated prevalence was 33.3% for striped dolphins and 31.8% for all cetaceans using the dilution of 1:160 and the cut-off of PI $\geq$ 40%. Further serum dilutions performed with *Brucella*-infected cases showed titers of 1:320 (n = 1), 1:640 (n = 2), 1:1280 (n = 2) and 1:5120 (n = 1). The PI for the different dilutions of each cetacean serum is shown in Supplementary File S1.

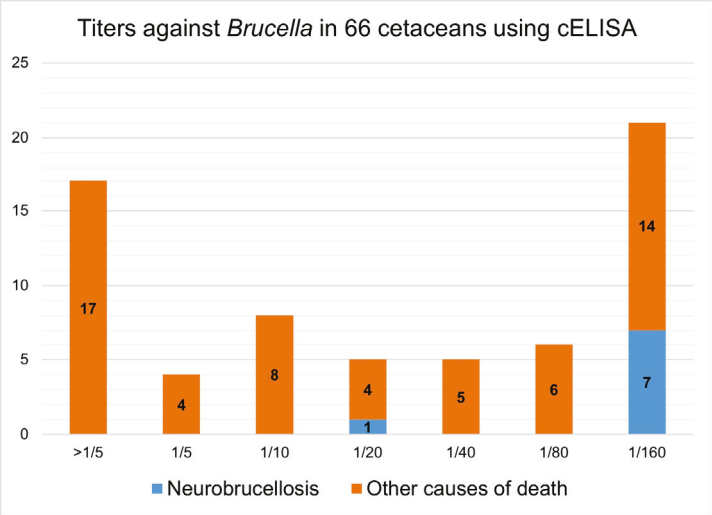


Figure 4. Antibody titers against *Brucella* using a cELISA in 66 cetaceans highlighting *Brucella*-infected cases. Vertical axis shows the absolute number of animals.

3.3.1. Serological Results Compared by Cause of Death

Cetaceans investigated serologically are classified by cause of death, species and cELISA results in Table 3. Seropositivity (at dilution 1:160) was only detected in striped dolphins and Risso's dolphins. Striped dolphins with neurobrucellosis (n = 8) had the highest proportion of seropositives (87.5%). High antibody titers (1:160), however, were also observed in striped dolphins dying from bycatch, CeMV infection, PEM and with cause of death classified as "other". Animals with neurobrucellosis showed a statistically significant higher proportion of seropositives compared to the groups of bycatch (4/15; 26.6%), striped dolphins not dying from neurobrucellosis (12/49; 24.5%) and the rest of cetaceans (14/66; 21.2%). Regarding other species, only 2/5 Risso's dolphins were seropositive, a calf dying from maternal separation and a bycaught adult (Table 2). None of the Risso's dolphins

investigated serologically showed lesions compatible with brucellosis, and in the two cases where culture was attempted, the results were negative.

Table 3. Antibody titers in the cELISA against *Brucella* LPS in serum samples of 66 cetaceans. The column on the right (%Pos) shows the percentage of seropositives (PI ≥ 40% at dilution 1:160) in each group. * In one dolphin, the cause of death was encephalitis by CeMV. ♦ Chronic forms of CeMV stranded in the period 2018–2021. Sc = *Stenella coeruleoalba*; Gg = *Grampus griseus*; Tt = *Tursiops truncatus*; Dd = *Delphinus delphis*; Gm = *Globicephala melas*.

Species	Cause of Death	n	Antibody Titer							
			>1:5	1:5	1:10	1:20	1:40	1:80	1:160	%Pos
Sc	Neurobrucellosis *	8				1			7	87.5%
	Bycatch	15	4	1	3		1	2	4	26.6%
	CeMV	12	5	1			1	1	4 ♦	33.3%
	Infectious/inflammatory	9	1	1	2	3		2		0%
	PEM	4		1	1				2	50%
	Mother–calf separation	2	1		1					0%
	Other	4	1			1			2	50%
	Unknown	3	1				2			0%
	TOTAL	57	13	4	7	5	4	5	19	33.3%
Gg	Sinusitis *Crassicauda*	3	2					1		0%
	Bycatch	1							1	100%
	Mother–calf separation	1							1	100%
	TOTAL	5	2					1	2	40%
Tt	Mother–calf separation	1	1							0%
	Infectious/inflammatory	1			1					0%
	TOTAL	2	1		1					0%
Dd	Unknown	1					1			0%
Gm	CeMV	1	1							0%
	TOTAL	66				45			21	31.8%

3.3.2. Serology by Age Class

The proportion of seropositive striped dolphins within the different age classes is shown in Table 4. Juveniles, compared to adults, presented a higher proportion of seropositivity (53.9 vs. 29.3%). They comprised the majority of neurobrucellosis cases (25 vs. 4.9%), and this difference was significant with $p < 0.019$. Seropositivity was 33% for both male and female striped dolphins.

Table 4. Seropositivity for *Brucella* (left column) and neurobrucellosis cases (right column) by age class. Serum was available in n = 57 striped dolphins. Right column shows the proportion of neurobrucellosis as cause of death in all striped dolphins, with or without serological analysis.

	Seropositives (%)	Neurobrucellosis (%)
Adults	12/41 (29.3%)	3/61 (4.9%)
Juveniles	7/13 (53.9%)	5/20 (25%)
Calves	0/3 (0%)	0/13 (0%)
Fetus	0	0/1 (0%)
Total	19/57 (33.3%)	8/97 (8.2%)

3.3.3. Brucella Serology in CeMV-Infected Cetaceans

A CeMV outbreak in the Northwestern Mediterranean Sea accounted for the death of 17 cetaceans from 2016 to 2021, including systemic and chronic CNS cases [15] (see Table 5).

The diagnosis was made with histopathology, a positive PCR and/or IHC result in the target organs. High titers against *Brucella* within this group were frequent in dolphins diagnosed with CeMV-chronic CNS forms. Only one of four CeMV cases, where *Brucella* isolation was attempted, yielded a positive result (N-319/16, stranded in 2016, with CNS lesions attributed to CeMV). In four of these cases, *Brucella* culture was attempted and was negative.

Table 5. Antibody titers against *Brucella* spp. in cetaceans infected with CeMV. * *Brucella* coinfection. Sc = *Stenella coeruleoalba*; Gm = *Globicephala melas*; J = juvenile; Ad = Adult.

ID	Species	Age Class	CeMV Form	Titer
N-319/16	Sc	J	Systemic *	1/160
N-044/17	Sc	J	Systemic	>1:5
N-045/17	Sc	J	Systemic	>1:5
N-077/17	Sc	J	Systemic	>1:5
N-454/17	Sc	J	Systemic	>1:5
N-488/17	Sc	Ad	Systemic	1/5
N-497/17	Sc	Ad	Systemic	1/10
N-604/17	Sc	Ad	Chronic	>1:5
N-001/18	Sc	Ad	Chronic	1/40
N-232/18	Sc	J	Chronic	1/160
N-293/18	Sc	Ad	Chronic	1/160
N-362/18	Sc	Ad	Chronic	1/160
N-361/19	Sc	J	Chronic	1/160
N-334/21	Sc	Ad	Chronic	1/80
N-023/21	Gm	J	Chronic	>1:5

4. Discussion

The results show that brucellosis is regularly detected in small cetaceans in the Northwestern Mediterranean Sea, and it is the most significant single bacterial cause of death in striped dolphins in the area, confirming previous similar findings from Mediterranean regions [12,15]. *B. ceti* infection and disease was diagnosed in nine out of one hundred twenty-three (7.3%) necropsied cetaceans, with this figure being the first estimated prevalence of the disease in dolphins from any Mediterranean coastal region. In eight striped dolphins, neurobrucellosis was deemed the primary cause of death, whereas *B. ceti* was considered a comorbidity in one striped dolphin with systemic CeMV infection and in a common bottlenose dolphin with *B. ceti* diskospondylitis and a CNS mucormycosis [8].

Understanding the pathogenesis of cetacean neurobrucellosis remains elusive, mostly due to the lack of knowledge about the types of immune responses elicited by *B. ceti* in healthy and in sick cetaceans. It is generally accepted that Th1 responses are relevant in controlling replication of intracellular bacteria. A strong humoral (Th2-mediated) response seems to be unprotective, with antibodies being a more useful indicator of exposure and infection than a proper defense mechanisms (for review, see [19,20]). Accordingly, a study with *B. melitensis* in mice suggested that antibodies are not decisive in the control of infection [21], although antibodies against LPS have proven to confer a certain protection in *B. abortus* [19,22]. As in other mammals, it may be hypothesized that cetaceans with a predominant Th1 response to *B. ceti* survive the infection, and a shift to a Th2 response constitutes the hallmark of disease progression. However, to our knowledge, the specific T cell response against *Brucella* sp. has never been measured in dolphins, and the role of serum antibodies against the bacteria is unknown. Several serologic tests have been used in cetacean species, either developed for terrestrial mammals or adapted to marine mammals [11,23–30]. These studies have shown a high seroprevalence of *Brucella*-infection, ranging from 7.6% to 60%, both in cetaceans and pinnipeds, in many places of the world. However, the Se and Sp of tests designed for terrestrial mammals have not been established for cetaceans, and this knowledge is hindered by the lack of reference panel sera for cetaceans. Bearing in mind these limitations, we applied a commercial cELISA for *Brucella*

diagnosis in cetaceans, not to establish Se and Sp values for this test, but rather to better define prevalence of *B. ceti* infection and disease, and to understand the practical utility of serologic results when applied to stranded cetaceans.

We observed a higher seropositivity in striped dolphins with neurobrucellosis than in the total of analyzed cetaceans and in striped dolphins dying from other causes, considering seropositivity when PI $\geq$ 40% at a serum dilution of 1:160. The causes of death in seropositive animals, however, were varied and included infectious and non-infectious causes, indicating that high antibody titers are not a synonym of active, pathology-related *Brucella* infection. If these cetaceans with high titers represent subclinical forms of latent *Brucella* infections, inducing humoral immunity remains to be studied. Antibodies in humans with brucellosis can persist several months after the remission of symptoms, clinical relapse [31,32] and, in areas with endemicity, repeated infections [31]. In rats inoculated with *B. abortus* antigens, antibodies are present a minimum of 120 days [33]. There is a report of a captive bottlenose dolphin with *Brucella* osteomyelitis with sustained high antibody titers against *Brucella* [34]. Considering this, it is possible that antibodies would be indicative of chronicity rather than accountable for disease development. In humans, whose pathogenesis of neurobrucellosis is often compared to cetaceans, neurobrucellosis is not the most common manifestation of disease [31,32] and occurs in subacute to chronic infections [35,36]. Thus, it is likely that the diagnosed cases presented in this work represent just the tip of the iceberg of an endemicity of *Brucella* infection in the Mediterranean, as suggested previously [15] and supported by the high seroprevalence reported in other studies around the world (see [4] for review).

The variable specificity of serological tests is often attributed to cross-reactions with the other LPS of Gram-negative bacteria. In terrestrial animals, *Campylobacter* spp., *Salmonella* spp., *Pasteurella* spp., *Yersinia enterocolytica* [11], *Francisella tularensis* and *Vibrio cholerae* [37] have been associated with cross-reactions. *Salmonella* spp. have been isolated from free-ranging cetaceans [38], but other terrestrial bacteria are not always found in marine environments. In the most common Gram-negative bacteria associated with marine mammals, the pathogenicity and roles in cross-reaction is unclear. In the seropositive dolphins of this paper, *Psychrobacter phenylpyruvicus* (N-28/21), *Photobacterium damselae* (N-557/17, N-232/18, N-42/18), *Pseudomonas* spp. (N-557/17), *Vibrio* sp. (N-232/18, N-329/18) and *Escherichia coli* (N-329/18) have been isolated.

The presence of high seropositivity in the cases of neurobrucellosis probably indicates that the humoral response is not effective against the pathogen. In our cases, Th1 response cytokines (IL-1 and TNFα) have been detected in *Brucella*-induced meningitis by immunohistochemistry, which could suggest a role of this type of response in brucellosis [39]. In these cases, for unknown reasons, cellular response is ineffective, as studied in other species [40]. Polymorphisms in some molecules of the immune system may also play a role in individual susceptibility [41,42].

Interestingly, the authors observed that juvenile striped dolphins were the age group with higher seroprevalence and proportion of neurobrucellosis. In our cases, this may be due to a larger contribution of anthropogenic interactions as cause of death for adults (21/61; 34.4%), diminishing the relative importance of neurobrucellosis. Immune immaturity as a predisposing cause for neurologic form of brucellosis in juveniles, however, cannot be discarded. Another hypothesis is the occurrence of vertical transmission, with consequent latency of *Brucella* in the tissues and reactivation when new stressors appear for the weaned animal. The results from this work contrast with some serologic studies in human patients, where they found a positive correlation between the age and seroprevalence of *Brucella* antibodies [43,44]. However, this may be due to adults being more exposed in work environment. In Italy and Costa Rica, similar results have been reported, with 6/8 striped dolphins with brucellosis being juveniles in Italy [12] and 28/51 in Costa Rica [45].

A cluster of *Brucella*-seropositive dolphins occurred in the period 2018–2021 in CNS-localized forms of CeMV (n = 5) (see Supplementary File S1). The authors speculate that the previous immune suppression of the systemic phase prompted the increased replication and

transmission of subclinical *Brucella*, without causing death, and the persistence of *Brucella* antibodies until the development of the chronic form of CeMV, when the immunosuppressive phase had resolved. Another hypothesis is that the acute phase transiently limited antibody production. At least in the present cases, there is no direct correlation between the massive immunosuppression in acute CeMV infection and the development of neurobrucellosis. In other publications, the two coinfections are more frequent, with 4/8 striped dolphins testing positive for both pathogens [12], although in others there was no correlation [46].

5. Conclusions

A seroprevalence of 31.8% against *Brucella* LPS antigens in cetaceans from the Catalan coast of the Mediterranean has been detected. This percentage is significantly higher in cetaceans with neurobrucellosis (87.5%), but there are also high titers in animals with other causes of death. Seropositive species include striped dolphins and Risso's dolphins. The prevalence of disease associated with *Brucella ceti* was 7.3%.

The cELISA designed for ruminants and pigs may be a potentially sensitive method in the serum samples of cetaceans to predict neurobrucellosis, but the specificity is probably low. This may reflect a proportion of subclinical carriers of the bacteria or the occurrence of cross-reactions. Cetaceans with chronic forms of CeMV seem to have higher antibody titers against *Brucella*. CeMV infection, in the acute immunosuppressive form, may enhance *Brucella* replication in carrier individuals and increase the horizontal transmission of the bacteria. More efforts are needed to dilucidate the epidemiology of the infection and the latency of bacteria in target organs. Research must continue to better understand this disease epidemiology and pathogenesis, a significant cause of mortality in our coast with the potential to alter the population dynamics of these protected species.

Supplementary Materials: The following supporting information can be downloaded at https://www.mdpi.com/article/10.3390/ani14162417/s1, File S1: Percentage of inhibition of all cELISA tested cetaceans; File S2: Biometric data, ancillary tests and cause of death of the 131 studied cetaceans.

Author Contributions: Conceptualization, M.D.; methodology, M.D. and L.M.; validation, M.D.; formal analysis, A.A.; investigation, M.D., S.W., L.P., L.G., A.P. and L.M.; resources, M.D.; data curation, L.M.; writing—original draft preparation, M.D., L.M. and M.C.-S.; writing—review and editing, A.P., S.W. and M.C.-S.; visualization, L.M.; supervision, M.D.; project administration, M.D.; funding acquisition, M.D. All authors have read and agreed to the published version of the manuscript.

Funding: This research was funded by Servei de Fauna i Flora (Generalitat de Catalunya) and Servei de Diagnòstic de Patologia Veterinària (Universitat Autònoma de Barcelona), permit number AG-2022-1439.

Institutional Review Board Statement: Not applicable (animals included in this study stranded in the coast and died naturally or were euthanized under authorized veterinary services).

Data Availability Statement: Data supporting reported results can be found in Supplementary Materials.

Acknowledgments: We thank Blanca Pérez and Aida Neira from the Servei de Diagnòstic de Patologia Veterinària, Universitat Autònoma de Barcelona, and Maite Martin and Marta Perez. We thank the brucellosis research group from CITA de Aragón (MJ de Miguel, S. Serrano, S. Andrés-Barranco and PM Muñoz) for the culture and identification of *Brucella* isolates. Thanks to Silvio Špičić Laboratory for Bacterial Zoonoses, Croatian Veterinary Institute, Zagreb, Croatia ST 27 for kindly providing DNA of *Brucella ceti* CRO350.

Conflicts of Interest: The authors declare no conflicts of interest.

References

1. Ewalt, D.R.; Payeur, J.B.; Martin, B.M.; Cummins, D.R.; Miller, W.G. Characteristics of a *Brucella* Species from a Bottlenose Dolphin (*Tursiops truncatus*). *J. Vet. Diagn. Investig.* **1994**, *6*, 448–452. [CrossRef] [PubMed]
2. Foster, G.; Osterman, B.S.; Godfroid, J.; Jacques, I.; Cloeckaert, A. *Brucella ceti* Sp. Nov. and *Brucella pinnipedialis* Sp. Nov. for *Brucella* strains with Cetaceans and Seals as Their Preferred Hosts. *Int. J. Syst. Evol. Microbiol.* **2007**, *57*, 2688–2693. [CrossRef]
3. Nymo, I.H.; Tryland, M.; Godfroid, J. A Review of *Brucella* Infection in Marine Mammals, with Special Emphasis on *Brucella pinnipedialis* in the Hooded Seal (*Cystophora cristata*). *Vet. Res.* **2011**, *42*, 93. [CrossRef] [PubMed]
4. Guzmán-Verri, C.; González-Barrientos, R.; Hernández-Mora, G.; Morales, J.-A.; Baquero-Calvo, E.; Chaves-Olarte, E.; Moreno, E. *Brucella ceti* and Brucellosis in Cetaceans. *Front. Cell. Infect. Microbiol.* **2012**, *2*, 3. [CrossRef] [PubMed]
5. Van Bressem, M.; Raga, A.; Di Guardo, G.; Jepson, P.; Duignan, P.; Siebert, U.; Barrett, T.; Santos, M.; Moreno, I.; Siciliano, S.; et al. Emerging Infectious Diseases in Cetaceans Worldwide and the Possible Role of Environmental Stressors. *Dis. Aquat. Organ.* **2009**, *86*, 143–157. [CrossRef]
6. Alba, P.; Terracciano, G.; Franco, A.; Lorenzetti, S.; Cocumelli, C.; Fichi, G.; Eleni, C.; Zygmunt, M.S.; Cloeckaert, A.; Battisti, A. The Presence of *Brucella ceti* ST26 in a Striped Dolphin (*Stenella coeruleoalba*) with Meningoencephalitis from the Mediterranean Sea. *Vet. Microbiol.* **2013**, *164*, 158–163. [CrossRef] [PubMed]
7. Garofolo, G.; Zilli, K.; Troiano, P.; Petrella, A.; Marotta, F.; Di Serafino, G.; Ancora, M.; Di Giannatale, E. *Brucella ceti* from Two Striped Dolphins Stranded on the Apulia Coastline, Italy. *J. Med. Microbiol.* **2014**, *63*, 325–329. [CrossRef]
8. Isidoro-Ayza, M.; Ruiz-Villalobos, N.; Pérez, L.; Guzmán-Verri, C.; Muñoz, P.M.; Alegre, F.; Barberán, M.; Chacón-Díaz, C.; Chaves-Olarte, E.; González-Barrientos, R.; et al. *Brucella ceti* Infection in Dolphins from the Western Mediterranean Sea. *BMC Vet. Res.* **2014**, *10*, 206. [CrossRef]
9. Cvetnić, Ž.; Duvnjak, S.; Đuras, M.; Gomerčić, T.; Reil, I.; Zdelar-Tuk, M.; Špičić, S. Evidence of *Brucella* Strain ST27 in Bottlenose Dolphin (*Tursiops truncatus*) in Europe. *Vet. Microbiol.* **2016**, *196*, 93–97. [CrossRef]
10. Grattarola, C.; Petrella, A.; Lucifora, G.; Di Francesco, G.; Di Nocera, F.; Pintore, A.; Cocumelli, C.; Terracciano, G.; Battisti, A.; Di Renzo, L.; et al. *Brucella ceti* Infection in Striped Dolphins from Italian Seas: Associated Lesions and Epidemiological Data. *Pathogens* **2023**, *12*, 1034. [CrossRef]
11. Van Bressem, M.; Van Waerebeek, K.; Raga, J.A.; Godfroid, J.; Brew, S.D.; MacMillan, A.P. Serological Evidence of *Brucella* Species Infection in Odontocetes from the South Pacific and the Mediterranean. *Vet. Rec.* **2001**, *148*, 657–661. [CrossRef]
12. Garofolo, G.; Petrella, A.; Lucifora, G.; Di Francesco, G.; Di Guardo, G.; Pautasso, A.; Iulini, B.; Varello, K.; Giorda, F.; Goria, M.; et al. Occurrence of *Brucella ceti* in Striped Dolphins from Italian Seas. *PLoS ONE* **2020**, *15*, e0240178. [CrossRef]
13. Pugliares, K.R.; Bogomolni, A.; Touhey, K.M.; Herzig, S.M.; Harry, C.T.; Moore, M.J. *Marine Mammal Necropsy: An Introductory Guide for Stranding Responders and Field Biologists*; Woods Hole Oceanographic Institution: Woods Hole, MA, USA, 2007.
14. Kuiken, T.; García-Hartmann, M. *Proceedings of the First European Cetacean Society Workshop on Cetacean Pathology: Dissection Techniques and Tissue Sampling, Leiden, The Netherlands, 13–14 September 1991*; European Cetacean Society: Leiden, The Netherlands, 1991; p. 39.
15. Cuvertoret-Sanz, M.; López-Figueroa, C.; O'Byrne, A.; Canturri, A.; Martí-Garcia, B.; Pintado, E.; Pérez, L.; Ganges, L.; Cobos, A.; Abarca, M.; et al. Causes of Cetacean Stranding and Death on the Catalonian Coast (Western Mediterranean Sea), 2012–2019. *Dis. Aquat. Organ.* **2020**, *142*, 239–253. [CrossRef]
16. López-Goñi, I.; García-Yoldi, D.; Marín, C.M.; De Miguel, M.J.; Barquero-Calvo, E.; Guzmán-Verri, C.; Albert, D.; Garin-Bastuji, B. New Bruce-Ladder Multiplex PCR Assay for the Biovar Typing of *Brucella suis* and the Discrimination of *Brucella suis* and *Brucella canis*. *Vet. Microbiol.* **2011**, *154*, 152–155. [CrossRef] [PubMed]
17. Calzada, N.; Aguilar, A.; Grau, E.; Lockyer, C. Patterns of Growth and Physical Maturity in the Western Mediterranean Striped Dolphin, *Stenella coeruleoalba* (Cetacea: Odontoceti). *Can. J. Zool.* **1997**, *75*, 632–637. [CrossRef]
18. Calzada, N.; Aguilar, A. Flipper Development in the Mediterranean Striped Dolphin (*Stenella coeruleoalba*). *Anat. Rec.* **1996**, *245*, 708–714. [CrossRef]
19. Dorneles, E.M.S.; Teixeira-Carvalho, A.; Araújo, M.S.S.; Sriranganathan, N.; Lage, A.P. Immune Response Triggered by Brucella Abortus Following Infection or Vaccination. *Vaccine* **2015**, *33*, 3659–3666. [CrossRef] [PubMed]
20. De Figueiredo, P.; Ficht, T.A.; Rice-Ficht, A.; Rossetti, C.A.; Adams, L.G. Pathogenesis and Immunobiology of Brucellosis. *Am. J. Pathol.* **2015**, *185*, 1505–1517. [CrossRef]
21. Dadelahi, A.S.; Abushahba, M.F.N.; Ponzilacqua-Silva, B.; Chambers, C.A.; Moley, C.R.; Lacey, C.A.; Dent, A.L.; Skyberg, J.A. Interactions between B Cells and T Follicular Regulatory Cells Enhance Susceptibility to Brucella Infection Independent of the Anti-*Brucella* Humoral Response. *PLoS Pathog.* **2023**, *19*, e1011672. [CrossRef] [PubMed]
22. Cloeckaert, A.; Jacques, I.; Bosseray, N.; Limet, J.N.; Bowden, R.; Dubray, G.; Plommet, M. Protection Conferred on Mice by Monoclonal Antibodies Directed against Outer-Membrane-Protein Antigens of *Brucella*. *J. Med. Microbiol.* **1991**, *34*, 175–180. [CrossRef]
23. Hernández-Mora, G.; Palacios-Alfaro, J.D.; González-Barrientos, R. Wildlife Reservoirs of Brucellosis: *Brucella* in Aquatic Environments. *Rev. Sci. Tech. Int. Off. Epizoot.* **2013**, *32*, 89–103. [CrossRef] [PubMed]
24. CMeegan, J.; Field, C.; Sidor, I.; Romano, T.; Casinghino, S.; Smith, C.R.; Kashinsky, L.; Fair, P.A.; Bossart, G.; Wells, R.; et al. Development, Validation, and Utilization of a Competitive Enzyme-Linked Immunosorbent Assay for the Detection of Antibodies against *Brucella* Species in Marine Mammals. *J. Vet. Diagn. Investig.* **2010**, *22*, 856–862. [CrossRef] [PubMed]

25. Prenger-Berninghoff, E.; Siebert, U.; Stede, M.; König, A.; Weiß, R.; Baljer, G. Incidence of *Brucella* Species in Marine Mammals of the German North Sea. *Dis. Aquat. Organ.* **2008**, *81*, 65–71. [CrossRef]
26. Lynch, M.; Duignan, P.J.; Taylor, T.; Nielsen, O.; Kirkwood, R.; Gibbens, J.; Arnould, J.P.Y. Epizootiology of *Brucella* Infection in Australian Fur Seals. *J. Wildl. Dis.* **2011**, *47*, 352–363. [CrossRef] [PubMed]
27. Norman, S.A.; Delaney, M.A.; Haman, K.H.; Thomas, A.C.; Godfroid, J.; Larsen, A.K.; Nymo, I.H.; Robbe-Austerman, S.; Quance, C.; Rhyan, J.C.; et al. Application of Real-Time Quantitative PCR Assays for Detecting Marine *Brucella* Spp. in Fish. *J. Vet. Diagn. Investig.* **2018**, *30*, 150–154. [CrossRef] [PubMed]
28. Hoover-Miller, A.; Dunn, J.; Field, C.; Blundell, G.; Atkinson, S. Seroprevalence of Brucella Antibodies in Harbor Seals in Alaska, USA, with Age, Regional, and Reproductive Comparisons. *Dis. Aquat. Organ.* **2017**, *126*, 1–12. [CrossRef]
29. Kershaw, J.; Stubberfield, E.; Foster, G.; Brownlow, A.; Hall, A.; Perrett, L. Exposure of Harbour Seals *Phoca vitulina* to *Brucella* in Declining Populations across Scotland. *Dis. Aquat. Organ.* **2017**, *126*, 13–23. [CrossRef] [PubMed]
30. Kroese, M.V.; Beckers, L.; Bisselink, Y.J.W.M.; Brasseur, S.; Van Tulden, P.W.; Koene, M.G.J.; Roest, H.I.J.; Ruuls, R.C.; Backer, J.A.; IJzer, J.; et al. *Brucella pinnipedialis* in Grey Seals (*Halichoerus gryphus*) and Harbor Seals (*Phoca vitulina*) in the Netherlands. *J. Wildl. Dis.* **2018**, *54*, 439. [CrossRef]
31. Ruiz-Mesa, J.D.; Sánchez-Gonzalez, J.; Reguera, J.M.; Martín, L.; Lopez-Palmero, S.; Colmenero, J.D. Rose Bengal Test: Diagnostic Yield and Use for the Rapid Diagnosis of Human Brucellosis in Emergency Departments in Endemic Areas. *Clin. Microbiol. Infect.* **2005**, *11*, 221–225. [CrossRef]
32. Casanova, A.; Ariza, J.; Rubio, M.; Masuet, C.; Díaz, R. BrucellaCapt versus Classical Tests in the Serological Diagnosis and Management of Human Brucellosis. *Clin. Vaccine Immunol.* **2009**, *16*, 844–851. [CrossRef]
33. Khatun, M.; Islam, A.; Baek, B.K. Comparative Analysis of Humoral Immune Response and Cognate Antigen Detection in Experimentally Infected Sprague Dawley Rats with *Brucella abortus* Biotype 1. *Vector-Borne Zoonotic Dis.* **2024**, *24*, 27–35. [CrossRef] [PubMed]
34. Goertz, C.E.C.; Frasca, S.; Bohach, G.A.; Cowan, D.F.; Buck, J.D.; French, R.A.; De Guise, S.; Maratea, J.; Hinckley, L.; Ewalt, D.; et al. Brucella Sp. Vertebral Osteomyelitis with Intercurrent Fatal *Staphylococcus aureus* Toxigenic Enteritis in a Bottlenose Dolphin (*Tursiops truncatus*). *J. Vet. Diagn. Investig.* **2011**, *23*, 845–851. [CrossRef] [PubMed]
35. Zhao, S.; Cheng, Y.; Liao, Y.; Zhang, Z.; Yin, X.; Shi, S. Treatment Efficacy and Risk Factors of Neurobrucellosis. *Med. Sci. Monit.* **2016**, *22*, 1005–1012. [CrossRef] [PubMed]
36. Soares, C.N.; Angelim, A.I.M.; Brandão, C.O.; Santos, R.Q.; Mehta, R.; Silva, M.T.T.D. Neurobrucellosis: The Great Mimicker. *Rev. Soc. Bras. Med. Trop.* **2022**, *55*, e0567-2021. [CrossRef] [PubMed]
37. Solís García Del Pozo, J.; Lorente Ortuño, S.; Navarro, E.; Solera, J. Detection of IgM Antibrucella Antibody in the Absence of IgGs: A Challenge for the Clinical Interpretation of *Brucella* Serology. *PLoS Negl. Trop. Dis.* **2014**, *8*, e3390. [CrossRef] [PubMed]
38. Grattarola, C.; Gallina, S.; Giorda, F.; Pautasso, A.; Ballardini, M.; Iulini, B.; Varello, K.; Goria, M.; Peletto, S.; Masoero, L.; et al. First Report of *Salmonella* 1,4,[5],12:I:- In Free-Ranging Striped Dolphins (*Stenella coeruleoalba*), Italy. *Sci. Rep.* **2019**, *9*, 6061. [CrossRef]
39. Rebollada-Merino, A.; Giorda, F.; Pumarola, M.; Martino, L.; Gomez-Buendia, A.; Romani-Cremaschi, U.; Casalone, C.; Mattioda, V.; Di Nocera, F.; Lucifora, G.; et al. Neurobrucellosis (*Brucella ceti*) in Striped Dolphins (*Stenella coeruleoalba*): Immunohistochemical Studies on Immune Response and Neuroinflammation. *Vet. Pathol.* **2024**, 03009858241250336, *online ahead of print*. [CrossRef]
40. Moreno, E.; Barquero-Calvo, E. The Role of Neutrophils in Brucellosis. *Microbiol. Mol. Biol. Rev.* **2020**, *84*, e00048-20. [CrossRef]
41. Bravo, M.J.; Colmenero, J.D.; Martín, J.; Alonso, A.; Caballero, A. Polymorphism of the Transmembrane Region of the MICA Gene and Human Brucellosis. *Tissue Antigens* **2007**, *69*, 358–360. [CrossRef]
42. Fu, J.; He, H.-Y.; Ojha, S.C.; Shi, H.; Sun, C.-F.; Deng, C.-L.; Sheng, Y.-J. Association of IL-6, IL-10 and TGF-B1 Gene Polymorphisms with Brucellosis: A Systematic Review with Meta-Analysis. *Microb. Pathog.* **2019**, *135*, 103640. [CrossRef]
43. Islam, M.A.; Khatun, M.M.; Werre, S.R.; Sriranganathan, N.; Boyle, S.M. A Review of *Brucella* Seroprevalence among Humans and Animals in Bangladesh with Special Emphasis on Epidemiology, Risk Factors and Control Opportunities. *Vet. Microbiol.* **2013**, *166*, 317–326. [CrossRef] [PubMed]
44. Abo-Shehada, M.N.; Odeh, J.S.; Abu-Essud, M.; Abuharfeil, N. Seroprevalence of Brucellosis among High Risk People in Northern Jordan. *Int. J. Epidemiol.* **1996**, *25*, 450–454. [CrossRef] [PubMed]
45. Roca-Monge, K.; González-Barrientos, R.; Suárez-Esquivel, M.; Palacios-Alfaro, J.D.; Castro-Ramírez, L.; Jiménez-Soto, M.; Cordero-Chavarría, M.; García-Párraga, D.; Barratclough, A.; Moreno, E.; et al. Age and Sexual Maturity Estimation of Stranded Striped Dolphins, Stenella Coeruleoalba, Infected with *Brucella ceti*. *Oceans* **2022**, *3*, 494–508. [CrossRef]
46. González-Barrientos, R.; Morales, J.-A.; Hernández-Mora, G.; Barquero-Calvo, E.; Guzmán-Verri, C.; Chaves-Olarte, E.; Moreno, E. Pathology of Striped Dolphins (*Stenella coeruleoalba*) Infected with *Brucella ceti*. *J. Comp. Pathol.* **2010**, *142*, 347–352. [CrossRef] [PubMed]

Disclaimer/Publisher's Note: The statements, opinions and data contained in all publications are solely those of the individual author(s) and contributor(s) and not of MDPI and/or the editor(s). MDPI and/or the editor(s) disclaim responsibility for any injury to people or property resulting from any ideas, methods, instructions or products referred to in the content.

animals

MDPI

Case Report

Disseminated Infection with *Aspergillus fumigatus* in a Scarlet Macaw Parrot (*Ara macao*)—A Case Report

Oana Irina Tanase [1], Geta Pavel [2], Ozana Maria Hritcu [2], Mihaela Anca Dascalu [1], Bianca Elena Bratuleanu [3], Cristina Mihaela Rimbu [1,3] and Florentina Daraban Bocaneti [1,*]

[1] Department of Public Health, Faculty of Veterinary Medicine, Iasi University of Life Sciences Ion Ionescu de la Brad, 700489 Iasi, Romania; crimbu@yahoo.com (C.M.R.)
[2] Department of Preclinics, Faculty of Veterinary Medicine, Iasi University of Life Sciences Ion Ionescu de la Brad, 700489 Iasi, Romania
[3] Regional Center of Advanced Research for Emerging Diseases, Zoonoses and Food Safety (ROVETEMERG), Iasi University of Life Sciences Ion Ionescu de la Brad, 700489 Iasi, Romania
* Correspondence: florentinabocaneti@yahoo.com

Simple Summary: Aspergillosis is an important fungal disease occurring in avian fauna, especially in birds kept in captivity. In *Psittaciformes*, severe disease occurs in the lungs and air sacs, with the development of white-to-yellow caseous nodules and plaques in the organs, in addition to greenish-grey fungal growth in the air sacs. Herein, we report the presence of disseminated infection with *Aspergillus fumigatus* in a 3-year-old male scarlet macaw parrot (*Ara macao*) that was presented to the Exotic Animal Clinic at the Faculty of Veterinary Medicine, Iași University of Life Sciences (Iași, Romania) for its postmortem examination. The confirmation of the fungal infection was achieved using histopathological, microbiological, and molecular methods. Since birds suffering from *Aspergillus* spp. do not always show respiratory issues, or their clinical signs are non-specific, this may create diagnostic difficulty for clinicians unfamiliar with the parrots' pathology. Therefore, for a definitive diagnosis, the demonstration of fungal presence by cytology or histopathology and its identification using culturing and molecular techniques is required.

Abstract: A 3-year-old male scarlet macaw parrot (*Ara macao*) was presented to the Exotic Animal Clinic at the Faculty of Veterinary Medicine, Iași University of Life Sciences (Iași, Romania) for its postmortem examination. According to the owner, the parrot had been raised only in captivity and after 5 days of inappetence, lethargy, and mild respiratory clinical signs, the parrot died. The post mortem examination revealed various-sized granulomas and caseous plaques in the lungs, air sacs, spleen, intestinal serosa, and liver. Microscopically, the granulomas were characterized by a necrotic center and the infiltration of numerous multinucleated giant cells and epithelioid-like cells and by the presence of hyphae typical of *Aspergillus* spp. Moreover, in the liver tissue, a diffuse inflammation, with numerous fungal hyphae, was noted. The fungal culture and the PCR assay allowed for the isolation and identification of *Aspergillus fumigatus* from the lung and liver samples. The macroscopical lesions and the histopathological findings, with the fungal isolation and molecular confirmation of *Aspergillus fumigatus* by nested PCR, provided the basis for the diagnosis of disseminated aspergillosis. To the authors' best knowledge, this is the first report of disseminated infection caused by *Aspergillus fumigatus* in a scarlet macaw parrot (*Ara macao*).

Keywords: mycosis; *Aspergillus*; macaw

1. Introduction

Aspergillosis is an important fungal disease in avian fauna. Out of the approximately 340 accepted *Aspergillus species* (*Aspergillus* spp.), only a small number are implicated in the development of avian aspergillosis [1]. According to recent studies, *Aspergillus fumigatus*

is by far the most prevalent species, representing up to 95% of all occurrences in both wild and domestic avian species [1,2]. Birds kept in captivity are more susceptible to acquiring an infection with *Aspergillus* spp. due to several factors related to environmental conditions (increased concentration of fungal spores precipitated by humid, warm, dirty, poorly ventilated air) or to host immunity (concurrent infections, virulence of the isolate, therapies, stress) [3,4]. The anatomy and physiology of the avian respiratory system is substantially distinct from that of the bronchoalveolar lungs of mammals. Given the small size (2–3 μm), inhaled *Aspergillus fumigatus* conidia is able to overcome the first physical barriers and profoundly penetrate into the respiratory system and subsequently, into the air sacs, which are particularly predisposed to contamination, since they are subjected to an airflow that facilitates particle deposition. In addition, avian species have few resident macrophages to eliminate corpora aliena and have an epithelial surface nearly lacking in a mucociliary transport mechanism [5]. When the immune response is less effective, the fungus can spread from the respiratory system via the circulatory system or by simple extension from the air sac wall to contiguous organs or cavities. Moreover, hematogenous transmission is achieved by hyphal penetration of the lung blood vessels and by means of macrophages transporting viable spores. Under appropriate aerobic conditions, fungal asexual reproduction within the air sacs is a common result, associated with plaques becoming velvety and changing color, depending on the *Aspergillus* spp. involved [6]. Microscopically, lesions are characterized by granulomatous inflammation associated with the fungal hyphae.

Acute infection, usually seen in young poultry, is defined by high morbidity and mortality, by respiratory signs, or by systemic disease in the visceral organs and the brain, while chronic respiratory infection is mostly seen in adult or captive birds, such raptors or parrots [7]. Furthermore, aspergillosis has been confirmed in various species of captive parrots, such in African grey parrots (*Psittacus erithacus*), blue-fronted Amazon parrots (*Amazona aestiva*), or Eclectus parrots (*Eclectus roratus*) [8–10]. In *Psittaciformes*, severe disease occurs with infection of the lower respiratory system (lungs and air sacs), resulting in the development of white-to-yellow caseous nodules and plaques in the organs, in addition to greenish-grey fungal growth in the air sacs [11]. Herein, we report the presence of disseminated infection with *Aspergillus fumigatus* in a scarlet macaw confirmed by histopathological, microbiological, and molecular methods.

2. Materials and Methods

2.1. Case Description

A 3-year-old male scarlet macaw (*Ara macao*) was presented to the Exotic Animal Clinic at the Faculty of Veterinary Medicine, Iași University of Life Sciences (Iași, Romania) in June 2021 for its postmortem examination. According to the owner, the parrot had been raised only in captivity and after 5 days of inappetence, lethargy, and mild respiratory clinical signs, the parrot suddenly died. No antemortem assays had been performed. A post-mortem examination was performed, and various-sized granules were noted in the internal organs. For the histopathological evaluation, tissue samples were collected from the lungs and liver, fixed in 10% buffered formalin, embedded in paraffin, sectioned at 5 μm, and stained with Masson's trichrome stain. Moreover, in order to visualize the suspected fungal hyphae, the sectioned samples were stained using periodic acid Schiff (PAS) staining. In parallel, for cytological examination, fresh smears from the lungs were prepared and routinely stained using the May–Grünwald–Giemsa method.

2.2. Isolation and Identification of Aspergillus spp.

Samples from the lungs and liver were cultured onto Sabouraud dextrose agar (Oxoid, Basingstoke, UK) and onto Mueller–Hinton agar with 5% sheep blood (Oxoid) and aerobically incubated at 37 °C for 7 days. *Aspergillus fumigatus* is a thermophilic species that can develop at temperatures of up to 55 °C, but can also survive up to 70 °C [12].

The suspected *Aspergillus fumigatus* isolate was obtained, and its macroscopic and microscopic morphologies, such as hyphae, conidial heads, and arrangements, were identified by lactophenol cotton blue staining, as previously described by Thom and Raper (1945) [13].

The conventional polymerase chain reaction (PCR) technique was performed on lungs and liver for the identification of *Aspergillus fumigatus*, following a protocol published by Sugita et al. (2004) [14]. Briefly, the DNA was extracted using the PureLink™ Genomic DNA Mini Kit, following the manufacture's instruction. The genus specific amplification was performed using the PCR Master Mix Platinum II Hot-Start Green (Invitrogen, Vilnius, Lithuania), 5 µL of extracted DNA, and 20 µM of primers ASAP1 (5′-CAGCGAGTACATCACCTTGG-3′) and ASAP2 (5′-CCATTGTTGAAAGTTTTAACTGATT-3′). The cycling conditions consisted of: an initial denaturation step at 94 °C for 4 min, 30 cycles of denaturation at 94 °C for 1 min, annealing at 55 °C for 2 min, and extension at 72 °C for 90 s, followed by a final extension step at 72 °C for 10 min. By nested PCR, for the specific amplification of the *A. fumigatus* ITS1 region, the primers ASPU (5′-GCCCGCCGTTTCGAC-3′) and AFI3 (5′-CCGTTGTTGAAAGTTTTAACTGATTAC-3′) were used, with a 1 µL PCR product used as a template. The cycling conditions consisted of: an initial denaturation step at 94 °C for 4 min, 25 cycles of denaturation at 94 °C for 1 min, annealing at 60 °C for 15 s, and extension at 72 °C for 15 s, followed by a final extension step at 72 °C for 10 min. The amplification products were visualized using 2% agarose gel electrophoresis.

3. Results

During the post mortem examination, extreme emaciation, with loss of body weight, was revealed. Various-sized granulomas and caseous plaques were observed in the lungs, air sacs, kidneys, spleen, intestinal serosa, and liver (Figure 1a,b).

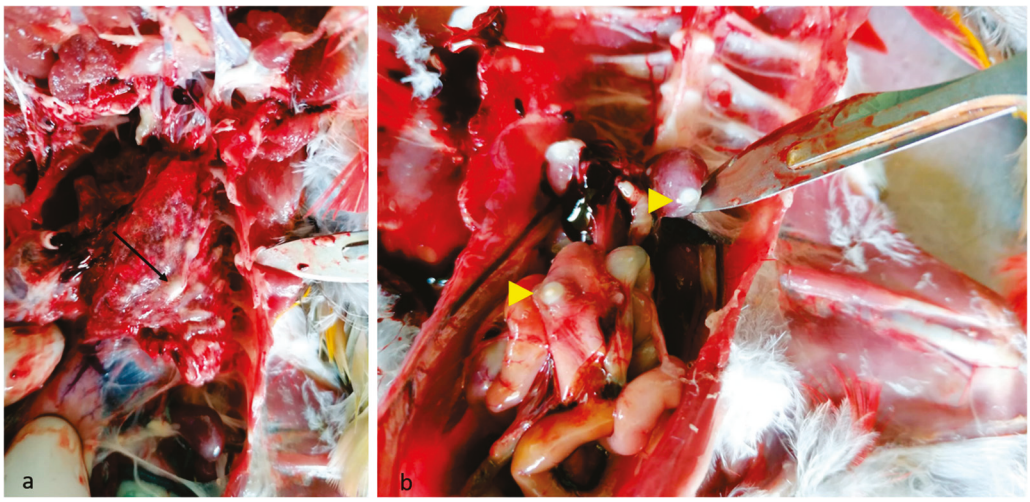


Figure 1. Macroscopic findings in parrot aspergillosis: (**a**) lungs showing fungal granulomas of various sizes (black arrows); (**b**) disseminated granulomas on spleen and intestinal serosa (yellow arrowheads).

The histopathological evaluation of the collected samples revealed areas of necrosis in the pulmonary parenchyma, characterized by infiltration of numerous multinucleated giant cells, epithelioid-like cells, fibrin heterophilic deposits, and hemosiderin granules. The necrotic areas were delimited from the surrounding tissue, while the bronchi spaces were blocked by inflammatory infiltrate (Figure 2a). Additionally, using PAS staining, numerous fungal hyphae with a characteristic architecture consisting of 45° dichotomous branches were observed within the necrotic and inflammatory areas of the affected lung parenchyma (Figure 2b).

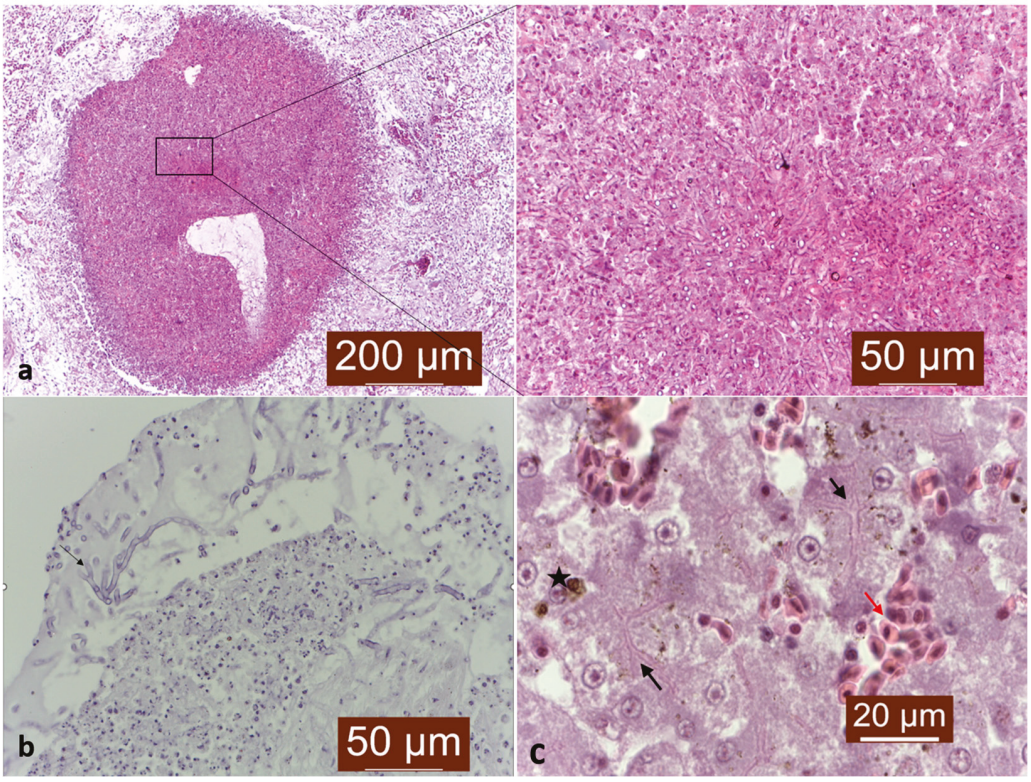


Figure 2. (**a**) Lung granuloma consisting of a central mass of necrotic exudate under Masson's trichrome staining and 20× magnification. Inset shows higher magnification of granulomas, with numerous fungal hyphae under Masson's trichrome staining and 40× magnification. (**b**) Fungal hyphae with a characteristic architecture consisting of 45° dichotomous branches in lung granuloma lesion, under PAS staining, 40× magnification. (**c**) Liver: fungal hyphae (black arrows), hemosiderin granules phagocytosis (black star), and congestion (red arrow) under Masson's trichrome staining and 100× magnification.

In liver tissue, a diffuse inflammation, characterized by a mild congestion with a significant hepatocyte necrosis, hemosiderin granules phagocytosis, and numerous fungal hyphae, were noted (Figure 2c).

Furthermore, the cytological examination of the lung smears revealed the presence of inflammatory cells consisting of numerous neutrophiles, macrophages, and lymphocytes. Moreover, atypical cells showing multinucleated giant cells (Figure 3a) with intensely vacuolated cytoplasm and undifferentiated walls, along with few fungal hyphae, have been identified (Figure 3b).

Following the cultivation on Sabouraud dextrose agar and Mueller–Hinton agar with 5% sheep blood media, the fungal presence in the lung and liver samples was confirmed, while according to the mycological descriptions, the causative *Aspergillus* spp. was identified as *Aspergillus fumigatus* on the basis of the following: (1) cultural characteristics—the presence of dense smoky colonies, gray-green in color with a slight creamy-white reverse (Figure 4a), and (2) microscopical morphology (revealed by lactophenol cotton blue staining)—septate hyphae and columnar conidia with a diameter from 2.5 to 3 µm, basipetally constructed in chains from a single palisade-like layer of phialides that were produced directly on broadly clavate vesicles in the absence of metulae (Figure 4c). These results were confirmed by PCR and nested PCR assays, in which an amplified product of 521 bp, corresponding to genus *Aspergillus*, and a product of 310 bp, corresponding to the *Aspergillus fumigatus* ITS1 region, respectively, were amplified in both the lung and liver samples and visualized by electrophoresis (Figure 4d).

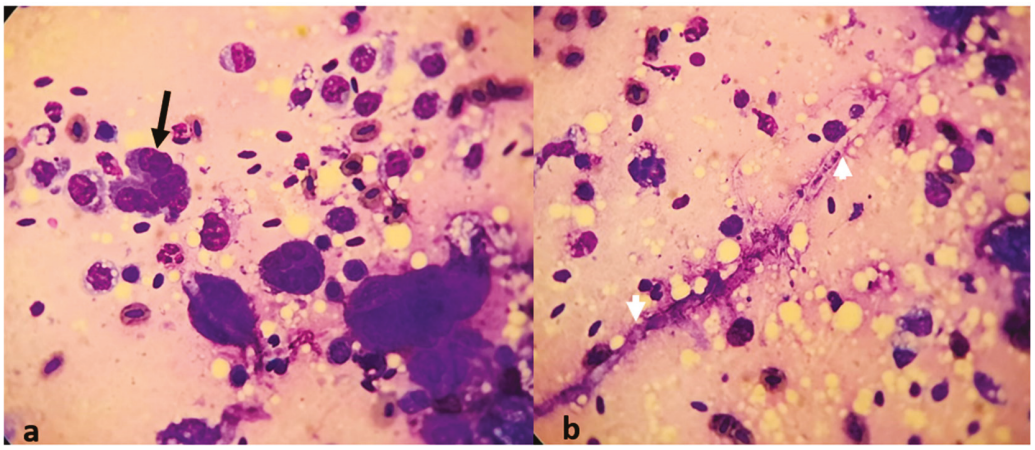


Figure 3. Cytology from the lung granuloma smears shows: (**a**) inflammatory cells and multinucleated giant cells (black arrow) under May–Grünwald–Giemsa staining, 40× magnification; (**b**) fungal hyphae (white arrowheads) under May-Grünwald Giemsa staining and 40× magnification.

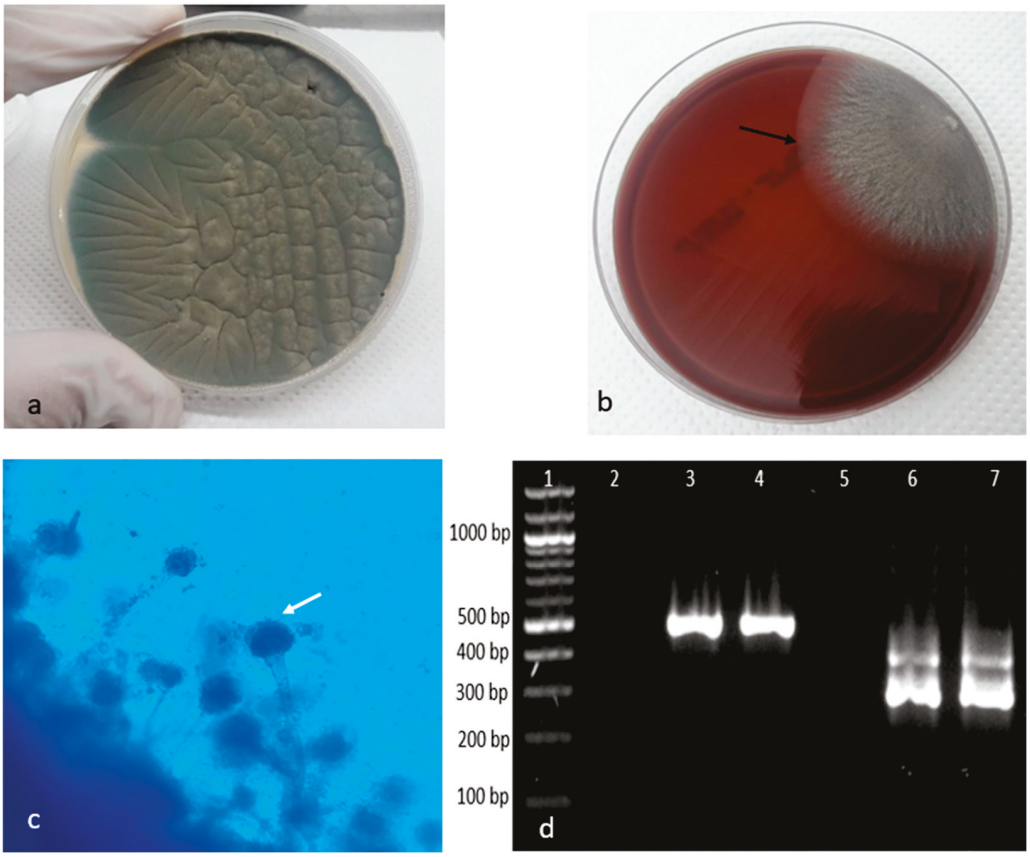


Figure 4. (**a**) Cultural characteristics of *Aspergillus fumigatus* colony: dense smoky and gray-green colonies on Sabouraud dextrose agar media; (**b**) cultural characteristics of *Aspergillus fumigatus* colony on Mueller–Hinton agar media showing gray-green colony (black arrow); (**c**) microscopical morphologies of *Aspergillus fumigatus* revealed by lactophenol cotton blue staining: typical columnar conidia heads (white arrow) showing characteristic form of vesicles under Lactophenol cotton blue staining, and ×20 magnification. (**d**) Molecular confirmation of genus *Aspergillus* and *Aspergillus fumigatus*: line 1: 1.2 kb molecular weight marker; lines 2 and 5 C-negative control; the product of 521 bp was amplified in line 3 (lung) and 4 (liver) samples by ASAP primers; using nested PCR, a product of 310 bp corresponding to *Aspergillus fumigatus* was obtained in the lung (line 6) and liver (line 7) samples using ASPU/AFI3 primers.

4. Discussion

Avian aspergillosis is described as a disease of captivity, with *Aspergillus fumigatus* and *Aspergillus flavus* mainly implicated as etiological agents, while their transmission occurs mostly via the respiratory route [10]. In our case, the infiltrate and the chronic lung parenchyma inflammation led to a progressive impaired air circulation, which eventually proved fatal. *Aspergillus* spp. is able to induce both granulomatous and diffuse lesions, consisting of some characteristic changes. Moreover, there is a high probability of finding both lesion types in the same affected organ, which may indicate that the dissemination route is not exclusively respiratory. In our case, the fresh examination of the lung granulomas using May–Grünwald–Giemsa staining demonstrated the characteristic branching structures of the *Aspergillus* spp. hyphae. Furthermore, the main lesions were identified in the lungs, where areas of necrosis, characterized by infiltration of numerous multinucleated giant cells, epithelioid-like cells, fibrin heterophilic deposits, and hemosiderin granules were noted, which may suggest that the path of conidia infection was via the respiratory route, which is stated to be the main avian infection route [3]. Beside lung infection, other organs are also reported to be affected by *Aspergillus* spp. In this regard, *Aspergillus* spp. was isolated from rib osteomyelitis in farmed ostriches, from sternum osteomyelitis in chickens, from ribs bone marrow in the African grey parrot, from kidneys in a swift parrot, from ocular lesions in domestic turkeys and Rufous owls, or from gizzard and liver lesions in the Java Finch [15–17]. Interestingly, in *Psittaciformes*, liver damage has not been associated with *Aspergillus* spp. infection. Accordingly, in an African grey parrot (*Psittacus erithacus*) infected with *Aspergillus fumigatus*, significant damage was found in the lungs, while no lesions were reported in the liver [4]. Moreover, a similar pattern was reported in a captive Eclestus parrot (*Eclestus roratus*) infected with *Aspergillus flavus* [10]. In our case, *Aspergillus* spp. hyphae were noted in the liver, which were accompanied by a diffuse inflammation, characterized by a mild congestion, with a significant hepatocyte necrosis and phagocytosis of the hemosiderin granules. To the authors' best knowledge, this is the first time that *Aspergillus fumigatus* has been associated with liver inflammation, suggesting a disseminated infection. The liver involvement demonstrated in this case may be explained by the small size of the conidia, enabling them to reach the lungs and its air sacs, and frequently, the caudal–thoracic and abdominal air sacs as well. When the immune system is not able to eliminate conidia, or when their accumulation is high, the infection progresses, with subsequent dissemination to the surrounding tissues, such those of the lungs, bronchi, liver, spleen, or intestinal serosa [3,4].

The identification of the *Aspergillus* spp. is of great importance in the confirmation of the avian aspergillosis diagnostic, since confusion may occur due to the lack of differences between the lesions induced by various species of *Aspergillus* such as *Aspergillus fumigatus*, *Aspergillus flavus*, *Aspergillus niger*, *Aspergillus nidulans*, or *Aspergillus restrictus* [10,17].

According to some authors, the simultaneous isolation of *Aspergillus* spp. with the demonstration of specific lesions plays a key role in the confirmation of the diagnostic [10,18,19]. As stated by Ref. [7], "due to the ubiquity of *Aspergillus* conidia, isolation of the fungi without the presence of lesions is not of diagnostic". In this case, the microscopical findings were further confirmed by the successful isolation of *Aspergillus fumigatus* on Sabouraud dextrose agar and Mueller–Hinton agar media and by its microscopical mycological morphology revealed by lactophenol cotton blue staining. Furthermore, the aforementioned diagnostic methods were completed by PCR using genus-specific and species-specific primers. According to Ref. [20], this approach, based on PCR detection for *Aspergillus* spp., is highly recommended for a definitive diagnosis, since this technique allows for the active demonstration of sensitivity and specificity (PCR 25%, culture 19.5%, microscopy 10%).

The histopathological findings for the macroscopical lesions, along with the fungal isolation and molecular confirmation of *Aspergillus fumigatus* by nested PCR, allowed for the diagnostic of disseminated aspergillosis.

It is important to note that the treatment of avian aspergillosis, when possible, is not always successful, for various reasons, including the following: (1) the diagnosis is confirmed in the late stages of the disease; (2) a narrow spectrum of antifungal drugs are available for avian species; (3) the available drugs may fail to penetrate the target tissues; (4) concurrent diseases and/or immunosuppression may be present [1]. Since aspergillosis occurrence in captive birds is known to depend on several factors, such as improper environmental conditions or host immunity, preventative measures play a crucial role. In this context, controlling the level of exposure and minimizing stressors are necessary. Moreover, a regular cleaning and disinfection of the nest areas, opening the canopy to increase the amount of sunlight reaching the floor of the aviaries, and ensuring proper ventilation, together with improved animal husbandry practices, can minimize stress in the environment, which in turn decreases the risk of aspergillosis [1].

5. Conclusions

Since birds suffering from *Aspergillus* spp. do not always show respiratory issues and considering that the clinical signs are non-specific, together, these challenges may create diagnostic difficulty for clinicians unfamiliar with the parrots' pathology. Therefore, for a definitive diagnosis, demonstration of fungal presence by cytology or histopathology, and its identification using culturing and molecular techniques, is required.

Author Contributions: O.I.T. contributed to necropsy diagnostics, study design, and manuscript revision; G.P. contributed to laboratory work and cytological examination; O.M.H. contributed to necropsy diagnostics and histopathological interpretation; M.A.D. contributed to study design and microbiological and molecular diagnosis; B.E.B. contributed to molecular diagnostics and manuscript revision; C.M.R. contributed to microbiological examination and manuscript revision; F.D.B. contributed to the study design, molecular diagnostics, and manuscript drafting and revision. O.I.T. and F.D.B. share the same rights for first authorship. All authors have read and agreed to the published version of the manuscript.

Funding: This study was supported by funds provided by Iasi University of Life Sciences Ion Ionescu de la Brad.

Institutional Review Board Statement: The animal study was reviewed and approved by the Romanian Faculty of Veterinary Science Ethics and Deontology Committee.

Informed Consent Statement: Written informed consent was obtained from the owner for participation of the animal in this study.

Data Availability Statement: The original contributions presented in the study are included in the article, further inquiries can be directed to the corresponding author.

Acknowledgments: The authors wish to thank the lab technician, Ioana Achirei, for her assistance in preparing the histopathological sections.

Conflicts of Interest: The authors declare no conflicts of interest.

References

1. Arné, P.; Risco-Castillo, V.; Jouvion, G.; Barzic, C.L.; Guillot, J. Aspergillosis in wild birds. *J. Fungi* **2021**, *7*, 241. [CrossRef] [PubMed]
2. Tell, L.A. Aspergillosis in mammals and birds: Impact on veterinary medicine. *Med. Mycol.* **2005**, *43* (Suppl. S1), S71–S73. [CrossRef] [PubMed]
3. Oglesbee, B.L. Mycotic diseases. In *Avian Medicine and Surgery*, 1st ed.; Altman, R.B., Chubb, S.L., Dorrestein, G.M., Quesenberry, K., Eds.; Publisher Saunders Company: Philadelphia, PA, USA, 1997; pp. 323–361.
4. De Oca, V.M.; Martínez, S.E.V.; Salinas, E.M.; Roberto, E.O.; Sánchez-Godoy, F. Pathological and mycological characterization of pulmonary *Aspergillus fumigatus* infection producing gliotoxin in a captive African grey parrot (*Psittacus erithacus*). *Braz. J. Vet. Pathol.* **2022**, *15*, 93–98. [CrossRef]
5. Maina, J.N. *The Lung-Air Sac System of Birds: Development, Structure, and Function*, 1st ed.; Springer: Berlin/Heidelberg, Germany; New York, NY, USA, 2005; pp. 159–174. [CrossRef]
6. Hauck, R.; Cray, C.; França, M. Spotlight on avian pathology: Aspergillosis. *Avian Pathol.* **2020**, *49*, 115–118. [CrossRef] [PubMed]

7. Kaplan, W.; Arnstein, P.; Ajello, L.; Chandler, F.; Watts, J.; Hicklin, M. Fatal aspergillosis in imported parrots. *Mycopathologia* **1975**, *56*, 25–29. [CrossRef] [PubMed]
8. Burr, E.W. Enzootic aspergillosis in wild red vented cockatoos in the Philippines. *Mycopathologia* **1981**, *73*, 21–28. [CrossRef] [PubMed]
9. Churria, C.D.G.; Reynaldi, F.; Origlia, J.; Marcantoni, H.; Píscopo, M.V.; Loyola, M.; Reinoso, E.H.; Petruccelli, M. Pulmonary aspergillosis due to *Aspergillus flavus* infection in a captive Eclectus Parrot (*Eclectus roratus*). *Braz. J. Vet. Pathol.* **2012**, *5*, 4–6.
10. Mihaylov, G.; Petrov, V.; Marutsov, P.; Simeonov, R.; Simeonova, G. A case of aspergillosis in a bearded vulture (*Gypaetos barbatus*). *Trakia J. Sci.* **2008**, *6*, 144–146.
11. Cacciuttolo, E.; Rossi, G.; Nardoni, S.; Legrottaglie, R.; Mani, P. Anatomopathological aspects of avian aspergillosis. *Vet. Res. Commun.* **2009**, *33*, 521–527. [CrossRef] [PubMed]
12. Latgé, J.P. *Aspergillus fumigatus* and aspergillosis. *Clin. Microbiol. Rev.* **1999**, *12*, 310–350. [CrossRef] [PubMed]
13. Thom, C.; Raper, K.B. *A Manual of the Aspergilli*; The Williams & Wilkins Company: Baltimore, MD, USA, 1945; pp. 148–155.
14. Sugita, C.; Makimura, K.; Uchida, K.; Yamaguchi, H.; Nagai, A. PCR identification system for the genus Aspergillus and three major pathogenic species: *Aspergillus fumigatus*, *Aspergillus flavus* and *Aspergillus niger*. *Med. Mycol.* **2004**, *42*, 433–437. [CrossRef] [PubMed]
15. Souza, L.R.; Santana, C.H.; Ribeiro, L.N.; Sousa, D.R.; Gomes, K.M.C.; Barroca, J.M.J.F.; Silva, M.B.G.; Santos, R.L. Pneumonia, airsacculitis and osteomyelitis caused by *Aspergillus fumigatus* in an African grey parrot (*Psittacus erithacus*)–case report. *Arq. Bras. Med. Vet. Zootec.* **2024**, *76*, 269–274. [CrossRef]
16. Arné, P.; Thierry, S.; Wang, D.; Deville, M.; Le Loc'h, G.; Desoutter, A.; Féménia, F.; Nieguitsila, A.; Huang, W.; Chermette, R.; et al. *Aspergillus fumigatus* in poultry. *Int. J. Microbiol.* **2011**, *2011*, 1–14. [CrossRef] [PubMed]
17. Talbot, J.J.; Thompson, P.; Vogelnest, L.; Barrs, V.R. Identification of pathogenic *Aspergillus* isolates from captive birds in Australia. *Med. Mycol.* **2018**, *56*, 1038–1041. [CrossRef] [PubMed]
18. Barton, J.T.; Daft, B.M.; Read, D.H.; Kinde, H.; Bickford, A.A. Tracheal aspergillosis in 6 1/2-week-old chickens caused by *Aspergillus flavus*. *Avian Dis.* **1992**, *36*, 1081–1085. [CrossRef] [PubMed]
19. Beernaert, L.A.; Pasmans, F.; Van Waeyenberghe, L.; Haesebrouck, F.; Martel, A. *Aspergillus* infections in birds: A review. *Avian Pathol.* **2010**, *39*, 325–331. [CrossRef] [PubMed]
20. Singh, R.; Singh, G.; Urhekar, A.D. Detection of *Aspergillus* Species by polymerase chain reaction. *Int. J. Curr. Microbiol. Appl. Sci.* **2016**, *5*, 254–260. [CrossRef]

Disclaimer/Publisher's Note: The statements, opinions and data contained in all publications are solely those of the individual author(s) and contributor(s) and not of MDPI and/or the editor(s). MDPI and/or the editor(s) disclaim responsibility for any injury to people or property resulting from any ideas, methods, instructions or products referred to in the content.

animals

MDPI

Article

Causes of Admission, Mortality and Pathological Findings in European Hedgehogs: Reports from Two University Centers in Italy and Switzerland

Ilaria Prandi [1,2,*], Eva Dervas [3], Elena Colombino [2,4], Giuseppe Bonaffini [1,2], Stefania Zanet [2], Riccardo Orusa [5], Serena Robetto [5], Massimo Vacchetta [6], Mitzy Mauthe von Degerfeld [1,2], Giuseppe Quaranta [1,2], Udo Hetzel [3] and Maria Teresa Capucchio [1,2,7]

[1] Centro Animali Non Convenzionali, Department of Veterinary Sciences, University of Turin, 10095 Grugliasco, Italy; giuseppe.bonaffini@unito.it (G.B.); mitzy.mauthe@unito.it (M.M.v.D.); giuseppe.quaranta@unito.it (G.Q.); mariateresa.capucchio@unito.it (M.T.C.)
[2] Department of Veterinary Sciences, University of Turin, 10095 Grugliasco, Italy; elena.colombino@edu.unito.it (E.C.); stefania.zanet@unito.it (S.Z.)
[3] Institute of Veterinary Pathology, Vetsuisse Faculty, University of Zurich, 8057 Zurich, Switzerland; eva.dervas@uzh.ch (E.D.); udo.hetzel@uzh.ch (U.H.)
[4] Patología y Sanidad Animal, Departamento Producción Sanidad Animal, Salud Pública Veterinaria y Ciencia y Tecnología de los Alimentos, Facultad de Veterinaria, Universidad CEU Cardenal Herrera, CEU Universities, 46115 Alfara del Patriarca, Spain
[5] National Reference Centre for Wild Animals Diseases (CeRMAS), S.C. Valle d'Aosta, Istituto Zooprofilattico Sperimentale del Piemonte, Liguria e Valle d'Aosta (IZSPLV), 11020 Quart, Italy; riccardo.orusa@izsto.it (R.O.); serena.robetto@izsto.it (S.R.)
[6] Centro Recupero Ricci "La Ninna", 12060 Novello, Italy; ninnaeisuoiamici@libero.it
[7] National Research Council of Italy-Institute of Sciences of Food Production (CNR-ISPA), 10095 Grugliasco, Italy
* Correspondence: ilaria.prandi@unito.it

Simple Summary: A decline in European hedgehog populations has been reported in several European countries over the past years. Human activities, along with global warming and infectious diseases, appear to be the main drivers of this phenomenon. The present study aimed to determine the major causes of mortality and the main pathological findings in European hedgehogs (*Erinaceus europaeus*) submitted to postmortem examination at two institutes of veterinary pathology, one located in Italy (Piedmont region) and one in Switzerland (Canton of Zurich). Hedgehogs were found in affected health status in the wild, mostly due to traumatic injury, poor overall condition and respiratory, gastrointestinal or neurological signs. The primary causes of death identified were infectious diseases and traumatic insults. The lungs were the most commonly affected organ, mainly displaying pneumonia, which was significantly associated with the presence of nematodes. These findings should be held in mind when treating the species presented to wildlife rescue centers and highlight the importance of proper education of the public on how to coexist and interact with hedgehog populations inhabiting urban areas.

Abstract: European hedgehogs (*Erinaceus europaeus*) are nocturnal insectivores frequently found in urban areas. In the last decades, their population has declined in various European countries and human activities have emerged as significant contributors to this trend. While the literature has mainly focused on trauma as the major cause of mortality, few authors have considered pathological findings. The present study is based on the results of full post-mortem examinations performed on 162 European hedgehogs in Italy and 109 in Switzerland. Unlike in previous studies, the main cause of mortality was infectious diseases (60.5%), followed by traumatic insults (27.7%). The lungs were the main organ affected, showing mostly lymphoplasmacytic (45.9%), granulomatous (18.1%) or suppurative (8.2%) pneumonia. Nematodes were detected in 57.2% of all lungs and were significantly associated with pneumonia (p-value < 0.001). To our knowledge, this is the first study to report infectious diseases as the main cause of hedgehog death, emphasizing the need for wildlife rescue centers to adopt appropriate diagnostic and therapeutic measures. Further research is necessary to

determine the broad range of infectious agents that affect this species and elucidate their interplay with the host. Finally, citizen sensitization should be implemented to promote responsible behaviors that could reduce human-related traumatic events.

Keywords: European hedgehogs; *Erinaceus europaeus*; causes of mortality; pathological findings; verminous pneumonia; wildlife rescue centers

1. Introduction

The European hedgehog (*Erinaceus europaeus*; Linnaeus, 1758) is a small nocturnal mammal [1] considered endemic in most parts of Europe [2]. It inhabits lowlands and hilly areas rich in grass, trees and fallen leaves [3–5].

Although classified as insectivores [6], with a diet mainly consisting of invertebrates (e.g., earthworms and slugs), hedgehogs have also been reported to feed on small vertebrates, bird eggs, fruits, plants and pet food found in urban gardens [3,6–8].

In winter, they enter hibernation [9], usually beginning in October–November and ending in March–April [9–11]. Hibernation length and climatic conditions also influence hedgehog reproduction. Hedgehogs begin mating in spring, soon after arousing from hibernation [9]. During the mating period, males expand their home range, leading to an increased risk of traumatic injuries, particularly from road accidents [7,10,12]. Females usually have one litter per year in colder climates, delivering four to five hoglets at the beginning of the summer [9,12]. However, in milder climates and when abundant food resources are available, or if their first litter is lost, female hedgehogs can mate again and deliver a second litter from August onwards [11]. Nonetheless, this can pose a risk for both adult females and hoglets, as they are consequently more dependent on acquiring adequate food resources to increase fat deposits and survive winter [13].

Hedgehogs exhibit synanthropic behavior [14], meaning that they reach higher densities in urban areas than in rural ones [5,15,16]. In anthropogenic environments, they can find more shelter possibilities, an abundance of both prey and pet food, a warmer microclimate and fewer wild predators (especially badgers) [5,13,15,17–19]. However, urban areas pose a number of risks to hedgehogs, including habitat fragmentation with a consequent reduction in their genetic diversity [5,16,18,20], an increased risk of road accidents, predation by domestic animals, trauma [5,19,21–23] and pesticide intoxication [24–26].

Over the last few decades, several authors have reported a gradual decrease in hedgehog populations in several European countries (e.g., United Kingdom, the Netherlands, Sweden and Switzerland) [16–18,27]. The reasons underlying this phenomenon appear to be multifactorial, with human activities proposed to play a major role, along with climate change, predation and infectious diseases [13,16,19]. In Zurich (Switzerland), hedgehog populations have been estimated to have declined by 40.6% over 25 years, accompanied by a 17.6% reduction in their distribution [16]. On the other hand, hedgehog populations in Italy are considered stable and are classified as Least Concern in the IUCN (International Union for Conservation of Nature) Red List of Italian Vertebrates [28]. However, it should be noted that, to our knowledge, quantitative data on Italian hedgehog populations are not available [29].

The causes of hedgehog mortality have been the topic of several studies, but the vast majority has focused on anthropogenic causes, especially road deaths [6,10,22,30–32], or analyzed admission and survival rates from wildlife rescue centers (WRCs) [11,13,33]. Only a few authors have taken data resulting from postmortem examinations into account, linking the cause of death with the main pathological findings, but nonetheless, obtaining different results [19,23]. These discrepancies in the main causes of mortality and the overall scarcity of studies reporting pathological findings in hedgehogs, along with the declining populations across Europe, prompted us to initiate this study.

The study aimed to describe the main causes of admission, mortality and pathological findings observed in European hedgehogs submitted for full post-mortem examination, including histological investigation.

2. Materials and Methods

This study was conducted at the Unit of Veterinary Pathology of the Department of Veterinary Sciences, University of Turin (Italy), and at the Institute for Veterinary Pathology of Vetsuisse Faculty, University of Zurich (Switzerland). The distance, in a beeline, between the two regions, calculated considering the two main cities (Turin and Zurich) as starting and ending points, is roughly 270 km [34].

2.1. Animal Origin

The Italian Unit of Veterinary Pathology analyzed wild European hedgehogs, dead or euthanized, for severe pathological conditions from 2018 to 2022 in two WRCs of the Piedmont region, North-Western Italy: Centro Animali Non Convenzionali (C.A.N.C.), a section of the Veterinary Teaching Hospital of Turin University specialized in the rescue of all wildlife species, located in Grugliasco (Turin province), and Centro Recupero Ricci La Ninna (La Ninna), a private WRC involved in the hospitalization and rehabilitation of hedgehogs, sited in Novello (Cuneo province). All these animals were found in Piedmont region by citizens or members of law enforcement agencies and brought to both centers because they were considered in need of medical assistance.

The Swiss Institute of Veterinary Pathology of Zurich examined all hedgehogs submitted for full post-mortem evaluation by private owners, WRCs or veterinary clinics. The animals were either found dead or died/were euthanized in animal facilities between 2011 and 2022.

2.2. Study Animals

For each animal, origin, sex, age (determined according to morphological characteristics [7,9,19] and divided into three categories—unweaned, juvenile and adult), body condition score (BCS, recorded on a scale of 1 to 5, with 1 being cachectic and 5 obese), the reason for collection from its habitat or the clinical signs displayed at the WRCs/veterinary clinics before death (if available) and the date of death were recorded.

According to previous publications, the reasons for admission were classified as follows: poor overall condition (apathy, weakness etc.), trauma, respiratory signs, gastrointestinal signs, neurological signs, neoplasia, random find/orphan, found dead and unknown [19,23]. The category "random find" includes all animals unnecessarily brought to WRCs by people from the public [13,19,33].

Animals were euthanized due to clinical deterioration and poor prognosis. In Italy, euthanasia was performed by induction of general anesthesia and intracardiac inoculation of a medicinal preparation consisting of mebezonium iodide, embutramide and tetracaine. In Switzerland, all submitted animals had either naturally deceased or had already been euthanized at WRCs or local veterinary clinics. Information on the exact method of euthanasia was not provided in the Swiss cases.

2.3. Pathological Examination

All animals underwent a full post-mortem examination. Italian hedgehogs were examined by PhD students in Veterinary Sciences overseen by a full professor in Veterinary Pathology. In Switzerland, all necropsies were performed by residents of the European College of Veterinary Pathologists (ECVP) supervised by ECVP diplomates. The main tissues (liver, spleen, intestine, kidneys, lungs, heart and brain) and additional organs showing gross alterations were collected and fixed in 10% buffered formalin for at least 24 h, embedded in paraffin blocks, sectioned at 3 µm, and routinely stained with hematoxylin and eosin (HE).

The most likely cause of death was established on the basis of both macroscopic and histological findings. Five main categories were determined: trauma/predation, infectious disease, starvation, neoplasia and unknown [19,23].

In Swiss reports, information on the cause of death was extracted from the "Diagnoses" and "Commentary" sections of necropsy reports.

2.4. Bacteriological and Parasitological Investigations

In selected cases, and in particular, in animals in which the organ lesions raised the suspicion of an infectious process, additional examinations were initiated. These included routine bacteriological investigations (for anaerobic and/or aerobic agents, depending on the submitted organ sample) in cases in which there was evidence of suppurative/fibrinous inflammation. When a bacterial species with known pathogenic potential was isolated and it was compatible with the macroscopic/histological lesions detected, it was considered the responsible agent of pathology.

In animals that were severely emaciated/cachectic and/or displayed evidence of gastroenteritis, parasites in the gastrointestinal tract or a verminous pneumonia, fecal samples were collected, submitted and examined via standard sedimentation and flotation protocols to identify parasitic structures. Due to cost limitations, only a subset of animals (n = 96 for parasitological and n = 17 for bacteriological examination) was subjected to further laboratory analyses.

2.5. Statistical Analysis and Data Presentation

Statistical analysis was performed using IBM SPSS Statistics software (version 29.0.1.0 (171)). Descriptive data are provided as frequencies. Given the qualitative nature of the variables, chi-squared test and Fisher's exact test (in case of two categories in both variables) were used to determine the possible presence of statistically significant differences between variables. The significance level was set at an alpha-value < 0.05.

In each Results subsection, descriptive statistics of collective data gathered from both countries and, if possible, associations between the different parameters are provided. In the subsection (Section 3.4), since most of the pathologic alterations affected only a small number of animals, the descriptive statistics on the pathological findings are reported collectively for all animals in both countries. In the last subsection (Section 3.4.5), because the examinations were performed only on a limited subset of animals, only descriptive statistics were provided and the country of origin was not considered.

3. Results

3.1. Descriptive Analysis

A total of 271 animals were included in the study. Of them, 162 animals (59.8%) originated from Italy and 109 animals (40.2%) from Switzerland. More specifically, with regards to Italian hedgehogs, 140 (51.7%) originated from C.A.N.C. and 22 animals (8.1%) from La Ninna WRC.

An overview of all population characteristics (sex, age and BCS) for each country of origin is provided in Table 1.

Tables 2–4 display the frequencies and percentages of hedgehog causes of admission and death, divided by the country of origin (Table 2), biological characteristics (sex, age and BCS; Table 3) and the season of mortality (Table 4).

Table 1. Population characteristics of the European hedgehogs included in the study, shown for both countries of origin. For Body Condition Score (BCS): Cachectic = 1/5; Decent = 2/5; Good = 3/5; Excellent = 4/5. No animals were scored 5/5 (obese); therefore, this category is not presented in the table.

		Sex						**Age**						**BCS**					
		Male		**Female**		**Unknown**		**Adult**		**Juvenile**		**Unweaned**		**Cachectic**		**Decent**		**Good**		**Excellent**	
		n	**%, [95% CI]**	**n**	**%, [95% CI]**	**n**	**%, [95% CI]**	**n**	**%, [95% CI]**	**n**	**%, [95% CI]**	**n**	**%, [95% CI]**	**n**	**%, [95% CI]**	**n**	**%, [95% CI]**	**n**	**%, [95% CI]**	**n**	**%, [95% CI]**
Country of origin	Italy	87	61.7, [53.1–69.8]	75	66.4, [56.9–75.0]	0	0.0, [0.0–19.5]	84	54.5, [46.3–62.6]	76	67.9, [58.3–76.4]	2	40.0, [5.2–85.3]	10	28.6, [14.6–46.3]	50	61.0, [49.6–71.6]	98	66.2, [58.0–73.8]	4	66.7, [22.3–95.7]
	Switzerland	54	38.3, [30.2–46.9]	38	33.6, [25.0–43.1]	17	100.0, [80.5–100.0]	70	45.5, [37.4–53.7]	36	32.1, [23.6–41.6]	3	60.0, [14.7–94.7]	25	71.4, [53.7–85.4]	32	39.0, [28.4–50.4]	50	33.8, [26.2–42.0]	2	33.3, [43.3–77.7]

Table 2. Frequencies and percentages of the causes of admission and death of all examined hedgehogs, shown for both countries of origin.

		Country of Origin			
		Italy		**Switzerland**	
		n	**%, [95% CI]**	**n**	**%, [95% CI]**
Cause of admission	Trauma/Predation	60	37.0, [29.6–45.0]	17	15.6, [9.4–23.8]
	Debilitation	56	34.6, [27.3–42.4]	19	17.4, [10.8–25.9]
	Found dead	3	1.9, [0.4–5.3]	27	24.8, [17.0–34.0]
	Respiratory signs	13	8.0, [4.3–13.3]	15	13.8, [7.9–21.7]
	Random find	23	14.2, [9.2–20.5]	0	0.0, [0.0–3.3]
	Gastrointestinal signs	2	1.2, [0.1–4.4]	12	11.0, [5.8–18.4]
	Neurological signs	0	0.0, [0.0–2.3]	6	5.5, [2.0–11.6]
	Neoplasia	2	1.2, [0.1–4.4]	0	0.0, [0.0–3.3]
	Unknown	3	1.9, [0.4–5.3]	13	11.9, [6.5–19.5]
Cause of death	Infectious disease	87	53.7, [45.7–61.6]	77	70.6, [61.2–79.0]
	Trauma/Predation	62	38.3, [30.8–46.2]	13	11.9, [6.5–19.5]
	Starvation	0	0.0, [0.0–2.3]	5	4.6, [1.5–10.4]
	Neoplasia	2	1.2, [0.1–4.4]	3	2.8, [0.6–7.8]
	Unknown	11	6.8, [3.4–11.8]	11	10.1, [5.1–17.3]

Table 3. Frequencies and percentages of the causes of admission and death of all examined hedgehogs, divided according to their biological characteristics (sex, age and BCS).

		Sex						Age						BCS					
		Male		Female		Unknown		Adult		Juvenile		Unweaned		Cachectic		Decent		Good		Excellent	
		n	%, [95% CI]	n	%, [95% CI]	n	%, [95% CI]	n	%, [95% CI]	n	%, [95% CI]	n	%, [95% CI]	n	%, [95% CI]	n	%, [95% CI]	n	%, [95% CI]	n	%, [95% CI]
Cause of admission	Trauma/ Predation	43	31.9, [24.1–40.4]	32	30.5, [21.9–40.2]	2	11.8, [1.5–36.4]	56	36.4, [28.8–44.5]	21	18.8, [12.0–27.2]	0	0.0, [0.0–52.2]	6	17.1, [6.6–33.6]	22	26.8, [17.6–37.8]	47	31.8, [24.4–40.0]	2	33.3, [4.3–77.7]
	Debilitation	37	27.4, [20.1–35.7]	35	33.3, [24.4–43.2]	3	17.6, [3.8–43.4]	34	22.1, [15.8–29.5]	40	35.7, [26.9–45.3]	1	20.0, [0.5–71.6]	9	25.7, [12.5–43.3]	29	35.4, [25.1–46.7]	37	25.0, [18.3–32.8]	0	0.0, [0.0–45.9]
	Found dead	14	10.4, [5.8–16.8]	8	7.6, [3.3–14.5]	8	47.1, [23.0–72.2]	13	8.4, [4.6–14.0]	16	14.3, [8.4–22.2]	1	20.0, [0.5–71.6]	7	20.0, [8.4–36.9]	8	9.6, [4.3–18.3]	15	10.1, [5.8–16.2]	0	0.0, [0.0–45.9]
	Respiratory signs	16	11.9, [6.9–18.5]	12	11.4, [6.0–19.1]	0	0.0, [0.0–19.5]	22	14.3, [9.2–20.8]	6	5.4, [2.0–11.3]	0	0.0, [0.0–52.2]	5	14.3, [4.8–30.3]	6	7.3, [2.7–15.2]	15	10.1, [5.8–16.2]	2	33.3, [4.3–77.7]
	Random find	14	10.4, [5.8–16.8]	9	8.6, [4.0–15.6]	0	0.0, [0.0–19.5]	3	1.9, [0.4–5.6]	18	16.1, [9.8–24.2]	2	40.0, [5.3–85.3]	1	2.9, [0.1–14.9]	7	8.5, [3.5–16.8]	15	10.1, [5.8–16.2]	0	0.0, [0.0–45.9]
	Gastrointestinal signs	8	5.9, [2.6–11.3]	5	4.8, [1.6–10.8]	1	5.9, [0.1–28.7]	8	5.2, [2.3–10.0]	5	4.5, [1.5–10.1]	1	20.0, [0.5–71.6]	2	5.7, [0.7–19.6]	4	4.9, [1.3–12.0]	8	5.4, [2.4–10.4]	0	0.0, [0.0–45.9]
	Neurological signs	2	1.5, [0.2–5.2]	3	2.9, [0.6–8.1]	1	5.9, [0.1–28.7]	4	2.6, [0.7–6.5]	2	1.8, [0.2–6.3]	0	0.0, [0.0–52.2]	0	0.0, [0.0–10.0]	3	3.7, [0.8–10.3]	3	2.0, [0.4–5.8]	0	0.0, [0.0–45.9]
	Neoplasia	1	0.7, [0.0–4.1]	1	1.0, [0.0–5.2]	0	0.0, [0.0–19.5]	2	1.3, [0.2–4.6]	0	0.0, [0.0–3.2]	0	0.0, [0.0–52.2]	0	0.0, [0.0–10.0]	1	1.2, [0.0–6.6]	0	0.0, [0.0–2.5]	1	16.7, [0.4–64.1]
	Unknown	6	4.4, [1.6–9.4]	8	7.6, [3.3–14.5]	2	11.8, [1.5–36.4]	12	7.8, [4.1–13.2]	4	3.6, [1.0–8.9]	0	0.0, [0.0–52.2]	5	14.3, [4.8–30.3]	2	2.4, [0.3–8.5]	8	5.4, [2.4–10.4]	1	16.7, [0.4–64.1]
Cause of death	Infectious disease	86	61.0, [52.4–69.1]	66	58.4%, [48.8–67.6]	12	70.6, [44.0–89.7]	89	57.8, [49.6–65.7]	70	62.5, [52.9–71.5]	5	100.0, [47.8–100.0]	22	62.9, [44.9–78.5]	53	64.6, [53.3–74.9]	86	58.1, [49.7–66.2]	3	50.0, [11.8–88.2]
	Trauma/ Predation	39	27.7, [20.5–35.8]	32	28.3, [20.2–37.6]	4	23.5, [6.8–49.9]	49	31.8, [24.6–39.8]	26	23.2, [15.8–32.1]	0	0.0, [0.0–52.2]	3	8.6, [1.8–23.1]	19	23.2, [14.6–33.8]	51	34.5, [26.8–42.7]	2	33.3, [4.3–77.7]
	Starvation	2	1.4, [0.2–5.0]	3	2.7, [0.6–7.6]	0	0.0, [0.0–19.5]	3	1.9, [0.4–5.6]	2	1.8, [0.2–6.3]	0	0.0, [0.0–52.2]	5	14.3, [4.8–30.3]	0	0.0, [0.0–4.4]	0	0.0, [0.0–2.5]	0	0.0, [0.0–45.9]
	Neoplasia	3	2.1, [6.1]	2	1.8, [0.2–6.2]	0	0.0, [0.0–19.5]	5	3.2, [1.2–7.4]	0	0.0, [0.0–3.2]	0	0.0, [0.0–52.2]	1	2.9, [0.1–14.9]	1	1.2, [0.0–6.6]	2	1.4, [0.1–4.8]	1	16.7, [0.4–64.1]
	Unknown	11	7.8, [4.0–13.5]	10	8.8, [4.3–15.6]	1	5.9, [0.1–28.7]	8	5.2, [2.3–10.0]	14	12.5, [7.0–20.1]	0	0.0, [0.0–52.2]	4	11.4, [3.2–26.7]	9	11.0, [5.1–19.8]	9	6.1, [2.8–11.2]	0	0.0, [0.0–45.9]

Table 4. Frequencies and percentages of the causes of death of all examined hedgehogs, shown for all four seasons. Winter = from 22nd December to 20th March; spring = from 21st March to 21st June; summer = from 22nd June to 22nd September; autumn = from 23rd September to 21st December.

		Cause of Death									
		Infectious Disease		**Neoplasia**		**Starvation**		**Trauma/Predation**		**Unknown**	
		n	**%, [95% CI]**	**n**	**%, [95% CI]**	**n**	**%, [95% CI]**	**n**	**%, [95% CI]**	**n**	**%, [95% CI]**
Season of death	Winter	19	11.6, [7.1–17.5]	1	20.0, [0.5–71.6]	1	20.0, [0.5–71.6]	2	2.7, [0.3–9.3]	3	13.6, [2.9–34.9]
	Spring	37	22.6, [16.4–29.7]	2	40.0, [5.3–85.3]	1	20.0, [0.5–71.6]	28	37.3, [26.4–49.3]	4	18.2, [5.2–40.3]
	Summer	60	36.6, [29.2–44.5]	0	0.0, [0.0–52.2]	3	60.0, [14.7–94.7]	27	36.0, [25.2–47.9]	10	45.5, [24.4–67.8]
	Autumn	45	27.4, [20.8–34.9]	2	40.0, [5.3–85.3]	0	0.0, [0.0–52.2]	14	18.7, [10.6–29.3]	5	22.7, [7.8–45.4]
	Unknown	3	1.8, [0.4–5.3]	0	0.0, [0.0–52.2]	0	0.0, [0.0–52.2]	4	5.3, [1.5–13.1]	0	0.0, [0.0–15.4]

Regarding the season of death, most hedgehogs died in summer (from 22nd June to 22nd September; n = 100, 36.9%), followed by spring (from 21st March to 21st June; n = 72, 26.6%), autumn (from 23rd September to 21st December; n = 66, 24.4%) and winter (from 22nd December to 20th March; n = 26, 9.6%). These data were not available for 7 animals (2.6%).

3.2. Causes of Admission

The main cause of hedgehog admission at veterinary clinics and WRCs of both countries was traumatic insults (n = 77, 28.4%, 95% CI: 23.1–34.2), followed by a poor overall condition (n = 75, 27.7%, 95% CI: 22.4–33.4), respiratory (n = 28, 10.3%, 95% CI: 7.0–14.6), gastrointestinal (n = 14, 5.2%, 95% CI: 2.9–8.5) or neurological signs (n = 6, 2.2%, 95% CI: 0.8–4.8) and random find without manifestation of specific clinical signs (n = 23, 8.5%, 95% CI: 5.5–12.5). A total of 30 animals were found dead or died prior to arrival at the centers (11.1%, 95% CI: 7.6–15.4), and for 16 individuals, the cause of admission was not recorded (5.9%, 95% CI: 3.4–9.4).

A significant association was observed between the cause of admission and the country of origin (p-value < 0.001, Cramer's V = 0.593). As shown in Table 2, in Italy, most animals were admitted due to a traumatic injury (37.0%) or debilitation (34.6%), while in Switzerland, most animals were found dead (24.8%), followed by manifestations of weakness (17.4%) and traumatic insults (15.6%).

Moreover, considering both countries together, the causes of admission were significantly associated with age classes (p-value < 0.001, Cramer's V = 0.298). Adult was the category with most animals admitted because of trauma (36.4%) or respiratory signs (14.3%) (see Table 3). In contrast, juveniles were mainly submitted due to the manifestation of weakness/debilitation (35.7%) or because they were found dead (or had died prior to therapeutic treatment; 14.3%). Unweaned animals were mainly randomly found (40%).

BCS also showed a significant association with the causes of admission (p-value = 0.002, Cramer's V = 0.240). Emaciated or thin animals were mainly admitted due to clinical manifestation of weakness (n = 38, 32.5%, 95% CI: 24.1–41.8), while animals with a good or excellent body condition mainly were submitted due to trauma (n = 49, 31.8%, 95% CI: 24.6–39.8).

No significant association was found between the sex and the cause of admission.

3.3. Causes of Death

The summary of the causes of death for both countries revealed that most hedgehogs died of infectious or parasitic diseases (n = 164, 60.5%, 95% CI: 54.4–66.4), followed by traumatic insults (n = 75, 27.7%, 95% CI: 22.4–33.4). Five animals out of 271 (1.8%, 95% CI: 0.6–4.3) died of starvation (determined due to severe cachexia and emptiness of the gastrointestinal tract) and another five (1.8%, 95% CI: 0.6–4.3) because of neoplasia. For 22 animals, the macroscopic and histologic analysis could not determine the cause of death with certainty (8.1%). Euthanasia was performed on 63 animals (23.2%).

A statistically significant association between the cause of death and the country of origin was detected (p-value < 0.001, Cramer's V = 0.325). In both countries infectious diseases were the most frequently reported cause of mortality (53.7% in Italy and 70.6% in Switzerland). On the other hand, as displayed in Table 2, a higher percentage of animals had died due to traumatic insults in Italy (38.3%), while only 13 animals were reported with trauma in Switzerland (11.9%).

Considering both countries together, a significant association was also present between the cause of mortality and BCS (p-value < 0.001, Cramer's V = 0.253). Infectious/parasitic disease was the main cause of mortality across all body categories (see Table 3). However, animals with a good or excellent body condition showed a higher percentage of traumatic insults (34.5% and 33.3%, respectively).

Age and season of death also appeared to be statistically related (p-value < 0.001, Cramer's V = 0.270), with adult animals mainly dying in spring (n = 58, 37.7%) and summer

(n = 41, 26.6%), and juveniles predominantly dying in summer (n = 54, 48.2%) and autumn (n = 36, 32.1%). Even if a statistical association was not found (p-value = 0.498), there was a trend for male hedgehogs to most frequently decease in summer (n = 47, 33.3%) and spring (n = 42, 29.8%), while females mainly had died in summer (n = 45, 40.2%) and autumn (n = 31, 27.7%).

No association was either present between the cause of death and the sex (p-value = 0.952), age (p-value = 0.103) or season (p-value = 0.130).

3.4. Pathological Findings

Histologic examination was performed on 257 hedgehogs (94.8%) and 14 animals (5.2%) were excluded due to either severe autolytic processes or because the cause of death could be clearly stated based on gross examination. The data reported refer to all animals analyzed, considering comprehensively both countries.

3.4.1. External Examination

Upon external gross examination, 65 animals (24.0%, 95% CI: 19.0–29.5) presented with ectoparasitic infestation. Ticks belonged to *Ixodes hexagonus* and *Ixodes ricinus*, while fleas were all *Archaeopsilla erinacei*, identified by means of taxonomic keys as part of a further research project [34–36]. The percentages of ectoparasite detection are reported in Table 5.

Table 5. Frequency and percentage of the main macroscopic findings identified in the inner organs.

Organ	Macroscopic Findings	n	%, [95% CI]
Ectoparasites	Co-infestation	25	9.2, [6.1–13.3]
	Myiasis	17	6.3, [3.7–9.9]
	Ticks	15	5.5, [3.1–9.0]
	Fleas	8	3.0, [1.3–5.7]
Lung	Granulomatous bronchopneumonia ± pleuritis	90	33.2, [27.6–39.2]
	Catarrhal bronchopneumonia ± pleuritis	55	20.3, [15.7–25.6]
	Hyperemia	26	9.6, [6.4–13-7]
	Suppurative bronchopneumonia ± pleuritis	14	5.2, [2.9–8.5]
	Hemorrhage	6	2.2, [0.8–4.8]
	Fibrinous pleuropneumonia	4	1.5, [0.4–3.7]
	Neoplasia	1	0.4, [0.0–2.0]
Liver	Hyperemia	11	4.1, [2.0–7.1]
	Lipidosis	11	4.1, [2.0–7.1]
	Chronic hepatitis/Perihepatitis	5	1.8, [0.6–4.3]
	Rupture	4	1.5, [0.4–3.7]
	Neoplasia	1	0.4, [0.0–2.0]
Skin	Laceration/Abrasion/Hemorrhage	48	17.7, [13.4–22.8]
	Dermatitis	17	6.3, [3.7–9.9]
	Abscess/Granuloma	9	3.3, [1.5–6.2]
Intestine	Catarrhal enteritis	20	7.4, [4.6–11.2]
	Herniation	4	1.5, [0.4–3.7]
	Hemorrhagic enteritis	3	1.1, [0.2, 3.2]
Mesenteric lymph nodes	Reactive hyperplasia	20	7.4, [4.6–11.2]

Table 5. *Cont.*

Organ	Macroscopic Findings	n	%, [95% CI]
Musculo-skeletal	Limb fracture/Luxation/Amputation	15	5.5, [3.1–9.0]
	Skull fracture	12	4.4, [2.3–7.6]
	Myositis/Osteitis	9	3.3, [1.5–6.2]
	Hemorrhage	8	3.0, [1.3–5.7]
	Polytrauma	4	1.5, [0.4–3.7]
Spleen	Congestion	16	5.9, [3.4–9.4]
	Neoplasia	3	1.1, [0.2, 3.2]
	Splenitis	3	1.1, [0.2, 3.2]
	Rupture	2	0.7, [0.1–2.6]
Kidneys	Interstitial nephritis/Glomerulonephritis	3	1.1, [0.2, 3.2]
	Hyperemia	2	0.7, [0.1–2.6]
	Neoplasia	2	0.7, [0.1–2.6]
	Petechiae	2	0.7, [0.1–2.6]
Stomach	Catharral gastritis	15	5.5, [3.1–9.0]
	Hemorrhagic gastritis	11	4.1, [2.0–7.1]
	Gastric ulcer	5	1.8, [0.6–4.3]
	Traumatic rupture	1	0.4, [0.0–2.0]
	Parasites	1	0.4, [0.0–2.0]
Brain	Hemorrhage	9	3.3, [1.5–6.2]
	Subdural hematoma	8	3.0, [1.3–5.7]
	Meningitis/meningoencephalitis	1	0.4, [0.0–2.0]
Heart	Fibrinous pericarditis	6	2.2, [0.8–4.8]
Urinary bladder	Suspected neurogenic bladder dysfunction	4	1.5, [0.4–3.7]
	Cystitis	2	0.7, [0.1–2.6]
Reproductive tract	Endometritis/Metritis	3	1.1, [0.2, 3.2]
	Balanoposthitis	1	0.4, [0.0–2.0]
Thoracic effusion	Serohemorrhagic	45	16.6, [12.4–21.6]
	Hemothorax	13	4.8, [2.6–8.1]
	Suppurative	6	2.2, [0.8–4.8]
	Serum-fibrinous	3	1.1, [0.2, 3.2]
Abdominal effusion	Serohemorrhagic	13	4.8, [2.6–8.1]
	Hemoabdomen	4	1.5, [0.4–3.7]
	Serofibrinous	2	0.7, [0.1–2.6]
	Suppurative	1	0.4, [0.0–2.0]

3.4.2. Inner Organs

The descriptions of the macroscopic and histologic lesions detected in the inner organs are reported in Tables 5 and 6 and are arranged based on the frequency in which each organ system was affected, ranging from most to less frequently interested. Figures 1 and 2 represent some of the macroscopic and histologic lesions detected, respectively.

Table 6. Frequency and percentage of the most frequent histologic findings identified in the inner organs. Histologic examination was not performed on 14 animals; therefore, these data are presented considering a total of 257 animals.

Organ	Histologic Findings	n	%, [95% CI]
Lung	Lymphoplasmacytic pneumonia ± pleuritis	118	45.9, [39.7–52.2]
	Granulomatous pneumonia ± pleuritis	49	18.1, [13.7–23.2]
	Suppurative pneumonia ± pleuritis	21	8.2, [5.1–12.2]
	Neoplasia	1	0.4, [0.0–0.2]
	Pulmonary parasites	147	57.2, [50.9–63.3]
Liver	Lymphoplasmacytic (cholangio)hepatitis	60	23.3, [18.3–29.0]
	Steatosis	12	4.7, [2.4–8.0]
	Suppurative/Mixed cellular (cholangio)hepatitis ± necrosis	9	3.5, [1.6–6.5]
	Granulomatous (cholangio)hepatitis	7	2.7, [1.1–5.5]
	Necrosis/Degeneration	7	2.7, [1.1–5.5]
	Neoplasia	3	1.2, [0.2–3.4]
Intestine	Lymphoplasmacytic enteritis	42	16.3, [12.0–21.4]
	Suppurative/necrotizing enteritis	13	5.1, [2.7–8.5]
	Intestinal parasites	35	13.6, [9.7–18.4]
Spleen	Extramedullary hematopoiesis	66	25.7, [20.5–31.5]
	Reactive hyperplasia of the white pulp	39	15.2, [11.0–20.2]
	Follicular depletion/rarefaction	3	1.2, [0.2–3.4]
	Neoplasia	3	1.2, [0.2–3.4]
	Splenitis	3	1.2, [0.2–3.4]
	Necrosis	1	0.4, [0.0–0.2]
Kidneys	Lymphoplasmacytic/granulomatous/suppurative nephritis	40	15.6, [11.4–20.6]
	Degeneration/Necrosis of tubuli	4	1.6, [0.4–3.9]
	Neoplasia	2	0.8, [0.1–2.8]
Brain	Suppurative (meningo)encephalitis	12	4.7, [2.4–8.0]
	Lymphoplasmacytic (meningo)encephalitis	11	4.3, [2.2–7.5]
	Hemorrhage	7	2.7, [1.1–5.5]
	Granulomatous (meningo)encephalitis	1	0.4, [0.0–0.2]
Heart	Lymphoplasmacytic epi-/myo-/endocarditis	11	4.3, [2.2–7.5]
	Suppurative myocarditis	5	1.9, [0.6–4.5]

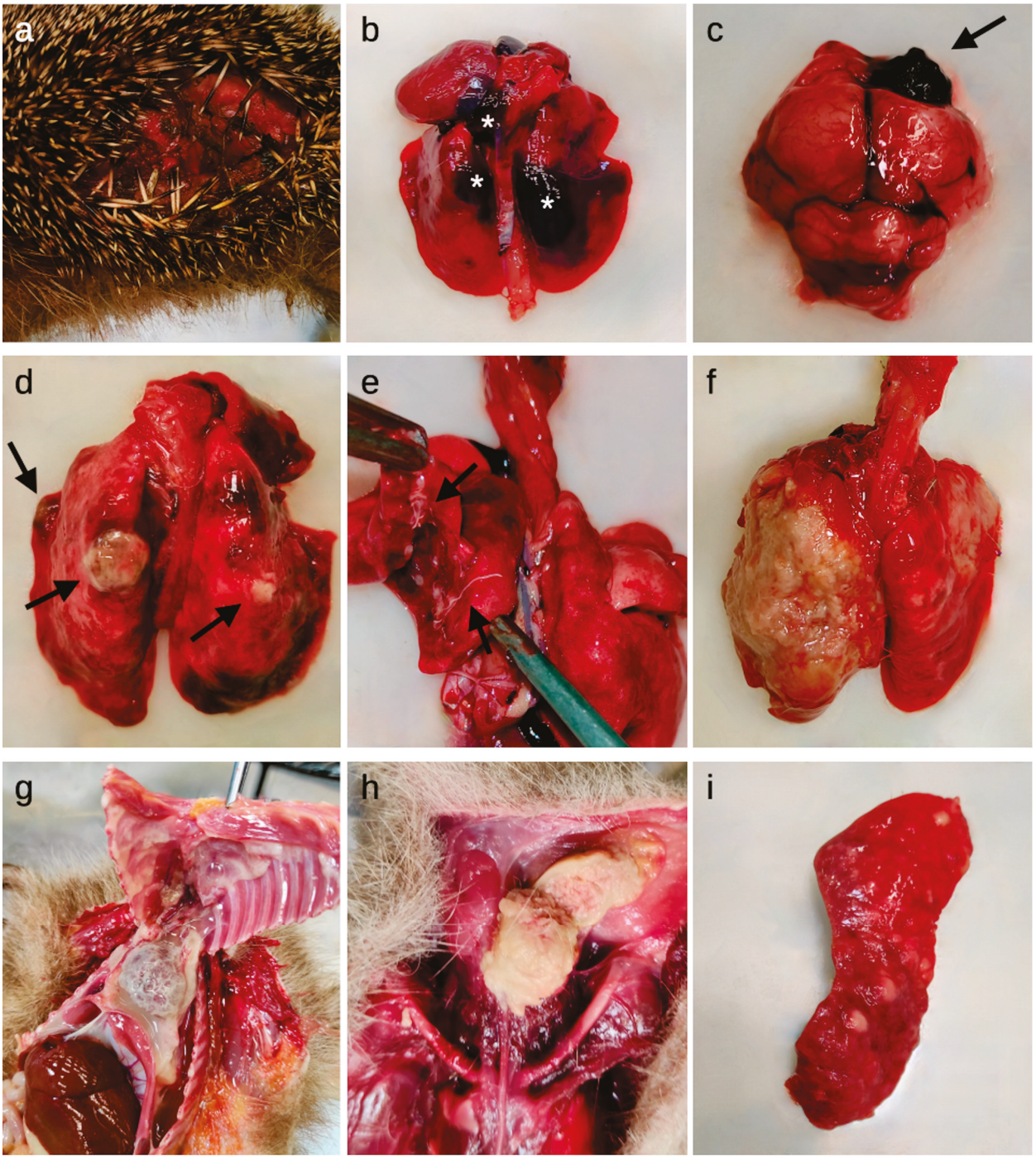


Figure 1. Macroscopic lesions detected in the studied European hedgehogs. (**a**) Skin: laceration of the lateral abdominal region; (**b**) Lungs: multifocal hemorrhages (asterisks) in the parenchyma; (**c**) Brain: focal hemorrhage in the right frontal lobe (arrow); (**d**) Lungs: multifocal granulomatous lesions (arrows) and hyperemia; (**e**) Lungs: lungworms (arrows) on the cut surface and in the bronchial lumina; (**f**) Lungs: severe diffuse fibrinous-suppurative pleuropneumonia; (**g**) Thoracic cavity: severe diffuse fibrinous pericarditis, pleuritis and serum-fibrinous thoracic effusion; (**h**) Ventral neck region: abscess; (**i**) Spleen: lymphoma.

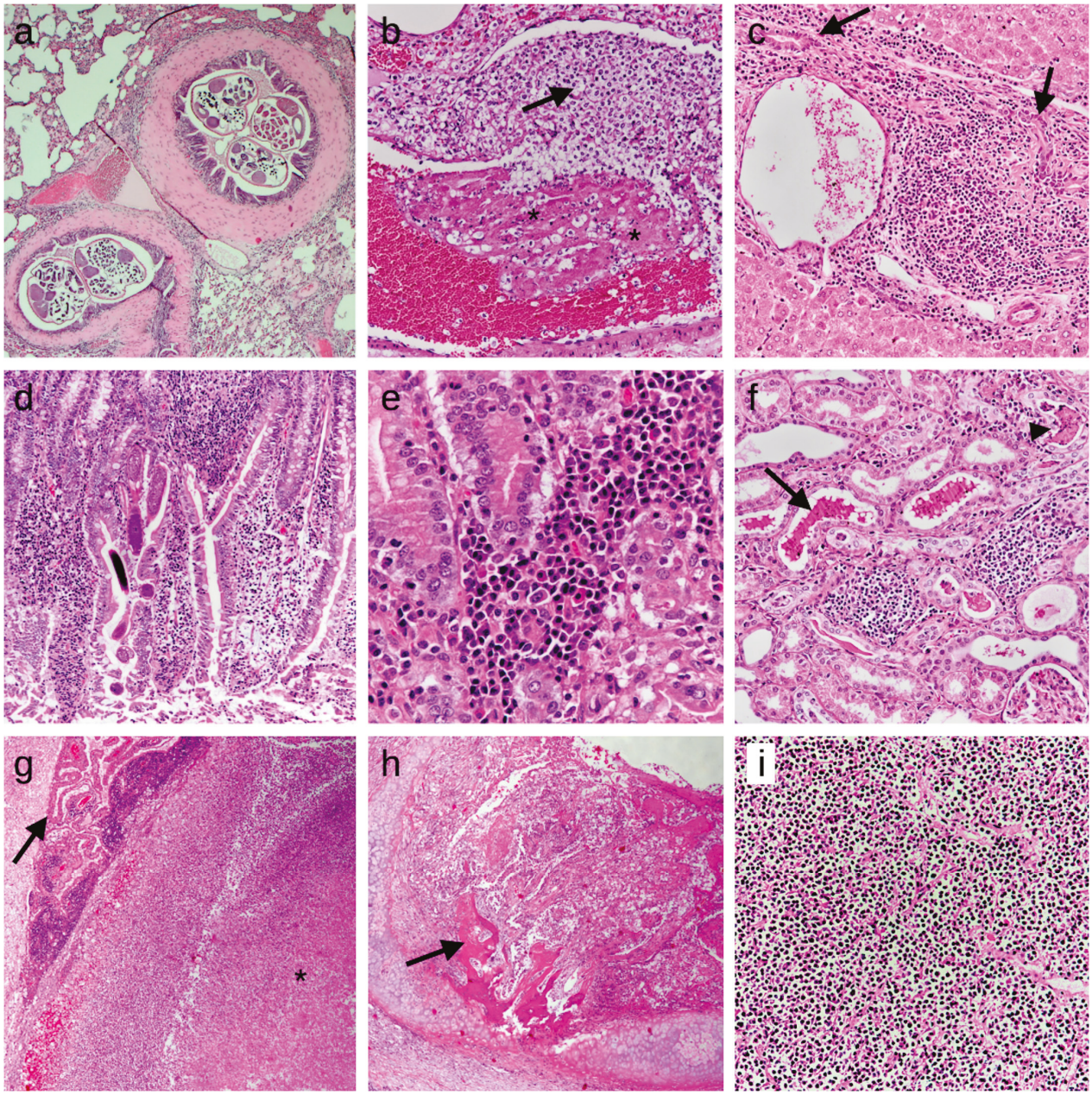


Figure 2. Histologic findings detected in the studied European hedgehogs. Lesions are shown according to the frequency of detection and the order in which they appear in the text. The first seven images represent inflammatory processes, while the last two are from neoplastic cases. HE stain. (**a**) Lung: lymphoplasmacytic bronchopneumonia with nematode slices in bronchial lumina, 50×; (**b**) Lung: presence of fibrin thrombi (asterisks) and immature neutrophils (arrow) attached to a pulmonary vessel wall, indicating septicemia/disseminated intravascular coagulation, 200×; (**c**) Liver: moderate chronic periportal hepatitis, characterized by infiltrations of lymphocytes and plasma cells and bile duct hyperplasia (arrows), 200×; (**d**) Intestine: moderate chronic enteritis with multiple larvae of nematodes in the mucosa, 100×; (**e**) Intestine: lymphocytes and plasma cells in the tela submucosae, 400×; (**f**) Kidney: mild chronic interstitial nephritis, characterized by infiltrations of lymphocytes and plasma cells. Also note the presence of chromoproteinuria (arrow) and cellular casts (arrowhead) in the tubular lumen, 200×; (**g**) Brain: focal abscess in the pons region (asterisk), compressing the choroid plexus (arrow), 50×; (**h**) Trachea: tracheal carcinoma, focally infiltrating the tracheal cartilage and showing focal osteoid formation (arrow), 25×; (**i**) Spleen: lymphoma, characterized by the presence of lymphoid neoplastic cells, entirely effacing the splenic architecture, 200×.

The lung was the most affected organ. In 57.2% of hedgehogs, cut sections of nematode eggs, larvae or adults were detected in the bronchial lumina (Figures 1e and 2a). A significant association was found between parasite presence and histologic findings (p-value < 0.001, Cramer's V = 0.525): in 91.8% (95% CI: 80.4–97.7) of the granulomatous pneumonia (n = 45), and in 65.3% (95% CI: 55.9–73.8) of the lymphoplasmacytic ones (n = 77), a concurrent presence of parasites was detected. In eight animals, the parasite presence was associated with lymphoplasmacytic laryngitis or tracheitis.

Cut sections of nematodes were detected in the intestinal lumen and/or in the mucosa of 35 animals (Figure 2d). A statistically significant association was observed between the presence of intestinal parasites and enteritis (p-value = 0.022, Cramer's V = 0.180).

Of the 74 animals affected by skin lesions, chronic, suppurative or ulcerative dermatitis was macroscopically reported in 17 animals (23.0%, 95% CI: 14.0–34.2) and subjected to histological examination. Of those animals, three cases presented multifocal epidermal ulcerations with degenerated neutrophils, bacterial colonies and mixed cellular infiltration in the subcutis. Three further animals showed chronic dermatitis with orthokeratotic hyperkeratosis, of which, two displayed intradermal presence of fungal spores and hyphae.

3.4.3. Body Cavities

The macroscopic findings detected in the body cavities are shown in Table 5 and Figure 1. Herniation of the abdominal organs was seen in four animals: three with lacerations of the abdominal wall with intestinal herniation and one with diaphragmatic intestinal herniation.

3.4.4. Neoplasia

Neoplasia was overall not common and led to the death of five animals (1.8%). Two hedgehogs were affected by lymphoma (Figures 1i and 2i); multifocally, the liver and spleen (and in one animal also the kidneys) were infiltrated by sheets of monomorphic round cells of 10–20 µm in diameter. Cells showed centrally located, heterochromatin-rich, round- to beam-shaped nuclei and sparse eosinophilic cytoplasm. Zero to one mitotic figure were detected in 10 high-power fields at highest magnification (400×).

One animal displayed an anaplastic tracheal carcinoma, characterized by a mucosal infiltration of small groups of pleomorphic neoplastic cells (Figure 2h). The polygonal cells possessed a moderate to abundant vacuolized cytoplasm, undefined margins, irregular nuclei with vesicular chromatin and a small nucleolus, with moderate to abundant anisocytosis and anisokaryosis and rare mitotic figures. Neutrophilic infiltration and necrotic foci were also present multifocally in the neoplasm.

One hedgehog showed multiple white, smooth, nodular proliferations on the thoracic wall, the abdominal serosal face of the diaphragm, kidneys and spleen. Histologically, the neoplasia showed features of a sarcoma, as it consisted of moderately pleomorphic elongated, spindeloid cells forming whorls and streams. Due to the combination of the macroscopic and histologic appearance of the neoplasia, the tentative diagnosis of a mesothelioma was made.

Another hedgehog was diagnosed with a sarcoma, that was presented as a nodule of 6 cm × 6 cm × 4 cm found in the subcutis of the left lateral abdominal region. Histologically, the proliferation was composed of spindle cells arranged in irregular streams and bundles with a variable amount of eosinophilic fibrillar cytoplasm, elongated to round nuclei and inconspicuous nucleoli. Rare mitotic figures were observed. Metastases of the neoplastic proliferations were found in the omentum majus, the liver, the spleen, the kidney, the lungs and the right submandibular lymph node.

3.4.5. Detection of Parasitic and Bacterial Infectious Agents

In 96 animals, fecal samples were submitted to coprological examination. From those, endoparasites could be detected in 77 samples (80.2%, 95% CI: 70.8–87.6). More specifically, 68 (88.3%, 95% CI: 79.0–94.5) animals were infested by *Capillaria* spp. (in most cases

these could be further identified as the species *Capillaria aerophila*), 37 (48.1%, 95% CI: 36.5–59.7) by *Crenosoma striatum*, 13 (16.9%, 95% CI: 9.3–27.1) by *Brachylaemus erinacei* and six (7.8%, 95% CI: 2.9–16.2) by *Cystoisospora* spp. Of all positive animals, 42 animals (54.5%, 95% CI: 42.8–65.9) displayed coinfection with at least two or all three of the addressed parasite species.

Bacteriological investigations were performed on 17 animals. *Clostridium perfringens*, *Enterococcus* spp. or *Enterobacteriaceae* were isolated from the gastrointestinal tract in three cases. In the respiratory tract, *Pasteurella* spp. and *Pasteurella multocida*, *Bacteroides fragilis*, *Salmonella enterica* serovar *enteritidis* or *Morganella morganii* were isolated from four animals. One hedgehog with multiple abscesses and peritonitis was positive for *Clostridium perfringens* type A. In nine further samples, no predominant bacterial agent could be cultivated, as only either a mixed bacterial flora or no bacteria (negative result) were reported.

4. Discussion

This study aimed to evaluate the causes of admission and mortality in European hedgehogs and to describe their main pathologic findings by means of a full postmortem examination, including histological investigation. This species is distributed throughout Europe and, as its presence is tightly connected to human settlements, it plays a crucial role in the human—wildlife interface. Recent studies have described a decline in the European hedgehog population in several European areas [16–18,27]. This prompted us to initiate the present study, by collecting and comparing data from two neighboring countries, Italy and Switzerland.

The Italian Piedmont region and Swiss Canton of Zurich are characterized by similar geographical features. Both regions are located in the subcontinental climatic European area, presenting mild summers and cold winters and seasonal fluctuations in temperature extremes [37]. Both countries are rich in rivers and lakes, while forest coverage accounts for approximately 30% in the Canton of Zurich and 37% in Piedmont [38,39]. Moreover, both regions are highly inhabited, with populated valleys characterized by marked land use and industrial development [38,40]. Climate change, as a global phenomenon, also affects both areas, and manifests as glacier melting, high-temperature peaks, reduction in rainfall and an increase in both intense rain and drought periods [41,42]. These similar characteristics allowed us to reduce the possible bias represented by the different geographic origins of the sampled animals and to facilitate the comparison of the obtained results.

In general, studies have pointed out that both climate change and human activities may contribute to a decline in hedgehog population [16,18]. More specifically, a recent study by Taucher indicated a decline in the population of European hedgehogs in the Canton of Zurich, which, among many other causes, was attributed to urban densification with consequent habitat fragmentation, changes in summer and winter temperatures, reductions in insect biomass, pesticide use and infectious diseases [16]. In addition, considering the geographic similarities between the two countries [29] and the lack of studies on the causes of mortality in Italian hedgehog populations, we considered this analysis fundamental, especially in the eye of possible future decline in population density.

In our study, the main causes of admission of the animals in both countries were traumatic insults, followed by debilitation, finding of a dead animal or death during transport, respiratory signs, and random findings. However, the frequencies of the causes of admission significantly differed between the two countries, with Italy constituting mainly traumatic insults (37.0%) and debilitation (34.6%), whereas in Switzerland, most of the examined hedgehogs were either found dead (24.8%) or displayed weakness (17.4%). This difference could be attributed to a possible bias related to the difference in the sequence of procedures preceding the examination of the carcasses: Italian hedgehogs were first submitted to the WRCs and—in the case of death or euthanasia—subsequently submitted for postmortem examination, while in Switzerland, all animals were directly submitted for necropsy by citizens, veterinary clinics or WRCs. Therefore, it could be less likely for

Italian citizens to bring animals to WRCs, when they are found dead or have already died during transport. In Italy, 38.3% of animals displayed lethal trauma, while this cause of death only accounted for 11.9% of examined hedgehogs in Switzerland. Although this information was not included in the statistical analysis, in most of the examined cases, the anamnesis indicated that trauma was most often related to car accidents, predation, entanglement or mowing-provoked lacerations. The difference in the frequency of trauma between the two countries could be attributed to differences in the urban environments of Italy and Switzerland. Indeed, areas with limited driving speed have been introduced in Zurich and in many other Swiss cities, where only a slight increase in the number of vehicles has been recorded [16]. In addition, Swiss citizens use public transport more frequently than in Italy, particularly in the Piedmont region (76.7% vs. 16.2%) [43,44]. These factors most likely contributed to the reduction in possible road traffic accidents. Moreover, Switzerland has a higher population density (215 inhabitants/km^2 on average, reaching over 400 inhabitants/km^2 in the Central Plateau, a geographical area where most of the population is located) [45] compared to the Piedmont region (168.4 inhabitants/km^2 and 325.1 inhabitants/km^2 in Turin province) [46]. This urban densification also led to a reduction in urban green spaces in Switzerland [16], limiting traumatic insults related to gardening-related activities (e.g., entanglement, mowing wounds, predation by domestic animals as dogs). Finally, the Swiss government has focused on promoting campaigns that help implement hedgehog-friendly gardens and educate citizens regarding responsible behavior towards this species, reducing the likelihood of human-related traumatic insults [47].

The causes of admission and death were also significantly associated with BCS. Traumas mainly affected animals with good or excellent body condition, which are more active than emaciated individuals and therefore cover larger areas, which simultaneously imposes a greater risk of being trapped, hit by cars or predated [7].

Traumatic insults mainly affected adults (65.3%) and were more frequent in the spring (37.3%) and summer (36.0%). It is important to note that male hedgehogs expand their territory in spring to mate, and that females are more active in summer, as they look for food resources (so as to increase their fat tissue deposition after or during lactation). In conclusion, our study supports the theory already stated by other authors, that increased locomotion related to the reproductive season can increase the probability of traumatic insults [6,7,10,12,13,32].

Infectious diseases mainly occurred in summer (36.6%) and autumn (27.4%). In these seasons, adults show reduced energy levels after the mating season (mainly males) or due to increased energy consumption during pregnancy and lactation (for female hedgehogs, which can deliver up to two litters in those seasons) [32]. Reductions in body conditions are known to predispose animals to infections, starvation and dehydration [32]. In addition, summer and autumn also represent the seasons in which juvenile hedgehogs start to disperse and search for food resources to build up adequate fat reserves prior to hibernation. The exploration of new territories also explains the high percentage of random finds of juveniles (16.1%) in our study. Indeed, citizens often wrongly believe that young animals found in the wild are abandoned or in danger and, therefore, needlessly submit them to WRCs. However, this can reduce their chances of survival [9,13].

The diagnosis of infectious disease was based on macroscopic and/or histologic detection of inflammatory infiltrates in at least one organ. In 39% of the cases in which an infection was diagnosed, the presence of leukocytes in the vessels of different organs, accompanied or not by the presence of fibrinous thrombi (indication of disseminated intravascular coagulation) and bacteria, justified the suspicion of terminal sepsis (Figure 2b). To our knowledge, this study is the first to report infectious diseases as the most frequent cause of mortality in European hedgehogs. In two other studies focusing on the results of full postmortem examinations in this species, traumatic insults of known or unknown origin were determined as the most frequent cause of mortality, leading to death in 41% of animals in the study by Zacharopoulou et al. [23], and in 32.7% in the study by Gracês et al. [19].

The first study determined infectious diseases caused by viruses or bacteria as the second most frequent cause of mortality (34%), followed by parasitism (11%), whereas infectious agents were responsible for 8.1% of hedgehog deaths in the study by Garcês et al. However, if we consider infectious and parasitic diseases together in Zacharopoulou's work, the overall prevalence is 45%, which is higher than the frequency of traumatic insults, and, therefore, would also constitute the first cause of mortality. In the study by Garcês et al. [19], the authors stated that histopathological examination was frequently impaired by severe autolysis or was not performed because of a lack of financial resources, thus possibly preventing the detection of lesions compatible with an infectious origin.

In all the addressed studies, verminous pneumonia (infection with lungworms) represented one of the most described infectious diseases in the European hedgehog [16,23,48]. In our study, the lungs were the most affected organ. The majority of animals showed lymphoplasmacytic pneumonia, followed by granulomatous and suppurative pneumonia. All types of pneumonia were significantly associated with the histological presence of parasites. This is in line with the results of fecal exams, which identified the presence of the nematodes *Crenosoma striatum* and *Capillaria aerophila*, both of which have already been described as the main agents of verminous pneumonia in hedgehogs [48]. Infection with both parasites has been associated with clinical signs such as weight loss, dry cough, nasal discharge, dyspnoea, wheezing and exercise intolerance [49]. Histologically, adult *Capillaria aerophila* nematodes are found either free in the airway lumen and/or within the airway epithelium, from the larynx to the bronchioles, as stated in a recent study on European hedgehogs originating from the Canton of Zurich. In this study, embedded worms and eggs of *Capillaria aerophila* were associated with epithelial hyperplasia or metaplasia of the respiratory epithelium [48]. In contrast, *Crenosoma striatum* adults were predominantly free in the lumen of bronchi and bronchioles, and their larvae were occasionally seen in granulomas in the pulmonary interstitium [48]. In accordance with previous studies, we also identified co-infection with these two parasite species [48–54]. Lungworm infection has also been reported to occur more frequently in adults than in juveniles [49,51,53], which is thought to be related to the shorter exposure time of young hedgehogs to the parasite's intermediate or paratenic hosts (e.g., earthworms and snails). This difference in age susceptibility also explains why the hedgehogs admitted due to the manifestation of respiratory clinical signs in our study were mainly adults (14.3%, compared to 5.4% juveniles).

The clinical relevance and significance of lungworm infection in hedgehogs have been controversial in previous studies. Although some authors have stated that lungworm infection is a main driver of hedgehog mortality [7,49,55], others have also associated parasites with subclinical infection/disease, indicating that a certain parasitic burden might represent a part of the hedgehog ecology [23,48]. In support of this hypothesis, Zacharopoulou et al. [23] reported that parasitism was associated with mortality in only 11% of animals. In accordance with the occasionally contradictory conclusions of previous studies, the interpretation of the clinical significance (and association with mortality) of lungworm infection was not always straightforward in the present study. Although a high number of deceased or euthanized animals displayed evidence of lungworm infection and a certain degree of associated pneumonia, the affected animals showed variation in their overall health condition. Hence, verminous pneumonia was detected in otherwise healthy animals (e.g., ones that had died due to a traumatic insult, without other histologic lesions in the inner organs) but also in hedgehogs displaying additional concurrent disease processes in other inner organs. In a small proportion of animals, verminous pneumonia was the only disease process noted on postmortem examination, highlighting its importance as a major contributor to mortality. Based on these results, we can hypothesize that, while in some cases, lungworm infection might not cause drastic alterations in host homeostasis, in other cases, it might represent the main agent of disease or promote the development and spread of other infectious agents, ultimately leading to the death of the animal. Nevertheless, the exact mechanism by which lungworms disrupt the host immune system or interact with other pathogens warrants further investigation.

Indeed, it has been reported that verminous pneumonia can be complicated by secondary bacterial infections (e.g., *Bordetella bronchiseptica* or *Pasteurella multocida*) that might subsequently lead hedgehogs to death [56]. This was also the case in two animals in our study, as *Pasteurella* spp. and *Pasteurella multocida* were isolated from the respiratory tract in addition to a lungworm infection being discovered. However, because of cost limitations, the majority of the lung samples were not subjected to bacteriological culture and it was not possible to test this hypothesis and to draw statistically significant conclusions on a possible lungworm—bacteria correlation. Therefore, further studies are needed to determine the effects of endoparasites and possible co-infections on the overall health of European hedgehogs.

Additionally, parasites detected in the enteric lumen displayed a statistically significant association with the presence of lymphoplasmacytic enteritis. European hedgehogs have been reported as hosts for several endoparasites [49,53]. Among these, *Capillaria* spp., *Physaloptera clausa* and *Brachylaemus erinacei* are the parasites most frequently found in the gastrointestinal tract, where they have been described in association with chronic non-suppurative gastroenteritis [49,51,54,57]. In our fecal exams, *Capillaria* spp. and *Brachylaemus erinacei* were detected, explaining the association between enteritis and parasite presence.

Infection with several bacterial pathogens has been described in European hedgehogs: *Bordetella bronchiseptica*, *Corynebacterium ulcerans*, *Escherichia coli, Klebsiella* spp., *Pasteurella* spp., *Pseudomonas* spp., *Staphylococcus* spp., *Streptococcus* spp. and *Yersinia* spp. have all been isolated from diseased hedgehogs [6,7,21]. In our study, bacterial isolation was performed on a limited number of samples (17). Most of these (nine) yielded mixed flora or no bacterial culture. In some samples (three), *Clostridium perfringens*, *Enterococcus* spp., or *Enterobacteriaceae* were isolated, but even though these species have been described as having zoonotic potential [58–60], we were not able to correlate them with the pathological lesions detected. In other animals (five), however, the bacterial isolation and the macroscopic and histological findings led us to conclude that the isolated species could be considered agents of disease. One animal affected by fibrinous pleuropneumonia tested positive for *Morganella morganii*. This opportunistic pathogen has been described in both animals and humans (with or without evidence of disease), and also has zoonotic potential [61]. In another hedgehog with a suspected septic process, *Salmonella enterica* serovar *enteritidis* was isolated from the lungs. *Salmonella* spp. was responsible for the death of two hedgehogs in Denmark [18] and *Salmonella enterica* serovar *enteritidis* was identified in systemic and pulmonary infections in European hedgehogs in Finland [6]. This particular serovar also has zoonotic potential and Lawson et al. have identified hedgehogs as sources of transmission of this pathogen to humans [62]. Hedgehogs, indeed, have been repeatedly reported as reservoirs for several zoonotic agents (e.g., MRSA *Staphylococcus aureus, Leptospira* spp. and several tick-borne pathogens) [21,63,64].

Overall, non-infectious lesions were uncommon in the examined hedgehogs, with 1.8% of all the animals displaying neoplasia. Similarly, Garcês and colleagues identified one case of neoplasia in 248 necropsied animals [19], whereas in Zacharopoulou's study neoplasia was found in 6% of all animals (2 out of 35) [23]. Similar to other mammalian species, different types of tumors have been reported in European hedgehogs, including mammary tumors [19,65], cutaneous malignant peripheral nerve sheath tumor and cortical adrenal gland adenoma [23], desmoplastic ganglioglioma [66], subcutaneous myxosarcoma [67] and lacrimal duct carcinoma [68]. In conclusion, neoplastic diseases appear to be rare in this species.

5. Conclusions

The present study examined the main causes of mortality and pathologic findings of European hedgehogs in Italian Piedmont region and the Swiss Canton of Zurich, regions characterized by similar geographical features. Trauma, especially road accidents or predation by domestic or wild animals, is the most common cause for submission of this species

to WRCs and a significant reason for mortality. Therefore, raising public awareness on how to effectively reduce interactions and successfully protect this species' habitat is of fundamental importance to reduce its mortality. Disseminating guidelines or educational campaigns could promote responsible behavior among citizens, providing information on how to create hedgehog-friendly gardens and the correct actions to take to reduce human-related traumatic events.

We also highlight the importance of infectious, and particularly parasitic, diseases contributing to hedgehog mortality, which should be considered when establishing an appropriate therapeutic approach. However, further microbiological studies are necessary to determine the main infectious agents found in this species. This is crucial not only for the overall health of this species but also considering the synanthropic behavior of hedgehogs and their contact with domestic animals and humans, to whom these pathogens could be transmitted. The role of endoparasites and their interaction with other infectious agents also warrants further investigation before establishing prophylactic measures. In light of the numerous reports indicating a decline in hedgehog populations in several European regions, frequent monitoring of the population health status is strongly needed in all countries.

Author Contributions: Conceptualization, I.P., E.D. and M.T.C.; methodology, I.P. and M.T.C.; formal analysis, I.P. and E.C.; investigation, I.P., E.D., E.C., S.Z., G.B., U.H. and M.T.C.; resources, M.M.v.D., M.V. and U.H.; writing—original draft preparation, I.P.; writing—review and editing, E.C., E.D., S.R. and M.T.C.; supervision, M.T.C. and G.Q.; project administration, M.T.C.; funding acquisition, R.O., S.R. and M.T.C. All authors have read and agreed to the published version of the manuscript.

Funding: This research was partially funded by the Italian Health Ministry Research Grants, Bando di Ricerca Corrente 2020 (Project n°: IZS PLV grant code 13/20 RC).

Institutional Review Board Statement: The use of material from these diagnostic cases for research purposes was authorized by document MeF-Ethik-2024-01 and protocol n.1511 approved on 9 February 2024 for Switzerland and Italy, respectively.

Informed Consent Statement: The full diagnostic postmortem examination was performed upon the caretaker's request. For these diagnosis-motivated necropsies, no ethical permission is required.

Data Availability Statement: The raw data that were analyzed in this article are available upon direct request to the authors.

Acknowledgments: We thank all the staff of the Institute for Veterinary Pathology of Zurich, of the Department of Veterinary Sciences (Veterinary Pathology sector) of Turin, of C.A.N.C. and of "La Ninna" centers for their technical support.

Conflicts of Interest: The authors declare no conflicts of interest.

References

1. Döpke, C. *Kasuistische Auswertung der Untersuchungen von Igeln (Erinaceus europaeus) im Einsendungsmaterial des Instituts für Pathologie von 1980 bis 2001*; Tierärztliche Hochschule: Hannover, Germany, 2002.
2. Amori, G.; Cassola, F. IUCN Red List European Hedgehog. Available online: https://www.iucnredlist.org/species/29650/2791303#geographic-range (accessed on 4 November 2023).
3. Delogu, M.; Cotti, C.; Lelli, D.; Sozzi, E.; Trogu, T.; Lavazza, A.; Garuti, G.; Castrucci, M.R.; Vaccari, G.; De Marco, M.A.; et al. Eco-Virological Preliminary Study of Potentially Emerging Pathogens in Hedgehogs (*Erinaceus europaeus*) Recovered at a Wildlife Treatment and Rehabilitation Center in Northern Italy. *Animals* **2020**, *10*, 407. [CrossRef] [PubMed]
4. Lapini, L. *Erinaceus europaeus*. In *The Atlas of European Mammals*; Mitchell-Jones, A.J., Amori, G., Bogdanowicz, W., Krystufek, B., Reijnders, P.J.H., Spitzenberger, F., Stubbe, M., Thissen, J.B.M., Vohralik, V., Zima, J., Eds.; Poyser: London, UK, 1999; pp. 38–40.
5. Pettett, C.E.; Moorhouse, T.P.; Johnson, P.J.; Macdonald, D.W. Factors Affecting Hedgehog (*Erinaceus europaeus*) Attraction to Rural Villages in Arable Landscapes. *Eur. J. Wildl. Res.* **2017**, *63*, 54. [CrossRef]
6. Rautio, A.; Isomursu, M.; Valtonen, A.; Hirvelä-Koski, V.; Kunnasranta, M. Mortality, Diseases and Diet of European Hedgehogs (*Erinaceus europaeus*) in an Urban Environment in Finland. *Mammal Res.* **2016**, *61*, 161–169. [CrossRef]
7. Bexton, S. Hedgehogs. In *BSAVA Manual of Wildlife Casualties*; Mullineaux, E., Keeble, E., Eds.; British Small Animal Veterinary Association: Glouchester, UK, 2016; pp. 117–132. ISBN 9781905319800.

8. Morris, P.A. The Effects of Supplementary Feeding on Movements of Hedgehogs (*Erinaceus europaeus*). *Mammal Rev.* **1985**, *15*, 23–32. [CrossRef]
9. Kadlecova, G.; Rasmussen, S.L.; Voslarova, E.; Vecerek, V. Differences in Mortality of Pre-Weaned and Post-Weaned Juvenile European Hedgehogs (*Erinaceus europaeus*) at Wildlife Rehabilitation Centres in the Czech Republic. *Animals* **2023**, *13*, 337. [CrossRef]
10. Haigh, A.; O'Riordan, R.M.; Butler, F. Hedgehog *Erinaceus europaeus* Mortality on Irish Roads. *Wildl. Biol.* **2014**, *20*, 155–160. [CrossRef]
11. Bunnell, T. The Incidence of Disease and Injury in Displaced Wild Hedgehogs (*Erinaceus europaeus*). *Lutra* **2001**, *44*, 3–14.
12. Jackson, D.B. The Breeding Biology of Introduced Hedgehogs (*Erinaceus europaeus*) on a Scottish Island: Lessons for Population Control and Bird Conservation. *J. Zool.* **2006**, *268*, 303–314. [CrossRef]
13. Lukešová, G.; Voslarova, E.; Vecerek, V.; Vucinic, M. Trends in Intake and Outcomes for European Hedgehog (*Erinaceus europaeus*) in the Czech Rescue Centers. *PLoS ONE* **2021**, *16*, e0248422. [CrossRef]
14. Bezerra-Santos, M.A.; Sgroi, G.; Mendoza-Roldan, J.A.; Khedri, J.; Camarda, A.; Iatta, R.; Sazmand, A.; Otranto, D. Ectoparasites of Hedgehogs: From Flea Mite Phoresy to Their Role as Vectors of Pathogens. *Int. J. Parasitol. Parasites Wildl.* **2021**, *15*, 95–104. [CrossRef]
15. Hubert, P.; Julliard, R.; Biagianti, S.; Poulle, M.L. Ecological Factors Driving the Higher Hedgehog (*Erinaceus europeaus*) Density in an Urban Area Compared to the Adjacent Rural Area. *Landsc. Urban Plan.* **2011**, *103*, 34–43. [CrossRef]
16. Taucher, A.L.; Gloor, S.; Dietrich, A.; Geiger, M.; Hegglin, D.; Bontadina, F. Decline in Distribution and Abundance: Urban Hedgehogs under Pressure. *Animals* **2020**, *10*, 1606. [CrossRef] [PubMed]
17. Van De Poel, J.L.; Dekker, J.; Van Langevelde, F. Dutch Hedgehogs *Erinaceus europaeus* Are Nowadays Mainly Found in Urban Areas, Possibly Due to the Negative Effects of Badgers Meles Meles. *Wildl. Biol.* **2015**, *21*, 51–55. [CrossRef]
18. Rasmussen, S.L.; Berg, T.B.; Dabelsteen, T.; Jones, O.R. The Ecology of Suburban Juvenile European Hedgehogs (*Erinaceus europaeus*) in Denmark. *Ecol. Evol.* **2019**, *9*, 13174–13187. [CrossRef]
19. Garcês, A.; Soeiro, V.; Lóio, S.; Sargo, R.; Sousa, L.; Silva, F.; Pires, I. Outcomes, Mortality Causes, and Pathological Findings in European Hedgehogs (*Erinaceus europaeus*, Linnaeus 1758): A Seventeen Year Retrospective Analysis in the North of Portugal. *Animals* **2020**, *10*, 1305. [CrossRef] [PubMed]
20. Hof, A.R.; Bright, P.W. The Value of Green-Spaces in Built-up Areas for Western Hedgehogs. *Lutra* **2009**, *52*, 69–82.
21. Ruszkowski, J.J.; Hetman, M.; Turlewicz-Podbielska, H.; Pomorska-Mól, M. Hedgehogs as a Potential Source of Zoonotic Pathogens—A Review and an Update of Knowledge. *Animals* **2021**, *11*, 1754. [CrossRef]
22. Huijser, M.P.; Bergers, P.J.M. The Effect of Roads and Traffic on Hedgehog (*Erinaceus europaeus*) Populations. *Biol. Conserv.* **2000**, *95*, 111–116. [CrossRef]
23. Zacharopoulou, M.; Guillaume, E.; Coupez, G.; Bleuart, C.; Le Loc'h, G.; Gaide, N. Causes of Mortality and Pathological Findings in European Hedgehogs (*Erinaceus europaeus*) Admitted to a Wildlife Care Centre in Southwestern France from 2019 to 2020. *J. Comp. Pathol.* **2022**, *190*, 19–29. [CrossRef]
24. Alomar, H.; Chabert, A.; Coeurdassier, M.; Vey, D.; Berny, P. Accumulation of Anticoagulant Rodenticides (Chlorophacinone, Bromadiolone and Brodifacoum) in a Non-Target Invertebrate, the Slug, *Deroceras reticulatum*. *Sci. Total Environ.* **2018**, *610–611*, 576–582. [CrossRef]
25. D'Havé, H.; Scheirs, J.; Covaci, A.; Schepens, P.; Verhagen, R.; De Coen, W. Nondestructive Pollution Exposure Assessment in the European Hedgehog (*Erinaceus europaeus*): III. Hair as an Indicator of Endogenous Organochlorine Compound Concentrations. *Environ. Toxicol. Chem.* **2006**, *25*, 158–167. [CrossRef] [PubMed]
26. Dowding, C.V.; Shore, R.F.; Worgan, A.; Baker, P.J.; Harris, S. Accumulation of Anticoagulant Rodenticides in a Non-Target Insectivore, the European Hedgehog (*Erinaceus europaeus*). *Environ. Pollut.* **2010**, *158*, 161–166. [CrossRef]
27. Hof, A.R.; Bright, P.W. Quantifying the Long-Term Decline of the West European Hedgehog in England by Subsampling Citizen-Science Datasets. *Eur. J. Wildl. Res.* **2016**, *62*, 407–413. [CrossRef]
28. Rondinini, C.; Battistoni, A.; Teofili, C. *Lista Rossa IUCN dei Vertebrati Italiani 2022*; Comitato Italiano IUCN e Ministero dell'Ambiente e della Sicurezza Energetica: Rome, Italy, 2022; Volume 30.
29. Rondinini, C.; Capasso, S. *Erinaceus europaeus*—Italian IUCN Red List. Available online: https://www.iucn.it/scheda.php?id=-944215748 (accessed on 13 November 2023).
30. Thrift, E.; Nouvellet, P.; Mathews, F. Plastic Entanglement Poses a Potential Hazard to European Hedgehogs *Erinaceus europaeus* in Great Britain. *Animals* **2023**, *13*, 2448. [CrossRef]
31. Moore, L.J.; Petrovan, S.O.; Baker, P.J.; Bates, A.J.; Hicks, H.L.; Perkins, S.E.; Yarnell, R.W. Impacts and Potential Mitigation of Road Mortality for Hedgehogs in Europe. *Animals* **2020**, *10*, 1523. [CrossRef]
32. Rasmussen, S.L.; Berg, T.B.; Martens, H.J.; Jones, O.R. Anyone Can Get Old—All You Have to Do Is Live Long Enough: Understanding Mortality and Life Expectancy in European Hedgehogs (*Erinaceus europaeus*). *Animals* **2023**, *13*, 626. [CrossRef]
33. Martínez, J.C.; Rosique, A.I.; Royo, M.S. Causes of Admission and Final Dispositions of Hedgehogs Admitted to Three Wildlife Rehabilitation Centers in Eastern Spain. *Hystrix* **2014**, *25*, 107–110. [CrossRef]
34. Otranto, D.; Dantas-Torres, F.; Santos-Silva, M.M. Ixodes Ricinus (Linnaeus, 1758) (Figs. 67−69). In *Ticks of Europe and North Africa: A Guide to Species Identification*; Estrada-Peña, A., Mihalca, A.D., Petney, T.N., Eds.; Springer International Publishing: Cham, Switzerland, 2017; pp. 189–195. ISBN 978-3-319-63760-0.

35. Sándor, A.D. Ixodes Hexagonus Leach, 1815 (Figs. 49–51). In *Ticks of Europe and North Africa: A Guide to Species Identification*; Estrada-Peña, A., Mihalca, A.D., Petney, T.N., Eds.; Springer International Publishing: Cham, Switzerland, 2017; pp. 147–151. ISBN 978-3-319-63760-0.
36. Smith, F.G.A. Siphonaptera. In *Handbooks for the Identification of British Insects*; Royal Entomological Society: St Albans, UK, 1957; Volume 6, pp. 1–94.
37. Il Clima in Europa. Available online: https://www.schededigeografia.net/Europa/europa_fisica/clima_europa.htm (accessed on 14 November 2023).
38. Wallenfeldt, J. Canton Zurich, Switzerland. Available online: https://www.britannica.com/place/Zurich-canton-Switzerland (accessed on 14 November 2023).
39. Foreste Del Piemonte, Economia e Ambiente. Available online: https://www.regione.piemonte.it/web/temi/ambiente-territorio/foreste/foreste-piemonte-economia-ambiente (accessed on 14 November 2023).
40. Tikkanen, A. Piedmont Region, Italy. Available online: https://www.britannica.com/place/Piedmont-region-Italy (accessed on 14 November 2023).
41. Landscape: In Brief. Available online: https://www.bafu.admin.ch/bafu/en/home/topics/landscape/in-brief.html (accessed on 14 November 2023).
42. Il Cambiamento Climatico in Piemonte. Available online: https://www.regione.piemonte.it/web/temi/ambiente-territorio/cambiamento-climatico/cambiamento-climatico-piemonte (accessed on 14 November 2023).
43. Fact Sheet: Facts & Figures Swiss Public Transport. Available online: https://www.mystsnet.com/en/download/fact-sheet-facts-figures-swiss-public-transport/ (accessed on 3 January 2024).
44. Trasporti e Mobilità Istat. Available online: https://www.istat.it/storage/politiche-sviluppo/Trasporti_mobilita.xls (accessed on 3 January 2024).
45. Urban and Rural Areas. Available online: https://www.eda.admin.ch/aboutswitzerland/en/home/gesellschaft/bevoelkerung/stadt-und-land.html (accessed on 3 January 2024).
46. Il Censimento Permanente Della Popolazione in Piemonte—Anno 2020. Available online: https://www.istat.it/it/archivio/268878 (accessed on 3 January 2024).
47. Igel Stadt Zürich. Available online: https://www.stadt-zuerich.ch/ted/de/index/gsz/beratung-und-wissen/tier-und-mensch/Igel.html (accessed on 4 January 2024).
48. Lehmann, S.; Dervas, E.; Ruiz Subira, A.; Eulenberger, U.; Gimmel, A.; Grimm, F.; Hetzel, U.; Kipar, A. Verminous Pneumonia in European Hedgehogs (*Erinaceus europaeus*). *Vet. Pathol.* **2023**, *61*, 256–268. [CrossRef]
49. Mariacher, A.; Santini, A.; Del Lesto, I.; Tonon, S.; Cardini, E.; Barone, A.; Eleni, C.; Fichi, G.; Perrucci, S. Endoparasite Infections of the European Hedgehog (*Erinaceus europaeus*) in Central Italy. *Animals* **2021**, *11*, 3171. [CrossRef]
50. Majeed, S.K.; Cooper, J.E. Lesions Associated with a *Capillaria* Infestation in the European Hedgehog (*Erinaceus europaeus*). *J. Comp. Pathol.* **1984**, *94*, 625–628. [CrossRef]
51. Majeed, S.K.; Morris, P.; Cooper, J.E. Occurrence of the Lungworms *Capillaria* and *Crenosoma* Spp. in British Hedgehogs (*Erinaceus europaeus*). *J. Comp. Pathol.* **1989**, *100*, 27–36. [CrossRef]
52. Poglayen, G.; Giannetto, S.; Scala, A.; Garippa, G.; Capelli, G.; Scaravelli, D.; Brianti, E.; Reeve, N.J. Helminths Found in Hedgehogs (*Erinaceus europaeus*) in Three Areas of Italy. *Vet. Rec.* **2003**, *152*, 22–24. [CrossRef] [PubMed]
53. Rasmussen, S.L.; Hallig, J.; van Wijk, R.E.; Petersen, H.H. An Investigation of Endoparasites and the Determinants of Parasite Infection in European Hedgehogs (*Erinaceus europaeus*) from Denmark. *Int. J. Parasitol. Parasites Wildl.* **2021**, *16*, 217–227. [CrossRef]
54. Pfäffle, M.; Černábolfíková, B.; Hulva, P.; Petney, T. Different Parasite Faunas in Sympatric Populations of Sister Hedgehog Species in a Secondary Contact Zone. *PLoS ONE* **2014**, *9*, e114030. [CrossRef]
55. Gaglio, G.; Allen, S.; Bowden, L.; Bryant, M.; Morgan, E.R. Parasites of European Hedgehogs (*Erinaceus europaeus*) in Britain: Epidemiological Study and Coprological Test Evaluation. *Eur. J. Wildl. Res.* **2010**, *56*, 839–844. [CrossRef]
56. Cousquer, G. Analysis of Tracheal Sputum for Diagnosing and Monitoring Verminous Pneumonia in Hedgehogs (*Erinaceus europaeus*). *Vet. Rec.* **2004**, *154*, 332–333. [CrossRef] [PubMed]
57. Gorgani-Firouzjaee, T.; Farshid, A.A.; Naem, S. First Ultrastructural Observations on Gastritis Caused by *Physaloptera clausa* (Spirurida: Physalopteridae) in Hedgehogs (*Erinaceus europeaus*). *Parasitol. Res.* **2015**, *114*, 3693–3698. [CrossRef]
58. Octavia, S.; Lan, R. The Family Enterobacteriaceae. In *The Prokaryotes*; Springer: Berlin, Heidelberg, 2014; pp. 225–286.
59. Mehdizadeh Gohari, I.; Navarro, M.A.; Li, J.; Shrestha, A.; Uzal, F.; McClane, B.A. Pathogenicity and Virulence of Clostridium Perfringens. *Virulence* **2021**, *12*, 723–753. [CrossRef]
60. Torres, C.; Alonso, C.A.; Ruiz-Ripa, L.; León-Sampedro, R.; Del Campo, R.; Coque, T.M. Antimicrobial Resistance in Enterococcus Spp. of Animal Origin. *Microbiol. Spectr.* **2018**, *6*, ARBA-0032-2018. [CrossRef]
61. Liu, H.; Zhu, J.; Hu, Q.; Rao, X. Morganella Morganii, a Non-Negligent Opportunistic Pathogen. *Int. J. Infect. Dis.* **2016**, *50*, 10–17. [CrossRef]
62. Lawson, B.; Franklinos, L.H.V.; Rodriguez-Ramos Fernandez, J.; Wend-Hansen, C.; Nair, S.; Macgregor, S.K.; John, S.K.; Pizzi, R.; Núñez, A.; Ashton, P.M.; et al. Salmonella Enteritidis ST183: Emerging and Endemic Biotypes Affecting Western European Hedgehogs (*Erinaceus europaeus*) and People in Great Britain. *Sci. Rep.* **2018**, *8*, 2449. [CrossRef]

63. Jota Baptista, C.; Oliveira, P.A.; Gonzalo-Orden, J.M.; Seixas, F. Do Urban Hedgehogs (*Erinaceus europaeus*) Represent a Relevant Source of Zoonotic Diseases? *Pathogens* **2023**, *12*, 268. [CrossRef]
64. Jota Baptista, C.V.; Seixas, F.; Gonzalo-Orden, J.M.; Oliveira, P.A. Can the European Hedgehog (*Erinaceus europaeus*) Be a Sentinel for One Health Concerns? *Biologics* **2021**, *1*, 61–69. [CrossRef]
65. Döpke, C.; Fehr, M.; Thiele, A.; Pohlenz, J.; Wohlsein, P. Morphological and Immunohistochemical Characterization of Spontaneous Mammary Tumours in European Hedgehogs (*Erinaceus europaeus*). *J. Comp. Pathol.* **2007**, *137*, 22–29. [CrossRef] [PubMed]
66. Ulrich, R.; Stan, A.C.; Fehr, M.; Mallig, C.; Puff, C. Desmoplastic Ganglioglioma of the Spinal Cord in a Western European Hedgehog (*Erinaceus europaeus*). *J. Vet. Diagn. Investig.* **2010**, *22*, 978–983. [CrossRef] [PubMed]
67. Singh, K.; Blas-Machado, U.; Cooper, E.J.; Caseltine, S.L.; Nordhausen, R. Spontaneous Subcutaneous Myxosarcoma in a Captive European Hedgehog (*Erinaceus europaeus*). *J. Vet. Diagn. Investig.* **2006**, *18*, 627–631. [CrossRef]
68. Kuonen, V.J.; Wilkie, D.A.; Morreale, R.J.; Oglesbee, B.; Barrett-Rephun, K. Unilateral Exophthalmia in a European Hedgehog (*Erinaceus europaeus*) Caused by a Lacrimal Ductal Carcinoma. *Vet. Ophthalmol.* **2002**, *5*, 161–165. [CrossRef]

Disclaimer/Publisher's Note: The statements, opinions and data contained in all publications are solely those of the individual author(s) and contributor(s) and not of MDPI and/or the editor(s). MDPI and/or the editor(s) disclaim responsibility for any injury to people or property resulting from any ideas, methods, instructions or products referred to in the content.

animals

MDPI

Brief Report

A Case of Severe Abomasal Sand Impaction in a Farmed White-Tailed Deer (*Odocoileus virginianus*) in Florida

Alireza Rahmani Shahraki [1], João H. J. Bittar [1], Samantha M. Wisely [2,3] and Juan M. Campos-Krauer [1,2,*]

[1] Department of Large Animal Clinical Sciences, College of Veterinary Medicine, University of Florida, Gainesville, FL 32611, USA; alirezarahmanish@ufl.edu (A.R.S.); jbittar@ufl.edu (J.H.J.B.)
[2] Department of Wildlife Ecology and Conservation, University of Florida, Gainesville, FL 32611, USA; wisely@ufl.edu
[3] Emerging Pathogens Institute, University of Florida, Gainesville, FL 32611, USA
* Correspondence: jmcampos@ufl.edu

Simple Summary: This case report presents a chronic abomasal sand impaction in a white-tailed deer in Florida. Abomasal impaction in ruminants can result from a low-quality diet or abnormal eating behavior. The farmer reported significant weight loss, abdominal enlargement, and general weakness in the deer. Post-mortem examination revealed a low body condition score, dehydration, and abdominal enlargement. Internal inspection identified pneumonia lesions in the left cranial lung lobe, which microbiological tests attributed to *Trueperella pyogenes*. Notable ruminal bloating was observed, characterized by gas accumulation. The abomasum was palpably firm and enlarged, predominantly filled with sand, except for a small ventral portion, with an estimated sand weight of approximately 5 kg. Although chronic sand impaction was suggested as the cause of death, it is posited that chronic sand-induced damage to the abomasal mucosal layer led to active subacute abomasitis, which compromised the animal's immune system and predisposed it to secondary infections.

Abstract: The University of Florida's Cervidae Health Research Initiative (CHeRI) conducted a post-mortem examination of a two-year-old white-tailed doe deceased at a northern Florida white-tailed deer farm. The carcass of the deer had notable emaciation and bloating. Upon opening of the carcass, there was pneumonia and the rumen was tympanic and enlarged. Additionally, the abomasum was distended and contained approximately 5 kg of sand. It is not uncommon for white-tailed deer to engage in geophagia (eating soil or sand), which typically does not result in diseases or fatalities. However, in this animal, we suspect a chronic process that created a physical barrier, hindering nutrient absorption and resulting in physical irritation of the abomasal mucosa with subsequent inflammation. This may have caused a disturbance in immune system function, allowing opportunistic bacteria to colonize and invade other organs, such as the lungs, contributing to the animal's death.

Keywords: deer; abomasal impaction; sand; Florida

1. Introduction

Abomasal impaction is characterized by the accumulation of compacted ingesta within the abomasum, resulting in distention and enlargement of the organ. This condition leads to decreased abomasal motility, and reduced rumen fluid flow and ingesta movement to the intestine, often accompanied by failure in the aboral transport mechanism [1,2]. Abomasal impaction can be a primary disorder that leads to the development of secondary conditions such as peritonitis [2]. The failure to pass fluid and ingesta to the intestine can result in dehydration, acid–base imbalances, and varying degrees of electrolyte imbalance, including metabolic alkalosis, hypochloremia, and hypokalemia. Weakness and decreased food intake are common consequences of abomasal disorders in farm animals such as

deer. In white-tailed deer, geophagia, the consumption of soil, is a relatively common behavior [3]. Geophagia involving natural mineral licks has been documented across North America [3–11]. These studies have consistently identified sodium (Na) as the most abundant mineral element present at these ungulate licks, alongside other essential minerals like sulfur (S), calcium (Ca), and magnesium (Mg) [3,5,6,12]. Furthermore, it is normal for young fawns to consume soil and for adults to engage in geophagia to acquire specific minerals and introduce beneficial bacteria into their gastrointestinal tract. In the vast majority of cases, geophagia does not lead to diseases or death [2]. Sand impaction is reported in various animal species, such as cattle, horses, and even elephants (*Elephas maximus*) [13,14]. Sand impaction can occur indirectly through consumption of contaminated food and water with sand [13]. Clinical signs of this progressive disease in different animal species include depression, anorexia, diarrhea, and scant feces [2]. Owners often report abdominal distention, loss of body weight, and weakness to rise. Initially, body temperature is usually normal, but due to negative energy balance, it may become subnormal after several days. Varying degrees of colic with mucosal damage are observed, often followed by bacterial infection, progressive endotoxemia, and ultimately death [15,16]. The aim of this manuscript is to report, for the first time, the occurrence of abomasal sand impaction in white-tailed deer (*Odocoileus virginianus*) in Florida.

2. Case History

A deer farmer in northern Florida reached out to the University of Florida's Cervidae Health Research Initiative (CHeRI) to request a post-mortem examination of a two-year-old white-tailed doe that was discovered deceased on the morning of 29 December 2017. The deer was stored in a walk-in refrigerator over 12 h until the necropsy was performed the following morning. Prior to its demise, the animal had a history of an enlarged abdomen for over four months and distinctive digestive noises, akin to sloshing, when it moved in its enclosure. Remarkably, these noises and the enlarged rumen did not seem to have a significant impact on the animal's overall health or reproductive success, aside from a notable weight loss. Four weeks before its demise, the doe underwent a successful laparoscopic artificial insemination, and it did not display any signs of illness until its death.

3. Necropsy and Lab Findings

The field necropsy procedures encompassed a thorough examination of the carcass. Upon external examination, the animal was notably lean and had lost body condition, and exhibited bloating. We found no external indications of trauma, wounds, parasites, or any abnormalities. The fur was dry and no secretions in the nose or mouth were observed. There were no signs of anemia, characterized by pale mucosal membranes in the oral cavity and eye. Additionally, the external reproductive organs appeared normal with no secretions.

Necropsy of the thoracic cavity revealed lung congestion, consolidation, and compartmentalization, with areas of blood and pus, particularly in the left cranial lung lobe, which exhibited a significant necrotic region measuring 5 to 6 cm (Figure 1). Samples from this area were collected for microbiology testing. Moreover, the heart was normal in size but showed signs of hyperemia and congestion. In the abdominal cavity the spleen was contracted, measuring only 11 cm in diameter and 1 cm in thickness throughout most of the organ. The kidneys were congested and all major organs appeared dehydrated, particularly liver and spleen.

The rumen exhibited marked bloating and contained a substantial amount of gas. The abomasum was enlarged and firm on palpation. Upon incising it was impacted with firm, clear sand, except for a small ventral area that contained a mixture of liquid food and sand on the red mucosa with minimal mucus (Figure 2). These findings indicated a chronic case of abomasal sand impaction. The sand, estimated to weigh 5 kg, exerted dependent pressure on the rumen, causing it to be displaced forward and potentially exerting significant pressure on the diaphragm.

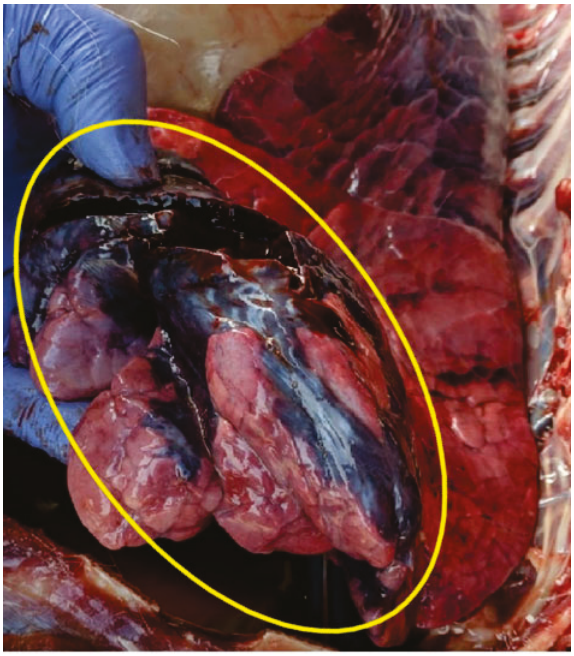


Figure 1. The yellow circle shows the lung lesion caused by *Trueperella pyogenes* in the white-tailed deer (*Odocoileus virginianus*) with severe abomasal sand impaction.

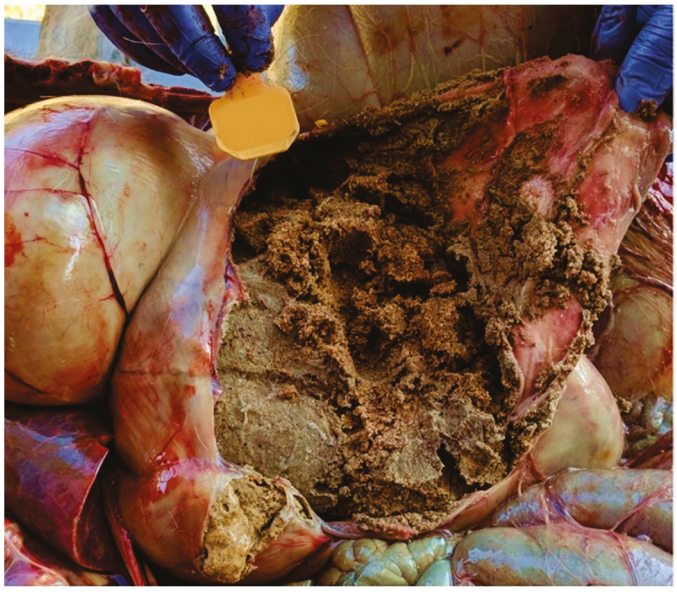


Figure 2. The open abomasum of a female white-tailed deer (*Odocoileus virginianus*). The deer suffered from chronic abomasal sand impaction. The ear tag included in the image as a reference is 5.08 cm by 4.12 cm.

The remaining portions of the gastrointestinal tract were normal. However, the small and large intestines were empty, containing only dry and hard fecal pellets in the rectum. No internal parasites were identified. All reproductive organs were normal and the doe was pregnant, with a 4 × 1.5 cm 20–25 days gestational fetus.

Samples of vital organs (lungs, heart, liver, kidney, spleen), blood, and fecal pellets were collected and stored at −80 °C freezer for subsequent laboratory analysis. Moreover, two nasal swabs and one rectal swab were obtained and stored in sterile 1.5 mL tubes and universal transport media (UTM) for further testing.

In accordance with the suspected disease, samples were submitted the University of Florida (UF) Microbiology, Parasitology, and Serology Diagnostic Laboratory of the College

of Veterinary Medicine. Blood samples were also sent to the Cervidae Health Research Initiative Molecular Ecology Lab at the University of Florida to be tested for epizootic hemorrhagic disease virus (EHDV), bluetongue virus (BTV), West Nile virus (WNV), and Eastern equine encephalitis (EEE) by RT-PCR [17–19], and the test results were negative.

Microbiology recovered heavy growth in the lungs of *Trueperella pyogenes*, a bacterium known to cause lesions and septicemia in white-tailed deer.

4. Discussion

Sand impaction is a chronic disease reported in domestic and wild animals [13,20]. The consumption of soil is a common behavior in white-tailed deer whose exact cause remains uncertain [21]. The ingestion of small amounts of soil is frequently observed in post-mortem examinations of calves and lambs [22]. This case represents the first report of severe abomasal sand impaction in an adult white-tailed deer in Florida. While chronic sand impaction was suggested as the cause of death, we believe that chronic subacute abomasitis may have contributed to immune suppression and predisposed the animal to secondary infections. This hypothesis aligns with existing literature [23]. *Trueperella pyogenes* is an opportunistic bacterium commonly found on mucosal surfaces, the rumen wall, and the upper respiratory system of deer and other farm animals [24,25]. Additionally, there is an association between intracranial abscesses in deer and the presence of *Trueperella pyogenes* [26]. In this case, we hypothesize that consistent inflammation in the abomasal wall, leading to an insufficient immune response, contributed to the lung lesions caused by *Trueperella pyogenes*. Reduced abomasal contractions and distended abomasum occurs in animals afflicted with abomasal impaction. Accumulation of sand in the abomasum can impact abomasal motility and contribute to hypomotility and eventually atony. This functional motility disorder can cause distention due to gas accumulation in the forestomach, especially in the rumen [13,27]. In this case, bloat was indicated in the owner's history and necropsy findings. The lesions in this doe were consistent with prior case reports [8,27]. More severe sand impaction can lead to partial or complete obstruction of the upper gastrointestinal tract, contributing to abdominal pain, decreased appetite, and scant feces [13,28]. The empty intestine in this case is consistent with other previous reports in the literature [1,27]. Additionally, severe dehydration and presumptive electrolyte imbalances occurred due to partial or complete obstruction in the upper alimentary tract, disrupting the natural passage of fluids from the abomasum into the duodenum. Previous case studies reported association between the occurrence of abomasal impaction and biochemical alteration in ruminants [29,30]. In this doe, post-mortem inspection revealed that the small intestines were empty, and the lack of chyme maybe attributed to the presence of hardened sand, which impeded the movement of food. Animals with abomasum obstruction due to sand or ingested feed often feature congestion and hyperemia in the serous layer of the organ [1,20]. In this case, petechiae and ecchymoses were observed on the serous layer of the impacted abomasum. The physical abrasion pressure exerted by sand likely induced mechanical damage to the abomasal wall, resulting in hemorrhage and inflammation, leading to alteration in blood vessel permeability. Furthermore, damage to the serosal layer of the abomasum and alterations in blood vessel permeability facilitate the entry of gastrointestinal microflora, particularly gram-negative bacteria, into the bloodstream. The lipopolysaccharide (LPS) of gram-negative bacteria plays a key role in the development of endotoxemia, affecting the animal's immune system. The persistence of endotoxemia can induce weakness and eventual death [13,31].

5. Conclusions

In conclusion, abomasal sand impaction contributed to severe obstruction of the abomasum (true stomach), impeded the normal passage of ingesta, and exposed the stomach contents to the mucosa. This resulted in reduced nutrient absorption, electrolytic imbalances, weight loss, and a compromised immune system. Mechanical damage or excoriation likely ensued from the abrasive action of sand against the stomach's mucosa

and submucosa, resulting in erosions and ulceration of the mucosa and these defects likely facilitated the invasion of microbes, potentially leading to endotoxemia and shock. The impacted stomach exerted physical pressure on surrounding organs, including the diaphragm and the respiratory system, potentially disrupting homeostasis, including splanchnic perfusion and pulmonary aeration. This may have contributed to lung lesions and infection.

Author Contributions: Conceptualization, J.M.C.-K. and A.R.S.; methodology, J.M.C.-K.; software, J.M.C.-K. and A.R.S.; validation, J.M.C.-K., J.H.J.B. and S.M.W.; formal analysis, J.M.C.-K. and A.R.S.; investigation, J.M.C.-K. and A.R.S.; resources, J.M.C.-K. and S.M.W.; data curation, J.M.C.-K. and S.M.W.; writing—original draft preparation, J.M.C.-K. and A.R.S.; writing—review and editing, J.M.C.-K., J.H.J.B. and S.M.W.; visualization, J.M.C.-K. and A.R.S.; supervision, J.M.C.-K., J.H.J.B. and S.M.W.; project administration, J.M.C.-K.; funding acquisition, J.M.C.-K. and S.M.W. All authors have read and agreed to the published version of the manuscript.

Funding: This research was funded by The University of Florida, Institute of Food and Agricultural Sciences, CHeRI, with funds provided by the Florida legislature (#6000CHERI).

Institutional Review Board Statement: Ethical approval was not required for this study as only a dead animal was examined.

Informed Consent Statement: Not applicable.

Data Availability Statement: Data are contained within the article.

Acknowledgments: We are grateful to all CHeRI technicians for their assistance. This study was made possible through the cooperation of farmed deer producers throughout Florida; we are grateful for their participation.

Conflicts of Interest: The authors declare no conflicts of interest.

References

1. Şimşek, A.; Sekin, S.; Içen, H.; Koçhan, A.; Çelik, Ö.; Yaman, T. Abomasal impaction due to sand accumulation in two cows. *Large Anim. Rev.* **2015**, *21*, 125–127.
2. Smith, B.P. *Large Animal Internal Medicine-E-Book*; Elsevier Health Sciences: Amsterdam, The Netherlands, 2014.
3. Knight, R.R.; Mudge, M.R. Characteristics of some natural licks in the Sun River area, Montana. *J. Wildl. Manag.* **1967**, *31*, 293. [CrossRef]
4. Hebert, D.; Im, C. Natural salt licks as a part of the ecology of the mountain goat. *Can. J. Zool.* **1971**, *49*, 605–610. [CrossRef] [PubMed]
5. Weeks, H.P.; Kirkpatrick, C.M. Adaptations of White-Tailed deer to naturally occurring sodium deficiencies. *J. Wildl. Manag.* **1976**, *40*, 610. [CrossRef]
6. Weeks, H.P. Characteristics of mineral licks and behavior of visiting White-Tailed deer in southern Indiana. *Am. Midl. Nat.* **1978**, *100*, 384. [CrossRef]
7. Fraser, D.A.; Reardon, E.J.; Dieken, F.; Loescher, B. Sampling problems and interpretation of chemical analysis of mineral springs used by wildlife. *J. Wildl. Manag.* **1980**, *44*, 623. [CrossRef]
8. Fraser, D.A.; Hristienko, H. Activity of moose and white-tailed deer at mineral springs. *Can. J. Zool.* **1981**, *59*, 1991–2000. [CrossRef]
9. Tankersley, N.G.; Gasaway, W.C. Mineral lick use by moose in Alaska. *Can. J. Zool.* **1983**, *61*, 2242–2249. [CrossRef]
10. Kreulen, D.A. Lick use by large herbivores: A review of benefits and banes of soil consumption. *Mammal Rev.* **1985**, *15*, 107–123. [CrossRef]
11. Risenhoover, K.L.; Peterson, R.O. Mineral licks as a sodium source for Isle Royale moose. *Oecologia* **1986**, *71*, 121–126. [CrossRef] [PubMed]
12. Jones, R.L.; Hanson, H.C. *Mineral Licks, Geophagy, and Biogeochemistry of North American Ungulates*, 1st ed.; Iowa State Pr: Ames, IA, USA, 1985.
13. Constable, P.D.; Hinchcliff, K.W.; Done, S.H.; Gruenberg, W. *Veterinary Medicine-E-Book: A Textbook of the Diseases of Cattle, Horses, Sheep, Pigs and Goats*; Elsevier Health Sciences: Amsterdam, The Netherlands, 2016.
14. Warren, K.; Bolton, J.R.; Swan, R.A.; Gaynor, W.C.; Pond, L. Treatment of gastrointestinal tract impaction of a 2-year-old Asian elephant (*Elephas maximus*). *Aust. Vet. J.* **1996**, *73*, 37–38. [CrossRef] [PubMed]
15. Johnston, J.; Freeman, D.E. Diseases and surgery of the large colon. *Vet. Clin. N. Am. Equine Pract.* **1997**, *13*, 317–340. [CrossRef] [PubMed]
16. Fowler, M.E.; Bravo, P.W. *Medicine and Surgery of Camelids*; John Wiley & Sons: Hoboken, NJ, USA, 2010.

17. Lambert, A.J.; Martin, D.A.; Lanciotti, R.S. Detection of North American Eastern and western equine encephalitis viruses by nucleic acid amplification assays. *J. Clin. Microbiol.* **2003**, *41*, 379–385. [CrossRef]
18. Lanciotti, R.S.; Kerst, A.J.; Nasci, R.S.; Godsey, M.S.; Mitchell, C.J.; Savage, H.M.; Komar, N.; Panella, N.A.; Allen, B.C.; Volpe, K.E.; et al. Rapid Detection of West Nile Virus from Human Clinical Specimens, Field-Collected Mosquitoes, and Avian Samples by a TaqMan Reverse Transcriptase-PCR Assay. *J. Clin. Microbiol.* **2000**, *38*, 4066–4071. [CrossRef] [PubMed]
19. Wernike, K.; Hoffmann, B.; Beer, M. Simultaneous detection of five notifiable viral diseases of cattle by single-tube multiplex real-time RT-PCR. *J. Virol. Methods* **2015**, *217*, 28–35. [CrossRef] [PubMed]
20. Teodoro, T.G.W.; Uzal, F.A.; Streitenberger, N.; Samol, M.A.; Henderson, E.E.; Asín, J. Colonic sand impaction with cecal rupture and peritonitis in an adult African savanna elephant, and review of noninfectious causes of gastrointestinal disease in elephants. *J. Vet. Diagn. Investig.* **2022**, *35*, 47–52. [CrossRef] [PubMed]
21. Neser, J.A.; De Vries, M.A.; De Vries, M.; Van Der Merwe, A.J.; Loock, A.H.; Smith, H.A.; Van Der Vyver, F.H.; Elsenbroek, J.H. Enzootic geophagia of calves and lambs in Northern Cape and Northwest and the possible role of chronic manganese poisoning. *S. Afr. J. Anim. Sci.* **2000**, *30*, 105–106. [CrossRef]
22. Graham, T.W.; Thurmond, M.; Mohr, F.C.; Holmberg, C.A.; Anderson, M.L.; Keen, C.L. Relationships between Maternal and Fetal Liver Copper, Iron, Manganese, and Zinc Concentrations and Fetal Development in California Holstein Dairy Cows. *J. Vet. Diagn. Investig.* **1994**, *6*, 77–87. [CrossRef] [PubMed]
23. Bonagura, V.R.; Rosenthal, D. Infections that cause secondary immune deficiency. In *Stiehm's Immune Deficiencies*; Academic Press: Cambridge, MA, USA, 2020; pp. 1035–1058.
24. Belser, E.H.; Cohen, B.S.; Osborn, D.A.; Keeler, S.P.; Russell, S.M.; Miller, K.V. Bacterial Fauna of the Forehead, Tongue, and Nasal Mucosa ofOdocoileus virginianus (White-Tailed Deer) in Georgia. *Southeast. Nat.* **2016**, *15*, 488–495. [CrossRef]
25. Narayanan, S.; Nagaraja, T.G.; Wallace, N.; Staats, J.; Chengappa, M.M.; Oberst, R.D. Biochemical and ribotypic comparison of Actinomyces pyogenes and A pyogenes-like organisms from liver abscesses, ruminal wall, and ruminal contents of cattle. *Am. J. Vet. Res.* **1998**, *59*, 271–276. [CrossRef] [PubMed]
26. Cohen, B.S.; Belser, E.H.; Keeler, S.P.; Yabsley, M.J.; Miller, K.V. Isolation and Genotypic Characterization of Trueperella (*Arcanobacterium*) pyogenes Recovered from Active Cranial Abscess Infections of Male White-Tailed Deer (*Odocoileus virginianus*). *J. Zoo Wildl. Med.* **2015**, *46*, 62–67. [CrossRef] [PubMed]
27. Reddy, B.S.; Sivajothi, S.; Swetha, K. Ultrasonographic assessment of effect of neostigmine on abomasal atony in young calves. *Buffalo Bull.* **2023**, *42*, 391. [CrossRef]
28. Ahn, S.; Shin, W.; Han, Y.; Bae, S.; Cho, C.-U.; Choi, S.; Oh, Y.; Kim, J.-T. Ruminal impaction with an indigestible foreign body in long-tailed goral (*Naemorhedus caudatus*). *Han-Gukgachugwisaenghakoeji* **2023**, *46*, 161–165. [CrossRef]
29. El-Ashker, M.; Salama, M.; El-Boshy, M.; El-Fadle, E.A.A. Significance of clinical observations and biochemical alterations in buffalo calves with dietary abomasal impaction. *BMC Vet. Res.* **2018**, *14*, 1. [CrossRef] [PubMed]
30. Yong, K.; Luo, Z.; Yang, Q.; Zhang, C.; QianLan, Z.; Hua, J.; Zhang, Y.; Cao, S. Case report: Abomasum impaction in beef cattle due to high intake of distillers' grain and treatment options in southwest China. *Front. Vet. Sci.* **2021**, *8*, 615871. [CrossRef] [PubMed]
31. Wittek, T.; Fürll, M.; Constable, P.D. Prevalence of Endotoxemia in Healthy Postparturient Dairy Cows and Cows with Abomasal Volvulus or Left Displaced Abomasum. *J. Vet. Intern. Med.* **2004**, *18*, 574–580. [CrossRef] [PubMed]

Disclaimer/Publisher's Note: The statements, opinions and data contained in all publications are solely those of the individual author(s) and contributor(s) and not of MDPI and/or the editor(s). MDPI and/or the editor(s) disclaim responsibility for any injury to people or property resulting from any ideas, methods, instructions or products referred to in the content.

animals

MDPI

Brief Report

Mycobacterium kansasii Infection in a Farmed White-Tailed Deer (*Odocoileus virginianus*) in Florida, USA

Sydney L. Cottingham [1], An-Chi Cheng [1], Pedro H. de Oliveira Viadanna [2,3], Kuttichantran Subramaniam [2,3], William F. Craft [4], Marley E. Iredale [4], Samantha M. Wisely [3,5] and Juan M. Campos Krauer [1,5,*]

[1] Department of Large Animal Clinical Sciences, College of Veterinary Medicine, University of Florida, Gainesville, FL 32611, USA; s.cottingham@ufl.edu (S.L.C.); anchicheng@ufl.edu (A.-C.C.)
[2] Department of Infectious Diseases and Immunology, College of Veterinary Medicine, University of Florida, Gainesville, FL 32611, USA; pedro.viadanna@wsu.edu (P.H.d.O.V.); kuttichantran@ufl.edu (K.S.)
[3] Emerging Pathogens Institute, University of Florida, Gainesville, FL 32611, USA; wisely@ufl.edu
[4] Department of Comparative, Diagnostic, and Population Medicine, College of Veterinary Medicine, University of Florida, Gainesville, FL 32611, USA; craftw@ufl.edu (W.F.C.); marley.iredale@ufl.edu (M.E.I.)
[5] Department of Wildlife Ecology and Conservation, University of Florida, Gainesville, FL 32611, USA
* Correspondence: jmcampos@ufl.edu; Tel.: +1-352-294-4327

Simple Summary: *Mycobacterium kansasii* is a zoonotic bacterial pathogen that can cause a chronic disease that resembles pulmonary tuberculosis in many mammals including humans, cattle, goats, black-tailed deer, white-tailed deer, Florida manatees, and rhesus monkeys. We identified the first case of *M. kansasii* infection in farmed white-tailed deer (*Odocoileus virginianus*) in Florida. We performed hematoxylin and eosin (H&E) staining, Ziehl–Neelsen (ZN) staining, PCR, and Sanger sequencing of the lung tissue after the animal was euthanized. The microscopic observations of the H&E-stained lung showed multifocal granuloma, while the ZN-stained tissue revealed low numbers of beaded, magenta-staining rod bacteria inside the granuloma formation. Molecular examination identified the presence of *Mycobacterium kansasii*. Although this was a sporadic case and there was no evidence that *M. kansasii* could be transmitted directly from animals to human beings, it is crucial to have basic biosecurity practices and management in place to prevent disease outbreaks and spillover.

Abstract: A 7-year-old farmed white-tailed deer doe was transported to a Levy County, Florida property and began to decline in health, exhibiting weight loss and pelvic limb weakness. The doe prematurely delivered live twin fawns, both of which later died. The doe was treated with corticosteroids, antibiotics, gastric cytoprotectants, and B vitamins but showed no improvement. The doe was euthanized, and a post mortem examination was performed under the University of Florida's Cervidae Health Research Initiative. We collected lung tissue after the animal was euthanized and performed histological evaluation, using H&E and Ziehl–Neelsen (ZN) staining, and molecular evaluation, using conventional PCR, followed by Sanger sequencing. The microscopic observations of the H&E-stained lung showed multifocal granuloma, while the ZN-stained tissue revealed low numbers of beaded, magenta-staining rod bacteria inside the granuloma formation. Molecular analysis identified the presence of *Mycobacterium kansasii*. This isolation of a non-tuberculous *Mycobacterium* in a white-tailed deer emphasizes the importance of specific pathogen identification in cases of tuberculosis-like disease in farmed and free-ranging cervids. We report the first case of *M. kansasii* infection in a farmed white-tailed deer (*Odocoileus virginianus*) in Florida. Although *M. kansasii* cases are sporadic in white-tailed deer, it is important to maintain farm biosecurity and prevent farmed cervids from contacting wildlife to prevent disease transmission.

Keywords: non-tuberculous *Mycobacterium*; pneumonia; captive cervid; deer farming

1. Introduction

Mycobacterium kansasii is a zoonotic pathogen capable of causing chronic, debilitating disease that resembles pulmonary tuberculosis. *M. kansasii* belongs to the phylum *Actinomycetota* and the family *Mycobacteriaceae* [1–3]. *M. kansasii* is an aerobic, Gram-positive, slow-growing, and photochromogenic species with a genome size of 6.4 Mb [4]. *M. kansasii* is classified as a non-tuberculous mycobacterium (NTM), distinguishing this species from the *Mycobacterium tuberculosis* complex (MTBC) [4]. *M. kansasii* is ubiquitous in the environment worldwide, particularly in soil and tap water [3,5].

M. kansasii was first described as an opportunistic pathogen in human patients with pulmonary disease resembling tuberculosis in Kansas, USA in the 1950s [6]. Clinical signs of *M. kansasii* in humans include anorexia, progressive weight loss, weakness, low-grade intermittent fever, and respiratory signs [7]. *M. kansasii* is more common in immunocompromised patients [8–11] and patients with existing pulmonary conditions, such as chronic obstructive pulmonary disease [12,13]. Human-to-human transmission of *M. kansasii* has not been confirmed [4,14].

M. kansasii is ubiquitous in the environment, yet is a rare pathogen in livestock and wildlife [4]. The clinical presentation of *M. kansasii* infection in animal hosts is highly variable, ranging from asymptomatic infection to overt clinical disease that may feature chronic weight loss, granulomatous pneumonia, bronchial lymphadenopathy, or cutaneous lesions [15–28]. Disease associated with *M. kansasii* infection has been reported in wild boar (*Sus scrofa*) [27], free-ranging black-tailed deer (*Odocoileus hemionus columbianus*) [17] and white-tailed deer (*Odocoileus virginianus*) [25], bonteboks (*Damaliscus pygargus dorcas*) [20], laboratory rhesus monkeys (*Macaca mulatta*) [22], captive Florida manatees (*Trichechus manatus*) [16], domestic goats (*Capra hircus*) [15], cattle (*Bos taurus*) [19,23,24,28], domestic cats (*Felis catus*) [26], Sichuan takins (*Budorcas taxicolortibetana*) [21], siamangs (*Hylobates syndactylus*) [21], and alpacas (*Vicugna pacos*) [18]. Herein, we report the first known case of *M. kansasii* infection in a farmed white-tailed deer.

2. Materials and Methods

In March 2018, an approximately 7-year-old farmed white-tailed deer doe was transported to a private property in Levy County, Florida. The owner of the doe reported progressive weight loss and pelvic limb weakness but did not initiate treatment as the doe was believed to be pregnant. The doe eventually delivered premature twin fawns, both of which died after birth. The owner administered a corticosteroid (intramuscular (IM), dexamethasone) at dosages varying between 4 and 12 mg daily for 28 days, a macrolide antibiotic (1.5 cc, IM, tylosin, Tylan 200 Injection, Elanco US, Inc., Greenfield, IN, USA), a gastric cytoprotectant (1 scoop, orally, sucralfate, Carafate©, Aspen Pharmacare, Durban, South Africa), supplemented B vitamin complex, vitamin B12, and thiamine at unknown dosages. Due to the lack of response to treatment, the doe was euthanized by the owner in August 2018. The University of Florida's Cervidae Health Research Initiative (CHeRI) was contacted to request a post mortem examination.

At necropsy, the doe presented in poor nutritional condition with a dull, rough-hair coat. The lungs were pale, with multifocal, 0.2–0.5 cm yellow-white-to-gray, granular, nodular lesions distributed across the pleural surface and throughout the parenchyma (Figure 1). The greatest density of nodular lesions was observed in the cranial lobes bilaterally. Paired lung, heart, liver, kidney, and spleen samples were chilled at 4 °C and fixed in 10% neutral buffered formalin. Fresh and fixed lung tissues were submitted to the University of Florida College of Veterinary Medicine Diagnostic Laboratories for histopathological and microbiological characterization.



(**a**) (**b**)

Figure 1. Gross appearance of the lungs in the *M. kansasii*-infected deer. (**a**) Open thoracic cavity demonstrating lungs with multifocal, granulomatous pneumonia. Arrows indicate granulomas. (**b**) Focal area of atelectasis with numerous granulomas.

Molecular Examination

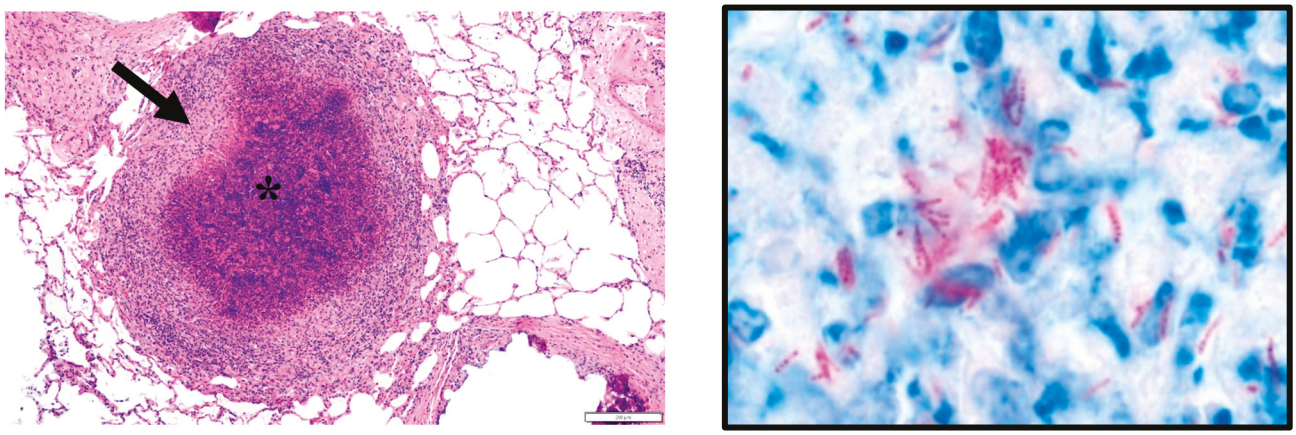
DNA from the lung and isolated bacteria was extracted using DNeasy Blood and Tissue Kit (Qiagen, Hilden, Germany) according to the manufacturer's instructions. Polymerase chain reaction (PCR) for *Mycobacterium* spp. was carried out using the primer pair KY18-KY75, which amplified a fragment (~500 bp) of the 16S rRNA [25]. Total reaction volumes were 30 µL, which consisted of 0.15 µL of Platinum Taq DNA Polymerase (Invitrogen), 3.0 µL of 10× PCR Buffer, 1.2 µL of 50 mM MgCl2, 0.6 µL of 10 mM dNTPs, 1.5 µL of 20 µM of each forward and reverse primer, 17.6 µL of molecular-grade water, and 4.5 µL of DNA template (100 ng). An initial denaturation step of 95 °C for 5 min was followed by 40 cycles of a 95 °C denaturation step for 5 s, a 55 °C annealing step for 5 s, a 68 °C extension step for 25 s, and a final extension step at 71 °C for 1 min. PCR products were subjected to gel electrophoresis using a 1% agarose gel stained with ethidium bromide. Amplicons of the expected size were purified using a QIAquick PCR Purification Kit (Qiagen). The concentration of purified amplicons was determined fluorometrically using a Qubit 3.0 Fluorometer and dsDNA BR Assay Kit (Life Technologies, Carlsbad, CA, USA) before submitting to Functional Biosciences, Inc. (Madison, WI, USA) for Sanger sequencing. The sequences were visualized and assembled using BioEdit 7.1.3.0.

3. Results

3.1. Microscopic Observations

Microscopically, the lung architecture was effaced by multifocal small-to-large granulomas with central areas of necrosis varying from caseous to lytic, with mild to prominent mineralization within necrotic centers (Figure 2). The necrotic centers were bordered by peripheral rims of epithelioid macrophages that often had finely vacuolated cytoplasm, low numbers of Langhans-type multinucleated giant cells, and scattered lymphocytes, plasma cells, and neutrophils. The granulomas were bordered by variable degrees of fibrosis, with more prominent fibrosis around granulomas with prominent central mineralization (likely indicating chronicity). The alveolar septa were mildly to moderately expanded by lymphocytes, plasma cells, macrophages, several neutrophils, small amounts of fibrin, and congested capillaries (interpreted as interstitial pneumonia). Ziehl–Neelsen staining revealed low numbers of approximately 5–15 µm long, occasionally beaded, slender, acid-fast rods that were extracellular and within macrophages and Langhans-type multinucleated

giant cells. Significant lesions were not detected in the heart, spleen, liver, and kidney. The presence of acid-fast rods within granulomas with caseous necrosis and mineralization was highly suggestive of infection with tuberculoid *Mycobacterium* spp. and prompted the molecular identification of the bacteria.



(**a**) (**b**)

Figure 2. Microscopic observations of lung tissue from the *M. kansasii*-infected deer. (**a**) H&E-stained histologic section of lung with a focal granuloma (bar = 200 μm); asterisk indicates necrotic center. Arrow indicates fibrous capsule with macrophages. (**b**) Ziehl–Neelsen acid-fast stain with low numbers of beaded, magenta-staining rod bacteria (bar = 10 μm).

3.2. Molecular Examination

A *Mycobacterium*-screening culture (Lowenstein–Jensen agar slants at 35–37 °C and 5% CO_2, and Middlebrook 7H11 agar at room temperature without added CO_2) isolated a rapid-growing *Mycobacterium* sp. at around 7 days after culturing. A collected colony and a fragment of the lung were tested for *Mycobacterium* using a specific PCR assay [17] followed by Sanger sequencing. The obtained sequence was 375 bp. A standard nucleotide–nucleotide BLAST (BLASTN) search revealed 100% query coverage and 99.48% identity to 79 strains/isolates of *Mycobacterium kansasii* within the National Center for Biotechnology Information GenBank database. *M. kansasii* is considered a slow-growing *Mycobacterium* species; however, PCR and Sanger sequencing conclusively confirmed the presence of this bacterium. Aerobic culture (general blood agar, chocolate agar, Columbia CNA agar, and MacConkey agar at 35–37 °C and 5% CO_2) of lung tissue found no growth at 24 h and very scant growth of mixed bacterial and fungal flora, without any clear predominance of the four morphotypes observed after an extended culture period.

4. Discussion

We report the first known isolation of *M. kansasii* from a farmed white-tailed deer. The histopathological changes observed in this case are consistent with lesions described in *M. kansasii* infections reported in a hunter-harvested, free-ranging black-tailed deer in Washington [17] and a free-ranging white-tailed deer in Louisiana [25]. *M. kansasii* more commonly infects immunocompromised individuals. Corticosteroids have known immunosuppressive activity, and oral dexamethasone is associated with the reactivation of latent *Mycobacterium* spp. infections in HIV patients. In this case, the history of extended corticosteroid therapy and transportation to a new facility may have produced an immunocompromised state that promoted the reactivation of a latent *M. kansasii* infection. No comorbidities were detected via post mortem examination or ancillary diagnostics, suggesting that *M. kansasii* was the primary cause of death. Though aerobic culture found bacterial and fungal flora in cultured lung tissue, microbial growth was scant, and no known pathogens were isolated.

5. Conclusions

This case highlights the importance of positively identifying mycobacterium species associated with tuberculous disease in captive or managed wildlife and underscores the risk of introducing disease agents when translocating livestock and captive wildlife. Mycobacteriosis associated with *M. kansasii* is not a reportable disease; however, bovine tuberculosis (bTB) caused by *Mycobacterium bovis* is a reportable zoonotic agent, and the diagnosis of bTB in captive and free-ranging wildlife has significant regulatory and public health implications for both livestock producers and wildlife managers. Identifying the *Mycobacteria* species associated with tuberculosis-like disease in captive wildlife is critical in mitigating risks to domestic livestock and free-ranging wildlife populations.

Despite *M. kansasii* not being a reportable disease, the pathogen still poses a risk as an opportunistic pathogen in immunocompromised humans. Deer farming brings humans into close contact with captive cervids, and this increased interaction between farmed cervids and human caretakers elevates the risk of transmission of potential zoonotic pathogens, including *M. kansasii*. It is crucial to maintain basic biosecurity and hygiene practices to reduce the risk of zoonotic disease transmission.

Author Contributions: Conceptualization, J.M.C.K. and S.L.C.; methodology, S.L.C., A.-C.C., P.H.d.O.V., K.S., W.F.C., M.E.I., J.M.C.K. and S.M.W.; software, P.H.d.O.V., A.-C.C. and K.S.; validation, S.L.C., J.M.C.K. and S.M.W.; formal analysis, S.L.C., P.H.d.O.V., K.S. and A.-C.C.; investigation, J.M.C.K., S.L.C., W.F.C., M.E.I. and K.S.; resources, J.M.C.K. and S.M.W.; data curation, S.L.C. and J.M.C.K.; writing—original draft preparation, S.L.C. and J.M.C.K.; writing—review and editing, S.L.C., J.M.C.K., W.F.C., M.E.I., K.S., P.H.d.O.V., A.-C.C. and S.M.W.; visualization, S.L.C. and J.M.C.K.; supervision, J.M.C.K. and S.M.W.; project administration, J.M.C.K.; funding acquisition, J.M.C.K. and S.M.W. All authors have read and agreed to the published version of the manuscript.

Funding: This research was funded by the University of Florida, Institute of Food and Agricultural Sciences, CHeRI, with funds provided by the Florida legislature #6000CHERI.

Institutional Review Board Statement: Not applicable.

Informed Consent Statement: Not applicable.

Data Availability Statement: Data are contained within the article.

Acknowledgments: We are grateful to all CHeRI technicians for their assistance. This study was made possible through the co-operation of farmed-deer producers throughout Florida; we are grateful for their participation.

Conflicts of Interest: The authors declare no conflicts of interest.

References

1. Wang, J.; McIntosh, F.; Radomski, N.; Dewar, K.; Simeone, R.; Enninga, J.; Brosch, R.; Rocha, E.P.; Veyrier, F.J.; Behr, M.A. Insights on the Emergence of *Mycobacterium tuberculosis* from the Analysis of *Mycobacterium kansasii*. *Genome Biol. Evol.* **2015**, *7*, 856–870. [CrossRef] [PubMed]
2. Machado, E.; Vasconcellos, S.E.G.; Cerdeira, C.; Gomes, L.L.; Junqueira, R.; Carvalho, L.D.; Ramos, J.P.; Redner, P.; Campos, C.E.D.; Caldas, P.C.S.; et al. Whole Genome Sequence of *Mycobacterium kansasii* Isolates of the Genotype 1 from Brazilian Patients with Pulmonary Disease Demonstrates Considerable Heterogeneity. *Mem. Inst. Oswaldo Cruz* **2018**, *113*, e180085. [CrossRef] [PubMed]
3. Luo, T.; Xu, P.; Zhang, Y.; Porter, J.L.; Ghanem, M.; Liu, Q.; Jiang, Y.; Li, J.; Miao, Q.; Hu, B.; et al. Population Genomics Provides Insights into the Evolution and Adaptation to Humans of the Waterborne Pathogen Mycobacterium Kansasii. *Nat. Commun.* **2021**, *12*, 2491. [CrossRef] [PubMed]
4. Pereira, A.C.; Ramos, B.; Reis, A.C.; Cunha, M.V. Non-Tuberculous Mycobacteria: Molecular and Physiological Bases of Virulence and Adaptation to Ecological Niches. *Microorganisms* **2020**, *8*, 1380. [CrossRef] [PubMed]
5. Vaerewijck, M.J.; Huys, G.; Palomino, J.C.; Swings, J.; Portaels, F. Mycobacteria in Drinking Water Distribution Systems: Ecology and Significance for Human Health. *FEMS Microbiol. Rev.* **2005**, *29*, 911–934. [CrossRef] [PubMed]
6. Buhler, V.B.; Pollak, A. Human Infection with Atypical Acid-Fast Organisms; Report of Two Cases with Pathologic Findings. *Am. J. Clin. Pathol.* **1953**, *23*, 363–374. [CrossRef] [PubMed]
7. Matveychuk, A.; Fuks, L.; Priess, R.; Hahim, I.; Shitrit, D. Clinical and Radiological Features of *Mycobacterium kansasii* and Other Ntm Infections. *Respir. Med.* **2012**, *106*, 1472–1477. [CrossRef] [PubMed]

8. Bloch, K.C.; Zwerling, L.; Pletcher, M.J.; Hahn, J.A.; Gerberding, J.L.; Ostroff, S.M.; Vugia, D.J.; Reingold, A.L. Incidence and Clinical Implications of Isolation of *Mycobacterium kansasii*: Results of a 5-Year, Population-Based Study. *Ann. Intern. Med.* **1998**, *129*, 698–704. [CrossRef] [PubMed]
9. Bhatt, K.; Banavathi, K. Mycobacterium Kansasii Osteomyelitis—A Masquerading Disease. *JMM Case Rep.* **2018**, *5*, e005114. [CrossRef]
10. Sheu, L.C.; Tran, T.M.; Jarlsberg, L.G.; Marras, T.K.; Daley, C.L.; Nahid, P. Non-Tuberculous Mycobacterial Infections at San Francisco General Hospital. *Clin. Respir. J.* **2015**, *9*, 436–442. [CrossRef]
11. Taillard, C.; Greub, G.; Weber, R.; Pfyffer, G.E.; Bodmer, T.; Zimmerli, S.; Frei, R.; Bassetti, S.; Rohner, P.; Piffaretti, J.C.; et al. Clinical Implications of Mycobacterium Kansasii Species Heterogeneity: Swiss National Survey. *J. Clin. Microbiol.* **2003**, *41*, 1240–1244. [CrossRef] [PubMed]
12. Davies, B.S.; Roberts, C.H.; Kaul, S.; Klein, J.L.; Milburn, H.J. Non-Tuberculous Slow-Growing Mycobacterial Pulmonary Infections in Non-Hiv-Infected Patients in South London. *Scand. J. Infect. Dis.* **2012**, *44*, 815–819. [CrossRef] [PubMed]
13. Arend, S.M.; de Palou, E.C.; de Haas, P.; Janssen, R.; Hoeve, M.A.; Verhard, E.M.; Ottenhoff, T.H.; van Soolingen, D.; van Dissel, J.T. Pneumonia Caused by *Mycobacterium kansasii* in a Series of Patients without Recognised Immune Defect. *Clin. Microbiol. Infect.* **2004**, *10*, 738–748. [CrossRef] [PubMed]
14. Ricketts, W.M.; O'Shaughnessy, T.C.; van Ingen, J. Human-to-Human Transmission of *Mycobacterium kansasii* or Victims of a Shared Source? *Eur. Respir. J.* **2014**, *44*, 1085–1087. [CrossRef] [PubMed]
15. Acosta, B.; Real, F.; Ferrer, O.; Deniz, S.; Poveda, B. Isolation of Mycobacterium Kansasii from a Tuberculin-Positive Goat. *Vet. Rec.* **1998**, *142*, 195–196. [CrossRef]
16. Sato, T.; Shibuya, H.; Ohba, S.; Nojiri, T.; Shirai, W. Mycobacteriosis in Two Captive Florida Manatees (Trichechus Manatus Latirostris). *J. Zoo Wildl. Med.* **2003**, *34*, 184–188. [PubMed]
17. Hall, P.B.; Bender, L.C.; Garner, M.M. Mycobacteriosis in a Black-Tailed Deer (*Odocoileus hemionus columbianus*) Caused by *Mycobacterium kansasii*. *J. Zoo Wildl. Med.* **2005**, *36*, 115–116. [CrossRef] [PubMed]
18. Braun, U.; Previtali, M.; Gautschi, A.; Forster, E.; Steininger, K.; Irmer, M.; Reichle, S.; Sydler, T.; Wiederkehr, D.; Ruetten, M.; et al. Sonographic Findings in an Alpaca with *Mycobacterium kansasii* Infection. *Schweiz. Arch. Tierheilkd.* **2009**, *151*, 287–290. [CrossRef]
19. Houlihan, M. Isolation of *Mycobacterium kansasii* from Calf Reactors in a Tb-Restricted Dairy Herd. *Vet. Rec.* **2010**, *166*, 272–273. [CrossRef]
20. Miller, M.; Terrell, S.; Lyashchenko, K.; Greenwald, R.; Harris, B.; Thomsen, B.V.; Fontenot, D.; Stetter, M.; Neiffer, D.; Fleming, G. Mycobacterium Kansasii Infection in a Bontebok (*Damaliscus pygaragus dorcas*) Herd: Diagnostic Challenges in Differentiating from the Mycobacterium Tuberculosis Complex. *J. Zoo Wildl. Med.* **2011**, *42*, 468–472. [CrossRef]
21. Thompson, K.A.; Campbell, M.; Levens, G.; Lim, A.; Bolin, S. *Mycobacterium kansasii* Infection in a Captive Sichuan Takin (*Budorcas taxicolortibetana*) and a Siamang (*Hylobates syndactylus*) at a Zoological Facility. *Vet. Rec. Case Rep.* **2016**, *4*, e000280. [CrossRef]
22. Shipley, S.T.; Johnson, D.K.; Roodgar, M.; Smith, D.G.; Montgomery, C.A.; Lloyd, S.M.; Higgins, J.A.; Kriel, E.H.; Klein, H.J.; Porter, W.P.; et al. Isolated from Tuberculin-Positive Rhesus Macaques (*Macaca mulatta*) in the Absence of Disease. *Comp. Med.* **2017**, *67*, 368–375. [PubMed]
23. Ghielmetti, G.; Friedel, U.; Scherrer, S.; Sarno, E.; Landolt, P.; Dietz, O.; Hilbe, M.; Zweifel, C.; Stephan, R. Non-Tuberculous *Mycobacteria* Isolated from Lymph Nodes and Faecal Samples of Healthy Slaughtered Cattle and the Abattoir Environment. *Transbound. Emerg. Dis.* **2018**, *65*, 711–718. [CrossRef]
24. Cerna, P.; Mitchell, J.L.; Lodzinska, J.; Cazzini, P.; Varjonen, K.; Gunn-Moore, D.A. Systemic Mycobacterium Kansasii Infection in Two Related Cats. *Pathogens* **2020**, *9*, 959. [CrossRef] [PubMed]
25. Ford, A.K.; Niedringhaus, K.D.; Anderson, A.N.; LaCour, J.M.; Nemeth, N.M. Disseminated Mycobacterium Kansasii Infection in a White-Tailed Deer and Implications for Public and Livestock Health. *J. Vet. Diagn. Investig.* **2020**, *32*, 147–151. [CrossRef] [PubMed]
26. Fukano, H.; Terazono, T.; Hirabayashi, A.; Yoshida, M.; Suzuki, M.; Wada, S.; Ishii, N.; Hoshino, Y. Human Pathogenic Mycobacterium Kansasii (Former Subtype I) with Zoonotic Potential Isolated from a Diseased Indoor Pet Cat, Japan. *Emerg. Microbes Infect.* **2021**, *10*, 220–222. [CrossRef] [PubMed]
27. Radulski, L.; Krajewska-Wedzina, M.; Lipiec, M.; Szulowski, K. Infection of a Free-Living Wild Boar (*Sus scrofa*) with a Bacterium from the *Mycobacterium kansasii* Complex. *Animals* **2022**, *12*, 964. [CrossRef]
28. Gomez-Buendia, A.; Alvarez, J.; Bezos, J.; Mourelo, J.; Amado, J.; Saez, J.L.; de Juan, L.; Romero, B. Non-Tuberculous Mycobacteria: Occurrence in Skin Test Cattle Reactors from Official Tuberculosis-Free Herds. *Front. Vet. Sci.* **2024**, *11*, 1361788. [CrossRef]

Disclaimer/Publisher's Note: The statements, opinions and data contained in all publications are solely those of the individual author(s) and contributor(s) and not of MDPI and/or the editor(s). MDPI and/or the editor(s) disclaim responsibility for any injury to people or property resulting from any ideas, methods, instructions or products referred to in the content.

animals

MDPI

Communication

Lack of Highly Pathogenic Avian Influenza H5N1 in the South Shetland Islands in Antarctica, Early 2023

Gabriela Muñoz [1,2], Vanessa Mendieta [1], Mauricio Ulloa [3,4], Belén Agüero [1,2], Cristian G. Torres [5], Lucas Kruger [6,7] and Victor Neira [1,*]

[1] Departamento de Medicina Preventiva Animal, Facultad de Ciencias Veterinarias y Pecuarias, Universidad de Chile, Santiago 8820808, Chile; munozbritogabriela@um.uchile.cl (G.M.); vmendietareis@gmail.com (V.M.); belen.aguero.a@gmail.com (B.A.)
[2] Programa de Doctorado en Ciencias Silvoagropecuarias y Veterinarias, Universidad de Chile, Santiago 8820808, Chile
[3] Veterinary Histology and Pathology, Institute of Animal Health and Food Safety, Veterinary School, University of Las Palmas de Gran Canaria, 35001 Las Palmas de Gran Canaria, Spain; mulloa@sernapesca.cl
[4] Servicio Nacional de Pesca y Acuicultura, Valparaíso 2340159, Chile
[5] Departamento de Ciencias Clínicas, Facultad de Ciencias Veterinarias y Pecuarias, Universidad de Chile, Santiago 8820808, Chile; crtorres@uchile.cl
[6] Instituto Antártico Chileno, Punta Arenas 6200000, Chile; lkruger@inach.cl
[7] Millennium Institute of Biodiversity of Antarctic and Subantarctic Ecosystems (BASE), Ñuñoa 7750000, Chile
* Correspondence: vneiraram@gmail.com; Tel.: +56-954069030

Simple Summary: A concerning highly pathogenic avian influenza caused widespread outbreaks among birds and wildlife at a global level. First identified in South America in October 2022 and linked to migratory birds, there's growing concern about virus spillover during bird migrations between the poles. The Arctic tern's migration from the Arctic to Antarctica raises concerns about its role in transmission. Even in Antarctica's seemingly untouched environment, diverse wildlife is at risk from the new strain of highly pathogenic avian influenza. Surveillance efforts started in the South Shetland Islands in January 2023, focusing on areas where penguins, birds, and marine mammals normally gather. Following Antarctic Treaty guidelines, observations and sample collection were conducted, revealing no signs of the virus in the region during that time lapse. These findings not only contribute to confirming the absence of the virus in Antarctica during the specified period but also emphasize the necessity for sustained surveillance and monitoring to safeguard the Antarctic ecosystem.

Abstract: In January 2023, an active surveillance initiative was undertaken in the South Shetland Islands, Antarctica, with the specific objective of ascertaining evidence for the presence of avian influenza, and specifically the highly pathogenic avian influenza virus subtype H5N1 (HPAIV H5N1). The investigation encompassed diverse locations, including Hanna Point (Livingston Island), Lions Rump (King George Island), and Base Escudero (King George Island), with targeted observations on marine mammals (southern elephant seals), flying birds (the kelp gull, snowy sheathbill and brown skua), and penguins (the chinstrap penguin and gentoo penguin). The study encompassed the examination of these sites for signs of mass mortality events possibly attributable to HPAIV H5N1, as well as sampling for influenza detection by means of real-time RT-PCR. Two hundred and seven (207) samples were collected, including 73 fecal samples obtained from the environment from marine mammals (predominantly feces of southern elephant seals), and 77 cloacal samples from penguins of the genus Pygoscelis (predominantly from the gentoo penguin). No evidence of mass mortality attributable to HPAIV H5N1 was observed, and all the collected samples tested negative for the presence of the virus, strongly suggesting the absence of the virus in the Antarctic territory during the specified period. This empirical evidence holds significant implications for both the ecological integrity of the region and the potential zoonotic threats, underscoring the importance of continued surveillance and monitoring in the Antarctic ecosystem.

Keywords: highly pathogenic avian influenza; H5N1; Antarctica; lack of detection

1. Introduction

The highly pathogenic avian influenza subtype H5NX, clade 2.3.4.4b, has caused global epidemic outbreaks affecting both wildlife and poultry populations [1]. This virulent virus has permeated avian and mammalian species, instigating mass mortality events across several continents. In October 2022, South America registered the first detection of the virus in wild birds, attributed to migratory birds, with multiple introductions reported [2].

Given that several species of seabirds occurring in Antarctica have the capability of long-range movement, including transequatorial migrating species capable of traveling from the Arctic to Antarctica, great concerns arise about the potential dissemination of the virus during migratory events directly between polar circles. Two species stand out as potential contributors to such transmission, notably the arctic tern (*Sterna paradisaea*), well-known for undertaking one of the longest migratory journeys from the Arctic to Antarctica [3,4], and the south polar skua (*Catharacta maccormicki*) which spends the austral winter off the North Atlantic and Pacific oceans, and in tropical/subtropical waters off the North Indian Ocean [5,6]. Additionally, several other species that breed in Antarctica with shorter migratory routes but dispersive migration behaviors, when connected, might facilitate the introduction of the virus into the Antarctic continent, such as southern giant petrels (*Macronectes giganteus*) [7], southern fulmars (*Fulmarus glacialoides*), cape petrels (*Daption capense*) [8], and brown skuas (*Catharacta lonbergii*) [9,10]. Southern giant petrels have recently been reported as being able to move from the Antarctic Peninsula to the coast of Tierra del Fuego in Argentina and Chile and back in a few days [7].

So far, only low-pathogenic avian influenza strains like H11N2 [11,12] and H5N5 LPAIV [13] have been reported in Antartica, but the rich wildlife in the region remains highly susceptible to the new strains of H5NX clade 2.3.4.4b. Recent reports outside Antarctica have documented mass mortality events in penguins and marine mammals, the most abundant species in Antarctica. Humboldt penguins *(Spheniscus humboldti*), South American sea lions (*Otaria flavescens*) [14], southern elephant seals (*Mirounga leonina*) in South America, and African penguins (*Spheniscus demersus*) in Africa [15], along with other species in the Northern Hemisphere, have also been severely affected.

In view of the potential introduction of H5NX clade 2.3.4.4b, we initiated active surveillance in January 2023, four months after the introduction of HPAIV H5N1 in South America. Our surveillance efforts were strategically concentrated on selected locations within the Southern Shetland Islands, where penguins, flying birds, and marine mammals converge.

2. Materials and Methods

2.1. Locations

In January 2023, we performed active surveillance looking for mass mortality events in the Antarctic wildlife attributable to HPAIV H5N1. The surveyed locations included were selected based on the available logistics and preferred locations of penguins and marine mammals. Such locations included Hanna Point, Livingston Island, and Lions Rump near Low Head at King George Island, and the western shore of the Fildes Peninsula near Teniente R. Marsh Airport. Hanna Point (−62.6544, −60.6133), presents a high concentration of wildlife, such as nesting gentoo penguins (*Pygoscelis papua*), chinstrap penguins (*Pygoscelis antarcticus*), southern giant petrels (*Macronectes giganteus*), and the presence of southern elephant seals (*Mirounga leonina*). Lions Rump, (−62.1333, −58.1167), an Antarctic Specially Protected Area (ASPA No 151, permit 892/2022 INACH), presents nesting of Adelie (*Pygoscelis adeliae*), chinstrap, and gentoo penguins, and a large number of southern elephant seals and fur seals (*Arctocephalus australis*) along the beaches. The western shore of the Fildes Peninsula (−62.197778, −58.993611) is occupied by a colony of southern elephant seals; other marine mammals such as the fur seal, the leopard seal

(*Hydrurga leptonyx*), and the Weddell seal (*Leptonychotes weddellii*) can also be observed. The surveillance team, made up of three individuals, fully adhered to Antarctic treaty guidelines when conducting the surveillance and monitoring of the selected locations, systematically observing and documenting the wildlife populations present. The locations are illustrated in Figure 1. The clinical observation and search for clinical signs of disease, such as respiratory, neurologic, or digestive syndromes, ref. [14] was performed by doctors of veterinary medicine.

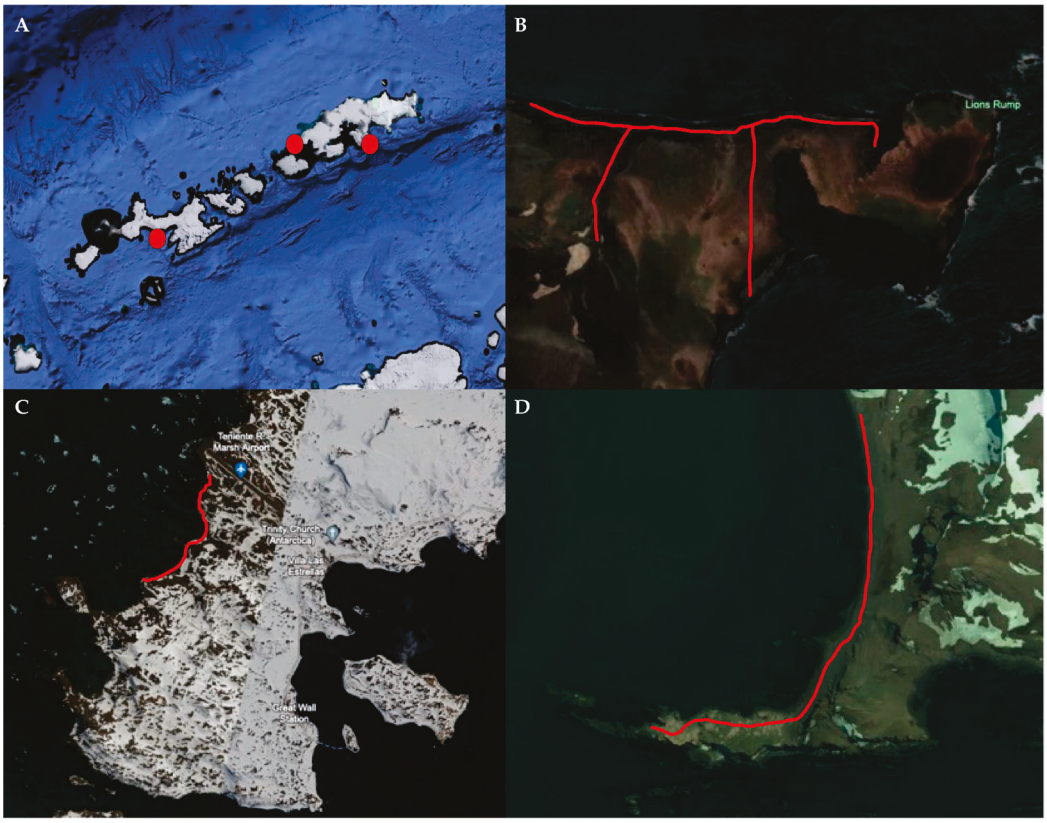


Figure 1. Image of the surveyed locations in the South Shetland Islands, Antarctica, captured from Google Earth. (**A**) South Shetland Islands with red dots that indicate the sampling locations. (**B**) Lions Rump in King George Island. (**C**) Fildes Peninsula in King George Island. (**D**) Hanna Point in Livingstone Island. The red line indicates the trekking route during the surveillance and monitoring activities. Captures are not to scale.

The rationale behind the sampling strategy is related to the known susceptibility of penguins and elephant seals to HPAIV. We recognize that the primary risk of avian influenza reaching Antarctica most likely stems from migratory birds that regularly nest on the continent. We anticipate that upon the virus's introduction, it would likely affect other at-risk species such as penguins and elephant seals. These species, which form substantial colonies, allow for more efficient evaluation and sample collection. This pattern is reflected in events observed in Peru, Argentina, and Chile in South America, where the introduction of the virus by migratory birds led to documented clinical observations of HPAIV penguins and marine mammals [16–18].

2.2. Sampling

A total of 207 samples, which consisted of 156 environmental samples and 51 cloacal samples, were collected to perform real-time reverse transcription-polymerase chain reaction (RT-PCR) targeting the M gene of the Influenza A virus. Specifically, at Hanna Point, Livingstone Island, a total of 80 samples were collected, including 53 from southern

elephant seals, 13 from kelp gulls, and smaller numbers from the snowy sheathbill (n = 3), chinstrap penguins (n = 3), and gentoo penguins (n = 8).

During sampling in Lions Rump, King George Island, a total of 104 samples were collected. Among these, 68 originated from southern elephant seals, and there were varying counts from gentoo penguins (n = 33), Adelie penguins (n = 2), and chinstrap penguins (n = 1). On the west coast of the Fildes Peninsula, King George Island, 23 samples were collected, including from southern elephant seals and an unidentified mammal (six environmental samples), and a brown skua (Direct). In the case of marine mammals and flying birds, fresh feces from the environment were meticulously collected, while cloacal samples were collected from clinically healthy penguins. To gather samples, we carefully surrounded the colonies, seeking out fresh feces. Using sterile cotton swabs, samples were preserved in minimum essential medium supplemented with antibiotic and antimycotic (Gibco™ 15240062), and kept in frozen storage until processing. For penguins, the collection of samples involved the capture of the animals by a doctor of veterinary medicine using a bird net and restraint. Subsequently, a cloacal swab was taken and preserved in viral transport media for further analysis. Environmental sampling for marine mammals and flying birds was carried out based on convenience. In contrast, a minimum of 30 individual cloacal samples were systematically collected from locations inhabited by penguins to evaluate disease freedom. This number (30) allows for the detection of at least one positive sample given a prevalence in the location equal to or less than 10%.

2.3. Diagnostic Testing

The samples were frozen upon arrival at the Animal Virology Lab, Facultad de Ciencias Veterinarias y Pecuarias, Universidad de Chile. The total RNA was extracted using TRIzol® LS Reagent (Invitrogen™, Carlsbad, CA, USA) following the manufacturer's recommendations. The real-time reverse transcription-polymerase chain reaction (real-time RT-PCR) with TaqMan probe (IDT) was performed, amplifying a conserved region of the matrix gene [19,20]. This protocol allows one to detect the generic Influenza A virus, which include Avian Influenza and HPAIVs.

Samples with a cycle threshold (Ct) below 35 were considered positive, between 35 and 40 inconclusive, and repeated Ct over 40 were considered negative. If a positive sample was obtained, a real-time RT-PCR with TaqMan probes for H5 2.3.4.4b clade confirmation using VSL-USDA protocols could be attempted.

3. Results

3.1. No Clinical Signs Related to HPAIV

The surveillance was performed by exploring all the colonies in each selected location (Figure 1). In Hanna Point, three large groups of elephant seals, a nesting colony of kelp gulls (*Larus dominicanus*), a nesting colony of giant petrels, and a large colony of gentoo penguins were observed. Notably, no evidence of unexpected mortality events, such as deceased animals or carcasses, were observed. The observed animals displayed normal behavior, and there were no discernible signs of evident disease. In Lions Rump, a large group of elephant seals and colonies of Adelie and gentoo penguins were observed to exhibit normal behavior, and no fresh dead animals or carcasses were observed. Likewise, no signs of disease were observed on the western shore of the Fildes Peninsula, where a group of southern elephant seals in good physical shape was identified. The animals presented in good condition and no mortality was identified. Fur seals were not observed during the surveillance.

3.2. Lack of Detection by Real-Time RT PCR

For the total of the samples analyzed, all resulted in a negative outcome for Influenza A detection. In the initial testing, only three samples resulted as suspect with Ct values ranging from 36.5 to 37.8, all obtained from gentoo penguin chicks; however, they resulted negative during the confirmation round. The complete sampling is summarized in Table 1.

Table 1. Overall sample collection in surveillance and monitoring activities. All samples tested negative for influenza identification.

Locations	Especies	Environmental	Direct	Total
Hanna Point, Livingstone Island	Southern elephant seal	53	0	53
	Kelp gull	13	0	13
	Snowy sheathbill	0	3	3
	Chinstrap penguin	0	3	3
	Gentoo penguin	0	8	8
Lions Rump, King George Island	Southern elephant seal	68	0	68
	Gentoo penguin	0	33	33
	Adelie penguin	0	1	1
	Chinstrap penguin	0	2	2
Fildes Peninsula western coast, King George Island	Southern elephant seal	16	0	16
	Unidentified mammal	6	0	6
	Brown skua	0	1	1
	Total	156	51	207

4. Discussion

The current outbreak of HPAIV H5N1, which began in 2022, has resulted in the deaths of a large number of seabirds across the Northern Hemisphere, Southern Africa, the Atlantic and Pacific Oceans, and throughout South America.

This study represents the first systematic effort to surveil the Influenza virus in Antarctica during 2023, focusing specifically on the South Shetland Islands near the Antarctic Peninsula in both avian and marine mammals. Fortunately, we neither observed clinical signs nor detected clinical or molecular evidence of the virus during surveillance in early 2023 at Lions Rump and Hanna Point, two distinctive areas for biodiversity in Antarctica inhabited by flying birds, penguins, and marine mammals, in any of the studied species. In a study primarily based on clinical observations in early 2023, no signs of the virus in the Antarctic and sub-Antarctic territories were reported either [21].

Migratory birds are pivotal in the global spread of HPAIV H5N1 [22]. The extensive infections documented in North America in 2022 indicate the potential for the virus to be transmitted over long distances, possibly even between polar regions. Although direct transmission over such vast distances is less common, there is substantial evidence of the virus's spread from North America to Chile and Peru, and its further dissemination to remote areas like Patagonia [2,14,16,18].

Arctic terns, known for their pole-to-pole migrations, provide a direct transmission route for HPAIV H5N1 from the Northern Hemisphere [3]. These birds, vulnerable to the Influenza A virus, have been confirmed as carriers of HPAIV H5N1 from September to December 2022 in the Northern Hemisphere [23], and massive mortality events in colonies on wild birds have been linked to this strain [24,25]. Moreover, HPAIV H5N1 has been completely sequenced from Arctic terns collected in Alaska, Wales, Denmark, Germany, Netherlands, England, and Scotland between 2022 and 2023 (Supplementary Information). Historical records also show the presence of H5NX in Arctic terns, with the first sequenced virus being H5N3 collected in 1975 (Supplementary Information). The evidence suggests that Arctic terns are highly susceptible to the virus, which can cause significant mortality; however, some individuals may resist and migrate while carrying the virus. In contrast, the south polar skua, another species that migrates between hemispheres, may be susceptible to Influenza infection, but there is currently no evidence of this.

The circumstantial evidence indicates that there was most likely no effective transmission of HPAIV H5N1 clade 2.3.4.4b in Antarctica during the summer of 2022/2023 in the Southern Hemisphere. Nevertheless, the virus could reach the continent directly from the Northern Hemisphere, most likely via Arctic terns.

Another possibility is short-distance dissemination. The virus is already in South America and is more than likely to be introduced to Antarctica through local migrations, very probably during this current 2023–2024 season. Species at risk for the introduction of the virus include, but are not limited to, southern giant petrels, southern fulmars, Cape petrels, and brown skuas. Of course, after introduction, other species such as penguins and marine mammals should be affected, as mentioned before. It is important to note that in Chile more than 50 avian species have tested positive [26].

Biologically speaking, the difference between HPAIV and low-pathogenic avian influenza virus (LPAIV) lies in the fact that HPAIV is a systemic infection, while LPAI remains localized in the respiratory and intestinal tract. In this study, cloacal swabs, a recommended choice for waterfowl, were used. This differs from gallinaceous poultry, for which oropharyngeal swabs are recommended; however, it is considered optimal to collect swabs from both anatomical areas [27]. In this study, the collection of oropharyngeal samples was not chosen due to the invasive nature of this technique, particularly in wild bird species. Instead, cloacal swabs and environmental fecal samples, representing a less intrusive option for sampling, were utilized.

The HPAIV H5N1 clade 2.3.4.4b is approaching Antarctica; it reached Tierra del Fuego, Chile, in April 2023 [26] (https://websag.azurewebsites.net/ia, accessed on 17 January 2024). Then, it was later confirmed in the Sub-Antarctic region, specifically in South Georgia [28], where mortalities in brown skuas, kelp gulls, and southern elephant seals were observed. The sequenced viruses from these events are linked to those from Chilean cases [28]. In the Falkland Islands, infections were confirmed in southern fulmars and black-browed albatrosses (*Thalassarche melanophris*). Due to the fact that all these species can reach Antarctica, the potential for the virus to spread is significant.

It is crucial to note that migratory wild birds pose a significant risk upon their next arrival, as opposed to the Procellariiformes, which constantly move throughout the region. Southern giant petrels, for example, can travel from the Antarctic Peninsula to the coast of Tierra del Fuego in Chile and Argentina and be back within a few days [7], even while tending to active nests. Due to their scavenging behavior, giant petrels are frequent visitors to penguin colonies and seal haul-out sites in Antarctica [29]. Immature southern giant petrels are often observed in the Magellan Strait, close to shore, and are known to interact with a variety of coastal species. There is no information on how these immature birds interact with conspecific adults year-round, but given the high mobility of the immature individuals, it is likely that some level of contact exists. Black-browed albatrosses also undertake foraging trips to the Antarctic Peninsula, and since at least one positive case has been reported in an albatross [30], they become another potential vector.

Finally, while elephant seal fatalities on Livingston Island are suspected, no positive detection of the virus has been confirmed, including the case of three dead elephant seals sampled by nasal and rectal swabs in Moltke Harbour [28]. However, a recent outbreak of HPAIV H5N1 in southern elephant seal pups was verified in Peninsula Valdés and adjacent areas of Argentina [18]. Additionally, the presence of leopard seals, which prey on birds such as penguins, introduces a new variable in the epidemiology of the disease, in that some species may contract the virus via the digestive route [14]. However, mammal-to-mammal transmission has recently been suggested [31].

Several iconic species could be affected by the HPAIV H5N1. Low-pathogenic avian influenza virus (LPAIV) subtype H11N2 is endemic among penguin populations, with low prevalence using direct molecular methods [11,12]. Reassortant strains with segments from South America [32], North America, and Eurasia [13] have also been detected. An LPAI H5N5 strain was identified in Antarctica in 2015 [12,13], suggesting its spread; however, it has not been detected ever since, indicating that non-adapted strains may die out. There is a possibility that penguins exhibit varying levels of susceptibility to HPAIV H5N1. Circumstantial evidence suggests that the Humboldt penguin may be more susceptible than the Magellanic penguin, due to the high impact in mortality rates of Humboldt penguins recorded in Chile (20%) during 2023 compared to Magellanic penguins (3%), where most

of the individuals have died from bycatch and so far no registered case from HPAI H5N1 virus has been registered, if we consider that both species share the same habitat along the south-eastern Pacific coast of Chile [33], a hypothesis that requires further confirmation.

Regarding marine mammals, the susceptibility of southern elephant seals has already been confirmed [18]. Regarding fur seals, the only confirmation of the virus has recently been reported in Uruguay [31]. From the above, it is evident that Antarctic pinnipeds are susceptible species that must necessarily be considered in new studies of Antarctica.

5. Conclusions

This study was conducted in January 2023 across three diverse wildlife locations in the South Shetland Islands. We relied on clinical observations and molecular detection to investigate the presence of HPAIV H5N1. However, we found no evidence of the virus. This research, along with other studies, strongly suggests that the virus did not reach the Antarctic continent in the last austral summer of 2022/2023. Although migratory birds, such as Arctic terns, were identified as potential vectors, no clinical signs of the virus were found during surveillance activities. It is important to highlight that the current findings may be influenced and limited by the sample size and specific locations covered during the study. To enhance the reliability of the results pertaining to the presence or absence of the virus, is necessary to increase the number of samples from various locations in a new study in the current season.

Importantly, endemic LPAIV viruses exhibit a different infection dynamic compared to HPAIV H5N5. HPAIV outbreaks are characterized by high morbidity and mortality, with the virus being detected in most of the affected and deceased animals. In this sense, expert clinical observations and molecular diagnostics are complementary strategies to determine the presence of this virus. Conversely, the previously detected endemic LPAIV H11N2 virus occurs with low prevalence in the absence of clinical signs. Hurt et al. in 2016 found one positive out of 295 samples in 2014, and one out of 493 in 2015 [12].

This research emphasizes the potential risk of introducing the virus from the Northern Hemisphere and currently from South America through local and long-distance migratory birds, highlighting the importance of ongoing surveillance efforts. As the virus poses a potential threat to nearby regions such as Tierra del Fuego and South Georgia, along with the possibility of future spread to Antarctica, it is imperative to expand the scope of surveillance activities.

The arrival of the virus in nearby sub-Antarctic regions and its potential spread underscores the need to understand and monitor transmission patterns in this unique environment. Given the susceptibility of various species, including Antarctic pinnipeds, continuous research is crucial to safeguard this delicate ecosystem. Having a robust and more comprehensive dataset through increased sampling is indispensable to the process of making informed decisions and developing effective strategies to prevent and manage the potential introduction of the HPAIV H5N1 to Antarctica.

Supplementary Materials: The following supporting information can be downloaded at: https://www.mdpi.com/article/10.3390/ani14071008/s1. HPAIV H5N1 sequenced from Arctic Terns collected in different countries between 2022 and 2023.

Author Contributions: Conceptualization, G.M. and V.N.; methodology, G.M, V.M., B.A. and V.N.; formal analysis, V.N.; investigation, G.M, V.M., B.A. and V.N.; resources, V.N.; data curation, G.M.; writing—original draft preparation, G.M., M.U., L.K. and V.N.; writing—review and editing, V.N.; project administration, V.N. and G.M.; funding acquisition, V.N. and C.G.T. All authors have read and agreed to the published version of the manuscript.

Funding: This work was supported by INACH Regular RT_08_21, ANID Fondecyt Regular 1211517 (VN). The funders had no role in study design, sample collection, data collection and analysis, the decision to publish, or in the preparation of the article. ANID Programa Beca Doctorado Nacional N° 21212316/2021 support was granted to B.A and 21220065/2022 to G.M.

Institutional Review Board Statement: The study was approved by the Institutional Ethics Committee of the University of Chile (CICUA) (protocol code 22603-VET-UCH, 25 July 2022).

Informed Consent Statement: Not applicable.

Data Availability Statement: Data are contained within the article and Supplementary Materials.

Acknowledgments: We thank the INACH personnel for supporting the sample collection and logistics. Thanks to Felipe Berrios for his support in sample processing.

Conflicts of Interest: The authors declare no conflicts of interest. The funders had no role in the study's design; in the collection, analyses, or interpretation of data; in the writing of the manuscript; or in the decision to publish the results.

References

1. Harvey, J.A.; Mullinax, J.M.; Runge, M.C.; Prosser, D.J. The Changing Dynamics of Highly Pathogenic Avian Influenza H5N1: Next Steps for Management & Science in North America. *Biol. Conserv.* **2023**, *282*, 110041. [CrossRef]
2. Ariyama, N.; Pardo-Roa, C.; Muñoz, G.; Aguayo, C.; Ávila, C.; Mathieu, C.; Brito, B.; Medina, R.; Johow, M.; Neira, V. Emergence and Rapid Dissemination of Highly Pathogenic Avian Influenza Virus H5N1 Clade 2.3.4.4b in Wild Birds, Chile. *bioRxiv* **2023**. [CrossRef]
3. Wong, J.B.; Lisovski, S.; Alisauskas, R.T.; English, W.; Giroux, M.-A.; Harrison, A.-L.; Kellett, D.; Lecomte, N.; Maftei, M.; Nagy-MacArthur, A.; et al. Arctic Terns from Circumpolar Breeding Colonies Share Common Migratory Routes. *Mar. Ecol. Prog. Ser.* **2021**, *671*, 191–206. [CrossRef]
4. Egevang, C.; Stenhouse, I.J.; Phillips, R.A.; Petersen, A.; Fox, J.W.; Silk, J.R.D. Tracking of Arctic Terns Sterna Paradisaea Reveals Longest Animal Migration. *Proc. Natl. Acad. Sci. USA* **2010**, *107*, 2078–2081. [CrossRef] [PubMed]
5. Kopp, M.; Peter, H.; Mustafa, O.; Lisovski, S.; Ritz, M.; Phillips, R.; Hahn, S. South Polar Skuas from a Single Breeding Population Overwinter in Different Oceans Though Show Similar Migration Patterns. *Mar. Ecol. Prog. Ser.* **2011**, *435*, 263–267. [CrossRef]
6. Weimerskirch, H.; Tarroux, A.; Chastel, O.; Delord, K.; Cherel, Y.; Descamps, S. Population-Specific Wintering Distributions of Adult South Polar Skuas over Three Oceans. *Mar. Ecol. Prog. Ser.* **2015**, *538*, 229–237. [CrossRef]
7. Finger, J.V.G.; Krüger, L.; Corá, D.H.; Petry, M.V. Habitat Selection of Southern Giant Petrels: Potential Environmental Monitors of the Antarctic Peninsula. *Antarct. Sci.* **2023**, *35*, 256–269. [CrossRef]
8. Delord, K.; Pinet, P.; Pinaud, D.; Barbraud, C.; De Grissac, S.; Lewden, A.; Cherel, Y.; Weimerskirch, H. Species-Specific Foraging Strategies and Segregation Mechanisms of Sympatric Antarctic Fulmarine Petrels throughout the Annual Cycle. *IBIS* **2016**, *158*, 569–586. [CrossRef]
9. Krietsch, J.; Hahn, S.; Kopp, M.; Phillips, R.; Peter, H.; Lisovski, S. Consistent Variation in Individual Migration Strategies of Brown Skuas. *Mar. Ecol. Prog. Ser.* **2017**, *578*, 213–225. [CrossRef]
10. Carneiro, A.; Manica, A.; Clay, T.; Silk, J.; King, M.; Phillips, R. Consistency in Migration Strategies and Habitat Preferences of Brown Skuas over Two Winters, a Decade Apart. *Mar. Ecol. Prog. Ser.* **2016**, *553*, 267–281. [CrossRef]
11. Ogrzewalska, M.; Couto Motta, F.; Resende, P.C.; Fumian, T.; Fonseca da Mendonça, A.C.; Appolinario Reis, L.; Lima Brandao, M.; Chame, M.; Arantes Gomes, I.L.; Mendonca Siqueira, M. Influenza A(H11N2) Virus Detection in Fecal Samples from Adélie (*Pygoscelis adeliae*) and Chinstrap (*Pygoscelis antarcticus*) Penguins, Penguin Island, Antarctica. *Microbiol. Spectr.* **2022**, *10*, e0142722. [CrossRef] [PubMed]
12. Hurt, A.C.; Su, Y.C.F.; Aban, M.; Peck, H.; Lau, H.; Baas, C.; Deng, Y.-M.; Spirason, N.; Ellström, P.; Hernandez, J.; et al. Evidence for the Introduction, Reassortment, and Persistence of Diverse Influenza A Viruses in Antarctica. *J. Virol.* **2016**, *90*, 9674–9682. [CrossRef] [PubMed]
13. Barriga, G.P.; Boric-Bargetto, D.; San Martin, M.C.; Neira, V.; van Bakel, H.; Thompsom, M.; Tapia, R.; Toro-Ascuy, D.; Moreno, L.; Vasquez, Y.; et al. Avian Influenza Virus H5 Strain with North American and Eurasian Lineage Genes in an Antarctic Penguin. *Emerg. Infect. Dis.* **2016**, *22*, 2221–2223. [CrossRef]
14. Ulloa, M.; Fernández, A.; Ariyama, N.; Colom-Rivero, A.; Rivera, C.; Nuñez, P.; Sanhueza, P.; Johow, M.; Araya, H.; Torres, J.C.; et al. Mass Mortality Event in South American Sea Lions (*Otaria flavescens*) Correlated to Highly Pathogenic Avian Influenza (HPAI) H5N1 Outbreak in Chile. *Vet. Q.* **2023**, *43*, 1–10. [CrossRef]
15. Molini, U.; Aikukutu, G.; Roux, J.-P.; Kemper, J.; Ntahonshikira, C.; Marruchella, G.; Khaiseb, S.; Cattoli, G.; Dundon, W.G. Avian Influenza H5N8 Outbreak in African Penguins (*Spheniscus demersus*), Namibia, 2019. *J. Wildl. Dis.* **2020**, *56*, 214–218. [CrossRef]
16. Pardo-Roa, C.; Nelson, M.I.; Ariyama, N.; Aguayo, C.; Almonacid, L.I.; Munoz, G.; Navarro, C.; Avila, C.; Ulloa, M.; Reyes, R.; et al. Cross-Species Transmission and PB2 Mammalian Adaptations of Highly Pathogenic Avian Influenza A/H5N1 Viruses in Chile. *bioRxiv* **2023**. [CrossRef]
17. Leguia, M.; Garcia-Glaessner, A.; Muñoz-Saavedra, B.; Juarez, D.; Barrera, P.; Calvo-Mac, C.; Jara, J.; Silva, W.; Ploog, K.; Amaro, L.; et al. Highly Pathogenic Avian Influenza A (H5N1) in Marine Mammals and Seabirds in Peru. *Nat. Commun.* **2023**, *14*, 5489. [CrossRef] [PubMed]
18. Campagna, C.; Uhart, M.; Falabella, V.; Campagna, J.; Zavattieri, V.; Vanstreels, R.E.T.; Lewis, M.N. Catastrophic Mortality of Southern Elephant Seals Caused by H5N1 Avian Influenza. *Mar. Mammal Sci.* **2024**, *40*, 322–325. [CrossRef]

19. Mena, J.; Brito, B.; Moreira, R.; Tadich, T.; González, I.; Cruces, J.; Ortega, R.; van Bakel, H.; Rathnasinghe, R.; Pizarro-Lucero, J.; et al. Reemergence of H3N8 Equine Influenza A Virus in Chile, 2018. *Transbound. Emerg. Dis.* **2018**, *65*, 1408–1415. [CrossRef]
20. Tapia, R.; García, V.; Mena, J.; Bucarey, S.; Medina, R.A.; Neira, V. Infection of Novel Reassortant H1N2 and H3N2 Swine Influenza A Viruses in the Guinea Pig Model. *Vet. Res.* **2018**, *49*, 73. [CrossRef]
21. Lisovski, S.; Günther, A.; Dewar, M.; Ainley, D.; Arce, R.; Ballard, G.; Belliure, J.; Boulinier, T.; Bennison, A.; Cary, C.; et al. No Evidence for Highly Pathogenic Avian Influenza Virus H5N1 (Clade 2.3.4.4b) in the Antarctic Region during the Austral Summer 2022/23. *bioRxiv* **2023**. [CrossRef]
22. Boulinier, T. Avian Influenza Spread and Seabird Movements between Colonies. *Trends Ecol. Evol.* **2023**, *38*, 391–395. [CrossRef]
23. European Food Safety Authority, European Centre for Disease Prevention and Control, European Union Reference Laboratory for Avian Influenza; Adlhoch, C.; Fusaro, A.; Gonzales, J.L.; Kuiken, T.; Marangon, S.; Niqueux, É.; Staubach, C.; Terregino, C.; Aznar, I.; et al. Avian Influenza Overview September–December 2022. *EFSA J.* **2023**, *21*, e07786. [CrossRef]
24. Giacinti, J.A.; Signore, A.V.; Jones, M.E.B.; Bourque, L.; Lair, S.; Jardine, C.; Stevens, B.; Bollinger, T.; Goldsmith, D.; British Columbia Wildlife AIV Surveillance Program (BC WASPs); et al. Avian Influenza Viruses in Wild Birds in Canada Following Incursions of Highly Pathogenic H5N1 Virus from Eurasia in 2021/2022. *bioRxiv* **2023**. [CrossRef]
25. Bird Flu Hits Northumberland Arctic Terns Colony. *BBC News*, 10 July 2023.
26. IA|SAG. Available online: https://websag.azurewebsites.net/ia (accessed on 18 December 2023).
27. Killian, M.L. Avian Influenza Virus Sample Types, Collection, and Handling. *Anim. Influenza Virus Methods Protoc.* **2020**, *2123*, 113–121. [CrossRef]
28. Bennison, A.; Byrne, A.M.P.; Reid, S.M.; Lynton-Jenkins, J.G.; Mollett, B.; Sliva, D.D.; Peers-Dent, J.; Finlayson, K.; Hall, R.; Blockley, F.; et al. Detection and Spread of High Pathogenicity Avian Influenza Virus H5N1 in the Antarctic Region. *bioRxiv* **2023**. [CrossRef]
29. Corá, D.H.; Finger, J.V.G.; Krüger, L. Coprophagic Behaviour of Southern Giant Petrels (*Macronectes giganteus*) during Breeding Period. *Polar Biol.* **2020**, *43*, 2111–2116. [CrossRef]
30. MAPPPD|Institute for Advanced Computational Science. Available online: https://www.stonybrook.edu/commcms/iacs/research/products/software/mapppd.php (accessed on 18 December 2023).
31. Tomás, G.; Marandino, A.; Panzera, Y.; Rodríguez, S.; Wallau, G.D.L.; Dezordi, F.; Pérez, R.; Bassetti, L.; Negro, R.; Williman, J.; et al. Highly Pathogenic Avian Influenza H5N1 Virus Infections in Pinnipeds and Seabirds in Uruguay: A Paradigm Shift to Virus Transmission in South America. *bioRxiv* **2023**. [CrossRef]
32. de Seixas, M.M.M.; de Araújo, J.; Krauss, S.; Fabrizio, T.; Walker, D.; Ometto, T.; Matsumiya Thomazelli, L.; Vanstreels, R.E.T.; Hurtado, R.F.; Krüger, L.; et al. H6N8 Avian Influenza Virus in Antarctic Seabirds Demonstrates Connectivity between South America and Antarctica. *Transbound. Emerg. Dis.* **2022**, *69*, e3436–e3446. [CrossRef]
33. Simeone, A.; Hiriart-Bertrand, L.; Reyes-Arriagada, R.; Halpern, M.; Dubach, J.; Wallace, R.; Pütz, K.; Lüthi, B. Heterospecific Pairing and Hybridization between Wild Humboldt and Magellanic Penguins in Southern Chile. *Condor* **2009**, *111*, 544–550. [CrossRef]

Disclaimer/Publisher's Note: The statements, opinions and data contained in all publications are solely those of the individual author(s) and contributor(s) and not of MDPI and/or the editor(s). MDPI and/or the editor(s) disclaim responsibility for any injury to people or property resulting from any ideas, methods, instructions or products referred to in the content.

animals

MDPI

Case Report

Ectopic Pregnancy and T-Cell Lymphoma in a Eurasian Red Squirrel (*Sciurus vulgaris*): Possible Comorbidity and a Comparative Pathology Perspective

Caterina Raso [1,*,†], Valentina Galietta [2,†], Claudia Eleni [2], Marco Innocenti [3], Niccolò Fonti [4], Tiziana Palmerini [2], Mauro Grillo [3], Pietro Calderini [1] and Elena Borgogni [1]

[1] Istituto Zooprofilattico Sperimentale del Lazio e Della Toscana "M. Aleandri", 02100 Rieti, Italy; pietro.calderini@izslt.it (P.C.); elena.borgogni@izslt.it (E.B.)
[2] Istituto Zooprofilattico Sperimentale del Lazio e Della Toscana "M. Aleandri", 00178 Roma, Italy; valentina.galietta@izslt.it (V.G.); claudia.eleni@izslt.it (C.E.); tiziana.palmerini@izslt.it (T.P.)
[3] UOC Igiene e Sanità Animale, ASL Rieti, 02100 Rieti, Italy; m.innocenti@asl.rieti.it (M.I.); m.grillo@asl.rieti.it (M.G.)
[4] Dipartimento di Scienze Veterinarie, Università di Pisa, Viale delle Piagge, 56124 Pisa, Italy; niccolo.fonti@phd.unipi.it
* Correspondence: caterina.raso@izslt.it
† These authors contributed equally to this work.

Simple Summary: *Sciurus vulgaris*, commonly known as the Eurasian red squirrel, is a wild rodent species widely distributed throughout Europe and currently classified as "least concern" by the International Union for Conservation of Nature (IUCN). Despite its conservation status, several threats, such as infectious diseases, habitat fragmentation and the introduction of the alien invasive species grey squirrel (*Sciurus carolinensis)*, could affect *S. vulgaris* populations. Ectopic pregnancy is a condition consisting of a pregnancy developing outside the uterus. Tumors affecting the reproductive tract are known to predispose to this condition. In this paper, we describe for the first time a case of lymphoma leading to an ectopic pregnancy in a Eurasian red squirrel. A deeper knowledge of the pathology of this species is important for estimating the impact of diseases on the *S. vulgaris* population. Moreover, wildlife can be a sentinel for pathologies that have environmental causes and that could affect other animals and humans that share the same environment. Thus, deeper knowledge of wildlife cancer incidence and the environmental and individual causes of cancer development is relevant from a comparative pathology perspective.

Abstract: Ectopic pregnancy (EP) is a life-threatening disease that affects humans and other mammals. Tumors causing ruptures of the reproductive tract have been identified as possible predisposing factors in human and veterinary medicine. We here describe a case of concomitant ectopic pregnancy and lymphoma in a Eurasian red squirrel found deceased in Italy and submitted to the public health laboratory Istituto Zooprofilattico Sperimentale del Lazio e della Toscana (IZSLT) for post-mortem examination. A full-term partially mummified ectopic fetus in the abdomen and a large fibrinonecrotic tubal scar adjacent to the right ovary were observed at necropsy. The tubal scar is likely the point of tubal rupture through which the fetus displaced. Histology revealed the presence of neoplastic cells referable to lymphoma infiltrating the ovary, spleen, small intestine, heart and peripancreatic adipose tissue. The lymphoma was further characterized as T-cell-type using immunohistochemistry. We suggest that the lymphoma, by involving the ovary, played a pathogenetic role in the development of a secondary EP by altering the genital tract at the structural and hormonal levels. To the best of our knowledge, this is the first report of concomitant ovarian lymphoma and EP in animals and humans in the literature.

Keywords: *Sciurus vulgaris*; ectopic pregnancy; T-cell lymphoma

1. Introduction

The Eurasian red squirrel *(Sciurus vulgaris)* is a rodent species with a large geographic and habitat range, which includes forests and urban environments from Europe to Asia. According to the International Union for Conservation of Nature (IUCN) [1], *S. vulgaris* falls under the Least Concern (LC) category. Despite its wide geographical distribution, several threats could impair its conservation status, such as emerging infectious diseases, habitat fragmentation and the introduction of the alien invasive eastern grey squirrel species (*Sciurus carolinensis)*, an important competitor for food and habitat [1]. Eurasian red squirrel offspring are born in February–April and May–August, with one to six individuals per litter [1,2] after a mean gestation length of 37.44 days [3]. Sciuridae have a hemochorial discoid placenta, similar to other rodents and primates, and a duplex uterus [4,5].

We here describe a case of concomitant occurrence of ectopic pregnancy (EP) and T-cell lymphoma in a Eurasian red squirrel found deceased in Italy. EP is a well-known life-threatening disease that affects humans and, although less frequently, other mammals [6]. It has been described in domestic [7–9], laboratory [10–13] and wild animals [14–16]. Two main EP types are recognized, tubal and abdominal pregnancy, depending on whether the gestation develops in the fallopian tubes or in the abdominal cavity, respectively. The etiopathogenesis of EP in animals has not been completely clarified. Several predisposing factors have been identified, including iatrogenic factors and surgical procedures [9,11,17], hormonal factors altering the normal ovum transport and implantation [6] and tumors and other spontaneous reproductive pathologies causing ruptures of the reproductive tract [15,18–21].

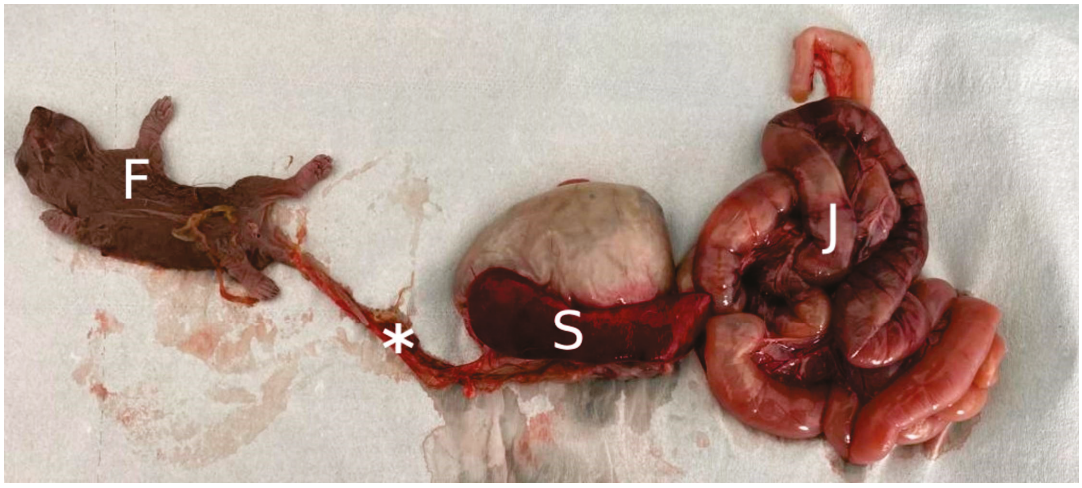
Lymphoma comprises a diverse group of hematopoietic malignancies that arise from the clonal proliferation of lymphocytes not only in the hematolymphoid system but also in extranodal sites [22]. It is one of the most frequent tumors in domestic animals [22,23] and laboratory rodents [24]. Several causes, such as individual factors, retroviruses, chemicals and irradiation, are involved in the etiology of lymphoma in rodents [24]. Oncogenesis results from the interplay between endogenous and exogenous genomic stressors: chronic inflammation, immune system, variation in cell biology between species and individuals, pathogen infection and environmental pollutants [25,26]. In veterinary medicine, most epitheliotropic lymphomas in the skin and the small intestine have a T-cell origin [23]. Moreover, most of the retrovirus-associated lymphomas of cats, mice and humans in the literature display a T-cell immunophenotype [23,24]. T-cell lymphoma has also been experimentally induced in genetically engineered mice using chemicals [24]. There are descriptions of multicentric and epitheliotropic lymphoma in red squirrels in the literature [27,28] and one record of a suspected EP [14], but no cases of concomitant ectopic pregnancy and lymphoma have been described, neither in *S. vulgaris* nor in other species or humans in the literature. This case report aims to unravel the possible comorbidity between the two conditions.

2. Materials and Methods

On 3 April 2023, an adult, female, free-ranging Eurasian red squirrel was found dead in Italy (42.41273700, 12.88127000) by the veterinary officers of the local health authority ASL of Rieti (Latium region, Central Italy). The day after its retrieval, the carcass was submitted to the territorial division of the public health laboratory Istituto Zooprofilattico Sperimentale del Lazio e della Toscana and underwent post-mortem examination. The body condition was estimated according to the score proposed by Ullman-Culleré and Folz for laboratory mice [29]. Samples of the ovaries, uterus, lung, heart, liver, spleen, kidney, intestine, pancreas and all the fetal organs were collected during the necropsy, fixed in 10% buffered formalin and routinely processed for histopathological examination. To further characterize the neoplasm, immunohistochemistry with polyclonal rabbit anti-human CD3 (Dako) and polyclonal rabbit anti-human CD20 (Thermo Fisher Scientific, Waltham, MA, USA) was performed on unstained sections of the affected organs using the labeled streptavidin–biotin (LSAB) peroxidase method.

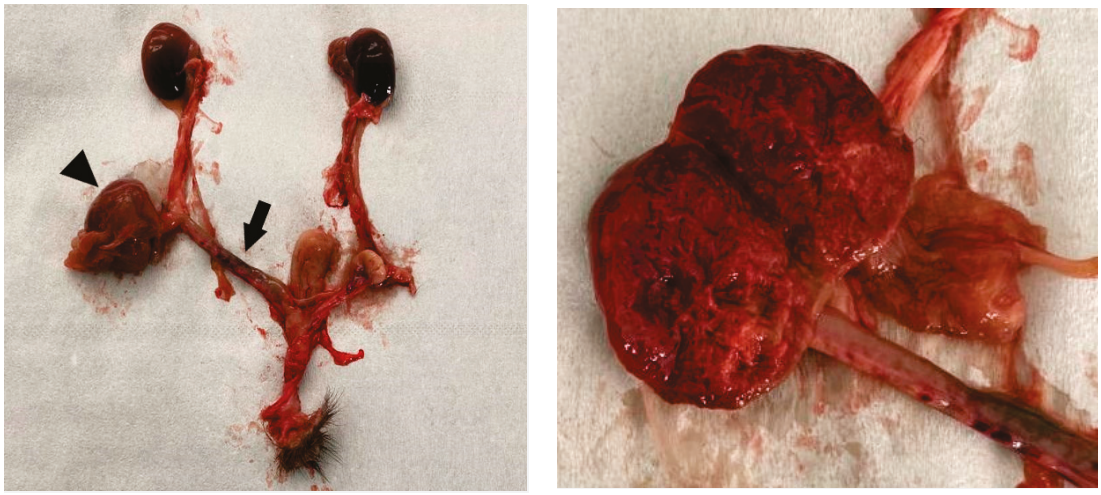
3. Results

The animal was in suboptimal body condition (BCS 2/5 [29]). Necropsy revealed the presence of a full-term fetus in the abdominal cavity. It measured 5 cm in crown–rump length, was early mummified, covered in a thin smooth yellow-grey serosal membrane, enveloped in the peritoneum and connected to the omentum through a thin fibrovascular band (Figure 1a). The fetal organs were almost fully developed, consistent with a late gestational stage, appeared autolytic and did not show macroscopically evident pathological findings. Gross examination of the adult squirrel's reproductive tract revealed moderate hyperemia of the right uterine horn wall and the presence of a soft reddish spherical mass measuring 1.5 cm, topographically adjacent to the right ovary and involving the tubal infundibulum wall (Figure 1b,c). A viable placenta was not present, neither enveloping the abdominal fetus nor in the uterus. Severe diffuse splenomegaly was observed, with symmetric enlargement and rounded edges of the organ. Other gross pathologic findings were severe segmental thickening of the jejunal wall, moderate diffuse catarrhal enteritis and enterocolitis and severe hyperemia of the corresponding serosa. Microscopically, a dense, not delimited, non-capsulated, infiltrative, round cell neoplasm referable to lymphoma was observed in the right ovary (Figure 2a), spleen (Figure S1) and small intestine (Figure 2b). Neoplastic cells were also visible in the peripancreatic adipose tissue (Figure S2) and in the small lymphatic vessels of the heart (Figure S3). Lymphoid cells had a nest-like arrangement in the ovarian parenchyma, while they diffusely infiltrated the other affected tissues. They were round to oval, with scant weakly basophilic cytoplasm. Nuclei were round to rarely indented, measured 1.5–2 times the volume of a red blood cell and showed peripheralized chromatin and one prominent basophilic nucleolus. Cellular pleomorphism was moderate, and the mitotic count ranged from two to four in 2.37 mm^2. Neoplastic cells stained positive for CD3 and negative for CD20 at the IHC, consistent with T-cell lymphoma (Figure 2c). Scattered lymphocytes expressing CD20 (B-cells) were present and attributed to secondary inflammation (Figure 2d). The periovarian spherical lesion was composed of fibrin, necrosis and erythrocytes and was consistent with a scar at the tubal level. Histologically, the fetal organs were altered by autolytic changes referable to mummification, thus preventing a thorough microscopic evaluation of the fetus.



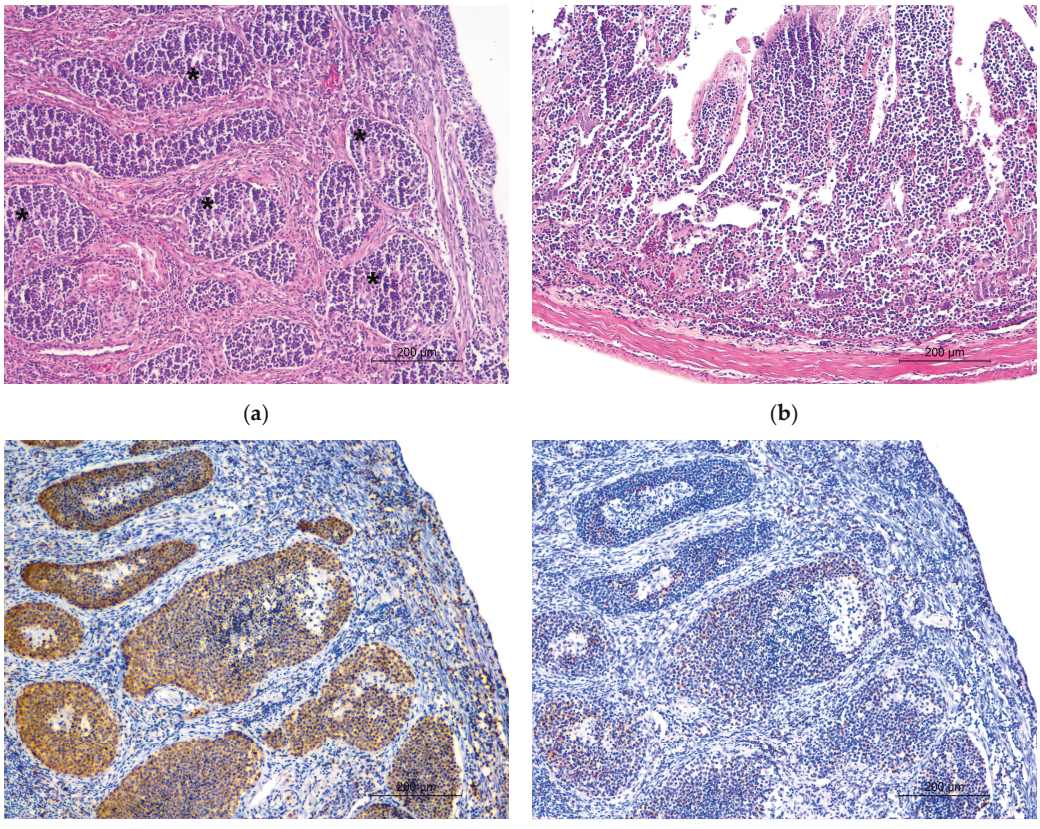
(**a**)

Figure 1. *Cont.*



(**b**) (**c**)

Figure 1. Gross findings at necropsy: (**a**) a thin fibrovascular cord (asterisk) connecting the full-term fetus (F) to the omentum; evident splenomegaly (S) and segmental enteropathy of the jejunum (J). (**b**) Genitourinary tract, gross: round lesion (black arrowhead) of 1.5 cm in diameter adjacent to the right ovary and hyperemia of the right uterine horn (black arrow). (**c**) Fibrin and necrotic-hemorrhagic tissue were evident on the cross-section of the periovarian tubal lesion.



(**a**) (**b**)

(**c**) (**d**)

Figure 2. Histological appearance of lymphoma in hematoxylin and eosin-stained sections: (**a**) neoplastic cells are arranged in irregular nest-like structures in the ovary (asterisk) and (**b**) diffusely infiltrate the lamina propria of the jejunum. Immunohistochemistry, ovary: neoplastic cells stain (**c**) positive (brown color) for CD3 and (**d**) negative for CD20 markers. (**d**) Scattered cells staining positive for CD20 are referable to inflammatory lymphocytes.

4. Discussion

The EP described in this case is referable to an abdominal pregnancy, similar to most of the diagnosed spontaneous ectopic pregnancies of mammals other than primates reported in the literature [6,8,10,12,13,16]. Based on the pathogenesis, abdominal pregnancy may be further subdivided into primary and secondary subtypes. In the primary subtype, fertilization or the first implantation of a fertilized oocyte occurs in the abdominal cavity, with placentation developing either on a peritoneal or an omental surface. In the secondary subtype, the fetus is expelled into the peritoneal cavity after implantation, following a rupture of the oviduct or uterus [6]. We can only hypothesize the underlying pathogenesis of the specific case reported in this paper. The ovarian neoplastic lesion altered the tubal structure at the periovarian level, predisposing to a rupture, followed by the displacement of the developing fetus from the gravid uterine horn to the abdominal cavity. Moreover, the ovarian neoplasm, by infiltrating the functional ovarian tissue, may have impaired the hormonal function and altered tubal motility, thus concurring the EP development [6,30]. Thus, our hypothesis is consistent with a secondary EP subtype: the fibrinonecrotic scar was likely the point of tubal rupture, and the ovarian lymphoma played a role in the development of the EP. Complete reimplantation of the placenta in the abdominal cavity or an internal abortion may occur following the loss of placental attachment caused by fetal escape into the abdominal cavity. We could not evaluate placental features as a viable placenta was not observable in our case, consistent with most of the records on abdominal pregnancy [6].

Although several cases of concomitant genital tract neoplasia and ectopic pregnancy have been described in human [18–21] and veterinary medicine [15], to our knowledge, no cases of concomitant lymphoma and ectopic pregnancy have been reported so far. The neoplasia described in this paper is a T-cell lymphoma involving the ovary, spleen, intestine, heart and peripancreatic tissue. In the literature, one case of multicentric lymphoma was recorded but not immunophenotyped [27], whereas one case of epitheliotropic lymphoma was characterized as T-cell in Eurasian red squirrels [28]. In our case, it was not possible to assess whether the lymphoma's primary site was the spleen, the jejunal Peyer plaques or the ovary or if it arose as a multicentric form.

Lymphomas are known to affect the ovarian tissue of domestic [31] and laboratory animals [32]. As in our case, ovarian lymphoma does not usually cause evident ovarian enlargement [33]. In cattle and humans, neoplastic foci were observed to develop within the corpora lutea [31,34], probably from the lymphocytes that physiologically surround the corpus luteum [33]. This pathogenetic process cannot be excluded in our case since a pregnancy corpus luteum was present and was infiltrated by the neoplastic cells. During pregnancy, lymphoma usually displays placental metastasis, leading to pregnancy complications and stillborn fetuses [35], but the absence of the placenta and fetal mummification prevented the evaluation of possible placental and fetal metastasis in this report.

Most of the oncogenetic mechanisms leading to the development of lymphoma are still unclear and hard to assess [23]. Interestingly, retroviruses are a possible cause of T-cell lymphoma in rodents [24]. We did not perform tests to exclude retroviruses in the reported case, but the possible correlation between retrovirus and lymphoma deserves further attention.

Examining tumors in several animal species sharing the same environment, including wildlife, can reveal species-specific mechanisms of cancer formation and cancer resistance and different responses to the same environmental stressors in different species [25,26]. Thus, synanthropic wildlife within a particular ecosystem can potentially play the role of both sentinels of environmental carcinogens and models of cancer development [26].

Knowledge of the health status of the majority of wildlife species is limited in most European countries [36]. As cancer in wildlife is mostly diagnosed by necropsy [37], the setup of networks for the detection of carcasses and systematic post-mortem examination of free-ranging species is crucial for understanding the impact of diseases, including cancer, and must be considered as a pillar in wildlife health surveillance programs.

5. Conclusions

To the best of our knowledge, this is the first reported case of concomitant lymphoma and secondary abdominal pregnancy. Our findings suggest that the ovarian lymphoma played a role in the development of the EP by altering the structure of the genital tract. By involving and altering the ovarian parenchyma, we suggest that the tumor could have also impaired the hormonal function of the corpus luteum in the maintenance of pregnancy, although this could not be confirmed by serial hormonal assays in the alive animal. Little is known about Eurasian red squirrel reproductive pathology and oncology, despite its affinity with other better-known rodents. Further studies are needed to estimate the incidence of lymphoma in red squirrels, concomitance with ectopic pregnancy and factors involved in tumorigenesis. A deeper knowledge of ecopathology is crucial for understanding the real impact of diseases on wildlife species from a conservation medicine perspective. Moreover, further studies are needed to clarify the environmental drivers of oncogenesis in the Eurasian red squirrel and other free-ranging wild species. The development of wildlife cancer registries and integration with other human and animal information systems would expand our knowledge on tumorigenesis and eventually help in identifying possible sentinels for environmental risk factors from a One Health perspective.

Supplementary Materials: The following supporting information can be downloaded at: https://www.mdpi.com/article/10.3390/ani14050731/s1, Figure S1: Lymphoma in the spleen; Figure S2: Neoplastic cells in the peripancreatic adipose tissue; Figure S3: Neoplastic cells in the small lymphatic vessels of the heart.

Author Contributions: Conceptualization, C.R., E.B. and M.I.; methodology, C.R., V.G. and C.E.; validation, C.R., V.G., C.E., M.I., N.F., T.P., M.G., P.C. and E.B.; formal analysis, C.R. and V.G.; investigation, C.R., V.G., C.E. and E.B.; resources, P.C. and C.E.; data curation, C.R., V.G., E.B. and T.P.; writing—original draft preparation, C.R. and V.G.; writing—review and editing, C.R., V.G., C.E., M.I., N.F. and E.B.; visualization, C.R. and V.G.; supervision, P.C., C.E. and M.G. All authors have read and agreed to the published version of the manuscript.

Funding: This research received no external funding.

Institutional Review Board Statement: This study did not require ethical approval.

Informed Consent Statement: Not applicable.

Data Availability Statement: The original contributions presented in this study are included in this article/Supplementary Materials. Further inquiries can be directed to the corresponding author.

Acknowledgments: The authors would like to thank Francesca Millanta for her scientific and technical support of this paper.

Conflicts of Interest: The authors declare no conflict of interest.

References

1. The IUCN Red List of Threatened Species. Available online: https://www.iucnredlist.org/species/221730864/221731049 (accessed on 24 December 2023).
2. Mari, V.; Martini, S.; Romeo, C.; Molinari, A.; Martinoli, A.; Tosi, G.; Wauters, L. Record litter size in the Eurasian Red Squirrel (*Sciurus vulgaris*). *Hystrix* **2008**, *19*, 62–65. [CrossRef]
3. Hayssen, V. Reproductive Effort in Squirrels: Ecological, Phylogenetic, Allometric, and Latitudinal Patterns. *J. Mammal.* **2008**, *89*, 582–606. [CrossRef]
4. Carter, A.M.; Enders, A.C. Placentation in mammals: Definitive placenta, yolk sac, and paraplacenta. *Theriogenology* **2016**, *86*, 278–287. [CrossRef] [PubMed]
5. Maranesi, M.; Bufalari, A.; Dall'Aglio, C.; Paoloni, D.; Moretti, G.; Crotti, S.; Manuali, E.; Stazi, M.; Bergamasco, F.; Cruciani, D.; et al. Reproductive Traits of an Invasive Alien Population of Grey Squirrel (*Sciurus carolinensis*) in Central Italy. *Animals* **2020**, *10*, 738. [CrossRef] [PubMed]
6. Corpa, J.M. Ectopic pregnancy in animals and humans. *Reproduction* **2006**, *131*, 631–640. [CrossRef]
7. Eddey, P.D. Ectopic pregnancy in an apparently healthy bitch. *J. Am. Anim. Hosp. Assoc.* **2012**, *48*, 194–197. [CrossRef] [PubMed]

8. Segura Gil, P.; Peris Palau, B.; Martínez Martínez, J.; Ortega Porcel, J.; Corpa Arenas, J.M. Abdominal pregnancies in farm rabbits. *Theriogenology* **2004**, *62*, 642–651. [CrossRef] [PubMed]
9. Rosset, E.; Galet, C.; Buff, S. A case report of an ectopic fetus in a cat. *J. Feline Med. Surg.* **2011**, *13*, 610–613. [CrossRef] [PubMed]
10. Tena-Betancourt, E.; Tena-Betancourt, C.A.; Zúniga-Muñoz, A.M.; Hernández-Godínez, B.; Ibáñez-Contreras, A.; Graullera-Rivera, V. Multiple extrauterine pregnancy with early and near full-term mummified fetuses in a New Zealand white rabbit (*Oryctolagus cuniculus*). *J. Am. Assoc. Lab. Anim. Sci.* **2014**, *53*, 204–207.
11. Brozos, C.; Karagiannis, I.; Kiossis, E.; Giadinis, N.D.; Boscos, C. Ectopic pregnancy through a caesarean scar in a ewe. *N. Z. Vet. J.* **2013**, *61*, 373–375. [CrossRef]
12. Gosden, R.G.; Russell, J.A. Spontaneous abdominal implantation in the rat with development to full term. *Lab. Anim.* **1981**, *15*, 379–380. [CrossRef] [PubMed]
13. Buckley, P.; Caine, A. A high incidence of abdominal pregnancy in the Djungarian hamster (*Phodopus sungorus*). *Reproduction* **1979**, *56*, 679–682. [CrossRef] [PubMed]
14. Simpson, V.R.; Hargreaves, J.; Butler, H.M.; Davison, N.J.; Everest, D.J. Causes of mortality and pathological lesions observed post-mortem in red squirrels (*Sciurus vulgaris*) in Great Britain. *BMC Vet. Res.* **2013**, *9*, 229. [CrossRef]
15. Fravel, V.A.; Lowenstine, L.J.; Koehne, A. Ectopic pregnancy with associated gestational choriocarcinoma in a California sea lion (Zalophus californianus). *Dis. Aquat. Org.* **2016**, *120*, 159–164. [CrossRef] [PubMed]
16. Hughes, K. Abdominal ectopic pregnancy and impaired postnatal mammary gland development, consistent with physiologic agalactia, in a wild European rabbit, Oryctolagus cuniculus. *Front. Vet. Sci.* **2019**, *6*, 254. [CrossRef]
17. Fylstra, D.L. Ectopic pregnancy after hysterectomy: A review and insight into etiology and prevention. *Fertil Steril.* **2010**, *94*, 431–435. [CrossRef]
18. Johnson, N.; Gist, W.; Akinlaja, O.; Gist, B. Bilateral ovarian teratomas with concurrent ectopic pregnancy at diagnostic laparoscopy. *Austin J. Womens Health* **2014**, *1*, 2. [CrossRef]
19. Liang, Y.F.; Zeng, J.C.; Ruan, J.B.; Kang, D.P.; Wang, L.M.; Chen, C.; Xu, J.F. Ovarian sclerosing stromal tumor in a young woman with ectopic pregnancy: Clinical, pathological, and immunohistochemical studies. *Int. J. Clin. Exp. Pathol.* **2014**, *7*, 456–459.
20. Inoue, T.; Nabeshima, K.; Shimao, Y.; Akiyama, Y.; Ohtsuka, T.; Koono, M. Tubal ectopic pregnancy associated with an adenomatoid tumor. *Pathol. Int.* **2001**, *51*, 211–214. [CrossRef]
21. Stewart, L.M.; Stewart, C.J.R.; Spilsbury, K.; Cohen, P.A.; Jordan, S. Association between pelvic inflammatory disease, infertility, ectopic pregnancy and the development of ovarian serous borderline tumor, mucinous borderline tumor and low-grade serous carcinoma. *Gynecol. Oncol.* **2020**, *156*, 611–615. [CrossRef]
22. Vail, D.M.; Thamm, D.H.; Liptak, J.M. Hematopoietic Tumors. In *Withrow and MacEwen's Small Animal Clinical Oncology*, 6th ed.; Published online; Elsevier Health Sciences: Amsterdam, The Netherlands, 2019; pp. 688–772.
23. Valli, V.E.O.; Kiupel, M.; Bienzle, D.; Wood, R.D. Hematopoietic system. In *Jubb, Kennedy, and Palmer's Pathology of Domestic Animals*, 6th ed.; W.B. Saunders: Philadelphia, PA, USA, 2016; Volume 3, pp. 102–268.
24. Ward, J.M. Lymphomas and leukemias in mice. *Exp. Toxicol. Pathol.* **2006**, *57*, 377–381. [CrossRef]
25. Seluanov, A.; Gladyshev, V.N.; Vijg, J.; Gorbunova, V. Mechanisms of cancer resistance in long-lived mammals. *Nat. Rev. Cancer* **2018**, *18*, 433–441. [CrossRef]
26. Pesavento, P.A.; Agnew, D.; Keel, M.K.; Woolard, K.D. Cancer in wildlife: Patterns of emergence. *Nat. Rev. Cancer* **2018**, *18*, 646–661. [CrossRef]
27. LaRose, J.P.; Meredith, A.L.; Everest, D.J.; Fiegna, C.; McInnes, C.J.; Shaw, D.J.; Milne, E.M. Epidemiological and postmortem findings in 262 red squirrels (*Sciurus vulgaris*) in Scotland, 2005 to 2009. *Vet. Rec.* **2010**, *167*, 297–302. [CrossRef] [PubMed]
28. Honnold, S.P.; Arun, I.; Saturday, G.; McLeod, C. Epitheliotropic lymphoma in a squirrel (*Sciurus* sp.). *J. Zoo Wildl. Med.* **2007**, *38*, 479–482. [CrossRef] [PubMed]
29. Ullman-Culleré, M.H.; Foltz, C.J. Body condition scoring: A rapid and accurate method for assessing health status in mice. *Comp. Med.* **1999**, *49*, 319–323.
30. Dialani, V.; Levine, D. Ectopic pregnancy: A review. *Ultrasound Q.* **2004**, *20*, 105–117. [CrossRef] [PubMed]
31. Schlafer, D.H.; Foster, R.A. Female Genital System. In *Jubb, Kennedy, and Palmer's Pathology of Domestic Animals*, 6th ed.; W.B. Saunders: Philadelphia, PA, USA, 2016; Volume 3, pp. 358–464.e1.
32. Willard-Mack, C.L.; Elmore, S.A.; Hall, W.C.; Harleman, J.; Kuper, C.F.; Losco, P.; Rehg, J.E.; Rühl-Fehlert, C.; Ward, J.M.; Weinstock, D.; et al. Nonproliferative and Proliferative Lesions of the Rat and Mouse Hematolymphoid System. *Toxicol. Pathol.* **2019**, *47*, 665–783. [CrossRef]
33. Monterroso, V.; Jaffe, E.S.; Merino, M.J.; Medeiros, L.J. Malignant lymphomas involving the ovary. A clinicopathologic analysis of 39 cases. *Am. J. Surg. Pathol.* **1993**, *17*, 154–170. [CrossRef] [PubMed]
34. Rajendran, T.; Kini, J.R.; Prasad, K. Primary Ovarian Non-Hodgkin's Lymphoma: An 18-year Retrospective Institutional Study and Review of Literature from India. *Cureus* **2023**, *15*, e40685. [CrossRef]
35. Masalunga, M.C.; Basa, R.L.; Damian, K.B.; Carnate, J.M. Metastatic Lymphomas of the Placenta: A Literature Review with an Illustrative Case. *Pediatr. Dev. Pathol.* **2023**, *27*, 67–76. [CrossRef] [PubMed]

36. Lawson, B.; Neimanis, A.; Lavazza, A.; López-Olvera, J.R.; Tavernier, P.; Billinis, C.; Duff, J.P.; Mladenov, D.T.; Rijks, J.M.; Savić, S.; et al. How to Start Up a National Wildlife Health Surveillance Programme. *Animals* **2021**, *11*, 2543. [CrossRef] [PubMed]
37. McAloose, D.; Newton, A. Wildlife cancer: A conservation perspective. *Nat. Rev. Cancer* **2009**, *9*, 517–526. [CrossRef] [PubMed]

Disclaimer/Publisher's Note: The statements, opinions and data contained in all publications are solely those of the individual author(s) and contributor(s) and not of MDPI and/or the editor(s). MDPI and/or the editor(s) disclaim responsibility for any injury to people or property resulting from any ideas, methods, instructions or products referred to in the content.

animals

MDPI

Article

Tumor and Tumor-like Lesions in Red Foxes (*Vulpes vulpes*) from Croatia

Šimun Naletilić [1], Ivan-Conrado Šoštarić-Zuckermann [2,*] and Željko Mihaljević [1]

[1] Croatian Veterinary Institute, Savska Cesta 143, 10000 Zagreb, Croatia; naletilic@veinst.hr (Š.N.); miha@veinst.hr (Ž.M.)
[2] Faculty of Veterinary Medicine, University of Zagreb, Heinzelova 55, 10000 Zagreb, Croatia
* Correspondence: isostaric@vef.unizg.hr

Simple Summary: The red fox (*Vulpes vulpes*), a member of the Canidae family, is found on all continents except Antarctica. In Croatia, red foxes are indigenous wild species that inhabit both the coastal and continental regions of the country. Neoplastic diseases are the leading cause of mortality in pet dogs, but wild members of the Canidae family can also develop tumors. Tumors in non-domestic canids are scarce; however, the true prevalence and diversity of these tumors are likely underestimated due to limited research. So far, only a limited number of tumors have been observed among the red fox population, either in their natural habitat or in captivity. The lack of wide-scale research on the incidence of neoplasia in the population of wild carnivora species in Croatia underscores the need for further investigation to enhance our understanding of tumors in foxes. In this study, conducted on a sample of 1890 red foxes, five tumor or tumor-like lesions were identified. These included two Meibomian gland adenomas, two collagenous hamartomas, and one teratoma. This research is the first of this kind in Croatia, shedding light on the occurrence and types of tumors in the red fox population.

Abstract: The red fox, found on all continents except Antarctica, occupies diverse habitats. In Croatia, it is an indigenous wild species with a population density of 0.7 animals per square kilometer. While tumors in wild animals from the Canidae family are scarce, the true prevalence and diversity of tumors are likely underestimated due to limited research. So far, a limited number of tumors have been observed among the red fox population, either in their natural habitat or in captivity. As part of the National Rabies Control Program, we examined 1890 red fox carcasses over a four-year period. Our focus was on identifying abnormalities on the skin and internal organs that suggest potential neoplastic proliferation. Five red foxes, three males and two females, were found to have growths resembling potential tumors. Their age distribution spanned from 2 to 7 years. Microscopic investigation revealed two collagenous hamartomas, two Meibomian gland adenomas, and one intra-abdominal teratoma within a cryptorchid testis. This retrospective study aims to provide a comprehensive description of tumor and tumor-like lesions observed in free-range red foxes from Croatia, marking the first research of its kind in Croatia.

Keywords: red fox; *Vulpes vulpes*; tumor; tumor-like lesion; Croatia

1. Introduction

The Canidae family comprises approximately 35 species, including the red fox (*Vulpes vulpes*), which is considered to be the most geographically widespread member of this family [1,2]. They are found on all continents except Antarctica and occupy diverse habitats, including urban areas and natural habitats, owing to their remarkable ability to adapt to various environments and food resources [2,3]. Red foxes in Croatia are considered indigenous wild species, with a population density estimated at 0.7 animals per square kilometer [4]. They are found in a wide range of habitats, including coastal and continental

areas, and are known to inhabit urban areas as well [3,4]. Due to their proximity to humans and domestic animals, such as dogs, they can potentially act as reservoirs for infectious and zoonotic agents [5]. Orphanhood is the most common cause of death in young foxes, while other categories of foxes most frequently die as a result of trauma or mange [6,7]. While these factors contribute to the mortality of different age categories of foxes, it is noteworthy that neoplastic diseases emerge as the primary cause of death in dogs in developed countries [8]. Considering these factors, especially given the shared family classification of foxes and dogs, it is useful to investigate the prevalence of tumors in the red fox population. The occurrence of neoplastic disease in wildlife has been observed to lead to substantial rates of morbidity and mortality [9]. Within nature, a small number of neoplasms occur that specifically target certain species of wild animals, thereby having a significant influence on the species' overall survival. One example is the devil facial tumor disease, a highly aggressive, transmissible, and inevitably lethal cancer that affects Tasmanian devils (*Sarcophilus harrisii*), resulting in an alarming 80 percent decline in their population [10,11]. Devil facial tumor disease is a naturally transmitted tumor that is spread through bites. It primarily affects the facial region and commonly metastasizes to nearby lymph nodes, lungs, and kidneys [11]. The second tumor that affects a significant portion of the fox population is adenocarcinoma of the ceruminous glands in the ear of endangered foxes (*Urocyon littoralis catalinae*) on Santa Catalina Island. This tumor affects approximately 48.9 to 52.2 percent of the fox population on the island. Its occurrence is linked to a chronic and long-term infection with ear mites, which leads to an extremely severe inflammatory reaction and hyperplasia in response to these mites [12]. The prevalence of cancer in captive animals has been noted to be greater in comparison to their counterparts in the wild [13]. The extended lifespan of captive animals can be attributed to improved veterinary management and care [13]. Tumors occurring in non-domestic canids are scarce, and the true prevalence and diversity of tumors are likely underestimated due to limited research [1]. It is generally accepted that the spectrum of tumor types seen in domestic dogs may also be present in wild species [1]. So far, only a limited number of neoplasms have been observed among the red fox population, both in their natural habitat and in captive settings, and there is a dearth of information regarding the prevalence of these tumors within this particular wild species. The majority of the documented cases consist of isolated reports of incidentally discovered tumors, with only a rare instance of their inclusion in comprehensive systematic investigations. Within 873 examined red foxes from Denmark, authors found only one tumor, which was apparently an insulin-producing islet cell tumor [14]. No instances of neoplasms were detected in a study conducted on a population of 530 red foxes in Germany [15]. A study conducted in Austria in 1999 identified the presence of mammary adenocarcinoma in a female red fox [15]. A publication in Italy documented a case of renal cell carcinoma in a red fox [16]. The occurrence of thyroid C-cell carcinoma with amyloid was documented in a 15-year-old red fox bred at Akita Ohmoriyama Zoo [17]. Individual case reports described the occurrence of adenosquamous carcinoma [18], seminoma, teratoma [19], and a lipoma [20]. There are also reported cases of tumors in the fennec fox (*Vulpes zerda*) and swift fox (*Vulpes velox*) that belong to the genus *Vulpes*. The fennec fox population has a significant incidence of hepatocellular carcinoma [21]. Furthermore, individual cases of tumors in the fennec fox have been documented, such as oral melanoma, thyroid gland adenoma [22], and nephroblastoma [23]. In addition, a single case of intestinal adenocarcinoma in a swift fox was also documented [24]. There is a lack of comparable research on the population of wild carnivora species in Croatia, but there have been two retrospective studies on the incidence of canine tumors in the dog population of Croatia. In the first study, an estimation of tumor prevalence was conducted in the overall canine population. The findings revealed that most of the tumors were malignant, with the primary sites of origin being the skin and subcutaneous tissues. This was followed by tumors originating from the mammary glands and the genital region. The prevailing tumor types identified in the study were mammary tubulopapillary carcinoma, mast cell tumor, and fibrosarcoma [25]. The second

study exclusively examined tumors found in indigenous Croatian dog breeds. The findings indicate that a majority of these tumors were malignant, with a higher prevalence observed in the skin, mammary glands, and hemolymphatic system [26].

Taking into consideration the aforementioned observations, the objective of this retrospective study is to provide a comprehensive description of tumor and tumor-like lesions observed in free-range red foxes from the central region of Croatia. This research, being the first of its kind conducted in Croatia and in this part of Europe, aims to enhance our understanding of tumor prevalence in wildlife and contribute valuable insights for conservation strategies.

2. Materials and Methods

A systematic examination was conducted on red fox (*Vulpes vulpes*) carcasses submitted to the Laboratory for Pathology at the Croatian Veterinary Institute in Zagreb over a four-year period, spanning from June 2019 to June 2023. These carcasses were obtained as part of the rabies control program mandated by the Croatian Ministry of Agriculture, Veterinary, and Food Safety Directorate. A methodical and thorough protocol was followed during the necropsy of all submitted carcasses. This protocol included a thorough examination of the skin and its formations, the external genitalia, the mucous membranes, and a systematic examination of the internal organs, beginning with the oral cavity and continuing through the neck, chest, abdominal cavity, and head. During the examination of deceased red fox specimens, special emphasis was placed on the detection of potential tumors. Based on the visual characteristics and growth patterns, these abnormalities were classified as tumors and tumor-like or nontumorous. All these tumor or tumor-like lesions were meticulously documented through photography and subsequently completely extracted and placed in adequate containers for fixation solution in 10% neutral formalin for a period of 24 to 48 h. A standard protocol for routine histology was followed, including dehydration, embedding in paraffin blocks, and cutting serial 4 μm thick slices. The sections were stained with hematoxylin and eosin and prepared for examination under a microscope.

Additionally, the sex of each fox with a tumor or tumor-like lesion was noted, and the age of each delivered fox was estimated using the teeth, following a previously established protocol [27].

Using an Axio Imager.A2 microscope (Zeiss, Oberkochen, Germany), all histology slides were examined, and images were captured with a Digicyte BigEye microscope camera.

3. Results

A total of 1890 fox carcasses were examined between June 2019 and June 2023 as part of the Croatian Ministry of Agriculture, Veterinary and Food Safety Directorate's rabies control program. There were eleven counties from which red foxes originated: Krapina-Zagorje, Varaždin, Međimurje, Karlovac, Lika-Senj, Sisak-Moslavina, Bjelovar-Bilogora, Brod-Posavina, Požega-Slavonia, and Dubrovnik-Neretva. Of all the foxes examined, 64% were killed during the legal hunt. In 32% of the foxes, trauma from a motor vehicle collision was the second cause of death. During the necropsy of only 4% of dead foxes discovered in public areas, it was found that the pathological alterations corresponded to infectious or parasitic diseases (Figure 1).

Following a thorough examination as outlined in the materials and methods, tumor or tumor-like lesions were found in five foxes (0.2645%; CI 0.08595–0.61628). Only five red fox carcasses out of the total number of foxes examined had growths that were classified as tumors or tumor-like (Table 1). All foxes with detected tumors or tumor-like lesions were killed during the legal hunt.

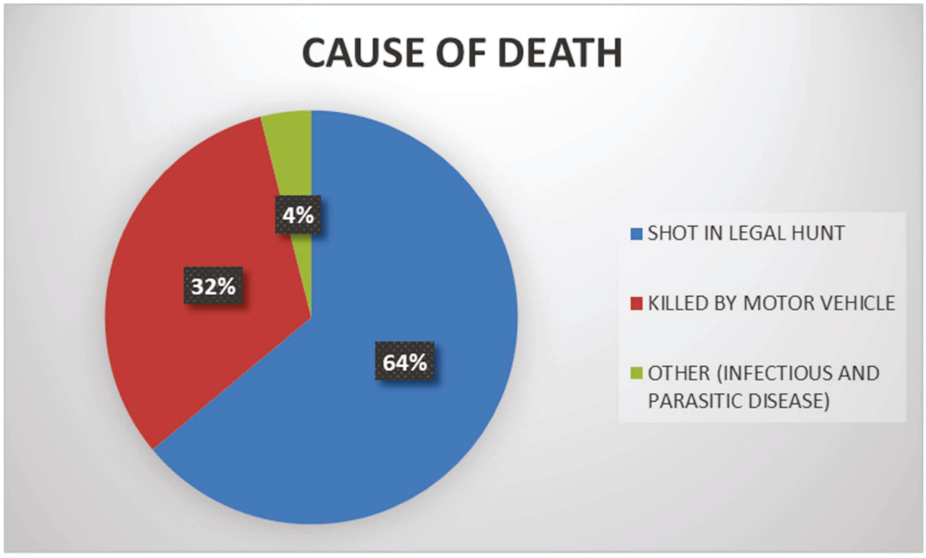


Figure 1. Causes of death in submitted foxes.

Most of the delivered foxes were between 1 and 3 years of age, but the range was from at least 1 month to more than 7 years (Figure 2).

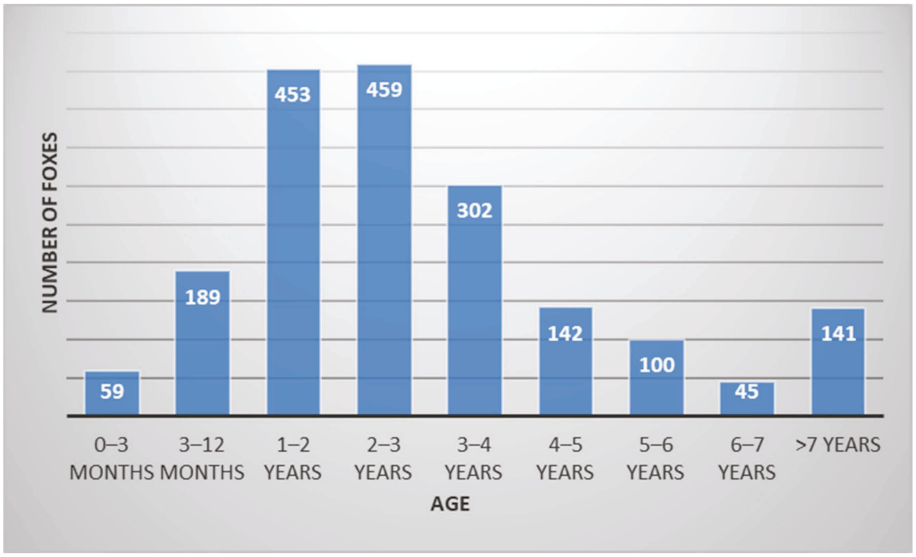


Figure 2. Age range of submitted foxes.

Table 1. Red foxes with detected tumor and tumor-like lesion; M-male; F- female.

Animals	Cause of Death	Sex	Age	Location of the Tumor/Tumor-like Lesion	Year of Necropsy	Diagnosis
Red fox (*Vulpes vulpes*)	Shot in legal hunt	M	2 years	Intraabdominal	2020	Teratoma
Red fox (*Vulpes vulpes*)	Shot in legal hunt	M	4 years	Upper eyelid	2021	Meibomian gland adenoma
Red fox (*Vulpes vulpes*)	Shot in legal hunt	F	4 years	Ventral abdomen	2022	Collagenous hamartoma
Red fox (*Vulpes vulpes*)	Shot in legal hunt	F	5 years	Lower eyelid	2023	Meibomian gland adenoma
Red fox (*Vulpes vulpes*)	Shot in legal hunt	M	7 years	Nose	2023	Collagenous hamartoma

Out of these five foxes, three were male, while the remaining two were female. The age distribution spanned from 2 to 7 years, with a mean age of 4.4 years, indicating a relatively young population. Within the five tumor/tumor-like lesions observed, four were located on the integumentary system, specifically in the regions encompassing the lower and upper eyelids, nose, and ventral abdomen. The fifth tumor was found within the abdominal cavity. Histological examination of the tumor/tumor-like lesions on the fox's skin revealed two of these as Meibomian gland adenomas (Figures 3 and 4), another two as collagenous hamartomas (Figures 5 and 6), while the intra-abdominal outgrowth was diagnosed as a teratoma (Figure 7) within a cryptorchid testis.

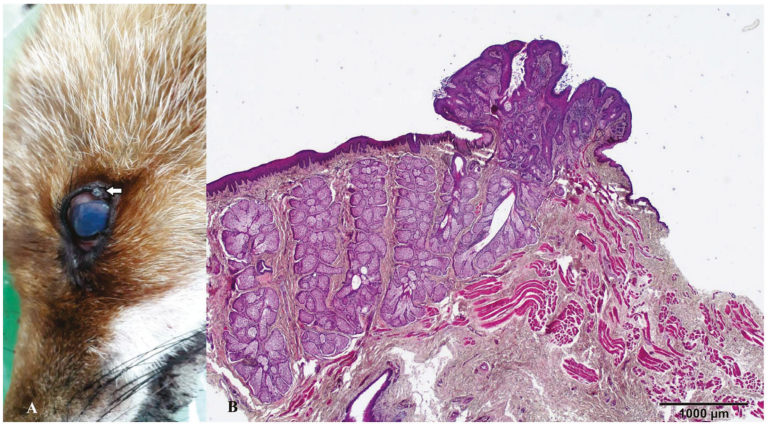


Figure 3. (**A**) Gross appearance of the Meibomian gland adenoma on the upper eyelid (arrow). (**B**) Microscopic appearance of the same lesion depicting a well-circumscribed, benign, intradermal lobular tumor.

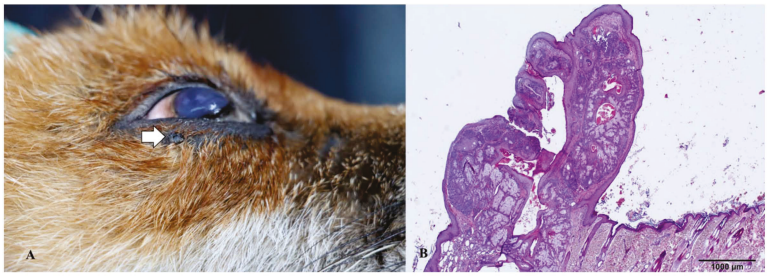


Figure 4. (**A**) Gross appearance of the Meibomian gland adenoma on the lower eyelid (arrow). (**B**) Microscopic appearance of the same lesion depicting a well-circumscribed, benign, intradermal lobular tumor with visible ductal dilation.

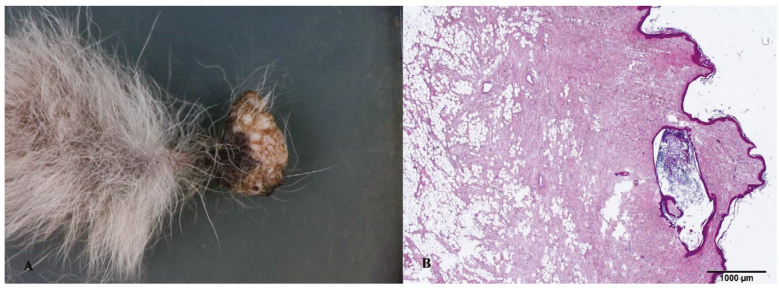


Figure 5. (**A**) Gross appearance of the collagenous hamartoma removed from the abdomen. (**B**) Microscopic appearance of the same lesion with visible bundles of cell-poor collagenous tissue with one dilated hair follicle.

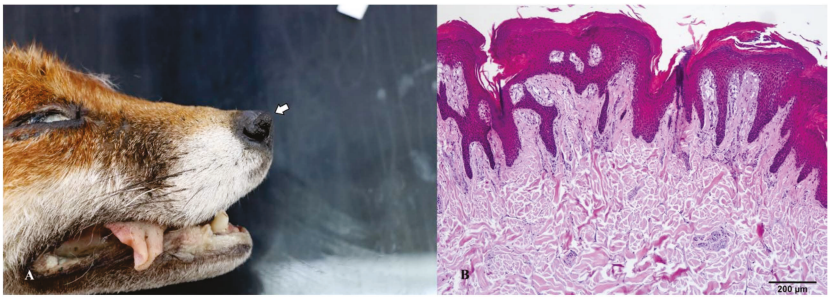


Figure 6. (**A**) Gross appearance of the collagenous hamartoma on the nose apex (arrow). (**B**) Microscopic picture with visible bundles of collagenous tissue and epidermal hyperkeratosis.

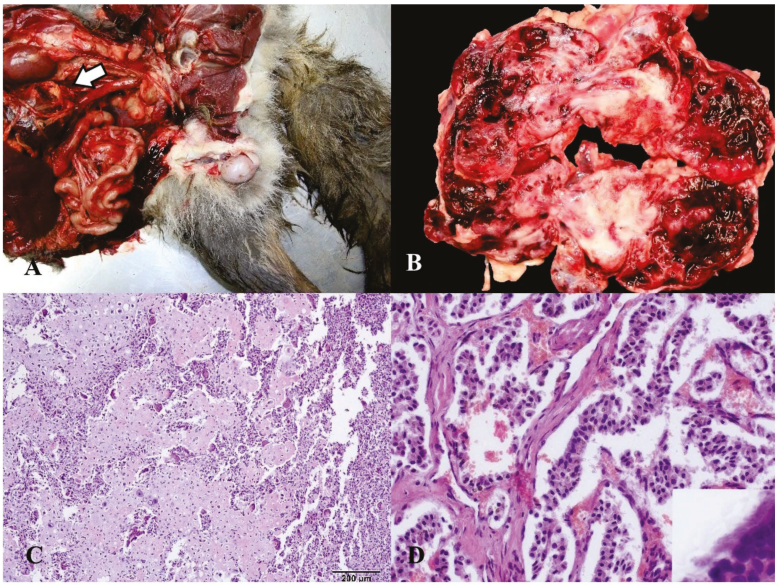


Figure 7. (**A**) Gross position of the teratoma inside the abdomen, between the spleen and kidney (arrow). (**B**) Cross section of teratoma with a central connective tissue and a vascular part with multiple blood spaces on both sides. (**C**) Microscopic appearance of the central part with cartilage formation, osteoid, and multinuclear osteoclasts. (**D**) Microscopic appearance of elongated, prism-shaped epithelial cells with well-developed cilia on their surface (insert photo).

The dermal structures present on the upper and lower eyelids exhibited a resemblance to a cauliflower, characterized by a polypoid morphology. On the cross section, these tumors were of gray to white color. The histological examination revealed a notable increase in the number of sebaceous glands, accompanied by a thin layer of non-proliferative cells, within a mild increase in the collagenous stroma. The presence of multifocal infiltration of inflammatory cells was also observed.

Collagenous mesenchymal structures were observed on the abdominal and nasal regions of two red fox specimens. The abdominal tumor-like lesion was characterized by a circular shape, accompanied by a stalk that connected the outgrowth with the abdominal skin. The observed cross-section exhibited a white-gray color, characterized by a connective tissue framework. The nasal outgrowth exhibited a prominent growth at the apex of the nose, resembling a horn. Upon closer inspection, the cross-sectional view revealed a white-gray color and a connective tissue arrangement. From a histological perspective, it can be observed that both tumor-like lesions consisted of excessive amounts of dermal collagen. The arrangement of the fiber pattern had a resemblance to the organization of collagen bundles in the dermis.

A teratoma was detected in a juvenile male with undescended testicles who was shot during legal hunting. The carcass exhibited moderate cachexia. There was a single testicle

located within the scrotum (a unilateral cryptorchid). Within the abdominal cavity, there was a mass that had an irregularly circular shape and a diameter of approximately 22 cm. This formation was connected to the mesentery through adhesions. The mass encompassed 25% of the abdominal cavity. The cross-section exhibited a central compact region, which was yellow and consisted of a connective tissue structure with multiple localized areas of mineralization. There was a vascular region on both sides that contained multiple blood-filled spaces. From a histological point of view, we observed regions of cartilage formation with osteoid and multinuclear osteoclasts. There were areas of connective tissue within the tumor's vascular region that frequently contained elongated, prism-shaped epithelial cells with well-developed cilia on their surfaces. The identification of two distinct cell types, each corresponding to one of the embryonic germ layers, led to the diagnosis of teratoma.

4. Discussion

Foxes, belong to the canid family and are the most numerous predator species found throughout Croatia [4]. According to many authors, they serve as potential reservoirs for a wide range of infectious diseases and zoonotic pathogens, including the rabies virus, *Trichinella* spp., *Echinococcus* spp., *Leptospira* [4,5,28,29], and *Salmonella* spp. [30]. The primary cause of mortality among foxes is commonly attributed to instances of being orphaned (33%), followed by trauma (27%), and sarcoptic mange (17%) [6]. The examination of observed pathological alterations in the organ systems of foxes in Germany revealed that the gastrointestinal system is the most commonly affected, followed by the respiratory, genitourinary, cardiovascular, integumentary, nervous, and lastly, the musculoskeletal system [2]. Based on the findings of these studies, it has been observed that foxes, along with other animal species, possess the potential to acquire various diseases with diverse origins. Due to the nature of our research, which focused on identifying tumors in foxes obtained through hunting or found dead on roads, only a limited number of foxes died from natural causes. Therefore, we are unable to make comparisons or assess the prevailing natural causes of death in the fox population in Croatia.

Tumors pose a significant risk to wild animals, with certain types leading to elevated mortality rates among specific vertebrate populations [9,31]. Viruses are responsible for a significant portion of these tumors [31].

To date, no research has been conducted in Croatia on this matter, thus precluding any direct comparison of findings with existing studies on tumor occurrence in wild animals that belong to the family Canidae. However, we will proceed to compare the obtained results with established data on tumor prevalence in domestic dogs within Croatia, as well as with data on reported tumors in foxes.

This study represents the initial investigation carried out in Croatia, aiming to analyze tumor and tumor-like lesions in red foxes within this specific region of Europe. In our study, it was observed that among a sample size of 1890 foxes, just five individuals had the presence of a tumor or tumor-like lesion, which was a comparatively elevated prevalence when compared to other regions in Europe. The salient feature of these findings is that all identified lesions were observed in red foxes living in their natural habitat, and furthermore, all tumors were classified as benign. This stands in contrast to previous studies where the majority of tumors in foxes were found to be malignant [15–18,21–24]. This number of only five animals with a tumor or tumor-like lesion is relatively low when compared with the considerably high incidence of tumors in canines, where it stands as the primary cause of mortality [8,25,26]. Three individuals were identified as males, representing 60% of the animals, while two individuals were identified as females (40%). Although this is a very small sample size, this is consistent with previous studies in foxes, which have shown a higher prevalence of tumors in male animals compared to females. When considering only red foxes in the reported cases, there is a higher incidence of tumors in female red foxes. Also, these findings correspond with previous studies conducted on dogs [25,26]. Although the population under examination encompassed a wide age spectrum, ranging from a few months to over 7 years, it is noteworthy that the group of foxes with the tumor had a

relatively young average age. In our study, a relatively young population (mean age 4.4 years) of foxes had tumors and tumor-like lesions, which contrasts findings in dogs, where tumors were predominantly observed in animals of middle or older age [8,25,26], but also most reports on tumor occurrences among foxes have highlighted a higher prevalence among older individuals, particularly those held in captivity [17,18,20–24]. The majority of these established tumorous lesions (80%) were found on the skin, while the remaining one was located in the abdomen (20%). This distribution aligns with findings from studies conducted on dogs, which have consistently reported a higher prevalence of skin tumors compared to tumors in other organ systems [25,26]. However, this does not align with the documented tumors in foxes, where only a single case of a cutaneous or subcutaneous tumor was described, this being subcutaneous lipoma [20].

In our study, it was observed that all skin tumors that were identified were benign tumors or tumor-like lesions, specifically meibomian gland adenoma and collagenous hamartoma. This corresponds with the previously documented data in foxes, where so far, no malignant skin tumors have been detected, and the only tumor detected was the previously mentioned lipoma case [20]. Interestingly, this contrasts with the data in dogs, where skin tumors are predominantly malignant [25,26].

Eyelid neoplasms are the predominant periocular tumors in elderly canines, with the majority being unilateral, benign, and slow-growing [32]. Meibomian gland adenoma arises from the tarsal glands (meibomian glands) on the inner aspect of the eyelid and is a frequently encountered benign neoplasm affecting the eyelids of canines [33]. Typically, they manifest as small, raised tumors with an irregular surface and a pink, grey, or black color [32,33], as in our cases. According to our research, solitary masses on the lower and upper eyelids represent 40% of all detected tumor lesions, or 50% of detected skin tumors.

Collagen hamartomas are common solitary and nodular tumor-like lesions in dogs [34,35]. Lesions can manifest on various regions of the body, although they are most commonly found on the head and limbs [34]. In the specific case of a red fox, we observed the presence of lesions on the nose, while in other instances, they were located in the caudal abdomen region. The histological findings in red foxes align with the hamartomas in dogs.

A tumor that was discovered inside the abdomen originated from an undescended testis in a 2-year-old fox. Cryptorchidism represents the prevailing anomaly in sexual development among juvenile males [36]. It occurs most often in stallions [37] but is also a frequent clinical finding in dogs [36]. Ninety percent of tumors of the male dog genital system are testicular tumors, which are the second most common type of tumor in male dogs [38]. The most prevalent type of tumor in the testis of dogs is Leydig cell tumor, but Sertoli cell tumor and seminoma are more prevalent in cryptorchids [36,39], which is not the case in this red fox where we detected testicular teratoma. Teratomas are uncommon tumors in dogs [40] that are formed of abnormal tissue originating from at least two, and frequently all three, germinal layers [37,41]. Typically, they are composed of histologically benign, well-differentiated tissue [42]. Macroscopically, this type of tumor is characterized by multiple cystic formations, often with the presence of hair and secretions containing mucoid or sebaceous substances, and solid masses of yellow and white composition consisting of fibrous, adipose, cartilaginous, and bony tissue [36], which corresponds to the macroscopic appearance of teratoma in our case. On histology, we detected tissues derived from two embryonic germ layers, which fulfills the criteria for the diagnosis of teratoma.

Arguably, the most influential factor of this study, skewing our results, was the young age of the examined fox population, which can be seen as a crucial limiting factor. The majority of foxes observed were either young individuals or mature juveniles, which contrasts with the data available for dogs, where the highest number of dogs affected by tumors are older animals. An additional aspect influencing the data is the inability to comprehensively study the entire fox population in Croatia, contrasting dogs, which are predominantly registered and supervised by their owners. The final factor that partially restricts the scope of the subject study is the potential occurrence of very small tumors either on the skin or within the internal organs, which might have been overlooked.

Despite the study's limitations, it must be emphasized that a substantial sample of foxes was analyzed, offering valuable insights into tumor occurrence in this wild animal species that is difficult to study. Undoubtedly, this study represents the initial research of its kind in Croatia, necessitating a more comprehensive and methodical examination to acquire additional data that will address the deficiencies identified by this study.

5. Conclusions

This study marks the inaugural investigation of its kind in Croatia, presenting a unique modality to explore tumorous and tumor-like lesions in foxes within this specific region of Europe. It lays the groundwork for future surveillance of these lesions in foxes living in their natural habitat. The identification of a limited number of tumors is likely linked to the young age of all the animals involved, since it is widely acknowledged that tumorous lesions predominantly appear in older canines.

To improve the accuracy of the analysis, it is crucial to systematically monitor the elderly fox population over an extended period of time. This will contribute to a more comprehensive understanding of the prevalence and nature of these lesions in the long term.

Author Contributions: Conceptualization, Š.N., I.-C.Š.-Z. and Ž.M.; methodology, Ž.M.; formal analysis, Š.N. and I.-C.Š.-Z.; investigation and pathological analysis Š.N.; data curation, Š.N. and Ž.M.; writing—original draft preparation, Š.N.; writing—review and editing, Š.N., I.-C.Š.-Z. and Ž.M.; supervision, I.-C.Š.-Z. and Ž.M. All authors have read and agreed to the published version of the manuscript.

Funding: This research received no external funding.

Institutional Review Board Statement: The authors confirm that the ethical policies of the journal, as outlined in the notes on the journal's author guidelines page, have been adhered to. All animals included in the study were collected according to an ongoing rabies annual monitoring program in Croatia prescribed by the Croatian Ministry of Agriculture, Veterinary and Food Safety Directorate. No animals were sacrificed specifically for the purpose of this study. This research did not involve any animal experiments.

Informed Consent Statement: Not applicable.

Data Availability Statement: The data presented in this study are available on request from the first author.

Acknowledgments: We express our gratitude to Angela Bradarić and Mario Maršić for their technical support.

Conflicts of Interest: The authors declare no conflicts of interest.

References

1. Terio, K.A.; McAloose, D.; St. Léger, J. *Pathology of Wildlife and Zoo Animals*; Academic Press: London, UK, 2018; pp. 229–262.
2. Lempp, C.; Jungwirth, N.; Grilo, M.L.; Reckendorf, A.; Ulrich, A.; van Neer, A.; Bodewes, R.; Pfankuche, V.M.; Bauer, C.; Osterhaus, A.D.M.E.; et al. Pathological Findings in the Red Fox (*Vulpes vulpes*), Stone Marten (*Martes foina*) and Raccoon Dog (*Nyctereutes procyonoides*), with Special Emphasis on Infectious and Zoonotic Agents in Northern Germany. *PLoS ONE* **2017**, *12*, e0175469. [CrossRef]
3. Galov, A.; Sindičić, M.; Andreanszky, T.; Čurković, S.; Dežđek, D.; Slavica, A.; Hartl, G.B.; Krueger, B. High Genetic Diversity and Low Population Structure in Red Foxes (*Vulpes vulpes*) from Croatia. *Mamm. Biol.* **2014**, *79*, 77–80. [CrossRef]
4. Slavica, A.; Severin, K.; Čač, Ž.; Cvetnić, Ž.; Lojkić, M.; Dežđek, D.; Konjević, D.; Pavlaka, M.; Bundišćak, Z. Model širenja silvatične bjesnoće na teritoriju Republike Hrvatske tijekom perioda od trideset godina. *Vet. Stanica* **2010**, *41*, 199–217.
5. Ebani, V.V.; Trebino, C.; Guardone, L.; Bertelloni, F.; Cagnoli, G.; Nardoni, S.; Sel, E.; Wilde, E.; Poli, A.; Mancianti, F. Occurrence of Bacterial and Protozoan Pathogens in Red Foxes (*Vulpes vulpes*) in Central Italy. *Animals* **2022**, *12*, 2891. [CrossRef]
6. Kelly, T.R.; Sleeman, J.M. Morbidity and Mortality of Red Foxes (*Vulpes vulpes*) and Gray Foxes (*Urocyon cinereoargenteus*) Admitted to the Wildlife Center of Virginia, 1993–2001. *J. Wildl. Dis.* **2003**, *39*, 467–469. [CrossRef]
7. Willebrand, T.; Samelius, G.; Walton, Z.; Odden, M.; Englund, J. Declining Survival Rates of Red Foxes *Vulpes vulpes* during the First Outbreak of Sarcoptic Mange in Sweden. *Wildl. Biol.* **2021**, *2022*, e01014. [CrossRef]
8. Dias-Pereira, P. Morbidity and Mortality in Elderly Dogs—A Model for Human Aging. *BMC Vet. Res.* **2022**, *18*, 457. [CrossRef]
9. McAloose, D.; Newton, A.L. Wildlife Cancer: A Conservation Perspective. *Nat. Rev. Cancer* **2009**, *9*, 517–526. [CrossRef] [PubMed]
10. Woods, G.M.; Lyons, A.B.; Bettiol, S.S. A Devil of a Transmissible Cancer. *Trop Med Infect Dis.* **2020**, *5*, 50. [CrossRef] [PubMed]

11. Pye, R.J.; Woods, G.M.; Kreiss, A. Devil Facial Tumor Disease. *Vet Pathol.* **2016**, *53*, 726–736. [CrossRef] [PubMed]
12. Vickers, T.W.; Clifford, D.L.; Garcelon, D.K.; King, J.L.; Duncan, C.L.; Gaffney, P.M.; Boyce, W.M. Pathology and Epidemiology of Ceruminous Gland Tumors among Endangered Santa Catalina Island Foxes (*Urocyon Littoralis Catalinae*) in the Channel Islands, USA. *PLoS ONE* **2015**, *10*, e0143211. [CrossRef]
13. Tidière, M.; Gaillard, J.M.; Berger, V.; Müller, D.W.H.; Bingaman Lackey, L.; Gimenez, O.; Clauss, M.; Lemaître, J.F. Comparative Analyses of Longevity and Senescence Reveal Variable Survival Benefits of Living in Zoos across Mammals. *Sci. Rep.* **2016**, *6*, 36361. [CrossRef]
14. Elvestad, K.; Henriques, U.V.; Kroustrup, J.P. Insulin-Producing Islet Cell Tumor in an Ectopic Pancreas of a Red Fox (*Vulpes vulpes*). *J. Wildl. Dis.* **1984**, *20*, 70–72. [CrossRef]
15. Janovsky, M.; Steineck, T. Adenocarcinoma of the Mammary Gland in a Red Fox from Austria. *J. Wildl. Dis.* **1999**, *35*, 392–394. [CrossRef]
16. Degli Uberti, B.; Mariani, U.; Restaino, G.; De Luca, G.; Anzalone, A.; Guida, M.; D'Alessio, N.; D'Amore, M. *Caso Report di un Carcinoma Renale in Una Volpe (Vulpes vulpes) in Regione Campania*; Società Italiana di Diagnostica di Laboratorio Veterinaria (SIDiLV): Perugia, Italy, 2018; p. 125.
17. Hirayama, K.; Kagawa, Y.; Nihtani, K.; Taniyama, H. Thyroid C-Cell Carcinoma with Amyloid in a Red Fox (*Vulpes vulpes schrenchki*). *Vet. Pathol.* **1999**, *36*, 342–344. [CrossRef]
18. Fukui, D.; Bando, G.; Ishikawa, Y.; Kadota, K. Adenosquamous Carcinoma with Cilium Formation, Mucin Production and Keratinization in the Nasal Cavity of a Red Fox (*Vulpes vulpes schrencki*). *J. Comp. Pathol.* **2007**, *137*, 142–145. [CrossRef] [PubMed]
19. Hayes, H.M.; Sass, B. Testis Neoplasia in Captive Wildlife Mammals: Comparative Aspects and Review. *J. Zoo Anim. Med.* **1987**, *18*, 162. [CrossRef]
20. Jeong, D.; Yang, J.; Kong, J.; Lee, B.; Lee, J.; Park, S.; Lee, S.; Seok, S.; Hong, I.; Lee, H.; et al. A Subcutaneous Lipoma in a Male Red Fox. *J. Vet. Clin.* **2015**, *32*, 278–281. [CrossRef]
21. Monahan, C.F.; Garner, M.M.; Kiupel, M. Hepatocellular neoplasms in captive fennec foxes (*Vulpes zerda*). *J. Zoo Wildl. Med.* **2018**, *49*, 996–1001. [CrossRef]
22. Gray, K.N.; Harwell, G.; Tsai, C.C. Multiple primary tumors in a fennec fox (*Fennecus zerda*). *J. Wildl. Dis.* **1982**, *18*, 369–371. [CrossRef] [PubMed]
23. Dillberger, J.E.; Citino, S.B. A Malignant Nephroblastoma in an Aged Fox (*Fennecus zerda*). *J. Comp. Pathol.* **1987**, *97*, 101–106. [CrossRef] [PubMed]
24. Choudhary, S.; Andrews, G.A.; Carpenter, J.W. Small intestinal adenocarcinoma with carcinomatosis in a swift fox (*Vulpes velox*). *J. Zoo Wildl. Med.* **2015**, *46*, 596–600. [CrossRef] [PubMed]
25. Šoštarić, I.-C.; Hohšteter, M.; Artukovi, B.; Sabo, R. Incidence and Types of Canine Tumours in Croatia. *Vet. Arhiv* **2013**, *83*, 31–45.
26. Zagradišnik, M.; Židak, H.; Huber, D.; Buhin, I.M.; Vlahović, D.; Severin, K.; Hohšteter, M. Pojavnost neoplazija u hrvatskih autohtonih pasmina pasa: Retrospektivna analiza tijekom desetogodišnjeg razdoblja. *Hrvat. Vet. Vjesn.* **2023**, *31*, 32–40.
27. Roulichová, J.; Anděra, M. Simple Method of Age Determination in Red Fox, *Vulpes vulpes*. *Folia Zool.* **2007**, *56*, 440–444.
28. Celva, R.; Crestanello, B.; Obber, F.; Dellamaria, D.; Trevisiol, K.; Bregoli, M.; Cenni, L.; Agreiter, A.; Danesi, P.; Hauffe, H.C.; et al. Assessing Red Fox (*Vulpes vulpes*) Demographics to Monitor Wildlife Diseases: A Spotlight on *Echinococcus multilocularis*. *Pathogens* **2022**, *12*, 60. [CrossRef] [PubMed]
29. Bandelj, P.; Blagus, R.; Vengušt, G.; Žele Vengušt, D. Wild Carnivore Survey of *Echinococcus* Species in Slovenia. *Animals* **2022**, *12*, 2223. [CrossRef]
30. Gambi, L.; Ravaioli, V.; Rossini, R.; Tranquillo, V.; Boscarino, A.; Mattei, S.; D'incau, M.; Tosi, G.; Fiorentini, L.; Donato, A.D. Prevalence of Different *Salmonella enterica* Subspecies and Serotypes in Wild Carnivores in Emilia-Romagna Region, Italy. *Animals* **2022**, *12*, 3368. [CrossRef]
31. Pesavento, P.A.; Agnew, D.; Keel, M.K.; Woolard, K.D. Cancer in Wildlife: Patterns of Emergence. *Nat. Rev. Cancer* **2018**, *18*, 646–661. [CrossRef]
32. Wang, S.-L.; Dawson, C.; Wei, L.-N.; Lin, C.-T. The Investigation of Histopathology and Locations of Excised Eyelid Masses in Dogs. *Vet. Rec. Open* **2019**, *6*, e000344. [CrossRef]
33. Goldschmidt, M.H.; Goldschmidt, K.H. Epithelial and Melanocytic Tumors of the Skin. In *Tumors in Domestic Animals*, 5th ed.; Meuten, D.J., Ed.; John Wiley & Sons Inc.: Ames, IA, USA, 2017; p. 111.
34. Hendrick, M.J. Mesenchymal Tumors of the Skin and Soft Tissues. In *Tumors in Domestic Animals*, 5th ed.; Meuten, D.J., Ed.; John Wiley & Sons Inc.: Ames, IA, USA, 2017; p. 152.
35. Gross, T.L.; Ihrke, P.J.; Walder, E.J.; Affolter, V.K. *Skin Diseases of the Dog and Cat: Clinical and Histopathologic Diagnosis*, 2nd ed.; Blackwell Science Ltd.: Oxford, UK, 2005; pp. 710–711.
36. Foster, R.A. Male Genital System. In *Jubb, Kennedy, and Palmer's Pathology of Domestic Animals*, 6th ed.; Maxie, M.G., Ed.; Elsevier: St. Louis, MO, USA, 2016; Volume 3, pp. 465–510.
37. Dalen, W.; Agnew, D.W.; MacLachlan, N.J. Tumors of the Genital Systems. In *Tumors in Domestic Animals*, 5th ed.; Meuten, D.J., Ed.; John Wiley & Sons Inc.: Ames, IA, USA, 2017; p. 711.
38. North, S.; Banks, T.; Straw, R. Tumors of the urogenital tract. In *Small Animal Oncology, an Introduction*; North, S., Banks, T., Straw, R., Eds.; Elsevier Saunders: Edinburgh, UK; London, UK; New York, NY, USA; Oxford, UK; Philadelphia, PA, USA; St. Louis, MO, USA; Sydney, Australia; Toronto, ON, Canada, 2009; pp. 151–172.

39. Morris, J.; Dobson, J. *Small Animal Oncology*, 1st ed.; Blackwell Science Ltd.: Oxford, UK, 2001.
40. Pêgas, G.R.A.; Monteiro, L.N.; Cassali, G.D. Extragonadal Malignant Teratoma in a Dog—Case Report. *Arq. Bras. Med. Vet. Zootec.* **2020**, *72*, 115–118. [CrossRef]
41. Makovicky, P.; Makarevich, A.; Makovicky, P.; Seidavi, A.; Vannucci, L.; Rimarova, K. Benign Ovarian Teratoma in the Dog with Predominantly Nervous Tissue: A Case Report. *Vet. Med.* **2022**, *67*, 99–104. [CrossRef]
42. Nagashima, Y.; Hoshi, K.; Tanaka, R.; Shibazaki, A.; Fujiwara, K.; Konno, K.; Machida, N.; Yamane, Y. Ovarian and Retroperitoneal Teratomas in a Dog. *J. Vet. Med. Sci.* **2000**, *62*, 793–795. [CrossRef] [PubMed]

Disclaimer/Publisher's Note: The statements, opinions and data contained in all publications are solely those of the individual author(s) and contributor(s) and not of MDPI and/or the editor(s). MDPI and/or the editor(s) disclaim responsibility for any injury to people or property resulting from any ideas, methods, instructions or products referred to in the content.

animals

MDPI

Communication

A Health Status Update of *Myocastor coypus* in Northern Italy

Arturo Nicoletti, Paola Pregel, Laura Starvaggi Cucuzza , Enrico Bollo and Frine Eleonora Scaglione *

Department of Veterinary Sciences, University of Turin, 10095 Grugliasco, TO, Italy; arturo.nicoletti1991@gmail.com (A.N.); paola.pregel@unito.it (P.P.); laura.starvaggicucuzza@unito.it (L.S.C.); enrico.bollo@unito.it (E.B.)

* Correspondence: frineeleonora.scaglione@unito.it; Tel.: +0039-0116709263

Simple Summary: Nutria (*Myocastor coypus*) is a pest animal present in Africa, Europe, North America and Asia that causes agricultural and ecological damages. Moreover, it has to be considered as a potential risk for public health. A health survey on a population of coypu of Northwest Italy has been carried out to evaluate its zoonotic risks. None of the animals were positive for Hepatitis E virus, Encephalomyocarditis virus, *Francisella* or *Neospora caninum*, whereas two animals tested positive for *Toxoplasma gondii*. Moreover, a high prevalence of histological lesions has been found. Coypu can act as a host for several pathogens, including important agents for human and animal health, and surveillance is necessary to fully understand the biological role and the importance of coypu as a disease reservoir in our country.

Abstract: *Myocastor coypus* is a pest animal present in Africa, Europe, North America and Asia that causes agricultural and ecological damages. Moreover, it has to be considered as a potential risk for public health. Forty-four coypus from the "Parco Naturale La Mandria" (Piedmont region, Northwest Italy) have been analysed. A complete necropsy and a whole histological evaluation of the liver, kidney and lung have been carried out on all the animals. Moreover, the positivity to Hepatitis E Virus (HEV), Encephalomyocarditis virus (EMCV), *Francisella* spp., *Toxoplasma gondii* and *Neospora caninum* have been investigated. None of the animal were positive for HEV, EMCV, *Francisella* spp. or *Neospora caninum*. Two animals tested positive for *Toxoplasma gondii*. A high presence of histological lesions has been identified in different organs, suggesting that lesions could be induced by different pathogens. As previously reported, coypu can act as a host for several pathogens, including important agents for human and animal health, and surveillance is necessary to fully understand the biological role and the importance of coypu as a disease reservoir in our country.

Keywords: nutria; ecological impact; health status; public health; *Toxoplasma gondii*; zoonoses

1. Introduction

The nutria, or coypu (*Myocastor coypus*), is a semiaquatic herbivorous rodent, originally native of South America, present currently in large feral populations in Africa, Europe, North America and Asia [1,2]. In Europe, the coypu was introduced principally for meat and fur production. In Italy the first introduction for fur farming dates back to 1928 by the National Institute of Rabbit husbandry in Alessandria (Piedmont, Northwest Italy) [3].

Coypu colonization of the natural environment is primarily due to intentional release actions and, minimally, to animals escaped from fur farms. During the following decades, coypu population, density and distribution have dramatically increased and, thanks to its ecological plasticity, even suboptimal habitats were colonized [4]. Due to its negative ecological impact, the coypu is currently considered a pest in the areas of introduction [5]. This animal usually lives next to water courses, in wetlands, riparian zones and coastlands [6]. Thereby, its burrowing behaviour undermines the banks of rivers, canals and dykes, whereas its feeding activity reduces plants' biodiversity and cover, altering the water's flowing speed and increasing the erosion of the banks [7].

Moreover, the damage to the habitat can negatively affect the reproduction of fishes, birds and invertebrates [8]. Coypu can also cause agricultural damages by feeding on crops, resulting in a great economic impact [9,10]. Due to the typical aspect of coypu ecology, this species is subjected to population control programs. Nevertheless, the population is still expanding [4,11].

Furthermore, the coypu can be infected by several pathogens and parasites. Some of them can be transmissible to humans and other animals. Several investigations focused on agents that might cause epizootics in wild populations and livestock, as well as in humans [5,12,13].

In this context, this research aims to evaluate the health status of the coypu in Northwest Italy and the presence of pathologies through gross necropsy examinations, histological and biomolecular investigations. The study focuses on viral, bacterial and parasitological pathogens, to investigate potential public health risks linked to coypu diffusion and to improve our knowledge about diseases affecting this species in the analysed area.

2. Materials and Methods

2.1. Animals and Samples Collection

Following the adoption of a regional animal containment programme (according to the D.G.R no. 74–6702 [08/03/2007] and subsequent amendments), 44 coypus from the "Parco Naturale La Mandria" (Piedmont region, Northwest Italy, 45°8′7″ N, 7°37′31″ E) were trapped with baited cage traps or shot. Trapped animals were euthanized with CO_2, according to Italian National Bioethics Committee guidelines and to law no. 157 (02/11/1992) and subsequent amendments. The sample included 25 males and 19 females. For each animal, biometric features as weight (kg) and foot length (cm) were collected. All animals were subjected to a standard necropsy procedure.

Samples of liver, kidney, lung and both eyeballs were fixed in 10% phosphate-buffered formalin for histological analysis and age determination.

Based on previous study in the same area [12], samples of liver, lung, heart and central nervous system (CNS) were collected and frozen at −20 °C for virological, bacteriological and parasitological investigations.

2.2. Age Estimation

Due to the impossibility of distinguishing between juveniles, adults and elderly by aspect, morphometric measures or dentition, the age was determined in 33 out of the 44 animals by dry eye-lens weight, according to the protocol proposed by Gosling and colleagues. In detail, the eyes were removed as soon after death as possible and placed in 10% buffered formalin. Eyes were kept in formalin for at least 1 month to allow the lens to harden. The lenses were extracted, and extraneous tissue was removed by rolling on absorbent paper and careful scraping with a blunt seeker. Any damaged lenses were discarded. Pairs of lenses were placed in a small crucible and dried in a forced draught at 80 °C for 22 h. Lenses were weighed on an analytical balance to an accuracy of 0.1 mg. The equation used to determine the age in months is log10 (age + 4.34 months) = 0.511 + 0.013 (mean lens weight) [14]. Based on the study of Pagnoni and Santolini [15], the animals were divided into two groups: juveniles (<8 months) and adults (8–12 months).

2.3. Histological Analysis

The fixed samples were routinely processed and paraffin embedded. Three µm sections were stained with haematoxylin and eosin (HE) and with von Kossa staining, if calcium salts precipitations in the tissue were suspected.

2.4. Virological Analysis

The total RNA was extracted from liver and heart samples using TRIzol® Reagent (Invitrogen™, ThermoFisher Scientific, Waltham, MA, USA), according to the manufacturer's instructions. RNA extracted from liver was tested for the presence of Hepatitis Virus E

(HEV) according to the protocol of Jothikumar [16]. Samples were considered negative for Ct (cycle threshold) values >38, doubtful if Ct was comprised between 36 and 38 and positive for Ct < 36. RNA extracted from heart was retrotranscribed through the High-Capacity cDNA Reverse Transcription Kit (Applied Biosystems™, ThermoFisher Scientific), and the obtained cDNAs were tested for the presence of the encephalomyocarditis virus (EMCV) using the protocol by Vanderhallen [17].

2.5. Bacteriological Analysis

The genomic DNA was extracted from liver samples using the QIAamp DNA Mini Kit (Qiagen, Hilden, Germany) according to the manufacturer's protocol. The extracted templates were amplified using a primer set specific for *Francisella* spp. [18]. Specimens collected from 39 lungs were plated onto 5% sheep Blood Agar and Gassner Agar and incubated for 24 h at 37 °C. Bacterial isolates were identified to species level by means of an automated system using Vitek® 2 Compact (bioMérieux, Inc., Durham, NC, USA), a testing system that combines an automated platform with an expansive database of clinically significant organisms.

2.6. Parasitological Analysis

Total genomic DNA was extracted from 25 mg of CNS homogenate, using the commercial kit NucleoSpin® Tissue (Macherey-Nagel, Düren, Germany). The extracted templates were tested for *Toxoplasma gondii* [19] and *Neospora caninum* [20]. PCR was performed as previously reported [21].

2.7. Statistical Analysis

Statistical analyses were performed using GraphPad Prism (version 10.0.1, GraphPad Software, La Jolla, CA, USA). Fisher's exact test was performed to determine non-random associations between sex and the recurrent pathologies detected in lung and kidney. A p value < 0.05 was considered statistically significant.

3. Results

3.1. Age Estimation

Out of 33 coypus considered for age determination, 32 were juveniles and only 1 was an adult (Table 1).

Table 1. Mean weight of the dry eye lens (mg), standard deviation, age in months and age class in tested coypus. NA: not applicable.

Coypus ID	Mean Weight (mg)	Standard Deviation (mg)	Age (Months)	Age Class
1	NA	NA	NA	NA
2	NA	NA	NA	NA
3	NA	NA	NA	NA
4	NA	NA	NA	NA
5	NA	NA	NA	NA
6	11.5	4.95	<1	Juvenile
7	7.5	4.95	<1	Juvenile
8	6	1.41	<1	Juvenile
9	7	1.41	<1	Juvenile
10	5.5	0.71	<1	Juvenile
11	NA	NA	NA	NA
12	NA	NA	NA	NA
13	35.5	9.19	5.0	Juvenile
14	34.5	2.12	4.8	Juvenile
15	46	NA	8.5	Adult
16	44	NA	7.8	Juvenile

Table 1. *Cont.*

Coypus ID	Mean Weight (mg)	Standard Deviation (mg)	Age (Months)	Age Class
17	36	NA	5.2	Juvenile
18	27.5	4.95	3.0	Juvenile
19	21	2.83	1.7	Juvenile
20	38	5.66	5.8	Juvenile
21	44	7.07	7.8	Juvenile
22	24.5	0.71	2.4	Juvenile
23	6	2.83	<1	Juvenile
24	13.5	2.12	0.5	Juvenile
25	13.5	4.95	0.5	Juvenile
26	13	1.41	0.4	Juvenile
27	6	4.24	<1	Juvenile
28	12.5	2.12	0.4	Juvenile
29	15.5	2.12	0.8	Juvenile
30	10.5	0.71	0.1	Juvenile
31	9.5	4.95	0.0	Juvenile
32	5	4.24	<1	Juvenile
33	20	5.66	1.6	Juvenile
34	10	0.00	0.0	Juvenile
35	21	2.83	1.7	Juvenile
36	28	2.83	3.2	Juvenile
37	7.5	0.71	<1	Juvenile
38	14	0.00	0.6	Juvenile
39	NA	NA	NA	NA
40	24.5	0.71	2.4	Juvenile
41	NA	NA	NA	NA
42	13.5	2.12	0.5	Juvenile
43	NA	NA	NA	NA
44	NA	NA	NA	NA

3.2. Histological Analysis

Out of 44 examined livers, 25 (56.8%) had no detectable microscopic lesions, whereas 18 (40.9%) showed one or more concurrent microscopic lesions (Table 2, Figures 1 and 2). One sample (2.3%) was autolytic and impossible to evaluate.

Table 2. Frequency and characteristics of the histological lesions detected in liver samples.

Lesion	Number of Samples Positive for the Lesion/Total Number of Microscopical Lesions (%)
Periportal lymphoid tissue activation	8/18 (44.4%)
Parenchymal lymphocytic infiltrate	7/18 (38.9%)
Perivascular lymphocytic infiltrate	3/18 (16.7%)
Macrophage infiltration	1/18 (5.6%)
Multifocal granuloma	1/18 (5.6%)

The evaluation of the kidneys showed 21 (47.7%) samples without lesions and 23 (52.3%) affected from one or more detectable microscopic lesions (Table 3, Figure 3). No statistically significant association between lymphocytic interstitial nephritis and sex or age was detected.

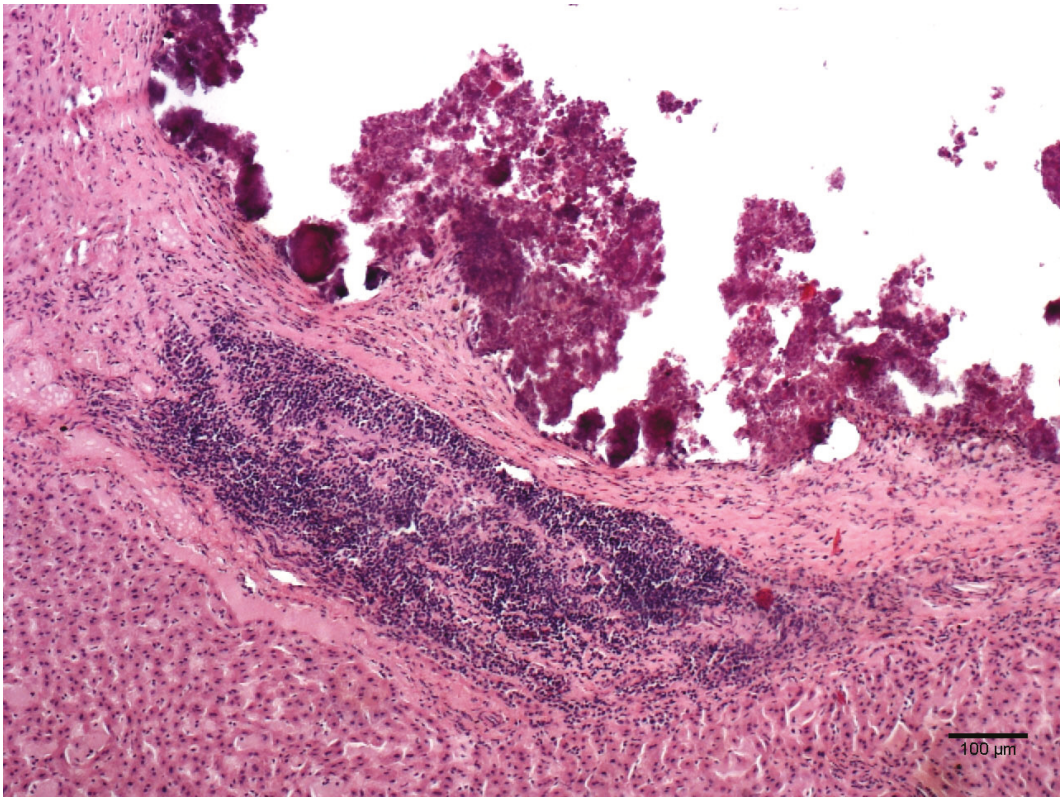


Figure 1. *Myocastor coypus* liver: granuloma with necrotic area surrounded by connective tissue and lymphocytic infiltrate (HE).

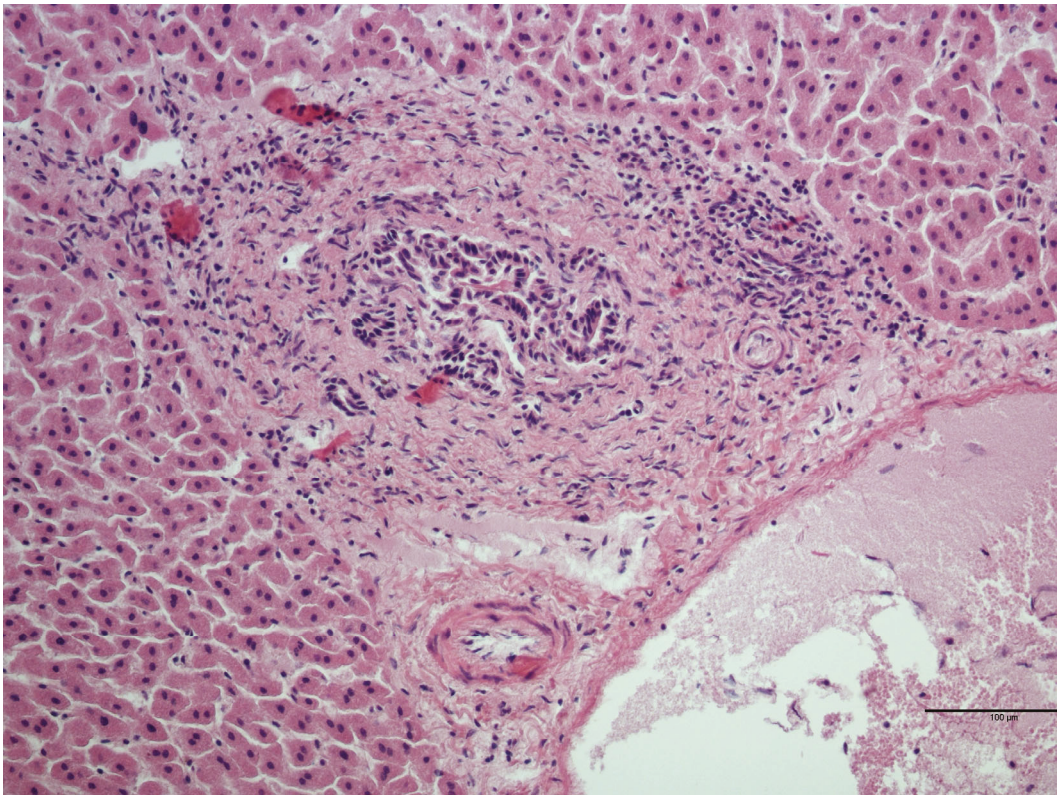


Figure 2. *Myocastor coypus* liver: mild activation of the periportal lymphoid tissue (HE).

Table 3. Frequency and characteristics of the histological lesions detected in kidney samples.

Lesion	Number of Samples Positive for the Lesion/Total Number of Microscopical Lesions (%)
Interstitial lymphocytic nephritis	20/23 (87.0%)
Urine crystals	2/23 (8.7%)
Perivascular lymphocytic infiltrate	1/23 (4.3%)
Cyst with focal lymphocytic infiltrate	1/23 (4.3%)
Interstitial lymphocytic and eosinophilic nephritis	1/23 (4.3%)
Lymphocytic infiltrate into perirenal fat	1/23 (4.3%)

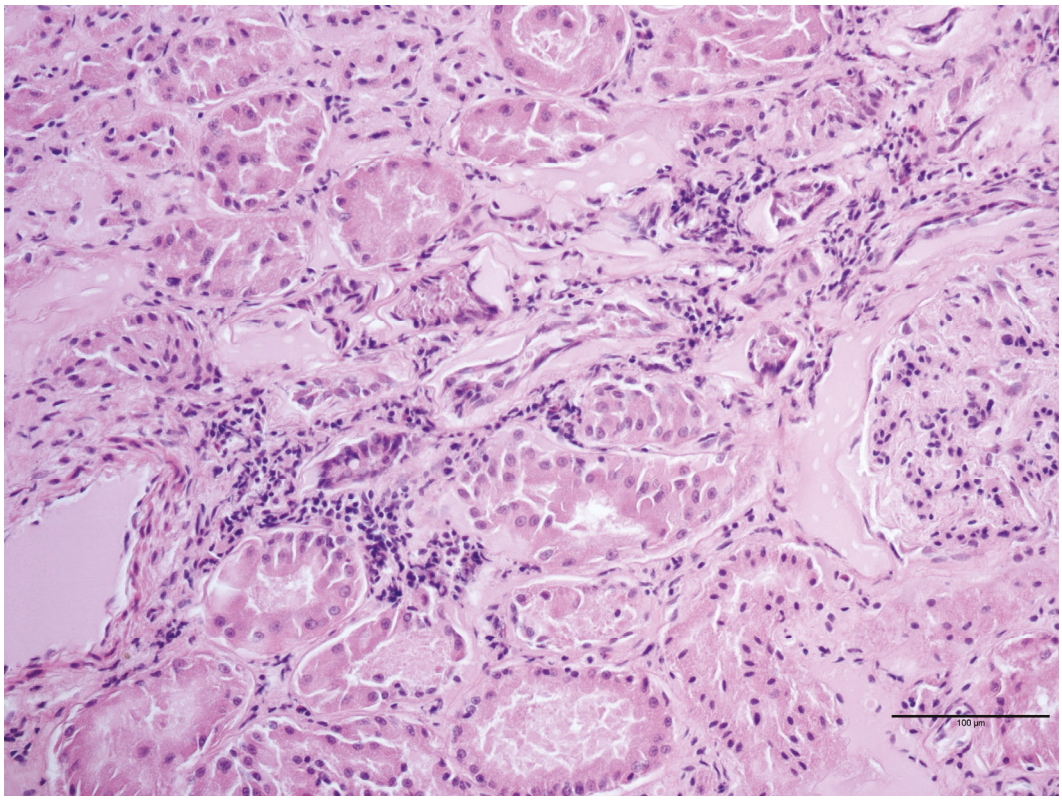


Figure 3. *Myocastor coypus* kidney: mild interstitial lymphoid nephritis (HE).

Each of the 44 examined lungs showed the presence of concomitant different lesions (Table 4, Figure 4). No statistically significant association was found between perivascular lymphocytic infiltrate or BALT activation and sex or age.

Table 4. Frequency and characteristics of the histological lesions detected in lung samples.

Lesion	Number of Samples Positive for the Lesion/Total Number of Microscopical Lesions (%)
Emphysema	44/44 (100%)
Oedema	36/44 (81.8%)
Parenchymal lymphocytic infiltrate	36/44 (81.8%)
Perivascular lymphocytic infiltrate	32/44 (72.7%)
BALT activation	27/44 (61.4%)
Alveolar thickening	12/44 (27.3%)
Atelectasis	9/44 (20.5%)

Table 4. *Cont.*

Lesion	Number of Samples Positive for the Lesion/Total Number of Microscopical Lesions (%)
Parenchymal lymphocytic and eosinophilic infiltrate	2/44 (4.5%)
Lymphocytic bronchitis	2/44 (4.5%)
Parenchymal neutrophilic infiltrate	1/44 (2.3%)
Focal haemorrhages	1/44 (2.3%)

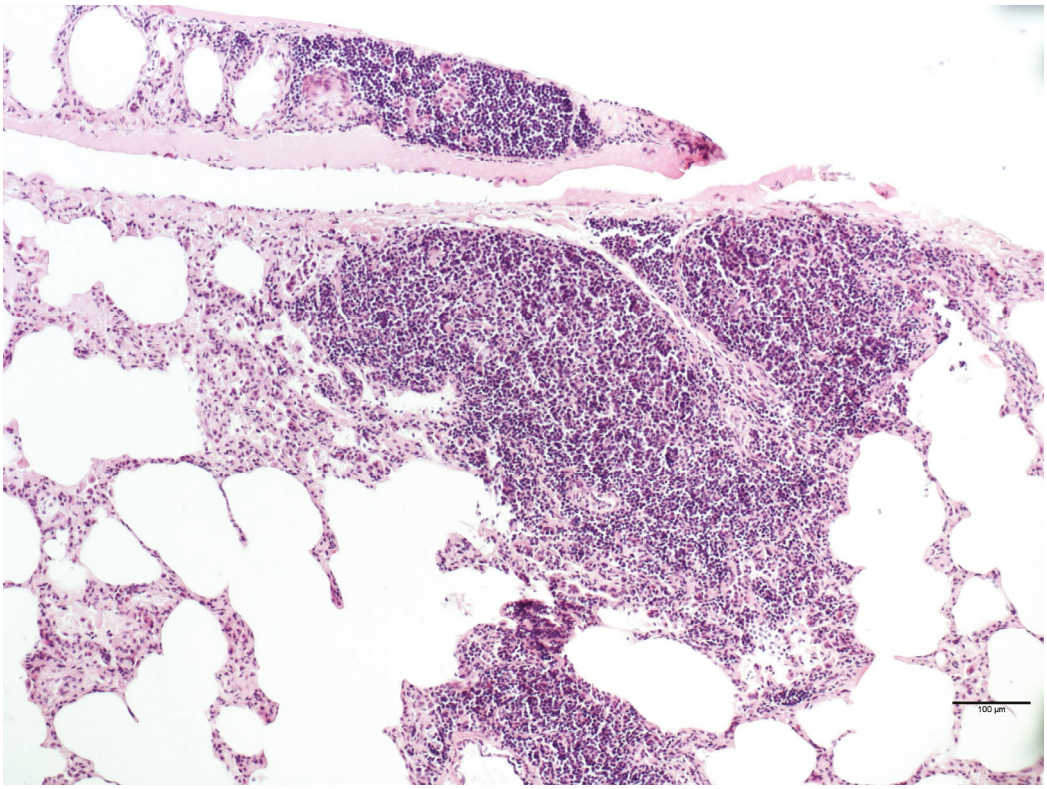


Figure 4. *Myocastor coypus* lung: severe parenchymal lymphocytic infiltrate (HE).

3.3. Bacteriological, Virological and Parasitological Analyses

None of the Samples Tested Positive for HEV or EMCV

None of the tested animals were positive for *Francisella* spp., while 25 out of 39 analysed lungs (64.1%) were positive in the bacteriological analysis. Six of them (15.4%) revealed polymicrobial infection. The bacterial species identification of the other 19 positive samples is listed in Table 5. Due to the conservation methods of the lung samples, it has to be considered that an underestimation of bacterial identification is possible.

Two out of the thirty-five (5.7%) analysed animals were positive for *T. gondii*, whereas *N. caninum* infection has never been detected.

Table 5. Isolated bacteria.

Isolated Bacteria	Number of Samples Positive/Total Number of Analysed Lungs (%)
Enterococcus spp.	4/19 (21.0%)
Enterococcus hirae	2/19 (10.5%)
Pseudomonas fluorescens	2/19 (10.5%)
Nocardia spp.	2/19 (10.5%)

Table 5. *Cont.*

Isolated Bacteria	Number of Samples Positive/Total Number of Analysed Lungs (%)
Enterococcus durans	1/19 (5.3%)
Pseudomonas mendocina	1/19 (5.3%)
Achromobacter xylosoxidans	1/19 (5.3%)
Brevibacillus laterosporus	1/19 (5.3%)
Corynebacterium propinquum	1/19 (5.3%)
Corynebacterium pseudodiphthericum	1/19 (5.3%)
Ochrobactrum anthropi	1/19 (5.3%)
Streptococcus aginosus	1/19 (5.3%)
Non-identifiable	1/19 (5.3%)

4. Discussion

All of the considered lungs had microscopical lesions. However, out of the 44 samples, only in 19 samples was it possible to isolate bacterial pathogens. Fifteen out of the nineteen (89.5%) analysed lungs showed the presence of lymphocytic infiltrates. Nine of them also showed the presence of lymphocytic infiltrate in the kidney and five of them in the liver. The other three individuals showed inflammatory lesions only in the liver.

As previously reported by Bollo and colleagues [12], cold and high humidity could be a predisposing factor for the high prevalence of pneumonia in wild coypu.

Histologically, kidneys mostly showed interstitial lymphocytic infiltrate (45.45%). This prevalence is higher than the one reported in another study conducted in the same region (10.1%) [12], and it could be caused by infection or immune-mediated diseases, such as Leptospirosis, as previously reported in other populations of coypu serologically investigated [12,22–24].

Livers showed microscopical lesions, with inflammatory infiltrations, mostly lymphocytic. The aetiology of those lesions can be related to inflammatory and degenerative processes, differently from the results obtained by Bollo and colleagues [12].

The investigation for EMCV's RNA was negative. In previous works, seropositivity against EMCV was found in Argentina [13] and Italy [12], whereas it was not detected in the USA [25].

PCR for *Francisella* spp. gave negative results. Similar results have been serologically obtained in two different studies made in Louisiana (USA) and Argentina, in which no antibodies against *F. tularensis* were found [13,25].

All the samples analysed for HEV and *Neospora caninum* were negative and, to the authors' best knowledge, positivity in this species has never been demonstrated.

Worthy of interest, two animals were positive for *Toxoplasma gondii*, which can infect all warm-blooded animals and is the aetiological agent of a major zoonosis. In the present research, one of the two animals found to be positive for *T. gondii* showed an interstitial lymphocytic nephritis and a lymphocytic perivascular and parenchymal infiltrate in the liver, even if, normally, animals challenged with *Toxoplasma* do not develop referable clinical signs [5,12]. The other positive animal showed no microscopical findings. The prevalence of *Toxoplasma* in the examined area (4.5%) is very low compared to Nardoni and colleagues' study (59.4%) [5]. A coypu infected with *Toxoplasma gondii* is a potential contagion source for other scavengers and can be used in the analysed area for monitoring the quantity of oocysts [5]. Human infection during pregnancy may be extremely dangerous for the foetus, and this parasite in immunocompromised patients can cause a life-threatening encephalitis [26]. New findings suggest that *Toxoplasma* can actually cause changes in memory, learning, behaviour and anxiety [27].

Currently, the coypu is mostly raised in South America for fur production. Meat consumption of the coypu is considered a by-product, but there are new studies that are considering coypu meat as a new novel and exotic food [28]. In this scenario, the

importance of coypu infections with *Toxoplasma* and other pathogens such as HEV acquires even more relevance.

5. Conclusions

In conclusion, the coypu is an acknowledged threat for both the environment and animals. It can act as a host for several pathogens, including important agents for human and animal health [5,9,12]. Therefore, further investigation for viral, bacterial and parasitic surveillance are necessary, to fully understand the biological role and the importance of coypu as a disease reservoir in our country.

Author Contributions: Conceptualization, A.N. and F.E.S.; methodology, L.S.C.; software, P.P.; validation, E.B.; formal analysis, A.N. and L.S.C.; investigation, F.E.S., A.N. and L.S.C.; writing—original draft preparation, A.N., F.E.S. and P.P.; writing—review and editing, F.E.S. and P.P.; supervision, E.B. All authors have read and agreed to the published version of the manuscript.

Funding: This research received no external funding.

Institutional Review Board Statement: Not applicable.

Informed Consent Statement: Not applicable.

Data Availability Statement: Data are contained within the article.

Conflicts of Interest: The authors declare no conflicts of interest.

References

1. Carter, J.; Leonard, B.P. A Review of the Literature on the Worldwide Distribution, Spread of, and Efforts to Eradicate the Coypu (*Myocastor Coypus*). *Wildl. Soc. Bull.* **2002**, *30*, 162–175.
2. Pedruzzi, L.; Schertler, A.; Giuntini, S.; Leggiero, I.; Mori, E. An Update on the Distribution of the Coypu, Myocastor Coypus, in Asia and Africa through Published Literature, Citizen-Science and Online Platforms. *Mamm. Biol.* **2022**, *102*, 109–118. [CrossRef]
3. Adriani, S.; Bonanni, M.; Amici, A. Study on the Presence and Perception of Coypu (*Myocastor coypus* Molina, 1782) in Three Areas of Lazio Region (Italy). *Jul.-Kühn-Arch.* **2011**, *432*, 49–50. [CrossRef]
4. Panzacchi, M.; Cocchi, R.; Genovesi, P.; Bertolino, S. Population Control of Coypu Myocastor Coypus in Italy Compared to Eradication in UK: A Cost-Benefit Analysis. *Wildl. Biol.* **2007**, *13*, 159–171. [CrossRef]
5. Nardoni, S.; Angelici, M.C.; Mugnaini, L.; Mancianti, F. Prevalence of Toxoplasma Gondii Infection in Myocastor Coypus in a Protected Italian Wetland. *Parasites Vectors* **2011**, *4*, 240. [CrossRef]
6. Robert, H.; Lafontaine, R.M.; Beudels-Jamar, R.C.; Delsinne, T.; Baiwy, E. *Risk Analysis of the Coypu Myocastor Coypus (Molina, 1792). Risk Analysis Report of Non-Native Organisms in Belgium*; Royal Belgian Institute of Natural Sciences: Brussels, Belgium, 2013. [CrossRef]
7. Kang, W.; Kim, G.; Park, Y. Habitat Suitability and Connectivity Modeling Predict Genetic Population Structure and Priority Control Areas for Invasive Nutria (*Myocastor Coypus*) in a Temperate River Basin. *PLoS ONE* **2022**, *17*, e0279082. [CrossRef] [PubMed]
8. GISD. Available online: http://www.iucngisd.org/gisd/ (accessed on 26 October 2023).
9. Barrat, J.; Richomme, C.; Moinet, M. The Accidental Release of Exotic Species from Breeding Colonies and Zoological Collections: -EN- -FR- Lâcher Accidentel d'espèces Exotiques à Partir de Colonies d'élevage et de Collections Zoologiques-ES-Liberación Accidental de Especies Exóticas de Colonias Reproductoras y Colecciones Zoológicas. *Rev. Sci. Tech. OIE* **2010**, *29*, 113–122. [CrossRef]
10. Wang, S.; Deng, T.; Zhang, J.; Li, Y. Global Economic Costs of Mammal Invasions. *Sci. Total Environ.* **2023**, *857*, 159479. [CrossRef]
11. Funzione Specializzata Tutela della Flora e della Fauna Ufficio Tecnico Gestionale. *Piano di Contenimento della Nutria (Myocastor coypus) sul Territorio della citta' Metropolitana di Torino Anni 2022–2026*; Funzione Specializzata Tutela della Flora e della Fauna Ufficio Tecnico Gestionale: Turin, Italy, 2021.
12. Bollo, E.; Pregel, P.; Gennero, S.; Pizzoni, E.; Rosati, S.; Nebbia, P.; Biolatti, B. Health Status of a Population of Nutria (*Myocastor Coypus*) Living in a Protected Area in Italy. *Res. Vet. Sci.* **2003**, *75*, 21–25. [CrossRef]
13. Martino, P.E.; Stanchi, N.O.; Silvestrini, M.; Brihuega, B.; Samartino, L.; Parrado, E. Seroprevalence for Selected Pathogens of Zoonotic Importance in Wild Nutria (*Myocastor Coypus*). *Eur. J. Wildl. Res.* **2014**, *60*, 551–554. [CrossRef]
14. Gosling, L.M.; Huson, L.W.; Addison, G.C. Age Estimation of Coypus (*Myocastor Coypus*) from Eye Lens Weight. *J. Appl. Ecol.* **1980**, *17*, 641. [CrossRef]
15. Pagnoni, G.A.; Santolini, R. Struttura di popolazione di nutria (*Myocastor coypus*) in un'area agricola della Pianura Padana Orientale. *Studi Trent. Sci. Nat.* **2011**, *88*, 45–52.

16. Jothikumar, N.; Cromeans, T.L.; Robertson, B.H.; Meng, X.J.; Hill, V.R. A Broadly Reactive One-Step Real-Time RT-PCR Assay for Rapid and Sensitive Detection of Hepatitis E Virus. *J. Virol. Methods* **2006**, *131*, 65–71. [CrossRef]
17. Vanderhallen, H.; Koenen, F. Identification of Encephalomyocarditis Virus in Clinical Samples by Reverse Transcription-PCR Followed by Genetic Typing Using Sequence Analysis. *J. Clin. Microbiol.* **1998**, *36*, 3463–3467. [CrossRef] [PubMed]
18. Forsman, M.; Sandstrom, G.; Sjostedt, A. Analysis of 16S Ribosomal DNA Sequences of Francisella Strains and Utilization for Determination of the Phylogeny of the Genus and for Identification of Strains by PCR. *Int. J. Syst. Bacteriol.* **1994**, *44*, 38–46. [CrossRef] [PubMed]
19. Homan, W.L.; Vercammen, M.; Braekeleer, J.D.; Verschueren, H. Identication of a 200- to 300-Fold Repetitive 529 Bp DNA Fragment in Toxoplasma Gondii, and Its Use for Diagnostic and Quantitative PCRp. *Int. J. Parasitol.* **2000**, *30*, 69–75. [CrossRef] [PubMed]
20. Romano, A.; Trisciuoglio, A.; Grande, D.; Ferroglio, E. Comparison of Two PCR Protocols for the Detection of Neospora Caninum DNA in Rodents. *Vet. Parasitol.* **2009**, *159*, 159–161. [CrossRef]
21. Ferroglio, E.; Bosio, F.; Trisciuoglio, A.; Zanet, S. Toxoplasma Gondii in Sympatric Wild Herbivores and Carnivores: Epidemiology of Infection in the Western Alps. *Parasit. Vectors* **2014**, *7*, 196. [CrossRef]
22. Zanzani, S.A.; Cerbo, A.D.; Gazzonis, A.L.; Epis, S.; Invernizzi, A.; Tagliabue, S.; Manfredi, M.T. Parasitic and Bacterial Infections of *Myocastor Coypus* in a Metropolitan Area of Northwestern Italy. *J. Wildl. Dis.* **2016**, *52*, 126–130. [CrossRef]
23. Ayral, F.; Kodjo, A.; Guédon, G.; Boué, F.; Richomme, C. Muskrats Are Greater Carriers of Pathogenic Leptospira than Coypus in Ecosystems with Temperate Climates. *PLoS ONE* **2020**, *15*, e0228577. [CrossRef]
24. Mazzotta, E.; Bellinati, L.; Bertasio, C.; Boniotti, M.B.; Lucchese, L.; Ceglie, L.; Martignago, F.; Leopardi, S.; Natale, A. Synanthropic and Wild Animals as Sentinels of Zoonotic Agents: A Study of Leptospira Genotypes Circulating in Northeastern Italy. *Int. J. Environ. Res. Public Health* **2023**, *20*, 3783. [CrossRef] [PubMed]
25. Howerth, E.W.; Reeves, A.J.; McElveen, M.R.; Austin, F.W. Survey for Selected Diseases in Nutria (*Myocastor Coypus*) from Louisiana. *J. Wildl. Dis.* **1994**, *30*, 450–453. [CrossRef] [PubMed]
26. Montoya, J.G.; Liesenfeld, O. Toxoplasmosis. *Lancet* **2004**, *363*, 1965–1976. [CrossRef] [PubMed]
27. Tyebji, S.; Seizova, S.; Hannan, A.J.; Tonkin, C.J. Toxoplasmosis: A Pathway to Neuropsychiatric Disorders. *Neurosci. Biobehav. Rev.* **2019**, *96*, 72–92. [CrossRef]
28. Saadoun, A.; Cabrera, M.C. A Review of Productive Parameters, Nutritive Value and Technological Characteristics of Farmed Nutria Meat (*Myocastor Coypus*). *Meat Sci.* **2019**, *148*, 137–149. [CrossRef]

Disclaimer/Publisher's Note: The statements, opinions and data contained in all publications are solely those of the individual author(s) and contributor(s) and not of MDPI and/or the editor(s). MDPI and/or the editor(s) disclaim responsibility for any injury to people or property resulting from any ideas, methods, instructions or products referred to in the content.

animals

MDPI

Article

Survey of *Mycobacterium* spp. in Eurasian Badgers (*Meles meles*) in Central Italy

Elga Ersilia Tieri *, Lucio Marino, Katiuscia Zilli, Cinzia Pompilii, Giovanni Di Teodoro, Antonio Cocco, Addolorato Ruberto, Michela Toro, Maria Teresa Mastrodomenico, Stefania Salucci and Fabrizio De Massis

Istituto Zooprofilattico Sperimentale dell'Abruzzo e del Molise 'G. Caporale' (IZS Teramo), Campo Boario, 64100 Teramo, Italy

* Correspondence: e.tieri@izs.it; Tel.: +39-0861-3321; Fax: +39-0861-332251

Simple Summary: The Eurasian badger (*Meles meles*) is a wild carnivore well adapted to the Abruzzo and Molise regions. During the 2013–2021 period, badger carcasses found dead or road-killed were systematically subjected to an anatomopathological examination and search for mycobacteria with the aim of ascertaining their presence in this species, given the absence of data in Italy. This study provides evidence of infection with the *Mycobacterium avium* subsp. *avium* (MAA) and *M. avium* subsp. *paratuberculosis* (*MAP*) in a small number of badgers. *M. bovis* does not seem to circulate within badger populations. This study suggests that in Central Italy, *Meles meles* should not play a role in the epidemiology of these mycobacteria under current epidemiological conditions.

Abstract: A survey to determine the presence of *Mycobacterium* spp. in the Abruzzo and Molise regions was conducted by testing samples from 124 badgers found dead or road-killed during the 2013–2021 period. Head lymph nodes were collected from all carcasses, as well as mediastinal lymph nodes from 20 of them, for bacteriological and molecular tests; tissues were inoculated onto a set of solid egg-based Lowenstein–Jensen media and in a liquid culture system (BACTEC) and were analyzed by polymerase chain reactions (PCRs). Organs and lymph nodes from 31 carcasses were collected for histological tests. During post-mortem examinations, macroscopic lesions consistent with a *Mycobacterium tuberculosis* complex (MTBC) and with nontuberculous mycobacteria (NTM) infections were not detected. Mycobacteria were isolated from four animals (3.22%). *M. avium* subsp. *avium* was isolated by head lymph nodes from two badgers (1.61%), *M. avium* subsp. *paratuberculosis* (0.80%) from one, and *Mycobacterium* spp. from another (0.80%). The significance of nontuberculous mycobacteria (NTM) in wildlife hosts in the absence of clinical signs and gross pathology has yet to be assessed. The most critical aspect came from isolates belonging to the *Mycobacterium avium* complex infection in wildlife due to the possible interference with tuberculin skin tests in cattle.

Keywords: badger; DNA typing; Italy; *Mycobacterium avium* subsp. *avium*; *Mycobacterium avium* subsp. *paratuberculosis*

1. Introduction

Mycobacteria are classified as tuberculosis mycobacteria capable of triggering tuberculosis in humans and animals, and they belong to the *Mycobacterium tuberculosis* complex (MTBC) group, including *M. bovis*, and in nontuberculous mycobacteria (NTM), which cause diseases other than tuberculosis. In the group of NTM, there are members of the *Mycobacterium avium* complex (MAC), which includes the species *Mycobacterium avium* and its subspecies *M. avium* subsp. *avium* (MAA) and *M. avium* subsp. *Paratuberculosis* (*MAP*) [1,2].

Wildlife is susceptible to the same infectious agents that affect livestock species, and where livestock is managed under extensive farming, cross-transmission may be favored [3].

The Eurasian badger (*Meles meles*) is widely distributed across Europe; however, from several countries, epidemiological information about tuberculosis on this species is lacking, making it difficult to assess the role of these badgers as a wildlife tuberculosis reservoir in Europe [4].

Meles meles seems to be involved in the transmission of *M. bovis* in cattle in the United Kingdom (UK) and Ireland, where badgers share pastures with cattle, which are extensively farmed [5,6]; in these territories, the tuberculosis prevalence is high in badgers and in cattle, probably due to the behavior, the high abundance, and the social group size with a greater number of individuals. Between 1998 and 2005, the prevalence rates of *M. bovis*, estimated by culture in the UK during the randomized badgers culling trial varied from 1.6% to 37.2%, with an average of 16.6%. In the same period, the badger population density was 3.92 badgers/Km^2, and on initial proactive culls, the mean estimated social group size was 5.44 ($\pm$4.27) [5]. In Ireland, in the period of 2002–2003, the prevalence of tuberculosis estimated by bacteriological examination of a wide range of anatomical site tissues of culled badgers was 43.2% [6]; in the period of 1993–2009, researchers reported a population density of 1.9 badgers/Km^2 and a social group size between 1.8 to 5.9 [7]. Although studies on badger tuberculosis differ both in the target population (road-killed or culled), in sample size, and in the diagnostic method used (gross lesion, culture, and PCR), the prevalence of the disease in the UK (6.4–11%) [8] and in Ireland (9–11%) [9] has recently decreased due to the control activities.

The prevalence of tuberculosis is lower in population badgers in France (4.57–5.14%) [10] and in Spain (4.23%) [11] than in Northern European countries. In France, the density of adult badgers was recently estimated to be between 1.66 and 7.86/Km^2, with an average of 3.84 and a social group size between 1.34 to 4.46 [12]. Studies carried out in the Iberian Peninsula seemed to indicate a social strategy based on well-defined social units composed of 2–4 adults and a density of 0.23–0.67 badgers/Km^2 in Spain [13] and of 0.53–0.94 badgers/Km^2 in Portugal [14], less dense than that found in Northern Europe.

Tuberculosis in the badger is a respiratory disease. In a review, Gallagher and Clifton-Hadley (2000) [15] described in detail the gross pathology and the pathogenesis of tuberculosis in badgers. They reported various investigations carried out in Britain and Ireland in which infected badgers showed mainly lung lesions and broncho mediastinal node lesions. However, in contrast with cattle, in which gross lymph node lesions accompany lung lesions in the great majority of cases, in the badger, this occurred in a minority of cases. The highest percentage of lesion frequencies was bronchial, retropharyngeal, mediastinal, prescapular, and popliteal [15].

Lung lesions of tuberculosis in badger may vary from nodules of 1–3 mm to widespread lobar disease where miliary tubercles coalesce to form large masses. Pleurisy, either nodular or unilateral pyothorax, nodular epicarditis, and pericarditis were found on occasion [15].

Other Mycobacteria were isolated from badgers. A total of 5 (7.35%) and 281 (0.51%) isolates of *M. avium* spp. were recovered from badgers during previous studies in Spain and in the UK, respectively, but none of the infected badgers showed lesions containing a large number of MAC bacilli, so the authors concluded that they may not have a significant role in the transmission of MAC organism [16].

In Italy, the ecology of *Meles meles* is different from that of Northern Europe, and livestock is managed under semi-extensive regimes. From the Italian national database of the Livestock Registry [17], it appears that, in 2021, in the Abruzzo and Molise regions, 3.80% and 1.46% of cattle, respectively, moved to pastures, while greater movements to pastures were recorded in Piedmont (34.76%) and Trentino alto Adige (10.71%) [17].

In Italy, badgers dig dens or use those dug by foxes and porcupines, and differently from what happens in Northern Europe, they exhibit a solitary behavior, not forming social groups sharing the same den [18].

One possible explanation for this great difference is that the mild and damp climate of the British Isles, with little snow cover and few dry periods, together with the high prevalence of pasture, provides ideal conditions for Earthworms *Lumbricus terrestris*, which

are their main prey. In continental Europe, including Italy, badgers have been found to specialize in very different foods, such as insects and fruits [19].

There are no studies on the density of badgers in the Abruzzo and Molise regions. Recent data document that in Northern Italy, social groups are formed by two to four adults, similar to what was described in Spain and Portugal. The badger density is 0.93–1.4/Km^2 [20], which is rather high compared with the data of the Iberian Peninsula [13,14].

The badger is distributed throughout the Italian peninsula, while it is absent in Sicily, Sardinia, and smaller islands. The habitats of the badger are forests both in the plains and in the mountains, up to 2000 m above sea level; it prefers deciduous or mixed woods, alternating with open, bushy, stony, and uncultivated areas [18]. The ability to live in different environments and to adapt its diet to very varied ecological conditions makes this species widespread and relatively common throughout Italy, from the Alpine and Apennine mountainous areas to the agricultural ones, where the extent of natural vegetation is limited, in the dense scrub environments as well as in coastal areas [18].

The Abruzzo and Molise regions are totally included in the distribution range of the badger in Italy. The Abruzzo region covers 10,800 Km^2, and the Molise region 4438 km^2 with an elevation ranging from the sea level, about 2900 m high for the former and about 2200 m for the latter.

In these regions, the variations in the vegetation cover are expressed along an altitudinal gradient corresponding to the climate gradient. The territory is mainly mountainous and hilly, and the plain consists of a narrow coastal strip. There are several ecosystems: the coastal plains include mainly urbanized and cultivated environments with fragmented natural habitats. Mixed forests (turkey oak, downy, and beech tree) are located throughout the sub-montane areas, while beech forests and montane shrublands and grasslands occur towards the higher elevations [21,22].

Meles meles is a species protected by European [23] and Italian laws [24]. However, although this species does not have particular conservation problems, the collection of samples for research purposes is only possible in the event of traffic accidents or natural death.

The aim of this study was to show the results of the analyses carried out to detect the presence of *Mycobacterium* spp., *M. tuberculosis* complex, *M. avium* subsp. *avium* e *M. avium* subsp. *paratuberculosis* in the European badger population residing in the Abruzzo and Molise regions.

2. Materials and Methods

2.1. Study Area and Sample Collection

Between 2013 and 2021, the carcasses of 124 badgers, including 113 adults and 11 juveniles (63 females and 61 males), mainly involved in road accidents in Abruzzo and Molise regions, were examined at IZS-Teramo. The carcasses were found in the following provinces: 65 in L'Aquila, 32 in Chieti, 15 in Teramo, 4 in Isernia, 5 in Pescara, and 3 in Campobasso.

A wide variety of methods were used to age badgers. These included techniques based on the fusion of tibial epiphyses, teeth sectioning, teeth wear, eye lens mass, and skull structure, but accurate aging of adult badgers remains problematic [25]. So, in this study, the classification into young and adult animals was carried out by measuring the distance from the tip of the nose to the base of the tail. Usually, in adult badgers, this distance is 61–73 cm (cm) [26]. Badgers with a length of less than 61 cm were considered young (Figure 1A,B).



Figure 1. (**A**) Young badger carcass with tip nose-base tail length < 61 cm; (**B**) adult badger carcass with tip nose-base tail length > 61 cm.

2.2. Post-Mortem and Histological Examination

Each carcass was subjected to an anatomopathological examination. Head lymph nodes were collected from all carcasses, and mediastinal lymph nodes from 20 of them were used for bacteriological and molecular tests in the search for *Mycobacterium* spp.

The bacteriological analysis was performed on a small number of tissues for each carcass; differently from the more sensitive approach described by Corner et al. (2012) [6], our diagnostic strategy is used to obtain initial information in undisturbed wild population at not an excessive cost to gain insights into epidemiological patterns in field studies, as supported by Delahay (2012) [27]. As relative indices of infection, we can use them to identify long-term trends in space and time in naturally infected populations.

Samples of lung, spleen, liver, and mesenteric lymph nodes were also collected from 31 carcasses and were fixed in 10% neutral buffered formalin, embedded in paraffin, and routinely processed for histology (hematoxylin and eosin staining—H&E).

2.3. Bacteriology

The lymph node tissue samples were individually homogenized, decontaminated with 5% sulfuric acid, and subjected to the culture test for the isolation of *Mycobacterium* spp. [28]; each homogenate was inoculated into the Lowenstein–Jensen (LJ) solid medium [28]; the homogenate was also inoculated in the liquid medium of the Bactec 9120 MB system, according to the method reported in the manufacturer's manual.

Growth on solid medium was monitored every week with visual examination. Instead, Bactec system warned the operator of the presence of positive samples by turning on a

warning light. The suspicious colonies, grown during the eight weeks of incubation, were picked up with a needle, placed on a glass slide, and subjected to staining using the Ziehl Neelsen procedure (ZN). Colonies of acid-fast bacteria, fuchsia-colored, were subjected to molecular identification by DNA amplification. The absence of growth of characteristic colonies was interpreted as negative.

2.4. DNA Extraction and IS6110 PCR

The search for *Mycobacterium tuberculosis* complex by direct tissue PCR was performed from the homogenized and decontaminated tissue samples used for culture isolation.

A 200 µL aliquot of homogenized Lymph node sample and tissue was submitted to mechanical lysis using 100 µg of glass beads (100 to 200 µm in diameter) in a Qiagen tissue lyser apparatus for 5 min at 30 Hz. Subsequently, the purification and extraction of the DNA was carried out by using Maxwell® 16 Tissue DNA Purification Kits (Technical handbook) and amplified with the PCR Multiplex technique through the specific amplification of a segment of 209 bp of the IS6110 insertion element according to the technique described by Boniotti et al. (2014) [29].

2.5. Genotyping of Mycobacterium spp. Isolates

For the identification of mycobacteria, BACTEC by-cultures containing colonies referable to *Mycobacterium* spp. and the isolates strains of *Mycobacterium* spp. have undergone DNA amplification with the DNA polymerase chain reaction (PCR) method [28,30–32]. The primers shown in Table 1 have been used for DNA amplification.

Table 1. List of the specific primers used for DNA amplification with PCR method.

***Mycobacterium* Target**	**Name of the Primer**	**Primer Sequencing**	**Target Gene**	**Amplicon Size**
Mycobacterium spp.	Mycgen-F	5′-AGAGTTTGATCCTGGCTCAG-3′	mbp70	1030 bp
	Mycgen-R	5′-TGCACACAGGCCACAAGGGA-3′		
M. tuberculosis complex	TB1-F	5′-GAACAATCCGGAGTTGACAA-3′	mbp70	372 bp
	TB1-R	5′-AGCACGCTGTCAATCATGTA-3′		
M. avium paratuberculosis	DMC1	5′-GATCGGAACGTCGGCTGGTCAGG-3′	IS900	217 bp
	DMC2	5′-GATCGCCTTGCTCATCGCTGCCG-3′		
M. avium avium	Mycgen-F	5′-AGAGTTTGATCCTGGCTCAG-3′	mbp70	180 bp
	Mycav-R	5′-ACCAGAAGACATGCGTCTTG-3′		

2.6. Statistical Analysis

Apparent prevalences of mycobacteria in these badgers were calculated and compared. Data from the Laboratory Information Management System were imported in MS Access® (Microsoft Access 2019, Redmond, Washington, DC, USA), which was used for cleaning and normalizing the dataset. The 95% credibility intervals (95% CI) with the indication of lower (l.c.l.) and upper (u.c.l.) credibility levels were calculated using a Bayesian approach with a beta distribution ($n + 1; n - s + 1$), where n is the total number of tested samples, and s is the tested positive samples [33].

3. Results

The anatomopathological and histological analyses did not reveal the presence of tuberculous lesions in the organs of the examined animals (Figure 2).

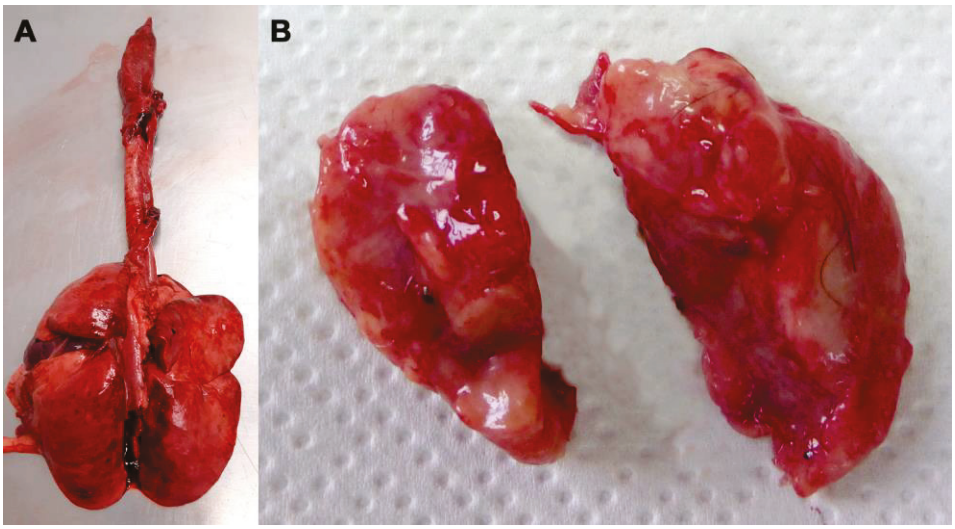


Figure 2. (**A**) Lungs and (**B**) retropharyngeal lymph nodes of road-killed badger without lesion of miliary tuberculosis.

In the 124 carcasses examined, mycobacteria were isolated from four animals (3.22%) (CI 95% 1.3–8.0), *M. avium* subsp. *avium* was isolated by head lymph nodes from two badgers (1.61%) (CI 95% 0.5–5.7), *M. avium* subsp. *paratuberculosis* (0.80%) (CI 95% 0.2–4.4) from one, and *Mycobacterium* spp. from another (0.80%) (CI 95% 0.2–4.4).

The largest number of carcasses was collected along the roads of the province of L'Aquila, near the municipalities of Sulmona and Alfedena, and in the province of Chieti, near the municipality of Guardiagrele and Lanciano, on secondary roads with little traffic (Figure 3). This is consistent with a study conducted in the Abruzzo region by Fabrizio et al. (2019) [34], which observed that the highest roadkill risk for badgers is characterized by intermediate values of both habitat suitability and landscape connectivity on isolated roads with little traffic rather than on large ones.

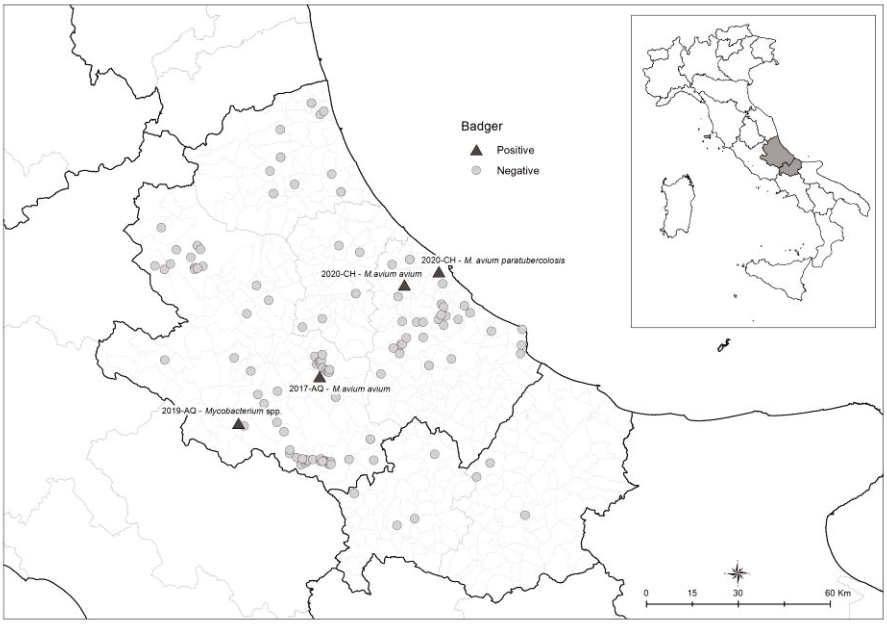


Figure 3. Map of tested and positive badgers in Abruzzo and Molise regions.

The search for *M. tuberculosis* complex from tissue homogenate with the PCR technique has resulted in negative for all the carcasses. The badger's information is reported in Table 2.

Table 2. Characteristics of mycobacteria positive badgers.

General Register Number	Date of Discovery	Municipality of Discovery	Sex	Age	Cause of Death	Tissues Examined	Methods	*Mycobacterium* Species
4860AZ2017	11 September 2017	Introdacqua (AQ)	F	Adult	Road-killed	Head lymph nodes	Culture+; BACTEC-PCR-	*M. avium* subsp. *avium*
4804AZ2019	4 September 2019	Collelongo (AQ)	F	Adult	Road-killed	Head lymph nodes	Culture+; BACTEC+ PCR-	*M.* spp.
41362TE2020	7 May 2020	Ortona (CH)	M	Adult	Predation	Head lymph nodes	Culture+; BACTEC+ PCR-	*M. avium* subsp. *paratuberculosis*
298930TE2020	26 November 2020	Vacri (CH)	M	Young	Road-killed	Head lymph nodes	Culture+; BACTEC+ PCR-	*M. avium* subsp. *avium*
						Mediastinal lymph nodes	Culture-; BACTEC-; PCR-	
						Lung	Histological exam: absence of tubercular lesion	

In the LJ medium, the colonies of the isolate mycobacteria were slow-growing ones (>2 weeks to form visible colonies), initially very small, about 1 mm in diameter, colorless, translucent, and convex with a smooth and shiny surface; after prolonged incubation, the colonies showed an opaque, wrinkled, and raised appearance (Figure 4A). They were ZN-positive staining (Figure 4B).

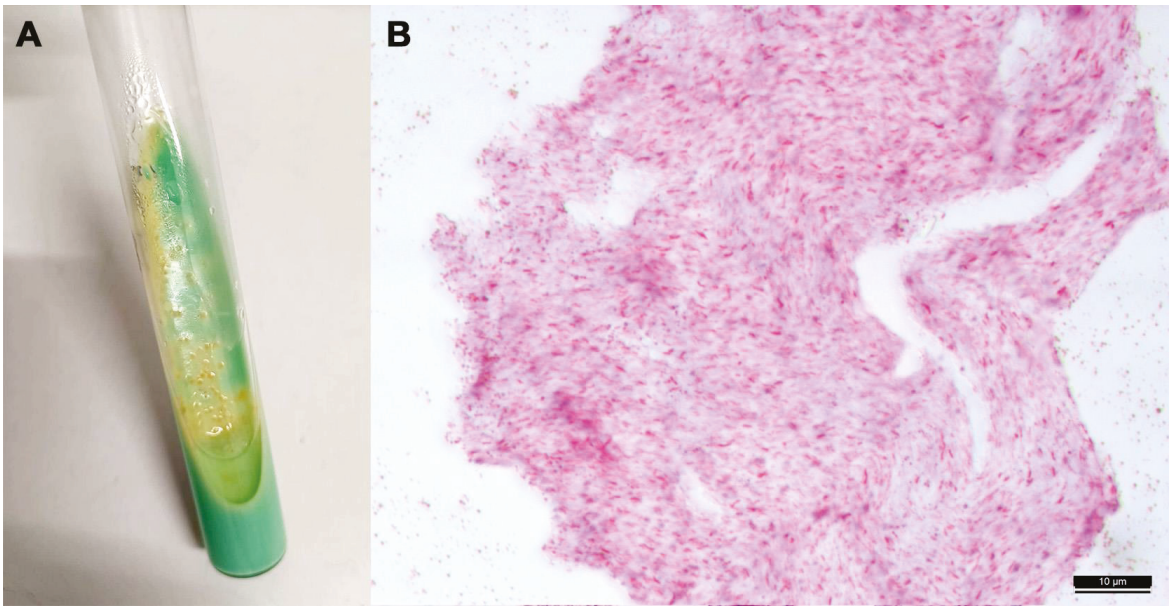


Figure 4. (**A**) Colonies of *Mycobacterium avium* subsp. *avium* grown on Lowenstein–Jensen medium; (**B**) Zielh–Neelsen positive staining of a suspected colony. Microscopic examination of the acid-fast smear reveals cells that are typically short and coccobacillary (100×).

4. Discussion

This study provides evidence of infection with the *M. avium* subsp. *avium* (MAA) and *M. avium* subsp. *paratuberculosis* (*MAP*) in badgers for the first time in Italy.

Infection with the MAC organism causes the formation of purulent, granulomatous, and caseous lesions [35], but no grossly visible lesions and no microscopic granuloma were observed in the four positive badgers identified in this Italian study. The lack of gross lesions in the tissues of the infected animals may be related to the phase of infection or to

the potential resistance to MAA and MAP of this species, as described for *M. bovis*. In all reports on necropsy examinations of badgers, a significant percentage of cases are counted in which there is *M. bovis* in the absence of macroscopic lesions (no visible lesions NVL) [15]. In these reports, from histological findings, *Meles meles* shows a containment phase early in the pathogenesis of the disease, which results in a lengthy period of latency, even including years [15]. Latent cases may never progress further, but in some badgers, this state may be triggered by stressors to a serious disease [15]. In a survey carried out in Spain, the five *M. avium*-positive badgers did not present macroscopic lesions, but on histological examinations of the retropharyngeal and sub-mandibular lymph nodes, they showed small granulomas, positive for mycobacterial antigens [16]. Although acid-fast bacilli were not observed on the ZN staining of the tissue sections, positive immunolabelling for mycobacterial antigens was detected in both macrophages and lymphocytes within granulomas [16].

M. avium subsp. *paratuberculosis* causes a chronic intestinal infection that affects domestic and wild ruminants, but several species were described as susceptible to the disease and reservoirs for transmission between wildlife and domestic animals. Infection is usually acquired through the fecal–oral route, standing the possibility of inter-species transmission through the ingestion of grass contaminated by infected feces from domestic and wildlife animals, especially deer and rabbits [36].

In livestock, MAP can cause serious biological and economic damage. MAP infection has been detected on farms worldwide [37]. Prevalence studies report the presence of MAP in the regions bordering Abruzzo and Molise in ovine farms in the Marche region [38] in sheep and goat farms in Apulia [39] and cow farms in Umbria and five regions of Southern Italy [40,41]. In Italian wildlife, *M. avium* subsp. *paratuberculosis* has been detected in many wild ruminants [42], and in wild boars (*Sus scrofa*) in Sardinia [43]. Paratuberculosis was reported in Europe mainly in cervids. However, the transmission of MAP between rabbits and cattle has been reported, and a high prevalence of paratuberculosis in the wild rabbit population may be associated with a high prevalence in domestic animals [42]. MAP reservoirs may exist locally, but their significance for paratuberculosis control in livestock is quite limited [36].

The most critical aspect derived from MAP and MAA infections in wildlife is the possible interference with tuberculosis diagnosis (skin test); this is thought to be due to the shared antigens between NTM and MTBC [36,44–47]. In Northern Italy, a study suggested a possible inter-species transmission of the same genotype of *M. avium* subsp. *paratuberculosis* among wild red deer (*Cervus elaphus*) and farm cattle, but a whole genome sequencing of isolates is necessary to confirm the data obtained from VNTR typing [48]. The results suggest that all isolates share an identical VNTR profile corresponding to the INMV1 genotype. The only variation was on the locus SSR2, but the utility of this last locus has already been questioned because of its instability [48].

Differently from what has been reported in the United Kingdom, Ireland, France, and Spain, the results obtained in this study suggest that in Central Italy, *M. bovis* does not seem to circulate within the badger population.

In the Abruzzo and Molise regions, *M. bovis* was occasionally found in wildlife. In March 2014, *M. bovis* was isolated from multiple organs of a free-ranging Marsican brown bear (*Ursus Arctos Marsicanus*) and deceased for systemic tuberculosis in the province of L'Aquila, the territory of Abruzzo, Lazio, and Molise National Park. The animal was found alive and showed severe, non-specific clinical signs and died soon after its discovery by park rangers. A presumptive diagnosis of tuberculosis was initially made from gross findings, especially on the enlarged necrotic mesenteric lymph nodes and rectal necrotic plaques. Histopathology confirmed the tubercular nature of the infection, showing specific granulomatous lesions with the presence of acid-fast bacilli. By molecular characterization, this isolate resulted in identical to isolates from an outbreak in semi-free-ranging bovine animals, which had been first detected in June 2012 in the Gioia dei Marsi municipality (AQ) [49]. It was ascertained that *M. bovis*-infected cattle had been grazing in the home

range of this bear since 2012. Some infected bovines died on pastures and were consumed by scavengers [49]. In 2023, *M. bovis* was isolated from the organs of a free-ranging red deer (*Cervus elaphus*) in the same municipality, and its molecular characterization is ongoing [Tieri, personal communication]. In the 2019–2022 period, MTBC bacteria were observed in four wild boars (three from Abruzzo and one from Molise regions), and the molecular identifications are ongoing [Tieri, personal communication].

To maintain the disease-free status from MTBC infection in these territories, a stricter application of health regulations in force is warranted to control the presence of bovine tuberculosis in areas where wildlife and cattle share the same pastures. Trades and the practice of summer translocation to mountain pastures should be fully considered among the risk factors for the introduction of bovine tuberculosis in protected areas [49].

Currently, in Italy, bovine tuberculosis prevalence is variable: regions located in the north and center of the Italian peninsula and in Sardinia are officially recognized as free, including, recently, Abruzzo and Molise (Regulation EU 2021/620 and subsequent amendments) [50], while the highest prevalence is recorded in the south and, above all, in Sicily (5.21%) [51]. In this insular region, where the badger is not present, studies have suggested that the Sicilian black pig (*Sus scrofa*) acts as a reservoir of bovine tuberculosis in the Nebrodi ecosystem (Messina province) [52,53]. The detection of *M. bovis* DNA in swine feces confirmed the active excretion of the pathogen through feces, highlighting the swine's role in environmental contamination [53].

5. Conclusions

Although this study found evidence of MAA and MAP bacteria in badgers, none of the infected animals showed lesions containing a large number of MAC bacilli, so *Meles meles* should not play a role in the epidemiology of MAC in the territory of the Abruzzo and Molise regions under current epidemiological conditions.

However, the detection of MAC in three badgers tested in this study suggests the possibility that this species, in the territories likely to be shared with cattle, could be a vehicle of these bacteria and, therefore, could potentially interfere with the surveillance activities carried out in the context of the National Eradication plan for tuberculosis in cattle. This leads to the possible consideration of the need for a systematical comparative antemortem screening test (skin test or IFN-y test) in the final steps of the eradication program.

Author Contributions: Conceptualization, E.E.T.; data curation, E.E.T., L.M. and K.Z.; formal analysis, E.E.T., L.M., K.Z., C.P., G.D.T., A.C., A.R., M.T., M.T.M. and S.S.; investigation, E.E.T., L.M. and S.S.; methodology K.Z.; resources, K.Z.; supervision E.E.T., L.M., S.S. and F.D.M.; visualization, S.S. and F.D.M.; writing—original draft preparation, E.E.T.; writing—review and editing, E.E.T. and F.D.M. All authors have read and agreed to the published version of the manuscript.

Funding: This research received no external funding.

Institutional Review Board Statement: Not applicable.

Informed Consent Statement: Not applicable.

Data Availability Statement: The data used in this study are the property of Istituto Zooprofilattico Sperimentale dell'Abruzzo e del Molise "G. Caporale", Italy, and thus not publicly available.

Conflicts of Interest: The authors declare no conflicts of interest.

References

1. Tortoli, E.; Fedrizzi, T.; Meehan, C.J.; Trovato, A.; Grottola, A.; Giacobazzi, E.; Serpini, G.F.; Tagliazucchi, S.; Fabio, A.; Bettua, C.; et al. The new phylogeny of the genus *Mycobacterium*: The old and the news. *Infect. Genet. Evol.* **2017**, *56*, 19–25. [CrossRef] [PubMed]
2. van Ingen, J.; Turenne, C.Y.; Tortoli, E.; Wallace, R.J.; Brown-Elliott, B.A. A definition of the *Mycobacterium avium* complex for taxonomical and clinical purposes, a review. *Int. J. Syst. Evol. Microbiol.* **2018**, *68*, 3666–3677. [CrossRef] [PubMed]
3. Gortázar, C.; Ferroglio, E.; Höfle, U.; Frölich, K.; Vicente, J. Diseases shared between wildlife and livestock: A European perspective. *Eur. J. Wildl. Res.* **2007**, *53*, 241–256. [CrossRef]

4. Reis, A.C.; Ramos, B.; Pereira, A.C.; Cunha, M.V. The hard numbers of tuberculosis epidemiology in wildlife: A meta-regression and systematic review. *Transbound. Emerg. Dis.* **2021**, *68*, 3257–3276. [CrossRef]
5. Bourne, F.J.; Donnelly, C.A.; Cox, D.R.; Gettinby, G.; McInerney, J.P.; Morrison, W.I.; Woodroffe, R. *The Scientific Evidence, a Science Base for a Sustainable Policy to Control TB in Cattle, an Epidemiological Investigation into Bovine Tuberculosis*; Final Report of the Independent Scientific Group on Cattle TB; DEFRA: London, UK, 2007; Available online: www.bovinetb.info/docs/final_report.pdf (accessed on 3 April 2023).
6. Corner, L.A.; O'Meara, D.; Costello, E.; Lesellier, S.; Gormley, E. The distribution of *Mycobacterium bovis* infection in naturally infected badgers. *Vet. J.* **2012**, *194*, 166–172. [CrossRef]
7. Byrne, A.W.; Sleeman, D.P.; O'Keeffe, J.; Davenport, J. The ecology of the European badger (*Meles meles*) in Ireland: A review. In *Biology and Environment: Proceedings of the Royal Irish Academy*; Royal Irish Academy: Dublin, Ireland, 2012; pp. 105–132.
8. Swift, B.M.C.; Barron, E.S.; Christley, R.; Corbetta, D.; Grau-Roma, L.; Jewell, C.; O'Cathail, C.; Mitchell, A.; Phoenix, J.; Prosser, A.; et al. Tuberculosis in badgers where the bovine tuberculosis epidemic is expanding in cattle in England. *Sci. Rep.* **2021**, *11*, 20995. [CrossRef] [PubMed]
9. Byrne, A.W.; Kenny, K.; Fogarty, U.; O'Keeffe, J.J.; More, S.J.; McGrath, G.; Teeling, M.; Martin, S.W.; Dohoo, I.R. Spatial and temporal analyses of metrics of tuberculosis infection in badgers (*Meles meles*) from the Republic of Ireland: Trends in apparent prevalence. *Prev. Vet. Med.* **2015**, *122*, 345–354. [CrossRef]
10. Réveillaud, É.; Desvaux, S.; Boschiroli, M.L.; Hars, J.; Faure, É.; Fediaevsky, A.; Cavalerie, L.; Chevalier, F.; Jabert, P.; Poliak, S.; et al. Infection of wildlife by *Mycobacterium bovis* in France assessment through a National Surveillance System, Sylvatub. *Front. Vet. Sci.* **2018**, *5*, 262. [CrossRef]
11. Blanco Vázquez, C.; Barral, T.D.; Romero, B.; Queipo, M.; Merediz, I.; Quirós, P.; Armenteros, J.Á.; Juste, R.; Domínguez, L.; Domínguez, M.; et al. spatial and temporal distribution of *Mycobacterium tuberculosis* Complex infection in Eurasian badger (*Meles meles*) and cattle in Asturias, Spain. *Animals* **2021**, *11*, 1294. [CrossRef]
12. Jacquier, M.; Vandel, J.M.; Léger, F. Breaking down population density into different components to better understand its spatial variation. *BMC Ecol. Evo.* **2021**, *21*, 82. [CrossRef]
13. Revilla, E.; Delibes, M.; Travaini, A.; Palomares, F. Physical and population parameters of the Eurasian badgers (*Meles meles* L.) from Mediterranean Spain. *Z. Saugetierkd.* **1999**, *64*, 269–276.
14. Silva, M.; Rosalino, L.M.; Alcobia, S.; Santos-Reis, M. Sett use, density and breeding phenology of badgers in Mediterranean agro-sylvo-pastoral systems. *Animals* **2021**, *11*, 2663. [CrossRef] [PubMed]
15. Gallagher, J.; Clifton-Hadley, R.S. Tuberculosis in badgers; a review of the disease and its significance for other animals. *Res. Vet. Sci.* **2000**, *69*, 203–217, Erratum in *Res. Vet. Sci.* **2001**, *70*, 179. [CrossRef]
16. Balseiro, A.; Merediz, I.; Sevilla, I.A.; García-Castro, C.; Gortázar, C.; Prieto, J.M.; Delahay, R.J. Infection of Eurasian badgers (*Meles meles*) with *Mycobacterium avium* complex (MAC) bacteria. *Vet. J.* **2011**, *188*, 231–233. [CrossRef]
17. Sistema Informativo Veterinario–Statistiche; Banca Dati Nazionale. Available online: https://www.vetinfo.it/j6_statistiche/#/ (accessed on 23 August 2023).
18. Pigozzi, G.; De Marinis, A.M. Meles meles (Linnaeus, 1758). In *Fauna d'Italia. Mammalia. III. Carnivora–Artiodactyla*; Boitani, L., Lovari, S., Vigna Taglianti, A., Eds.; Calderini: Bologna, Italy, 2003; pp. 158–167.
19. Johnson, D.D.P.; Macdonald, D.W.; Dickman, A.J. Analysis and review of models of the sociobiology of the Mustelidae. *Mammal. Rev.* **2000**, *30*, 171–196. [CrossRef]
20. Balestrieri, A.; Cardarelli, E.; Pandini, M.; Remonti, L.; Saino, N.; Prigioni, C. Spatial organisation of European badger (*Meles meles*) in Northern Italy as assessed by camera-trapping. *Eur. J. Wildl. Res.* **2016**, *62*, 219–226. [CrossRef]
21. Regione Molise. Piano Forestale Regionale. *Studio di Incidenza Ambientale.* 2017. Available online: https://www.regione.molise.it/flex/cm/pages/ServeAttachment.php/L/IT/D/8%252F8%252F6%252FD.d08fdf775275ec8fb3a7/P/BLOB:ID=327/E/pdf?mode=download (accessed on 23 August 2023).
22. Pirone, G.; Frattaroli, A.R.; Ciaschetti, G.; Di Martino, L. La vegetazione d'Abruzzo. In *Abruzzo Rapporto Sullo Stato Dell'Ambiente 2018*; Carsa: Pescara, Italy, 2018; pp. 159–200. Available online: https://www.artaabruzzo.it/download/pubblicazioni/relaz_stato_ambiente_abruzzo_2018.pdf (accessed on 23 August 2023).
23. Bern Convention. Convention on the Conservation of European Wildlife and Natural Habitats. Treaty No. 104. Convention on the Conservation of European Wildlife and Natural Habitats. Council of Europe, 1979. Available online: www.coe.int/en/web/bern-convention/ (accessed on 2 April 2023).
24. National Law (Italy) n. 503, 05/08/1981. Ratifica ed Esecuzione della Convenzione Relativa alla Conservazione Della vita Selvatica e Dell'ambiente Naturale in Europa, Con Allegati, Adottata a Berna il 19 Settembre 1979. Off. J. 250, 11/09/1981. Available online: https://www.normattiva.it/uri-res/N2Ls?urn:nir:stato:legge:1981-08-05;503 (accessed on 23 August 2023).
25. Anderson, R.M.; Trewhella, W. Population dynamics of the badger (*Meles meles*) and the epidemiology of bovine tuberculosis (*Mycobacterium bovis*). *Philos. Trans. R. Soc. Lond. B Biol. Sci.* **1985**, *310*, 327–381.
26. Bertusi, M.G.; Tosetti, T. Tasso (*Meles meles*). In *Mammiferi d'Italia*; Grafis: Bologna, Italy, 1986.
27. Delahay, R.J. A forensic investigation of *Mycobacterium bovis* infection in badgers. *Vet. J.* **2012**, *194*, 135–136. [CrossRef]
28. World Organization for Animal Health. Bovine Tuberculosis. In *Manual of Diagnostic Tests and Vaccines for Terrestrial Animals*; OIE: Paris, France, 2018; pp. 1058–1074.

29. Boniotti, M.B.; Gaffuri, A.; Gelmetti, D.; Tagliabue, S.; Chiari, M.; Mangeli, A.; Spisani, M.; Nassuato, C.; Gibelli, L.; Sacchi, C.; et al. Detection and molecular characterization of *Mycobacterium microti* isolates in wild boar from Northern Italy. *J. Clin. Microbiol.* **2014**, *52*, 2834–2843. [CrossRef]
30. Collins, D.M.; Stephens, D.M.; de Lisle, G.W. Comparison of polymerase chain reaction tests and faecal culture for detecting *Mycobacterium paratuberculosis* in bovine faeces. *Vet. Microbiol.* **1993**, *36*, 289–299. [CrossRef]
31. Kulski, J.K.; Khinsoe, C.; Pryce, T.; Christiansen, K. Use of a multiplex PCR to detect and identify *Mycobacterium avium* and *M. intracellular* in blood culture fluids of AIDS patients. *J. Clin. Microbiol.* **1995**, *33*, 668–674. [CrossRef] [PubMed]
32. Wilton, S.; Cousins, D. Detection and identification of multiple mycobacterial pathogens by DNA amplification in a single tube. *PCR Methods Appl.* **1992**, *1*, 269–273. [CrossRef] [PubMed]
33. Sivia, D.S. *Data Analysis: A Bayesian Tutorial*; Oxford University Press: Oxford, UK, 1996.
34. Fabrizio, M.; Di Febbraro, M.; D'Amico, M.; Frate, L.; Roscioni, F.; Loy, A. Habitat suitability vs. landscape connectivity determining roadkill risk at a regional scale: A case study on European badger (*Meles meles*). *Eur. J. Wildl. Res.* **2019**, *65*, 7. [CrossRef]
35. Glawischnig, W.; Steineck, T.; Spergser, J. Infections caused by *Mycobacterium avium* subspecies *avium*, *hominissuis*, and *paratuberculosis* in free-ranging red deer (*Cervus elaphus hippelaphus*) in Austria, 2001–2004. *J. Wildl. Dis.* **2006**, *42*, 724–731. [CrossRef] [PubMed]
36. Carta, T.; Álvarez, J.; Pérez de la Lastra, J.M.; Gortázar, C. Wildlife and paratuberculosis: A review. *Res. Vet. Sci.* **2013**, *94*, 191–197. [CrossRef]
37. Whittington, R.; Donat, K.; Weber, M.F.; Kelton, D.; Nielsen, S.S.; Eisenberg, S.; Arrigoni, N.; Juste, R.; Sáez, J.L.; Dhand, N.; et al. Control of paratuberculosis: Who, why and how. A review of 48 countries. *BMC Vet. Res.* **2019**, *15*, 198. [CrossRef]
38. Attili, A.R.; Ngu Ngwa, V.; Preziuso, S.; Pacifici, L.; Domesi, A.; Cuteri, V. Ovine paratuberculosis: A seroprevalence study in dairy flocks reared in the Marche region, Italy. *Vet. Med. Int.* **2011**, *2011*, 782875.
39. Iarussi, F.; Paradies, P.; Sardaro, R.; Rubino, G.; Scaltrito, D.; Pieragostini, E.; Petazzi, F. Epidemiology and risk factors of *Mycobacterium avium* subspecies *paratuberculosis* in semi-extensive dairy sheep and goat farms of Apulia, Southern Italy. *Small Rumin. Res.* **2019**, *177*, 89–96. [CrossRef]
40. Cenci-Goga, B.T.; Vescera, F.; Paolotto, P.; McCrindle, C.M.; Roberti, U. Seroprevalence of *Mycobacterium avium* subspecies *paratuberculosis* in cows in Umbria, Italy. *Vet. Rec.* **2010**, *167*, 577–578. [CrossRef]
41. Marchetti, G.; Ricchi, M.; Serraino, A.; Giacometti, F.; Bonfante, E.; Arrigoni, N. Prevalence of *Mycobacterium avium* subsp. *paratuberculosis* in milk and dairy cattle in Southern Italy: Preliminary results. *Ital. J. Food Saf.* **2013**, *2*, e35. Available online: https://www.pagepressjournals.org/index.php/ijfs/article/view/ijfs.2013.e35 (accessed on 23 August 2023).
42. Fanelli, A.; Buonavoglia, D.; Pleite, C.M.C.; Tizzani, P. Paratuberculosis at European scale: An overview from 2010 to 2017. *Vet. Ital.* **2020**, *56*, 13–21.
43. Zanetti, S.; Bua, A.; Molicotti, P.; Delogu, G.; Mura, A.; Ortu, S.; Sechi, L.A. Identification of mycobacterial infections in wild boars in Northern Sardinia, Italy. *Acta Vet. Hung.* **2008**, *56*, 145–152. [CrossRef] [PubMed]
44. Barry, C.; Corbett, D.; Bakker, D.; Andersen, P.; McNair, J.; Strain, S. The effect of *Mycobacterium avium* Complex infections on routine *Mycobacterium bovis* diagnostic tests. *Vet. Med. Int.* **2011**, *2011*, 145092. [CrossRef] [PubMed]
45. Byrne, A.W.; Graham, J.; Milne, G.; Guelbenzu-Gonzalo, M.; Strain, S. Is there a relationship between bovine Tuberculosis (bTB) herd breakdown risk and *Mycobacterium avium* subsp. *paratuberculosis* status? An investigation in bTB chronically and non-chronically infected herds. *Front. Vet. Sci.* **2019**, *6*, 30. [PubMed]
46. Picasso-Risso, C.; Grau, A.; Bakker, D.; Nacar, J.; Mínguez, O.; Perez, A.; Alvarez, J. Association between results of diagnostic tests for bovine tuberculosis and Johne's disease in cattle. *Vet. Rec.* **2019**, *185*, 693. [CrossRef]
47. Stabel, J.R.; Waters, W.R.; Bannantine, J.P.; Palmer, M.V. Comparative cellular immune responses in calves after infection with *Mycobacterium avium* subsp. *paratuberculosis*, *M. avium* subsp. *avium*, *M. kansasii* and *M. bovis*. *Vet. Immunol. Immunopathol.* **2021**, *237*, 110268. [CrossRef]
48. Galiero, A.; Leo, S.; Garbarino, C.; Arrigoni, N.; Russo, S.; Giacomelli, S.; Bianchi, A.; Trevisiol, K.; Idrizi, I.; Daka, G.; et al. Mycobacterium aviumsubsp. paratuberculosis isolated from wild red deer (*Cervus elaphus*) in Northern Italy. *Vet Microbiol.* **2018**, *217*, 167–172. [CrossRef]
49. Fico, R.; Mariacher, A.; Franco, A.; Eleni, C.; Ciarrocca, E.; Pacciarini, M.L.; Battisti, A. Systemic tuberculosis by MYCOBACTERIUM BOVIS in a free-ranging MARSICAN brown bear (URSUS ARCTOS MARSICANUS): A Case report. *BMC Vet. Res.* **2019**, *15*, 152. [CrossRef]
50. European Regulation EU 2021/620 Commission Implementing Regulation (EU) 2021/620 of 15 April 2021 Laying Down Rules for the Application of Regulation (EU) 2016/429 of the European Parliament and of the Council as Regards the Approval of the Disease-Free and Non-Vaccination Status of Certain Member States or Zones or Compartments Thereof as Regards Certain Listed Diseases and the Approval of Eradication Programmes for Those Listed Diseases. Available online: https://eur-lex.europa.eu/legal-content/EN/TXT/?uri=CELEX:02021R0620-20231127 (accessed on 21 December 2023).
51. Abbate, J.M.; Arfuso, F.; Iaria, C.; Arestia, G.; Lanteri, G. Prevalence of Bovine Tuberculosis in Slaughtered Cattle in Sicily, Southern Italy. *Animals* **2020**, *10*, 1473. [CrossRef]

52. Di Marco, V.; Mazzone, P.; Capucchio, M.T.; Boniotti, M.B.; Aronica, V.; Russo, M.; Fiasconaro, M.; Cifani, N.; Corneli, S.; Biasibetti, E.; et al. Epidemiological significance of the domestic black pig (*Sus scrofa*) in maintenance of bovine tuberculosis in Sicily. *J. Clin. Microbiol.* **2012**, *50*, 1209–1218. [CrossRef]
53. Amato, B.; Di Marco Lo Presti, V.; Gerace, E.; Capucchio, M.T.; Vitale, M.; Zanghì, P.; Pacciarini, M.L.; Marianelli, C.; Boniotti, M.B. Molecular epidemiology of Mycobacterium tuberculosis complex strains isolated from livestock and wild animals in Italy suggests the need for a different eradication strategy for bovine tuberculosis. *Transbound. Emerg. Dis.* **2018**, *65*, e416–e424. [CrossRef] [PubMed]

Disclaimer/Publisher's Note: The statements, opinions and data contained in all publications are solely those of the individual author(s) and contributor(s) and not of MDPI and/or the editor(s). MDPI and/or the editor(s) disclaim responsibility for any injury to people or property resulting from any ideas, methods, instructions or products referred to in the content.

animals

MDPI

Case Report

Adhesive Bowel Obstruction (ABO) in a Stranded Narrow-Ridged Finless Porpoise (*Neophocaena asiaeorientalis sunameri*)

Sung Bin Lee [1,†], Adams Hei Long Yuen [1,2,†], Young Min Lee [1], Sang Wha Kim [3,4], Sunmin Kim [5], Cherry Tsz Ching Poon [6], Won Joon Jung [1], Sib Sankar Giri [1], Sang Guen Kim [7], Su Jin Jo [1], Jae Hong Park [1], Mae Hyun Hwang [1], Jong-pil Seo [8], Seongjun Choe [5], Byung Yeop Kim [9,*] and Se Chang Park [1,*]

[1] Laboratory of Aquatic Biomedicine, College of Veterinary Medicine, Research Institute for Veterinary Science, Seoul National University, Seoul 08826, Republic of Korea; lsbin1129@snu.ac.kr (S.B.L.); mushhama@snu.ac.kr (Y.M.L.); cwj0125@snu.ac.kr (W.J.J.); ssgiri@snu.ac.kr (S.S.G.); ssjjone@snu.ac.kr (S.J.J.); jaehong139@snu.ac.kr (J.H.P.); ghkdao@snu.ac.kr (M.H.H.)
[2] Radiotherapy and Oncology Centre, Gleneagles Hospital Hong Kong, Wong Chuk Hang, Hong Kong SAR, China; yhladams@hotmail.com
[3] Department of Microbiology and Immunology, Institute of Endemic Disease, College of Medicine, Seoul National University, Seoul 03080, Republic of Korea; sangwhakim@kangwon.ac.kr
[4] College of Veterinary Medicine, Institute of Veterinary Science, Kangwon National University, Chuncheon 24341, Republic of Korea
[5] Department of Parasitology, Parasite Research Center, International Parasite Resource Bank, School of Medicine, Chungbuk National University, Cheongju 28644, Republic of Korea; xsunminx@gmail.com (S.K.); vetazmo@gmail.com (S.C.)
[6] Department of Surgery, Queen Mary Hospital, Pokfulam, Hong Kong SAR, China; poontccherry@gmail.com
[7] Department of Biological Sciences, Kyonggi University, Suwon 16227, Republic of Korea; imagine0518@kyonggi.ac.kr
[8] College of Veterinary Medicine, Veterinary Medical Research Institute, Jeju National University, Jeju 63243, Republic of Korea; jpseo@jejunu.ac.kr
[9] Department of Marine Industry and Maritime Police, College of Ocean Science, Jeju National University, Jeju 63243, Republic of Korea
* Correspondence: kimby@jejunu.ac.kr (B.Y.K.); parksec@snu.ac.kr (S.C.P.)
† These authors contributed equally to this study.

Simple Summary: This study demonstrates the clinical and radiological presentation of intestinal adhesions and obstructions in a stranded narrow-ridged finless porpoise and discusses the possible cause of death. The main reason for the intestinal lesions was likely related to parasitic infection; however, further studies should be conducted to determine the relationship between parasitic infections and adhesive bowel obstruction. This is the first case study report of intestinal adhesions and obstructions in a narrow-ridged finless porpoise, and it provides a valuable reference for confirming a diagnosis of adhesive bowel obstruction using post-mortem computed tomography (PMCT).

Abstract: In this case report, we present a rare occurrence of a narrow-ridged finless porpoise (*Neophocaena asiaeorientalis sunameri*), discovered on the coast of Jeju Island, Republic of Korea, that was afflicted with adhesive bowel obstruction (ABO), a life-threatening condition that has scarcely been reported in cetaceans. Diagnosis of ABO was confirmed via radiological and clinical assessments. Post-mortem computed tomography and necropsy revealed ABO between two loops of the jejunum at the L8 level. The mesenteric tissue covering the intestinal lesion was severely thickened with increased tension. Both bowel loops were fixed to the mesentery and acutely angulated, leading to asymmetrical thickening of the cross-sectional bowel walls. The intestinal lumen was stenosed because of pressure from the firm mesenteric band, and no fecal matter was observed in the lumen of the posterior bowel or rectum. Calcified nodules were detected, and histological analysis suggested parasitic or suspected post-parasitic infections. The primary cause of the intestinal lesions is presumed to be a reaction related to parasitic infection. However, further investigations would establish a definitive

link between parasitic infections and ABO in this species. This case highlights the importance of studying rare medical conditions in wildlife, providing valuable insights into marine mammal health.

Keywords: adhesive bowel obstruction; intestinal adhesion; stenosis; diagnostic imaging techniques; narrow-ridged finless porpoise; *Neophocaena asiaeorientalis sunameri*; cetaceans

1. Introduction

Cetaceans have a long gastrointestinal (GI) tract, enabling them to feed on prey of lower caloric value [1], whereas their intestines possess a dependent blood supply from the aorta via the mesenteric artery. However, the long course of the GI tract and the highly mobile mesenteric arterial supply are prone to adhesive bowel obstruction (ABO), which can result in fatal intestinal necrosis and sudden death [2,3].

Unlike domestic animals that often attract greater research attention, ABO is difficult to be detected and measured in wildlife, particularly in cetaceans. Most published records related to ABO in cetaceans were discovered using surgery in captive animals [4] or necropsy in wild animals [5,6]. The study of wildlife health is confronted with numerous impediments, including limitations in the available materials, the behavioral aspects of the animals, as well as considerations in zoology and ecology [7,8]. Consequently, the underlying pathogenesis of this disease in cetaceans is still not fully understood. To seek better understanding of the causes of death and underlying pathology, cetaceans stranded in South Korean waters have been routinely assessed using post-mortem computed tomography (PMCT) to provide additional information complementing the findings of conventional necropsy [9,10]. In this case report, we present a case of ABO in a stranded narrow-ridged finless porpoise and demonstrate the relevant necropsy and PMCT findings.

2. Case Description

On 14 December 2021, an adult female narrow-ridged finless porpoise (NRFP) (154.8 cm) was stranded on the northern coast of Jeju Island in the Republic of Korea (33°52.667′ N 126°56.450′ E; Figure 1). The carcass was fresh, and no scavengers were found upon retrieval (code 2) [11]. To minimize post-mortem changes, the carcass was immediately transported to the freezer at the College of Ocean Science (Jeju National University, Jeju-si, Jeju-do, Republic of Korea) upon retrieval, and frozen at −22 °C until further examination. Ethical review and approval were not required because this study did not alter aspects of the animal's life.

The PMCT was performed using an Aquilion Lightning 16-row, 32-slice helical CT system (Aquilion Lightning, Canon Medical Systems, Otawara, Japan). The scanning parameters were set to 120 kVp and 200 mAs, with a 1 mm slice thickness, and the scanned field of view (sFOV) was 600 mm. The reconstructed PMCT images were assessed using the open-source Digital Imaging and Communications in Medicine (DICOM) viewing software Horos, version 3.3.6 (RRID:SCR_017340). The PMCT multiplanar reconstruction imaging revealed calcified lesions in the gastric wall, rectus abdominis, and left mammary gland, suggesting systemic parasitic infections.

Using a pulmonary image window (WL-500/WW1400), an extensive ground-glass opacity pattern associated with pulmonary infection was observed in both lungs. Gas accumulation was observed in the pleural cavity and pericardium, which led to the suspicion of pneumothorax and pneumopericardium, respectively. The stomach contents were observed, indicating that the porpoise actively foraged before death (Figure 2B); however, the bowel was empty.

The acute-angled pattern of the intestine (approximately at the L8 level) made up of proximal dilated and distal collapsed bowel loops, with one transition point, was observed (Figure 2C, yellow arrow), which was suggestive of ABO being caused by matted adhesions (WL300/WW3500). Mild hyperattenuation, representing fibrotic scar tissue, was observed at the mesentery where adhesion occurred (Figure 2D) (WL16/WW3500). Radiological

findings suggested that the intestinal loop of the carcass may have experienced a resolved intestinal infection.

Necropsy of the carcass was performed at the Jeju office of the Korea Fisheries Resources Agency (FIRA; Hallim-eup, Jeju, Republic of Korea) on 20 July 2022. During the necropsy of the NRFP, all samples that were suspected to contribute to the cause of death were preserved in 70% ethanol and/or 10% neutral buffered formalin for molecular analysis and histopathological examination, respectively. All the collected samples were transported to the Laboratory of Aquatic Biomedicine (LAB; Seoul National University, Gwanak-gu, Seoul, Republic of Korea), and further analyzed. The formalin-fixed lesions were cut into appropriate sizes, and tissue slides were produced by the Korea Vet Lab (Seongnam, Korea). The samples were embedded into paraffin and sectioned into 5 µm. The sliced tissues were stained using hematoxylin and eosin (H&E), gram, PAS, and Perls Prussian blue to detect histological changes. All tissue slides were analyzed by veterinary pathologists (Antech Diagnostics, Fountain Valley, CA, USA). Parasites were isolated and collected from the tympanic bullae, lungs, liver, gastrointestinal tract, and left mammary glands. Species identification of the parasites was conducted using morphological and genetic analysis at the Parasite Research Center and International Parasite Resource Bank (Chungbuk National University, Seowon-gu, Cheongju, Republic of Korea) [12,13].

Foamy fluid was not observed in the respiratory system. Tension pneumothorax was observed in both lungs, particularly in the left lung. Multiple firm nodules were isolated from the muscles near the left mammary gland (2.9 × 3.7 cm), the outer wall of the forestomach (1.85 × 1.4 cm; 2.3 × 1.1 cm), and the peritoneum (6.0 × 3.1 cm; 4.0 × 3.2 cm) near the genital slit. Based on molecular examination, the nodules near the left mammary gland and peritoneum were identified as *Crassicauda* sp. remains among caseous debris [14]. Although parasitic infection in the forestomach nodules was confirmed in histopathological examination, the species was not identified. The nematode *Anisakis* sp. larvae were identified in the stomachs of the NRFP. The intestine exhibited the presence of *Anisakis* sp. larvae, *Diphyllobothrium fuhrmanni*, and *Synthesium nipponicum*.

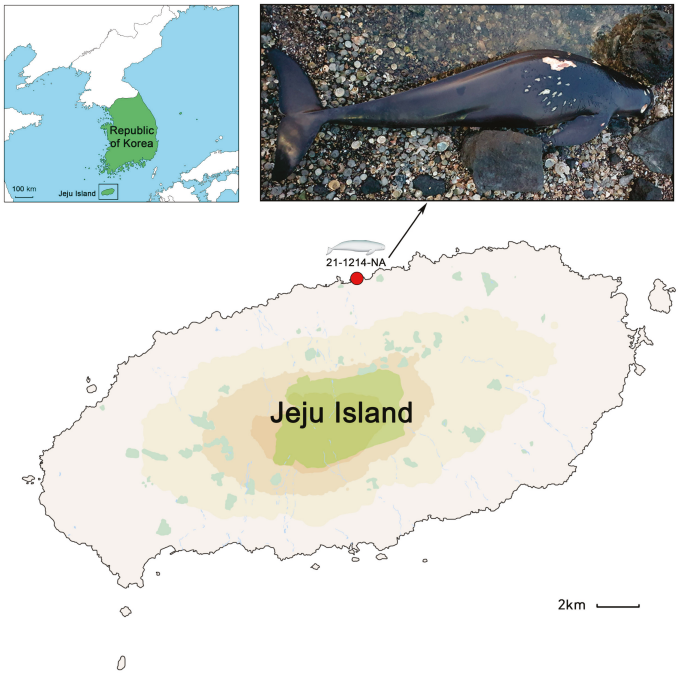


Figure 1. The stranding location of specimen 21-1214-NA. The carcass was discovered on the beach near Hwabukpogu Port Lighthouse in fresh condition (33°52.667′ N 126°56.450′ E).

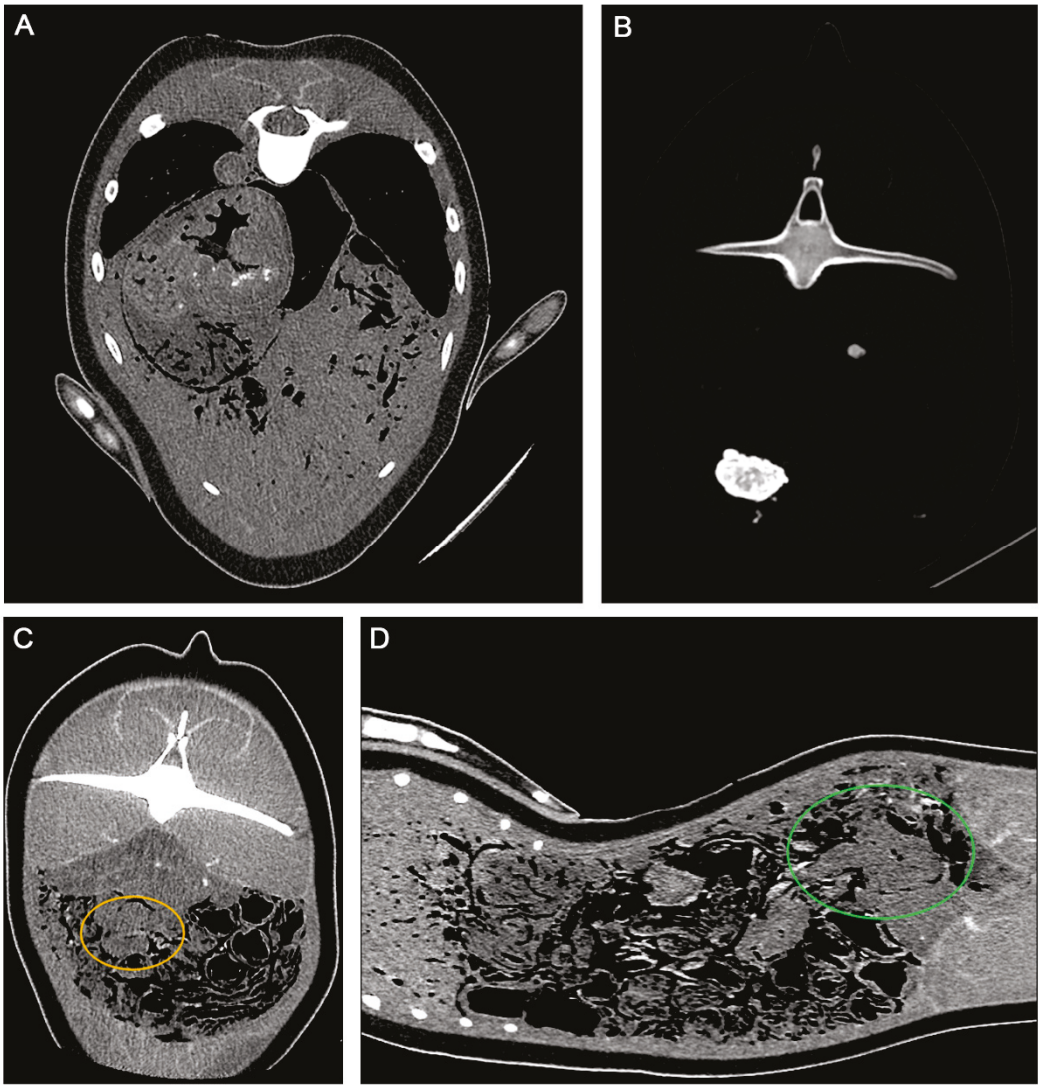


Figure 2. Post-mortem computed tomography (PMCT) images of the individual with suspicion of intestinal adhesion: (**A**) axial PMCT image (WL330/WW830) showing multiple hyperattenuated lesions secondary to parasitic infections. The lesion was an intramuscular nodule near the left mammary gland. (**B**) Using an abdominal PMCT algorithm (WL40/WW350), the forestomach content was observable in a coronal PMCT image, suggesting that the porpoise was actively foraging before death. (**C**) Axial PMCT image (WL40/WW350) showing acute angulation of both bowel loops (orange circle). (**D**) Coronal PMCT image (WL40/WW350) showing mild hyperattenuation in the stenosed intestine, suggestive of fibrotic scar tissue (green circle).

Congestion was observed in the pyloric sphincter of the fundic stomach, which was enlarged. Enteroenteric adhesions were observed between the anterior and posterior jejunum loops (Figure 3A). Two small bowel loops were stenosed (Figure 3B) by the firm mesentery band, which was severely thickened and indurated with increased tension, acute angulation, and asymmetrical wall thickening (Figure 3C,D). The anterior small bowel before the adhesion point demonstrated an enlarged sign, whereas the posterior parts showed normal signs without fecal matter. The transverse sections of the adhered intestines showed inflammation in the serosa layer, which was chronically encapsulated by central inflammatory cells and cellular debris (Figure 3E). No pathogens were identified upon histological examination. In the thickened mesentery band, agglomerates of pigment-loaded macrophages (Figure 3F) were observed. Microabscesses, which are possible traces

of migrating parasites [15], were scattered throughout the tissue with mineralization. Finally, no parasites were detected.

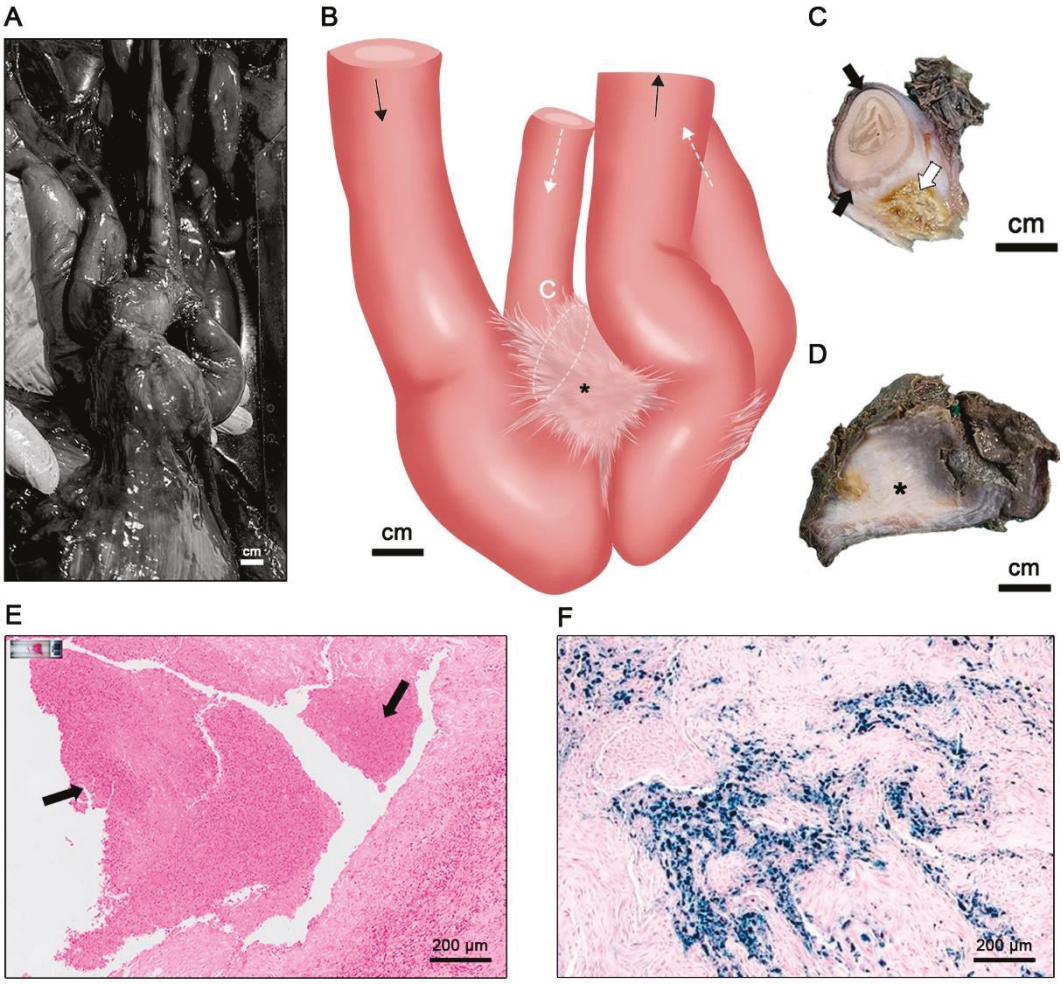


Figure 3. The intestinal lesions of 21-1214-NA. (**A**,**B**) Enteroenteric adhesion was observed between two loops of the anterior and posterior jejunum (**B** was illustrated by S.B.L.). The direction of passage of intraluminal food is indicated by arrows, with black arrows representing the anterior jejunum and white arrows representing the posterior jejunum. The adhesive mesenteric lesion is denoted by an asterisk (*). The loops demonstrated stenosis with (**C**) acute angulation by (**D**) the thickened mesentery band with the adhesive lesion indicated by an asterisk (*). Cross-sectioned intestine loops had asymmetrical thickening of the wall (black arrows in (**C**)) and the mesentery was filled with calcified material (white arrow in (**C**)). Inflammatory cells were centrally infiltrated in the serosa layer of the loops (black arrows in (**E**)). No pathogen was identified in gross examination. (**F**) In the thickened mesentery band, agglomerates of hemosiderin-loaded macrophages were found using Perls Prussian blue staining.

3. Discussion

In mammals, extensive reports have indicated that ABO is associated with cardinal symptoms such as acute or chronic abdominal pain, vomiting, and decreased oral input [16–18]. We believe that these complications may have also affected the NRFP in the present report. The NRFP may have suffered from persistent abdominal pain as a result of ABO. This would have caused the NRFP to regurgitate and vomit whenever it consumed food, and this would be evidenced by fundic gastritis, the presence of stomach content, and the absence of bowel content. Eventually, failure of food passage through the stomach to

the bowel would have led to inanition, electrolyte depletion, and consequently, the death of the NRFP [19].

Mesenteric fibrosis and stenosis caused by chronic hemorrhage were observed in the reported NRFP, as evidenced by the presence of hemosiderin-loaded macrophages [20]. The etiology of mesenteric fibrosis and stenosis in cetaceans remains incompletely understood, primarily attributed to the scarcity of pertinent disease cases and information. It is hypothesized, however, that localized injury to the mesentery and consequent inflammation may trigger the activation of the fibrinocoagulative pathway [21]. The activated cellular turnover triggers increased infiltration of inflammatory cells and fibrinogen deposition. Consequently, the formation of a fibrous matrix, infiltration of fibroblasts, and consequent fibrin formation lead to permanent adhesion. In the presently reported NRFP, no external scarring was found on the body, indicating mesenteric fibrosis and stenosis resulting from traumatic injury could be ruled out.

The parasitic reaction resulting from *Crassicauda* sp. or *Anisakis* sp. infection could also have been a potential contributing factor to the mesenteric fibrosis and stenosis in this NRFP. This supposition is based on the presence of the parasite within the peritoneum and muscles near the mammary glands, as well as the existence of multiple parasitic or post-parasitic nodules and cysts throughout the body [22,23]. While previous studies have primarily classified *Crassicauda* spp. as endoparasites, they have demonstrated the ability to infect tissues or organs outside their typical habitats [24]. For instance, in Cuvier's beaked whales (*Ziphius cavirostris*), mesenteric arteritis caused by *Crassicauda* sp. infection led to jejunum–mesentery adhesions [25]. In contrast, prior studies have reported instances of small bowel obstruction in humans resulting from acute enteric anisakiasis following the consumption of raw seafood [26,27]. Enteric anisakiasis is a rare occurrence, accounting for 4.1% of human anisakiasis cases [28], and the symptoms observed in these human cases align with those identified in the NRFP of this study, including focal stenosis, wall thickening, and inflammatory changes in the jejunum. Although direct parasitic invasion of the bowel wall was not observed in the intestinal lesions of the NRFP, the occurrence of ABO could be attributed to an acute anaphylactic allergic reaction [29], given the presence of *Anisakis* sp. larvae in the intestine, a rarity in this species as well. However, further investigations are necessary to establish a causal link between intestinal adhesions, parasitic infections, and the life cycle of *Crassicauda* spp. and *Anisakis* spp. in narrow-ridged finless porpoises (*N. asiaeorientalis sunameri*).

In recent years, active research has been conducted on the indirect assessment of wildlife disease processes in free-ranging wild animals using various techniques such as satellite remote sensing, camera traps, and echolocation signals [30–32]. However, the underwater environment presents physical and technical challenges such as limited visibility, underwater acoustic sensor networks, and wireless equipment setup difficulties [33–35]. Particularly, in the case of finless porpoises, the absence of dorsal fins and their inconspicuous swimming behavior, scarcely exhibiting aerial body parts, pose significant limitations in disease monitoring, contributing to a slower pace of research compared to terrestrial animal disease assessments [36]. Due to these limitations, we are conducting disease-monitoring examinations using cetacean carcasses. Specifically, post-mortem computed tomography (PMCT) has emerged as a standard initial screening procedure for cetaceans in Korean waters. It provides non-invasive assessment and strong evidence to demonstrate various pathological conditions in cetaceans. The datasets obtained from PMCT can be easily stored digitally, allowing requests for a second opinion or retrospective examination. However, the diagnosis of ABO using PMCT is highly dependent on the operator. The best practice for diagnosing ABO is using CT scanning with contrast media to enhance the density differences between lesions and the surrounding parenchyma. Contrast-enhanced post-mortem computed tomography requires a roller pump to allow good perfusion of the blood vessels and to ease the visibility of ABO. Unfortunately, the imaging center does not currently have a roller pump, making the application of contrast media impossible in this case. Therefore, the operators must be familiar with the anatomy of NRFPs, as well as

the use of PMCT reconstruction techniques, to accurately locate the affected site. In this study, PMCT procedures and image evaluations were performed under the guidance of a board-certified radiographer (A.H.L.Y.) with over 7 years of experience in post-mortem cetacean imaging. It is crucial that operators are accurately trained to implement the diagnostic capabilities of computed tomography to diagnose ABO in cetaceans.

To the best of our knowledge, the published literature lacks any reference to the applicability of imaging modalities in diagnosing intestinal adhesion and stenosis in NRFPs. Computed tomography is a frequently used modality for identifying intestinal adhesions in humans. It can be used to track the level of intestinal adhesion by identifying the "whirl" sign, the fat notch sign, the beak sign, and the small bowel feces sign [37]. Together with the cardinal symptoms of intestinal obstruction such as abdominal pain, nausea or vomiting, and absolute constipation, diagnosis of intestinal adhesions in living organisms can be much more straightforward. However, in the case of a dead organism, obtaining information regarding clinical symptoms becomes impossible. In the present study, our group adopted the PMCT workflow and imaging parameters with reference to Yuen et al. [9,10] for the diagnosis of abdominal gas embolism and upper aerodigestive tract obstruction. We found that mesenteric fibrosis was a significant radiological sign to propose the presence of intestinal adhesion, which was confirmed via necropsy. In the future, research should be directed at obtaining a standardized CT imaging sign for the diagnosis of intestinal adhesion.

Cetaceans serve as umbrella species at the top of the marine ecosystem [38,39], playing a crucial role as keystone species that define the entire environmental conditions [40], including various factors such as micro-plastics, contaminants, epidemics, and pollution [41,42]. However, the NRFP is currently listed as an endangered species on the International Union for Conservation of Nature (IUCN) Red List, reflecting a significant decline in its population in recent years [43]. To address this issue, it is imperative to establish a continuous monitoring system for the NRFP population and the emergence of diseases within the marine environment of Korean seawater. This case report aims to contribute to further veterinary studies of NRFPs by providing insights into the pathology and living conditions of NRFPs in the Korean sea.

4. Conclusions

This case report documents ABO in an NRFP, and it uses PMCT as an adjunct to confirm this fatal condition, which we diagnosed via necropsy. PMCT has emerged as a standard initial screening procedure and non-invasive assessment for cetaceans in Korean seawaters. The findings highlight the merit of utilizing CT for the identification of ABO in cetaceans; therefore, this report will serve as a reference for the diagnosis of ABO in live or dead cetaceans. The etiology of this ABO case is postulated to involve parasitic infection, akin to instances in humans; however, this remains unclear, necessitating further investigation. The health and pathology of the population of NRFPs in Korean seawater, classified as an endangered species, should undergo continuous monitoring. We believe that this study can offer insights for further comprehensive investigations.

Author Contributions: Conceptualization, S.C.P., B.Y.K., S.B.L. and A.H.L.Y.; methodology, S.B.L., A.H.L.Y., S.S.G., S.G.K., J.-p.S., S.C. and B.Y.K.; data curation and formal analysis, S.B.L., A.H.L.Y., Y.M.L., S.W.K., S.K., C.T.C.P., W.J.J., S.J.J., J.H.P. and M.H.H.; writing—original draft preparation, S.B.L. and A.H.L.Y.; writing—review and editing, B.Y.K. and S.C.P. All authors have read and agreed to the published version of the manuscript.

Funding: This study was supported by the National Research Foundation of Korea (NRF2022R1A2C100811412).

Institutional Review Board Statement: Ethical review and approval were waived for this study since this necropsy study did not alter aspects of the animal's life.

Informed Consent Statement: Not applicable.

Data Availability Statement: Substantial research data from this study have been presented in the paper. Access to original data is available on request.

Acknowledgments: We thank Jeju's conservation efforts as a part of the Jeju Islands Cetacean Stranding Network. We thank Byung Yeop Kim at the Department of Marine Industry and Maritime Police, the College of Ocean Science, Jeju National University, and Se Chang Park at the College of Veterinary Medicine and Research Institute for Veterinary Science, Seoul National University, for their suggestions and discussion.

Conflicts of Interest: The authors declare no conflict of interest. The funders had no role in the design of the study; in the collection, analyses, or interpretation of data; in the writing of the manuscript; or in the decision to publish the results.

References

1. Estes, J.A. (Ed.) *Whales, Whaling, and Ocean Ecosystems*; University of California Press: Berkeley, CA, USA, 2006.
2. Begeman, L.; Leger, J.S.; Blyde, D.J.; Jauniaux, T.P.; Lair, S.; Lovewell, G.; Raverty, S.; Seibel, H.; Siebert, U.; Staggs, S.L.; et al. Intestinal volvulus in cetaceans. *Vet. Pathol.* **2012**, *50*, 590–596. [CrossRef]
3. Cummings, C.O.; Pirie, G.; Sasaki, E.; Wakamatsu, N. Gastric dilatation-volvulus in two North American river otters (*Lontra canadensis*). *Vet. Rec. Case Rep.* **2021**, *9*, e96. [CrossRef]
4. Rosenberg, J.F.; Haulena, M.; Bailey, J.E.; Hendrickson, D.A.; Ivančić, M.; Raverty, S.A. Emergency anesthesia and exploratory laparotomy in a compromised pacific white-sided dolphin (*Lagenorhynchus obliquidens*). *J. Zoo Wildl. Med.* **2017**, *48*, 581–585. [CrossRef]
5. Anderson, H.F.; Rawson, A.J. Volvulus with necrosis of intestine in Stenella attenuata. *Mar. Mammal Sci.* **1997**, *13*, 147–149. [CrossRef]
6. Scaglione, F.E.; Bollo, E.; Pregel, P.; Chiappino, L.; Sereno, A.; Mignone, W.; Guarda, F. Heart pathologies in dolphins stranded along the northwestern Italian coast. *Dis. Aquat. Org.* **2013**, *107*, 31–36. [CrossRef]
7. Stallknecht, D.E. *Impediments to Wildlife Disease Surveillance, Research, and Diagnostics. Wildlife and Emerging Zoonotic Diseases: The Biology, Circumstances and Consequences of Cross-Species Transmission*; Springer: Berlin/Heidelberg, Germany, 2007; pp. 445–461.
8. Ryser-Degiorgis, M.P. Wildlife health investigations: Needs, challenges and recommendations. *BMC Vet. Res.* **2013**, *9*, 223. [CrossRef] [PubMed]
9. Yuen, A.H.L.; Kim, S.W.; Lee, S.B.; Lee, S.; Lee, Y.R.; Kim, S.M.; Poon, C.T.C.; Kwon, J.; Jung, W.J.; Giri, S.S.; et al. Radiological investigation of gas embolism in the East Asian finless porpoise (*Neophocaena asiaeorientalis sunameri*). *Front. Mar. Sci.* **2022**, *9*, 711174. [CrossRef]
10. Yuen, A.H.L.; Lee, S.B.; Kim, S.W.; Lee, Y.M.; Kim, D.G.; Poon, C.T.C.; Seo, J.-P.; Baeck, G.W.; Kim, B.Y.; Park, S.C. Fatal upper aerodigestive tract obstruction in an East Asian finless porpoise (*Neophocaena asiaeorientalis sunameri*): Findings in post-mortem computed tomography. *Forensic Sci. Med. Pathol.* **2023**, *19*, 1–8. [CrossRef]
11. Geraci, J.R.; Lounsbury, V.J. *Marine Mammals Ashore: A Field Guide for Strandings*; National Aquarium in Baltimore: Baltimore, MD, USA, 2005.
12. Wan, X.L.; Zheng, J.S.; Li, W.X.; Zeng, X.Y.; Yang, J.W.; Hao, Y.J.; Wang, D. Parasitic infections in the East Asian finless porpoise *Neophocaena asiaeorientalis sunameri* living off the Chinese Yellow/Bohai Sea coast. *Dis. Aquat. Org.* **2017**, *125*, 63–71. [CrossRef]
13. Kim, S.; Youn, H.; Lee, K.; Lee, H.; Kim, M.J.; Kang, Y.; Choe, S.; Georgieva, S. Novel morphological and molecular data for *Nasitrema* spp. (Digenea: Brachycladiidae) in the East Asian finless porpoise (*Neophocaena asiaeorientalis sunameri*). *Front. Mar. Sci.* **2023**, *10*, 1187451. [CrossRef]
14. Lempereur, L.; Delobelle, M.; Doom, M.; Haelters, J.; Levy, E.; Losson, B.; Jauniaux, T. *Crassicauda boopis* in a fin whale (*Balaenoptera physalus*) ship-struck in the eastern North Atlantic Ocean. *Parasitol. Open* **2017**, *3*, e9. [CrossRef]
15. Ilić, T.; Debeljak, M.; Prodanović, R.; Bogunovic, D. Epizootiological and clinical significance of *Stephanurus dentatus* nematode in swine. *Arch. Vet. Sci.* **2022**, *15*, 5–19. [CrossRef]
16. Menzies, D.; Ellis, H. Intestinal obstruction from adhesions--how big is the problem? *Ann. R. Coll. Surg. Engl.* **1990**, *72*, 60. [PubMed]
17. Eggleston, R.B.; Mueller, P.E. Prevention and treatment of gastrointestinal adhesions. *Vet. Clin. North Am. Equine Pract.* **2003**, *19*, 741–763. [CrossRef] [PubMed]
18. Hyun, J.E.; Han, H.J. Small Bowel Obstruction Induced by Concurrent Postoperative Intra-Abdominal Adhesions and Small Bowel Fecal Materials in a Young Dog. *Vet. Sci.* **2021**, *8*, 83. [CrossRef] [PubMed]
19. Tong, J.W.V.; Lingam, P.; Shelat, V.G. Adhesive small bowel obstruction—An update. *Acute Med. Surg.* **2020**, *7*, e587. [CrossRef]
20. Franklin, S.D.; Fierro, J.; Hysinger, E.B.; Phinizy, P.A.; Piccione, J. Hemosiderin-laden macrophages in bronchoalveolar lavage samples of children with bronchopulmonary dysplasia. *J. Pediatr.* **2023**, *253*, 79–85. [CrossRef]
21. Byard, R.W.; Heath, K. Mesenteric fibrosis—A histologic marker of previous blunt abdominal trauma in early childhood. *Int. J. Legal Med.* **2010**, *124*, 71–73. [CrossRef]
22. Azizi, H.; Nourani, H.; Moradi, A. Infestation and pathological lesions of some lymph nodes induced by *Linguatula serrata* nymphs in sheep slaughtered in Shahrekord Area (Southwest Iran). *Asian Pac. J. Trop. Biomed.* **2015**, *5*, 574–578. [CrossRef]

23. Tatz, A.J.; Segev, G.; Steinman, A.; Berlin, D.; Milgram, J.; Kelmer, G. Surgical treatment for acute small intestinal obstruction caused by *Parascaris equorum* infection in 15 horses (2002–2011). *Equine Vet. J.* **2012**, *44*, 111–114. [CrossRef]
24. Carvalho, V.L.; Bevilaqua, C.M.L.; Iñiguez, A.M.; Mathews-Cascon, H.; Ribeiro, F.B.; Pessoa, L.M.B.; de Lima Silva, F.J. Metazoan parasites of cetaceans off the northeastern coast of Brazil. *Vet. Parasitol.* **2010**, *173*, 116–122. [CrossRef] [PubMed]
25. Díaz-Delgado, J.; Fernández, A.; Xuriach, A.; Sierra, E.; Bernaldo de Quirós, Y.; Mompeo, B.; Pérez, L.; Andrada, M.; Marigo, J.; Catão-Dias, J.L.; et al. Verminous arteritis due to *Crassicauda* sp. in Cuvier's beaked whales (*Ziphius cavirostris*). *Vet. Pathol.* **2016**, *53*, 1233–1240. [CrossRef] [PubMed]
26. Kang, D.B.; Oh, J.T.; Park, W.C.; Lee, J.K. Small bowel obstruction caused by acute invasive enteric anisakiasis. *Korean J. Gastroenterol.* **2010**, *56*, 192–195. [CrossRef]
27. Sasaki, T.; Fukumori, D.; Matsumoto, H.; Ohmori, H.; Yamamoto, F. Small bowel obstruction caused by anisakiasis of the small intestine: Report of a case. *Surg. Today.* **2003**, *33*, 123–125. [CrossRef]
28. Ishikura, H. Anisakis. *Rinshou Syokaki Naika (Clin. Gastroenterol.)* **1991**, *6*, 1052–1060.
29. Caramello, P.; Vitali, A.; Canta, F.; Caldana, A.; Santi, F.; Caputo, A.; Lipani, F.; Balbiano, R. Intestinal localization of anisakiasis manifested as acute abdomen. *Clin. Microbiol. Infect.* **2003**, *9*, 734–737. [CrossRef]
30. Orusa, T.; Orusa, R.; Viani, A.; Carella, E.; Borgogno Mondino, E. Geomatics and EO data to support wildlife diseases assessment at landscape level: A pilot experience to map infectious keratoconjunctivitis in chamois and phenological trends in Aosta Valley (NW Italy). *Remote Sens.* **2020**, *12*, 3542. [CrossRef]
31. Caravaggi, A.; Burton, A.C.; Clark, D.A.; Fisher, J.T.; Grass, A.; Green, S.; Hobaiter, C.; Hofmeester, T.R.; Kalan, A.K.; Rabaiotti, D.; et al. A review of factors to consider when using camera traps to study animal behavior to inform wildlife ecology and conservation. *Conserv. Sci. Pract.* **2020**, *2*, e239. [CrossRef]
32. Ogawa, M.; Kimura, S.S. Variations in echolocation click characteristics of finless porpoise in response to day/night and absence/presence of vessel noise. *PLoS ONE* **2023**, *18*, e0288513. [CrossRef]
33. Akyildiz, I.F.; Pompili, D.; Melodia, T. Underwater acoustic sensor networks: Research challenges. *Ad Hoc Netw.* **2005**, *3*, 257–279. [CrossRef]
34. Stephenson, P.J. Technological advances in biodiversity monitoring: Applicability, opportunities and challenges. *Curr. Opin. Environ. Sustain.* **2020**, *45*, 36–41. [CrossRef]
35. Hussey, N.E.; Kessel, S.T.; Aarestrup, K.; Cooke, S.J.; Cowley, P.D.; Fisk, A.T.; Harcourt, R.G.; Holland, K.N.; Iverson, S.J.; Kocik, J.F.; et al. Aquatic animal telemetry: A panoramic window into the underwater world. *Science* **2015**, *348*, 1255642. [CrossRef] [PubMed]
36. Kimura, S.; Akamatsu, T.; Wang, K.; Wang, D.; Li, S.; Dong, S.; Arai, N. Comparison of stationary acoustic monitoring and visual observation of finless porpoises. *J. Acoust. Soc. Am.* **2009**, *125*, 547–553. [CrossRef] [PubMed]
37. Gopireddy, D.R.; Soule, E.; Arif-Tiwari, H.; Sharma, S.; Kanmaniraja, D.; Jain, K.; Lall, C. Spectrum of CT findings related to bowel adhesions without bowel obstruction: A comprehensive imaging review. *J. Clin. Imaging Sci.* **2020**, *10*, 80. [CrossRef] [PubMed]
38. Copello, J.M.; Bellazzi, G.; Cazenave, J.; Visser, I.N. Argentinean orca (*Orcinus orca*) as an umbrella species: Conservation & management benefits. In *Contributions to the Global Management and Conservation of Marine Mammals*; Editora Artemis: Curitiba, Brazil, 2021; pp. 1–27. [CrossRef]
39. Tardin, R.H.; Chun, Y.; Jenkins, C.N.; Maciel, I.S.; Simão, S.M.; Alves, M.A.S. Environment and anthropogenic activities influence cetacean habitat use in southeastern Brazil. *Mar. Ecol. Prog.* **2019**, *616*, 197–210. [CrossRef]
40. Parsons, E.C.M.; Baulch, S.; Bechshoft, T.; Bellazzi, G.; Bouchet, P.; Cosentino, A.M.; Godard-Codding, C.; Gulland, F.; Hoffmann-Kuhnt, M.; Hoyt, E.; et al. Key research questions of global importance for cetacean conservation. *Endanger. Species Res.* **2015**, *27*, 113–118. [CrossRef]
41. Alava, J.J. Modeling the bioaccumulation and biomagnification potential of microplastics in a cetacean foodweb of the northeastern pacific: A prospective tool to assess the risk exposure to plastic particles. *Front. Mar. Sci.* **2020**, *7*, 566101. [CrossRef]
42. Méndez-Fernandez, P.; Spitz, J.; Dars, C.; Dabin, W.; Mahfouz, C.; André, J.M.; Chouvelon, T.; Authier, M.; Caurant, F. Two cetacean species reveal different long-term trends for toxic trace elements in European Atlantic French waters. *Chemosphere* **2022**, *294*, 133676. [CrossRef]
43. Lee, S.M.; Park, K.J.; Kim, B.Y.; Min, M.S.; Lee, H.; Lee, M.Y. Genetic diversity and population demography of narrow-ridged finless porpoises from South Korea on the basis of mitochondrial DNA variation: Implications for its conservation in East Asia. *Mar. Mammal Sci.* **2019**, *35*, 574–594. [CrossRef]

Disclaimer/Publisher's Note: The statements, opinions and data contained in all publications are solely those of the individual author(s) and contributor(s) and not of MDPI and/or the editor(s). MDPI and/or the editor(s) disclaim responsibility for any injury to people or property resulting from any ideas, methods, instructions or products referred to in the content.

animals

MDPI

Article

Prevalence and Characterization of Dental and Skull-Bone Pathologies of the Raccoon Dog (*Nyctereutes procyonoides*) in Lithuania

Eugenijus Jurgelėnas [1,*], Indrė Jasinevičiūtė [1] and Linas Daugnora [2]

[1] Department of Anatomy and Physiology, Veterinary Academy, Lithuanian University of Health Sciences, Tilžės 18, LT-47181 Kaunas, Lithuania; indre.jasineviciute@lsmu.lt
[2] Institute of Baltic Region History and Archaeology, Klaipėda University, Herkaus Manto 84, LT-92294 Klaipėda, Lithuania; daugnora@gmail.com
* Correspondence: eugenijus.jurgelenas@lsmu.lt

Simple Summary: The raccoon dog, a species introduced in Lithuania in 1950, has become an invasive species in the Baltic countries and has established itself as one of the prominent carnivores in the region. The primary objective of this study is to identify and compare dental and skull-bone pathologies between male and female raccoon dogs. The predominant pathology observed was tooth absence, with the majority of cases involving the absence of the mandibular third molar. Additionally, various stages of inflammation in the tissues surrounding the teeth were also noteworthy pathologies. Furthermore, our findings indicate that males exhibit a significantly higher prevalence of dental and skull-bone pathologies compared to females.

Abstract: The present investigation endeavours to discern dental and non-dental pathologies affecting cranial structures of raccoon dogs, while focusing on cases of periodontitis. Furthermore, the study aims to conduct a comparative analysis based on sex and the nature of the pathologies encountered. The number of investigated skulls amounted to 126, including 76 males and 50 females. The predominant pathology identified was hypodontia, which accounted for 26.7% of males and 20% of females. Notably, the majority of hypodontia cases involved the absence of the mandibular third molar. Another noteworthy pathology was various stages of periodontitis, with rates ranging from 21.3% in males to 8% in females. Other pathologies, like tooth fractures and abrasion, were significantly less encountered. Excessive bone formation was relatively abundant and localized in specific areas—the parietal bone and the occipital regions. This tendency was observed in 8% of male cases and 6% of females. We found that the total number of dental and skull-bone pathologies is significantly more common in males than in females ($p = 0.003$). Additionally, the total number of various cases of periodontitis is more common in males too ($p = 0.04$).

Keywords: Canidae; raccoon dog; teeth; non-dental pathology; maxilla; mandible

1. Introduction

The raccoon dog (*Nyctereutes procyonoides*), an invasive species introduced in Lithuania in 1950, has established a significant presence following migration from Belarus and Latvia. Presently, the raccoon dog stands as one of the prevailing carnivores in the Baltic countries [1]. The native range of this species extends from northern Indochina through the eastern provinces of China and the Korean Peninsula to the south-east corner of Russia and Mongolia [2]. Maximum life span is seven to eight years, with a record in captivity of 13 years. Only about 1% of raccoon dogs live to five years, and 88% of the young (in Finland) die before their first year [3]. Morphologically, raccoon dogs exhibit a customary dental formula, as most other canids, characterized by the following dentition pattern: I 3/3, C 1/1, P 4/4, M 2/3 [3].

Pathologies of the teeth and periodontium of wild carnivores have been studied intensively [4,5]. Comprehensive investigations focusing on dental pathologies among members of the Canidae family have been conducted extensively in various European nations. Noteworthy studies of dental pathologies in red foxes have been researched in Poland [6] and the Czech Republic [7]. Moreover, similar studies were carried out on wolves in Latvia [8]. However, most of them include changes in the number of crown damage: abrasion, tooth fractures, and discoloration [9]. Previous studies lack pathologies of periodontal tissue of wild carnivores. Moreover, existing studies on dental pathologies often lack standardization and present incomplete methodologies [10]. In this study, a meticulous and structured approach was employed to evaluate dental and periodontal pathologies, facilitating expanded research even with limited sample sizes. Although wolf teeth pathologies were analyzed using the dental evaluation methodology, the author strongly recommends its application for assessing dental pathologies in other Canidae species [11]. Several skulls of representatives of the canine family have been studied using standard evaluation, including grey foxes [12], wolves [13], and kit foxes [14]. Notably, most of these studies were carried out in the USA.

Non-dental pathologies of the skulls of wild carnivores are poorly studied. Few studies examine the pathologies of wolves' and coyotes' skeletons (including skulls) [15]. A primarily methodologically detailed study of non-dental pathologies of lynx was carried out in Croatia [16]. Many studies are devoted to the changes in the shape of the foramen magnum in domestic dogs, including fossils [17], but such studies are scarce regarding wild carnivores.

The pathologies of the skeletons of representatives of the canine family are studied in Lithuania by the authors of the present article. Recently, we conducted a detailed study of teeth and non-dental pathologies in red foxes [18]. Since raccoon dogs breed in a limited area, their dental and non-dental pathologies are studied very poorly, especially in Europe. Even though the dental pathologies of Japanese raccoon dogs were analyzed, the mentioned subspecies do not live in Europe [19]. Available sources show that a preliminary study was carried out in Latvia where only 35 skulls of raccoon dogs were used, and only the changes in the number of teeth and crowns were examined [20].

This study conducted by our research team forms part of an ongoing series of investigations. The primary objective of this particular study was to examine both dental and non-dental pathologies among all members of the Canidae family residing in Lithuania. Additionally, our intention is to consolidate and synthesize the findings from these studies in the future, allowing for comparative analysis with data obtained from other countries.

The present study aims to identify the pathologies of the teeth, periodontium, and skull bones in males and females of raccoon dogs and to compare the obtained data by sex and the type of pathologies found.

2. Material and Methods

The study material was used from the Kaunas Tadas Ivanauskas Museum of Zoology collection of skulls of raccoon dogs (*Nyctereutes procyonoides*). Skulls were collected in the territory of the Republic of Lithuania from 1955. Sources of the collection were hunters and expeditors who found cadavers of animals. The collection of skulls is inventoried and has a registration card with the following parameters of the body: length, weight, and sex. In males, the penile bone (os penis) was attached with a registration card to confirm sex. Only the skulls of adult raccoon dogs were evaluated in the research. The maturity of the raccoon dogs' skulls was determined by the closure of the presphenoid–vomer and basisphenoid–presphenoid sutures [12].

A total of 126 skulls and mandibles were included in this investigation, comprising 76 males and 50 females. The study comprehensively assessed and documented pathological alterations across various anatomical positions of the skulls. These pathological changes were meticulously described and captured through photography for thorough examination and analysis.

The methodology employed for evaluating dental conditions in this study was adapted from the approach described by Janssens et al. (2016) [11]. Specifically, the description provided by Evenhuis et al. (2018) [12] served as the foundation for assessing abrasion/attrition, periapical lesions, and also the temporomandibular joint pathologies. Notably, we excluded stage 1 of abrasion/attrition because the enamel fracture in the prepared skulls is potentially artefactual. Bone fractures and excessive bone formation were analyzed based on *Jubb, Kennedy & Palmer's Pathology of Domestic Animals* [21]. Meanwhile, the investigation into changes of shape of the foramen magnum relied on the insights presented in *Miller's Anatomy of the Dog* [22], and Janeczek et al. (2011) [23]. The categories encompassing all pathologies are presented in Table 1, providing a comprehensive overview of the pathological conditions.

Table 1. Descriptions of dental and non-dental pathologies.

Categories	Sub-Categories	Short Explanation
Dental pathologies		
Abnormal number of teeth	Hypodontia	No alveolus present (genetic)
	Traumatic	A tooth is missing, and the alveolus is visible and deformed
	Excessive teeth	Polyodontia/hyperdontia (genetic)
Tooth fractures	Uncomplicated crown (or crown-root) fracture	Fracture without pulp exposure
	Complicated crown (or crown-root) fracture	Fractures with pulp exposure
Attrition/abrasion	Stage 2	Exposure of dentine on the cuspal tip, without tertiary dentine formation
	Stage 3	Exposure of dentine on the cuspal tip, with tertiary dentine formation
	Stage 4	Pulp cavity exposure secondary to attrition/abrasion
Enamel hypoplasia	Mild	Brownish enamel discoloration
	Severe	Part of tooth is enamel free, dentine visible
Periapical lesions	–	Macroscopically visible periapical bone loss, root tip resorption, sinus tract formation originating periapically, or obvious focal periosteal reaction overlying the apex
Periodontal disease	Stage 2	Less than 25% loss of alveolar bone
	Stage 3	More than 25% but less than 50% loss of alveolar bone
	Stage 4	More than 50% loss of alveolar bone
Non-dental pathologies		
Temporomandibular joint (TMP) osteoarthritis	Mild	Evidence of early periarticular new bone formation/osteophytes with minimal or no subchondral bone change
	Moderate	Periarticular new bone formation and/or subchondral bone changes
	Severe	All previously described signs are present and more pronounced; subchondral bone lysis present; partial or complete ankylosis may be observed
Bone fractures	–	–
Excessive bone formation	–	Exostosis or osteophytes.
Shape changes of the foramen magnum	–	Deviations from the typical shape of the foramen magnum—oval or circular. A visible notch to any side is fixed as an abnormality.

To validate the observed pathological changes, a subset of cases underwent digital X-ray imaging. Digital X-ray imaging was conducted at a private small animal clinic Ltd. "VetPet LT", using Amadeo V–AX stationary system. Descriptive studies were employed to examine data. For the comparison, the percentages were calculated. The statistical data analysis was performed using SPSS 24.0. Statistical comparison between males and females was evaluated via the Chi-square test. Statistically, the significant parameter was when $p < 0.05$.

3. Results

3.1. Dental Pathologies in Male Raccoon Dogs

An abnormal number of teeth. Pathologies related to the number of teeth were investigated, with no inclusion of hyperdontia identified in the sample. Only a single case of traumatic dental lost (left canine tooth) was detected. Details regarding cases of hypodontia are presented in Figure 1, which also provides information on their distribution in the maxilla and mandible.

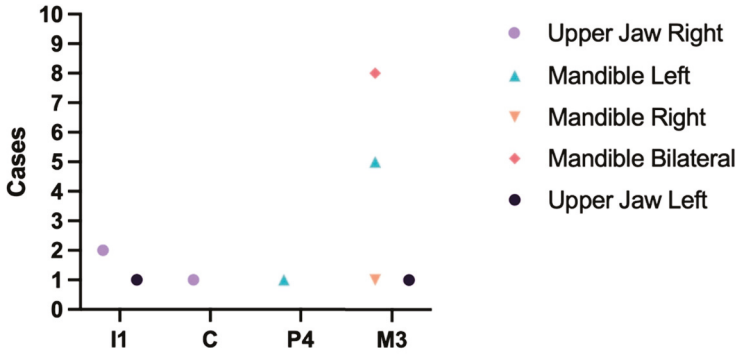


Figure 1. Distribution of cases of hypodontia in males. Blue triangle—Mandible left (Figure 2).

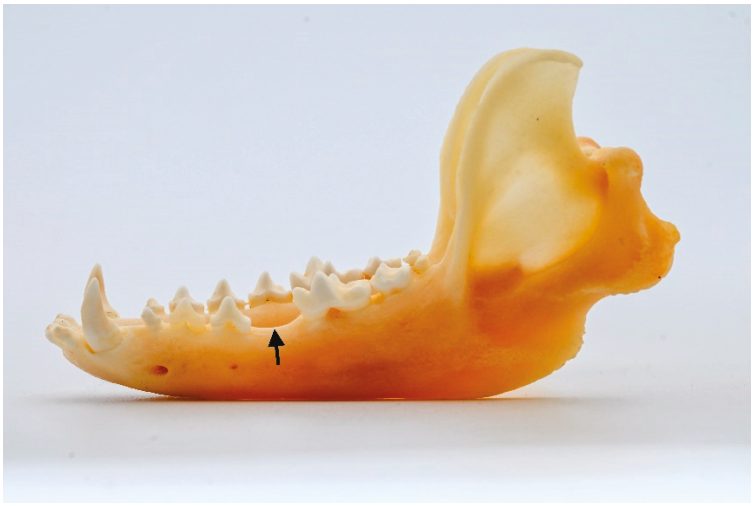


Figure 2. ID M–4688, male. Approx. length—90 mm. Absence of the P4 (arrow) in the left mandible of the raccoon dog.

Tooth fractures. No instances of uncomplicated crown (or crown-root) fractures were detected in the study sample. However, a total of eight cases of complicated crown fractures were identified. Among the affected teeth, the majority were upper incisive teeth (five cases), and also canine and premolar teeth. It should be noted that questionable cases of dental fractures, which may arise during skull preparation, were excluded from the analysis.

Attrition/abrasion. Among the observed cases, a total of seven cases of various stages of abrasion were identified. Specifically, four cases were categorized as stage 2 abrasion, two cases as stage 3, and one case as stage 4. The canine teeth were the most commonly affected. Additionally, a case of stage 3, and one case of stage 4 were multiple abrasions of the upper and lower premolar and molar teeth.

No instances of enamel hypoplasia were detected in the study sample. Moreover, no cases of periapical lesions were found in the examined specimens

Periodontal disease. A total of 16 cases of various stages of periodontitis were observed. Stage 2 periodontitis was the most prevalent, with 13 cases (see Figure 3). Also, two cases

of stage 3 periodontitis were detected (see Figure 4). The typical affected regions included the maxilla, ranging from P^3 to M^2, and the mandible, spanning from P_4 to M_3.



Figure 3. ID M–0951, male. Approx. length—120 mm. Second-stage periodontitis in the molar and premolar regions in the maxilla and mandible of the raccoon dog (marked with a dashed red line).

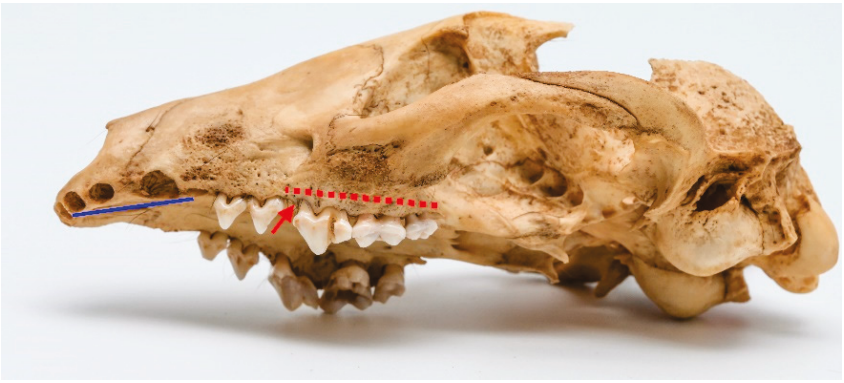
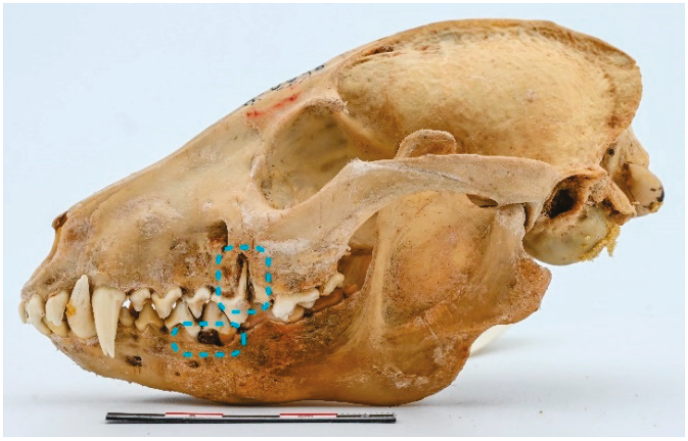


Figure 4. ID MP–2704, male. Approx. length—120 mm. Third-stage periodontitis with local dehiscence (marked by red arrow) in the molar and premolar regions of the raccoon dog (marked with dashed red line). Note: the blue line marks the artefactual teeth loss.

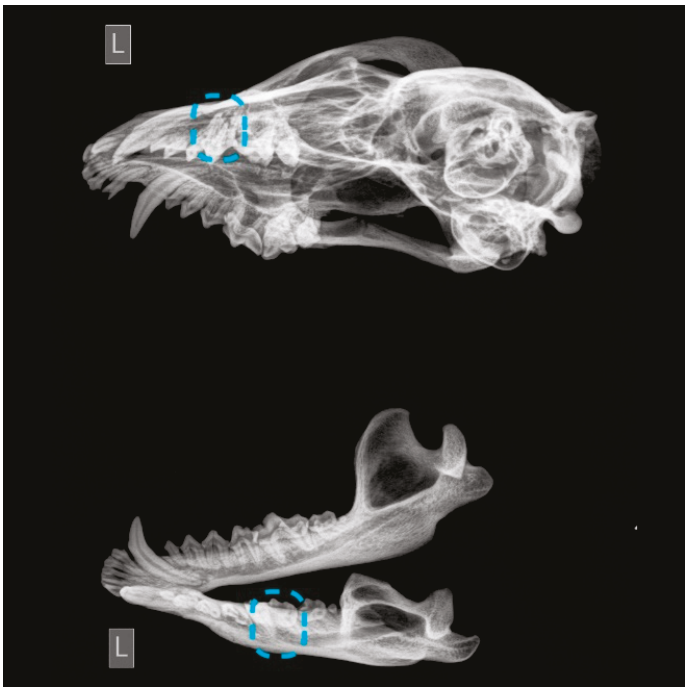
Among observed cases, only one clear instance of stage 4 periodontitis was detected (ID M–0948; Figure 5a,b). The periapical bone resorption had developed around the length of the buccal root of P^4. Furthermore, severe periodontitis characterized by significant bone resorption was observed around P^3 as well. A milder stage of periodontitis was identified around I^3, C, M^1, and M^1 of the left maxilla.

In the left mandible, both P_3 and P_4 exhibited pronounced effects of late-stage periodontitis, with the extent of bone resorption in the periapical area surrounding the roots of these teeth. The molar teeth on the left mandible displayed a comparatively lower degree of periodontitis, yet some loss of surrounding bone was evident.

Non-dental pathologies in male raccoon dogs. Fractures of skull bones and atypical shapes of the foramen magnum were not detected in any of the examined specimens. Two skulls were affected by a mild stage of temporomandibular joint osteoarthritis, while no moderate or severe cases were observed. Excessive bone formation pathologies were the predominant category in this group (Table 2). A total of six cases were identified, and each case will be described individually.



(**a**)



(**b**)

Figure 5. ID M–0948, male. (**a**) Approx. length—120 mm. Fourth-stage periodontitis with local dehiscence (marked by a blue square) of the left mandible and maxilla in the skull of the raccoon dog. (**b**) X-ray of fourth-stage periodontitis with local dehiscence (marked by a blue square) of the left mandible and maxilla in the skull of a raccoon dog.

Table 2. Description of excessive bone formation pathological findings in males.

ID	Pathological Findings
M–0798	Spike-like osteophytes on external sagittal crest and temporal line.
M–0947	Small osteophytes on the nuchal crest, partial disappearance of the right side of the nuchal crest.
M–0943	Osteophytes on left side of zygomatic arch.
M–0792	Small osteophytes on external sagittal crest concentrated caudally (Figure 6).
M–1224	Osteophytes on external sagittal crest, caudal aspect.
M–2438	Osteophytes on nuchal crest, left side more concentrated.

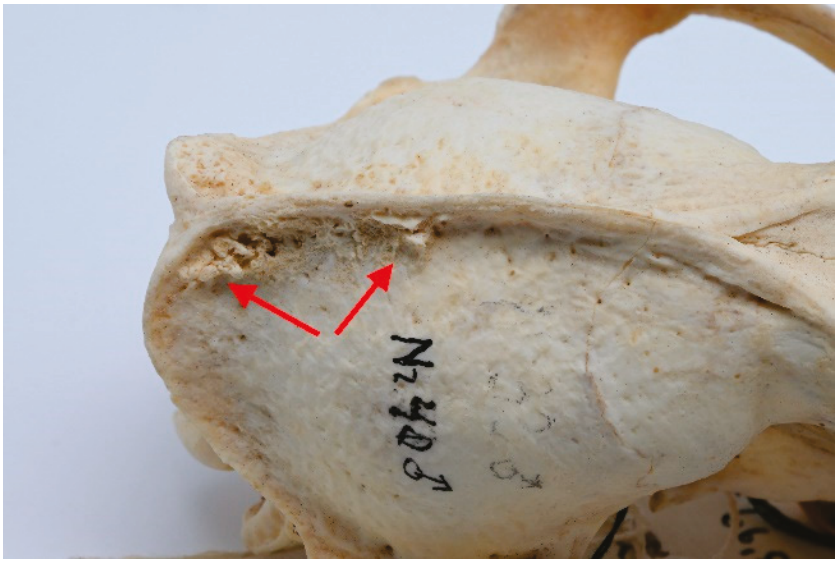


Figure 6. ID M–0792, male. Approx. length—65 mm. Osteophytes of the external sagittal crest (marked by red arrows).

Other findings. One particular skull (ID M–3392; Figure 7a,b) is severely affected and includes a lot of various kinds of dental and non-dental pathologies. This case warrants a detailed description of its specific findings. An absence of third lower molar teeth was detected. Complicated horizontal dental fracture with necrotic pulp and severe periapical alveolar resorption is present in P^4 and rostral root of M^1 of the left side of the maxilla. Furthermore, third-stage periodontitis with mild alveolar resorption affects all premolar and molar teeth, and attrition affects the left side's lower and upper canine teeth. A similar pattern of periodontitis is evident on the left mandible. Moreover, multiple osteophytes had developed in the region of the zygomatic bone and external sagittal crest and nuchal crest.

3.2. Dental Pathologies in Female Raccoon Dogs

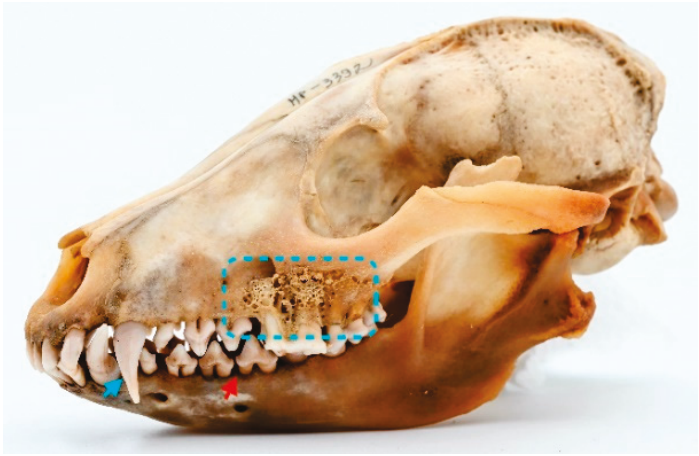
An abnormal number of teeth. Figure 8 provides an overview of the findings in relation to dental numerical anomalies. Similar to the males' skulls, no cases of excessive teeth were observed among the female specimens. Hence, the table exclusively displays cases of hypodontia. Furthermore, no traumatic dental-loss cases were detected in the female raccoon dogs.

Tooth fractures. Similar to the male specimens, no cases of uncomplicated crown fractures or crown-root fractures were found. However, two skulls exhibited complicated crown fractures. In one skull, the crown of left I1 and I2 was fractured, while the other one had fractures in both the left and right I1.

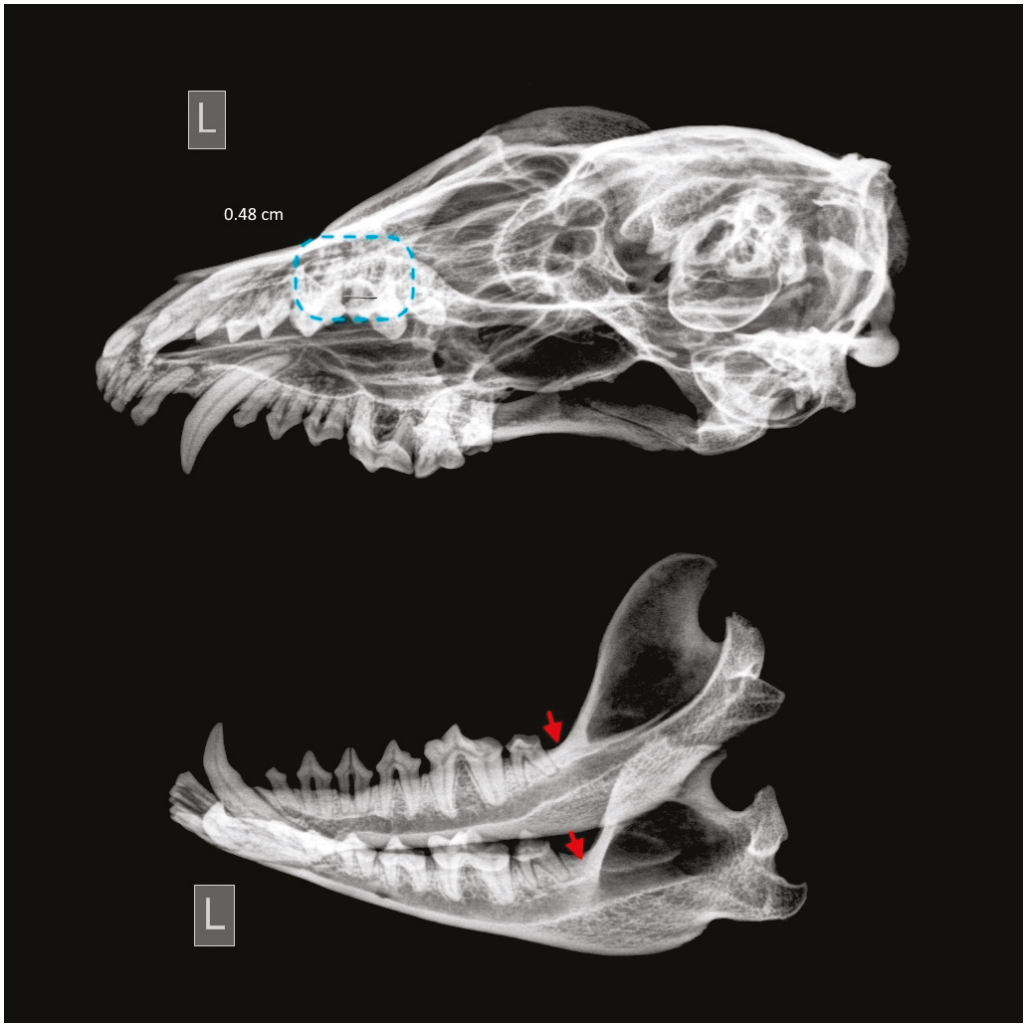
Attrition/abrasion. In total, we found eight cases of various stages of abrasion. Among them, five cases of stage 2 abrasion, one case of stage 3, and two cases of stage 4. The stage 2 abrasion primarily affected the caudal surface of the upper canine teeth. Additionally, one case of stage 3 and one case of stage 4 abrasion were founded on the upper and lower premolar and molar teeth.

Multiple teeth were affected in one skull (ID M–0796; Figure 9a,b). Almost all teeth were severely worn and were categorized as stage 4 abrasion.

Enamel hypoplasia was not detected in the female raccoon dog skulls examined in this study. Regarding periapical lesions, only one case was identified (ID M–578; Figure 10). In the mandible, the bone tissue around the M_1 was strongly affected, and resulted in porosity.



(**a**)



(**b**)

Figure 7. ID M–3392, male. (**a**) Approx. length—120 mm. Third-stage periodontitis with complicated hori-zontal dental fracture and periapical bone resorption (marked by a blue square) in the raccoon dog's left side of the maxilla. Blue arrow shows the attrition of the left upper canine tooth, and red arrow shows the mild alveolar resorption. (**b**) X-ray of third-stage periodontitis with complicated hori-zontal dental fracture and periapical bone resorption (marked by a blue square) in the raccoon dog's left side of the maxilla. Red arrows show the absence of the lower third molar tooth. No tooth buds were found.

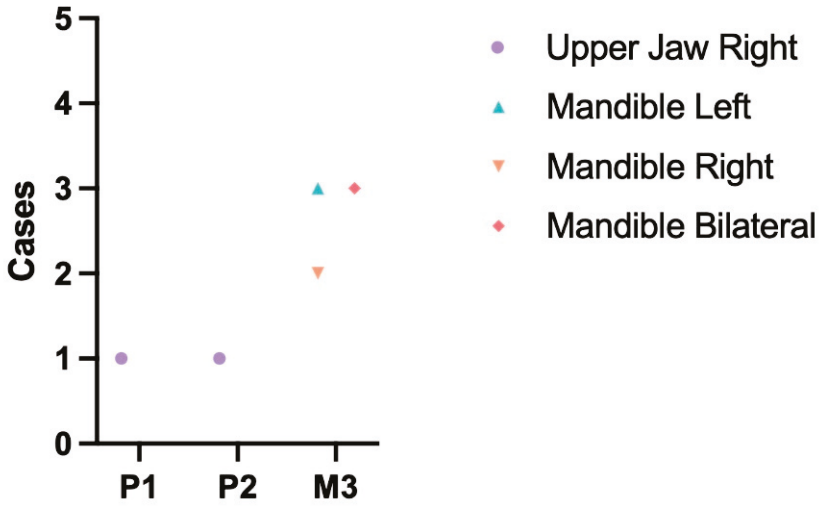


Figure 8. Distribution of cases of hypodontia in males.

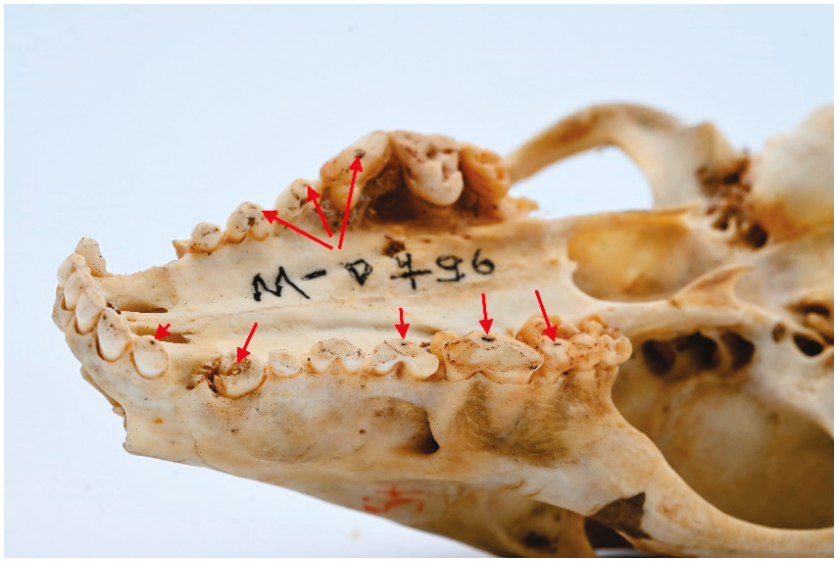
Periodontal disease. There were fewer cases of periodontitis in females' skulls. In total, four cases of various stages of periodontitis were detected; from them, two cases of stage 2, and separate cases of stage 3, and stage 4 were detected. These cases of periodontitis were predominantly located in the maxillary region, spanning from P^4 to M^2.

Non-dental pathologies in female raccoon dogs. Non-dental pathologies in female raccoon dogs were relatively minimal. No bone fractures or atypical shapes of the foramen magnum were found. Additionally, no signs of temporomandibular joint changes were detected in the female skulls. Similar to the male skulls, the primary non-dental pathology observed was excessive bone formation, with three cases detected (Table 3).



(**a**)

Figure 9. *Cont.*



(**b**)

Figure 9. ID M–0796, female. (**a**) Approx. length—125 mm. Multiple abrasions (arrows) in the skull of the raccoon dog, lateral view. Note: blue square marks the artefactual tooth loss. (**b**) Approx. length—70 mm. Multiple abrasions (arrows) in the skull of the raccoon dog, ventral view.

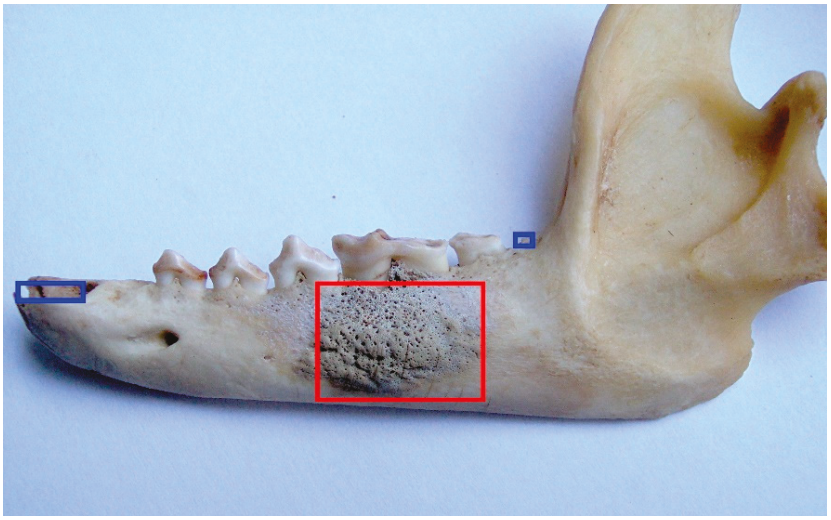


Figure 10. ID M–578, female. Approx. length—90 mm. Left-mandible porous bone tissue around the M1 (marked in red rectangle). Note: blue squares mark the artefactual tooth loss.

Table 3. Description of excessive-bone-formation pathological findings in females.

ID	Pathology Description
M–0808	Small dot-like osteophytes covering almost all of the parietal bone.
M–615	Spike-like osteophytes concentrated on the external sagittal crest, particularly between the external sagittal crest and temporal line.
M–2165	Osteophytes on the external sagittal crest, with a higher concentration near the connection with the nuchal crest.

3.3. Statistical Analysis

In total, 126 skulls with mandibles were examined, comprising 76 males and 50 females. Among the studied raccoon-dog specimens, a substantial proportion of 89 skulls (70.6%)

exhibited various pathologies, including both dental and non-dental conditions. Specifically, the prevalence of pathologies was higher in males, with 61 cases (80.3%), compared to females, with 28 cases (56%).

The research findings revealed that pathologies of skulls in males were more common than in females ($\chi^2 = 8.55$, $p = 0.003$). A similar situation was revealed when we included dental and periodontal disease only (note: male skull ID M–3392 was excluded from the future statistics). Pathologies in males, 52 (69.3%), were more common than in females, 25 (50%) ($\chi^2 = 4.74$, $p = 0.02$). Non-dental pathologies in males, 8 (10.7%), were slightly more common than in females, 3 (6%), but there was no statistical significance ($\chi^2 = 0.81$, $p = 0.36$).

Distributions of dental and periodontal disease in the maxilla, mandible, and both jaws are presented in Table 4 Remarkably, pathologies affecting both jaws were more prevalent in males than in females.

Table 4. Distribution of dental and periodontal pathologies in various parts of the skull.

Sex	Maxilla	Mandible	Located in Both Jaws
Males (n = 75)	16 (21.3%)	17 (22.7%)	19 (25.3%)
Females (n = 50)	13 (26%)	9 (18%)	3 (6%)
χ^2	0.36 ($p = 0.54$)	0.39 ($p = 0.52$)	7.73 ($p = 0.005$)

The investigation of various types of dental and skull-bone pathologies, as summarized in Table 5, revealed only one statistically significant difference between males and females. Specifically, the overall prevalence of periodontal disease was found to be higher in males compared to females ($p = 0.04$).

Table 5. Statistical significance and distribution of pathologies.

Pathology	Males n = 75	Females n = 50	χ^2
Hypodontia (total)	20 (26.7%)	10 (20%)	0.73; $p = 0.39$
Hypodontia—M^3 only	14 (18.7%)	8 (16%)	0.14; $p = 0.70$
Traumatic tooth loss	1 (1.3%)	0	0.67; $p = 0.41$
Tooth fractures	8 (10.6%)	2 (4%)	1.81; $p = 0.17$
Abrasion (total)	7 (9.3%)	8 (16%)	1.26; $p = 0.26$
Periapical lesions	0	1 (2%)	1.51; $p = 0.21$
Periodontitis (total)	16 (21.3%)	4 (8%)	3.96; $p = 0.04$
Periodontitis (stages 3 and 4 only)	3 (4%)	2 (4%)	0.00; $p = 1$
Excessive bone formation	6 (8%)	3 (6%)	0.17; $p = 0.67$
TMP osteoarthritis	2 (2.7%)	0	1.35; $p = 0.24$

4. Discussion

Hypodontia emerged as a prevalent pathology in our study, with isolated cases observed in both males and females. Only isolated cases of lack of incisors, canine, and molar teeth occurred in males and females, and hypodontia of the mandibular M_3 molar tooth was the dominant one. This pattern should not come as a surprise since hypodontia of the mandibular M_3 molar tooth is also very common in other representatives of the canine family. In our previous study, after examining 230 skulls of red foxes, we found that the lack of a mandibular M_3 molar tooth was the most common compared to the lack of other teeth and accounted for 6.19% of cases in males and 7.69% in females [18]. A similar trend has been found in wolves. Of the 187 skulls studied, hypodontia accounted for 2.1%, of which M_3 deficiency was the most common [8].

Hypodontia is a commonly observed condition in raccoon dogs, and its distribution pattern differs to some extent from other species. In Japanese raccoon dogs (*Nyctereutes procynoides viverrinus*), out of 179 skulls studied, hypodontia was found in 35. Similar to

our findings, M_3-molar-tooth deficiency prevailed, but another common hypodontia was a deficiency of both upper and lower teeth P1, which we found in our study only in one skull [19]. Interestingly, a significant disparity of results was found in the neighboring country Latvia where only one hypodontia was found in the 35 skulls of raccoon dogs studied. A lack of the premolar instead of the third molar was detected in the case [20]. Regarding the causes of hypodontia, we believe that all the cases identified in our study are of genetic origin rather than resulting from trauma. This implies that the affected teeth never erupted. In general, when it comes to hypodontia of M_3, the loss of this tooth does not have a significant impact on survival. For carnivores, the canine, especially the carnassial teeth, are considered of primary importance [7]. We did not observe any lack of these critical teeth in our study.

In our study, only one case was described as a traumatic dental loss, specifically the loss of the left canine tooth in male skulls. No cases of traumatic dental loss were detected in the female skulls examined. It is worth noting that in other studies focusing on raccoon dogs, researchers usually do not separate dental losses into subcategories. However, when examining other animal species such as wolves, traumatic dental loss was detected more frequently. This pathology was detected in 9 skulls of 40 (22.5%) [11].

Our findings revealed that tooth fractures were observed in 10.66% of male skulls and 4% of female skulls. Unfortunately, there is limited information available regarding tooth fractures specifically in raccoon dogs from other countries. Research of other canids shows that tooth fractures are quite common. Yanagisawa et al. (2019) [14] found that tooth fractures in kit foxes (*Vulpes macrotis*) was found in 56.2% of specimens. Similar to our study, the dominant type was complicated crown fractures. In 187 grey-wolf skulls, Andersone and Ozolins (2000) [8] found that only two skulls had broken teeth. As in our study, incisors and canine teeth were the most common fractured teeth.

In contrast to many studies on teeth pathologies that often include cases of hyperdontia, our research did not identify a single case of hyperdontia in the examined raccoon dog skulls. Hyperdontia, the presence of an excessive number of teeth, was not observed in any of the specimens in our study. The same tendency was noticed in another study conducted in Latvia [20]. The trend is not unexpected since in skulls of other representatives of the canine family, only isolated cases of hyperdontia are detected. About 2% of the cases were found in red foxes [6]. However, in the studies examining raccoon dogs of another subspecies (*Nyctereutes procynoides viverrinus*), hyperdontia was quite common. In a study based on analyzing 179 skulls, hyperdontia accounted for 4.5% of teeth pathologies. In a similar study of 82 skulls, hyperdontia was identified in 6 skulls [19,24]. Asahara (2016) [25], who found that in 153 studied skulls of raccoon dogs, M_4 extra tooth accounted for 2.61% of the pathologies, also gives a plausible explanation of the causes of hyperdontia. It is mainly associated with the high content of insects in the diet. The higher the range of insects, the larger the additional molars that are necessary for crushing chitin. Nutrition studies conducted in Lithuania showed that in the warm season, plants (raspberry, bilberry) and amphibians predominate in the diet of raccoon dogs. In the cold season, ungulate carrion (*Sus scrofa*, cervids), plants, and, in a smaller quantity, rodents make up the bulk of raccoon dogs' diet [26]. To summarize, insects do not form a significant part of the diet in Lithuania.

As for damage to the surface of the dental crown, we found 7 (9.3%) cases tooth abrasion in males and 8 (16%) instances in females. Typical abrasion of the caudal side of the canine tooth and multiple premolars and molar teeth abrasions were found. Analogous cases are also detected in other species of canines. Abrasion of the exact nature were seen in our study in local red foxes [18]. The abrasion of the canine tooth can be explained by cage-biter syndrome, whereas the high content of sand can explain multiple abrasion of the teeth in food [11].

Periapical lesions were found to be rare in raccoon dogs based on our research findings. No individual cases of periapical lesions were found in the male skull, except in a severely affected skull (ID M–3392) together with another pathology. In females, only one skull had

a clear case of periapical lesion. In other canids, the occurrence rate of this pathology is from only 0.4% in grey fox [12] to 5.3% in arctic fox [27].

Regarding periodontitis, our study revealed a significant difference in the number of cases between males and females. Males exhibited 16 cases of various stages of periodontitis, whereas females had only 4 cases. The predominant stage of periodontitis was stage 2, which was more common in males than in females. Stages 3 and 4 divide between sexes almost equally. The number of cases found in raccoon-dog populations in other countries remains uncertain, as there is a severe shortage of studies of periodontal diseases. Therefore, we must rely on similar studies of different species of the canine family. Evenhuis et al. (2018) [12] found that almost half of the specimens (n = 276, 48.7%) displayed some degree of bony change consistent with periodontitis after studying 569 of the skulls of grey foxes (*Urocyon cinereoargenteus*). Within the study, a group of 226 (39.7%) specimens displayed bony change suggestive of stage 2 periodontitis, 120 (21.1%) with stage 3, and 13 (2.3%) with stage 4. In our study, the number of detected cases of stage 2 periodontitis is much lower. The limitation of our study lies in the relatively smaller amount of material available. In addition, we included only obvious cases, while we rejected dubious ones. It has to be admitted that the diagnosis of stage 2 periodontitis when examining the bone material is complicated.

Similar to our previous study on red foxes, we also investigated non-dental pathologies in raccoon-dog skulls. In our previous study of red foxes, we found small numbers of varied pathologies, among them one bone fracture and two cases of an atypical form of the foramen magnum [18]. However, in the current study, we did not identify such pathologies. This should come as no surprise since both skull fractures and the atypical form of the foramen magnum is usually critical in terms of survival. The atypical condition of the foramen magnum adversely affects the spinal cord, resulting in neurological disorders [23].

Temporomandibular joint osteoarthritis is a rare pathology observed in the Canidae family. Evenhuis et al. (2018) [12] found that none of the specimens of grey foxes have any sign of TMJ osteoarthritis. In the kit foxes, 5.9% of the specimens have a sign of low-grade temporomandibular joint osteoarthritis [14]. In our study, TMP osteoarthritis occurs only in 2.7% of males and not at all in females.

In the present study, we found a wide variety of bone growths—osteophytes in specific areas of the skull, i.e., external sagittal crest, nuchal crest, and the zygomatic bone. These areas were affected in both males and females. Although there were more of these pathologies in the skulls of males than in the skulls of females, the difference was not statistically significant. Unfortunately, there are very few studies of non-dental pathologies. Gomerčić et al. (2009) [16] examined 58 skulls of Eurasian lynx (*Lynx lynx*) and identified non-dental pathologies only in 2 skulls. In this study, lesions were found in the area of the frontal bone, and only in 1 skull were there bony outgrowths that covered the frontal bone's zygomatic process.

The interpretation of osteophytes in specific areas presents challenges. However, it can be hypothesized that the proliferation of osteophytes in the external sagittal crest and the nuchal crest is associated with the attachment sites of certain muscles. Evans and de Lahunta (2013) [22] propose that the external sagittal crest forms the medial boundary of the temporal fossa, a large area on the external surface of the cranium from which the temporal muscle originates. Consequently, the development of the osteophytes of the external sagittal crest can be attributed to the development of the temporal muscle and increased load.

The assessment of the differences between males and females did not reveal statistically significant differences in almost any category of pathologies, except for the total number of periodontitis cases, which was more common in males than in females ($p < 0.05$). A slight tendency for pathologies is more common in males than females, which is observed in hypodontia and tooth fractures. Also, pathologies are more commonly located in both jaws in males than in females ($p = 0.005$), but not in only maxilla or mandible. Consequently, it can be concluded that the prevalence of dental and non-dental pathologies in the population

of raccoon dogs is not dependent on sex. This finding aligns with the results obtained from the examination of red-fox populations, where no statistically significant differences were found, except in the category of multiple pathologies [18]. This trend is observed in most other canine family studies. Szuma (1999) [6], who studied the pathologies of the teeth of red foxes, also did not find statistically significant differences in individual categories, although dental pathologies were generally more common in males. Similarly, in our study, we found that dental pathologies are more common in males than in females ($p = 0.02$).

5. Conclusions

In conclusion, the prevalence of dental pathologies in raccoon dogs in Lithuania appears to be comparable to findings from studies conducted in other countries. Admittedly, the lack of similar studies was significant, and the comparison of data had to be based mainly on data from studies of the Japanese subspecies. Hypodontia of the mandibular third molar tooth could be singled out, which is the most common pathology and coincides with the data of studies of most representatives of the canine family. Furthermore, a notable result of this study is the identification of an abundant but only singular dominant type of non-dental pathology. The observed increase in bone tissue proliferation is relatively significant in the occipital- and parietal-bone areas and prompts a more detailed study of the causes of these pathologies in the future.

Author Contributions: Conceptualization, E.J. and L.D.; methodology, E.J. and I.J.; formal analysis, E.J.; data curation, E.J. and L.D.; writing–original draft preparation, E.J.; writing–review and editing, E.J. and I.J.; visualization, E.J., I.J. and L.D.; supervision, E.J., I.J. and L.D. All authors have read and agreed to the published version of the manuscript.

Funding: This research received no external funding.

Institutional Review Board Statement: Not applicable.

Informed Consent Statement: Not applicable.

Data Availability Statement: Authors can confirm that all relevant data are included in the article and are available from the corresponding author upon reasonable request.

Acknowledgments: We want to thank the Curator of the Mammal Department of Kaunas Tadas Ivanauskas Museum of Zoology, Vaclovas Gedminas, for support in our research and Kazimieras Martinaitis, Head of Accounting and Storage of the Collections Department, for photographs. We also thank the small animal clinic "VetPet LT" for taking X-ray images.

Conflicts of Interest: The authors declare no conflict of interest.

References

1. Kauhala, K. Introduced Carnivores in Europe with Special Reference to Central and Northern Europe. *Wildl. Biol.* **1996**, *2*, 197–204. [CrossRef]
2. Kauhala, K.; Saeki, M. Nyctereutes Procyonoides. The IUCN Red List of Threatened Species 2016: E.T14925A85658776. 2016. Available online: https://doi.org/10.2305/IUCN.UK.2016-1.RLTS.T14925A85658776.en (accessed on 22 July 2023).
3. Sillero, C.; Hoffmann, M.; Macdonald, D. *Canids: Foxes, Wolves, Jackals and Dogs. Status Survey and Conservation Action Plan*; IUCN-The World Conservation Union: Gland, Switzerland, 2004.
4. Pires, A.; Caldeira, I.; Petrucci-Fonseca, F.; Viegas, I.; Viegas, C.; Bastos-Silveira, C.; Requicha, J. Dental Pathology of the Wild Iberian Wolf (*Canis lupus* Signatus): The Study of a 20th Century Portuguese Museum Collection. *Vet. Anim. Sci.* **2020**, *9*, 100100. [CrossRef]
5. Losey, R.J.; Jessup, E.; Nomokonova, T.; Sablin, M. Craniomandibular Trauma and Tooth Loss in Northern Dogs and Wolves: Implications for the Archaeological Study of Dog Husbandry and Domestication. *PLoS ONE* **2014**, *9*, e99746. [CrossRef]
6. Szuma, E. Dental Abnormalities in the Red Fox Vulpes Vulpes from Poland. *Acta Theriol.* **1999**, *44*, 393–412. [CrossRef]
7. Nentvichová, M.; Anděra, M. Dental Anomalies and Dental Variations in the Red FoxVulpes Vulpes in the Czech Republic. *Acta Theriol.* **2008**, *53*, 217–228. [CrossRef]
8. Andersone, Ž.; Ozolins, J. Craniometrical Characteristics and Dental Anomalies in Wolves *Canis lupus* from Latvia. *Acta Theriol.* **2000**, *45*, 549–558. [CrossRef]
9. Van Valkenburgh, B.; White, P.A. Naturally-Occurring Tooth Wear, Tooth Fracture, and Cranial Injuries in Large Carnivores from Zambia. *PeerJ* **2021**, *9*, e11313. [CrossRef]

10. Buchalczyk, T.; Dynowski, J.; Szteyn, S. Variations in Number of Teeth and Asymmetry of the Skull in the Wolf. *Acta Theriol.* **1981**, *26*, 23–30. [CrossRef]
11. Janssens, L.; Verhaert, L.; Berkowic, D.; Adriaens, D. A Standardized Framework for Examination of Oral Lesions in Wolf Skulls (Carnivora: Canidae: *Canis lupus*). *J. Mammal.* **2016**, *97*, 1111–1124. [CrossRef]
12. Evenhuis, J.V.; Zisman, I.; Kass, P.H.; Verstraete, F.J.M. Dental Pathology of the Grey Fox (*Urocyon cinereoargenteus*). *J. Comp. Path.* **2018**, *158*, 39–50. [CrossRef]
13. Döring, S.; Arzi, B.; Winer, J.N.; Kass, P.H.; Verstraete, F.J.M. Dental and Temporomandibular Joint Pathology of the Grey Wolf (*Canis lupus*). *J. Comp. Pathol.* **2018**, *160*, 56–70. [CrossRef] [PubMed]
14. Yanagisawa, N.; Wilson, R.E.; Kass, P.H.; Verstraete, F.J.M. Dental and Temporomandibular Joint Pathology of the Kit Fox (*Vulpes macrotis*). *J. Comp. Pathol.* **2019**, *167*, 60–72. [CrossRef] [PubMed]
15. Wobeser, G. Traumatic, Degenerative, and Developmental Lesions in Wolves and Coyotes from Saskatchewan. *J. Wildl. Dis.* **1992**, *28*, 268–275. [CrossRef] [PubMed]
16. Gomerčić, T.; Đuras, M.; Pavlović, A.; Kusak, J.; Sindičić, M.; Huber, D. Variation in Teeth Number, Teeth and Skull Disorders in Eurasian Lynx, Lynx Lynx from Croatia. *Folia Zool.* **2009**, *58*, 57–65.
17. Onar, V.; Pazvant, G.; Ince, N.; Alpak, H.; Janeczek, M.; Kızıltan, Z. Morphometric Analysis of the Foramen Magnum of Byzantine Dogs Excavated in Istanbul Yenikapi at the Site of Theodosius Harbour. *Mediterr. Archaeol. Archaeom.* **2013**, *13*, 135–142.
18. Jurgelėnas, E.; Zakienė, I.; Daugnora, L. Dental and Skull Bone Pathologies of the Red Fox (*Vulpes vulpes*) in Lithuania. *J. Vertebr. Biol.* **2020**, *69*, 1–12. [CrossRef]
19. Harada, Y.; Ogawa, K.; Mori, S.; Kobayashi, S.; Kubo, H.; Kiyosue, T. Variations of Dentition in Raccoon Dogs (*Nyctereutes procynoides viverrinus* T.) Anomalies in Number of the Teeth. *Shika Kiso Igakkai Zasshi* **1989**, *31*, 257–264. [CrossRef]
20. Putnina, A.; Mugurevics, A. Dental Pathologies of Foxes (*Vulpes vulpes*) and Raccoon Dogs (*Nyctereutes procyonoides* Gray) in Latvia. In Proceedings of the Animals Health Food Hygiene, Jelgava, Latvia, 14 November 2008.
21. Maxie, M.G. *Jubb, Kennedy & Palmer's Pathology of Domestic Animals: Volume 1*; Elsevier Health Sciences: Amsterdam, The Netherlands, 2015; ISBN 978-0-7020-6842-3.
22. Evans, H.E.; de Lahunta, A. *Miller's Anatomy of the Dog–E-Book*; Elsevier Health Sciences: Amsterdam, The Netherlands, 2013; ISBN 978-0-323-26623-9.
23. Janeczek, M.; Chrószcz, A.; Czerski, A. Morphological Investigations of the Occipital Area in Adult American Staffordshire Terriers. *Anat. Histol. Embryol.* **2011**, *40*, 278–282. [CrossRef]
24. Harada, Y.; Imoto, H.; Yamada, H.; Yamamoto, T.; Yamada, T. Supernumerary Teeth in Anterior Molars of Raccoon Dogs. *Jpn. J. Oral Biol.* **1979**, *21*, 309–316. [CrossRef]
25. Asahara, M. The Origin of the Lower Fourth Molar in Canids, Inferred by Individual Variation. *PeerJ* **2016**, *4*, e2689. [CrossRef]
26. Baltrūnaitė, L. Diet and Winter Habitat Use of the Red Fox, Pine Marten and Raccoon Dog in Dzūkija National Park, Lithuania. *Acta Zool. Litu.* **2006**, *16*, 46–53. [CrossRef]
27. Evenhuis, J.V.; Shirley Kot, C.C.; Arzi, B.; Kass, P.H.; Verstraete, F.J.M. Dental and Temporomandibular Joint Pathology of the Arctic Fox (*Vulpes lagopus*). *J. Comp. Pathol.* **2023**, *201*, 87–99. [CrossRef] [PubMed]

Disclaimer/Publisher's Note: The statements, opinions and data contained in all publications are solely those of the individual author(s) and contributor(s) and not of MDPI and/or the editor(s). MDPI and/or the editor(s) disclaim responsibility for any injury to people or property resulting from any ideas, methods, instructions or products referred to in the content.

animals

MDPI

Article

Cetacean Intracytoplasmic Eosinophilic Globules: A Cytomorphological, Histological, Histochemical, Immunohistochemical, and Proteomic Characterization

Antonio Fernández [1], Nakita Câmara [1,2,3,*], Eva Sierra [1], Manuel Arbelo [1], Yara Bernaldo de Quirós [1], Paul D. Jepson [4], Rob Deaville [4], Josué Díaz-Delgado [1,*], Cristian Suárez-Santana [1], Ayoze Castro [1,2], Julia N. Hernández [1] and Ana Godinho [1,5]

[1] Veterinary Histology and Pathology, Atlantic Center for Cetacean Research, University Institute of Animal Health and Food Safety (IUSA), Veterinary School, University of Las Palmas de Gran Canaria, Calle Transmontaña, s/n, 35416 Arucas, Canary Islands, Spain; antonio.fernandez@ulpgc.es (A.F.); eva.sierra@ulpgc.es (E.S.); manuel.arbelo@ulpgc.es (M.A.); yara.bernaldo@ulpgc.es (Y.B.d.Q.); cristian.suarez@ulpgc.es (C.S.-S.); ayoze.castro@ulpgc.es (A.C.); julia.hernandez@ulpgc.es (J.N.H.); ana_godinho@yahoo.com (A.G.)
[2] The Oceanic Platform of the Canary Islands (PLOCAN), Carretera de Taliarte, s/n, 35200 Telde, Canary Islands, Spain
[3] Loro Parque Foundation, Avenida Loro Parque, s/n, 38400 Puerto de la Cruz, Canary Islands, Spain
[4] Zoological Society of London, Institute of Zoology, Regent's Park, London NW1 4RY, UK; jepsonic.paul@gmail.com (P.D.J.); rob.deaville@ioz.ac.uk (R.D.)
[5] Rua Central de Gandra, University Institute of Health Sciences (IUCS)-CESPU, 4585-116 Gandra, Portugal
* Correspondence: nakita.camara@ulpgc.es or nakita.camara@plocan.eu (N.C.); josue.diaz101@alu.ulpgc.es or j.diazdelgado@surrey.ac.uk (J.D.-D.); Tel.: +34-611-050-008 (N.C.); +1-979-450-6041 (J.D.-D.)

Simple Summary: The presence of round to oval, single to multiple, hyaline eosinophilic globules inside the cytoplasmic of the hepatocytes of cetaceans are unknown. Therefore, this article aims to describe their occurrence and characterize their features using different laboratorial techniques. A total of 95 out of 115 cetaceans (83%) from 16 different species exhibited intracytoplasmic eosinophilic globules (IEGs) within the hepatocytes. These globules were positive for fibrinogen (FB, 97%), albumin (Alb, 85%), and α1-antitrypsine (A1AT, 53%), with the positivity for FB and A1AT correlated with live-stranding, hepatic congestion and a good nutritional status. The IEGs in 36 cetaceans that died due to bycatch were, all except one, FB-positive and A1AT-negative. The IEGs exhibited morphologic and compositional variations at the ultrastructural level, suggesting various stages of development. The proteomic analyses confirmed an association between the IEGs and acute phase proteins, suggesting a relationship between acute stress (i.e., bycatch), disease, and cellular protective mechanisms.

Abstract: The nature, etiopathogenesis, and clinicopathologic relevance of the prevalent intracytoplasmic eosinophilic globules (IEGs) within hepatocytes of cetaceans are unknown. This study aims to evaluate the presence and characterize the IEGs in the hepatocytes of cetaceans using histochemical and immunohistochemical electron microscopy, Western blot, lectin histochemistry, and matrix-assisted laser desorption/ionization time-of-flight mass spectrometry techniques. A total of 95/115 (83%) animals (16 species) exhibited histologically evident intracytoplasmic round to oval, single to multiple, hyaline eosinophilic globules within the hepatocytes. These globules were largely PAS-positive, diastase resistant, and were immunopositive for fibrinogen (FB, 97%), albumin (Alb, 85%), and α1-antitrypsine (A1AT, 53%). The IEG positivity for FB and A1AT were correlated with live-stranding, hepatic congestion and a good nutritional status. The cetaceans lacking IEGs were consistently dead stranded and had poor body conditions. The IEGs in 36 bycaught cetaceans were, all except one, FB-positive and A1AT-negative. The IEGs exhibited morphologic and compositional variations at the ultrastructural level, suggesting various stages of development and/or etiopathogenesis(es). The glycocalyx analysis suggested an FB- and A1AT-glycosylation pattern variability between cetaceans and other animals. The proteomic analyses confirmed an association between the IEGs and acute phase proteins, suggesting a relationship between acute stress (i.e., bycatch), disease,

and cellular protective mechanisms, allowing pathologists to correlate this morphological change using the acute hepatocytic cell response under certain stress conditions.

Keywords: albumin; α1-antitrypsine; bycatch; cetacean; fibrinogen; intracytoplasmic hyaline globules; live-stranding; liver; marine mammal pathology

1. Introduction

Many diseases known in humans and animals are characterized by protein alterations and intracellular or extracellular aggregation [1]. The presence of intracellular inclusions (aggregates of stainable substances) [2] has been extensively described and multiple studies have investigated their nature and their relationship with disease [3–8]. For instance, intracytoplasmic globules may be identified in an α1-antitrypsine deficiency [9], Alzheimer's disease [10], Parkison's disease [11], amyloidosis [12], endotoxemia [13], toxicity [14], iatrogenic origin [15], endoplasmic storage diseases [6], a variety of tumor types [16–18], hepatectomy [19], hepatic congestion [20], congestive heart failure, and hypoxia [18]. Additionally, some authors have further speculated that intracytoplasmic clear globules appear as a postmortem phenomenon in animals that died of anoxia (or asphyxia), because of the increased venous blood pressure just before and continuing for some time after death [21]. Furthermore, such intracytoplasmic inclusions may receive different names based on their morphologic features (e.g., hyaline bodies [4,20], pale bodies [22]), nature (e.g., α1-antitripsine [A1AT] [23], fibrinogen [FB] [5,6], complement factors [5]), and discoverers (e.g., Mallory–Denk bodies [24], Lafora bodies [25]).

Protein aggregations are usually the result of structural modifications of proteins by both mutations and cellular oxidative damage [26]. In the liver, a classic example is the Mallory–Denk body seen in steatohepatitis as well as in other conditions, such as iatrogenic hepatotoxicity, cholestatic disorders and some hepatocellular neoplasms [8,27]. Furthermore, structurally normal yet overexpressed proteins may also accumulate [28]. These aggregates can also be identified as structures with poor conformation leading to chaperones such as ubiquitin (Ub) that identify them and lead to their degradation [8,29]. These accumulations of poorly formed or excess proteins usually occur in the endoplasmic reticulum and are caused by mechanisms that impede the normal transport of proteins to the Golgi apparatus [30]. Various methodologies, including histochemical (e.g., periodic acid–Schiff [PAS], Shikata, acid fuchsin) stains, immunomarkers (e.g., P62, Ub, intermediate filament proteins keratins 8 and 18), and ultrastructural analyses, have been used to characterize and discern between these inclusions [31,32]. The presence of hyaline globules in cetacean hepatocytes (hereafter referred to as intracytoplasmic eosinophilic globules [IEGs]) has been previously described [33,34]. In 1993, Kennedy et al. identified PAS-diastase-resistant (PAS-d) IEGs in two striped dolphins (*Stenella coeruleoalba*) with a morbillivirus infection [34]. These IEGs also had "pink points" (PPs) highlighted by phosphotungstic acid hematoxylin (PTAH). The electron microscopy results revealed that the IEGs were 4–8 μm in diameter and were irregularly delineated by a membrane. The authors proposed that the IEGs had a possible lysosomal origin, containing glycoproteins. The presence of morbilliviral particles was ruled out. Further, in 2004, Jaber et al. described IEGs in 33 of 135 animals representing nine different cetacean species, including odontocetes and mysticetes [35]. However, the nature, etiopathogenesis, and relevance of the prevalent IEGs within the hepatocytes remain unknown. To partially fill in this knowledge gap, this study aims to investigate the presence and characterize the nature of IEGs in the hepatocytes of cetaceans.

2. Materials and Methods

2.1. Selection Criteria, Biologic, and Epidemiologic Data

A total of 155 free-ranging cetaceans (18 species) with appropriate carcass conditions (very fresh, fresh, and mild autolysis) were employed in this study. The analyzed animals were

115 cetaceans stranded in the Canary Islands between 1992 and 2008 (including seven bycaught delphinids) and 40 harbor porpoises (*Phocoena phocoena*) stranded on the shores of the United Kingdom. The biologic data (age class, sex, body condition, carcass condition, morphometrics) and stranding conditions for each individual were recorded systematically [36–38]. Permission for the management of the stranded cetaceans in the Canary Islands was issued by the environmental department of the Canary Islands' Government and the Spanish Ministry of Environment. The possession of the bodies and/or the samples collected from protected species (in this particular case, cetaceans) in England, by the aegis of the Institute of Zoology coordinated Cetacean Strandings Investigation Programme, was authorized under the Natural England Class License CL-01 (https://www.gov.uk/government/publications/licence-to-possess-plants-and-animals-for-scientific-purposes/licence-to-possess-and-transport-dead-specimens-of-annex-iv-and-iib-species-cl01#annex-b{-}{-}-research-establishments, accessed on 1 May 2023). No experiments were performed on live animals since our work was based on dead stranded cetaceans, including bycaught animals and some animals that had been stranded alive but died shortly after.

2.2. Pathologic Examinations

These animals were necropsied following the standardized protocols [36–38]. Representative tissue samples (random cross-sectional samples) of the main organs were collected. However, this study focused on the liver, where samples of 1 cm^3 in size were collected from two or more regions, depending on the size of the liver and the presence/absence of gross lesions.

2.3. Histopathology

The tissue samples were fixed in 10% neutral buffered formalin (for a minimum of 24 h), embedded in paraffin wax, and processed routinely. The sections (3 μm) were stained with hematoxylin and eosin (H&E) for the histologic examination. The PAS (for polysaccharides [e.g., glycogen] and mucosubstances [e.g., glycoproteins, glycolipids, and mucins]) with and without diastase treatment (diastase breaks down glycogen), reticulin (for reticular fibers), Hall's (for bilirubin), chromotrope aniline blue trichrome (CAB) (for collagen), and Perl's Prussian blue (for iron) stains were conducted to better characterize the IEGs. A subjective grading scale (mild, moderate, marked) was applied.

2.4. Immunohistochemical Analysis

For the immunohistochemical (IHC) analysis, we employed primary polyclonal antibodies against A1AT (1:500, Dako, Santa Clara, CA, USA), FB (1:200, Dako), Alb (1:1000, Abcam, Cambridge, UK), and cytokeratin (CK8/18) (1:20, Euro-Diagnostica, Arnhem, The Netherlands). Briefly, the tissue sections were treated with proteinase for 7 min (A1AT, FB) or citrate for 10 min (Alb, CK8/18) and incubated for 30 min using a 10% normal swine serum before an overnight incubation with the primary antibodies. The sections were then incubated using swine anti-rabbit (A1AT, FB), donkey anti-sheep (Alb) or rabbit anti-mouse (CK 8/18) sera for 30 min at room temperature. For the visualization, the Strept ABC Complex (Dako) was applied for 1 h, followed by 3-amino-9-ethyl-carbazole (Sigma, St. Louis, MI, USA). For the positive controls, internal cases from our database were used. In the case of the negative controls, sequential sections of the positive control tissues were incubated using a nonimmune homologous serum instead of the primary antibody.

2.5. Ultrastructural Analysis

Transmission electron microscopy (TEM) was performed on the liver sections of eight dolphins (five species) that had IEGs labeled for FB and/or A1AT by the IHC analysis. The formalin-fixed samples were postfixed in a suspension using 2.5% glutaraldehyde in a 0.1 M phosphate buffer (pH 7.2). Further, using osmium tetroxide, they were stained with 1% uranyl acetate and embedded in epon (Epon 812, Fluka Chemie AG, Industriestrasse 25, CH 9470 Buchs, Switzerland). Semi-thin sections were stained with Toluidine blue. Then,

ultra-thin sections were cut at 50 nm, contrasted using lead citrate, and observed under a Zeiss EM912 TEM. For the TEM interpretation and comparative purposes, liver samples without IEGs were used. A subjective grading scale (mild, moderate, marked) was applied.

2.6. Histochemistry, Western Blot, and Mass Spectrometry Analyses

A total of 23 liver samples from live-stranding, acute, and chronic disease and bycaught cases were selected. For the glycobiology analysis, formalin-fixed paraffin-embedded sections (3 μm) were incubated in a 10% bovine serum albumin for 30 min and incubated with six monoclonal primary antibodies (lectins) (Vector Laboratories, Burlingame, CA, USA), namely Sambucus nigra lectin (SNA), Phaseolus vulgaris erythroagglutinin (PHA-E), wheat germ agglutinin (WGA), Phaseolus vulgaris leucoagglutinin (PHA-L), Datura stramonium lectin (DSL), and Galanthus nivalis agglutinin (GNA) for 1 h at room temperature. The sections were washed three times for 5 min in a phosphate-buffered saline (PBS) and incubated for 45 min in the Strept ABC Complex (Vector Laboratories, Burlingame, CA, USA). Then, 3,3′-diaminobenzidine (Sigma, St. Louis, MI, USA) was applied after two washes of 5 min in the PBS. A subjective grading scale (mild, moderate, marked) was applied to describe the extension of the lesions.

For the proteomic analysis, fresh frozen liver samples were homogenized and placed in a HEPES sucrose buffer solution (985 μL) with phenylmethanesulfonyl fluoride (10 μL) and dithiothreitol (5 μL) at a low temperature, allowing for cell lysis to occur without protein denaturation. The samples were centrifuged at 7000× *g* rpm at 4 °C for 10 min, and the supernatant was recovered. The proteins were then quantified in an ELISA plate reader using the Bradford method at 595 nm absorbance. For electrophoresis, three 10% polyacrylamide gels were prepared. Two were used to perform the Western blot technique, while the other was stained with Comassi Blue for the matrix-assisted laser desorption/ionization time-of-flight mass spectrometry (MALDI-TOF) techniques.

For the Western blot analysis, gels were placed on a stirring plate and 20 volts and 90 amps were applied overnight at 4 °C for their transfer. The following day, the membrane along with the proteins were removed and stained with Ponceau Red to detect the bands and select the molecular weights of interest. After washing in distilled water and a tris-buffered saline with polysorbate 20 (TBST), the membrane was blocked with 10% milk for 1 h, and the primary antibodies (FB and A1AT) were incubated overnight. The next day, the membranes were washed using TBST and blocked with 0.5% skimmed milk for 20 min. Subsequently, the membranes were incubated with the secondary antibody (anti-rabbit, 1:3000) for 1 h. For visualization, the membranes were washed using TBST and SuperSignal® (Thermo Scientific, Rockford, IL, USA) was added by stirring in the dark for 5 min.

For the MALDI-TOF analysis, the bands of greatest interest were cut out of the polyacrylamide gel once they were stained with Coomasie Blue. The selection was conducted by locating the bands with the highest protein concentration and the bands that did not appear consistently in all the samples. Subsequently, the gel was broken using ammonium bicarbonate 50 mM and acetonitrile (5%) and stirred for 15 min. The supernatant was removed, and the operation was repeated twice using ammonium bicarbonate (50 mM) and acetonitrile (50%). The supernatant was removed and immersed in 100 μL acetonitrile (100%). A SpeedVac was used for 20 min to dry the samples. DIEGsstion was achieved by adding trypsin 10 ng/μL to each sample with a volume adjustment (5 to 20 μL per sample). Next, 50 μL of a 20 Mm ammonium bicarbonate was added and the samples were incubated overnight at 37 °C. For the peptide extraction and crystallization, the samples were centrifuged lightly, and the supernatant was collected. Then, 60 μL of acetonitrile (60%) and trifluoroacetic acid (TFA, 0.1%) were added to the samples and stirred for 30 min at room temperature. The procedure was repeated twice. The supernatant was collected and dried for 2 h using the SpeedVac. Once the samples were dried, they were washed using acetonitrile (60%) and TFA (0.1%), followed by TFA (0.1%) alone. Next, the samples were aspirated using a Ziptop c18 pipette tip, which previously aspirated acetonitrile (100%) and TFA (0.1%). After aspirating the samples with cyanohydroxycinnamic acid 5 mg/mL

in acetonitrile (50%) and TFA (0.1%), 1.2 µL of the solution was aspirated and applied to the plate for crystallization and the MALDI-TOF analysis. The peptide mass fingerprinting results were obtained and entered into two databases (SwissProt and nrNCBI) for the identification of the peptides and the corresponding proteins using a taxonomic selection ("other mammals").

2.7. Statistical Analysis

Fisher's exact test was performed to evaluate the potential associations between the presence of IEGs and the body condition, IEGs and congestion, IEGs and meningoencephalitides, meningoencephalitides and IEG–A1T1 positivity, meningoencephalitides and IEG–FB positivity, IEG–FB positivity and natural and anthropogenic pathologies, and IEG–A1T1 positivity and natural and anthropogenic pathologies.

3. Results

3.1. Study Population and Epidemiology of IEGs

A total of 95 of 115 (83%) animals, including 16 species, presented IEGs (Table 1).

Table 1. Cetaceans with intracytoplasmic eosinophilic globules (IEGs) within the hepatocytes and liver congestion.

Species	Stranded Cetaceans			Livers with IEGs	Liver Congestion [1]
	Alive	Dead	Total		
Balaenoptera physalus	1	0	1	1/1	0/1
Delphinus delphis	8	10	18	15/18	15/18
Globicephala macrorhynchus	2	1	3	2/3	3/3
Grampus griseus	1	1	2	2/2	2/2
Kogia breviceps	0	5	5	3/5	3/5
Kogia simus	0	1	1	1/1	1/1
Lagenodelphis hosei	0	1	1	1/1	0/1
Mesoplodon densirostris	2	0	2	2/2	2/2
Mesoplodon europaeus	2	1	3	2/3	2/3
Phocoena phocoena	0	1	1	0/1	1/1
Physeter macrocephalus	0	4	4	3/4	3/4
Pseudorca crassidens	2	1	3	3/3	2/3
Stenella coerulealba	13	18	31	27/31	27/31
Stenella longirostris	1	2	3	0/3	3/3
Stenella frontalis	9	12	21	18/21	19/21
Steno bredanensis	1	1	2	2/2	2/2
Tursiops truncatus	5	7	12	12/12	12/12
Ziphius cavirostris	1	1	2	1/2	1/2
Total	48	67	115	95/115	98/115

[1] Livers with moderate to marked sinusoid congestion.

The sex distribution was male (62), female (48), not recorded (5). The age distribution was fetus/neonate/calf (15), juvenile/subadult (26), adult (57), and not recorded (17). From the 115 animals, 48 (42%) were live stranded and 67 (58%) were dead stranded. A total of 36 animals were bycaught (UK, n = 29; Canary Islands, n = 7). The detailed biologic and epidemiologic data of these animals are recorded in Supplemental Table S1. IEGs were more prevalent in the live-stranded animals (90%) with acute liver congestion (Fisher test, p-value < 0.001) and in the individuals that had a good nutritional status (Fisher test, p-value = 0.025). No sex or age bias was noted (Fisher test, p-value = 0.842; and Chi-square test, p-value = 0.489, respectively). The bycaught animals presented a milder hepatic congestion compared to the live-stranded animals.

3.2. Histologic and Immunohistochemical Features of IEGs

The IEGs had varying morphologic features, ranged from 3 μm to 8 μm in diameter, were pale (occasionally noticeable as "optically empty", bearing some resemblance to lipid macrovacuoles) to bright with thin to dense homogeneous to granular eosinophilic material that often displaced the nucleus to the periphery (signet-ring-like morphology), and had rare fibrillary structures (Figure 1). In some instances, they seemed to have a clear halo. The IEGs tended to be larger in the livers with marked congestion, typically spanning the entire cytoplasm and peripheralizing the nucleus.

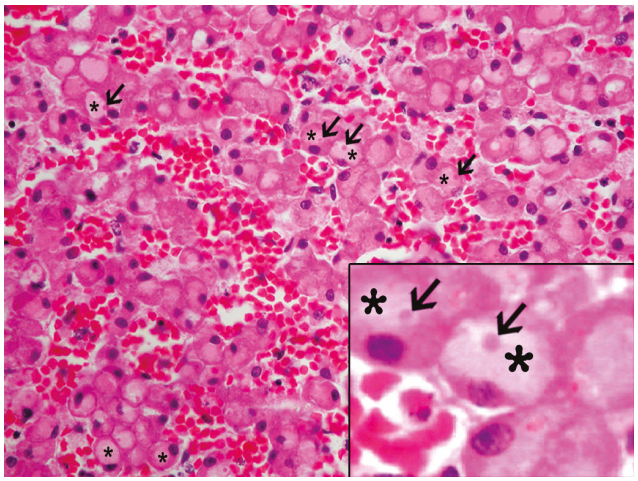


Figure 1. Histologic features of the intracytoplasmic eosinophilic globules (IEGs) in cetaceans. Common bottlenose dolphin, *Tursiops truncatus*. Sinusoids were variably distended; hepatocytes had intracytoplasmic IEGs (*) and "pink points" (PPs) (arrows). Hematoxylin and eosin (H&E) 40×. Inset: common bottlenose dolphin, *Tursiops truncatus.* Detail of the IEGs (*) within hepatocyte and PPs (arrows). H&E 80×.

The IEGs were consistently yet variably highlighted by the PAS (95/95, 100%), and in 72 of 95 (76%) animals, the IEGs were PAS-d resistant (Figure 2).

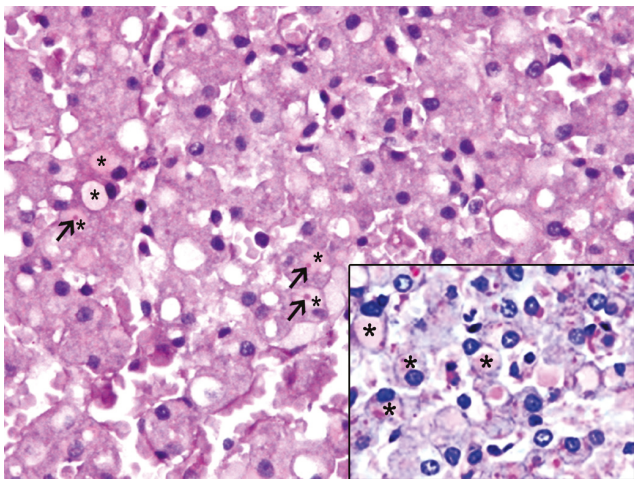


Figure 2. Histologic features of the intracytoplasmic eosinophilic globules (IEGs) in cetaceans. Common bottlenose dolphin, *Tursiops truncatus.* The IEGs (*) and PPs (arrows) were variably highlighted by the periodic acid–Schiff (PAS). PAS 40×. Inset: Common dolphin, *Delphinus delphis*. The IEGs (*) were largely resistant to PAS-diastase (PAS-d), clearly marked with a pinkish color. PAS-d 40×.

The IEGs in 91 of the 95 (96%) animals had single, and rarely dual, central to peripheral bright, dense eosinophilic stippling (hereafter referred as to "pink points" [PPs]). The PPs

were consistently PAS-d resistant. A moderate to marked congestion, primarily within the centrilobular areas, was observed in 90.9% of the livers with IEGs, whereas varying degrees of congestion was seen in 31.2% of the livers without IEGs.

The IEGs were immunopositive for FB (92/95, 97%) (Figure 3a), Alb (90/95, 90%) (Figure 3b), and A1AT (51/95, 54%) (Figure 3c) (Tables S1 and S2).

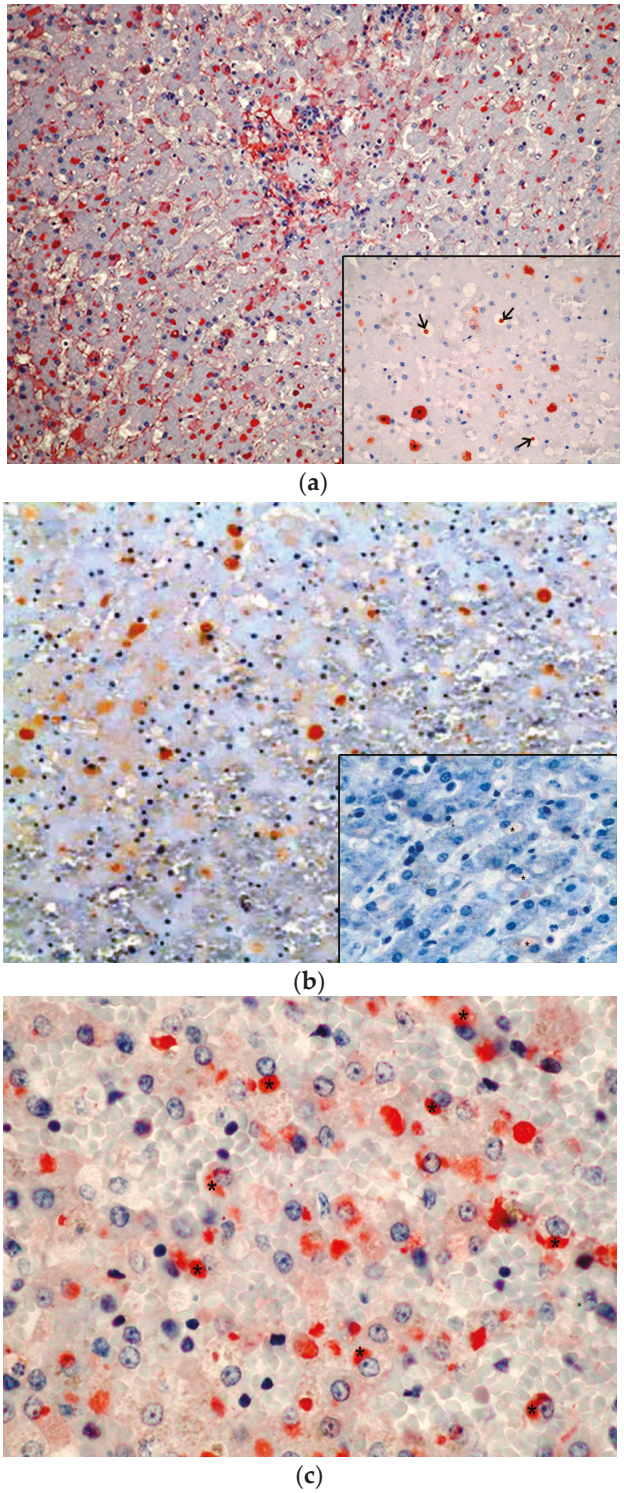


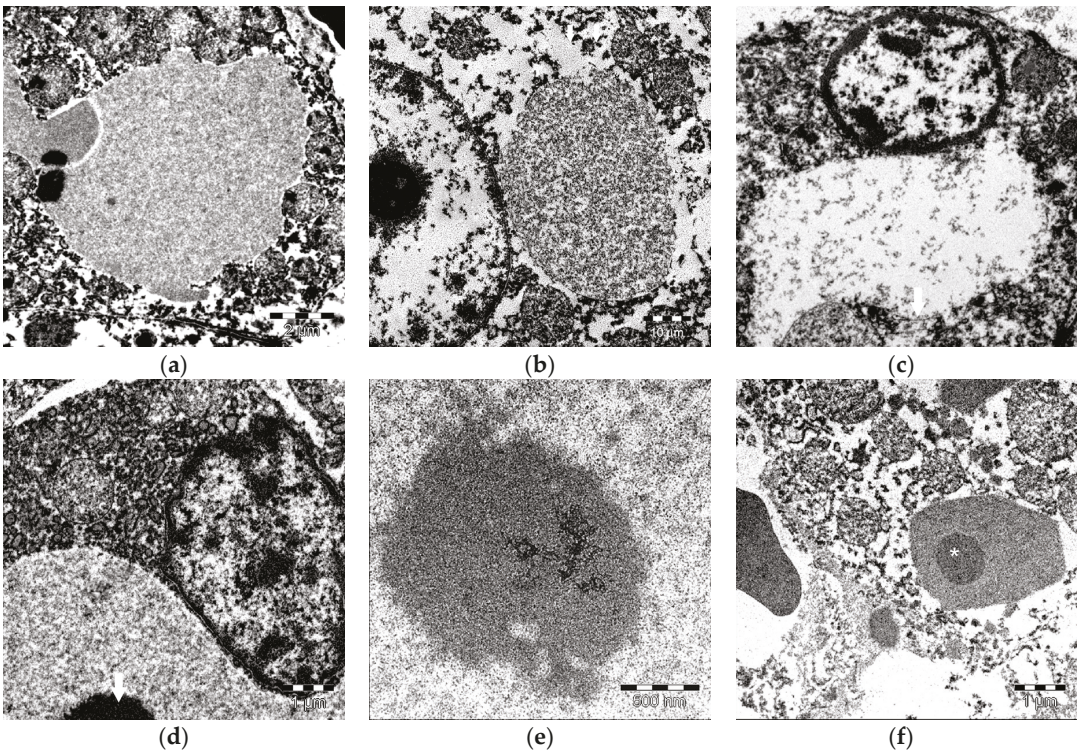
Figure 3. Immunohistological features of the intracytoplasmic eosinophilic globules (IEGs) in cetaceans. (**a**) Common dolphin, *Delphinus delphis*. The IEGs were labeled by an anti-fibrinogen (FB)

antibody, presenting a red color. The IHC for FB 20×. Inset: common dolphin, *Delphinus delphis*. Detail of the FB-positive IEGs (*) and the PPs (arrows). The IHC for FB 40×. (**b**) Dwarf sperm whale, *Kogia sima*. The IEGs were labeled by an anti-albumin (Alb) antibody. The IHC for Alb 20×. Inset: common dolphin, *Delphinus delphis*. Detail of the Alb-positive IEGs (*). The IHC for Alb 40×. (**c**) Striped dolphin, *Stenella frontalis*. The IEGs (*) were labeled by an α-1-antritrypsin (A1AT) antibody, demonstrating a positive red color. The IHC for A1AT 40×.

The IEGs–FB positivity was more prevalent in the animals that died due to natural causes. However, the same correlation was not found with the IEGs–A1AT positivity (Fisher test, p-value = 0.006 and p-value = 0.079, respectively). Nevertheless, the IEGs–A1AT positivity was associated with the individuals that presented meningoencephalitis (Fisher test, p-value = 0.024).

3.3. Ultrastructural Features of IEGs

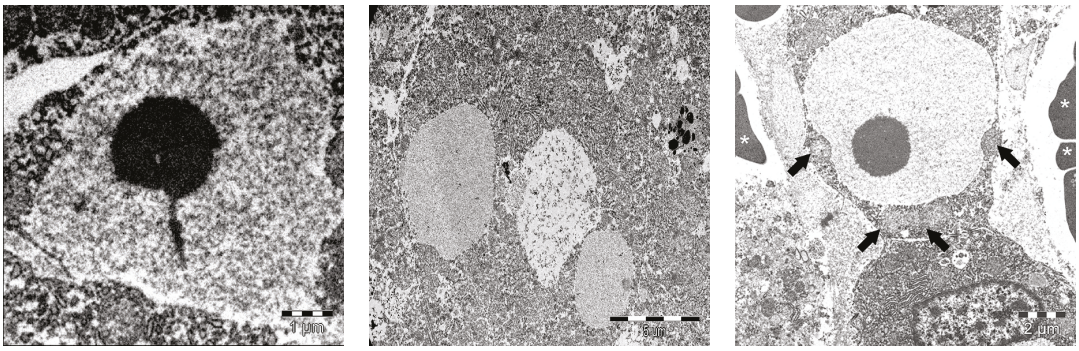
Ultrastructurally, the IEGs exhibited a variable content and morphology. Some had a thin, homogenous, moderately electrodense granular material (Figure 4a), while others had a coarse, moderately electrodense granular material (Figure 4b) or a scattered thick granular electrolucent material (Figure 4c). Some IEGs were bound by a limiting membrane (Figure 4b,c). The IEGs ranged from 3 μm to 8 μm, often peripheralizing the nucleus (Figure 4d). The PPs ranged from 0.9 μm to 2.5 μm and were composed of a granular, thick electrodense material that lacked a limiting membrane (Figure 4e). The PPs often comprised a large portion of the IEGs (Figure 4f). Some of the PPs had radial projections of an identical electrodense granular material (Figure 4g). Most of the IEGs had a single PP; however, some had two. The PPs and IEGs diameters were correlated positively. In the bycaught animals, the IEGs were not morphologically dissimilar to those observed under other circumstances. Single or multiple IEGs were seen in the hepatocytes of bycaught porpoises (Figure 4h), often having a finely granular, homogeneous, and slightly electrodense material. The IEGs contours were variable. Some were lined by organelles, e.g., mitochondria, peroxisomes (Figure 4i). PPs were also detected in the bycaught animals. No additional structural abnormalities were detected in the affected hepatocytes.



(**a**) (**b**) (**c**)

(**d**) (**e**) (**f**)

Figure 4. *Cont*.



(**g**) (**h**) (**i**)

Figure 4. Ultrastructural features of the intracytoplasmic eosinophilic globules (IEGs) within the hepatocytes in cetaceans. Transmission electron microscopy (TEM). (**a**) Common dolphin, *Delphinus delphis*. The IEGs with a fine, moderately electrodense granular material lacking limiting membrane. 4000×. (**b**) Striped dolphin, *Stenella coeruleoalba*. Small IEGs with a granular, moderately electrodense material and a focally preserved, thin limiting membrane (arrows). 5000×. (**c**) Spotted dolphin, *Stenella frontalis*. The IEGs with a fine, scattered, mildly electrodense granular material and a focally preserved limiting membrane (arrow). 4000×. (**d**) Common bottlenose dolphin, *Tursiops truncatus*. The IEGs with a fine, moderately electrodense granular material peripheralizing the nucleus (asterisk). A fragment of a "pink point" (PP) is noted (arrow). 6300×. (**e**) Harbor porpoise, *Phocoena phocoena*. Electrodense PP lacking a limiting membrane. 20,000×. (**f**) Harbor porpoise, *Phocoena phocoena*. Large PP (asterisk) within a relatively small IEG. 4000×. (**g**) Harbor porpoise, *Phocoena phocoena*. Electrodense PP with a focal fibrillary projection within the IEG. (**h**) Harbor porpoise, *Phocoena phocoena*. Three IEGs of varying electrodensities within a hepatocyte. 6300×. (**i**) Harbor porpoise, *Phocoena phocoena*. Two PPs within an IEG; note the adjacent mitochondria (arrows). The asterisks indicate erythrocytes within sinusoidal spaces. 5000×.

3.4. Histochemistry, Western Blot, and Mass Spectrometry Analyses

The glycobiology techniques revealed that the PPs were PAS-d resistant, had a stippling crown highlighted by a reticulin stain, and showed a red refringent staining pattern with CAB staining that was compatible with megamitochondria (Figure 5). The accumulation of glycogen within the IEGs was seen in 15 livers. The lectin histochemistry panel (Table S3) in the liver sections from three animals revealed IEGs that were consistently positive for SNA and PHA-E, and had varying staining for GNA, PHA-L, and DSA (Figure S1). The IEGs had positivity for SNA in 8/15 and PHA-E in 13/15 cases. WGA was consistently negative.

The Western blot analysis revealed specific bands for the studied proteins. Three bands corresponding to the alpha-, beta-, and gamma-chains of FB and one band corresponding to A1AT were identified (Figure S2). As expected, the anti-FB antibody identified bands of different molecular weights corresponding to the alpha-, beta-, and gamma-chains of FB and the FB-derived peptides.

A total of 19 proteins with a statistical significance were identified from 17 bands in the polyacrylamide gel (Figure S3 and Table S4). The identified proteins were serum albumin, protein disulfide-isomerase, catalase, protein disulfide isomerase-associated 3, calreticulin, carbamoyl-phosphate synthetase 1 (two isoforms), endoplasmin, formyltetrahydrofolate dehydrogenase isoform a, betaine-homocysteine methyltransferase, beta-actin, actin, alanine-glyoxylate aminotransferase, ornithine carbamoyltransferase, arginase 1, ferritin L subunit, methionine adenosyltransferase I, and glutathione S-transferase. Mitochondrial proteins were abundant, such as carbamoyl-phosphate synthetase 1, alanine-glyoxylate aminotransferase, and ornithine carbamoyltransferase, among others, as well as other proteins involved in the urea cycle, such as arginase 1, ornithine carbamoyltransferase, and carbamoyl-phosphate synthetase 1.

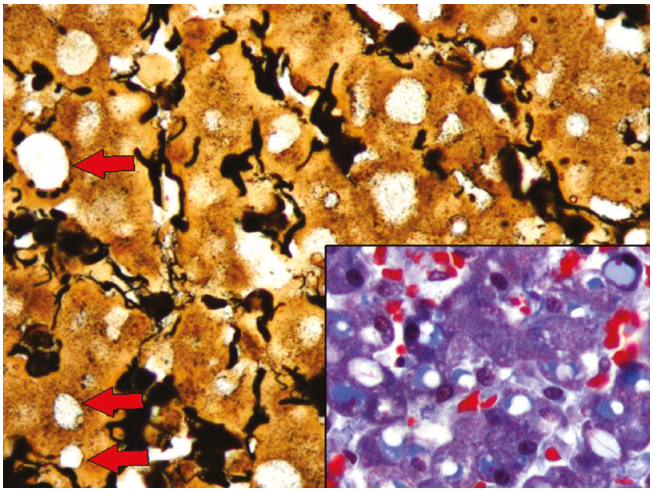


Figure 5. Reticulin technique. Detail of the hepatic intralobular reticulin fiber framework and adjacent hepatocytes harboring IEGs. Some IEGs had a thin peripheral stippling highlighted by a reticulin stain (arrows). Reticulin 40×. Inset: PPs (fibrillary strands in the longitudinal section) were stained red by chromotrope aniline blue trichrome (CAB). CAB 40×.

4. Discussion

This study assessed the presence of and characterized IEGs in cetaceans using histologic, immunohistochemical, ultrastructural, histochemistry and proteomic analyses. In this study, IEGs were prevalent in odontocetes and mysticetes, particularly in live-stranded animals with evidence of acute hemodynamic alterations (e.g., acute passive hepatic congestion) and a good nutritional status. The lower frequency of IEGs in animals with poor body conditions could be related to a liver protein synthesis compromise [39]. No species or sex bias was observed. However, IEGs were more prevalent in adult and subadult animals, probably due to overrepresentation. Regardless, these results suggest that animals of any age may possess etiopathogenic mechanisms that lead to IEG formation. A wide variety of cetacean species were affected and these had readily evident morphologic, biologic, and behavioral differences. Therefore, IEGs should be considered non-species-specific, which agrees with the observations in humans and some terrestrial animals [3,24,40,41]. IEGs were observed in animals subjected to stressful factors, including fatal anthropogenic interactions, e.g., bycatch, and acute and chronic disease processes.

The IEGs were similar across species and conditions. However, they presented slight morphologic and tinctorial variations, including consistent PPs. The IEGs were largely PAS-d resistant, which agreed with a previous study [34] and suggested that glycoproteins and/or glycolipids are components of IEGs [34,42]. Glycoproteins such as FB might also be non-resistant to PAS-d [5,6]. The accumulation of glycogen within the IEGs was seen in 15 livers. Such findings were frequently associated with acute and subacute hepatic injuries [43]. The IEGs tended to be larger in livers with marked congestion, typically spanning the entire cytoplasm and peripheralizing the nucleus. Hyaline, FB-positive, and A1AT-positive globules directly associated with liver congestion were described in livers from human autopsies, as well as in rats in which vacuoles were formed within the cytoplasm of the hepatocytes and metamorphosed into hyaline globules by condensation [4,19]. In a study conducted on rats, the formation of IEGs was observed within a 24 h period after the induction of hepatic congestion. After a reestablished circulation, half of the vacuoles had disappeared, while the other half underwent a metamorphosis, transforming into hyaline globules from the condensation of its content [19]. After 24 h of circulatory recovery, very few IEGs were observed, which confirmed the reversibility of the process [19]. A comparative approach would lend support to the potential reversibility for the IEGs in our study set, which is further supported by seemingly healthy cytological features based on

the TEM examinations. Liver congestion or ischemia may also involve the production of other proteins, such as heat shock proteins [44].

The acute phase proteins (APPs) may be classified as positive or negative, depending on their serum concentrations during inflammation or hemostatic disturbances. The positive APPs included FB and A1AT, among others, whereas Alb was considered a negative APP [45]. In this study, the IEGs were largely immunopositive for FB and Alb (90%), and to a lesser extent for A1AT. The IEGs were consistently negative for CK8/18 and ubiquitin ruling out a compositional analogy to Mallory bodies and intracytoplasmic hyaline bodies [8,31,46,47].

FB-positive IEGs were more prevalent in congested centrilobular areas and live-stranded animals, suggesting an association with hemodynamic alterations [4,48]. The PPs were largely negative for FB; however, some showed a peripheral halo-like labeling. In hypoxic/ischemic liver disease, secondary to a reduced cardiac output, a rapid decrease in the serum FB ensued with a parallel increase in the liver FB due to a higher production of FB (and other APPs) in the hepatocytes [49]. The high prevalence of the FB-positive IGEs observed in this study and the increased FB expression recorded after a variety of liver injuries lends support to a non-specific hepatic injury response mechanism hypothesis [50].

Alb is the most abundant serum protein in mammals. It is a polypeptide and when mutated it may present glycosylated dominions [51,52]. The Alb values and consequently the albumin:globulin ratio are high in cetaceans compared to domestic animals [53]. In cachexia or profound malnutrition, protein production is impaired. In such circumstances, positive APPs such as FB and A1AT may increase, while negative APPs such as albumin may decrease [54]. The Alb-positive IEGs were more prevalent in the congested areas and included homogeneous and "optically empty" IEGs within the hepatocytes. The serum albumin is not a standout marker of liver disease in marine mammals. However, in cases of dehydration and shock [e.g., under "stranding stress response" (SSR)] [55–60], a high level of serum albumin may be detected [53]. By contrast, alpha-globulins such as haptoglobin, lipoproteins, and antitrypsin are important markers of acute inflammatory disease in some marine mammals and may be elevated in inflammatory and infectious diseases prior to clinical signs [53].

A1AT is a stress protein with direct defensive functions in the liver that can reduce cellular apoptosis in hepatic sinusoids in cases of hypothermia and hypoxia-reoxygenation [61]. Therefore, the A1TA positivity may be interpreted as a hepatocellular protection mechanism, and in many cases, coexists with the FB accumulation [62]. In humans, under normal conditions, the liver secretes 34 mg/kg/24 h of A1AT, which can be increased between three and five times in inflammatory and infectious processes [63]. In this study, 54% of the stranded cetaceans had A1AT-positive IEGs. Nearly half of them were live-stranded animals. In this study the presence the A1AT-positive IEGs was statistically correlated with meningoencephalitis. In humans, A1AT is increased in the serum and cerebrospinal fluid in cases of bacterial, but not viral, meningitis [30]. Meningoencephalitis in cetaceans is caused mainly by bacteria (*Brucella* sp.), viruses (*Morbillivirus* sp.), and parasitosis (trematodes) [36,37]. However, in these cases, virological and/or bacteriological studies have not been carried out, so the possible etiopathogenic relationship should be investigated in the future, given its possible diagnostic value. None of these cases had lesions that were suggestive of an A1AT deficiency [9,23,64,65]. A1AT-positive IEGs were common in livers of alcoholic patients [23]. Interestingly, A1AT appeared to be detectable later than FB based on lack of detection in the IEGs of bycaught porpoises (acutely dead by asphyxia).

All the bycaught animals in this study, except for one neonate, had FB-positive and A1AT-negative IEGs. Death by asphyxia in bycaught animals may take between 3 and 6 min [48]. Unlike terrestrial animals, cetaceans' voluntary respiration may impede "reflex inspiration" (expected to occur in humans and terrestrial animals), resulting in a state of unconsciousness and death from hypoxia [66]. While pulmonary congestion, edema, and emphysema may be common in bycaught porpoises, hepatic congestion may be more variable [48,67]. In this study, the bycaught animals presented milder hepatic congestion

compared to live-stranded animals. In bycaught dolphins, severe stress may result in a rapid and massive formation of IEGs. The absence of the A1AT positivity in these cases could be explained by a short course of severe stress and systemic hypoxia leading to death in fatal net entanglements [48,67]. A sudden increase in catecholamines, vasoactive factors, and capture myopathy-related damage may also play a role in these cases [48,67,68].

Either stranded off the Canary Islands or the United Kingdom, we confirmed the IEGs using transmission electron microscopy with slight morphologic variations, including number (one to two), size, electrodensity, presence or lack of limiting membranes, and adjacent organelles. The ultrastructural studies on the intracytoplasmic hyaline globules in various disease processes showed most cases to be composed of filamentous material [27]. In our study, only granular content was observed, though the state of preservation of the samples may have compromised their ultrastructure. It is known that in cases of poor A1AT conformation, intracytoplasmic globules may be surrounded by a membrane [62]. This may also be noted in FB-positive globules [69]. In this study, we observed IEGs with and without a membrane, which could suggest the existence of different IEG-developing mechanisms and, plausibly, uncharacterized globular materials. TEM was performed on the samples which were fixed in formalin, which might have resulted in certain artifacts that could have confounded the interpretation of TEM results. Future studies are warranted since it was described that 30% of the newly synthesized proteins may have been poorly assembled and could have been retained in the endoplasmic reticulum [70]. We hypothesize that altered protein maturation/folding could be a mechanism underlying the IEG formation in cetaceans.

The study of cellular glycocalyx allowed for a better understanding of cellular metabolism [71]. For instance, poorly formed A1AT requires the alteration of a mannose moiety to modify the structure of carbohydrates and to be recognized for its degradation [72]. We used lectin histochemistry to identify the carbohydrate structures since they constituted a group of proteins and glycoproteins with the ability to connect to sugar chains [73]. In cases of hypoxic and ischemic stress, there is an increase in glucose, which contributes to the synthesis of O-link β-N-acetylglucosamine (O-GlcNac) [74]. This type of glycosylation aided in the preservation of mitochondria by reducing cell death in mice [75]. On the other hand, O-GlcNac also increased thermotolerance, increasing its levels before an increase in heat shock protein (HSP) synthesis occurred [76]. This modulated the regulation of HSPs, particularly HSP90, as well as other stress-induced proteins, favoring protein stabilization and preventing their aggregation [77]. In this study, we used WGA to detect O-GlcNac, which participated in anti-stress mechanisms [78].

In this study, the IEGs were consistently positive for SNA and PHA-E, and had varying staining for GNA, PHA-L, and DSA. The known glycosylation patterns for the FB-positive hyaline globules would anticipate the positivity for SNA and the negativity for PHA-E [79]. However, we observed that the IEGSs had an SNA positivity in 8/15 and a PHA-E positivity in 13/15 cases. It was possible that the SNA-negative animals (7/15) could have expressed only the α chain of FB, based on the type of glycosylation. The IEGs were largely negative for WGA, as only one bycaught porpoise showed WGA-positive IEGs. This could be interpreted as a cellular response to a stressful situation, such as net entanglement, and affirmed an association with a stress response. As a preliminary conclusion on the glycobiology analysis results, it seems plausible that glycosylation of the different protein chains of FB and A1AT may be different from in the glycosylation in other mammals and/or that these were modified by metabolic factors. Future studies should address the sugar chain identification in FB of A1AT in cetaceans.

The etiopathogenic mechanisms that could play primary roles in the IEG development in cetaceans may be associated with (a) live-stranding-related phenomena, namely severe acute passive congestion due to body compression against the substrate and SSR [55–60], and (b) individual factors (species, age, nutritional status, health status). The body compression at beaching results in an impeded systemic venous return and systemic venous hypertension, primarily in the caudal vena cava and peritoneal viscera. This is particularly significant in the liver, which is supported by histologic alterations that are consistent with

acute centrilobular (passive) congestion and may result in the accumulation of substances that cannot be excreted into the sinusoidal spaces. Under such circumstances, proteins and other molecules may leak into the space of Disse from the hepatocytes and sinusoid capillaries, as observed in rats [40]. The venous compression in rats resulted in IEGs within 3–6 h. However, the IEGs may be resolved 24 h after the subsequent vascular decompression (reperfusion). These data lend support to the reversibility of IEGs. In humans, IEGs have also been described under passive congestion in deaths by severe mechanical compression [80]. Along with other experimental studies, these highlight the relevance of hemodynamic disturbances in the IEG development, typically involving increased pressure at the caudal/inferior vena cava and subsequent hepatic congestion [19]. Interestingly, the vacuoles with a morphologic similarity to the present IEGs and the hepatocellular globules in other studies in various species were interpreted as a postmortem phenomenon in rats that were euthanized using CO_2 in closed chambers [40]. The change has been variably reported and attributed to the postmortem effects of anoxia, inadequate exsanguination, or delay in necropsy. Two critical factors for postmortem hepatocyte vacuolation are hepatic anoxia, which increases the permeability of the hepatocytes, and high venous or intrahepatic blood pressure, which forces sinusoidal plasma into the hepatocytes to form the vacuoles [21]. With these two factors, the hepatocyte vacuoles were much larger and developed faster [21,81,82]. The venous blood pressure rose sharply during the first 5–10 min and persisted for hours after death, a time period coincident with the vacuole development in animals that die of anoxia or asphyxia [21]. In contrast, if the animals were bled immediately after death, the hepatocyte vacuoles were not observed, presumably due to the prevention of an increase in the venous or intrahepatic blood pressure [81,82]. In our study, we did not control the variable time-after-death necropsy and the fixation of the tissue. Therefore, those conclusions cannot be ratified. However, these vacuoles were not present in all the specimens and certainly in not all the routine cases.

Cetacean live strandings should be understood as potential life-threatening situations prompting physiopathological mechanisms for the preservation of hemostasis (the basis of SSR) [55–60]. These may include peripheral vasoconstriction (leading to local or multiorgan hypoxia) to maintain a perfusion to the vital organs, such as the heart and brain [68]. If prolonged, venous congestion and arterial peripheral vasoconstriction can ensue and may lead to ischemic hypoxia in various organs, including the liver. We believe this is a major player for IEG development. Further negative factors in live-stranding events would include individual hyperthermia, which may also prompt APP production [83] or cause reperfusion injury.

Moreover, pre-existing or concomitant disease processes may influence IEG development. Along with other studies [84], this reinforces the idea that more proteins can be produced and found in the liver in stranded cetaceans that are subject to severe stressors. For instance, in septicemia, the liver increases APP production (e.g., FB and A1AT) as well as coagulation factors [85]. A lack of an A1AT expression in the FB-positive IEGs was observed in poor nutritional statuses, senility, infectious and neoplastic diseases, and in live-stranded animals. A1AT was commonly seen in animals with a variety of pathologic processes, such as septicemia, infectious meningoencephalitis, and parasitic sinusitis, which was in agreement with previous observations in natural and experimental diseases in humans and other animals [30,85].

PPs were previously described by Kennedy et al. in 1993 and Jaber et al. in 2004 [34,35]. The reports of structures comparable to PPs in humans and other animals include FB-III hyaline globules [69], type-III Mallory bodies [27], and structures observed in humans with cardiac dysfunction [86] and rats with autolysis [40]. Nevertheless, the significance of these structures is still unknown. The strong red refringence of PPs due to trichrome stain suggested megamitochondria [86,87]. However, this was ruled out by the TEM analysis. The PPs were shown to be composed of glycosylated elements and were present in the FB- and A1AT-positive IEGs. We surmised that the PPs in cetaceans were part of

protein metabolism aggregation and participated in the morphologic signature of the stress response in cetaceans [88].

In the mammalian liver, 74% of the proteins are membrane proteins and only 11% correspond to cytosol proteins. When detected in a serum, it is a sign of mitochondrial damage, and consequently, cellular damage [89]. Endoplasmin (also known as HSP90) is directly related to situations of cellular stress, such as oxidative stress, and is normally associated with heat stress [90]. We detected endoplasmin using the MALDI-TOF analysis and it was likely related to live stranding and high environmental temperatures and/or individual hyperthermia. We also identified two types of disulfide isomerase protein, as well as calreticulin. The former was one of the stress proteins belonging to the endoplasmic reticulum response that acts in cases of oxidative stress [91]. These proteins belonged to a family of isomerases. A1AT was identified as one of the substrates for these enzymes [92]. Calreticulin, a soluble endoplasmic reticulum protein, acted through connections to proteins with conformation problems or that needed to be degraded, such as A1AT [92–94]. Both results corroborated the abundant presence of A1AT in the IEGs in stranded cetaceans and indicated that the cetacean hepatocytes may behave in a similar way to other species that exhibit an aggregation of A1TA [92–94]. The proteomic analysis in cetaceans remained comparatively limited [95–98]. The integration of the omics technologies, including proteomics, will be of great benefit to assess and understand the complexity and intricacy of the SSR and the signatures of disease in cetaceans. Such knowledge could advance cetacean care and conservation initiatives as well as environmental issues.

5. Conclusions

In summary, the combination of the histologic, immunohistochemical, glycosylation, Western blot, and proteomic analyses allowed for characterization of IEGs in stranded cetaceans. The IEG composition included APPs, primarily FB, Alb, and A1AT. The IEGs were interpreted as a potentially reversible response to stress and hepatic injury, and IEGs should be considered part of the stress response signature along with other biomarkers and pathologic findings in cetaceans. The relevant etiopathogenic mechanisms contributing to IEG development were associated with live-stranding-related phenomena, namely severe acute passive congestion and SSR, bycatch stress, and individual factors, from which the nutritional status and pre-existing diseases appear to be more important. While further research is warranted to fully characterize the composition of and assess the clinicopathologic relevance of IEGs in cetaceans, these results open new venues and contribute to a better understanding of cellular response to injury and protective phenomena in cetaceans, contributing to the advancement of integrative marine environment biomonitoring.

Supplementary Materials: The following supporting information can be downloaded at: https://www.mdpi.com/article/10.3390/ani13132130/s1, Table S1: Biologic, epidemiologic, and pathologic data of 115 cetaceans stranded in the Canary Islands included in this study; Table S2: Histochemical and immunohistochemical analysis of the intracytoplasmic eosinophilic globules (IEGs) included in this study; Table S3: Qualitative assessment of the lectin histochemistry labeling pattern, mild +, moderate ++, marked +++; Figure S1: Lectin-immunohistochemical features of intracytoplasmic eosinophilic globules (IEGs) in cetaceans. SNA, Sambucus nigra lectin; PHA-E, Phaseolus vulgaris erythroagglutinin; WGA, wheat germ agglutinin; PHA-L, Phaseolus vulgaris leucoagglutinin, DSL, Datura stramonium lectin; GNA, Galanthus nivalis agglutinin. Harbor porpoise, *Phocoena phocoena*, (a) through (e). Short-finned pilot whale, *Globicephala macrorhynchus*, (f) through (j). Spinner dolphin, *Stenella longirostris*, (k) through (o). (a) Canalicular pattern. (b) Globular pattern. (c) Canalicular pattern. (d) Labeling within Kupffer cells. (e) Globular and canalicular pattern. (f) Diffuse pattern. (g) Globular pattern. (h) Diffuse pattern. (i) Labeling within Kupffer cells. (j) Globular, canalicular and diffuse patterns. (k) Canalicular pattern. (l) Labeling along sinusoidal surface. (m) Canalicular and diffuse patterns. (n) Labeling within Kupffer cells. (o) Canalicular pattern; Figure S2: Western blot. Fibrinogen (left) and α1-antitrypsine (right); Figure S3: 10% acrylamide gel with markings of the 17 points from which the proteins were extracted; Table S4: Peptide mass fingerprinting (PMF) results.

Author Contributions: Conceptualization, A.F. and A.G.; methodology, validation, formal analysis, and investigation A.F., N.C., P.D.J., R.D. and A.G.; resources, data, and sample collection, A.F., N.C., E.S., M.A., Y.B.d.Q., P.D.J., R.D., J.D.-D., C.S.-S., A.C., J.N.H. and A.G.; writing—original draft preparation, N.C., J.D.-D. and A.G.; writing—review and editing, A.F., N.C., J.D.-D. and A.G.; supervision, A.F.; project administration, A.F., N.C. and A.G.; funding acquisition, A.F., N.C. and A.G. All authors have read and agreed to the published version of the manuscript.

Funding: Part of this research work was supported by grants [Postgraduate Grant for the Completion of Doctoral Theses of the Modality B2 (ref TES2005/255 supported by Canary Islands Research Agency Innovation and Information Society); Predoctoral Grant and Postdoctoral Period for Training of Research Personnel (ref BES 2016 076907 supported by the Ministry of Economy and Competitiveness); the Catalina Ruiz Postdoctoral Fellowship for Training of Research Personnel 2021 (ref APCR 2021010020 supported by Canary Islands Government)] and research projects [National project titled assessment of the health status of three species of resident cetaceans in the Canary archipelago: *Physeter macrocephalus*, *Tursiops truncatus*, *Globicephala macrorhynchus*] supported by the Ministry of Science and Technology (ref REN 2002-04162-C02-01); Embolic Pathology (gas) in Cetaceans (PEGCET 3, PEGCET 4 and PEGCET 5) supported by the Ministry of Economy and Competitiveness and the Ministry of Science, Innovation and Universities, respectively (ref CGL 2015 71498 P, PGC2018-101226-B-100 and PID2021-127687NB-I00)].

Institutional Review Board Statement: Not applicable.

Informed Consent Statement: No consent was obtained from the fishermen, as the bodies were relayed onto the Zoological Society of London for examination by a third party. Nevertheless, in terms of licensing for their work on strandings in the UK, they operate under a class license issued by Natural England, which covers them for possession of bodies/samples from protected species.

Data Availability Statement: Data sharing is not applicable for this article.

Acknowledgments: The authors wish to thank Celso Reis, Head of Glycobiology in Cancer at i3S/Ipatimup, University of Porto, and his team. We would like to thank Manolo Carrillo, Vidal Martin, and Marisa Tejedor for their collaboration in the Canary Islands Network (Canary Islands Government).

Conflicts of Interest: The authors declare no conflict of interest. The funders had no role in the design of the study; in the collection, analyses, or interpretation of the data; in the writing of the manuscript; or in the decision to publish the results.

Abbreviations

Alb	Albumin
APP	Acute phase proteins
A1AT	α1-antitrypsine
CAB	Chromotrope aniline blue trichrome
CK	Cytokeratin
DSL	Datura stramonium lectin
FB	Fibrinogen
GNA	Galanthus nivalis agglutinin
HSP	Heat shock protein
H&E	Hematoxylin and eosin
IHC	Immunohistochemical
IEGs	Intracytoplasmic eosinophilic globules
MALDI-TOF	Matrix-assisted laser desorption/ionization time-of-flight mass spectrometry
O-GlcNac	O-link β-N-acetylglucosamine
PAS	Periodic acid–Schiff
PAS-d	Periodic acid–Schiff-diastase
PBS	Phosphate-buffered saline
PHA-E	Phaseolus vulgaris erythroagglutinin
PHA-L	Phaseolus vulgaris leucoagglutinin
PP	Pink point
PTAH	Phosphotungstic acid hematoxylin
SNA	Sambucus nigra lectin
SSR	Stranding stress response

TBST	Tris-buffered saline and polysorbate
TEM	Transmission electron microscopy
TFA	Trifluoroacetic acid
WGA	Wheat germ agglutinin

References

1. Scheckel, C.; Aguzzi, A. Prions, Prionoids and Protein Misfolding Disorders. *Nat. Rev. Genet.* **2018**, *19*, 405–418. [CrossRef] [PubMed]
2. Strnad, P.; Nuraldeen, R.; Guldiken, N.; Hartmann, D.; Mahajan, V.; Denk, H.; Haybaeck, J. Broad Spectrum of Hepatocyte Inclusions in Humans, Animals, and Experimental Models. *Compr. Physiol.* **2013**, *3*, 1393–1436. [CrossRef] [PubMed]
3. Boyd, K.L.; Latimer, K.S. Hepatic Hyaline Globules in an Eclectus Parrot (*Eclectus Roratus*). *J. Vet. Diagn. Investig.* **2001**, *13*, 270–272. [CrossRef] [PubMed]
4. Klatt, E.C.; Koss, M.N.; Young, T.S.; Macauley, L.; Martin, S.E. Hepatic Hyaline Globules Associated with Passive Congestion. *Arch. Pathol. Lab. Med.* **1988**, *112*, 510–513.
5. Ng, I.O.; Ng, M.; Lai, E.C.; Wu, P.C. Endoplasmic Storage Disease of Liver: Characterization of Intracytoplasmic Hyaline Inclusions. *Histopathology* **1989**, *15*, 473–481. [CrossRef]
6. Storch, W. Immunohistological Investigations of PAS-Negative Globular Intracisternal Hyalin in Human Liver Biopsy Specimens. *Virchows Arch. B Cell Pathol. Incl. Mol. Pathol.* **1985**, *48*, 155–165. [CrossRef]
7. Stumptner, C.; Heid, H.; Fuchsbichler, A.; Hauser, H.; Mischinger, H.J.; Zatloukal, K.; Denk, H. Analysis of Intracytoplasmic Hyaline Bodies in a Hepatocellular Carcinoma. Demonstration of P62 as Major Constituent. *Am. J. Pathol.* **1999**, *154*, 1701–1710. [CrossRef]
8. Zatloukal, K.; French, S.W.; Stumptner, C.; Strnad, P.; Harada, M.; Toivola, D.M.; Cadrin, M.; Omary, M.B. From Mallory to Mallory-Denk Bodies: What, How and Why? *Exp. Cell Res.* **2007**, *313*, 2033–2049. [CrossRef]
9. Bradfield, J.W.; Blenkinsopp, W.K. Alpha-1-Antitrypsin Globules in the Liver and PiM Phenotype. *J. Clin. Pathol.* **1977**, *30*, 464–466. [CrossRef]
10. Wegiel, J.; Wisniewski, H.M. Rosenthal Fibers, Eosinophilic Inclusions, and Anchorage Densities with Desmosome-like Structures in Astrocytes in Alzheimer's Disease. *Acta Neuropathol.* **1994**, *87*, 355–361. [CrossRef]
11. Takahashi, H.; Wakabayashi, K. The Cellular Pathology of Parkinson's Disease. *Neuropathology* **2001**, *21*, 315–322. [CrossRef]
12. Li, W.M. Histopathology of Primary Cutaneous Amyloidoses and Systemic Amyloidosis. *Clin. Dermatol.* **1990**, *8*, 30–35. [CrossRef] [PubMed]
13. Holmes, D.D.; Smith, P.D. Inclusion Bodies in Hepatic Cytoplasm of Dogs and Rats after Administering Endotoxin. *Am. J. Vet. Res.* **1969**, *30*, 811–815. [PubMed]
14. Bull, L.B. The Histological Evidence of Liver Damage from Pyrrolizidine Alkaloids: Megalocytosis of the Liver Cells and Inclusion Globules. *Aust. Vet. J.* **1955**, *31*, 33–40. [CrossRef]
15. Hashimoto, K.; Hoshii, Y.; Takahashi, M.; Mitsuno, S.; Hanai, N.; Watanabe, Y.; Ishihara, T. Use of a Monoclonal Antibody against Lafora Bodies for the Immunocytochemical Study of Ground-Glass Inclusions in Hepatocytes Due to Cyanamide. *Histopathology* **2001**, *39*, 60–65. [CrossRef] [PubMed]
16. Chan, J.K.C. The Wonderful Colors of the Hematoxylin-Eosin Stain in Diagnostic Surgical Pathology. *Int. J. Surg. Pathol.* **2014**, *22*, 12–32. [CrossRef] [PubMed]
17. Al-Nafussi, A.I.; Hughes, D.E.; Williams, A.R. Hyaline Globules in Ovarian Tumours. *Histopathology* **1993**, *23*, 563–566. [CrossRef]
18. Reymundo, C.; Toro, M.; Morales, C.; López-Beltrán, A.; Nogales, F.; Nogales, F.J. Hyaline Globules in Uterine Malignant Mixed Müllerian Tumours. A Diagnostic Aid? *Pathol. Res. Pract.* **1993**, *189*, 1063–1066. [CrossRef]
19. Shibayama, Y.; Yahara, M.; Saitoh, M.; Nakata, K. The Pathogenesis of Hyaline Globules in Liver Cells after Partial Hepatectomy in Rats. *Exp. Mol. Pathol.* **1991**, *54*, 41–46. [CrossRef]
20. Shibayama, Y.; Yahara, M.; Nakata, K. The Fate of Vacuolation in Liver Cells with Special Reference to Hyaline Globules. *J. Pathol.* **1990**, *162*, 335–340. [CrossRef]
21. Trowell, O.A. The Experimental Production of Watery Vacuolation of the Liver. *J. Physiol.* **1946**, *105*, 268–297. [CrossRef] [PubMed]
22. Moon, W.S.; Yu, H.C.; Chung, M.J.; Kang, M.J.; Lee, D.G. Pale Bodies in Hepatocellular Carcinoma. *J. Korean Med. Sci.* **2000**, *15*, 516–520. [CrossRef]
23. Pariente, E.A.; Degott, C.; Martin, J.P.; Feldmann, G.; Potet, F.; Benhamou, J.P. Hepatocytic PAS-Positive Diastase-Resistance Inclusions in the Absence of Alpha-1-Antitrypsin Deficiency--High Prevalence in Alcoholic Cirrhosis. *Am. J. Clin. Pathol.* **1981**, *76*, 299–302. [CrossRef]
24. Mallory, F.B. Cirrhosis of the Liver: Five Different Types of Lesions from Which It May Arise. *Bull. Johns Hopkins Hosp.* **1911**, *22*, 69–74.
25. Lafora, G.R.; Glueck, B. Beitrag Zur Histopathologie Der Myoklonischen Epilepsie. *Z. Gesamte Neurol. Psychiatr.* **1911**, *6*, 15. [CrossRef]
26. Lévy, E.; El Banna, N.; Baïlle, D.; Heneman-Masurel, A.; Truchet, S.; Rezaei, H.; Huang, M.-E.; Béringue, V.; Martin, D.; Vernis, L. Causative Links between Protein Aggregation and Oxidative Stress: A Review. *Int. J. Mol. Sci.* **2019**, *20*, 3896. [CrossRef]

27. Denk, H.; Stumptner, C.; Fuchsbichler, A.; Müller, T.; Farr, G.; Müller, W.; Terracciano, L.; Zatloukal, K. Are the Mallory Bodies and Intracellular Hyaline Bodies in Neoplastic and Non-Neoplastic Hepatocytes Related? *J. Pathol.* **2006**, *208*, 653–661. [CrossRef]
28. Weids, A.J.; Ibstedt, S.; Tamás, M.J.; Grant, C.M. Distinct Stress Conditions Result in Aggregation of Proteins with Similar Properties. *Sci. Rep.* **2016**, *6*, 24554. [CrossRef]
29. McClellan, A.J.; Tam, S.; Kaganovich, D.; Frydman, J. Protein Quality Control: Chaperones Culling Corrupt Conformations. *Nat. Cell Biol.* **2005**, *7*, 736–741. [CrossRef]
30. Paradowski, M.; Lobos, M.; Kuydowicz, J.; Krakowiak, M.; Kubasiewicz-Ujma, B. Acute Phase Proteins in Serum and Cerebrospinal Fluid in the Course of Bacterial Meningitis. *Clin. Biochem.* **1995**, *28*, 459–466. [CrossRef]
31. Denk, H.; Stumptner, C.; Zatloukal, K. Mallory Bodies Revisited. *J. Hepatol.* **2000**, *32*, 689–702. [CrossRef] [PubMed]
32. Kurtovic, E.; Limaiem, F. *Mallory Bodies*; StatPearls Publishing: Treasure Island, FL, USA, 2023.
33. Domingo, M.; Visa, J.; Pumarola, M.; Marco, A.J.; Ferrer, L.; Rabanal, R.; Kennedy, S. Pathologic and Immunocytochemical Studies of Morbillivirus Infection in Striped Dolphins (*Stenella Coeruleoalba*). *Vet. Pathol.* **1992**, *29*, 1–10. [CrossRef]
34. Kennedy, S.; Di Guardo, G.; McConnell, S.; Moffett, D.; Agrimi, U. Histological, Histochemical and Ultrastructural Features of Hyaline Inclusions in Hepatocytes of Striped Dolphins (*Stenella coeruleoalba*). *J. Comp. Pathol.* **1993**, *109*, 179–185. [CrossRef]
35. Jaber, J.R.; Pérez, J.; Arbelo, M.; Andrada, M.; Hidalgo, M.; Gómez-Villamandos, J.C.; Van Den Ingh, T.; Fernández, A. Hepatic Lesions in Cetaceans Stranded in the Canary Islands. *Vet. Pathol.* **2004**, *41*, 147–153. [CrossRef]
36. Arbelo, M.; de los Monteros, A.; Herráez, P.; Andrada Borzollino, M.; Sierra, E.; Rodríguez Guisado, F.; Jepson, P.; Fernández, A. Pathology and Causes of Death of Stranded Cetaceans in the Canary Islands (1999–2005). *Dis. Aquat. Organ.* **2013**, *103*, 87–99. [CrossRef] [PubMed]
37. Díaz-Delgado, J.; Fernández, A.; Sierra, E.; Sacchini, S.; Andrada, M.; Vela, A.I.; Quesada-Canales, Ó.; Paz, Y.; Zucca, D.; Groch, K.; et al. Pathologic Findings and Causes of Death of Stranded Cetaceans in the Canary Islands (2006–2012). *PLoS ONE* **2018**, *13*, e0204444. [CrossRef] [PubMed]
38. Geraci, J.R.; Lounsbury, V.J. *Marine Mammals Ashore: A Field Guide for Strandings*; National Aquarium: Baltimore, MD, USA, 2005; ISBN 0977460908.
39. Hall, J.E.; Hall, M.E. Chapter 70: Protein Metabolism. In *Guyton and Hall Textbook of Medical Physiology*; Elsevier Health Sciences: Amsterdam, The Netherlands, 2020; pp. 865–870. ISBN 0323640036.
40. Li, X.; Elwell, M.R.; Ryan, A.M.; Ochoa, R. Morphogenesis of Postmortem Hepatocyte Vacuolation and Liver Weight Increases in Sprague-Dawley Rats. *Toxicol. Pathol.* **2003**, *31*, 682–688. [CrossRef]
41. Yamada, M.; Nakamura, K.; Nakajima, Y.; Yamamoto, M.; Komae, H.; Okuda, K.; Tsuji, M.; Arai, M. Ground-Glass Hepatocytes in Fibrinogen Storage Disease in Japanese Black Calves. *J. Comp. Pathol.* **2002**, *126*, 95–99. [CrossRef]
42. Bancroft, J.D.; Stevens, A. *Theory and Practice of Histological Techniques*; Churchill Livingstone: New York, NY, USA, 1996.
43. Nayak, N.C.; Sathar, S.A.; Mughal, S.; Duttagupta, S.; Mathur, M.; Chopra, P. The Nature and Significance of Liver Cell Vacuolation Following Hepatocellular Injury—An Analysis Based on Observations on Rats Rendered Tolerant to Hepatotoxic Damage. *Virchows Arch.* **1996**, *428*, 353–365. [CrossRef]
44. Dai, C.-L.; Xia, Z.-L.; Kume, M.; Yamamoto, Y.; Yamagami, K.; Ozaki, N.; Yamaoka, Y. Heat Shock Protein 72 Normothermic Ischemia, and the Impact of Congested Portal Blood Reperfusion on Rat Liver. *World J. Gastroenterol.* **2001**, *7*, 415. [CrossRef]
45. Gruys, E.; Toussaint, M.J.M.; Niewold, T.A.; Koopmans, S.J. Acute Phase Reaction and Acute Phase Proteins. *J. Zhejiang Univ. B* **2005**, *6*, 1045–1056. [CrossRef]
46. Hanada, S.; Strnad, P.; Brunt, E.M.; Omary, M.B. The Genetic Background Modulates Susceptibility to Mouse Liver Mallory-Denk Body Formation and Liver Injury. *Hepatology* **2008**, *48*, 943–952. [CrossRef] [PubMed]
47. Stumptner, C.; Fuchsbichler, A.; Zatloukal, K.; Denk, H. In Vitro Production of Mallory Bodies and Intracellular Hyaline Bodies: The Central Role of Sequestosome 1/P62. *Hepatology* **2007**, *46*, 851–860. [CrossRef]
48. Soulsbury, C.D.; Iossa, G.; Harris, S. The Animal Welfare Implications of Cetacean Deaths in Fisheries. In *A University of Bristol Report to the Whale and Dolphin Conservation Society (WDC)*; University of Bristol: Bristol, UK, 2008.
49. Cellarier, G.; Bonal, J.; Bouchiat, C.; Talard, P.; Dussarat, G. V Acute Ischemic Liver. *Press. Med.* **1995**, *24*, 1418–1420.
50. Neubauer, K.; Knittel, T.; Armbrust, T.; Ramadori, G. Accumulation and Cellular Localization of Fibrinogen/Fibrin during Shortterm and Longterm Rat Liver Injury. *Gastroenterology* **1995**, *108*, 1124–1135. [CrossRef] [PubMed]
51. Kragh-Hansen, U.; Donaldson, D.; Jensen, P.H. The Glycan Structure of Albumin Redhill, a Glycosylated Variant of Human Serum Albumin. *Biochim. Biophys. Acta (BBA) Protein Struct. Mol. Enzymol.* **2001**, *1550*, 20–26. [CrossRef]
52. Sugio, S.; Kashima, A.; Mochizuki, S.; Noda, M.; Kobayashi, K. Crystal Structure of Human Serum Albumin at 2.5 Å Resolution. *Protein Eng.* **1999**, *12*, 439–446. [CrossRef]
53. Dierauf, L.; Gulland, F.M.D. *CRC Handbook of Marine Mammal Medicine: Health, Disease, and Rehabilitation*; CRC Press: Boca Raton, FL, USA, 2001; ISBN 1420041630.
54. Barber, M.D.; Preston, T.; McMillan, D.C.; Slater, C.; Ross, J.A.; Fearon, K.C.H. Modulation of the Liver Export Protein Synthetic Response to Feeding by an N− 3 Fatty-Acid-Enriched Nutritional Supplement Is Associated with Anabolism in Cachectic Cancer Patients. *Clin. Sci.* **2004**, *106*, 359–364. [CrossRef]
55. Câmara, N.; Sierra, E.; Fernández-Maldonado, C.; Espinosa De Los Monteros, A.; Arbelo, M.; Fernández, A.; Herráez, P. Stress Cardiomyopathy in Stranded Cetaceans: A Histological, Histochemical and Immunohistochemical Study. *Vet. Rec.* **2019**, *185*, 694. [CrossRef]

56. Câmara, N.; Sierra, E.; Fernández, A.; Arbelo, M.; Andrada, M.; Monteros, A.E.D.L.; Herráez, P. Increased Plasma Cardiac Troponin I in Live-Stranded Cetaceans: Correlation with Pathological Findings of Acute Cardiac Injury. *Sci. Rep.* **2020**, *10*, 1555. [CrossRef]
57. Câmara, N.; Sierra, E.; Fernández, A.; Arbelo, M.; Bernaldo de Quirós, Y.; Arregui, M.; Consoli, F.; Herráez, P. Capture Myopathy and Stress Cardiomyopathy in a Live-Stranded Risso's Dolphin (Grampus Griseus) in Rehabilitation. *Animals* **2020**, *10*, 220. [CrossRef]
58. Câmara, N.; Sierra, E.; Fernández, A.; Suárez-Santana, C.M.; Puig-Lozano, R.; Arbelo, M.; Herráez, P. Skeletal and Cardiac Rhabdomyolysis in a Live-Stranded Neonatal Bryde's Whale with Fetal Distress. *Front. Vet. Sci.* **2019**, *6*, 476. [CrossRef] [PubMed]
59. Herráez, P.; Espinosa de los Monteros, A.; Fernández, A.; Edwards, J.F.; Sacchini, S.; Sierra, E. Capture Myopathy in Live-Stranded Cetaceans. *Vet. J.* **2013**, *196*, 181–188. [CrossRef]
60. Herráez, P.; Sierra, E.; Arbelo, M.; Jaber, J.R.; Espinosa De Los Monteros, A.; Fernández, A. Rhabdomyolysis and Myoglobinuric Nephrosis (Capture Myopathy) in a Striped Dolphin. *J. Wildl. Dis. Wildl. Dis. Assoc.* **2007**, *43*, 770–774. [CrossRef] [PubMed]
61. Yang, H.; Zhang, W.-J.; Wu, L.-Q.; Gu, F.; Ye, L.-Y.; Li, J.; Xu, S.-Q.; Xu, Y.-P.; Lou, J.-N. Protection of Liver Sinusoidal Endothelial Cells from Hypoxia-Reoxygenation Induced Apoptosis by Alpha-1 Antitrypsin in Vitro. *Zhonghua Yi Xue Za Zhi* **2005**, *85*, 106–110. [PubMed]
62. Granell, S.; Baldini, G.; Mohammad, S.; Nicolin, V.; Narducci, P.; Storrie, B.; Baldini, G. Sequestration of Mutated A1-Antitrypsin into Inclusion Bodies Is a Cell-Protective Mechanism to Maintain Endoplasmic Reticulum Function. *Mol. Biol. Cell* **2008**, *19*, 572–586. [CrossRef] [PubMed]
63. Vidal, R.; Blanco, I.; Casas, F.; Jardí, R.; Miratvilles, M.; de Pacientes, C.D.R.N. Diagnóstico y Tratamiento Del Déficit de Alfa-1-Antitripsina. *Arch. Bronconeumol.* **2006**, *42*, 645–659. [CrossRef] [PubMed]
64. Laurell, C.-B.; Eriksson, S. The Electrophoretic α; 1-Globulin Pattern of Serum in α; 1-Antitrypsin Deficiency. *Scand. J. Clin. Lab. Investig.* **1963**, *15*, 132–140. [CrossRef]
65. Sharp, H.L.; Bridges, R.A.; Krivit, W.; Freier, E.F. Cirrhosis Associated with Alpha-1-Antitrypsin Deficiency: A Previously Unrecognized Inherited Disorder. *J. Lab. Clin. Med.* **1969**, *73*, 934–939.
66. Parkes, M.J. Breath-holding and Its Breakpoint. *Exp. Physiol.* **2006**, *91*, 1–15. [CrossRef]
67. Siebert, U.; Tolley, K.; Vikingsson, G.A.; Olafsdottir, D.; Lehnert, K.; Weiss, R.; Baumgärtner, W. Pathological Findings in Harbour Porpoises (*Phocoena Phocoena*) from Norwegian and Icelandic Waters. *J. Comp. Pathol.* **2006**, *134*, 134–142. [CrossRef]
68. Cowan, D.F.; Curry, B.E. Histopathology of the Alarm Reaction in Small Odontocetes. *J. Comp. Pathol.* **2008**, *139*, 24–33. [CrossRef] [PubMed]
69. Simsek, Z.; Ekinci, O.; Cindoruk, M.; Karakan, T.; Degertekin, B.; Akyol, G.; Unal, S. Fibrinogen Storage Disease without Hypofibrinogenemia Associated with Estrogen Therapy. *BMC Gastroenterol.* **2005**, *5*, 36. [CrossRef] [PubMed]
70. Ji, C. Dissection of Endoplasmic Reticulum Stress Signaling in Alcoholic and Non-alcoholic Liver Injury. *J. Gastroenterol. Hepatol.* **2008**, *23*, S16–S24. [CrossRef] [PubMed]
71. Varki, A.; Cummings, R.; Esko, J.; Freeze, H.; Hart, G.; Marth, J. Proteoglycans and Glycosaminoglycans. In *Essentials of Glycobiology*; Cold Spring Harbor Laboratory Press: Cold Spring Harbor, NY, USA, 1999.
72. Hosokawa, N.; Tremblay, L.O.; You, Z.; Herscovics, A.; Wada, I.; Nagata, K. Enhancement of Endoplasmic Reticulum (ER) Degradation of Misfolded Null Hong Kong A1-Antitrypsin by Human ER Mannosidase I. *J. Biol. Chem.* **2003**, *278*, 26287–26294. [CrossRef]
73. McMillan, P.N.; Hixson, D.C.; Hevey, K.A.; Naik, S.; Jauregui, H.O. Hepatocyte Cell Surface Polarity as Demonstrated by Lectin Binding. *J. Histochem. Cytochem. Off. J. Histochem. Soc.* **1988**, *36*, 1561–1571. [CrossRef] [PubMed]
74. Chatham, J.C.; Marchase, R.B. The Role of Protein O-Linked Beta-N-Acetylglucosamine in Mediating Cardiac Stress Responses. *Biochim. Biophys. Acta* **2010**, *1800*, 57–66. [CrossRef] [PubMed]
75. Jones, S.P.; Zachara, N.E.; Ngoh, G.A.; Hill, B.G.; Teshima, Y.; Bhatnagar, A.; Hart, G.W.; Marbán, E. Cardioprotection by N-Acetylglucosamine Linkage to Cellular Proteins. *Circulation* **2008**, *117*, 1172–1182. [CrossRef] [PubMed]
76. Sohn, K.-C.; Lee, K.-Y.; Park, J.E.; Do, S.-I. OGT Functions as a Catalytic Chaperone under Heat Stress Response: A Unique Defense Role of OGT in Hyperthermia. *Biochem. Biophys. Res. Commun.* **2004**, *322*, 1045–1051. [CrossRef]
77. Zachara, N.E.; O'Donnell, N.; Cheung, W.D.; Mercer, J.J.; Marth, J.D.; Hart, G.W. Dynamic O-GlcNAc Modification of Nucleocytoplasmic Proteins in Response to Stress. A Survival Response of Mammalian Cells. *J. Biol. Chem.* **2004**, *279*, 30133–30142. [CrossRef]
78. Housley, M.P.; Rodgers, J.T.; Udeshi, N.D.; Kelly, T.J.; Shabanowitz, J.; Hunt, D.F.; Puigserver, P.; Hart, G.W. O-GlcNAc Regulates FoxO Activation in Response to Glucose. *J. Biol. Chem.* **2008**, *283*, 16283–16292. [CrossRef] [PubMed]
79. L'Hôte, C.; Berger, S.; Bourgerie, S.; Duval-Iflah, Y.; Julien, R.; Karamanos, Y. Use of Porcine Fibrinogen as a Model Glycoprotein to Study the Binding Specificity of the Three Variants of K88 Lectin. *Infect. Immun.* **1995**, *63*, 1927–1932. [CrossRef]
80. Saukko, P.; Knight, B. The Pathology of Wounds. In *Knight's Forensic Pathology*; CRC Pres: Boca Raton, FL, USA, 2004; pp. 136–173. ISBN 9781444115383.
81. Kimura, M.; Abe, M. Histology of Postmortem Changes in Rat Livers to Ascertain Hour of Death. *Int. J. Tissue React.* **1994**, *16*, 139–150.
82. Sykes, B.I.; Penny, E.; Purchase, I.F. Hepatocyte Vacuolation and Increased Liver Weight Occurring in Anoxic Rats. *Toxicol. Appl. Pharmacol.* **1976**, *36*, 31–39. [CrossRef]

83. Lei, L.; Yu, J.; Bao, E. Expression of Heat Shock Protein 90 (Hsp90) and Transcription of Its Corresponding MRNA in Broilers Exposed to High Temperature. *Br. Poult. Sci.* **2009**, *50*, 504–511. [CrossRef]
84. Southern, S.; Allen, A.; Kellar, N. Molecular Signature of Physiological Stress in Dolphins Based on Protein Expression Profiling of Skin. 2002. Available online: https://www.researchgate.net/publication/268397040_MOLECULAR_SIGNATURE_OF_PHYSIOLOGICAL_STRESS_IN_DOLPHINS_BASED_ON_PROTEIN_EXPRESSION_PROFILING_OF_SKIN (accessed on 21 January 2023).
85. Dhainaut, J.F.; Marin, N.; Mignon, A.; Vinsonneau, C. Hepatic Response to Sepsis: Interaction between Coagulation and Inflammatory Processes. *Crit. Care Med.* **2001**, *29*, S42–S47. [CrossRef]
86. Underwood, J.C. Light and Electron Microscopy of Globular Hyaline Inclusions in Liver Cells. *J. Clin. Pathol.* **1972**, *25*, 821–826. [CrossRef]
87. Junge, J.; Horn, T.; Christoffersen, P. Megamitochondria as a Diagnostic Marker for Alcohol Induced Centrilobular and Periportal Fibrosis in the Liver. *Virchows Arch. A. Pathol. Anat. Histopathol.* **1987**, *410*, 553–558. [CrossRef] [PubMed]
88. Kopito, R.R. Aggresomes, Inclusion Bodies and Protein Aggregation. *Trends Cell Biol.* **2000**, *10*, 524–530. [CrossRef] [PubMed]
89. Crouser, E.D.; Julian, M.W.; Huff, J.E.; Struck, J.; Cook, C.H. Carbamoyl Phosphate Synthase-1: A Marker of Mitochondrial Damage and Depletion in the Liver during Sepsis. *Crit. Care Med.* **2006**, *34*, 2439–2446. [CrossRef]
90. Spees, J.L.; Chang, S.A.; Snyder, M.J.; Chang, E.S. Thermal Acclimation and Stress in the American Lobster, Homarus Americanus: Equivalent Temperature Shifts Elicit Unique Gene Expression Patterns for Molecular Chaperones and Polyubiquitin. *Cell Stress Chaperones* **2002**, *7*, 97–106. [CrossRef] [PubMed]
91. Huang, T.-S.; Olsvik, P.A.; Krøvel, A.; Tung, H.; Torstensen, B.E. Stress-Induced Expression of Protein Disulfide Isomerase Associated 3 (PDIA3) in Atlantic Salmon (*Salmo salar* L.). *Comp. Biochem. Physiol. B Biochem. Mol. Biol.* **2009**, *154*, 435–442. [CrossRef] [PubMed]
92. Horibe, T.; Gomi, M.; Iguchi, D.; Ito, H.; Kitamura, Y.; Masuoka, T.; Tsujimoto, I.; Kimura, T.; Kikuchi, M. Different Contributions of the Three CXXC Motifs of Human Protein-Disulfide Isomerase-Related Protein to Isomerase Activity and Oxidative Refolding. *J. Biol. Chem.* **2004**, *279*, 4604–4611. [CrossRef] [PubMed]
93. Ellgaard, L.; Helenius, A. ER Quality Control: Towards an Understanding at the Molecular Level. *Curr. Opin. Cell Biol.* **2001**, *13*, 431–437. [CrossRef] [PubMed]
94. Wickner, S.; Maurizi, M.R.; Gottesman, S. Posttranslational Quality Control: Folding, Refolding, and Degrading Proteins. *Science* **1999**, *286*, 1888–1893. [CrossRef] [PubMed]
95. Bergfelt, D.; Lippolis, J.; Vandenplas, M.; Davis, S.; Miller, B.; Madan, R.; Kline, M.; Martinez, M.; Sanchez-Okrucky, R.; Almeida, A. Preliminary Analysis of the Proteome of Exhaled Breath Condensate in Bottlenose Dolphins (*Tursiops truncatus*). *Aquat. Mamm.* **2018**, *44*, 256–266. [CrossRef]
96. Desoubeaux, G.; Piqueras, M.D.C.; Le-Bert, C.; Fravel, V.; Clauss, T.; Delaune, A.J.; Daniels, R.; Jensen, E.D.; Flower, J.E.; Bossart, G.D.; et al. Labeled Quantitative Mass Spectrometry to Study the Host Response during Aspergillosis in the Common Bottlenose Dolphin (*Tursiops truncatus*). *Vet. Microbiol.* **2019**, *232*, 42–49. [CrossRef]
97. Kershaw, J.L.; Botting, C.H.; Brownlow, A.; Hall, A.J. Not Just Fat: Investigating the Proteome of Cetacean Blubber Tissue. *Conserv. Physiol.* **2018**, *6*, coy003. [CrossRef]
98. Mancia, A. New Technologies for Monitoring Marine Mammal Health. In *Marine Mammal Ecotoxicology*; Academic Press: Cambridge, MA, USA, 2018; pp. 291–320.

Disclaimer/Publisher's Note: The statements, opinions and data contained in all publications are solely those of the individual author(s) and contributor(s) and not of MDPI and/or the editor(s). MDPI and/or the editor(s) disclaim responsibility for any injury to people or property resulting from any ideas, methods, instructions or products referred to in the content.

MDPI AG
Grosspeteranlage 5
4052 Basel
Switzerland
Tel.: +41 61 683 77 34

Animals Editorial Office
E-mail: animals@mdpi.com
www.mdpi.com/journal/animals



Disclaimer/Publisher's Note: The title and front matter of this reprint are at the discretion of the Guest Editors. The publisher is not responsible for their content or any associated concerns. The statements, opinions and data contained in all individual articles are solely those of the individual Editors and contributors and not of MDPI. MDPI disclaims responsibility for any injury to people or property resulting from any ideas, methods, instructions or products referred to in the content.





Academic Open
Access Publishing

mdpi.com

ISBN 978-3-7258-9176-4